Natural Killer cells in cirrhosis and hepatocellular carcinoma and the role of LLT1 in the Liver and in hepatocellular carcinoma

Dr Naveenta Kumar

Wellcome Trust Clinical Research Fellow

Imperial College London

Division of Medicine

Department of Hepatology

Supervisors: Professor Salim Khakoo, Professor Rob Goldin, Late Dr Harry Antoniades

Thesis submitted for the degree of Doctor of Philosophy

Declaration of Originality

I declare that the content of this thesis is the result of my own work. The laboratory work, analysis, illustrations and written work were all performed by myself except where otherwise specified in the text.

Copyright Declaration

The copyright of this thesis rests with the author. Unless otherwise indicated, the contents are licenced under a Creative Commons Attribution Non-Commercial 4.0 International Licence (CC BY-NC).

Under this licence, you may copy and redistribute the material in any medium or format. You may also create and distribute modified version of the work. This is on the condition that: you credit the author and do not use it, or any derivative works, for a commercial purpose.

When reusing or sharing this work, ensure you make the licence terms clear to others by naming the licence and linking to the licence text. Where a work has been adapted, you should indicate that the work has been changed and describe those changes.

Please seek permission from the copyright holder for uses of this work that are not included in this licence or permitted under UK Copyright Law.

Abstract

Hepatocellular carcinoma (HCC) is a major complication of cirrhosis and liver disease secondary to alcohol related and non-alcohol related fatty liver disease (NAFLD) is a growing concern. Work identifying cancer specific or immunomodulatory antigens is key to rapidly advancing immunotherapeutic options. Natural Killer (NK) cells provide potent anti-pathogen and tumour surveillance responses. Harnessing NK cells is an exciting prospect as they are capable of direct cytotoxicity and mediate antibody-dependent cellular cytotoxicity. However, understanding pre-existing modifications to NK cells in cirrhosis is key to understanding the role of NK cells in disease and how they can be modified.

Peripheral blood and intrahepatic NK cells from patients with liver disease of a non-viral aetiology were characterised using flow cytometry, Nanostring technology and tissue culture techniques and compared to healthy controls. NK cells were hypofunctional, with reduced expression of key activating receptors NKp46, DNAM-1, and CD16 and an upregulation in inhibitory receptor CD161 in disease. NKp30 was associated with reduced cytotoxicity in NAFLD. The expansion of a CD56dimNK cell subpopulation in cirrhosis and HCC was identified, with reduced expression of CD16, increased expression of liver-homing CXCR6 and CCR5, preserved cytotoxic function but impaired cytokine production. Furthermore, having identified an increased proportion of CD161+ NK cells in cirrhosis, I demonstrated the increased expression of the ligand LLT1 on liver tissue in cirrhosis using immunohistochemistry and real-time quantitative PCR. By generating LLT1 overexpressing Huh7 cells, I demonstrated that LLT1 inhibits NK cell degranulation. Lastly, I demonstrated that tumour growth factor beta (TGFβ), a key cytokine in the pathogenesis of fibrosis, may result in the upregulation of LLT1 in the liver.

Overall the data describes an inhibitory profile of NK cells in cirrhosis with impaired function, identifies a novel dysfunctional CD56dimCD16+/-NK cell subpopulation in cirrhosis and HCC and identifies an inhibitory pathway important in cirrhosis.

Acknowledgements

I would like to thank Professor Salim Khakoo for all his kindness, guidance and support, not only pertaining to this work but also with navigating training and career choices. He has always been available despite being in a different city, has nurtured my love of science and taught me to be more confident in my achievements. Professor Goldin has also been very supportive throughout my time at Imperial, always available to talk and guide me through the tough times research has brought. I would like to acknowledge Dr Marco Purbhoo, an excellent scientist, who was my initial supervisor before he left Imperial after the first two months of my first year of research. And of course, I would like to thank Dr Harry Antoniades, who took over as a supervisor late in my second year and who passed away a few months into my fourth year. Harry always challenged me to challenge myself. He is missed dearly.

I'd like to thank the Wellcome Trust, for supporting me by funding this with a clinical research training fellowship award. I would like to thank my wonderful lab colleagues, especially Dr Fouzia Sadiq and Dr Mina Aletrari who taught me many techniques before they left Imperial, and Dr Wafa Khamri for all her help. The Liver Immunology lab group at Imperial College have been of infinite support, with regards to practical aspects within the laboratory and more recently with moral support. I would like to thank Dr Lucia Possamai, Dr Sujit Mukherjee, Dr Arjuna Singanayagam, Dr Rooshi Nathwani, Dr Evangelos Triantafyllou, Dr Fanny Lebosse and Dr Nikhil Vergis for making my time in research such an enjoyable experience. Professor Thursz has always provided support throughout my time in research and I am very appreciative of this. I would also like to thank Professor Nigel Heaton for all his support at the King's College Hospital site.

I would like to thank my mother and my wonderful late father for their guidance, and my sisters for allowing me to vent my stresses. Finally, I would like to dedicate this thesis to my wonderful husband Devesh and my gorgeous daughter Aradhya, who have honestly put up with so much, with my late night finishes in the laboratory, early morning starts and processing tissue into the weekends. They have patiently waited for me to get to the end of this chapter of my life, and I look forward to spending a lot more quality time with them.

Abstracts and Publications relating to this research

Publications:

Hepatitis B viral replication influences the expression of natural killer cell ligands

Lemonica Koumbi, Teresa Pollicino, Giovanni Raimondo, **Naveenta Kumar,** Peter Karayiannis, Salim I. Khakoo**,**

Ann Gastroenterol. Jul-Sep 2016;29(3):348-57.doi: 10.20524/aog.2016.0036. Epub 2016 Apr 25

Respiratory syncytial virus infection, TLR3 ligands and pro-inflammatory cytokines induce CD161 ligand LLT1 expression on the respiratory epithelium.

Satkunanathan S, **Kumar N**, Bajorek M, Purbhoo MA, Culley FJ.

J Virol. 2013 Dec 18 PMID: 24352438

Abstracts:

The LLT1-CD161 interaction: An important inhibitory interaction for NK cells in cirrhosis

Naveenta Kumar, Fouzia Sadiq, Sujit Mukherjee, Wafa Khamri, Fanny Lebosse, Ameet Dhar, Marco Purbhoo, Rob Goldin, Mark Thursz, Harry Antoniades, Salim Khakoo

Oral presentation at International Liver congress 2019, Vienna

Circulating NK cells in cirrhosis are hypofunctional with an expanded inhibitory, immature, liver-homing CD56dimCD16+/- NK cell proportion.

Naveenta Kumar, Wafa Khamri, Fouzia Sadiq, Evangelos Triantafyllou, Fanny Lebosse, Sujit Mukherjee, Ameet Dhar, Mark Thursz, Harry Antoniades, Salim Khakoo

Abstract, Awarded Young Investigator Registration Bursary, presented at the International Liver Congress, 2018

Circulating Natural Killer cells in Hepatocellular Carcinoma are hypofunctional with an exhausted phenotype

Naveenta Kumar, Wafa Khamri, Fouzia Sadiq, Oltin T. Pop, Sujit Mukherjee, Ameet Dhar, Rohini Sharma, Shahid A. Khan, Mark R. Thursz, Charalambos G. Antoniades, Salim Khakoo

Abstract, 2017, HEPATOLOGY, VOLUME 66, NUMBER 1 (SUPPL); 353A

A Novel inhibitory NK cell subpopulation is expanded in Cirrhosis

Naveenta Kumar, Wafa Khamri, Fouzia Sadiq, Fanny Lebosse, Rooshi Nathwani, Arjuna Singanayagam, Ameet Dhar, Mark R. Thursz, Charalambos G. Antoniades, Salim Khakoo,

Abstract, 2017, HEPATOLOGY, VOLUME 66, NUMBER 1 (SUPPL); 355A

A novel population of immunosuppressive CD8 T cells is expanded in patients with decompensated liver disease

F. Lebosse, **N. Kumar,** O. Pop, R. Nathwani, A. Singanayagam, S. Mukherjee, T.Z. Hou, A. Quaglia, F. Zoulim, J. Wendon, M. Thursz, A. Dhar, W. Khamri, C.G. Antoniades

Abstract, 2017, Journal of Hepatology, Vol. 66, Issue 1, S146

LLT1 is upregulated in Hepatocellular carcinoma and inhibits NK cell cytotoxicity

Kumar N, Mroz A, Aletrari M, Goldin R, Purbhoo M

Abstract awarded Poster of distinction, Gut Jun 2014, 63 (Suppl 1) A92; DOI: 10.1136/gutjnl-2014-307263.195

List of Abbreviations

ACLF Acute on chronic liver failure

AD Acute decompensation of cirrhosis

ADCC Antibody-dependent cell-mediated cytotoxicity

AFP Alpha-foetoprotein

AICL Activation-Induced C-Type Lectin

ALD Alcohol-Related Liver Disease

ALF Acute Liver Failure

ALT Alanine transaminase

ANOVA Analysis of Variance

APC Antigen presenting cell

AST Aspartate transaminase

BSA Bovine serum albumin

BCLC Barcelona Clinic Liver Cancer

CCL CC-chemokine ligand

CCR CC-chemokine receptor

CCRL CC-chemokine receptor-like

CD Cluster of differentiation

cDNA Complimentary Deoxyribonucleic Acid

CLEC2D C-type Lectin Domain Family 2 member D

CMV Cytomegalovirus

CO2 Carbon dioxide

CRC Colorectal carcinoma

CT Threshold cycle

CXCL Chemokine ligand

CXCR Chemokine receptor

DMEM Dulbecco's modified eagle medium

DMSO Dimethyl sulfoxide

DNA Deoxyribonucleic acid

DNAM DNAX accessory molecule

EDTA Ethylene diamine tetraacetic Acid

ELISA Enzyme-linked immuno sorbent assay

Eomes Eomesodermin

E:T Effector to target ratio

FACS Fluorescence-activated cell sorting

FasL Fas ligand

FCS Fetal calf serum

FcRγ Fc receptor γ-chain

FDR False discovery rate

FITC Fluorescein isothiocyanate

FMO Fluorescence Minus One

GM-CSF Granulocyte-macrophage colony-stimulating factor

GZM Granzyme

HBV Hepatitis B virus

HCC Hepatocellular carcinoma

hCMV Human cytomegalovirus

HCV Hepatitis C virus

HEPES Hydroxy ethyl piperazine ethane sulfonic acid

HIV Human immunodeficiency virus

HLA Human leukocyte Antigen

HLA-DR Human leukocyte Antigen – antigen D related

HSECs Hepatic sinusoidal endothelial cells

ICAM Intracellular adhesion molecule

IFNγ Interferon gamma

IL Interleukin

ILC Innate-like lymphocytes

INR International Normalised Ratio

IQR Interquartile range

ITAM Immunoreceptor Tyrosine-Based Activation Motifs

ITIM Immunoreceptor Tyrosine-Based Inhibitory Motif

ITGA Integrin alpha

JAK Janus kinase

KIR Killer cell immunoglobulin like receptors

KLRG1 Killer Cell Lectin-Like Receptor G1

LAMP Lysosomal-associated membrane protein

LFA-1 Lymphocyte Adhesion Molecule-1

LILR Leukocyte Immunoglobulin-Like Receptor

LIF Leukaemia inhibitory factor

LLT1 Lectin like transcript 1

MAPK Mitogen Activated Protein Kinase

MELD Model Of End Stage Liver Disease score

MELD-Na MELD sodium score

MFI Median fluorescence intensity

MHC Major histocompatibility complex

MIC MHC class I chain related molecule

MIP Macrophage inflammatory protein

MNC Mononuclear cells

mRNA Messenger ribonucleic acid

mTOR Mechanistic target of rapamycin

NAFLD Non-alcoholic fatty liver disease

NASH Non-alcoholic steatohepatitis

NCAM Neural cell adhesion molecule

NFILS Nuclear factor, interleukin 3 regulated

NFκB Nuclear factor kappa-light-chain-enhancer of activated B cells

NK Natural killer

PAMP Pathogen associated molecular patterns

PBMCs Peripheral blood mononuclear cells

PBS Phosphate buffered saline

PCR Polymerase chain reaction

PE Phycoerythrin

PFA Paraformaldehyde

PMA Phorbol 12- myristate 13-acetate

PMA/I Phorbol 12- myristate 13-acetate and ionomycin

PRF Perforin

PVR Paraformaldehyde

qRT-PCR Quantitative Real Time Reverse Transcription Polymerase Chain Reaction

RANTES Regulated on activation, normal T expressed and secreted

REC Research ethics committee

RNA Ribonucleic acid

ROR RAR-related orphan receptor

ROS Reactive oxygen species

RPMI Roswell park memorial institute medium

SD Standard Deviation

S1PR1 Sphingosine-1-phosphate receptor 1

STAT Signal transducer and activator of transcription

T-bet T-box expressed in T cells

TCR T Cell Receptor

TGF Transforming growth factor

Th T helper

TIGIT T-cell immunoreceptor with immunoglobulin and ITIM domains

TLR Toll-like receptor

TNF Tissue necrosis factor

TRAIL Tumour necrosis factor–related apoptosis-inducing ligand

ΔΔ CT Delta-Delta CT

Contents

NATURAL KILLER CELLS IN CIRRHOSIS AND HEPATOCELLULAR CARCINOMA AND THE ROLE OF LLT1 IN THE LIVER AND IN HEPATOCELLULAR CARCINOMA 1

DECLARATION OF ORIGINALITY 2

COPYRIGHT DECLARATION 2

ABSTRACT 3

ACKNOWLEDGEMENTS 4

ABSTRACTS AND PUBLICATIONS RELATING TO THIS RESEARCH 5

PUBLICATIONS: 5
ABSTRACTS: 5

LIST OF ABBREVIATIONS 7

1. INTRODUCTION 22

1.1 THE BURDEN OF LIVER DISEASE AND HEPATOCELLULAR CARCINOMA 22
1.1.1 DIAGNOSIS AND CURRENT THERAPEUTIC OPTIONS FOR HCC 22
1.1.2 PATHOGENESIS OF HCC 24
1.2 IMMUNE DYSFUNCTION IN CIRRHOSIS AND HCC 26
1.2.1 THE IMMUNOLOGICAL ROLE OF THE NORMAL LIVER 27
1.2.2 IMMUNE DYSFUNCTION IN CIRRHOSIS 29
1.2.3 THE TUMOUR MICROENVIRONMENT 30
1.2.4 IMMUNOTHERAPY IN HEPATOCELLULAR CARCINOMA 32
1.3 NK CELLS 33
1.3.1 NK CELL DEVELOPMENT 34
1.3.2 NK CELL EDUCATION 36
1.3.3 THE CIRCULATING NK CELL PHENOTYPE IN HEALTH 36
1.3.4 NK CELL EFFECTOR FUNCTIONS 39
1.3.5 CROSS TALK WITH OTHER IMMUNE CELLS 40
1.3.6 NK CELLS WITHIN THE HEALTHY LIVER 41
1.3.7 FUNCTIONAL ROLES OF NK CELLS IN ANTI-VIRAL, ANTI-PATHOGEN AND ANTI-TUMOURAL RESPONSES 43
1.3.8 NK CELLS IN LIVER DISEASE 45
1.4 HYPOTHESIS 56
1.5 THESIS AIMS 56

2. MATERIALS AND METHODS 57

2.1. ETHICS 57
2.2 SUBJECT SELECTION AND SAMPLE COLLECTION 57
2.2.1 PATIENT RECRUITMENT AND SAMPLE COLLECTION 57
2.2.2 HEALTHY CONTROLS 58
2.3. SAMPLE PROCESSING 58
2.3.1 WHOLE BLOOD PROCESSING 58
2.3.2 LIVER TISSUE PROCESSING 58
2.4 CELL LINES AND CELL CULTURE 59
2.4.1 K562 59
2.4.2 HUH7 59

2.4.3 HepG2 59
2.4.4 Jurkat 59
2.4.5 Raji Cells 60
Cell culture and reagents 60
2.5 NK cell phenotyping 62
2.5.1 Ex-vivo phenotyping using flow cytometry 62
2.5.2 Phenotyping following co-culture with K562 target cells 63
2.5.3 Phenotyping following co-culture with Huh7 cells 63
2.5.4 Phenotyping following incubation in serum from patients with cirrhosis 65
2.5.5 Gene expression analysis 65
2.6 NK cell functional assays 69
2.6.1 CD107a, Interferon gamma (IFNγ) and Tumour necrosis factor alpha (TNFa) in all NK cells 69
2.6.2 CD107a in NK cell subpopulations determined by CD56/CD16 expression 71
2.6.3 Ex-vivo Perforin and Granzyme B staining 71
2.6.4 Cytokine secretion 72
2.7 Immunohistochemistry 73
2.7.1 LLT1 expression and scoring and analysis by Image J 73
2.7.2 Double staining protocol to ascertain LLT1 co-localisation 78
2.8 Quantitative real-time PCR for LLT1 expression 79
2.9 Elisa for serum analysis for LLT1 79
2.10 LLT1 surface expression on liver cell lines 80
2.11 Stimulation of liver cell lines to upregulate LLT1 surface expression 81
2.12 LLT1 cloning and transfection 82
2.13 Co-culture of PBMCs with Huh7-LLT1 YFP transfectants 84
2.14 Clinical data 85
2.15 Statistical analysis 85

3. RESULTS: PHENOTYPIC AND FUNCTIONAL ANALYSIS OF NK CELLS IN PATIENTS WITH CIRRHOSIS AND HCC 86

3.1 Introduction 86
3.1 Characterising NK cell phenotype and function 87
3.1.1 Surface receptor expression 96
3.1.6 CXCR6 expression 157
3.1.7 Surface receptor co-expression 168
3.2 NK cell function 179
3.2.1 Singular NK cell responses to target cells 179
3.2.2 Polyfunctional NK cell responses to target cells 190
3.2.3 CD56bright and CD56dim NK cell responses to target cells 197
3.2.4 Correlation of NK cell functional responses with cirrhosis status and cirrhosis aetiology 206
3.2.5 NK cell surface receptor correlation with functional responses 218
3.3 Gene expression 223
3.3.1 Comparison of gene expression in CD56dimCD16++ NK cells in the circulation in health and in disease 224
3.3.2 Comparison of gene expression in CD56brightCD16- NK cells in the circulation in health and in disease 228
3.3.3 Gene-set enrichment analysis 233
3.3.2 Comparison of gene expression of intrahepatic NK cell subpopulations and circulating NK cell subpopulations 242
3.4 Discussion 252

4. RESULTS: CHARACTERISING THE CIRCULATING CD56DIMCD16+/- NK CELL SUBPOPULATION IN CIRRHOSIS 259

4.1 INTRODUCTION 259
4.2 CD56DIMCD16+/- NK CELL PHENOTYPE AND FUNCTION 261
4.2.1 SURFACE EXPRESSION OF ACTIVATING RECEPTORS ON NK CELL SUBPOPULATIONS 261
4.2.2 SURFACE EXPRESSION OF THE INHIBITORY RECEPTOR CD161 ON NK CELL SUBPOPULATIONS 274
4.2.3 SURFACE EXPRESSION OF LIVER HOMING RECEPTOR CXCR6 AND INTRAHEPATIC MARKERS 276
4.2.4 GENE EXPRESSION ANALYSES OF CIRCULATING CD56DIMCD16+/- CELLS IN CIRRHOSIS 289
4.2.5 CD56DIMCD16+/- NK CELL MATURITY 303
4.2.6 EFFECTOR FUNCTION IN CIRCULATING CD56DIMCD16+/- NK CELLS IN CIRRHOSIS 312
4.3 INDUCTION OF THE CD56DIMCD16+/- NK CELL SUBPOPULATION 319
4.3.1 CULTURE OF HEALTHY PBMCS IN MEDIA SUPPLEMENTED WITH SERA 319
4.3.2 POST-ACTIVATION PROFILE FOLLOWING INCUBATION WITH K562 TARGET CELLS 321
4.3.3 POST-ACTIVATION PHENOTYPE FOLLOWING CO-CULTURE WITH HUH7 CELLS 328
4.4 DISCUSSION 336

5. CHAPTER 5: LLT1 EXPRESSION IN THE LIVER AND INTERACTION WITH CD161+ NK CELLS 341

5.1 INTRODUCTION 341
5.2 LLT1 EXPRESSION IS UP-REGULATED ON LIVER EPITHELIUM IN CIRRHOSIS AND HEPATOCELLULAR CARCINOMA 343
5.2.1 LLT1 EXPRESSION ON LIVER TISSUE DETERMINED BY IMMUNOHISTOCHEMISTRY 343
5.2.2 LLT1 EXPRESSION ON LIVER TISSUE AS DETERMINED BY QUANTITATIVE REAL-TIME PCR 360
5.2.3 SOLUBLE LLT1 EXPRESSION 365
5.3 CD161 EXPRESSION ON IMMUNE CELLS 367
5.3.1 CD161 EXPRESSION ON CIRCULATING AND LIVER INFILTRATING NK CELLS 367
5.3.2 CD161 EXPRESSION ON CIRCULATING AND LIVER INFILTRATING T CELLS 378
5.4 FUNCTIONAL CONSEQUENCES OF THE LLT1-CD161 INTERACTION 404
5.4.1 LLT1 CAUSES A REDUCTION IN THE CYTOTOXIC CAPACITY OF NK CELLS 404
5.5 MECHANISM FOR LLT1 UP-REGULATION ON HEPATOCYTES 408
5.6 DISCUSSION 413

6. FINAL DISCUSSION AND CONCLUSION 418

6.1 NOVEL FINDINGS 418
6.2 FUTURE DIRECTIONS 422

7. REFERENCES 424

8. APPENDICES 459

8.1 LIST OF GENES ADDED TO THE NANOSTRING IMMUNOLOGY PANEL 459
8.2 SEQUENCE CONFIRMING CORRECT CLONING OF LLT1 AND CD161 460
8.3 APPENDIX C – CLINICAL PARAMETER CORRELATED WITH NK RECEPTOR EXPRESSION IN CIRCULATING NK CELLS IN PATIENTS WITH CIRRHOSIS AND PATIENTS WITH CIRRHOSIS AND HCC. 461
8.4 APPENDIX D - DIFFERENTIAL GENE EXPRESSION ANALYSES 464
8.5 COMPARISON OF SURFACE EXPRESSION OF RECEPTORS IN CIRCULATORY AND INTRAHEPATIC NK CELLS SUBPOPULATIONS 478
APPENDIX 8.6 CYTOKINE PRODUCTION IN NK CELL SUBSETS FOLLOWING PMA/IONOMYCIN STIMULATION 494
8.7 IMMUNOHISTOCHEMISTRY FOR LLT1 IN CHOLANGIOCARCINOMA 496

List of Figures

Figure 1 Stages of NK cell development (Adapted from Abel et al, 2018 and Scoville et al, 2017) 35
Figure 2 NK cell receptors. 38
Figure 3 Gating strategy for cell sorting NK cell subpopulations based on CD56 and CD16 expression 67
Figure 4 LLT1 Immunohistochemistry scoring system for LLT1 expression in the liver. Formalin fixed 75
Figure 5 Gating strategy for NK cells from peripheral blood mononuclear cells (PBMCs) and intrahepatic mononuclear cells (IMNCs). 92
Figure 6 The proportion of circulating peripheral blood mononuclear cells (PBMCs) that are NK cells. 94
Figure 7 The proportion of intrahepatic mononuclear cells (IMNCs) that are NK cells. 95
Figure 8 Paired analysis demonstrating that a greater proportion of intrahepatic mononuclear cells are NK cells in comparison to the proportion of circulating peripheral blood mononuclear cells that are NK cells. 96
Figure 9 NKG2D expression on NK cells. Gating strategy for NKG2D on NK cells using flow cytometry. 97
Figure 10 NKG2D expression on circulating NK cells.. 99
Figure 11 Comparisons of NKG2D expression in cirrhosis and HCC delineated by underlying aetiology. 100
Figure 12 NKG2D expression on circulating NK cells in cirrhosis and underlying MELD-Na score and Child-Pugh classification. 102
Figure 13 NKG2D expression on circulating NK cells in individuals with HCC analysed by Barcelona Clinic Liver Cancer (BCLC) classification.. 103
Figure 14 NKG2D expression on intrahepatic NK cells. 104
Figure 15 Gating strategy for DNAM-1+NK cells using flow cytometry. 106
Figure 16 DNAM-1 expression on circulating NK cells. 108
Figure 17 Comparing the proportion of circulating DNAM-1+NK cells in cirrhosis and in HCC delineated by underlying aetiology.. 109
Figure 18 DNAM-1 expression on circulating NK cells in cirrhosis and underlying MELD-Na score and Child-Pugh classification. 111
Figure 19 The proportion of DNAM-1+NK cells in the circulation in patients with HCC on a background of cirrhosis categorised by BCLC staging. 112
Figure 20 DNAM-1 expression on intrahepatic NK cells. Graph displays the percentage of NK cells expressing DNAM-1. 113
Figure 21 NKp30 and NKp46 expression. 115
Figure 22 NKp30 expression on circulating NK cells. 117
Figure 23 Comparisons of NKp30 expression in cirrhosis and HCC delineated by underlying aetiology. 118
Figure 24 NKp30 expression on circulating NK cells in cirrhosis and underlying MELD-Na score and Child-Pugh classification. 120
Figure 25 NKp30 expression on circulating NK cells in individuals with HCC analysed by Barcelona Clinic Liver Cancer (BCLC) classification.. 121
Figure 26 NKp30 expression (median fluorescence intensity) on circulating NK cells in cirrhosis correlated negatively with patient age (spearman rank correlation) 122
Figure 27 NKp30 expression on intrahepatic NK cells. 124
Figure 28 NKp46 expression on circulating NK cells. 126

Figure 29 Comparisons of NKp46 expression in cirrhosis and HCC delineated by underlying aetiology. 127
Figure 30 NKp46 expression on circulating NK cells in cirrhosis and underlying MELD-Na score and Child-Pugh classification. 129
Figure 31 NKp46 expression (median fluorescence intensity) on circulating NK cells in individuals with HCC analysed by Barcelona Clinic Liver Cancer (BCLC) classification.. 130
Figure 32 NKp46 expression on intrahepatic NK cells... 131
Figure 33 Gating strategy for circulating and intrahepatic CD161+NK cells using flow cytometry.... 133
Figure 34 CD161 expression on circulating NK cells. 135
Figure 35 Comparing the proportion of circulating CD161+NK cells in cirrhosis and in HCC delineated by underlying aetiology..... 136
Figure 36 CD161 expression on circulating NK cells in cirrhosis and underlying MELD-Na score and Child-Pugh classification. 138
Figure 37 The proportion of CD161+NK cells in the circulation in patients with HCC on a background of cirrhosis categorised by BCLC staging..... 140
Figure 38 CD161 expression on intrahepatic NK cells. Graph displays the percentage of CD161+NK cells. 141
Figure 39 Gating strategy for CD3-CD56+ NK cell subpopulations based on CD16 expression..... 143
Figure 40 CD56 and CD16 gating applied to peripheral blood and intrahepatic samples..... 144
Figure 41 CD16 expression on circulating CD56dim NK cells..... 145
Figure 42 CD16 expression on circulating CD56bright NK cells. 146
Figure 43 Circulating proportions of CD56dimCD16+/- NK cells. 148
Figure 44 A comparison of the proportion of circulating CD56dimCD16+/- NK cells in cirrhosis and HCC of differing aetiologies. 150
Figure 45 Circulating CD56dimCD16+/-NK cells in cirrhosis and underlying MELD-Na score and Child-Pugh classification. 152
Figure 46 The proportion of CD56dimCD16+/-NK cells in the circulation in patients with HCC on a background of cirrhosis categorised by BCLC staging..... 154
Figure 47 The proportion of intrahepatic CD56dimCD16+/-NK cells and comparison with circulating proportions of CD56dimCD16+/-NK cells. 156
Figure 48 Gating strategy for circulating and intrahepatic CXCR6+NK cells using flow cytometry.... 158
Figure 49 CXCR6 expression on circulating NK cells. Graphs demonstrate the percentage of all circulating NK cells that express CXCR6.. 160
Figure 50 Comparing the proportion of circulating CXCR6+NK cells in cirrhosis and in HCC delineated by underlying aetiology..... 161
Figure 51 CXCR6 expression on circulating NK cells in cirrhosis and underlying MELD-Na score and Child-Pugh classification. 163
Figure 52 The proportion of CXCR6+NK cells in the circulation in patients with HCC on a background of cirrhosis categorised by BCLC staging..... 164
Figure 53 CXCR6 expression on intrahepatic NK cells..... 166
Figure 54 Activating receptor co-expression on circulating NK cells in patients with hepatocellular carcinoma with cirrhosis secondary to underlying metabolic dysfunction-associated steatotic liver disease (MASLD HCC)..... 170
Figure 55 Activating receptor co-expression on circulating NK cells in patients with hepatocellular carcinoma and underlying cirrhosis secondary to alcohol related liver disease (ALD HCC)..... 171
Figure 56 NKp46 expression on circulating NK cells correlated negatively with the proportion of circulating NK cells that were CD56dimCD16+/- in patients with hepatocellular carcinoma (HCC).. 173

Figure 57 CD161 expression correlates with activating receptors NKp30, NKG2D and DNAM-1 on circulating NK cells in patients with hepatocellular carcinoma (HCC) and underlying cirrhosis secondary to metabolic dysfunction-associated steatotic liver disease (MASLD). 176
Figure 58 CXCR6 expression negatively correlated with DNAM-1 expression and CD161 expression on circulating NK cells in patients with Hepatocellular carcinoma (HCC) on a background of cirrhosis secondary to metabolic dysfunction-associated steatotic liver disease (MASLD). 177
Figure 59 Gating strategy for NK cells and functional experiments. 180
Figure 60 Optimisation for functional NK cell experiments..... 183
Figure 61 Degranulation (CD107a expression) in circulating NK cells in response to K562 and HepG2 target cells..... 185
Figure 62 Interferon gamma (IFNγ) production in circulating NK cells in response to K562 and HepG2 target cells..... 187
Figure 63 Tumour necrosis alpha (TNFα) production in circulating NK cells in response to K562 and HepG2 target cells..... 189
Figure 64 Gating strategy to identify polyfunctional NK cells with the capacity to produce a cytotoxic and cytokine response to target cells.. 190
Figure 65 Polyfunctional circulating NK cell responses to target cells. 192
Figure 66 Combined peripheral blood NK cell cytotoxic and interferon gamma responses to target cells. 194
Figure 67 Combined peripheral blood NK cell cytotoxic and tumour necrosis alpha responses to target cells..... 196
Figure 68 Gating strategy for CD56bright and CD56dim NK cells..... 197
Figure 69 Comparing the NK cell cytotoxicity response (by measuring CD107a expression) in CD56dim and CD56bright NK cells in healthy volunteers and patient groups against K562 target cells.. 199
Figure 70 Comparing interferon gamma (IFNγ) response in CD56dim and CD56bright NK cells in healthy volunteers and patient groups against K562 target cells. 201
Figure 71 Comparing tumour necrosis factor alpha (TNFα) response in CD56dim and CD56bright NK cells in healthy volunteers and patient groups against K562 target cells. 203
Figure 72 Comparing the capacity for a polyfunctional response in CD56dim and CD56bright NK cells in healthy volunteers and patient groups against K562 target cells. 205
Figure 73 CD107a expression in NK cells from patients with cirrhosis does not correlate with underlying cirrhosis status. 207
Figure 74 Interferon gamma (IFNγ) production in NK cells from patients with cirrhosis does not correlate with underlying cirrhosis status. 209
Figure 75 Tumour necrosis factor alpha (TNFα) production in NK cells from patients with cirrhosis does not correlate with underlying cirrhosis status. 211
Figure 76 Comparison of CD107a expression in NK cells in patients with alcohol related liver disease (ALD) and metabolic dysfunction-associated steatotic liver disease (MASLD)..... 213
Figure 77 Comparison of interferon gamma(IFNγ) production in NK cells in patients with alcohol related liver disease (ALD) and metabolic dysfunction-associated steatotic liver disease (MASLD)..215
Figure 78 Comparison of tumour necrosis factor alpha(TNFα) production in NK cells in patients with alcohol related liver disease (ALD) and metabolic dysfunction-associated steatotic liver disease (MASLD). 217
Figure 79 NKp30 expression inversely correlated with NK cell functional responses in patients with hepatocellular carcinoma (HCC) on a background of cirrhosis secondary to metabolic dysfunction-associated steatotic liver disease (MASLD)..... 220

Figure 80 NKp30 expression correlated with NK cell degranulation and interferon gamma (IFNγ) production in circulating NK cells from patients with cirrhosis secondary to alcohol related liver disease (ALD). 222
Figure 81 Differential gene expression in circulating CD56dimCD16++NK cells in MASLD cirrhosis when compared to CD56dimCD16++NK cells from healthy donors. 226
Figure 82 Differential gene expression in circulating CD56dimCD16++ NK cells in ALD cirrhosis when compared to CD56dimCD16++NK cells from healthy donors. 227
Figure 83 Differential gene expression in circulating CD56dimCD16++NK cells in MASLD HCC when compared to CD56dimCD16++NK cells from healthy donors. 228
Figure 84 Differential gene expression in circulating CD56brightCD16-NK cells in MASLD cirrhosis when compared to CD56brightCD16-NK cells from healthy donors. 230
Figure 85 Differential gene expression in circulating CD56brightCD16-NK cells in ALD cirrhosis when compared to CD56brightCD16-NK cells from healthy donors. 231
Figure 86 Differential gene expression in circulating CD56brightCD16-NK cells in MASLD HCC when compared to CD56brightCD16-NK cells from patients with MASLD cirrhosis. 232
Figure 87 Gene enrichment pathway analysis, comparing circulating CD56dimCD16++NK cells in patients with MASLD cirrhosis (n=4) with CD56dimCD16++NK cells from healthy volunteers (n=3). 234
Figure 88 Gene enrichment pathway analysis, comparing circulating CD56dimCD16++NK cells in patients with ALD cirrhosis (n=3) with CD56dimCD16++NK cells from healthy volunteers (n=3).. 235
Figure 89 Gene enrichment pathway analysis, comparing circulating CD56dimCD16++NK cells in patients with MASLD HCC (n=3) with CD56dimCD16++NK cells from patients with MASLD cirrhosis (n=4).. 237
Figure 90 Predicted effects of differential gene expression on NK cell signalling in circulating CD56dimCD16++ NK cells in MASLD cirrhosis when compared to healthy NK cells. 240
Figure 91 Upstream regulators in circulating CD56dimCD16++ NK cells in cirrhosis secondary to metabolic dysfunction-associated steatotic liver disease (MASLD cirrhosis). 241
Figure 92 Gene expression in intrahepatic CD56dimCD16++ NK cells from patients MASLD cirrhosis compared to circulating CD56dimCD16++ NK cells from patients with MASLD cirrhosis. 244
Figure 93 Downregulated genes in intrahepatic CD56brightCD16- NK cells when compared to circulating CD56brightCD16- NK cells. 247
Figure 94 Upregulated genes in intrahepatic CD56brightCD16- NK cells when compared to circulating CD56brightCD16- NK cells. 249
Figure 95 Gene enrichment pathway analysis, comparing intrahepatic CD56dimCD16++NK cells in patients with MASLD cirrhosis (n=3) with circulating CD56dimCD16++NK cells from patients with MASLD cirrhosis (n=3; non-paired samples).. 250
Figure 96 Gene enrichment pathway analysis, comparing intrahepatic CD56brightCD16-NK cells in patients with MASLD cirrhosis (n=3) with circulating CD56brightCD16-NK cells from patients with MASLD cirrhosis (n=3; non-paired samples). 251
Figure 97 DNAM-1 expression in NK cell subsets defined by CD56 and CD16 expression in the circulation and in the liver in cirrhosis.. 263
Figure 98 A comparison of DNAM-1 expression on CD56dimCD16+/- NK cells in patients with cirrhosis secondary to alcohol related liver disease (ALD) and metabolic dysfunction-associated steatotic liver disease (MASLD).. 265
Figure 99 NKG2D expression in NK cell subsets defined by CD56 and CD16 expression in the circulation and in the liver in cirrhosis.. 266
Figure 100 A comparison of NKG2D expression on CD56dimCD16+/- NK cells in patients with cirrhosis secondary to alcohol related liver disease (ALD) and metabolic dysfunction-associated steatotic liver disease (MASLD). 268

Figure 101 NKp46 expression in NK cell subsets defined by CD56 and CD16 expression in the circulation and in the liver in cirrhosis. 269
Figure 102 A comparison of NKp46 expression on CD56dimCD16+/- NK cells in patients with cirrhosis secondary to alcohol related liver disease (ALD) and metabolic dysfunction-associated steatotic liver disease (MASLD). 270
Figure 103 NKp30 expression in NK cell subsets defined by CD56 and CD16 expression in the circulation and in the liver in cirrhosis. 272
Figure 104 A comparison of NKp30 expression on CD56dimCD16+/- NK cells in patients with cirrhosis secondary to alcohol related liver disease (ALD) and metabolic dysfunction-associated steatotic liver disease (MASLD). 273
Figure 105 CD161 expression in NK cell subsets defined by CD56 and CD16 expression in the circulation and in the liver in cirrhosis.. 275
Figure 106 A comparison of CD161 expression on CD56dimCD16+/- NK cells in patients with cirrhosis secondary to alcohol related liver disease (ALD) and metabolic dysfunction-associated steatotic liver disease (MASLD).. 276
Figure 107 CXCR6 expression in NK cell subsets defined by CD56 and CD16 expression in the circulation and in the liver in cirrhosis. 278
Figure 108 A comparison of CXCR6 expression on CD56dimCD16+/- NK cells in patients with cirrhosis secondary to alcohol related liver disease (ALD) with metabolic dysfunction-associated steatotic liver disease (MASLD). 280
Figure 109 Gating strategies for surface receptors CXCR6, CCR5 and CD49a. 282
Figure 110 CCR5 expression in NK cell subsets defined by CD56 and CD16 expression in the circulation and in the liver in cirrhosis. 284
Figure 111 CD49a expression in NK cell subsets defined by CD56 and CD16 expression in the circulation and in the liver in cirrhosis. 286
Figure 112 Tbet and EOMES expression in circulating and intrahepatic NK cells in cirrhosis. 288
Figure 113 Differential gene expression in circulating NK cell subpopulations in patients with Metabolic dysfunction-associated liver dysfunction (MASLD) cirrhosis. 292
Figure 114 Differential gene expression in circulating NK cell subpopulations in patients with Alcohol related liver disease (ALD) cirrhosis 293
Figure 115 Differential gene expression in circulating NK cell subpopulations in patients with HCC on a background of MASLD cirrhosis 295
Figure 116 Gene enrichment pathway analysis, comparing circulating CD56dimCD16+/-NK cells with CD56dimCD16++ NK cells in patients with MASLD cirrhosis (n=4).. 297
Figure 117 Gene enrichment pathway analysis, comparing circulating CD56dimCD16+/-NK cells with CD56brightCD16-NK cells in patients with MASLD cirrhosis (n=4). 299
Figure 118 Gene enrichment pathway analysis, comparing circulating CD56dimCD16++NK cells with CD56brightCD16-NK cells in patients with MASLD cirrhosis (n=4). 300
Figure 119 Predicted activation or inhibition of upstream transcriptional regulators and molecules that may result in the differential gene expression profile seen in CD56dimCD16+/-NK cells i.e. predicted 'upstream regulators' for the CD56dimCD16+/- NK cell subpopulation (using Ingenuity Pathway Analysis software, Qiagen). 301
Figure 120 Gating strategy for CD57, NKG2C and KLRG1. 304
Figure 121 Gating strategy for IL7R and NKG2A. 305
Figure 122 Gating strategy for TCF1. 305
Figure 123 CD57 expression in NK cell subsets defined by CD56 and CD16 expression in the circulation in cirrhosis.. 306

Figure 124 NKG2A and NKG2C expression in NK cell subsets defined by CD56 and CD16 expression in the circulation in cirrhosis. 307
Figure 125 KLRG1 and IL7R expression in NK cell subsets defined by CD56 and CD16 expression in the circulation in cirrhosis. 309
Figure 126 TCF1 expression in NK cell subsets defined by CD56 and CD16 expression in the circulation in cirrhosis. 311
Figure 127 Gating strategy for Perforin and Granzyme B. 312
Figure 128 Perforin and Granzyme B within in NK cell subsets defined by CD56 and CD16 expression in the circulation in cirrhosis. 314
Figure 129 Cytokine expression in isolated sorted NK cells. 316
Figure 130 CD107a expression on pre-sorted NK cell subsets from patients with cirrhosis following incubation with K562 target cells. 318
Figure 131 CD56dimCD16+/- NK cells as a proportion of all circulating NK cells following incubation with sera from healthy donors and patients. 320
Figure 132 CD56 and CD16 expression on NK cells ex-vivo prior to incubation with K562 target cells (Pre-Activation profile, graph on left) and following incubation with K562 target cells (Post-Activation profile. Graph on right). 321
Figure 133 CD56dimCD16+/- NK cells are increased in proportion following activation. 322
Figure 134 CD56dimCD16+/- NK cell proportions post-activation with K562 target cells. 323
Figure 135 Receptor expression on the induced CD56dimCD16+/- NK cell subset following a 4 hour co-culture with K562 target cells. 326
Figure 136 Receptor expression on the induced CD56dimCD16+/- NK cell subset following a 48 hour co-culture with K562 target cells. 328
Figure 137 Huh7 cells with or without heat damage. 329
Figure 138 Post activation phenotype in healthy peripheral blood NK cells incubated with Huh7 cells for 48 hours. 330
Figure 139 CXCR6 expression on NK cell subsets following 48hour co-culture with Huh7 cells. 331
Figure 140 CD161 expression on NK cell subsets following 48hour co-culture with Huh7 cells. 333
Figure 141 DNAM-1 expression on NK cell subsets following 48hour co-culture with Huh7 cells. 335
Figure 142 Immunohistochemistry demonstrating LLT1 expression in normal liver. 345
Figure 143 Immunohistochemistry demonstrating LLT1 expression on formalin fixed paraffin embedded (FFPE) liver tissue. 346
Figure 144 LLT1 is upregulated in the liver in disease. 349
Figure 145 LLT1 expression is increased on hepatocytes in cirrhosis of all aetiologies. 351
Figure 146 LLT1 expression in cirrhosis and Hepatocellular carcinoma (HCC) separated by underlying aetiology (viral or non-viral aetiology). 352
Figure 147 LLT1 expression in HCC tumour tissue and adjacent background liver tissue and distal background liver tissue in patients with underlying cirrhosis. 354
Figure 148 Immunohistochemistry LLT1 expression scores in HCC tumour tissue in patients with underlying cirrhosis depending on the presence of vascular invasion and tumour differentiation. 356
Figure 149 Characterisation of LLT1 expressing cells in normal liver. 358
Figure 150 The co-localisation of LLT1 on sinusoidal and perisinusoidal cells with other markers. 359
Figure 151 LLT1 expression is increased in patients with cirrhosis and variable in patients with HCC on a background of cirrhosis. 362
Figure 152 LLT1 expression in patients with HCC without underlying cirrhosis. 364
Figure 153 ELISA to detect soluble LLT1 expression in serum from healthy donors (n=10), patients with cirrhosis (n=17), and patients with hepatocellular carcinoma (HCC) with underlying cirrhosis (n=13). 366

Figure 154 Gating strategy for checkpoint inhibitors on CD161+ NK cells.. 369
Figure 155 PD-1 expression on CD161+ NK cells. 371
Figure 156 BTLA expression on CD161+ NK cells.. 373
Figure 157 CD25 expression on CD161+ NK cells. 375
Figure 158 CTLA-4 expression on CD161+ NK cells.. 377
Figure 159 Gating strategy for identifying CD3+CD8+CD161^{hi}Vα7.2+ MAIT cells and the subsequent proportions of these cells that have PD-1, CTLA-4, BTLA and CD25 surface expression..... 379
Figure 160 Gating strategy for identifying CD3+CD4+CD161+ T cells and the subsequent proportions of these cells that have PD-1, CTLA-4, BTLA and CD25 surface expression..... 380
Figure 161 Percentage of mononuclear cells that are CD3+CD56-T cells in the circulation and in the liver. 382
Figure 162 The percentage of CD3+CD56-T cells that are MAIT cells in the circulation and in the liver. 384
Figure 163 The percentage of CD3+CD56-T cells that are CD4+CD161+T cells in the circulation and in the liver. 386
Figure 164 PD-1 expression on MAIT cells.. 388
Figure 165 PD-1 expression on CD4+CD161+T cells. 390
Figure 166 BTLA expression on MAIT cells.. 392
Figure 167 BTLA expression on CD4+CD161+T cells.. 394
Figure 168 CTLA-4 expression on MAIT cells.. 396
Figure 169 CTLA-4 expression on CD4+CD161+T cells.. 398
Figure 170 CD25 expression on MAIT cells.. 400
Figure 171 CD25 expression on CD4+CD161+T cells. 402
Figure 172 LLT1 expression in cell lines and transfection efficiency of Huh7 cells resulting in Huh7-LLT1 YFP transfectants. 405
Figure 173 Gating strategy to assess CD107a expression in CD161+ and CD161- NK cells. 406
Figure 174 LLT1 inhibits degranulation in CD161+NK cells. 407
Figure 175 LLT1 surface expression on Huh7 cells post stimulation with Interleukins. 409
Figure 176 LLT1 surface expression on Huh7 cells post stimulation with TLR agonists.. 410
Figure 177 Tumour growth factor beta (TGF-β) upregulates LLT1 expression on liver cell lines.. 411
Figure 178 Tumour growth factor beta (TGF-β) upregulates LLT1 expression on Huh7 cells. 412

List of Tables

Table 1 NK cell frequencies and cytotoxicity in NAFLD and NASH studies 50
Table 2 Studies on NK cells in patients with HCC. HCC:Hepatocellular carcinoma, MDSC:myeloid derived suppressor cells, Treg:T regulatory cells, ... 53
Table 3 Phenotyping flow cytometry antibody panels. 61
Table 4 Functional flow cytometry antibody panels 71
Table 5 Weighted scoring system, resulting in higher scores for tissue sections demonstrating stronger staining of LLT1 by immunohistochemistry. 77
Table 6 Antibodies used for double staining liver tissue 78
Table 7 Cytokine and TLR ligands used to stimulate Huh7 cells for 48hours (concentrations in R10 medium). 81
Table 8 Population characteristics of peripheral blood samples used for phenotyping experiments. 89
Table 9 Population characteristics for liver samples from which intrahepatic mononuclear cells were extracted for phenotyping. 91
Table 10 Population characteristics of peripheral blood samples used for functional experiments. 181
Table 11 Characteristics of patients from whom samples were utilised for gene expression profiling using Nansostring technology. 224
Table 12 Characteristics of patients from whom peripheral blood samples were used to determine CCR5, CD49a, Tbet and EOMES expression on NK cell subsets. 280
Table 13 Characteristics of patients with cirrhosis from whom peripheral blood samples were used to determine if there was surface expression of CD57, NKG2C, NKG2A, IL7R, KLRG1 and TCF1. 303
Table 14 Characteristics of patients with cirrhosis from whom peripheral blood samples were used to determine the ex-vivo perforin and granzyme B content. 313
Table 15 Summary of phenotypic and functional characteristics of the CD56dimCD16+/- NK cell subpopulation in cirrhosis comparison to classical NK cell subpopulations (CD56dimCD16++ and CD56brightCD16- NK cells) 337
Table 16 Demographics and clinical data for patients from whom liver LLT1 expression was determined using immunohistochemistry. 344
Table 17 Demographics and clinical data for patients from whom liver tissue samples were used for quantitative PCR for LLT1 expression. 361
Table 18 Demographics and clinical data of patients and healthy donors from whom serum samples were taken to detect circulating soluble LLT1. 365
Table 19 Demographics of patients and healthy volunteers from whom peripheral blood samples were used for NK cell and T cell phenotyping.. 368

1. Introduction

1.1 The burden of liver disease and Hepatocellular carcinoma

Liver disease remains a significant cause for morbidity and mortality globally (Devarbhavi et al., 2023). Liver cancer remains the 6th most common cancer worldwide (https://www.wcrf.org/preventing-cancer/cancer-statistics/liver-cancer-statistics/). Despite advances in the treatment of viral hepatitis, hepatitis B infection and cirrhosis related to hepatitis C remain leading causes of hepatocellular carcinoma globally (J. Llovet et al., 2021), with the incidence of hepatocellular carcinoma 2 to 3 fold greater in men than women (Sung et al., 2021). However in England, premature liver related death from alcohol related liver disease has continued to rise over the last 20 years (latest statistics from The Office of Health Improvement & Disparities, https://www.gov.uk/government/statistics/liver-disease-profile-april-2024-update). Furthermore, The World Health organisation determined that obesity rates in adolescents have quadrupled since 1990, giving concern to the rise of morbidity from metabolic dysfunction-associated liver disease and liver damage from concomitant alcohol consumption(Hart et al., 2010).

1.1.1 Diagnosis and current therapeutic options for HCC

Patients with cirrhosis have a higher risk of developing HCC (Tarao et al., 2019). Surveillance of patients with known cirrhosis is recommended with liver ultrasound (Galle et al., 2018). However, the sensitivity of ultrasound surveillance alone is dependent on operator and patient factors, such as obesity, with sensitivity estimated to be 51-87% (Ayoub et al., 2019). Biomarkers such as α-fetoprotein (AFP) in addition to US can increase sensitivity (Ayoub et al., 2019). Radiological diagnostic features of HCC consist of arterialisation of tumours that demonstrate wash out in comparison to the surrouding non-tumour cirrhotic liver in the portal phase on triple phase cross sectional imaging. Histological confirmation can be sought, particularly for lesions arising in non-cirrhotic livers, and to guide therapy.

Current management strategies for HCC in the UK are based on the Barcelona clinic liver cancer (BCLC) staging criteria (Dufour et al., 2012; Bruno Sangro et al., 2024). Staging is based on liver function as assessed using the Child-Pugh status, Eastern Cooperative Oncology Group (ECOG) performance status and the tumour burden. Resection and transplantation are curative options for some, but despite the use of the Duvoux criteria to allow downstaging of disease, many patients remain outside of transplantation criteria with an advanced Child-

Pugh score, multifocal and advanced disease or a poor performance status. In addition, those post-resection are still at risk of HCC, with a high recurrence rate due to remaining underlying viral infection, chronic inflammation and cirrhosis (Portolani et al., 2006). Alternatives such a radiofrequency ablation and transarterial chemoembolization may also be offered, as stated in the BCLC guidance.

The updated European Society of Medical Oncology (ESMO) guidance has included newer therapies, such as selective internal radiation therapy (SIRT), which can be considered in disease limited to the liver, with preserved liver function and in whom first line therapy with embolisation or systemic therapy is not appropriate, and stereotactic ablative radiotherapy (SABR) for tumours with a high risk of failure of traditional resection or ablative techniques due to tumour location (Vogel et al., 2018, 2021). Other therapies, such as irreversible elcetroporation (IRE) cannot be recommended yet as standard therapy without further evidence (Sugimoto et al., 2020).

For those presenting with advanced disease, there is currently also a paucity of chemotherapy alternatives on offer. Atezolizumab and bevacizumab are currently recommended as first line treatment for those with advanced HCC and portal invasion or extrahepatic metastases with preserved liver function and performance status (Vogel et al., 2021). Atezolizumab is a monoclonal antibody against PD-L1 and bevacizumab is a monoclonal antibody to vascular endothelial growth factor (VEGF) in the circulation (Finn et al., 2020). PD-L1 is often overexpressed on tumour tissue and is a recognised checkpoint inhibitor of T cell function, with VEGF involved in abnormal angiogenesis required for tumour growth and survival (Finn et al., 2020). However, 20% of patients do not respond to this treatment regimen and need to move onto secondline treatments (Vogel et al., 2021). Sorafenib, a multi-tyrosine kinase inhibitor, has been demonstrated to increase the median overall survival by approximately 3 months, though these patients had Child's Pugh A status and a good performance score (Eastern cooperative oncology group ECOG 2 or less)(Palmer, 2008). Levantinib (multikinase inhibitor against VEGF), has been compared to sorafenib and not demonstrated inferiority, and has only been evaluated as a first line therapy (Vogel et al., 2021). A few other multikinase inhibitors, such as Regorafenib, Cabozantinib and Ramicurimab, are reserved for potential second line therapy as per recently updated European Society for Medical Oncology (ESMO) Guidelines (Vogel et al., 2021).

Further immunotherapeutic options are being explored (Pardee & Butterfield, 2012; Sawada et al., 2013). Monotherapy with nivolumab (anti-PD1 therapy) did not show benefit when compared to sorafenib in terms of improving overall survival (Yau et al., 2022), and monotherapy with pembolizumab for patients previously treated with sorafenib in the KEYNOTE-224 phase III did not demonstrate significant improvement in progression free survival compared to best supportive care (Finn et al., 2019; Vogel et al., 2021). Further immunotherapies, including adoptive cell transfer, combination therapy with multikinase inhibitors and therapeutic vaccines are being explored (Palmer et al., 2009; Bruno Sangro et al., 2021; Vogt et al., 2014). Furthermore, combinations of immunotherapy and locoregional treatments or surgical treatments are another avenue being explored (e.g. PRIMER-1 trial delivering pembrolizumab (PD-1 inhibitor) and or lenvatinib in combination with surgical resection in patients with HCC).

Key evident pitfalls in managing HCC include patients presenting late with advanced disease, a high risk of recurrence of HCC following therapy due to a background of a scarred cirrhotic liver and the paucity of therapeutic options for patients with advanced disease. In order to identify novel targets for therapy, we must first understand the pathophysiology of HCC and the immune environment.

1.1.2 Pathogenesis of HCC

Cirrhosis is recognised to be associated with an increased risk of developing HCC regardless of the underlying aetiology of cirrhosis (Tarao et al., 2019). Mechanisms resulting in the pathogenesis of cirrhosis that appear to be aetiology independent include repetitive cycles of liver damage, inflammation, regeneration and repair, leading ultimately to chronic inflammation, stellate cell activation, extensive fibrosis and regenerative nodule formation (Farazi & Depinho, 2006). Telomere shortening is associated with cirrhosis and contributes to genetic instability (Farazi & Depinho, 2006). Furthermore, genetic and epigenetic alterations including the loss of p53, telomerase reactivation, over expression of receptor tyrosine kinases and abnormal DNA methylation have been identified to contribute to the pathogenesis of HCC (Farazi & Depinho, 2006; Ramakrishna et al., 2013a).

However, despite these common processes leading to HCC, HCC demonstrates vast intratumoural heterogeneity (Faivre et al., 2020; Q. Zhang et al., 2020). This is in part determined by aetiology specific mechanisms associated with the pathogenesis of HCC. Furthermore, HCC can arise without established cirrhosis, for example, as seen in HCC associated with aflatoxin ingestion, viral hepatitis and non-alcohol related liver disease (NAFLD) (Desai et al., 2019; Farazi & Depinho, 2006).

The hepatropic viruses Hepatitis B (HBV) and Hepatitis C (HCV) can result in chronic inflammation leading to cirrhosis. HBV DNA integration can result in deletion of tumour suppressor genes and genes integral to the cell cycle, including p53 and telomerase reverse transcriptase (Farazi & Depinho, 2006). HCC associated with HBV are classified as proliferative tumours with an aggressive, poorly differentiated phenotype (J. Llovet et al., 2021). The Hepatitis B x antigen (HBx) plays a regulatory role in viral replication, interacting with transcription factors to sustain viral replication whilst promoting cell survival by inhibiting apoptosis (Rawat & Bouchard, 2015). HBx has also been demonstrated to interfere with DNA repair processes, directly binding with p53, promoting angiogenesis by upregulating vascular endothelial growth factor (VEGF) and promoting vascular invasion and metastasis (Ali et al., 2014; Z. He et al., 2017; J. M. Llovet et al., 2021). Hence there is a greater risk of HCC in HBV infected individuals, regardless of whether there is established underlying cirrhosis. In HCV related HCC, the HCV core protein can cause steatosis, promote cell proliferation and increase reactive oxygen species in addition to inducing fibrosis and cirrhosis (Goto et al., 2020; Moriya et al., 1997; Okuda et al., 2002). There is also some evidence from transgenic mice studies that non-structural HCV proteins NS3 and NS5A can promote cell transformation (Goto et al., 2020). Like HBV, HCV can also interfere with key transcription factors, such as the HCV core protein activating hypoxia -inducible factor 1 alpha (HIF1α) in turn upregulating VEGF and promoting angiogenesis, and plays a role in aberrant epigenetic methylation (Goto et al., 2020; Hassan et al., 2009; Toh et al., 2019).

Carcinogenic processes specific to alcohol related liver disease (ALD) include the generation of the liver damaging intermediate, acetaldehyde, during the metabolism of alcohol; reactive oxygen species, from alcohol metabolism and abnormal iron metabolism, accentuating oxidative mediated stress; alcohol mediated hypomethylation and epigenetic alterations

(Ganne-Carrié & Nahon, 2019). Susceptibility to HCC from these pathogenic processes is further modulated by the presence of specific gene variations (Nahon & Zucman-Rossi, 2012).

Steatohepatitis is a feature of alcohol related hepatitis and hepatitis secondary to metabolic dysfunction-associated steatotic liver disease (MASLD). A single nucleotide polymorphism (SNP) in the PNPLA3 allele (adiponutrin/platin-like phospholipase 3) has been associated with steatosis in both alcohol related liver disease and MASLD and specifically with an increased risk of HCC on a background of cirrhosis secondary to these two aetiologies (Ganne-Carrié & Nahon, 2019; Romeo et al., 2008; Singal et al., 2014). Other SNPs, including TM6SF2, are associated with the promotion of steatosis in both ALD and MASLD but not specifically with the progression of HCC (Ganne-Carrié & Nahon, 2019; Grgurevic et al., 2021).

Metabolic syndrome and diabetes can in itself be associated with promoting the pathogenesis of HCC. Hyperinsulinaemia, associated with insulin resistance in metabolic syndrome, drives cell proliferation via stimulation of oncogenes c-fos and c-jun via mitogen-activated protein kinase (MAPK) pathways (Grgurevic et al., 2021). Furthermore, hyperinsulinaemia promotes steatosis and induced reactive oxygen species secondary to increased oxidation of free fatty acids (Grgurevic et al., 2021; J. Llovet et al., 2021). This results in repeated cell damage and apoptosis whilst simultaneously driving proliferation.

Immunological changes, both aetiology dependent and aetiology independent, resulting immune escape of transformed cells are also imperative in the evolution of HCC. In order to understand these changes, it is vital to understand the underlying immune profile of the liver, its role as a tolerogenic organ and alterations in the immune milieu in chronic liver disease.

1.2 Immune dysfunction in cirrhosis and HCC

The predisposition to infections and the recognition of cirrhosis as a premalignant state requiring screening for HCC suggests underlying immune dysfunction and suboptimal host anti-tumour immune responses in cirrhosis. Understanding immunological adaptations that may arise in cirrhosis is key to developing novel anti-cancer therapies for HCC in the context of cirrhosis.

1.2.1 The immunological role of the normal liver

The liver contains a rich myriad of immune cells that, along with non-haematopoietic cells within the liver, provide a tolerogenic environment whilst also retaining the capacity to produce potent local and systemic immunological responses when required.

Liver resident immune cells line the sinusoidal spaces (Freitas-Lopes et al., 2017). The liver lymphoid population comprises of Natural Killer (NK) cells, forming up to of 50% of the liver lymphoid population compared to 10-15% of the peripheral blood circulation, NKT cells and T cells (Hudspeth et al., 2016b). Kupffer cells, liver resident macrophages, form the largest population of tissue resident macrophages in the body (Robinson et al., 2016). Dendritic cells are enriched also within the liver and myeloid suppressor cells have been demonstrated as being expanded in disease (Robinson et al., 2016). In addition to the immune cell populations, hepatocytes and other epithelial cells are also able to produce immune responses. Hepatocytes express all toll-like receptors (TLRs), has the capacity to directly produce interleukin 6 (IL-6) and produce acute phase proteins in response to the activation of STAT3 (Nakamoto & Kanai, 2014; Z. Zhou et al., 2016). Furthermore, hepatocytes also can generate acute phase proteins via the activation of NF-κB secondary to stimlation by interleukin 1 beta (IL-1β) (Z. Zhou et al., 2016). Liver sinusoidal endothelial cells (LSECs) also play a pivotal role through by expressing pattern recognition receptors (PRRs) including TLRs (Nakamoto & Kanai, 2014; Robinson et al., 2016). Hepatic stellate cells are known to have a key role in disease and fibrogenesis in response to transforming growth factor beta (TGFβ).

The normal state of the liver is that of an immune tolerogenic environment, allowing the exposure of immune cells and hepatocytes residing within the liver to multiple antigens via the portal circulation, but inhibiting unfavourable immune responses (Bowen et al., 2004; Thomson & Knolle, 2010). Blood from the portal venous system containing antigens from food and gut commensals flows through the sinusoidal spaces, is filtered through liver sinusoidal endothelial cells to pass through to hepatocytes before draining out via central veins (Robinson et al., 2016). Pathogen associated molecular patterns (PAMPs) and damage associated molecular patterns (DAMPs) within the portal vein blood are recognised by PRRs found on hepatocytes and Kupffer cells, phagocytosed and removed without producing an inflammatory response (Robinson et al., 2016). The ability to recognise and phagocytose

these antigens without producing a potent immune response is in part reliant on the balance of pro- and anti-inflammatory cytokines within the liver. Interleukin 10 (IL-10) produced by Kupffer cells and dendritic cells reduce the expression of MHC class II on surrounding antigen presenting cells (APCs) thereby limiting any stimulation of the adaptive CD4 T cell response (Robinson et al., 2016; Thomson & Knolle, 2010). Furthermore, LSECs, hepatocytes and dendritic cells present antigen to T cells via MHC class I, without co-stimulation to activate T cells, thereby inducing tolerance (Robinson et al., 2016; Thomson & Knolle, 2010).

However, the liver is able to produce potent local adaptive and innate immune responses when required. In response to pathogens, Kupffer cells produce an array of pro-inflammatory chemokines and cytokines, including IL-6, interleukin 1 (IL-1) and tumour necrosis factor alpha (TNFα) (Robinson et al., 2016). Liver resident cells recruit circulating immune cells by two mechanisms. Firstly, immune cells may be recuited from the blood supply in an antigen specific manner, by antigen presentation on MHC class I by LSECs and dendritic cells (Thomson & Knolle, 2010). Secondly, the upregulation of certain chemokines and chemokine receptors on LSECs can result in the engagement of passing lymphoid cells within the sinusoidal space, for example, CCR5 and CXCR6 engagement of T cells and NK cells (Hudspeth et al., 2016b; Thomson & Knolle, 2010). Hepatocyte death can occur, either by the direct effect of toxins (necrosis) or due to the indirect effect of pathogen clearance and inflammation (J. Li et al., 2019). The liver can regenerate by hepatocyte proliferation, the differentiation of liver progenitor cells and by the production of extracellular matrix components by activated hepatic stellate cells (J. Li et al., 2019; Robinson et al., 2016). Pro-inflammatory cytokines, coupled with TGFβ, activate hepatic stellate cells and induce the secretion of extracellular matrix components and growth factors (J. Li et al., 2019; Robinson et al., 2016). However, this process is tightly regulated by matrix metalloproteinases (MMPs), secreted by activated liver macrophages, which in turn breakdown these extracellular matrix components (Roeb, 2018). Activated macrophages also reduce tissue inhibitors of metalloproteinases (TIMPs) that promote fibrosis, while activated NK cells delete activated hepatic stellate cells via tumour necrosis factor-related apoptosis inducing ligand (TRAIL), NKG2D activation and Fas ligand (FasL) (Robinson et al., 2016; Roeb, 2018).

1.2.2 Immune dysfunction in cirrhosis

Cirrhosis is associated with low grade systemic inflammation in the compensated state, which is escalated in acute on chronic liver failure (ACLF) (Albillos et al., 2022). There are several mechanisms culminating to this chronic activation of the immune system. Dysbiosis in the gut results in an alteration of the gut microbiota in cirrhosis (Albillos et al., 2022). This, coupled with the increase in gut permeability results in the alteration of and increase in the PAMPs that are presented via the portal circulation (Albillos et al., 2022; Pijls et al., 2014). Furthermore, continued chemical insults from alcohol, viruses and steatosis results in hepatocyte damage and the increased release of DAMPs locally (Albillos et al., 2022). This increased influx of DAMPs and PAMPs detected via PRRs on Kupffer cells and LSECs triggers the activation and release of pro-inflammatory cytokines (Albillos et al., 2022). The proinflammatory response is mediated by the construction of structures called inflammasomes, with the nucleotide-binding oligomerisation domain (NOD)-like receptors family pyrin containing 3 (NLRP3) inflammasome having been characterised within Kupffer cells and hepatocytes in viral hepatitis, ALD and MASLD (Ramakrishna et al., 2013b; X. Wu et al., 2017). NLRP3 activation results in the release of caspase 1, which cleaves and results in the release of pro-inflammatory IL-1β, IL-18 and IL-1α (X. Wu et al., 2017). Furthermore, circulating monocytes are recruited into the injured liver, further releasing pro-inflammatory cytokines (TNFα, interferon (IFN) gamma, IL-6) and propagating liver damage, whilst also releasing TGFβ and activating hepatic stellate cells to promote fibrosis (Tacke, 2012).

However, there is evidence that there is systemic immune dysfunction in cirrhosis. Circulating proinflammatory CD14+CD16+ monocytes are expanded in patients with cirrhosis, however, these monocytes demonstrate attenuated phagocytic effector functions (Albillos et al., 2022; Tacke, 2012). Circulating neutrophils in patients with cirrhosis demonstrate impaired phagocytosis with increased production of reactive oxygen species, impaired adhesion and migration (Irvine et al., 2019). Patients with cirrhosis are demonstrably lymphopaenic (Matos et al., 2013; Tuchendler et al., 2018). Cytotoxic T cells have been demonstrated to express exhaustion markers PD-1 and Tim-3 (Albillos et al., 2022; Markwick et al., 2015) and induce dysfunction in monocytes and neutrophils (Lebossé et al., 2019).

The systemic hyporesponsiveness in immunity in advanced cirrhosis is thought to culminate from perisistent activation followed by ultimate tolerance and exhaustion of immune cells

following the release of DAMPs from the liver and PAMPs from increased gut permeability coupled with the reduction in the capacity for the damaged liver to produce acute phase proteins (Albillos et al., 2022; Irvine et al., 2019). This immune dysfuction and relative innumodeficiency has been associated with the frequent episodes of sepsis in patients with cirrhosis (Strnad et al., 2017) and may also result in the predisposition to developing liver cancers.

1.2.3 The Tumour Microenvironment

Cytotoxic immune cells, such as NK cells and CD8+ T cells are involved in tumour surveillance, eliminating tumour cells identified directly by abnormal cell surface receptor expression, abnormal expression of antigens via MHC-1, and by antigen presentation from professional APCs (G. P. Dunn et al., 2002; Swann & Smyth, 2007). Increased populations of tumour infiltrating CD8+ T cells and NK cells are associated with a favourable prognosis in HCC (Ringelhan et al., 2018). Conversely, tumour cells that acquire mutations may escape from immune cell surveillance and elimination (G. P. Dunn et al., 2002; Swann & Smyth, 2007). There is sufficient evidence to suggest that the interplay between tumour cells and non-tumour cells residing within and around the tumour, results in a modulation of the non-malignant cells and the local environment to promote tumour survival and growth: a phenomenon known as the 'Tumour Microenvironment' (Balkwill et al., 2012; Fridman et al., 2012; Mbeunkui & Johann, 2009). Within this HCC tumour microenvironment, key cells that accumulate and support tumour survival include tumour asscociated macrophages, myeloid derived suppressor cells and T regulatory cells (J. Zhou et al., 2021).

<u>Tumour associated macrophages (TAMs)</u>

TAMs have an immunosuppressive phenotype, characterised by producing IL10, IL6 and TGFβ with lower levels of IL12 (Porta et al., 2009). An increased density of TAMs intra- or peri-tumoural has been asscociated with poor prognosis in HCC (Ding et al., 2009; Kong et al., 2013). TAMs promote angiogenesis and can enhance metastases through promoting migration and invasion (Wan et al., 2015). TAMs may recruit T regulatory cells (Tregs) via TGFβ and CCL22 secretion, further promoting tumour growth (D. Wang et al., 2019). Within the

liver, the pro-inflammatory activation of STAT3 and NF-κB via IL-6 and TNFα respectively, as discussed above, have been associated with the development of HCC, with TAMs sustaining the secretion of these pro-inflammatory cytokines (Ringelhan et al., 2018; Weston et al., 2019). However, activation of the NLRP3 inflammasome has been associated with protective effects against HCC development in some studies (C. Shi et al., 2020). Furthermore, cross talk between monocytes and NK cells have been suggested as a mechanism for rendering tumour infiltrating NK cells hypofunctional (Y. Wu et al., 2013).

Tumour infiltrating T cells

An increased density of intratumour CD8+T cells are associated with a better prognosis while an increased density of intratumoural Tregs is associated with a poorer overall survival in HCC (Schoenberg et al., 2021; Yu et al., 2020). Tumour infiltrating CD8+ T cell cytotoxicity and IFNγ secretion is suppressed by Tregs in HCC, with the upregulation of PDL1 on Tregs (Langhans et al., 2015; J. Llovet et al., 2021). Expression of PDL1 on HCC tumour tissue further suppresses CD8+T cell functional responses, with an increased proportion of PD-1+CD8+T cells in the circulation being associated with disease progression (F. Shi et al., 2011). Furthermore, circulating tumour cells in HCC directly secrete CCL5, recruiting Tregs to create an immunosuppressive environment in the circulation, allowing seeding and metastasis of circulating tumour cells (Y.-F. Sun et al., 2021). Single cell RNA sequencing has also identified CTLA-4 expression on tumour infiltrating CD8+ T cells (C. Zheng et al., 2017). As discussed above, circulatory immune cells in patients with cirrhosis also display an activated and exhausted phenotype with effector dysfunction. T cell exhaustion is further compounded by chronic infection with hepatropic viruses (HBV and HCV), where an increased proportion of Tregs may be found, thus reducing tumour surveillance capacity (Jinan He et al., 2024; Ringelhan et al., 2018).

Myeloid derived suppressor cells (MDSCs)

MDSCs are expanded in the circulation of patients with HCC and asscociated with poorer outcomes in HCC (Lu et al., 2019; Weston et al., 2019). There are 2 subsets of MDSCs: monocytic (M-MDSC) and polymorphonuclear (PMN-MDSC) and they are activated via TGFβ, IFNγ, IL13 or IL4 (Cassetta et al., 2020; Gabrilovich & Nagaraj, 2009). MDSCs reportedly inhibit T cell proliferation, inhibit NK cell cytotoxicity and activate T regulatory cells via the

production of multiple factors, including consumption of arginase-1 and cysteine, production of nitric oxide synthase, TGFβ, IL-10 and indoleamine 2.3-dioxygenase (IDO) (Lu et al., 2019; Zea et al., 2005).

Neutrophils

Tumour associated neutrophils (TANs) have been described to have the capacity to have pro- and antitumour effects depending on the cyokine environment within the tumour (Coffelt et al., 2016). Anti-tumour effects include reactive oxygen species (ROS) production, cross talk with monocytes to promote IL-12 production and subsequent NK cell activation, and chemokine production (Kotsari et al., 2023). However through the production of CCL2 and CCL17, TAN have been shown to attract macrophages and Tregs in turn promoting tumour growth (S.-L. Zhou et al., 2016). Peritumoural TANs have also been decribed to express PD-L1 thereby inhibiting T cells (G. He et al., 2015). TANs also have the capacity to display myeloid derived suppressor cell activity (Furumaya et al., 2020).

The role of NK cells in HCC is discussed further below.

It is important to understand the non-immune cell components that contribute to the tumour microenvironment also: cancer associated fibroblasts, liver sinusoidal cells and cytokines. Cancer associated fibroblasts, derived from activated hepatic stellate cells or directly from cancer cells, promote angiogenesis, produce extracellular matrix and secrete growth factors (Yin et al., 2024; J. Zhang et al., 2020).

1.2.4 Immunotherapy in Hepatocellular carcinoma

The heterogeneity of HCC, combined with the immunosuppressive tumour microenvironment described, and the lack of predictive biomarkers to predict response to immunotherapy make successful targeting with treatments difficult. In addition, the presence of cirrhosis and liver dysfunction from different underlying aetiologies adds another layer of complexity. Initial immunotherapy trials focussed on the use of a single agent but neither showed superiority to sorafenib in terms of overall survival: nivolumab (anti-PD1) in the Phase III CheckMate459 trial (Yau et al., 2022) and pembrolizumab (anti-PD1) in the Phase III KEYNOTE-240 (Finn et al., 2019). Current first line immunotherapy for advanced HCC involves dual therapy with atezolizumab and bevacizumab, targeting PD-1 checkpoint-mediated inhibition and exhaustion of tumour infiltrating T cells and angiogenesis via anti-VEGF inhibitor respectively

(Finn et al., 2020). Ipilimumab (CTLA-4 inhibitor) in combination with nivolumab (phase III checkmate 9DW trial has now demonstrated an improved overall survival against sorafenib or Lenvatinib (NCT04039607). Durvalumab (PD-L1 inhibitor) and tremelimumab (CTLA-4 inhibitor) (Phase III HIMALAYA trial) has also shown benefit over sorafenib (B. Sangro et al., 2024).

Given the success of combination immunotherapy in patients with advanced disease, immunotherapy trials are currently running looking at adjuvant treatment to prevent recurrence following treatment. The IMbrave 050 has reported that patients receiving atezolizumab and bevacizumab had a better recurrence free survival (Qin et al., 2023).

The neoadjuvant use of immunotherapy is also being explored for patients undergoing surgery for HCC e.g. PRIMER-1 trial (NCT05185739) is currently investigating the use of pembrolizumab (PD-1 inhibitor) and/or Lenvatinib for 6 weeks prior to surgery to improve recurrence free survival (Childs et al., 2024).

Other avenues under exploration include combination immunotherapy and locoregional therapy: EMERALD1 reported an improved performance free survival period for patients having durvalumab and bevacizumab and trans-arterial chemoembolization (TACE) versus TACE alone (Lencioni et al., 2024).

Adoptive cell transfers, like chimeric antigen receptor T (CAR-T) cells (Mandlik et al., 2023) are an exciting research avenue. T cell receptors are manufactured to recognise specific anti-tumour antigen, thereby directing the T cells to the tumour (Aggeletopoulou et al., 2024). However understanding not only the tumour environment, but also the underpinning immunological changes established in cirrhosis is essential to overcome the underlying immunosuppressive environment.

1.3 NK cells

Natural Killer (NK) cells are innate lymphocytes with important anti-pathogen and anti-tumour responses. NK cells were initially discovered in mice, coining the term ‘natural’ killer cells due to the rapid, antigen-independent onset of cytotoxicity against leukaemia cells (Kiessling et al., 1975). NK cells account for 5-15% of peripheral blood lymphocytes, but are

concentrated within liver tissue, accounting for up to 50% of liver resident lymphocytes (Gao et al., 2008).

1.3.1 NK cell development

Innate lymphoid cells (ILCs) can be categorised into five types: NK cells, ILC1, ILC2, ILC3 and lymphoid tissue inducer cells. NK cells and ILC1 share many functional and phenotypical features. Both cell types have the capacity to produce interferon gamma, kill via the expression of tumour necrosis factor related apoptosis inducing ligand (TRAIL) and express CD56 and NKp46 (Panda & Colonna, 2019). However, NK cells are found in the circulation as well as within tissue, whereas ILC1 cells are thought to be tissue resident cells only, expressing tissue homing markers including CD69, CD49a and CD103 (Panda & Colonna, 2019). Differential expression of transcription factors T-bet, EOMES and Hobit are also seen but expression is can vary based on location and type of NK cell and ILC1 (Panda & Colonna, 2019).

NK cells are derived from a common progenitor cell (Figure 1). NK cells are thought to arise within the bone marrow, but can mature in secondary lymphoid tissue, including lymph nodes (Abel et al., 2018). Hematopoietic stem cells acquire CD45RA expression, and subsequently acquire IL7R, CD38, CD7 and CD10 to differentiate into common lymphoid progenitor cells (CLPs). Acquisition of IL-2Rβ (CD122) demarcates differentiation into NK cells and CD56 expression classically identifies NK cells, with CD56bright NK cells thought of as a less mature subset of NK cells and CD56dim NK cells as the mature NK cells (Abel et al., 2018; Scoville et al., 2017). However, the identification of a CD56negative subset of NK cells expanded in Human Immunodeficiency Virus infection and a CD56dimCD16negative subset in aplastic patients with stem cell transplants challenges this and indicates other possible routes of differentiation (Cao et al., 2022; Roberto et al., 2018). NK cells are deemed terminally mature with the expression of CD16, CD57 and killer immunoglobulin receptors (Abel et al., 2018; Mikulak et al., 2019). Expression of NKG2C/CD94 in mature NK cells has been associated with an adaptive memory phenotype (Lopez-Vergès et al., 2011).

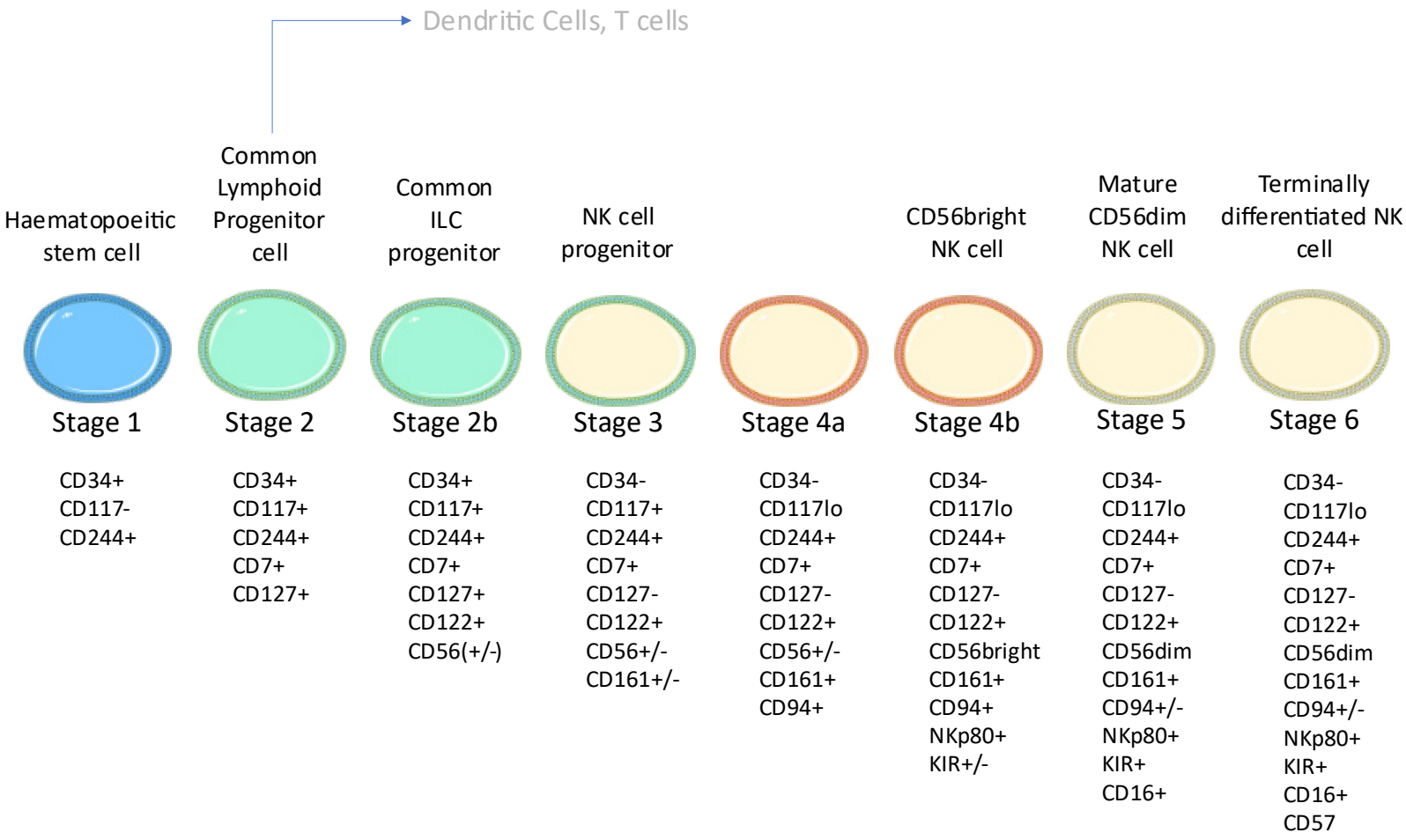


Figure 1 Stages of NK cell development (Adapted from Abel et al, 2018 and Scoville et al, 2017)

1.3.2 NK cell education

During NK cell development, NK cells are classically licenced following exposure to cells expressing major histocompatibility complex class 1 (MHC1) molecules. In brief, NK cells express a variety of killer immunoglobulin-like receptors (KIRs) that demonstrate heterogeneity, allowing the recognition of a multitude of self MHC1 molecules. The interaction of KIR with specific MHC1 ligands, delivers a potent inhibitory signal to the NK cell allowing functional maturity. The now licenced NK cell is inhibited by cells expressing the same self MHC1 ligands, and mounts a potent cytotoxic response to other cells lacking that specific MHC1 i.e. cells 'missing self' MHC1 (Y. He & Tian, 2017; S. Kim et al., 2005). NK cells that do not encounter MHC1 ligands for the KIRs they express do not learn this inhibitory response but also do not become functionally mature, and hence do not mount cytotoxic responses to healthy cells. Hence both licenced and unlicenced NK cells have a self-tolerance (S. Kim et al., 2005). Furthermore, Zamora et al demonstrate that while licenced NK cells function as potent effector cells in the context of viral infection, unlicenced cells can act as helper cells, migrating to lymph nodes and producing GM-CSF to promote dendritic cell activation and thus T cell activation (Zamora et al., 2017).

Other inhibitory receptors, such as NKG2A expressed on NK cells may also play a role in education, as NKG2A+ NK cells can show increased responsiveness to target cells not expressing HLA-E, the ligand for NKG2A (Y. He & Tian, 2017). However, education via classical MHC1 results in NK cells with the ability to deliver potent cytotoxic and cytokine responses, whereas education solely via non-classical MHC results in NK cells with cytotoxic capacity but weak cytokine producing capacity (Y. He & Tian, 2017). This suggests that the strength of inhibition varies by receptor type and influences education (Brodin et al., 2009).

1.3.3 The circulating NK cell phenotype in health

Circulating NK cells are classically defined as CD3- negative, differentiating them from T cells, and CD56+ innate lymphocytes. They are further defined as mature CD56dim NK cells with predominantly cytotoxic capacity, forming 90% of circulating NK cells, and the less mature CD56bright NK subpopulation with the capacity to produce potent cytokine responses.

Activation is dependent on the balance of inhibitory and stimulatory signals mediated by cell surface receptors and allows immediate directed cytotoxic responses resulting in the elimination of infected and transformed cells. Surface receptors can be classified into C-type lectins (including NKG2D, NKG2A), natural cytotoxicity receptors (NCRs including NKp46, NKp30, NKp44), killer-immunoglobulin like receptors (KIR), and activating receptors such as 2B4, DNAM-1 and CD16 (see Figure 2).

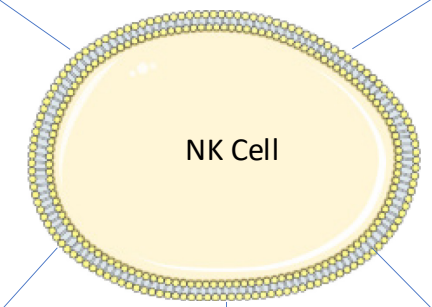
CD16 is highly expressed on mature circulating NK cells, and binds to the Fc portion of immunoglobulins, triggering antibody dependent NK cell mediated cytotoxcity (ADCC). NKG2D is a powerful activating receptor, binding to stress-induced ligands (MIC-A, MIC-B, ULBP) upregulated on the cell surface of transformed cells and infected cells. The NCRs are also potent activating receptors. Co-enagement of NK cell activating receptors can result in synergy with activation of cytotoxicity (Bryceson et al., 2006b).

However, there is evidence that receptors can have more than one action. NKG2D can activate different responses in NK cells depending on which isoform is expressed and the which ligand is engaged (Silva-Santos & Strid, 2018). Furthermore, repeated prolonged exposure to NKG2D ligands has been associated with a downregulation of NKG2D and impairment of NKG2D related cytotoxicity (Coudert et al., 2005; Oppenheim et al., 2005). Dendritic cells can exert an inhibitory role on NK cells via IL-10 secretion and engagement of the NKp46 receptor, an NCR receptor usually deemed to have an activating role (Spallanzani et al., 2015).

There is also emerging evidence that combinations of receptors on NK cell subsets influence the overall functional role of the NK cell. In mice, NK cell subsets expressing CD27, NKG2A and DNAM-1 together delineate NK cells preferentially delivering cytotoxic responses against tumour cell lines, while NK cells expressing CD11b and KLRG1 produce interferon gamma in response to tumour cell lines (Rocca et al., 2022).

KIR Inhibitory receptors	Ligand
KIR2DL1	HLA-C2
KIR2DL2	HLA-C1, HLA-C2
KIR2DL3	HLA-C1, HLA-C2
KIR2DL5	
KIR3DL1	HLA-Bw4
KIR3DL2	HLA-A3, HLA-A11
KIR3DL3	HHLA2

KIR Activating receptors	Ligand
KIR2DS1	HLA-C2
KIR2DS2	HLA-A11, HLA-C1
KIR2DS3	
KIR2DS4	HLA-Cw4, HLAC*05:01
KIR2DS5	
KIR3DS1	HLA-Bw4
KIR2DL4	HLA-G



NCR	Ligand
NKp46	Viral haemagglutinins, heparin, neuroaminidase
NKp30	B7H6, BAT3, hCMV-pp65
NKp44	Viral haemagglutinins

C-type Lectin	Ligand
CD161	LLT1
NKG2A-CD94	HLA-E
NKG2C-CD94	HLA-E
NKG2D	MICA, MICB,
NKG2E-CD94	HLA-E
KLRG1	E-cadherin, N-cadherin
NKp80	AICL

Other	Ligand
CD16	Fc portion of Immunoglobulin
2B4	CD48
LILRB1	MHC-1, UL18
DNAM-1	PVR
CD96	PVR
TIGIT	PVR
LAIR1	Collagen
CD160	HVEM

Figure 2 NK cell receptors. KIR: Killer immunoglobulin receptor, HLA: Human leucocyte antigen, HHLA: Human Endogenous Retrovirus-H Long Terminal Repeat-Associating Protein 2, KLRG1: Killer cell lectin-like receptor subfamily G member 1, LILRB1: Leukocyte Immunoglobulin Like Receptor B1, TIGIT: T cell immunoreceptor with Ig and ITIM domains, PVR: Poliovirus receptor, DNAM-1: DNAX accessory molecule 1, LAIR1: Leukocyte-associated immunoglobulin-like receptor 1, MHC: Major histocompatibility complex, MIC: MHC class I chain-related protein, AICL: Activation induced C-type lectin

1.3.4 NK cell effector functions

NK cells execute effector functions via a variety of routes to mediate anti-tumour and anti-pathogen responses.

1.3.4.1 NK cell mediated cytotoxicity

NK cells contain preformed lytic granules containing perforin, granzyme, granulysin, Fas ligand (FasL) and TNF-related apoptosis inducing ligand (TRAIL) as well as small peptides and defensins (Krzewski & Coligan, 2012). NK cells mediate cytotoxicity through directed lytic granule release (Topham & Hewitt, 2009). Activated NK cells engage with target cells and establish an immune synapse, with stabilisation of the synapse via the engagement of integrins with ligands on the target cell (Bryceson et al., 2006a; Orange, 2008; Riteau et al., 2003). If there is a lack of inhibitory signalling from the engagement of KIR at the immune synapse, activating signals trigger a cytoskeletal reorganisation resulting in polarisation of the microtubule organising centre, movement of the lysosomes containing the lytic granules towards the immune synapse and the directed release of lytic granules towards the target cell (Orange, 2008). Degranulation is measured indirectly by the increase of LAMP-1/CD107a expression on the NK cell surface following the fusion of LAMP-1 lined lysosomes with the NK cell surface following exocytosis of the lytic granules (Alter et al., 2004).

Once delivered towards the target cell, perforin proceeds to be inserted via calcium dependent process into the target cell membrane, generating pores, while granzymes result in the generation of reactive oxygen species resulting in mitochondrial and DNA damage (Krzewski & Coligan, 2012). Granulysin serves as a chemoattractant for other immune cells, while peptides and defensins within the granules can aid anti-microbial responses via macrophage activation (Krensky & Clayberger, 2009; Krzewski & Coligan, 2012).

FasL and TRAIL engage with death receptors Fas and TRAIL-receptor (TRAIL-R) expressed on target cells, inducing caspase dependent apoptosis of the target cell (S. Wang & El-Deiry, 2003; Zamai et al., 1998). Fas and TRAIL-R can be upregulated on target cells via IFNγ secretion by NK cells (Abel et al., 2018). FasL is also expressed on the NK cell surface, and can be induced following NK cell CD16 engagement (Bloom et al., 1999).

Furthermore, NK cells have the capacity for antibody dependent cell mediated cytotoxicity via CD16 mediated NK cell activation, upon CD16 binding the Fc portion of antibodies that

have opsonised infected or transformed cells, effectively triggering cytotoxic effector functions directed towards the infected cell (O Mandelboim et al., 1999). This in particular makes the NK cell a cell of interest in delivering antibody mediated cancer immunotherapies (N. Kumar & Khakoo, 2018b).

1.3.4.2 NK cell secretion of cytokines and chemokines

NK cells have the capacity to produce the pro-inflammatory cytokines interferon gamma (IFNγ), Tumour necrosis factor alpha (TNFα) and GM-CSF on activation (Arase et al., 1996; Levitt et al., 1991; Paya et al., 1988). Furthermore, NK cells can produce chemokines CCL3 (MIP1α), CCL4 (MIP1β), CCL5 (RANTES), XCL1 and CXCL8 (Abel et al., 2018) and there is evidence that on encounter with target cells, release of these chemokines precedes the release of IFNγ and TNFα, with single activating receptor engagement by target cells being sufficient for chemokine release, but multiple receptors engagement being required for IFNγ and TNFα release (Fauriat et al., 2010).

Whilst the pro-inflammatory cytokines and chemokine attract other immune cells, activating and supporting anti-pathogen responses, NK cells also have the capacity to produce interleukin 10 (IL-10), demonstrating a potentially anti-inflammatory role of NK cells, by reducing dendritic cell activation and inhibiting T cell activation particularly in chronic viral infections (Martinez-Espinosa et al., 2022).

1.3.5 Cross talk with other immune cells

NK cells can directly interact with other immune cells to promote a pro-imflammatory response. NK cell interactions with dendritic cells and monocytes have been well characterised, with antigen presentation via MHC class II molecules and secretion of interleukin 12 (IL-12) by dendritic cells and monocytes resulting in the activation of NK cells (Ferlazzo & Morandi, 2014). Activated NK cells produce IFNγ, which in turn promotes anti-pathogen monocyte effector functions (Ferlazzo & Morandi, 2014; Oth et al., 2018). Furthermore, interleukin 15 (IL-15) production and transpresentation by dendritic cells further promotes NK cell survival, which can be modulated by co-engagement of inhibitory NK cell receptors (Anton et al., 2015; Lucas et al., 2007). Direct interactions have been documented with dendritic cells via the NKp30 receptor to promote dendritic cell maturation

but also to delete immature dendritic cells (Castriconi et al., 2003; Vitale et al., 2005). Activated NK cells releasing IFNγ and TNFα reciprocally provide stimulation to dendritic cells to enhance IL-12 production and promote a TH1 immune response (Ferlazzo & Morandi, 2014). NK cell mediated cytotoxicity results in the release of further antigens, promoting antigen presentation to mount an adaptive T cell response.

However, NK cell interactions can also be regulatory and limit immune responses. Activated CD8+ T cells can be susceptible to NK cell cytotoxicity through the upregulation of NKG2D ligands and DNAM-1 ligands (Pallmer & Oxenius, 2016). NK cell mediated deletion of T cells is can be important feature in chronic viral infections, as seen in chronic HBV infection with TRAIL mediated killing of HBV specific CD8 T cells (Peppa et al., 2013). T regulatory (Treg) cells may have a negative impact in return on NK cell function, which may be important in chronic viral infections or cancers where the Treg population is expanded (Pallmer & Oxenius, 2016). Whilst interleukin 2 (IL-2) promotes NK cell activation and cytotoxicity, Treg cells limit the availability of IL-2 and thus regulate the NK cell response (Gasteiger et al., 2013).

1.3.6 NK cells within the healthy liver

1.3.6.1 Phenotype

Natural Killer (NK) cells account for thirty to fifty percent of liver lymphocytes (Gao et al., 2008). Unlike circulating NK cells, CD56bright NK cells make up a greater proportion of liver resident NK cells, but differ from circulating CD56bright NK cells with an increased expression of the liver homing surface receptors CXCR6, CCR5, CD69 and transciption factor EOMES but with a lower expression of the transcription factor T-bet in comparison to circulating NK cells (Marquardt et al., 2015; Stegmann et al., 2016). A subset of liver NK cells have also been reported to express CD49a (T. Hydes et al., 2017; Marquardt et al., 2015). The upregulation of transcription factors Hobit and Blimp has also been described as key in the upregulation of CD69 and driving tissue residency in NK cells (Mackay et al., 2016).

Hepatic NK cells may be derived from different precursors to circulatory NK cells and this may account for why liver resident NK cells are typically CD56bright NK cells with a tissue homing repertoire of cell surface molecules (Mikulak et al., 2019).

As described earlier, liver resident NK cells are long-lived, found lining sinusoidal spaces and are not thought to enter circulation following engagement through CXCR3, CCR5 and CXCR6 ligands expressed within the liver sinusoids, with CCL3+ Kupffer cells, CCL5+ sinusoidal T and NK cells and CXCL16+LSECs (Cuff et al., 2016; Hudspeth et al., 2016a; Pallett et al., 2020).

Whilst circulating blood CD56bright NK cells are thought to be less mature than CD56dim NK cells, there is evidence that circulating NK cells may be a precursor for CD56bright liver resident NK cells. Circulating NK cells in adults can be recuited to the liver and, once engaged in liver sinusoids, these recruited NK cells upregulate EOMES and demonstrate a liver resident NK cell phenotype (Cuff et al., 2016).

1.3.6.2 Effector Functions

Liver resident NK cells also significantly differ with regards to effector function in comparison to circulating NK cells. Liver resident NK cells must maintain hyporesponsiveness in order to maintain a tolerogenic environment within the liver (Mikulak et al., 2019). TRAIL and FasL are upregulated on liver NK cells indicating that NK cell-mediated apoptosis may play a bigger role in the liver (Tang et al., 2016). IL-10 from Kupffer cells inhibits NK cell pro-inflammatory responses. Furthermore the engagement of NKG2A by HLA-E molecules on hepatocytes promotes TGF- secretion by NK cells which in turn modulates dendritic cell function and supports the expansion of Treg cells (Jinushi et al., 2007). Treg cells additionally produce IL-10 and TGF further inhibiting NK cells and promoting tolerogenesis (Mikulak et al., 2019; Pedroza-Pacheco et al., 2013). In addition, exposure of NK cells to apoptotic cells results in the production of TGF by NK cells, and an attenuated IFNγ response following NK cell stimulation (Chong et al., 2010). Furthermore, these NK cells in turn suppress CD4+T cell proliferation via NKp46 engagement (Chong et al., 2010).

There is also evidence that liver resident NK cells may have adaptive properties as demonstrated by their ability to function like memory cells. Studies on mouse NK cells in the context of murine cytomegalovirus infection demonstrated that CD57+NKG2C+NK cells may have memory like responses on re-infection with CMV (Lopez-Vergès et al., 2011; J. C. Sun et al., 2009). Pre-activating human NK cells with IL-12, IL-15 and IL-18 followed by a prolonged rest period resulted in cytokine induced memory like NK cells (Tarannum & Romee, 2021). Furthermore, these NK cells were able to pass on their abilities to daughter cells, partly explained by epigenetic modifications within the cytokine induced memory like NK cells (Pahl

et al., 2018). However, interestingly these memory NK cells are CXCR6+ liver resident NK cells (Paust et al., 2010), and the transcription factor aryl hydrocarbon receptor in mice has been demonstrated as being upregulated in these cells (L. H. Zhang et al., 2016).

1.3.7 Functional roles of NK cells in anti-viral, anti-pathogen and anti-tumoural responses

NK cell effector functions described above play a vital role in anti-pathogen responses, having the capacity for direct cytotoxicity in response to virally infected cells, and releasing cytokines, such as interferon gamma, aiding monocyte/macrophage recruitment and activation essential in anti-bacterial responses. NK cells also play a pivotal role in tumour surveillance, having the capacity to lyse transformed cells. General NK cell effector functions will be discussed below, followed by specific NK cell responses in liver disease.

1.3.7.1 NK cell anti-viral and anti-pathogen responses

NK cells are powerful effectors in acute viral infections, predominantly due to their capacity for IFNγ production and direct cytotoxicity following the engagement of activating NCRs via ligands expressed on infected cells (Barrow et al., 2019; Van Erp et al., 2019). Virally infected NK cells may evade antigen recognition by T cells by downregulating MHC class I, but this results in a loss of inhibition of NK cells via KIR as described above (Waggoner et al., 2016). In addition, the upregulation of death ligands (FasL and TRAIL) on infected cells may also trigger NK cell mediated apoptosis (Van Erp et al., 2019; Waggoner et al., 2016). In addition, NK cells produce potent antibody mediated direct cell cytotoxicity following the engagement of CD16 by infected cells opsonised with antibody, as described above (Ofer Mandelboim et al., 1999).

With regards to bacterial infections, NK cells are activated by IL-12 secreted by monocytes, and in turn support monocyte function via the production of IFNγ, activating monocytes and recruiting monocytes and cascading immune cell recuitment (Souza-Fonseca-Guimaraes et al., 2012). NK cells also express TLR and cytotoxicity can be directly induced in response to the detection of PAMPs (Noh et al., 2020). TLR4 enagagement by lipopolysaccharide promotes IFNγ production and enhances NK cell cytotoxicity (Lauzon et al., 2006). NK cells also produce alpha defensins and LL37, anti-bacterial peptides important in the chemoattraction of adaptive T cells (Agerberth et al., 2000).

1.3.7.2 NK cell tumour Surveillance and anti-tumour responses

NK cells provide an efficient first line response to tumours cells (Y. Li & Sun, 2018). Tumour cells often downregulate MHC-1 expression, allowing escape from CD8+ T cell cytotoxicity. However, this triggers a powerful anti-tumour NK cell response from licenced NK cells, in keeping with the 'missing self hypothesis' (Raulet & Vance, 2006). Tumour cells often upregulate stress ligands, such as MHC Class I polypeptide-related sequence A and B (MICA and MICB) that readily engage NKG2D, a powerful activating NK cell receptor. Cross talk with dendritic cells supports the activation and maturation of dendritic cells and promotes antigen presentation to mount CD8+T cell responses as described above.

The increased activity of NK cells is associated with a reduced occurrence of cancer, thereby supporting the role of NK cells intumour surveillance (Imai et al., 2000; Muntasell et al., 2017). Similarly, reduced tumour infiltrating NK cells in solid tumours is associated with poor outcomes in multiple different cancers (Eckl et al., 2012; Habif et al., 2019; Tartter, 1987). Furthermore, infiltrating NK cells can be modulated negatively in the tumour microenvironment, thereby allowing the tumour to persist. Le Maux Chansac *et al.* examined NK cells residing within lung tumour tissue, and found that although these NK cells were capable of cell cytotoxicity when incubated with the MHC-1 negative cell line K562, these same NK cells were unable to lyse the autologous lung tumour also deficient in MHC-1 (Le Maux Chansac et al., 2005). This was predominantly due to an up-regulation of inhibitory ligands by the lung adenocarcinoma (Le Maux Chansac et al., 2005). In addition, Platonova *et al.* examined the phenotype and function of intratumoural NK cells residing within non-small cell lung cancers and, when comparing them to those from peripheral blood or non-tumour tissue, found the NK cell repertoire was altered with a down-regulation of activating receptor expression, including NKG2D and DNAM-1, and a lack of expression of some MHC-1 receptors, rendering these NK cells hypofunctional within the tumour microenvironment (Platonova et al., 2011). Tumours may also express inhibitory ligands on tumour cells, as exemplified by the up-regulation of CD137L expression on acute myeloid leukemia cells, which interacts with the inhibitory receptor CD137 on NK cells (Baessler et al., 2010).

1.3.8 NK cells in Liver disease

1.3.8.1 Viral hepatitis

Hepatitis C (HCV) results in chronic infection in 80% of people infected, and untreated can result in cirrhosis in approximately 20% of patients and HCC in up to 4% of patients (Lauer & Walker, 2001; M. H. Lee et al., 2014). At the beginning of 2020, an estimated 56.8 million people across the world were affected by HCV, and with the novel direct acting antiviral agents now available, there is a global drive to eliminate HCV (Blach et al., 2022). NK cell modulation and HCV mediated evasion from NK cell cytotoxicity in part explains the ability of HCV to persist in the human host.

Genetic polymorphisms in KIR and their HLA ligands are associated with differing outcomes, with KIR2DL3/HLA-C1, KIR2DL3/HLA-Cw*03 and KIR3DS1/HLABw4 being associated with an increased incidence of spontaneous resolution to infection (De Re et al., 2015; Khakoo et al., 2004; Knapp et al., 2010), while KIR2DS2/HLA-C1, KIR2DL2/HLA-C1, KIR2DS3/HLA-C2, KIR3DL1/HLABw4 and KIR2DS4/KIR2DS1/KIR2DL1 rs35440472-A with HLA-C rs1130838-A are associated with negative outcomes, including increased susceptibility to infection with HCV and/or chronicity and/or HCC (De Re et al., 2015; Dring et al., 2011; Shen et al., 2021; Umemura et al., 2021). The KIR3DL1/HLABw4 combination in particular is strongly associated with the development of HCC in patients with HCV related cirrhosis (Umemura et al., 2021). Combinations of KIR and HLA can have a significant impact on viral clearance following treatment with directly acting anti-viral therapies, with patients carrying KIR2DL3/HLAC1C1 responding to treatment and those carrying KIR2DL2/HLAC1C2 not responding to treatment (Vidal-Castiñeira et al., 2010).

KIR may work synergistically with other NK cell receptors. Patients regularly injecting substances and who are at high risk of contracting HCV but remain negative for HCV infection had an increased proportion of KIR2DL3+NKG2A- NK cells (Thoens et al., 2014). As patients with HCV infection demonstrated an upregulation of HLA-E expression in the liver, the reduced expression of NKG2A on circulating NK cells may confer protection to contracting HCV (Thoens et al., 2014).

Other NK cell receptors also play a role in acute and chronic HCV infection, although the reported changes seen in chronic HCV infection are inconsistent across studies (Cheent &

Khakoo, 2011; H. R. Rosen & Golden-Mason, 2020). Overall, many studies have demonstrated that in chronic HCV infection, both circulating NK cells and intrahepatic NK cells are reduced in proportion to healthy controls (Bonorino et al., 2009; Meier et al., 2005; Barbara Oliviero et al., 2009; Pembroke et al., 2014). The HCV NS3 protein can attenuate NK cell function by downregulating the NCRs NKp46 and NKp30 (Yang et al., 2017). Worryingly, attenuated NK cell effector functions following exposure to the HCV core protein, do not appear to recover following clearance of HCV (Golden-Mason et al., 2014), implying that NK cell dysfunction may persist for some time following viral clearance (H. R. Rosen & Golden-Mason, 2020). Within the liver, cross talk with Treg cells may also promote fibrosis, with activated hepatic stellate cells demonstrating a reduced expression of MIC A and MIC B following incubation with Treg cells, resulting in reduced killing by NK cells (Langhans et al., 2015). Intrahepatic NK cells are also altered, demonstrating reduced TRAIL expression (Varchetta et al., 2012).

Interestingly, TRAIL expression on intrahepatic NK cells in HBV infection is upregulated, unfortunately resulting in hepatocyte death while mediating anti-HBV responses within the liver (C. Dunn et al., 2007). Furthermore, CD8+T cell deletion by NK cells has been characterised in chronic HBV infection, with TRAIL-R2 being upregulated on HBV specific CD8 T cells and triggering TRAIL-mediated NK cell cytotoxicity (Peppa et al., 2013), indicating that some NK cell responses in HBV infection may not be desirable and may contribute to persistence (Maini & Peppa, 2013).

While NK cell cytotoxicity appears to be maintained in circulating and intrahepatic NK cells in chronic HBV infection, the production of IFNγ and TNFα is impaired (Barbara Oliviero et al., 2009; Peppa et al., 2010). Furthermore, there is some evidence that inhibitory receptors, including T cell immunoglobulin and mucin domain containing 3 (TIM3) and NKG2A, are upregulated on NK cells (Ju et al., 2010; F. Li et al., 2013). Gene expression analysis demonstrates similarities between these dysfunctional NK cells and exhausted T cells (Marotel et al., 2021).

1.3.8.2 Autoimmune Liver Disease

Autoimmune liver disease encompasses a range of diseases, sometimes with overlap, including autoimmune hepatitis (AIH), primary biliary cholangitis (PBC) and primary sclerosing cholangitis (PSC).

Whilst NK cells constitute approximately half of the liver lymphocyte population, there is little evidence regarding the role of NK cells in AIH, with pathology attributed mainly to the adaptive immune system (M. Liu et al., 2021; Mikulak et al., 2019). However, polyIC mediated liver injury in mice resulted in NK cell enrichment in the liver and a resulting autoimmune hepatitis in mice (Dong et al., 2004). In patients with AIH, intrahepatic CD56bright NK cells reduced significantly in proportion following corticosteroid therapy, and a significant proportion of these NK cells were CD161 positive (Jeffery et al., 2018).

In patients with PBC, NK cytotoxicity in peripheral and intrahepatic NK cells remains preserved and even enhanced (Y. Chuang et al., 2006; M. Liu et al., 2021). NK cells surrounding destroyed biliary epithelium in PBC are increased in number (Shimoda et al., 2011) and appear to be constitutively activated (T. J. Hydes et al., 2019).

In PSC, there is an increase in peripheral circulating NK cells (Panasiuk et al., 2004), and certain genetic variations in MICA (*MICA5.1*) and MICB (*MICB24*), ligands for the activating NK cell receptor, are associated with an increased susceptibility to developing PSC (Wiencke, 2001). In both PBC and PSC, TRAIL mediated apoptosis appears to be the most likely pathway for NK cell mediated autoreactivity (Takeda et al., 2008).

1.3.8.3 Alcohol related Liver disease

Alcohol related liver disease (ALD) is a major cause of morbidity and mortality. Updated statistics on liver disease in England from the Office for Health Improvement and Disparities (April 2024 update, https://www.gov.uk/government/statistics/liver-disease-profile-april-2024-update/liver-disease-profile-april-2024-update) reveal that the rate of premature deaths from liver disease has risen by 40% from 2001 to 2022, with the number of deaths from ALD increasing by 61.3% in England since 2003.

Alcohol related liver disease is associated with impaired cytotoxic NK cell function (F J Laso et al., 1997; Pan et al., 2006). Patients dependent on alcohol, without underlying liver disease,

had reduced perforin expression within NK cells in comparison to healthy volunteers (Perney et al., 2003), suggesting that alcohol or related metabolites can have direct detrimental effects on NK cell function. However, it is unclear at what stage of ALD and the development of fibrosis that NK cell dysfunction becomes apparent. NK cells in patients consuming alcohol chronically in excess but without liver fibrosis reveal activated circulating NK cells with increased cytotoxicity (Francisco Javier Laso et al., 2010). However, in patients with alcohol related hepatitis, NK cells have been described as either with impaired cytotoxicity (Støy et al., 2015) or found to have increased cytotoxicity contributing to severe alcohol related hepatitis (Sehgal et al., 2020).

Cui et al demonstrate that NK cells provide protective mechanisms as NK cell depletion in these mice resulted in an increase in hepatic steatosis, and beneficial effects were mediated by IFNγ release from NK cells (Cui et al., 2017). NK cell mediated killing of activated hepatic stellate cells as an anti-fibrotic mechanism is also impaired, again via impaired IFNγ secretion, in alcohol related liver disease mouse models (Jeong et al., 2008). Furthermore, cross talk with NKT10 cells, a subset of invariant NKT cells with the capacity to produce IL-10, is thought to inhibit NK cell function as demonstrated in a mouse model with alcohol induced liver disease (Cui et al., 2017).

1.3.8.4 Metabolic dysfunction-associated Liver Disease

The nomenclature for non-alcohol related fatty liver disease was updated to metabolic dysfunction-associated steatotic liver disease (MASLD) following the mounting evidence of the condition being associated with a more global multi-system metabolic syndrome, with strong associations with diabetes, cardiovascular and renal disease (L. A. Adams et al., 2017; Eslam et al., 2020; Rinella et al., 2023; Targher et al., 2021, 2024). The term MetALD was also coined to recognise the separate population of patients with a combination of MASLD and an increased alcohol intake for whom outcomes from the disease and disease progression may differ from patients with simple MASLD (Rinella et al., 2023).

In MASLD, the evidence for NK cells remains contradictory, and this may be in part due to the broad spectrum of disease, from simple steatosis to a pro-inflammatory steatohepatitis characterised by an increase in intrahepatic Kupffer cells, neutrophils, activated CD8+T cells and TH17 T cells (Martínez-Chantar et al., 2021). While the majority of studies report a reduced frequency and reduced cytotoxicity of circulating NK cells in obese patients

(Martínez-Chantar et al., 2021; Michelet et al., 2018; Viel et al., 2017), studies on NK cells in MASLD and metabolic dysfunction-associated steatohepatitis (MASH) are less congruent (Table 1).

With regards to NK cell receptors, while some studies found an increased expression of the activating NKG2D receptor on NK cells in MASH (Kahraman et al., 2010; Stiglund et al., 2019), other studies found a reduced expression of NKG2D in MASLD (Diedrich et al., 2020). Reduced expression of NKp46 and NKp30 and increased expression of inhibitory/exhaustion markers including Siglec 7 and 9, TIGIT, PD-1 and ILT2 have also been described (Sakamoto et al., 2021).

In addition, the altered metabolic environment in MASLD may play a role in reprogramming NK cell function. NK cell cytokine production and degranulation is reliant on aerobic glycolysis and oxidative phosphorylation, and mTOR (the mammalian target of rapamycin) is involved in upregulating these processes (Martínez-Chantar et al., 2021). TGFβ has been demonstrated to reduce NK cell metabolism through reduced mTOR signalling in obese mice (Cuff et al., 2019).

Table 1 NK cell frequencies and cytotoxicity in NAFLD and NASH studies

DISEASE COMPARISON	NK CELL NUMBER/PROPORTION	NK CELL CYTOTOXICITY	
MASLD VS MASH	No difference in peripheral blood NK cell number	No difference in peripheral blood	(Stiglund et al., 2019)
MASLD VS HEALTHY	Increased NK cells in peripheral blood in patients with F4 fibrosis	Peripheral blood NK cytotoxicity inversely correlates with liver fibrosis	(Amer et al., 2018)
MASLD VS HEALTHY		Liver NK cell degranulation inversely correlates with liver fibrosis	(Cuff et al., 2019)
MASLD VS MASH	Increased intrahepatic NK cells in MASH vs MASLD		(Kahraman et al., 2010)
MASLD VS HEALTHY	Reduced NK cells in the peripheral blood in MASLD	Reduced degranulation in CD56dim NK cell subset	(Sakamoto et al., 2021)
MASLD VS HEALTHY	Increased liver stiffness on fibroscan correlated negatively with intrahepatic NK cells Reduced numbers of NK cells in peripheral blood		(Diedrich et al., 2020)

1.3.8.4 Hepatocellular carcinoma and NK cell related immune dysregulation

Solid tumours with reduced numbers of infiltrating NK cells have been associated with poor prognosis as described above. Altered NK cell numbers, activity and receptor expression has also been demonstrated in HCC as detailed in Table 2 below (Cai et al., 2008; W. L. Chuang et al., 1990; Y. Wu et al., 2013). The interactions resulting in hypofunctional NK cells are not fully understood. Chew et al describe an immunosuppressive gradient across the tumour microenvironment, where NK cells, with an increased IL10 production and reduced Granzmye B production, are recruited to the tumour microenvironment to join an enriched population of Treg and exhausted CD8+PD-1+T cells (Chew et al., 2017). NK cell crosstalk with other cells of the tumour and stromal immune infiltrate may account for some of the phenotypic and functional changes seen in NK cells. Macrophage and NK cell peri- and intra-tumoural interactions in HCC via the 2B4 reeceptor on NK cells results in an initial NK cell activation but

then a rapid subsequent exhaustion of NK cells (Y. Wu et al., 2013). Myeloid derived suppressor cells that are expanded in HCC have been demonstrated to interact with NKp30 on NK cells but inhibit NK cell function (Hoechst et al., 2009). Interactions with fibroblasts derived from HCC tumour tissue have induced dysfunctional NK cells in vitro (T. Li et al., 2012). T-regulatory (Treg) cells also inhibit NK cell function in the context of HCC, with loss of anti-tumour responsesin NK cells from patients with higher proportions of Treg cells (Cai et al., 2008).

Modulation of NK cell receptor expression has been described in HCC and associated with NK cell dysfunction. NKG2D expression has been demonstrated to be important for effective NK mediated tumour surveillance (Guerra et al., 2008). NKG2D expression has been described as altered in HCC many independent studies (Jinushi et al., 2005; Mantovani et al., 2019; Sheppard et al., 2017; Zecca et al., 2021). Jinushi et al., describe soluble MICA levels that are elevated in some patients with HCC and corresponding peripheral blood NK cells had lower levels of NKG2D expression and impaired activation (Jinushi et al., 2005). ULBP1 has also been described in the serum of patients with HCC but has been associated with improved survival (Easom et al., 2020; Kamimura et al., 2012), while soluble MICA has been associated with poorer outcomes (Jinushi et al., 2005; V. Kumar et al., 2012). Further conflicting evidence comes from Sheppard et al who describe a mouse model where NKG2D sufficient mice demonstrate accelerated tumour growth with the recruitement of CD8+ T cells in comparison to NKG2D deficient mice (Sheppard et al., 2017). Conflicting evidence for NKp30 expression in HCC is partly explained by an alteration in the isomer expressed in HCC, with an increase in the inhibitory NKp30 variant being expressed in HCC (Mantovani et al., 2019).

More recent studies imply a regulatory and possibly pathogenic role of NK cells in HCC. Zecca et al describe a CD49a+ NK cell tumour infiltrating subset, that have a increased expression of NCRs, a lower expression of NKG2D and demonstrate reduced NK cell cytotoxicity and TNFα production. The CD49a+NK subset is also EOMES+, unlike liver resident NK cells that are classically TbetHiEOMESlo (Zecca et al., 2021). CD49a+EOMES+ NK cells have been described in the decidua, in increased abundance early in pregnancy, where the role of these NK cells is thought to promote angiogenesis to support a successful pregnancy (Montaldo et al., 2016; Zecca et al., 2021). This pro-angiogenic NK cell subset found within HCC tumour tissue raises the question of whether NK cells are beneficial or pathogenic in this context, and if promoting

NK cell function with targeted immunotherapy would be beneficial for the patient or detrimental.

Some studies have demonstrated an increase in NK cell function following treatment being associated with better outcomes. Patients with 5 year recurrence free survivals following adjuvant sorafenib in the STORM trial had higher intratumoural NK cells (Pinyol et al., 2019). Sorafenib has also been shown to inhibit the release of MICA from tumour cells, thereby mitigating the effects of soluble MICA (Kohga et al., 2010). Patients following radiofrequency ablation demonstrated an increase in circulating NK cells expressing activating receptors and increased effector responses, and this correlated with an improved disease free survival, supporting the hypothesis that promoting NK cell function in patients with HCC is beneficial (Zerbini et al., 2010).

Table 2 Studies on NK cells in patients with HCC. HCC:Hepatocellular carcinoma, MDSC:myeloid derived suppressor cells, Treg:T regulatory cells,

COMPARISON	SITE	NK CELL NUMBER	NK CELL FUNCTION	NK CELL RECEPTORS/NK CELL CROSSTALK	
HCC VS HBV CIRRHOSIS VS HEALTHY	Blood		Reduced cytotoxcity in HCC and non-HCC cirrhosis compared to healthy Cytotoxicity inversely correlates with advanced HCC/vascular invasion		(W. L. Chuang et al., 1990)
HCC VS HEALTHY	Blood		Reduced cytotoxicity in HCC	MDSC inhibit NK cells via NKp30	(Hoechst et al., 2009)
HCC VS HEALTHY	Blood Tumour	Reduced CD56dimCD16+ NK cells in blood and tumour	Reduced cytotoxicity in HCC and reduced IFNγ production in blood and tumour	Treg cells inhibit NK cells	(Cai et al., 2008)
HCC VS HEALTHY	Blood	Reduced numbers of NK cells in blood			(Fathy et al., 2009)
HCC TUMOUR VS NON TUMOUR TISSUE	Liver	Reduced numbers of NK cells in tumour and in patients with metastases		Increased Treg cells in tumour	(Guo et al., 2012)

COMPARISON	SITE	NK CELL NUMBER	NK CELL FUNCTION	NK CELL RECEPTORS/NK CELL CROSSTALK	
HCC TUMOUR VS NON TUMOUR TISSUE	Liver	Reduced numbers of CD56brightNK cells in tumour	Reduced TNFα and IFNγ by tumour infiltrating NK cells	Crostalk with stromal monocytes via 2B4 receptor activates and induces NK cell dysfunction	(Y. Wu et al., 2013)
HCC	Blood		Reduced cytotoxicity by NKG2Dlo NK cells from patients with HCC and soluble MICA in serum	Reduced maturation/activation of DC by NK cells pre-treated with soluble MICA NKG2D downregulated in patients with HCC and soluble MICA in serum	(Jinushi et al., 2005)
HCC	Fibroblast from HCC tumour tissue			HCC tumour tissue derived fibroblasts inhibit peripheral blood NK cell Granzyme B and perforin production via Prostaglandin E2 and IDO expression	(T. Li et al., 2012)
HCC POST TREATMENT VS CIRRHOSIS VS HEALTHY	Blood		Reduced NK cell cytotoxicity in patients with worse outcomes following HCC treatment	NK cells coexpressing NKG2A, NKp46 and NKp30 associated with worse outcomes following curative HCC treatment NK cells with increased granzyme B and CD3ζ associated with better outcomes	(Cariani et al., 2016)
HCC VS HEALTHY	Liver		Increased CD96 on NK cells with increased IL-10, TGFβ, low gene expression of Tbet, IL-15, perforin, granzyme and reduced production of IFNγ and TNFα	Increased CD96 on intratumoural NK or CD155 on tumour tissue associated with poorer outcomes	(H. Sun, Huang, et al., 2019)

COMPARISON	SITE	NK CELL NUMBER	NK CELL FUNCTION	NK CELL RECEPTORS/NK CELL CROSSTALK	
HCC	Liver	Increased CD49a+ NK cells in HCC tumour tissue correlates with poor prognosis		Increased PD-1, CD96 and TIGIT on CD49a+ NK cells within tumour tissue	(H. Sun, Liu, et al., 2019)
HCC	Blood Liver			Decreased NKp30, reduced NKG2D, increased TIM3 in peripheral blood NKp30+NK cells expressed the inhibitory variant of NKp30 in advanced HCC Increased soluble B7-H6 in advanced HCC	(Mantovani et al., 2019)
HCC PRE TREATMENT AND HCC POST RFA	Blood	No difference	No difference Increased risk of HCC recurrence if proportion of NK cells producing IFNγ is <45% at 1 month post RFA		(H. A. Lee et al., 2021)
HCC VS HEALTHY	Liver	Reduced liver resident CXCR6+ NK cells within tumour - Intratumour NK cells mostly TbetHiEOMESlo	Reduced NK cell cytotoxicity Reduced TNFα production	Increased CD49+EOMES+NK subset in HCC Higher expression of NKp46, NKp30, NKp44 Lower expression of NKG2D	(Zecca et al., 2021) NK regulatory

1.4 Hypothesis

Whilst NK cells have been demonstrated to be dysfunctional in HCC, it is important to understand at what point of the disease process NK cell dysfunction arises and at what point tumour surveillance may be impaired as this has important consequences for potential immunotherapeutics. I propose that NK cell modulations occur before HCC arises, resulting in hyporesponsive NK cells in keeping with cirrhosis associated immune dysfunction and with cirrhosis being a premalignant state.

While NK cell dysfunction is well characterised in viral hepatitis, it is not clear at which stage in steatotic liver disease NK cell dysfunction arises and if changes seen in cirrhosis secondary to steatotic liver disease persist in patients who develop HCC.

1.5 Thesis Aims

1. Characterise NK cells in patients with cirrhosis and in HCC and underlying cirrhosis secondary to non-viral liver disease with deep phenotyping (protein expression and gene expression) and functional analysis of circulating and intrahepatic NK cells in cirrhosis and HCC.
2. Investigate the CD56dimCD16+/- NK cell subpopulation that is expanded in cirrhosis and HCC
3. Clarify the role of the inhibitory CD161-LLT1 interaction in cirrhosis and HCC

2. Materials and Methods

2.1.Ethics

Ethical approval for the use of patient samples for this study was sought and granted by the Research Ethics Committee for London (City & East, REC reference 15/LO/0363).

2.2 Subject selection and sample collection

2.2.1 Patient recruitment and sample collection

Patients with cirrhosis, hepatocellular carcinoma (HCC), or undergoing surgery for a liver resection but without underlying cirrhosis or HCC were recruited and consented from outpatient clinics at Imperial College NHS Healthcare Trust (St Mary's Hospital and Hammersmith Hospital) and Kings College Hospital. Patients with non-alcoholic fatty liver disease (NAFLD) who were not cirrhotic (biopsy proven Metavir score <4 or with a fibroscan score of <7kPa) were also consented as a control group. All patients were given the relevant patient information sheet (Appendices A-C) and gave informed written consent to participate (Appendices D-F). Patients awaiting liver transplantation were consulted via telephone and posted patient information sheets if they consented verbally. Formal written consent was then taken when the patient subsequently attended an outpatient clinic appointment or was called in to hospital prior to transplantation. Criteria deeming patients eligible to participate were aged over 18 years with capacity to give informed consent.

Peripheral venous blood was taken from participants in sodium heparin blood bottles and serum separating tubes (SST). Up to a volume of 40ml of blood was taken and processed. The maximum time between venesection and blood processing was 4 hours. Liver tissue from surgical liver resections or whole liver explants were either taken fresh immediately to the histopathologist for examination or placed on ice in a cold room (at 4°C) until the histopathologist could examine the liver tissue. Subsequently, any liver tissue deemed surplus to diagnosis by the histopathologist was then processed for mononuclear cell extraction. The maximum time between liver resection/removal and liver tissue processing was 16 hours.

2.2.2 Healthy controls

Healthy volunteers were recruited and written consent taken. After informed consent blood samples were obtained from individuals who had no known history of liver disease and no regular medication use. For all of the assays described, each experiment comprised healthy control samples alongside the patient samples, in order to control for any assay-to-assay variation.

2.3. Sample Processing

2.3.1 Whole blood processing

Blood from sodium heparin tubes was diluted with one volume of phosphate-buffered saline (Gibco™ PBS, pH 7.4, Thermofisher Scientific). This diluted blood was layered over Ficoll-Paque™ PLUS Media (GE Healthcare) (30mls diluted blood over 15mls Ficoll-Paque™ PLUS Media) and spun at 2000rpm for 20mins without brakes. Peripheral blood mononuclear cells (PBMCs) were thus harvested via density centrifugation, resuspended in sterile heat-inactivated fetal calf serum (FCS, Lonza) with 10% dimethyl sulfoxide (DMSO) and stored in controlled containers (Nalgene® Mr. Frosty® Cryo 1°C freezing containers) at -80°C for 8-24 hours, before being transferred to liquid nitrogen at -190°C. When required for assays or phenotyping, the cells were thawed at 37°C, rapidly transferred and washed in RPMI 1640 medium (Thermofisher Scientific) and resuspended in RPMI 1640 supplemented with 10% FCS and 1% penicillin-streptomycin and 2mM L-glutamine (Thermofisher Scientific), henceforth referred to as R10 culture medium.

Blood collected in serum separating tubes was spun at 1800rpm for 10minutes. The serum was stored at -80°C in 500ul aliquots.

2.3.2 Liver tissue processing

Liver tissue was washed in 500mls of PBS, diced into 5mm^3 pieces and transferred into RPMI 1640 medium supplemented with 10% FCS. Tissue and media was then transferred to gentleMACS C-tubes and mechanically dissociated using a

gentleMACS™ Dissociator (mouse-spleen program 03, Miltenyi Biotech). The subsequent liver tissue slurry was then filtered through a 70µm mesh and then spun at 50rcf for 5mins to pellet any remaining large hepatocyte debris. The supernatant was then filtered again through a 35µm filter, and then layered over Ficoll-Paque™ PLUS Media (GE Healthcare) (30mls of supernatant over 15mls Ficoll-Paque™ PLUS Media) and the liver mononuclear cells (LMNCs) extracted by density centrifugation. The liver mononuclear cells were washed, any remaining red blood cells lysed using ACK lysis buffer (Thermofisher Scientific), and stored in CryoStor® cell cryopreservation media (CS10, Sigma-Aldrich) in controlled cooling containers (Nalgene® Mr. Frosty® Cryo 1°C freezing containers) at -80°C for 8-24hours before being transferred to liquid nitrogen at -190°C.

2.4 Cell lines and cell culture

2.4.1 K562

The K562 cell line is a human erythroleukaemic cell line derived from a patient with chronic myeloid leukaemia. These cells do not express surface MHC class I and are therefore readily killed by NK cells (Koeffler & Golde, 1980).

2.4.2 Huh7

The Huh7 cell line is an hepatocellular carcinoma cell line, derived originally from a patient with a well-differentiated hepatocellular carcinoma and established by Nakabayshi, H. and Sato, J (Nakabayashi et al., 1982).

2.4.3 HepG2

The HepG2 cell line is another hepatocellular carcinoma cell line, derived from a patient with a well-differentiated tumour (Aden et al., 1979).

2.4.4 Jurkat

The Jurkat cell line is a T cell lymphocyte cell line derived from a patient with a T cell leukaemia (Schwenk & Schneider, 1975).

2.4.5 Raji Cells

The Raji cell line is a B cell line, derived from a patient with Burkitt's lymphoma(Pulvertaft, 1965).

Cell culture and reagents

Cell lines were cultured and maintained in R10 culture medium (RPMI medium (Gibco, ThermoFisher Scientific) supplemented with 10% heat inactivated foetal calf serum and 1% penicillin/streptomycin) at 37°C under 5% CO2. These were maintained in logarithmic phase at neutral pH by diluting the cultures at a 1 in 10 dilution every 72 hours in the case of K562 cells, or when cells had reach 80% to 90% confluence in the case of Huh7 and HepG2 cells. Adherent cell lines were detached from culture flasks using trypsin-EDTA (0.25%) solution (ThermoFisher Scientific, 25200072).

Table 3 Phenotyping flow cytometry antibody panels.

Laser	*Phenotyping panel 1*	*Phenotyping panel 2*	*Liver Panel*	*Maturity panel 1*	*Maturity panel 2*
405 450/50	CD3- eF 450 (SK7, 48-0036-41, ThermoFisher)	CD3- eF 450 (SK7, 48-0036-41, ThermoFisher)	CD16 V450 (644490, 3G8, BD)	CD16 V450 (644490, 3G8, BD)	CD16 V450 (644490, 3G8, BD)
405 525/50	Fixable Viability Dye eF 506 (65-0866-14, ThermoFisher)	CD4- BV510 (566804, BD)	Fixable Viability Dye eF 506 (65-0866-14, ThermoFisher)	Fixable Viability Dye eF 506 (65-0866-14, ThermoFisher)	Fixable Viability Dye eF 506 (65-0866-14, ThermoFisher)
405 610/20	NKp30 BV605 (563384, BD)			IL7R (562662, BD)	
405 660/20		BTLA-BV650 (564803, BD)			
405 710/50	DNAM-1 BV11 (752659, BD)		CCR5 BV711 (2D7, 563395, BD)		
405 780/60	NKp46 BV786 (563329, BD)	PD-1 – BV786 (741018, BD)			
488 530/30	NKG2D FITC (11-5878-42, ThermoFisher)	CD56-FITC (11-0566-42, ThermoFisher)		NKG2C AF488 (FAB138G-100, R&D)	
488 575/26		CTLA-4 PE (12-1529-42, ThermoFisher)	CD56 PE (CMSSB, 12-0567, ThermoFisher)	NKG2A PE (FAB1059P-100, R&D)	CD56 PE (CMSSB, 12-0567, ThermoFisher)
488 610/20	CD161 PE-eF 610 (61-1619-41, ThermoFisher)	CD161 PE-e 610 (61-1619-41, ThermoFisher)	EOMES PE-eF610 (WD1928, 61-4877, ThermoFisher)	KLRG1 PE eF 610 (61-9488-42, ThermoFisher)	
488 695/40	CD16 PerCP-e710 (Clone 3G8, 46-0166-41, ThermoFisher)	Va7.2 PerCP-Cy5.5 (use 5ul)	CD3 (clone SK7) PerCP-eFluor 710 (ThermoFisher)	CD3 (clone SK7) PerCP-eFluor 710 (Thermofisher)	CD3 (clone SK7) PerCP-eF 710 (ThermoFisher)
488 780/60	CD56 PE-Cy7 (CMSSB, 25-0567-41, ThermoFisher)	CD25 PE-Cy7 (25-0257-42, ThermoFisher)	T-Bet PE-Cy7 (4B10, 25-5825, ThermoFisher)	CD56 PE-Cy7 (CMSSB, 25-0567-41, ThermoFisher)	
633 670/14	CXCR6 AF647 (SA051D1, Biolegend)	CD8- APC (47-0088-42, ThermoFisher)	CD49a (328314, Biolegend)	CD57 APC (359610, Biolegend)	TCF-1 (566693, BD)
633 780/60		Fixable Viability Dye eF 780 (65-0856-18, ThermoFisher)			

2.5 NK cell phenotyping

2.5.1 Ex-vivo phenotyping using flow cytometry

PBMCs for phenotyping were thawed rapidly at 37°C, washed initially in Gibco RPMI 1640 medium (ThermoFisher Scientific) and then phosphate-buffered saline (PBS, Sigma-Aldrich) and resuspended in PBS. $5x10^5$ cells were aliquoted in a 100µl volume into wells of a 96 well plate. LMNCs were also thawed and washed as above but resuspended at $2x10^5$ cells per 100µl per well. The cells were then stained for viability (fixable viability dye 506 or fixable viability dye 780, Thermofisher Scientific) for 20mins at 4°C. Following this, the cells were washed initially with PBS, and then again with flow cytometry staining buffer containing foetal bovine serum and 0.09% sodium azide (eBioscience™ Flow Cytometry Staining Buffer, Thermofisher Scientific), before being incubated with a blocking buffer (10% human AB serum (Sigma-Aldrich) in flow cytometry staining buffer (Thermofisher Scientific) for 20mins at 4°C. Following this, the cells were resuspended in a pre-mixed cocktail of fluorescently conjugated antibodies and BD brilliant staining buffer (Becton Dickinson) in a final volume of 100µl for 20mins at 4°C. The pre-mixed cocktails of antibody panels are detailed in Table 1 above. Control wells were stained with the above cocktail of antibodies excluding one antibody (fluorescence minus one), and one well remained unstained. Quantities of antibodies to be used were initially optimised to ensure that maximal staining (percentage positive population and mean/median fluorescent intensity of the positive) was achieved with minimal non-specific binding. Finally, the cells were washed twice with flow cytometry staining buffer (eBioscience™, Thermofisher Scientific), resuspended in a final volume of 150µl of flow cytometry staining buffer and acquired by flow cytometry.

Intracellular staining where required (i.e. for transcription factors TCF-1, Tbet, EOMES) was undertaken after surface staining as follows. The cells were washed twice in flow cytometry staining buffer (eBioscience™, Thermofisher Scientific) and fixed in eBioscience™ IC Fixation Buffer (Thermofisher Scientific) containing 2% paraformaldehyde for 30mins at 4°C. Cells were then permeabilised with two washes in eBioscience™ Permeabilization Buffer (10X) containing saponin (Thermofisher Scientific), and subsequently blocked again by resuspending the cells in 100µl of

permeabilisation buffer with 2% Human AB serum (Sigma-Aldrich) for 20mins at 4°C. Following this, antibodies for the transcription factors were added directly to each well and incubated for a further 20mins at 4°C. Cells were then washed again in permeabilisation buffer, followed by flow cytometry staining buffer, and then resuspended in a final volume of 150µl of flow cytometry staining buffer (eBioscience™, Thermofisher Scientific) and acquired immediately by flow cytometry.

2.5.2 Phenotyping following co-culture with K562 target cells

PBMCs were thawed rapidly at 37°C, washed initially in RPMI 1640 medium, then resuspended in R10 medium at a concentration of $1x10^6$ cells/ml and stimulated for 16hours at 37°C in 5% CO_2 with IL-15 (Thermofisher Scientific) at a concentration of 1ng/ml. The following day the IL-15 containing medium was removed from the PBMCs, and the PBMCs were resuspended at a concentration of $5x10^5$ cells/100µl in fresh R10 media. K562 target cells were suspended in R10 medium at a concentration of $1x10^5$ cells/100µl, and 100µl of this was added to the PBMCs, resulting in a PBMC:K562 ratio of 5:1 in a final volume of 200µl in a 96 well U bottom plate. Cells were then incubated at 37°C in 5% CO_2 for either 4 hours or 48 hours. Two wells were plated for each donor with $5x10^5$ PBMCs alone in 200µl of R10 media and no K562 target cells, as controls for the 4 hour incubation and the 48 hour incubation. Surface phenotyping of NK cells were then undertaken at the end of each incubation as described above with phenotyping panel 1 (see Table 3) and acquired by flow cytometry.

2.5.3 Phenotyping following co-culture with Huh7 cells

PBMCs were thawed rapidly at 37°C, washed initially in RPMI 1640 medium, then resuspended in R10 medium at a concentration of $1x10^6$ cells/ml and stimulated for 16hours at 37°C in 5% CO_2 with IL-15 at a concentration of 1ng/ml. The following day the IL-15 containing medium was removed from the PBMCs, and the PBMCs were resuspended at a concentration of $1x10^6$ cells per 100µl in fresh R10 media. Huh7 cells were plated as follows to achieve either direct co-culture, indirect co-culture or heat damaged Huh7 co-culture conditions.

2.5.3.1 Direct Huh7 and PBMC co-culture

Huh7 cells were plated the day before at $2x10^5$ cells per well in a volume of 500µl of R10 medium in a flat bottom 24 well plate, allowing the cells 16 hours to incubate at 37°C in 5% CO_2 to adhere to the well and provide an 80-90% confluent lining to the well. Following this, all media was aspirated from the well lined with Huh7 cells, and 100µl of the resuspended PBMCs in R10 were placed in each well, resulting in a 5:1 PBMC:Huh7 ratio. One well was plated with 100µl of the resuspended PBMCs alone for each donor in R10 (i.e. without any Huh7 cells). The volume of media in all wells was made up to 500µl in total by adding fresh R10 media, and the plate incubated at 37°C in 5% CO_2 for 48hours.

2.5.3.2 Indirect Huh7 and PBMC co-culture

Huh7 cells were plated the day before at $2x10^5$ cells per well in a volume of 500µl of R10 medium in a flat bottom 24 well plate, allowing the target cells 16hours to incubate at 37°C in 5% CO_2 to adhere to the well and provide an 80-90% confluent lining to the well. Following this, all media was aspirated from the wells lined with Huh7 cells, and replaced with 500µl of fresh R10 media. Polycarbonate cell culture inserts with 0.4µm pores (ThermoFisher Scientific) were gently placed within each well above and not touching the adhered Huh7 cells. $1x10^6$ PBMCs were seeded in a 200µl volume of fresh R10 media onto the cell culture inserts, maintaining at PBMC:Huh7 ration of 5:1. One well was set up as above for each PBMC donor but without Huh7 cells (ie 500µl of fresh R10 media in a well with $1x10^6$ PBMCs seeded onto a cell culture insert placed within the well). The plate was incubated at 37°C in 5% CO_2 for 48hours.

2.5.3.3 Heat-damaged Huh 7 and PBMC co-culture

Huh7 cells were suspended at a concentration of $4.5x10^5$ cells per ml of R10 media, and exposed to 70°C in a heated water bath for one minute. Huh7 cells were then resuspended in the same media in which they were exposed to 70°C and plated at $2x10^5$ cells per well (400µl of the media with suspended Huh7 cells) in a flat bottom 24 well plate, allowing the cells 16 hours to incubate at 37°C in 5% CO_2. Following this, 100µl of the resuspended PBMCs in R10 were added to each well, resulting in a 5:1

PBMC:Huh7 ratio in a 500µl volume of media. One well was plated with PBMCs only for each donor (no Huh7 cells) in 500µl of fresh media. The plate was incubated at 37°C in 5% CO_2 for 48hours.

Surface phenotyping of NK cells were then undertaken at the end of each incubation as described above with phenotyping panel 1 (see Table 3) and acquired by flow cytometry.

2.5.4 Phenotyping following incubation in serum from patients with cirrhosis

Healthy PBMCs from three donors were incubated at 37°C in 5% CO_2 for 48 hours in Gibco RPMI 1640 medium (ThermoFisher) supplemented with 1% penicillin-streptomycin (Gibco™, ThermoFisher) and 25% serum from healthy donors (n=4) or patients with cirrhosis (n=6) ($5x10^5$ PBMCs in 500µl of media). Controls for each PBMC donor included RPMI 1640 medium supplemented with 25% heat inactivated human AB serum (Sigma-Aldrich) and RPMI 1640 medium supplemented with 25% foetal bovine serum (Gibco™, ThermoFisher). PBMCs were then surface stained with NK phenotyping panel 1 as described above and acquired using flow cytometry.

2.5.5 Gene expression analysis

2.5.5.1 Cell sorting

PBMCs and MNCs were thawed rapidly at 37°C, washed initially in Gibco RPMI 1640 medium (ThermoFisher Scientific) and then PBS, and resuspended in PBS (MilliporeSigma, St Louis, Missouri, USA). The cells were then stained for viability (fixable viability dye 506, ThermoFisher Scientific) for 20mins at 4°C. Following this, the cells were washed initially with PBS, and then again with flow cytometry staining buffer containing foetal bovine serum and 0.09% sodium azide (eBioscience™ Flow Cytometry Staining Buffer, Thermofisher Scientific), before being incubated with a blocking buffer (10% human AB serum (Sigma-Aldrich) in flow cytometry staining buffer (Thermofisher Scientific) for 20mins at 4°C. Following this, the cells were resuspended in a pre-mixed cocktail of fluorescently conjugated antibodies and BD brilliant staining buffer (Becton Dickinson) in a final volume of 100µl for 20mins at 4°C.

The pre-mixed cocktail of antibodies were as follows, mixed as 5µl of antibody per million cells in a maximum staining volume of 100µl per 5million cells: eFluor405-CD3 (eBioscience™, Thermofisher Scientific), PerCP eFluor710-CD16 (eBioscience™, Thermofisher Scientific) and PE-Cy7-CD56 (eBioscience™, Thermofisher Scientific. Controls of 1 x 10^6 PBMCs were stained as follows: a) with the above cocktail of antibodies excluding one antibody (fluorescence minus one), b) single stained with only one antibody, c) one control remained stained with the fixable viability dye only and d) one control remained unstained. Finally, the cells were washed twice with flow cytometry staining buffer (eBioscience™, Thermofisher Scientific), resuspended in 100µl of flow cytometry staining buffer per 5million cells and kept on ice. Cells were sorted using the BD FACS Aria II and collected in fresh R10 media at 4°C. Gating was as demonstrated in figure 3, gating initially on lymphocytes and singlet cells as identified on forward and side scatter plots, then live cells, then CD3 negative cells, then CD56 positive cells. The following subpopulations were sorted and collected: CD56dimCD16++ NK cells, CD56dimCD16+/- NK cells and CD56brightCD16- NK cells.

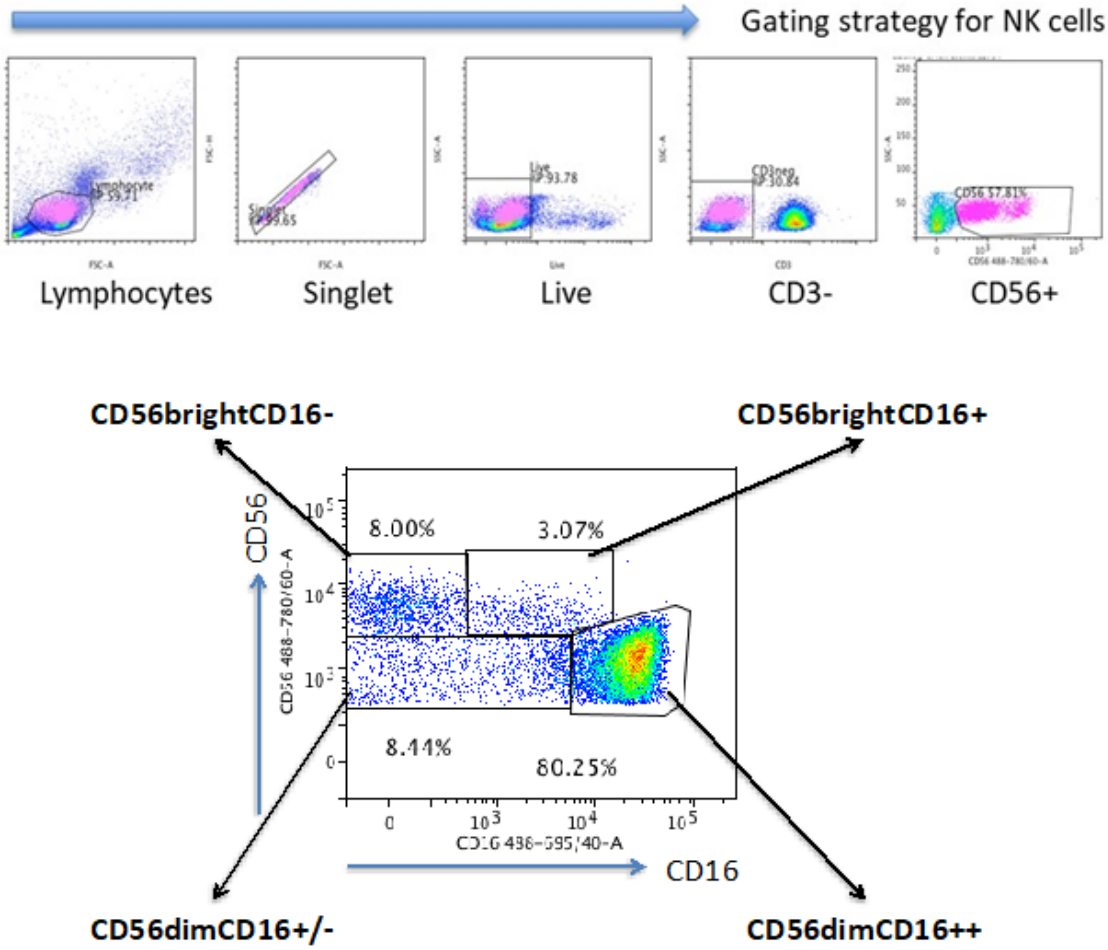


Figure 3 Gating strategy for cell sorting NK cell subpopulations based on CD56 and CD16 expression.

2.5.5.2 Gene expression and Nanostring analysis

Sorted NK cell subpopulations were lysed at a concentration of 20 000 cells per 1µl of buffer RLT (RLT lysis buffer, Qiagen, Germany) and stored at -80°C. Gene expression analysis was performed using NanoString nCounter® GX Human Immunology V2 assay (NanoString Technologies, Inc., Seattle, WA), consisting of a 594 immunology-related gene panel, that was customised with a further 30 genes, and housekeeping control genes (see Appendix A for the customised gene panel). The cell lysates were transported on ice to the NanoString facility at University College London for the NanoString team to process as follows: Cell lysates were incubated with NanoString reporter probes, labelled with a barcode, and capture probes, labelled with biotin, at 65°C for 18 hours overnight. This allowed hybridisation of the NanoString reporter probes and capture probes to the target RNA in the cell lysate. These probe-target

complexes were then immobilised on a cartridge via the biotin on the capture probe, and the fluorescently labelled barcodes on the reporter probes were scanned using the nCounter® Digital Analyser at the UCL NanoString Facility (University College London, UK). Reporter code count (RCC) files were generated for each sample, reporting the number of copies of each of the genes found in each sample. This NanoString data was analysed using nSolver® analysis software v4.0, normalising gene expression with the use of housekeeping genes and subtracting negative controls from the normalised data. Normalised data was compared between NK cell subpopulations, in disease and in health, to reveal differential expression of genes where gene expression levels were greater than 30, with $p<0.05$ and false discovery rate (FDR <0.05) (calculated using the Benjamini-Hochberg approach) and a fold change of greater than 2.

Gene enrichment analysis, to determine which pathways were upregulated or downregulated in disease compared to health and between NK cell subpopulations, was undertaken using two platforms: ReactomeGSA (version 89) and Ingenuity Pathway Analysis software (version 24.0, Qiagen).

2.6 NK cell functional assays

2.6.1 CD107a, Interferon gamma (IFNγ) and Tumour necrosis factor alpha (TNFα) in all NK cells

PBMCs for functional assays were thawed rapidly at 37°C, washed initially in Gibco RPMI 1640 medium, then resuspended in R10 medium at a concentration of $1x10^6$ cells/ml and stimulated for 16hours at 37°C in 5% CO_2 with IL-15 at a concentration of 1ng/ml. The following day the IL-15 containing medium was removed from the PBMCs, and the PBMCs were resuspended at a concentration of $5x10^5$ cells per 100µl in fresh R10 containing anti APC-H7-CD107a antibody (eBioscience™, Thermofisher Scientific) at a concentration of 1µl antibody per million cells. As with the phenotyping assays, all antibody concentrations used in the functional assays were optimised to allow maximal binding but minimise non-specific staining. K562 target cells were suspended in R10 medium at a concentration of $1x10^5$ cells/100µl, and 100µl of this was added to the PBMCs, resulting in a PBMC:Target ratio of 5:1 in a final volume of 200µl in a 96 well U bottom plate. This optimal ratio was pre-determined by titration of PBMC:Target ratios ranging from 1:1 to 20:1. In one control well, K562 targets were not added to the PBMCs, but the volume was made up to 200µl by adding fresh R10 medium. This allowed the assessment of baseline spontaneous degranulation and IFNγ and TNFα production in PBMCs without target cells. The cells were incubated at 37°C in 5% CO_2 for 1 hour, after which cell transport protein inhibitor (eBioscience™ Protein Transport Inhibitor Cocktail (500X), Thermofisher Scientific) was added to the wells to prevent internalisation of the membrane bound CD107a and allowing accumulation of intracellular cytokines. After a further 3 hours incubation at 37°C in 5% CO_2, the cells were washed, resuspended in PBS and stained with fixable viability dye 506 (eBioscience™, Thermofisher Scientific) for 20mins at 4°C, and then washed and incubated with blocking buffer as described above. The PBMCs were then surface stained with monoclonal antibodies in BD brilliant staining buffer (Becton Dickinson) in a final volume of 100µl as follows: PerCP eFluor710-CD3 (eBioscience™, Thermofisher Scientific), V450-CD16 (Becton Dickinson), PE-Cy7 CD56 (eBioscience™, Thermofisher Scientific). The cells were washed twice in flow cytometry staining buffer (eBioscience™, Thermofisher Scientific) and fixed in eBioscience™ IC Fixation

Buffer (Thermofisher Scientific) containing 2% paraformaldehyde for 30mins at 4°C. Cells were then permeabilised with two washes in eBioscience™ Permeabilization Buffer (10X) containing saponin (Thermofisher Scientific), and subsequently blocked again by resuspending the cells in 100µl of permeabilisation buffer with 2% Human AB serum (Sigma-Aldrich) for 20mins at 4°C. Following this, anti PE-IFNγ and anti-Alexa fluor700-TNFα were added directly to each well and incubated for a further 20mins at 4°C. Cells were then washed again in permeabilisation buffer, followed by flow cytometry staining buffer, and then resuspended in a final volume of 150µl of flow cytometry staining buffer (eBioscience™, Thermofisher Scientific) and acquired immediately by flow cytometry.

Huh7 or HepG2 target cells were plated the day before at $2x10^5$ target cells per well in a volume of 500µl of R10 medium in a flat bottom 24 well plate, allowing the target cells 16hours to adhere to the well and provide an 80-90% confluent lining to the well. Following this, the media from each target lined well was removed and replaced with 200µl of PBMCs with anti-CD107a antibody in R10 medium prepared as described above at a concentration of $5x10^5$ cells per 100µl, resulting in a 5:1 PBMC:target ratio. The cells were incubated at 37°C in 5% CO_2 for 1 hour, after which cell transport protein inhibitor (eBioscience™ Protein Transport Inhibitor Cocktail (500X), Thermofisher Scientific) was added to the wells and incubated for a further 3 hours at 37°C in 5% CO_2. Surface staining for NK cell CD107a expression and intracellular staining for TNFα and IFNγ was undertaken as described above and acquired immediately by flow cytometry.

Table 4 Functional flow cytometry antibody panels

Laser	*Functional NK Panel*	*Perforin and Granzyme panel*
405 450/50	CD16 V450 (644490, 3G8, BD)	CD16 V450 (644490, 3G8, BD)
405 525/50	Fixable Viability Dye eF 506 (65-0866-14, ThermoFisher)	Fixable Viability Dye eF 506 (65-0866-14, ThermoFisher)
405 610/20		
405 660/20		
405 710/50		
405 780/60		
488 530/30		
488 575/26	IFNgamma PE (502509, Biolegend)	Perforin PE (353304, Biolegend)
488 610/20		
488 695/40	CD3 (clone SK7) PerCP-eFluor 710 ThermoFisher	CD3 (clone SK7) PerCP-eFluor 710 ThermoFisher
488 780/60	CD56 PE-Cy7 (CMSSB, 25-0567-41, ThermoFisher)	CD56 PE-Cy7 (CMSSB, 25-0567-41, ThermoFisher)
633 670/14		Granzyme B APC (372204, Biolegend)
633 730/45	TNF alpha Alexa Fluor 700 (502928, Biolegend)	
633 780/60	CD107a APC-H7 (561343, BD)	

2.6.2 CD107a in NK cell subpopulations determined by CD56/CD16 expression

Peripheral blood mononuclear cells from patients with cirrhosis (n=3) were sorted into NK cell subpopulations based on CD56 and CD16 expression as demonstrated in Figure 2.1 and as described above. Isolated NK cell subpopulations were incubated for 12 hours with IL-15 (1ng/ml) and then co-cultured for 1 hour in fresh R10 media supplemented with 1µl APC-H7-CD107a antibody (eBioscience™, Thermofisher Scientific) per million cells with K562 target cells in a 1:1 ratio. Cell transport protein inhibitor (eBioscience™ Protein Transport Inhibitor Cocktail (500X), Thermofisher Scientific) was added at this point, and then incubated for a further 3 hours. Cells were then washed and resuspended in 150µl of flow cytometry staining buffer and acquired immediately by flow cytometry to detect CD107a expression.

2.6.3 Ex-vivo Perforin and Granzyme B staining

PBMCs and LMNCs were prepared, stained with fixable viability dye 506 (eBioscience™, Thermofisher Scientific) and incubated in blocking buffer as described above for phenotyping. Surface staining was then performed using the following antibodies in a final volume of 100µl: PerCP eFluor710-CD3 (eBioscience™,

Thermofisher Scientific), V450-CD16 (Becton Dickinson) and PE-Cy7- CD56 (eBioscience™, Thermofisher Scientific). The cells were washed twice in flow cytometry staining buffer (eBioscience™, Thermofisher Scientific) and fixed in eBioscience™ IC Fixation Buffer (Thermofisher Scientific) containing 2% paraformaldehyde for 30mins at 4°C. Cells were permeabilised with two washes in eBioscience™ Permeabilization Buffer (10X) containing saponin (Thermofisher Scientific), and subsequently blocked again by resuspending the cells in 100µl of permeabilisation buffer with 2% Human AB serum (Sigma-Aldrich) for 20mins at 4°C. Following this, anti PE-Perforin and anti APC-Granzyme B were added directly to each well and incubated for a further 20mins at 4°C. Cells were then washed in permeabilisation buffer, followed by flow cytometry staining buffer, and then resuspended in a final volume of 150µl of flow cytometry staining buffer (eBioscience™, Thermofisher Scientific) and acquired immediately by flow cytometry.

2.6.4 Cytokine secretion

PBMCs from patients with cirrhosis (n=3) were sorted into NK cell subpopulations based on CD56 and CD16 expression as demonstrated in Figure 1 and as described above. The isolated NK cell subpopulations were then stimulated with PMA (50ng/ml, MilliporeSigma, St Louis, Missouri, USA) and ionomycin (500ng/ml, MilliporeSigma, St Louis, Missouri, USA) in duplicates for four hours. The supernatants were then collected and cytokine secretion assessed using a V-plex Proinflammatory Panel 1 kit (MSD, Maryland, USA), a multiplex cytokine detection system detecting 10 different cytokines (TNFα, IFNγ, IL-1β, IL-2, IL-4, IL-6, IL-8, IL-10, IL-12p70, IL-13). The assays were performed in duplicate and the plate read using a QuickPlex SQ 120 instrument (MSD), with data downloaded using DISCOVERY WORKBENCH® 4.0 software.

2.7 Immunohistochemistry

2.7.1 LLT1 expression and scoring and analysis by Image J

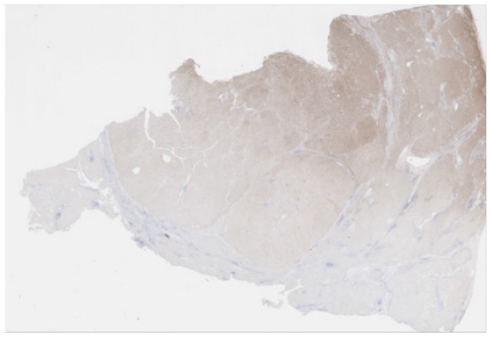
LLT1/CLEC2D mouse monoclonal antibody (M01, clone 4C7 (Abnova, Taiwan)) was tested in different dilutions and optimised on formalin fixed and paraffin embedded (FFPE) liver tissue (3um in thickness), using salivary tissue as a positive control as recommended by the antibody manufacturer (Abnova, Taiwan). A dilution of 1 in 4000 was determined to give best yield with no background staining.

FFPE blocks of normal liver tissue margins from resections for colorectal metastases and cirrhotic liver tissue from liver biopsies were identified. Liver tissue from resections demonstrating HCC and background liver tissue blocks from the same patients were also identified. These FFPE blocks were cut in 3µm sections and mounted on slides. Slides were stained for LLT1 (1:4000) in batches using automated staining to minimise variability using a Leica BOND-III instrument (Leica Biosystems, Wetzlar Germany) and selecting the BOND Epitope Retrieval Solution 1 (Leica Biosystems, Wetzlar Germany), a citrate based pH6 solution for heat induced epitope retrieval. Control slides used with each batch (salivary tissue as a positive control, unstained slides as a negative control). The antibody was developed with BOND DAB enhancer (Leica Biosystems, Wetzlar Germany) and counterstained with haematoxylin. Consecutive slides were stained with Haematoxylin and Eosin (Dako CoverStainer, Agilent, UK).

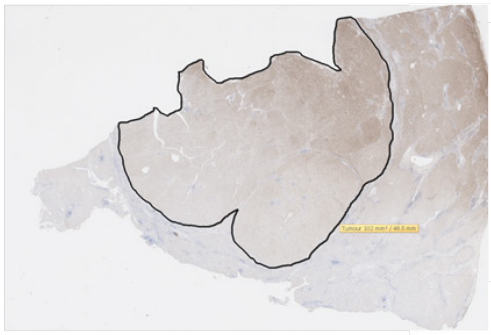
These tissue slides were then scanned in their entirety, and images analysed using NDP.view 2.4.26 and ImageJ v1.48 software. Images were reviewed to characterise the nature and location of LLT1 staining within liver tissue. The total area of tissue (tumour and non-tumour) was outlined and measured using ImageJ software. An automated scoring system was devised to reduce bias and attempt to quantify staining. Strength of staining of LLT1 was determined using the positive and negative control slides, and contrast ranges set correlating to negative, weak, moderate and strongly positive using ImageJ software. The area of the tissue section covered by each contrast range was measured using ImageJ, and then calculated as a percentage of the total area initially measured (Figure 4). A score of 0-3 was assigned to each contrast range, with 0 for areas negative for LLT1, 1 for areas weakly staining for LLT1,

2 for areas staining moderately for LLT1 and 3 for areas strongly positive for LLT1 (Table 5). This was then multiplied by the area, as a percentage of the total area of tissue, corresponding to each contrast range to provide an overall score for LLT1 staining (Table 5).

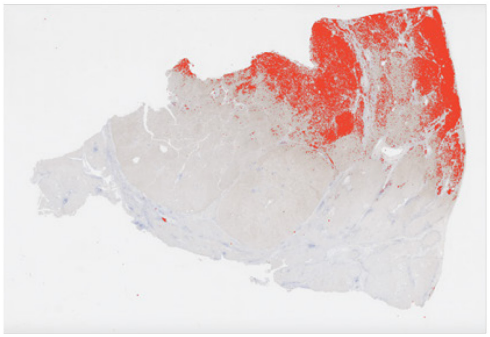
A



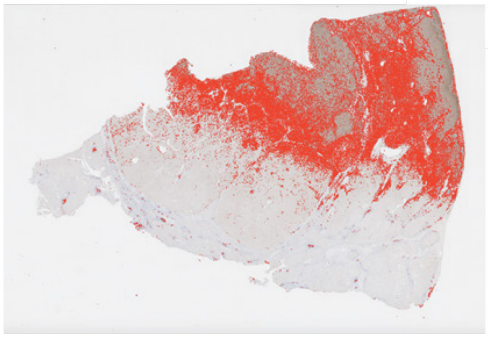
B



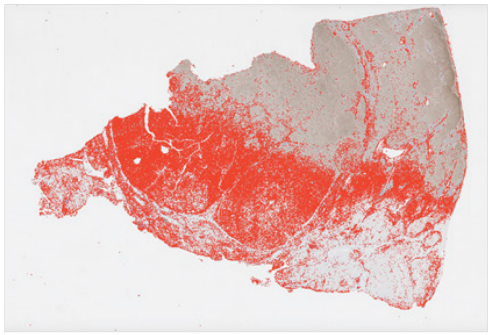
C



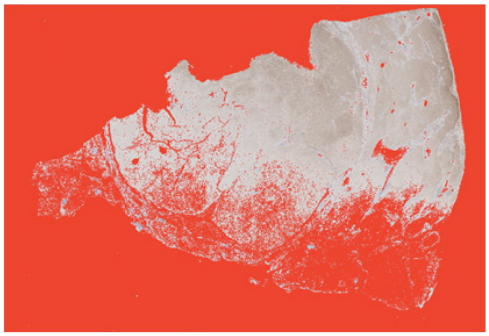
Strong Positive



Moderate Positive



Weak Positive



Negative

D

	Contrast thresholds at 0.45x magnification
Strong positive	0-181
Moderate positive	182-200
Weak positive	201-230
Negative	231-255

Figure 4 LLT1 Immunohistochemistry scoring system for LLT1 expression in the liver. ***Formalin fixed paraffin embedded (FFPE) blocks of liver tissue demonstrating normal liver margins from liver resections for indications other than Hepatocellular carcinoma (HCC) (e.g. liver resections***

for colorectal metastases), cirrhosis, HCC and paired background liver tissue from patients with HCC were identified. Slides were prepared using 3µm sections of tissue from these FFPE blocks, with slides stained for LLT1 (1:4000 dilution, Abnova) and consecutive slides stained with haematoxylin and eosin (H&E). A) Original scanned image of whole slide demonstrating LLT1 expression using immunohistochemistry on a section of tissue from a liver resection for HCC on a background of cirrhosis. The image demonstrates an area of tumour tissue and background non-tumour margins. Image displayed at 0.45x magnification. B) The total area of tissue on the slide was outlined and measured using ImageJ software for healthy liver tissue, cirrhotic liver tissue (for patients without HCC), background non-tumour liver tissue for patients with HCC and tumour tissue for patients with HCC. This image (picture B) demonstrates the total area of HCC tumour tissue outlined in black. The total area was measured using ImageJ software with the image at 0.45x magnification. C) and D) demonstrate contrast thresholds for each strength of staining (strong, moderate, weak, negative), set using negative and positive controls for each batch of slides stained. C) The red areas demonstrate the area on the slide with the allocated staining intensity for LLT1 (strong, moderate, weak, negative intensity of staining for LLT1) set by contrast ranges in table D). As the ImageJ software was used to analyse the entire image, the background white area of the slide without tissue also appeared red when the negative staining threshold was set. The total area of tissue highlighted as red was measured as the area corresponding to that contrast level i.e. in this example, the total area highlighted as red within the tumour area initially outlined (picture B) was measured by ImageJ for each contrast level. The measured area of liver tissue for each contrast range on each slide was calculated as a percentage of the total area of liver tissue on that slide for healthy livers and for cirrhotic livers without HCC. As a result, for each slide, the area of tissue staining negative, weak positive, moderate positive and strong positive was calculated as a percentage of the total tissue area on that slide. For slides with tumour tissue, as demonstrated in this figure, the area of tumour tissue at each contrast range (corresponding to strong, moderate, weak, negative intensity of staining for LLT1) as defined by table D) were then calculated as a percentage of the total tumour tissue area measured on that slide using ImageJ software.

Table 5 Weighted scoring system, resulting in higher scores for tissue sections demonstrating stronger staining of LLT1 by immunohistochemistry. The area of liver tissue at each staining intensity for LLT1 was calculated as a percentage of the total area of liver tissue on that slide as described in Figure 4. The percentage of liver tissue demonstrating each intensity level of staining for LLT1 was then multiplied by the corresponding weighted score for that intensity of staining as per the table below. A total score was calculated by adding all of the scores at each staining intensity. The higher the score, the higher the overall intensity of LLT1 staining in the liver tissue for that patient sample.

Weighted Score	*Intensity of staining*	*Area corresponding to the intensity of staining (as a % of the total area of tissue on the slide)*	*Weighted score multiplied by area corresponding to intensity of staining (as a % of the total area of tissue on the slide)*
0	*Negative*	*Area a*	*0 x Area a*
1	*Weak*	*Area b*	*1 x Area b*
2	*Moderate*	*Area c*	*2 x Area c*
3	*Strong*	*Area d*	*3 x Area d*
		Total area = a + b + c + d = 100%	*Total Score (minimum score 0, maximum score 300) = (0 x a) + (1 x b) + (2 x c) + (3 x d)*

2.7.2 Double staining protocol to ascertain LLT1 co-localisation

Table 6 Antibodies used for double staining liver tissue

ANTIBODY	SUPPLIER AND CATALOGUE NUMBER	DILUTION
LLT1	Abnova, H00029121-M01	1/4000
CD68 CLONE KP1	Dako, M0814	1/2000
CD3 CLONE LN10	Novocastra, NCL-L-CD3-565	1/100
CD20 CLONE L26	Dako, M0755	1/100
VIMENTIN CLONE V9	Novocastra, NCL-L-VIM-V9	1/100

Double staining of normal liver tissue slides was undertaken by the Pathology Translational Technology Platform service at UCL. In brief, 3µm paraffin sections of normal liver tissue margins from liver resections for colorectal metastases (n=3) underwent automated dewaxing (Leica Bond Dewax AR9222, Leica Biosystems, Wetzlar Germany). Automated antigen retrieval was then performed on the sections; Leica Bond Epitope retrieval solution 2 (pH9, AR9640, Leica Biosystems, Wetzlar Germany) was applied to the slides and they were heated to 100 degrees Celsius for 30 minutes.

LLT1 antibody (Abnova, H00029121-M01) was applied to the slides at a dilution of 1/4000 and incubated at room temperature for 30 minutes. The antibody was developed with Bond Red Refine Detection Kit (catalogue number DS9390, Leica Biosystems, Wetzlar Germany). The secondary antibody (CD3, 1/100; CD20, 1/100; CD68, 1/2000; or Vimentin, 1/100) was then applied and incubated for 30 minutes. Bond Post Primary AP and Bond Polymer AP were applied. The slides were then removed from the Bond-RX automated immunostainers (Leica Biosystems) and completed by hand: Vector Blue AP stain (Vector Labs SK-5300) was applied and developed manually, visually confirming using a microscope. Once the stain was sufficiently developed, the reaction was stopped by rinsing the slides in distilled water. Slides were then allowed to air dry and were mounted in Vector Mount Permanent Mounting Media (Vector Labs H-5000). Control slides were single stained for each primary antibody.

Images were captured and analysed using Nuance Multispectral Imaging System 3.0.2 (PerkinElmer, UK).

2.8 Quantitative real-time PCR for LLT1 expression

Liver tissue samples from resection specimens or explants undertaken for HCC and cirrhosis, and normal margins from liver resections undertaken for indications other than primary liver cancer, were snap frozen and stored in liquid nitrogen at –190°C.

Tissue samples were thawed and RNA extracted following mechanical homogenisation using a TissueRuptor II as per the Qiagen RNeasy plus Mini kit following the manufacturer's instructions (Qiagen, Germany), eluting the RNA in 50µl volume of RNAse free water (Qiagen). RNA was then transcribed into complementary DNA (cDNA) using the Qiagen Omniscript kit following the manufacturer's protocol (Qiagen, Germany), using Oligo dT primers.

Real time reverse transcription (RT)-PCR for LLT1 expression (CLEC2D gene) was performed using a TaqMan gene expression assay, multiplexing FAM dye-labelled LLT1 probe (ThermoFisher, Hs00203174_m1) with VIC dye-labelled GAPDH (glyceraldehyde-3-phosphate dehydrogenase, ThermoFisher, Hs02786624_g1) probe (GAPDH used as an endogenous control). Each sample was run in duplicate with the difference in threshold cycles for LLT1 and GAPDH calculated for each sample (ΔC_T) and the difference in ΔC_T between normal liver, cirrhotic liver and HCC tumour tissue samples ($\Delta\Delta C_T$). Reactions were run for 40 cycles, C_T values averaged across replicates. The fold change in LLT1 expression was expressed as $2^{\Delta\Delta CT}$. Statistical comparisons were made using Mann-Whitney tests, with Wilcoxon matched-pairs signed rank test used for samples from the same donor i.e. HCC tumour tissue and paired background liver tissue.

2.9 Elisa for serum analysis for LLT1

Serum samples from patients with cirrhosis were screened for soluble LLT1 expression using an ELISA based assay as follows. Serum samples from 10 healthy donors, 17

patients with cirrhosis not currently acutely decompensated and 13 patients with treatment naïve HCC were collected and stored in 100 aliquots at -80 following centrifugation of fresh blood in serum separating tubes. A C type lectin domain family 2 member D (CLEC2D) ELISA kit (Mybiosource, San Diego, US, MBS7213167) was purchased. Serum samples were diluted 1:2 with the assay buffer and plated in duplicate on the assay plate that is pre-coated with a CLEC2D-HRP conjugate, with control standards diluted as per the manufacturer's protocol. Following incubation, the assay plate was decanted and washed 5 times, a subtracted for HRP added and then a stop solution added. The intensity of colour was measured using a plate spectrophotometer, with a standard curve generated from the standard controls and with CLEC2D concentrations calculated from this standard curve. Statistical analysis was performed using the non-parametric Mann-Whitney test between groups.

2.10 LLT1 surface expression on liver cell lines

Huh7 cells and HepG2 cells were surface stained as follows to determine surface LLT1 expression. HepG2 cells and Huh7 cells were detached from the T25 culture flasks by removal of the R10 culture medium and incubation at 37°C in 5% CO_2 for 2 minutes with 2mls of PBS supplemented with 5mM EDTA (ethylenediaminetetraacetic acid) and 0.1% BSA (Bovine serum albumin, Sigma-Aldrich). Trypsin-EDTA was not used to detach cells as this was found to cleave cells surface proteins. Huh7 cells and HepG2 cells were washed twice in PBS. $1x10^5$ HepG2 cells and $1x10^5$ Huh7 cells were resuspended in 1ml of PBS and 1µl of fixable viability dye 506 (ThermoFisher Scientific, 65-0866-18) for 20minutes at 4°C. The cells were washed with flow cytometry staining buffer containing foetal bovine serum and 0.09% sodium azide (eBioscience™ Flow Cytometry Staining Buffer, Thermofisher Scientific), before being incubated with a blocking buffer (10% human AB serum (Sigma-Aldrich) in flow cytometry staining buffer (Thermofisher Scientific)) for 20mins at 4°C. Cells were resuspended with 5µl of an unconjugated primary antibody against LLT1 (M01, mouse anti human LLT1 monoclonal clone 4C7 (H00029121-M01, Abnova, Taiwan) or goat anti-human OCIL/CLEC2D polyclonal antibody (AF3480, R&D systems, Minnesota, US)) in 100µl of

flow cytometry staining buffer for 20mins at 4°C. Cells were washed twice with flow cytometry staining buffer and resuspended in 5µl of a corresponding fluorescent secondary antibody (goat anti-mouse alexa fluor 633 (ThermoFisher Scientific, A-21146) or rabbit anti-goat alexa fluor 633 (ThermoFisher Scientific A-21086)) diluted in 100µl of flow cytometry staining buffer for 20mins at 4°C. Cells were washed twice in flow cytometry staining buffer and resuspended in 200µl of flow cytometry staining buffer an acquired immediately by flow cytometry.

2.11 Stimulation of liver cell lines to upregulate LLT1 surface expression

$2x10^5$ Huh7 cells were plated per well in a 24 well plate with 2mls of R10 complete media and incubated at 37°C in 5% CO_2 for 16hours. The media was then supplemented with cytokines or toll-like receptor (TLR) agonists as detailed in the table below. Each stimulation was performed in duplicate, for 48 hours, with two wells remaining unstimulated in R10 media alone. Following the 48 hour stimulation, the media was aspirated off the Huh7 cells from each well, washed by layering on 1ml of PBS into each well and aspirating the PBS, and detached by and then incubating each well in 500µl of PBS supplemented with 5mM EDTA for 2 minutes at 37°C in 5% CO_2. Cells were then washed with PBS, stained with a fixable viability dye and proceeded to determine surface expression of LLT1 as described above.

Table 7 Cytokine and TLR ligands used to stimulate Huh7 cells for 48hours (concentrations in R10 medium).

Cytokines	TLR ligands
IL 1β 10ng/ml	Pam 1µg/ml (TLR1/2 agonist)
IL4 100ng/ml	HKLM 10^8/ml (TLR2 agonist)
IL5 50ng/ml	Poly I:C 5µg/ml (TLR3)
IL6 1ng/ml	Poly I:C LMW 5µg/ml (TLR3 agonist)
IL10 100ng/ml	LPS 1µg/ml (TLR4 agonist)
IL12 20ng/ml	FLAST 100ng/ml (TLR5 agonist)
IL17 50ng/ml	FSL-1 100ng/ml (TLR6/2 agonist)
IL22 100ng/ml	Imiquimod 1µg/ml (TLR7 agonist)
TNFα 10ng/ml	ssRNA 2.5µg/ml (TLR8 agonist)
TGF beta 10ng/ml	ODN 2006 5µM (TLR9 agonist)
IFNγ 50units/ml	

2.12 LLT1 cloning and transfection

Human LLT-1 were cloned by RT-PCR from cDNA created following reverse transcription of RNA extracted from healthy donor PBMCs as follows. RNA was extracted following the manufacturer's protocol using a Qiagen RNeasy Mini Kit (Qiagen, Germany). LLT-1 was amplified from this cDNA with PCR using primers 5'-CGTGTACAAGGGAGGCGGTTCAATGCATGACAGTAACAATGTGG-3' and CAAATCAGATATACATGTCTAGAGCGGCCGCTCGAGCG-3' (ThermoFisher Scientific) and the resulting LLT1 DNA product was ran using electrophoresis on an 1% agarose gel (1g agarose, 10ml x5 Tris-borate-ethylenediaminetetraacetic acid buffer) and subsequently purified following gel extraction with the QIAquick Gel Extraction kit using the manufacturer's protocol (Qiagen). LLT1 was N-terminally tagged with fluorescent proteins by cloning the LLT1 DNA and the pcDNA3.1 vector (ThermoFisher Scientific, V79520) containing enhanced yellow fluorescent protein (EYFP). This was achieved by digesting the LLT1 DNA product following gel extraction and the pcDNA3.1 vector with BsrG1 (ThermoFisher Scientific, ER0931) and Xho1 (ThermoFisher Scientific, ER0691) at 37°C for 1 hour. The digested products were run on an agarose gel, purified by gel extraction and ligated for 1 hour at room temperature. The resulting plasmid DNA was used to transform preprepared chemically competent *Escherichia coli* dh5α cells by incubating them together at 4°C for 30mins, then 42°C for 2 minutes followed by rapid cooling on ice for 2 minutes. 100µl of Luria broth (Gibco, Thermofisher) was added and the transformed cells were plated on to selective agar plates and cultures at 37°C overnight. Miniprep cultures, from single colonies grown on these plates, were cultured in 10ml of Luria broth supplemented with antibiotics (0.1mg/ml ampicillin) overnight at 37°C. Plasmid DNA was extracted from miniprep cultures using a QIAprep Spin Miniprep Kit (Qiagen) following the manufacturer's instructions and eluted in 50µl of RNAse free water. The plasmid DNA was sequenced to ensure the correct transcript for LLT1 had been cloned.

The pcDNA3.1 vector with the YFP tagged LLT1 insert was then digested with BamH1

(ThermoFisher, ER0051) and Xho1 to cleave the LLT1-YFP tagged insert. The LLT1-YFP insert was then ligated as described above with a predigested pIB2 plasmid vector (Gift from M. Purbhoo) (predigested with BamH1 and Xho1). The pIB2 vector with the LLT1-YFP insert was used to transform competent cells as described above, plated on selective agar plates and cultured at 37°C. Miniprep cultures from single colonies were cultured the next day in 10ml of Luria broth supplemented with 0.1mg/ml of ampicillin as described above and the subsequent plasmid DNA extracted using the QIAprep Spin Miniprep Kit (Qiagen).

Phoenix amphotrophic cells, a retroviral packaging cell line encoding gag-pol and env DNA, were cultured in R10 media until they reached 80% confluence in a 6 well plate. 10µg of the pIB2 vector with the LLT1-YFP insert was mixed with 10µl of Plus Reagent (ThermoFisher, 11514015) and 8µl lipofectamine (ThermoFisher Scientific, 18324012) in 200µl of OPTI-MEM (Gibco, ThermoFisher, 31985062) for 15 minutes at room temperature under a sterile tissue culture hood. The R10 media was carefully aspirated from the plate containing the adhered Phoenix cells, and the vector/lipofectamine/OPTI-MEM mixture was gently placed over the Phoenix cells, with an additional 800µl of OPTI-MEM to bring the volume up to 1ml. The Phoenix cells were incubated at 37°C in 5% CO_2 for 4 hours before adding 5mls of R10 media and incubated overnight. The next day, the medium was aspirated and replaced with 2mls of serum free OPTI-MEM and incubated at 37°C in 5% CO_2 for a further 24 hours. Following this, the supernatant was aspirated, collecting all the retroviruses containing the pIB2-LLT1-YFP DNA manufactured by the Pheonix cells, and filtered through a 45µm filter. Lipofectamine (8µl) and Plus Reagent (10µl) was added to the retrovirus containing aspirate and incubated at room temperature under a sterile hood for 15minutes. The retrovirus/lipofectamine mixture was then placed directly on to Huh7 cells plated in a 6 well plate at 80% confluence. The plate was spun at a low speed (500G for 60 minutes). The plate was then incubated at at 37°C in 5% CO_2 for overnight (10hours). The next morning, the retrovirus/lipofectamine mixture was aspirated and removed, the Huh7 cells washed in complete R10 media and left to incubate overnight again at 37°C in 5% CO_2 before being transferred to a larger T25 flask. Huh7 cells were subsequently examined under a confocal microscope to ensure

they had been transfected and were expressing LLT1-YFP. Huh7-LLT1 YFP transfectants were selected for by adding 5 µg/ml Blasticidin (ThermoFisher Scientific) to the R10 media for 48hours.

2.13 Co-culture of PBMCs with Huh7-LLT1 YFP transfectants

In order to assess whether LLT1 expression had an effect on NK cell cytotoxicity, PBMCs were co-cultured with Huh7 cells that express LLT1 constitutionally at a low level and Huh7-LLT1 YFP transfectants that express LLT1 at a higher level as follows. In brief, Huh7 cells and Huh7-LLT1 YFP cells were plated the day before at $2x10^5$ cells per well in a volume of 500µl of R10 medium in a flat bottom 24 well plate, allowing the target cells 16hours to incubate at 37°C in 5% CO_2 to adhere to the well and provide an 80-90% confluent lining to the well. PBMCs from three different healthy donors were thawed rapidly at 37°C, washed initially in Gibco RPMI 1640 medium, then resuspended in R10 medium at a concentration of $1x10^6$ cells/ml and stimulated for 16hours at 37°C in 5% CO_2 with IL-15 at a concentration of 1ng/ml. The following day the IL-15 containing medium was removed from the PBMCs, and the PBMCs were resuspended at a concentration of $5x10^5$ cells/100µl in fresh R10 media. Following this, the media from each target lined well was removed and replaced with 200µl of PBMCs with anti-CD107a antibody in R10 medium prepared as described above at a concentration of $5x10^5$ cells per 100µl, resulting in a 5:1 PBMC:target ratio (see section – CD107a assay). The cells were incubated at 37°C in 5% CO_2 for 1 hour, after which cell transport protein inhibitor (eBioscience™ Protein Transport Inhibitor Cocktail (500X), Thermofisher Scientific) was added to the wells and incubated for a further 3 hours at 37°C in 5% CO_2. PBMC to target wells were set up in triplicate. Surface staining for NK cell CD107a expression was undertaken as described above and acquired immediately by flow cytometry. Jurkat cells were used as a control target due to the lack of expression of LLT1 as determined by flow cytometry using an unconjugated monoclonal primary antibody against LLT1 (M01, clone 4C7 (Abnova, Taiwan)) with an anti-mouse fluorescent secondary antibody as described above.

The difference between CD107a expression was calculated between CD161-NK cells and CD161+NK cells against each cell type. Statistical comparisons were made between groups using Mann-Whitney tests.

2.14 Clinical data

Patient information was recorded from clinical notes and database records. Data collected for cirrhotic patients included: age, sex, Child Pugh status, MELD-Na score at time of recruitment and underlying aetiology of liver disease. Laboratory data collected included serum alanine transaminase (ALT), aspartate transaminase (AST), total), albumin, internationalised normalised ratio (INR), platelet count, neutrophil and white cell count, sodium and creatinine. For patients with HCC, the Barcelona Clinic Liver cancer staging (BCLC) was also recorded. Phenotypic and functional data was correlated to these clinical parameters using Spearman rank correlation.

2.15 Statistical analysis

Data acquired by flow cytometry was analysed using Flowlogic v7 software (Inivai, Miltenyi biotech). Statistical data analysis was performed using GraphPad Prism version 7.0c software (GraphPad Software Inc, U.S.A). Descriptive statistics are shown as median± interquartile range. Comparisons between groups were made using the non-parametric Mann-Whitney test or Kruskal-Wallis test with Dunn's multiple comparisons tests as appropriate. Paired analyses used the non-parametric Wilcoxon signed rank test. All tests were two-tailed and a probability value (p-value) of less than 0.05 was considered significant. All error bars on graphs demonstrate the interquartile range. For differential gene expression and pathway enrichment analysis, p values and the false discovery rate (FDR) were calculated using the Benjamini-Hochberg approach using nSolver® analysis software v4.0 and ReactomeGSA (version 89).

3. Results: Phenotypic and Functional analysis of NK cells in patients with cirrhosis and HCC

3.1 Introduction

NK cell function and activation depends on a complex interplay between activating and inhibitory signals from NK cell surface receptors (Paul & Lal, 2017; Sivori et al., 2019). NK cells are potently inhibited by MHC class I molecules expressed on the cell surface (Ewen et al., 2018). Loss of MHC class I is common immune escape mechanism in cancer, allowing malignant cells to evade detection of abnormal by CD8+T cells (Dhatchinamoorthy et al., 2021). However, upon encountering NK cells, this loss of MHC class I expression on transformed cells results in the release of NK cells from inhibition (Marcus et al., 2014; Raulet & Vance, 2006). Furthermore, transformed, damaged and infected cells up-regulate stress-induced surface molecules, which may in turn engage with activating NK cell receptors (Sivori et al., 2019). The combination of loss of inhibitory signalling, coupled with NK cell activating receptor engagement with surface antigens on transformed cells results in NK cell activation.

However, NK cell activity may be attenuated despite the lack of MHC class I expression on target transformed cells and this has been described in many different cancers, including solid tumours of the lung and liver, as well as leukaemia (Baessler et al., 2010; Cai et al., 2008; Le Maux Chansac et al., 2005; Platonova et al., 2011; C. Sun et al., 2015; Y. Wu et al., 2013). The induced expression of ligands for inhibitory receptors on malignant cells, often coupled with the down-regulation of activating receptors on NK cells have been associated with NK cell dysfunction in these tumours.

Changes in the NK cell surface receptor repertoire have also been described in chronic hepatropic viral infections, such as hepatitis B and hepatitis C infection, and associated with NK cell dysfunction(Fisicaro et al., 2019; B Oliviero et al., 2009; Strunz et al., 2018). Whilst NK cell surface receptor changes have been well characterised in viral hepatitis, due to the important anti-viral role of NK cells, NK cell receptor alterations

in cirrhosis and hepatocellular carcinoma (HCC) of a non-viral aetiology have been less well documented.

The aim of this chapter is therefore to:

1. Delineate and characterise any phenotypical changes seen in NK cells in cirrhosis with and without HCC of a non-viral aetiology
2. Delineate and characterise any functional deficits seen in NK cells in cirrhosis with and without HCC of a non-viral aetiology.
3. Define any key differences between circulating peripheral NK cells and intrahepatic NK cells in disease in cirrhosis.

3.1 Characterising NK cell phenotype and function

To investigate if individuals with cirrhosis with or without HCC have reduced immunosurveillance potential I performed a phenotypic analysis of NK cells.

Peripheral blood mononuclear cells (PBMCs) and intrahepatic mononuclear cells (IMNCs) were extracted and purified by density centrifugation, and surface receptor expression evaluated using flow cytometry, as outlined in the methods. Peripheral blood samples were analysed from the following patient groups: outpatients with cirrhosis (cirrhosis group, n=35); patients with HCC on a background of cirrhosis (HCC group, n=29); and healthy volunteers (n=32, Table 8). Patients with autoimmune liver disease and viral hepatitis were excluded and only patients with an underlying aetiology of alcohol related liver disease (ALD) or metabolic dysfunction-associated steatotic liver disease (MASLD) were included. Patients with HCC were treatment naïve and had a background of cirrhosis secondary to ALD or MASLD. Peripheral blood samples from patients with MASLD but without cirrhosis, as determined by liver biopsy (ISHAK score <4 or Metavir <F3) and/or a liver stiffness score of less than 7kPa, were also analysed (n=7).

Preliminary data was used to inform a power calculation to determine the smallest sample size needed to see functional differences between peripheral blood NK cells

from patients compared to healthy volunteers. Preliminary data demonstrated that the mean proportion of circulating healthy NK cells expressing CD107a, a marker of NK cell degranulation, against K562 target cells, was 67% (standard deviation 10%, based on healthy volunteer samples from 10 donors). Based on this, a priori power calculation was performed to calculate the minimum sample size required to demonstrate a 15% reduction in functional response (CD107a expression) in patients compared to healthy controls. Using G*Power version 3.1.9.7 (Faul et al., 2007), the minimum sample size in each group to detect this difference was calculated to be 7 patients (effect size 1.5, Wilcoxon-Mann-Whitney comparison test, 0.05 probability of a type-I error, 80% power, one-tailed test). Thus the obtained sample size of 22 healthy patients, 22 patients with cirrhosis (14 with ALD, 8 with MASLD) and 16 HCC patients (8 with ALD, 8 with MASLD) was adequate for detecting a reduction in functional response.

IMNCs were extracted from liver resection tissue or liver explants with HCC (from both the tumour tissue and the surrounding liver background margins), with or without underlying cirrhosis (6 patients with HCC on a background of cirrhosis, 4 patients with HCC but without cirrhosis), or from explants with cirrhosis only (4 patients). All patients had liver disease of a non-viral aetiology and again patients with autoimmune liver disease and viral hepatitis were excluded. Patients with an underlying aetiology of ALD or MASLD were included. The presence of cirrhosis in the background liver tissue was determined by a histopathologist. All patients with HCC were treatment naïve. IMNCs extracted from histologically normal liver margins from resections undertaken for colorectal metastases were used as representative for healthy IMNCs (7 patients) (see Table 9). Again, liver tissue used was determined to be disease free by a histopathologist prior to extraction of IMNCs.

Table 8 Population characteristics of peripheral blood samples used for phenotyping experiments. All patients had liver disease of a non-viral aetiology. (HCC= patient group with treatment naïve, non-viral cirrhosis with hepatocellular carcinoma; ALD= alcohol related liver disease; MASLD= metabolic dysfunction-associated steatotic liver disease; MASLD (non-cirrhotic) = patients with liver stiffness score of <7kPa and/or biopsy proven fibrosis score of F2 or less; BCLC staging= Barcelona clinic Liver Cancer staging; p values calculated using non-parametric Mann Whitney analyses).

	Healthy	**Cirrhosis**	**HCC**	**MASLD** (non-cirrhotic)	**Healthy vs. Cirrhosis (p value)**	**Healthy vs. HCC (p value)**	**Cirrhosis vs. HCC (p value)**
Total number	32	35	29	7			
Age, years mean, (range)	41 (23-62)	57 (26-79)	72 (57-84)	54 (43-69)	**p<0.0001** ****	**p<0.0001** ****	**p<0.0001** ****
Male n, (%)	21, (70.0%)	23, (65.7%)	24 (82.8%)	5 (71.4%)			
Child-Pugh (CP) Score: CPA n, (%)		13 (37.1%)	24 (82.8%)				
CPB n, (%)		14 (40.0%)	1 (3.4%)				
CPC n, (%)		8 (22.9%)	4 (13.8%)				
MELD-Na score mean, (range)		12 (6-23)	10 (6-18)				p=0.42
Aetiology:							
ALD n, (%)		26 (74.3%)	11 (37.9%)				
MASLD n, (%)		8 (22.9%)	15 (51.7%)				
Other(haemochromatosis+ALD) n, (%)		1 (2.90%)	3 (10.3%)				
BCLC staging:							
BCLC 0 n, (%)			4 (13.8%)				
BCLC A n, (%)			4 (13.8%)				
BCLC B n, (%)			8 (27.6%)				
BCLC C n, (%)			8 (27.6%)				
BCLC D n. (%)			5 (17.2%)				

	Healthy	Cirrhosis	HCC	MASLD (non-cirrhotic)	Healthy vs. Cirrhosis (p value)	Healthy vs. HCC (p value)	Cirrhosis vs. HCC (p value)
Bilirubin (total) (µmol/L)							p=0.09
mean, (range)		27.4 (5-97)	20.8 (3-82)	7.43 (2-13)			
Platelets (10^9/L)							p=0.97
mean, (range)		156 (35-313)	178 (33-735)	216 (140-257)			
INR							p=0.07
mean, (range)		1.29 (1.0-2.2)	1.19 (0.93-1.7)	1.03 (0.93-1.1)			
Albumin (g/L)							p=0.06
mean, (range)		32.4 (18-42)	35.5 (21-46)	40.7 (34-43)			
ALT (IU/L)							p=0.25
mean, (range)		35.1 (6-114)	40 (10-202)	46.9 (15-93)			
Creatinine (µmol/L)							p=0.31
mean, (range)		84.2 (43-160)	91 (44-171)	69.1 (64-99)			
AFP (µg/L)							
mean, (range)			12498 (2-264917)				
Lymphocyte count (10^9/L)							p=0.69
mean, (range)		1.5 (0.2-3.5)	1.2 (0.2-2.1)	2.34 (1-3.9)			

Table 9 Population characteristics for liver samples from which intrahepatic mononuclear cells were extracted for phenotyping. All patients with cirrhosis and/or HCC had underlying liver disease of a non-viral aetiology. The presence of cirrhosis was determined by histological evaluation by the histopathologist. All patients with HCC were treatment naïve. Healthy liver tissue was taken from background liver from resections for colorectal metastases and determined to be healthy by histological examination by a histopathologist.

	Healthy	HCC without cirrhosis	Cirrhosis	HCC with cirrhosis
Total number	7	4	4	6
Age (mean, (range))	60 (50-68)	60 (53-68)	50 (44-56)	61 (53-67)
Male (n, (% of total))	2 (28.6%)	2 (50.0%)	3 (75.0%)	5 (83.3%)
AFP (mean,(range)		91 (2-212)		11 (2-28)
Aetiology:				
ALD (n)		0	2	4
MASLD (n)		1	1	1
Mixed ALD+MASLD (n)		1	1	1
Other (Haemochromatosis+ALD) (n)		2	0	0

Following extraction of PBMCs and IMNCs via density centrifugation as described in the methods, NK cells were identified using flow cytometry methods following surface staining with fluorescently conjugated antibodies (Phenotyping panel 1, Table 3). In brief, mononuclear cells were labelled with a viability dye followed by a cocktail of fluorescently conjugated anti-CD3 and anti-CD56 antibodies. NK cells were sequentially identified using flow cytometry gating strategy shown in Figure 5.

The proportion of NK cells and the expression of individual NK cell receptor was compared between patient groups, with statistical analyses between these groups using non-parametric Mann-Whitney tests, or Kruskal-Wallis test with Dunn's multiple comparisons if comparing multiple groups. Receptor co-expression and expression against clinical composite scores was correlated using a Spearman rank correlation. Paired comparisons between circulating and intrahepatic NK cells in the same individuals were made using the non-parametric Wilcoxon matched-pairs signed rank test. P values are denoted on the figures and tables below as follows: * $p<0.05$, **

p<0.01, *** p<0.001, **** p<0.0001. Error bars on the figures demonstrate the interquartile range, with bars representing the median value for the dataset.

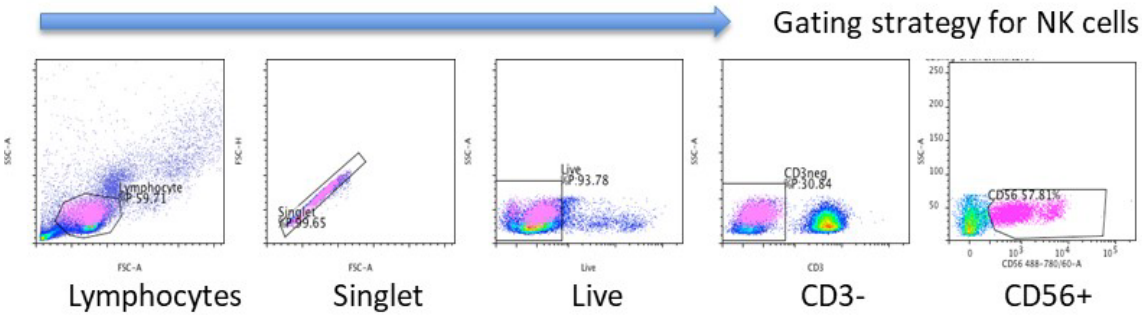
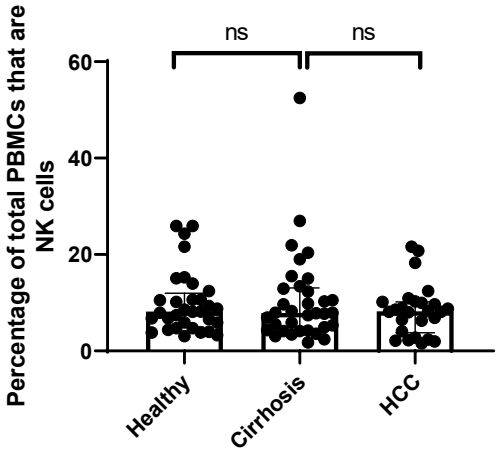


Figure 5 Gating strategy for NK cells from peripheral blood mononuclear cells (PBMCs) and intrahepatic mononuclear cells (IMNCs). Following staining of PBMCs and IMNCs with an amine binding viability dye, PBMCs and IMNCs were surface stained with fluorescently labelled anti-CD3 and anti-CD56 anti-human antibodies (Phenotyping Panel 1, Table 3). CD3-CD56+ NK cells were identified as follows using flow cytometry: lymphocytes were identified using a forward and side scatter density plot; singlet cells were then gated on; live cells were identified; CD3 negative cells were then selected and subsequently CD56 positive cells (NK cells) were then selected.

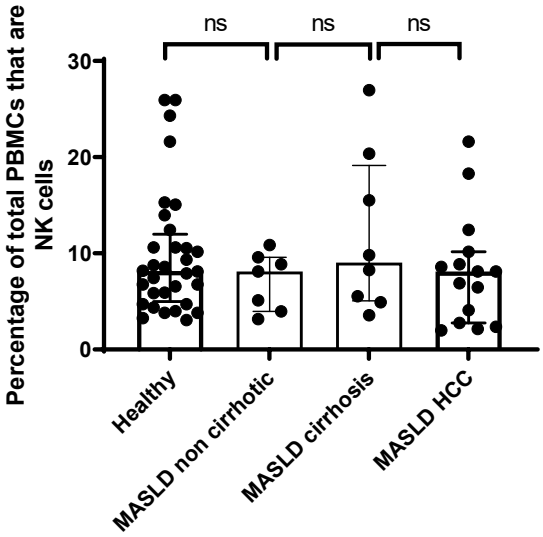
There was no significant difference in the circulating proportion of lymphocytes that were NK cells in health or disease. Separating patients with ALD and MASLD cirrhosis and ALD and MASLD HCC on a background of cirrhosis again did not reveal a significant difference in circulating proportion of NK cells (Figure 6). Further comparisons between CD56dim NK cells and CD56bright NK cells did not show a significant difference between healthy and patient groups in the circulation or in the liver *(data not shown).*

Proportion of circulating peripheral blood mononuclear cells that are NK cells

A Percentage of PBMCs that are NK cells



B Percentage of PBMCs that are NK cells in MASLD



C Percentage of PBMCs that are NK cells in ALD

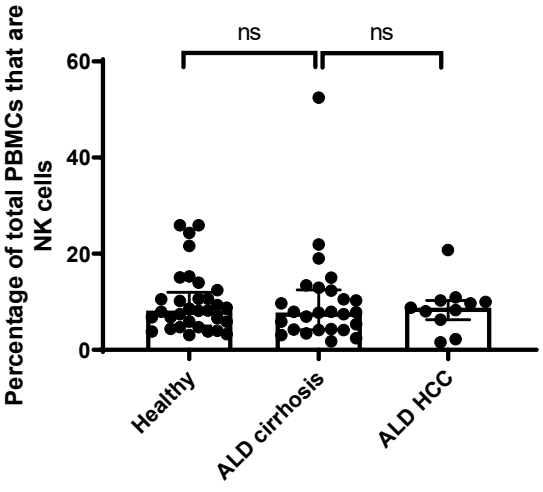


Figure 6 The proportion of circulating peripheral blood mononuclear cells (PBMCs) that are NK cells. The percentage of circulating PBMCs that were CD3-CD56+ NK cells was determined following surface staining for CD3 and CD56 with fluorescently conjugated antibodies and subsequent flow cytometry (Phenotyping panel 1, Table 3). A) There were no significant differences in the proportion of circulating NK cells in patients with cirrhosis or hepatocellular carcinoma (HCC) in comparison to healthy individuals. B) There were no significant differences in the circulating proportions of NK cells in healthy individuals in comparison with patients with metabolic dysfunction-associated steatotic liver disease (MASLD) with or without cirrhosis (MASLD (non-cirrhotic) and MASLD cirrhosis respectively) and patients with HCC on a background of MASLD cirrhosis (MASLD HCC). C) There were no significant differences in the circulating proportions of NK cells in healthy individuals in comparison with patients with alcohol related liver disease (ALD) with cirrhosis (ALD cirrhosis) and patients with HCC on a background of ALD related cirrhosis (ALD HCC). Comparisons were made using the non-parametric Mann Whitney test. Error bars represent the interquartile range.

Comparisons of the proportion of intrahepatic mononuclear cells that were NK cells did not reveal a difference between the different patient populations (Figure 7). However, there was an increased proportion of intrahepatic mononuclear cells that were NK cells (median range 28%-55% across patient groups) in comparison to circulating mononuclear cells that were NK cells (median range 7.8%-8.2% across healthy individuals and patient groups) in keeping with published data (Figure 8).

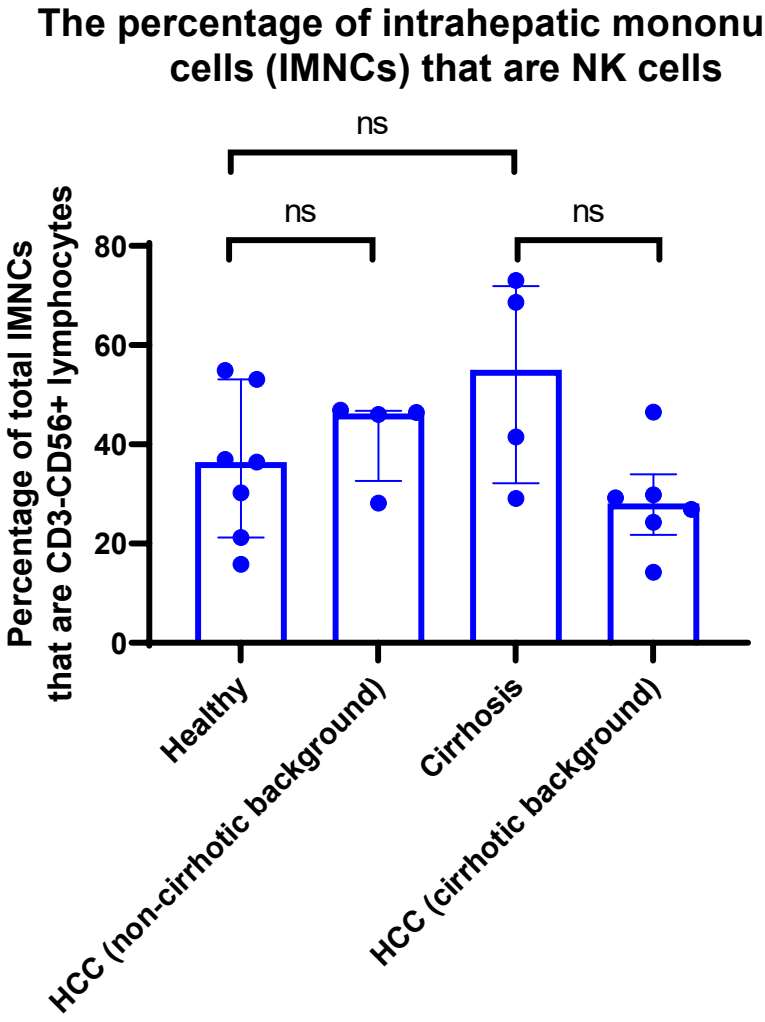


Figure 7 The proportion of intrahepatic mononuclear cells (IMNCs) that are NK cells. The percentage of total IMNCs that were CD3-CD56+ NK cells was determined following surface staining for CD3 and CD56 with fluorescently conjugated antibodies and subsequent flow cytometry (Phenotyping panel 1, Table 3). There was no significant difference in the proportion of intrahepatic NK cells in healthy liver (Healthy, n=7) in comparison to patients with HCC without cirrhosis (HCC, non-cirrhotic background, n=4), HCC with cirrhosis (HCC, cirrhotic background, n=6) and patients with cirrhosis (Cirrhosis, n=4). Comparisons were made using the non-parametric Mann Whitney test. Error bars represent the interquartile range.

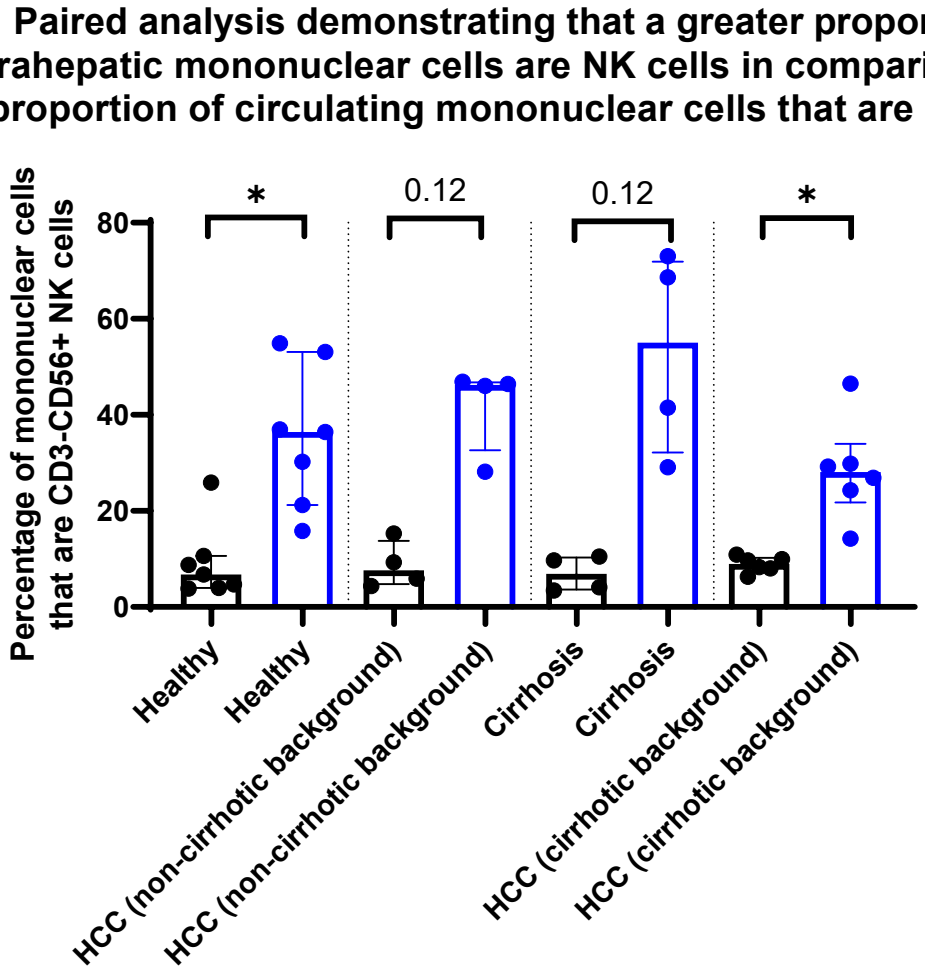


*Figure 8 Paired analysis demonstrating that a greater proportion of intrahepatic mononuclear cells are NK cells in comparison to the proportion of circulating peripheral blood mononuclear cells that are NK cells. Peripheral blood mononuclear cells (PBMCs) and intrahepatic mononuclear cells (IMNCs) from the same donors were stained to identify NK cells (Phenotyping panel 1, Table 3). The proportion of circulating and intrahepatic NK cells were compared. Comparisons were made using the Wilcoxon matched-pairs signed rank test. Error bars represent the interquartile range. P values are denoted on the figures as follows: * p<0.05). (Intrahepatic data is in blue; circulating data in black; graph displays individual values; patient demographics described in Table 9).*

3.1.1 Surface receptor expression

PBMCs and IMNCs were stained with fluorescently conjugated antibodies for the activating receptors NKG2D, DNAM-1, NKp30, NKp46, CD16, inhibitory receptor

CD161 and the liver homing receptor CXCR6 and phenotyped by flow cytometry (Phenotyping Panel 1, described in Chapter 2, Table 3).

3.1.1.1 Activating receptors - NKG2D and DNAM-1 expression

NKG2D is well recognised to be down-regulated in cancer due to shedding of NKG2D ligands by tumours (Masahisa et al., 2005). To investigate this, I studied NKG2D expression on circulating and intrahepatic NK cells in healthy individuals, individuals with cirrhosis and individuals with HCC on a background of cirrhosis.

NKG2D expression was not altered in cirrhosis or HCC of a non-viral aetiology in comparison to healthy donors (Figure 10). NKG2D expression was further analysed separating CD56dim and CD56bright NK cells, but again did not show altered expression in circulating NK cells.

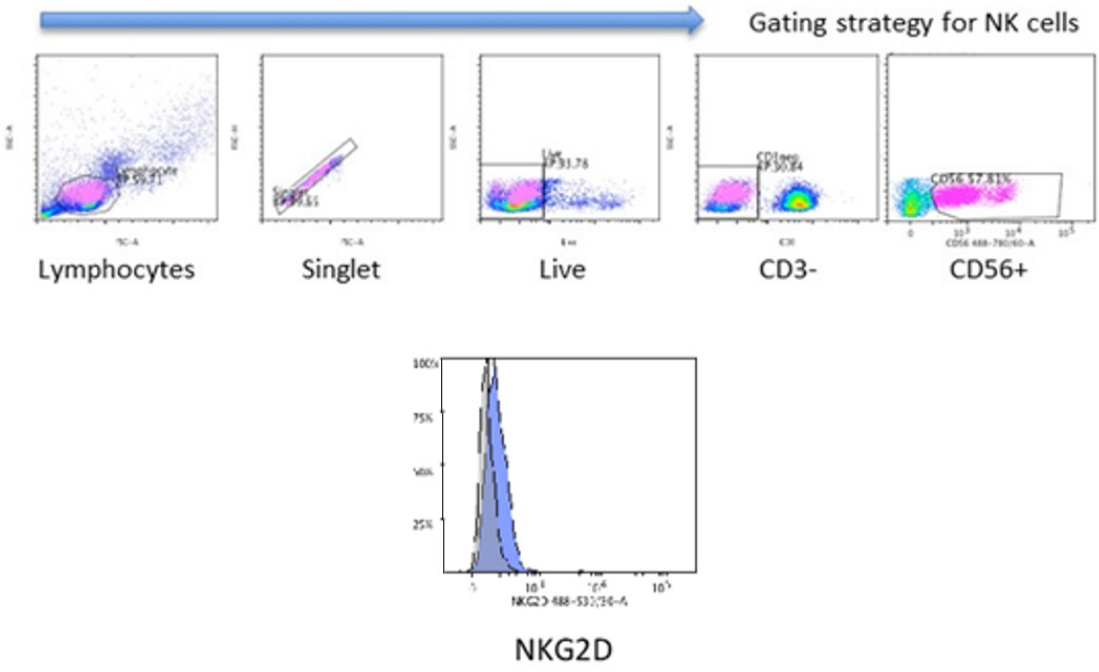
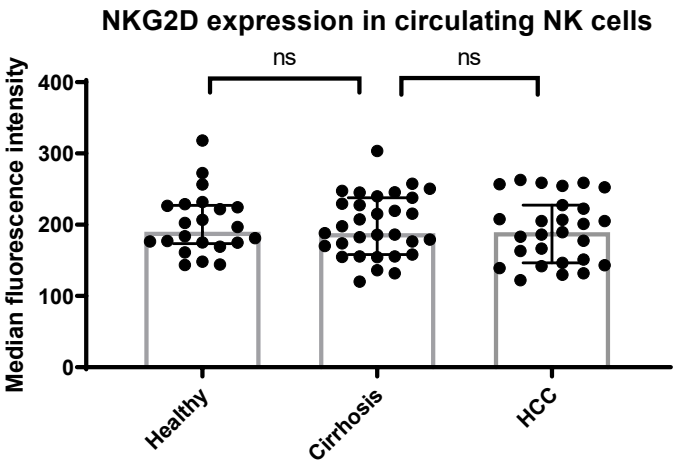


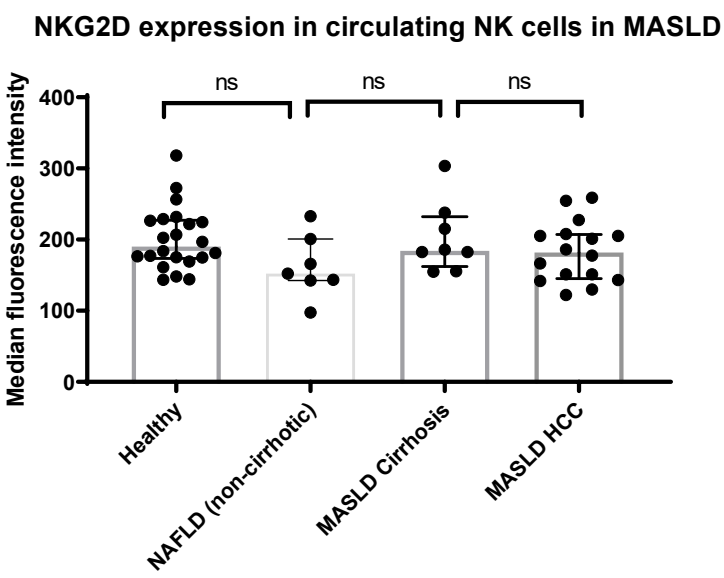
Figure 9 NKG2D expression on NK cells. Gating strategy for NKG2D on NK cells using flow cytometry. Following gating for lymphocytes, singlet gating and live cells, CD3-CD56+ NK cells were selected. The median fluorescence intensity (MFI) of all NK cells was determined (NKG2D staining in blue, fluorescence minus one (FMO) control in grey). The MFI for the FMO was subtracted from the MFI measured for NKG2D to calculate the true MFI for NKG2D.

Surface expression of NKG2D on circulating NK cells

A



B



C

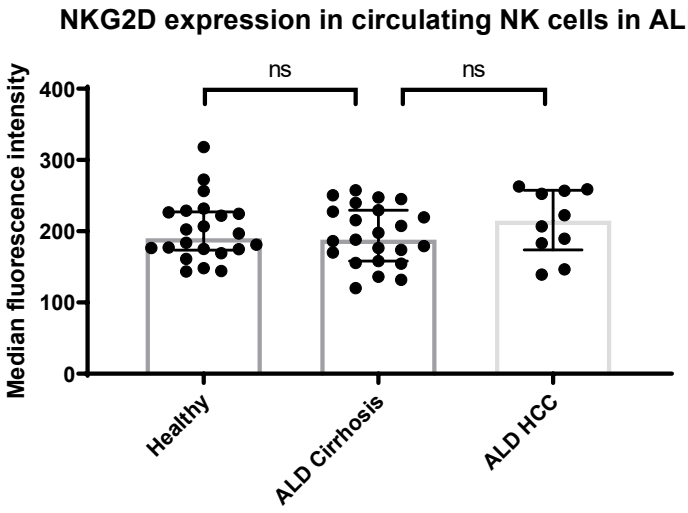


Figure 10 NKG2D expression on circulating NK cells. A) The median fluorescence intensity (MFI) of NKG2D on all circulating NK cells in healthy volunteers, patients with cirrhosis and patients with hepatocellular carcinoma (HCC) on a background of cirrhosis. B) The MFI of NKG2D expression on NK cells from healthy volunteers in comparison to patients with MASLD without cirrhosis (MASLD (non-cirrhotic)), MASLD with cirrhosis (MASLD cirrhosis) and MASLD cirrhosis with HCC (MASLD HCC). C) The median fluorescence intensity of NKG2D expression on NK cells from healthy volunteers in comparison to patients with ALD cirrhosis and patients with ALD cirrhosis and HCC (ALD HCC). (MASLD = metabolic dysfunction-associated steatotic liver disease; ALD= Alcohol related fatty liver disease; HCC= Hepatocellular carcinoma). No significant differences were seen when comparing NKG2D expression between healthy individuals and patients with cirrhosis, and when comparing patients with cirrhosis with patients with HCC. Graphs display individual values and the median value. Comparisons between groups have been made using the Mann-Whitney test. Error bars represent the interquartile range.

The cirrhosis and HCC groups were further separated by aetiology and NKG2D expression compared (Figure 10). There were no significant differences in NKG2D expression in patients with underlying MASLD or ALD.

Direct comparisons of the MASLD and ALD cirrhosis groups and HCC groups did not reveal any differences in NKG2D expression and the underlying aetiology of the disease (Figure 11).

NKG2D surface expression on circulating NK cells and underlying disease aetiology

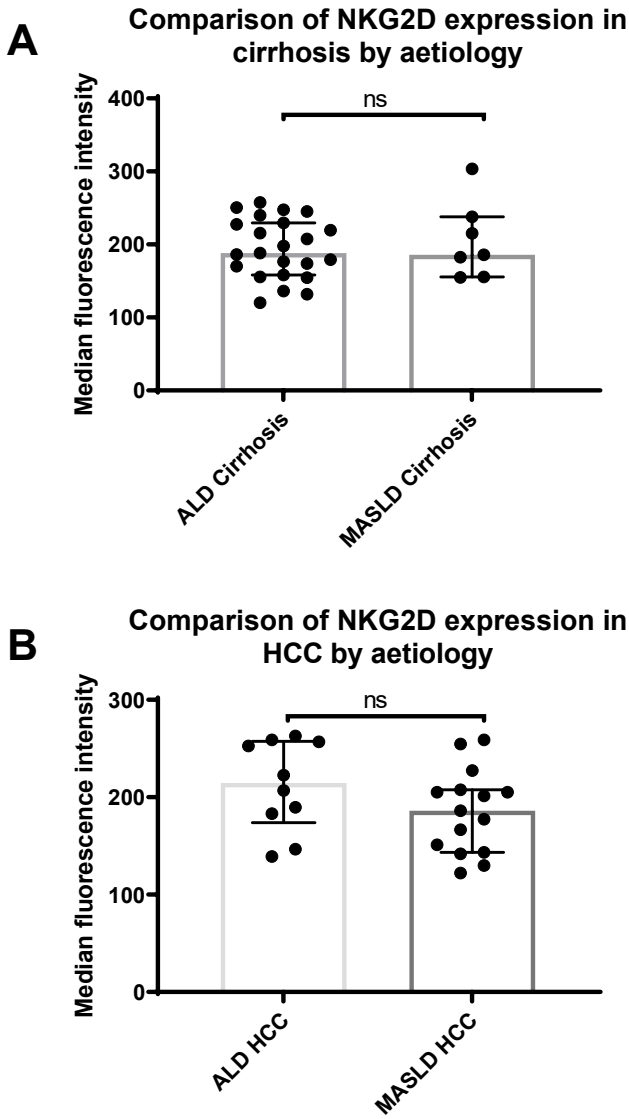


Figure 11 *Comparisons of NKG2D expression in cirrhosis and HCC delineated by underlying aetiology. A) NKG2D expression (median fluorescence intensity, MFI) on circulating NK cells was compared in patients with cirrhosis secondary to alcohol related liver disease (ALD cirrhosis) with patients with cirrhosis secondary to metabolic dysfunction-associated steatotic liver disease (MASLD cirrhosis). There were no significant differences in NKG2D expression on circulating NK cells in patients with ALD cirrhosis compared to MASLD cirrhosis. B) NKG2D expression (MFI) was compared between patients with HCC secondary to ALD cirrhosis (ALD HCC) and patients with HCC secondary to MASLD cirrhosis (MASLD HCC). There were no significant differences in NKG2D expression on circulating NK cells from patients with ALD HCC*

compared to MASLD HCC. (Graphs display individual values and the median value. Comparisons between groups have been made using the Mann-Whitney test. Error bars represent the interquartile range).

NKG2D expression on circulating NK cells and underlying cirrhosis status

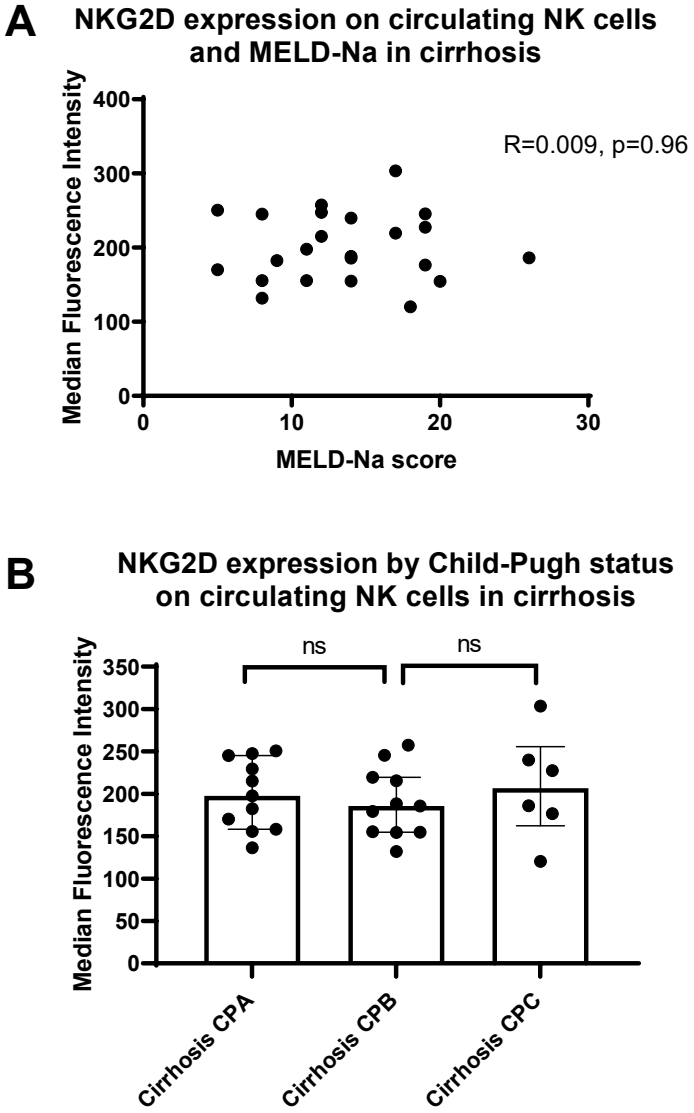


Figure 12 NKG2D expression on circulating NK cells in cirrhosis and underlying MELD-Na score and Child-Pugh classification. NKG2D expression (median fluorescence intensity) on circulating NK cells was determined in patients with cirrhosis. A) NKG2D expression did not correlate with MELD-Na score in patients with cirrhosis without HCC (spearman rank correlation). B) There were no differences in NKG2D expression on circulating NK cells in patients with cirrhosis categorised by Child-Pugh status (CPA= Child-Pugh A, CPB = Child-Pugh B, CPC = Child-Pugh C). (Graphs display individual values, and the median value is also displayed on the bar graph. Comparisons between groups have been made using the Mann-Whitney test. Error bars represent the interquartile range). Analyses were repeated for

patients with MASLD cirrhosis and for ALD cirrhosis but did not demonstrate correlation with MELD-Na or significance between Child-Pugh status.

NKG2D expression did not correlate with cirrhosis staging by Child-Pugh status or by MELD-Na score in patients with cirrhosis without HCC (Figure 12). NKG2D expression on NK cells did not correlate with any clinical parameters (Appendix 8.3, table 8.1). There were no differences in NKG2D expression when comparing patients with HCC with different BCLC (Barcelona Clinic Liver Cancer) staging (Figure 13), though sample numbers in each subgroup were too small measure differences.

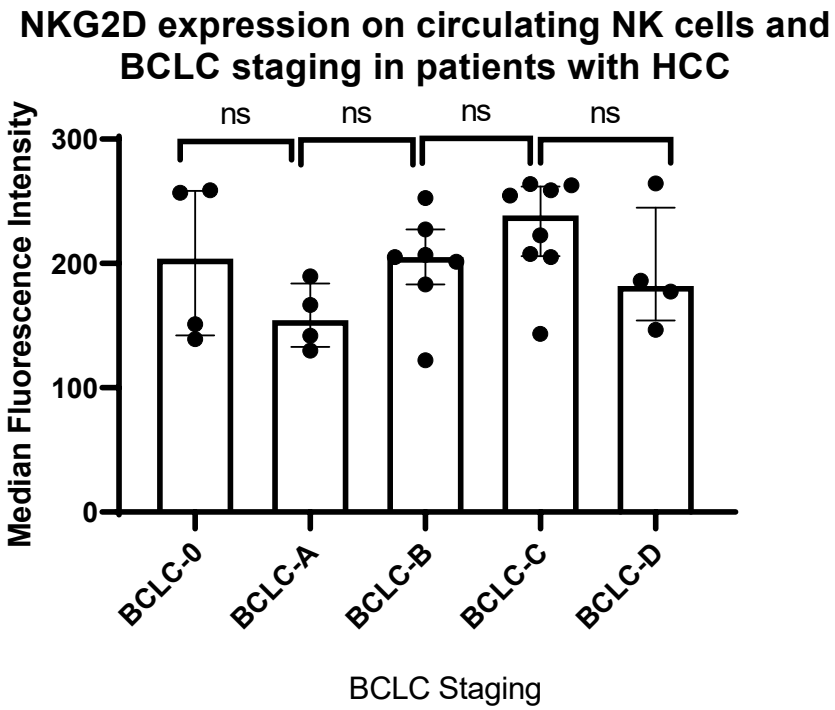


Figure 13 NKG2D expression on circulating NK cells in individuals with HCC analysed by Barcelona Clinic Liver Cancer (BCLC) classification. Comparisons between groups with different stages did not reveal a difference in NKG2D expression (Kruskal-Wallis test with Dunn's multiple comparisons). (Graphs display individual values and the median value. Error bars represent the interquartile range).

NKG2D expression was determined on intrahepatic NK cells and compared to circulating NK cells from the same patient donors (Figure 14).

Surface expression of NKG2D on intrahepatic NK cells

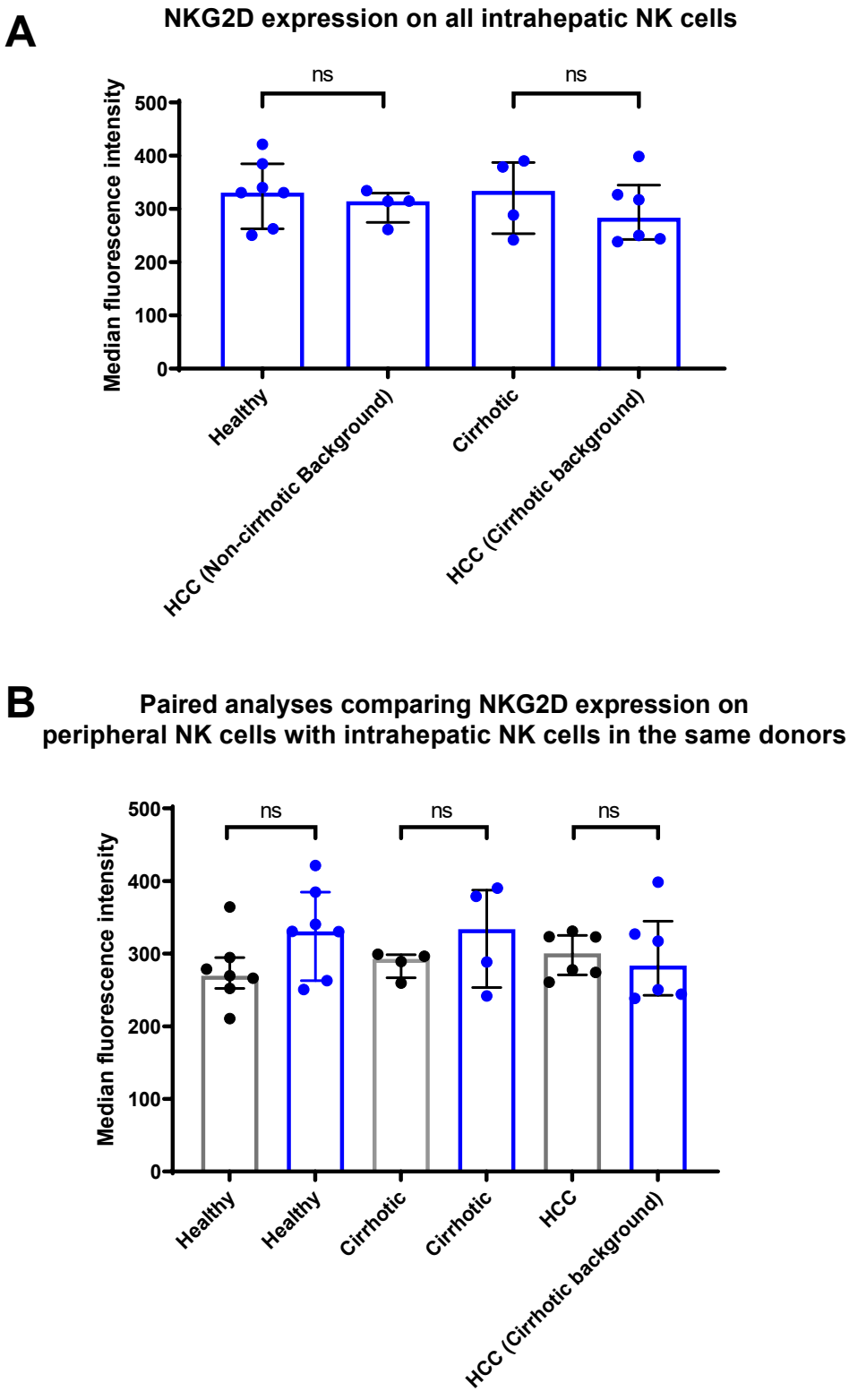


Figure 14 NKG2D expression on intrahepatic NK cells. A) Intrahepatic NK cell expression of NKG2D (median fluorescence intensity). Comparisons between groups have been made using

the Mann-Whitney test. B) Comparison of NKG2D expression in circulating NK cells (data in black) compared to intrahepatic NK cells (data in blue) from the same donor. NKG2D expression was determined on circulating NK cells from patients and compared to the intrahepatic NK cell expression of NKG2D from the same patient. Comparisons were made using the non-parametric Wilcoxon matched-pairs signed rank test. Graphs display individual values and the median value. Error bars represent the interquartile range.

Intrahepatic NK cells from patients with cirrhosis and HCC with or without cirrhosis did not show altered expression of NKG2D compared to healthy intrahepatic NK cells, although sample numbers were too small to draw conclusions (Figure 14A). Comparisons between circulating NK cells and intrahepatic NK cells in healthy samples, patients with cirrhosis and patients with HCC on a background of cirrhosis did not reveal differences in NKG2D expression (Figure 14B).

CD155, the ligand for NK cell activating receptor DNAM-1, has been identified as upregulated on HCC tissue (Duan et al., 2019) and hence DNAM-1 expression on NK cells in healthy individuals, patients with cirrhosis and patients with HCC on a background of cirrhosis was determined to see if there is differential expression of DNAM-1 in disease. DNAM-1 was determined using the gating strategy below, identifying the percentage of NK cells expressing DNAM-1 (Figure 15).

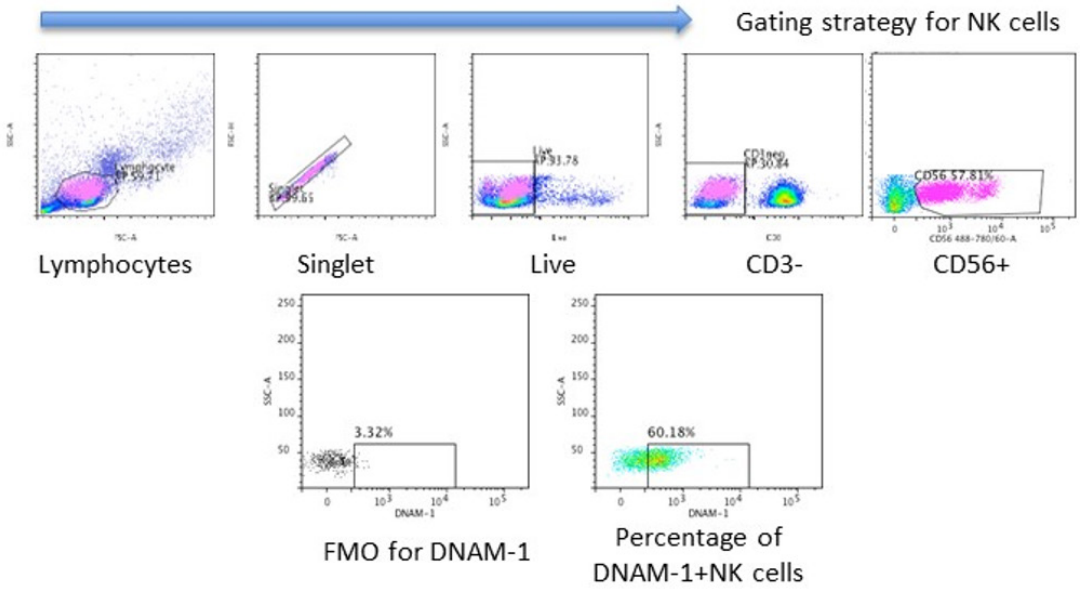
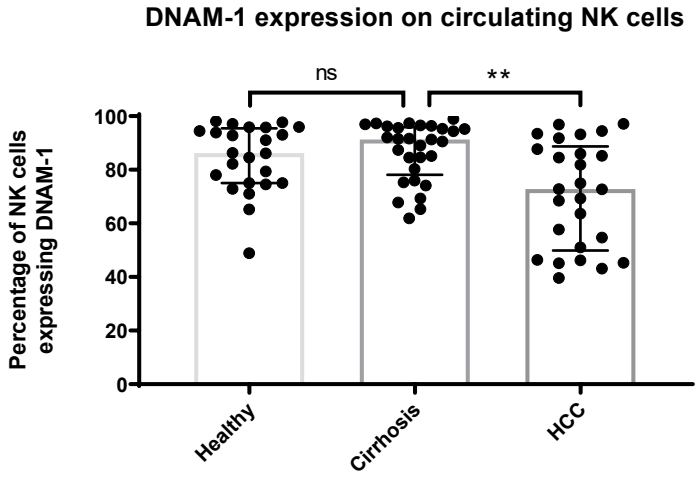


Figure 15 Gating strategy for DNAM-1+NK cells using flow cytometry. Following gating for lymphocytes, singlet gating and live cells, CD3-CD56+ NK cells were selected. The percentage of NK cells expressing DNAM-1 was determined using a fluorescence minus one (FMO) control.

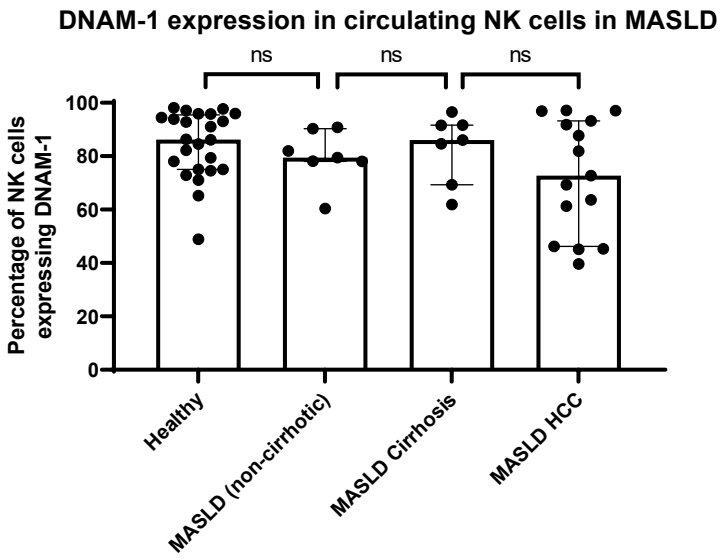
The proportion of DNAM-1+NK cells was reduced in patients with HCC on a background of cirrhosis in comparison to patients with cirrhosis only, while there was no difference between NK cell expression of DNAM-1 when comparing patients with cirrhosis and healthy volunteers (Figure 16 A). However, on separating patients by their underlying aetiology of disease, although there was a downward trend in DNAM-1 expression in HCC with an underlying MASLD or ALD aetiology compared to patients with cirrhosis of the same aetiology, the difference lost significance. There was broad variation in the expression of DNAM-1 in patients with HCC regardless of aetiology (Figure 16 B and 16 C).

Surface expression of DNAM-1 on circulating NK cells

A



B



C

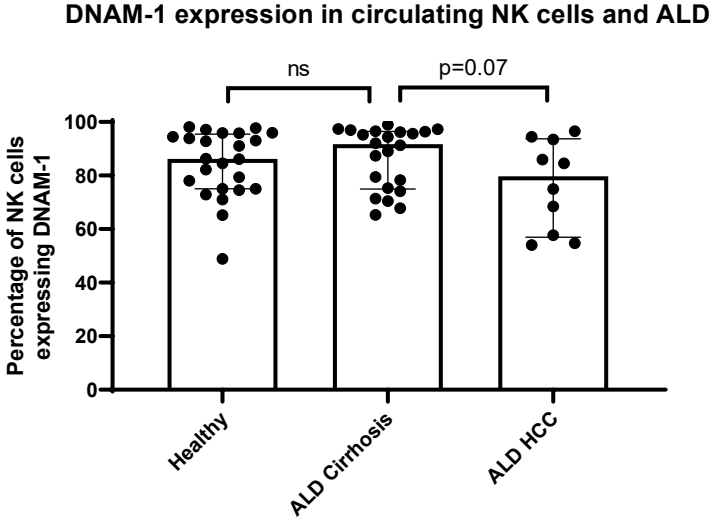


*Figure 16 DNAM-1 expression on circulating NK cells. A) DNAM-1+NK cells as a proportion of all circulating NK cells in healthy volunteers, patients with cirrhosis of a non-viral aetiology and patients with treatment naïve, non-viral hepatocellular carcinoma (HCC). Patients in HCC group had a significantly lower expression of DNAM-1 expression compared to patients with cirrhosis without HCC. B) DNAM-1+NK cells as a proportion of all NK cells from healthy volunteers in comparison to patients with MASLD without cirrhosis (MASLD (non-cirrhotic)), MASLD with cirrhosis (MASLD cirrhosis) and MASLD cirrhosis with HCC (MASLD HCC). C) DNAM-1+NK cells as a proportion of all NK cells from healthy volunteers in comparison to patients with ALD cirrhosis and patients with ALD cirrhosis and HCC. There were no significant differences in DNAM-1 expression in HCC or cirrhosis when analysing groups separated by underlying aetiology (MASLD or ALD). (MASLD = metabolic dysfunction-associated steatotic liver disease; ALD= Alcohol related fatty liver disease; HCC= Hepatocellular carcinoma). (Graphs display individual values and the median value and comparisons between groups have been made using the Mann-Whitney test. Error bars represent the interquartile range. P values are denoted on the figures as follows: * p<0.05, ** p<0.01, *** p<0.001, **** p<0.0001).*

The DNAM-1+NK cell proportion was not significantly different in patients with cirrhosis with or without HCC secondary to ALD compared to patients with cirrhosis and HCC secondary to MASLD (Figure 17).

DNAM-1 surface expression on circulating NK cells and underlying disease aetiology

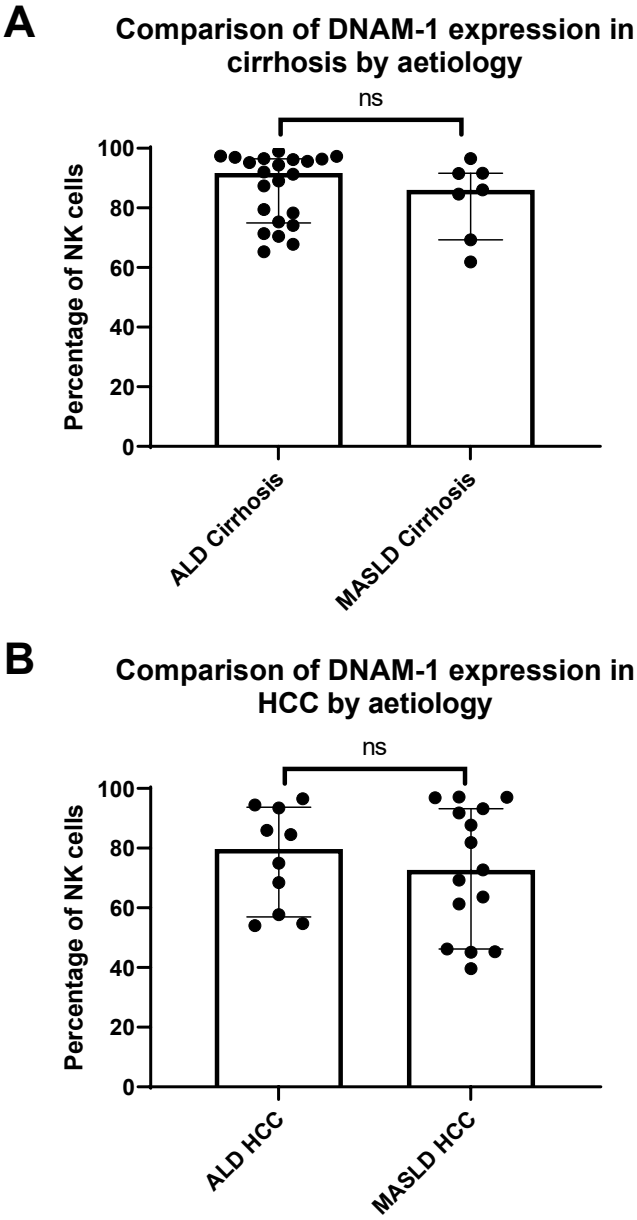


Figure 17 Comparing the proportion of circulating DNAM-1+NK cells in cirrhosis and in HCC delineated by underlying aetiology. Graphs display the percentage of circulating NK cells expressing DNAM-1. A) The proportion of circulating DNAM-1+NK cells in patients with cirrhosis secondary to ALD (ALD cirrhosis) was compared to patients with cirrhosis secondary to MASLD (MASLD cirrhosis). Comparisons between patients with ALD cirrhosis and patients with MASLD cirrhosis did not reveal a difference in the circulating DNAM-1+NK cell proportion. B) The proportion of circulating DNAM-1+NK cells in patients with HCC secondary to ALD cirrhosis (ALD HCC) was compared to patients with HCC secondary to MASLD cirrhosis (MASLD

HCC). Comparisons between these two groups of patients with HCC did not reveal a significant difference in the circulating proportion of DNAM-1+ NK cells. (MASLD = metabolic dysfunction-associated steatotic liver disease; ALD= Alcohol related fatty liver disease; HCC= Hepatocellular carcinoma) (Graphs display individual values and the median value. Comparisons between groups are made using the Mann-Whitney test. Error bars represent the interquartile range).

The proportion of DNAM-1+NK cells in the circulation did not vary in patients with cirrhosis categorised by Child-Pugh status, nor did it correlate with the MELD-Na score (Figure 18). There were also no significant differences in the proportion of DNAM-1+NK cells in the circulation of patients with HCC despite the underlying BCLC staging (Figure 19). DNAM-1 expression in the circulation did not correlate with any clinical parameters (Appendix 8.3, table 8.2).

DNAM-1 expression on circulating NK cells and underlying cirrhosis status

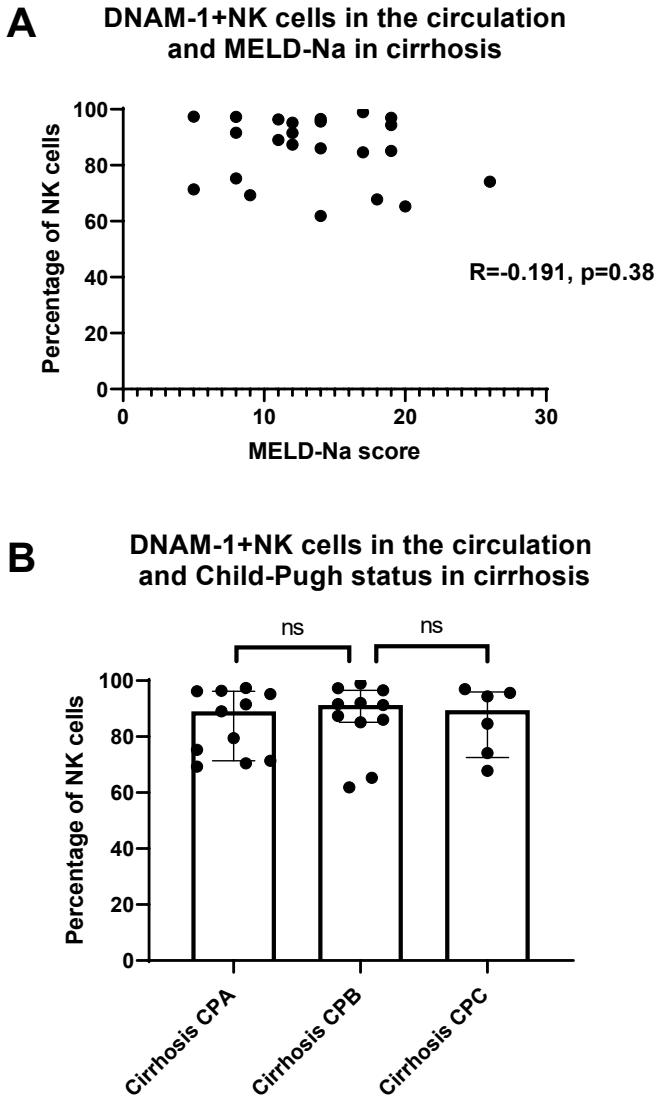


*Figure 18 DNAM-1 expression on circulating NK cells in cirrhosis and underlying MELD-Na score and Child-Pugh classification. DNAM-1+ circulating NK cells were determined in patients with cirrhosis. Graphs display the percentage of circulating NK cells that expressed DNAM-1. A) DNAM-1+NK cell proportion did not correlate with MELD-Na score in patients with cirrhosis without HCC (spearman rank correlation). B) The circulating DNAM-1+ve NK cell proportion in patients with cirrhosis did not differ by underlying Child-Pugh status (CPA= Child-Pugh A, CPB = Child-Pugh B, CPC = Child-Pugh C). (Graphs display individual values, and the median value is also displayed on the bar graph. Comparisons between groups have been made using the Mann-Whitney test. Error bars represent the interquartile range. P values are denoted on the figures as follows: * p<0.05, ** p<0.01, *** p<0.001, **** p<0.0001). Analyses were repeated*

for patients with MASLD cirrhosis and for ALD cirrhosis but did not demonstrate correlation with MELD-Na or significance between Child-Pugh status.

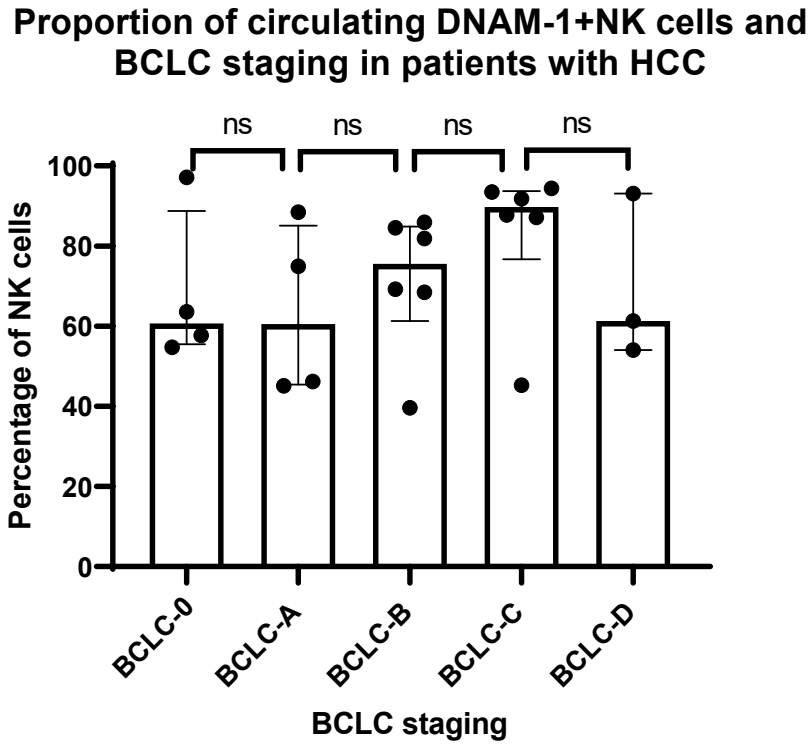


Figure 19 The proportion of DNAM-1+NK cells in the circulation in patients with HCC on a background of cirrhosis categorised by BCLC staging. Graph displays the percentage of circulating NK cells expressing DNAM-1. Comparisons between groups with different stages did not reveal a difference in the circulating proportion of NK cells that express DNAM-1 (Kruskal-Wallis test with Dunn's multiple comparisons). (Graphs display individual values and the median value. Error bars represent the interquartile range).

Again, no differences were seen in DNAM-1 expression on intrahepatic NK cells, however sample sizes were too small to draw significant comparisons (Figure 20A). Overall the proportion of DNAM-1+ intrahepatic NK cells was lower than the circulating proportion of DNAM-1+NK cells in healthy states, but significance was lost when comparing patients with cirrhosis or HCC (Figure 20B).

Surface expression of DNAM-1 on intrahepatic NK cells

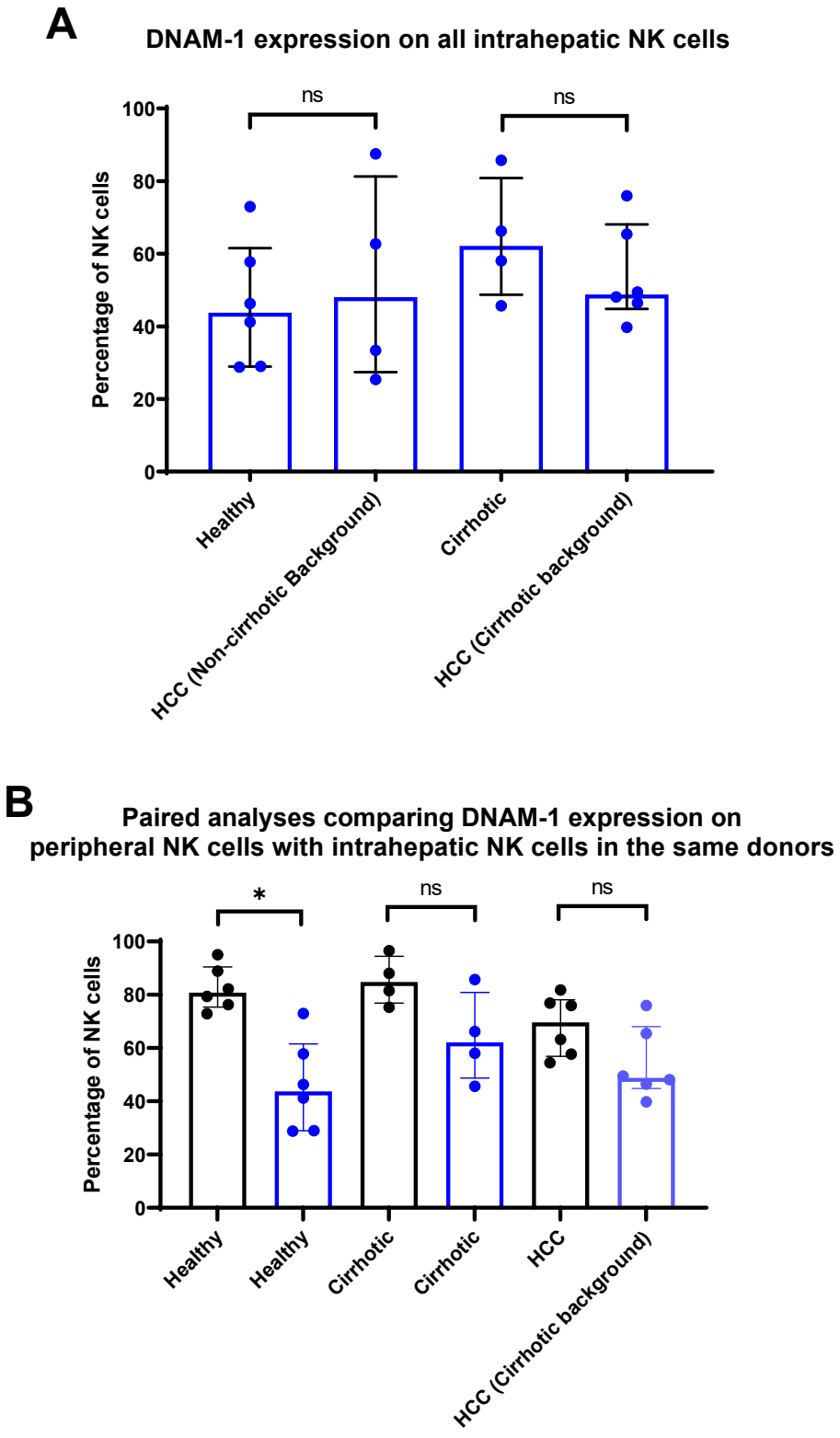


Figure 20 DNAM-1 expression on intrahepatic NK cells. Graph displays the percentage of NK cells expressing DNAM-1. A) DNAM-1 expression on intrahepatic NK cells, expressed as a

*proportion of total intrahepatic NK cells. Comparisons are made using the non-parametric Mann Whitney tests. B) Comparison of DNAM-1 expression in circulating NK cells (data in black) compared to intrahepatic NK cells (data in blue) from the same donor. DNAM-1 expression was determined on circulating NK cells from patients and compared to the intrahepatic NK cell expression of DNAM-1 from the same patient. Comparisons were made using the non-parametric Wilcoxon matched-pairs signed rank test. Graphs display individual values and the median value. Error bars represent the interquartile range .P values are denoted on the figures as follows: * p<0.05, ** p<0.01, *** p<0.001, **** p<0.0001).*

3.1.2 NCR expression- NKp46 and NKp30 expression

Variation in the expression of NKp30 and NKp46 has been described in patients with HCC, with reduced expression of NKp46 corresponding to poorer outcomes in HCC, and NKp30 being associated with an inhibitory role in NK cell function (Cariani et al., 2016; Hoechst et al., 2009; Mantovani et al., 2019; Zecca et al., 2021). Therefore, the expression of natural cytotoxicity receptors (NCR) NKp30 and NKp46 was determined using flow cytometry in patients with HCC on a background of cirrhosis and compared with patients with cirrhosis only to ascertain if changes in expression were seen in cirrhosis also. Comparisons were made with healthy individuals also to determine whether disease aetiology made a difference to receptor expression. As all NK cells express NKp46 and NKp30 (Barrow et al., 2019), the median fluorescence intensity for each receptor was determined on all NK cells (Figure 21; antibodies used as per Phenotyping Panel 1, Table 3).

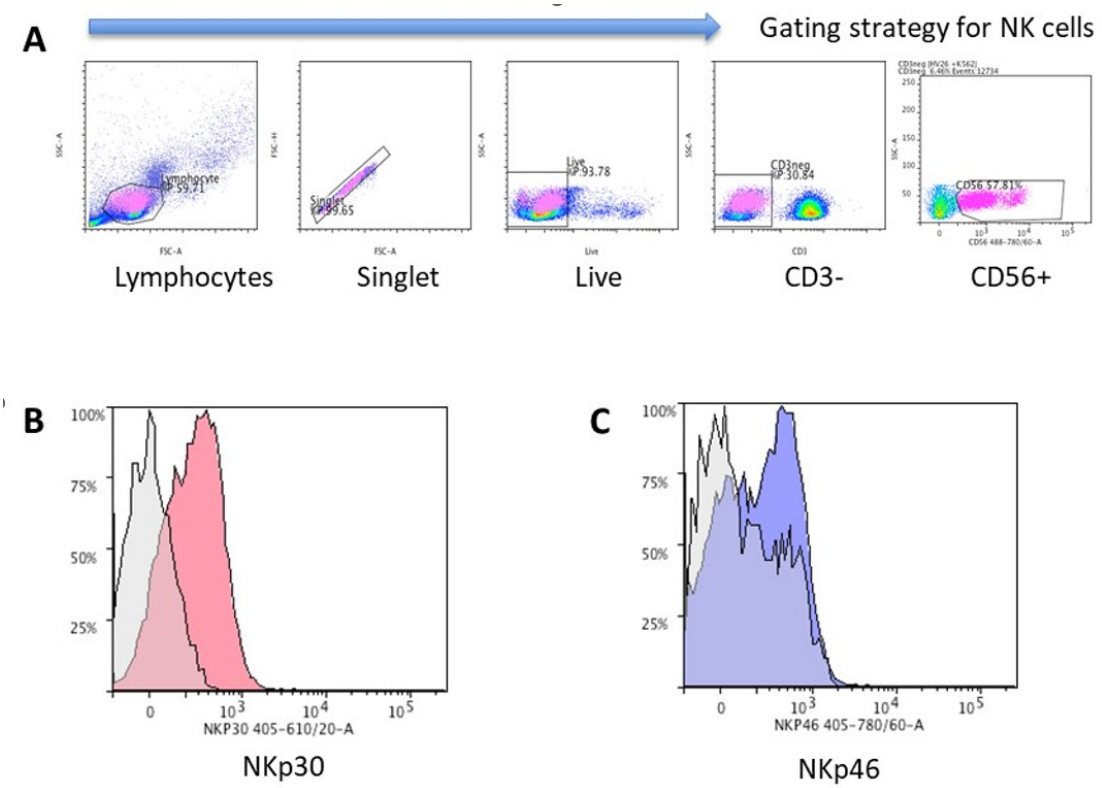
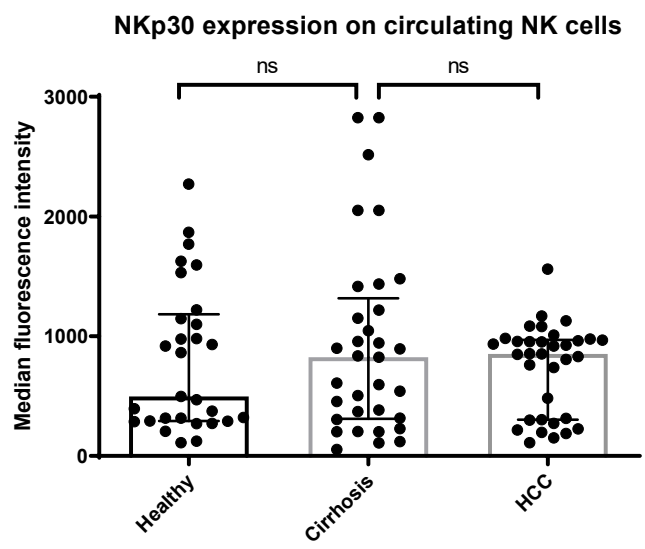


Figure 21 NKp30 and NKp46 expression. A) Gating strategy for NK cells (CD3-CD56+ live lymphocytes). B) The median fluorescence intensity (MFI) was measured for all NK cells for NKp30 and for NKp46 (C). The fluorescence minus one (FMO) method was used to determine positive staining (FMO shown in grey on graphs B and C, NKp30 staining shown in red on graph B and NKp46 staining shown in blue on graph C). The MFI for the FMO was subtracted from the total MFI for stained cells to measure true positive MFI for each receptor.

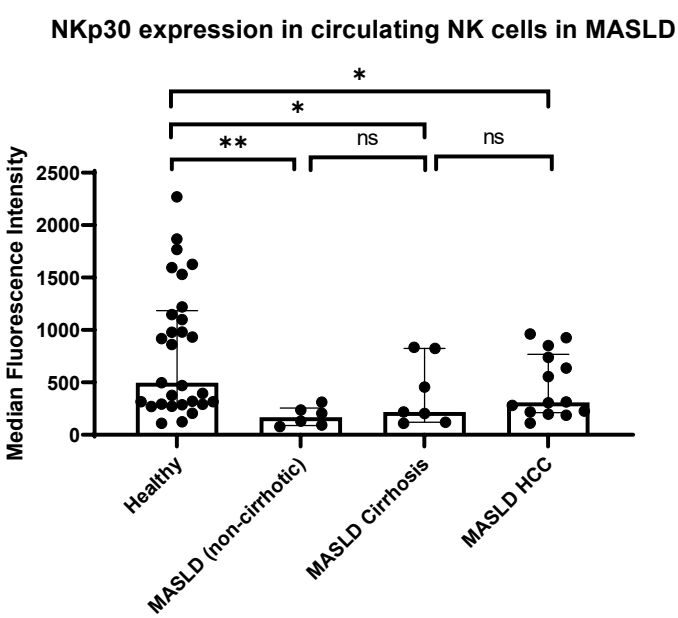
Differences in NKp30 expression were not statistically significant when comparing healthy to cirrhosis states, and cirrhosis to HCC states without separation of the underlying aetiology (Figure 22A). On further analysis by underlying aetiology, there was a significantly lower expression of NKp30 on circulating NK cells in patients with MASLD cirrhosis and with MASLD HCC on a background of cirrhosis group in comparison to healthy volunteers (217 vs. 496, MASLD cirrhosis vs. healthy, p=0.0356; 309 vs. 496, MASLD HCC vs. healthy, p=0.0495; MFI values, Figure 22B). This reduced expression of NKp30 was also seen in patients with MASLD without cirrhosis in comparison to healthy individuals (Figure 22B).

Surface expression of NKp30 on circulating NK cells

A



B



C

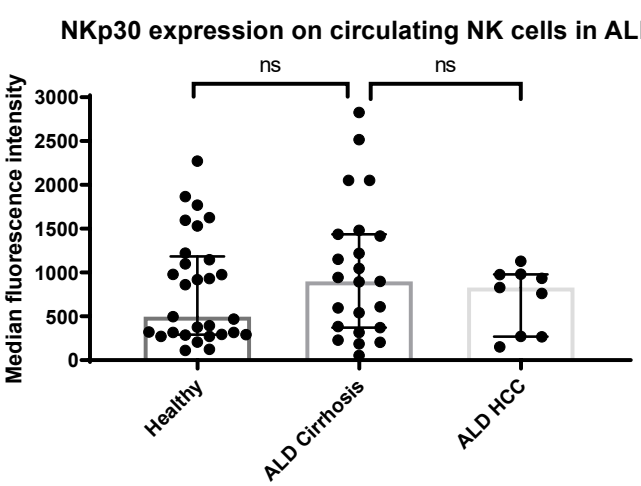


*Figure 22 NKp30 expression on circulating NK cells. A) The median fluorescence intensity (MFI) of NKp30 on all circulating NK cells in healthy volunteers, patients with cirrhosis and patients with hepatocellular carcinoma (HCC) on a background of cirrhosis. No significant differences were seen for NKp30 expression between groups. B) The MFI of NKp30 expression on NK cells from healthy volunteers in comparison to patients with MASLD without cirrhosis (MASLD (non-cirrhotic)), MASLD with cirrhosis (MASLD cirrhosis) and MASLD cirrhosis with HCC (MASLD HCC). There was an overall reduced expression of NKp30 in patients with MASLD regardless of whether there was underlying fibrosis or HCC in comparison to healthy volunteers. C) The MFI of NKp30 expression on NK cells from healthy volunteers in comparison to patients with ALD cirrhosis and patients with ALD cirrhosis and HCC (ALD HCC). There were no significant differences in NKp30 expression between groups. (MASLD = metabolic dysfunction-associated steatotic liver disease; ALD= Alcohol related fatty liver disease; HCC= Hepatocellular carcinoma). Graphs display individual values and the median value. Comparisons between groups have been made using the Mann-Whitney test. Error bars represent the interquartile range. P values are denoted on the figures as follows: * p<0.05, ** p<0.01, *** p<0.001, **** p<0.0001.*

NKp30 expression on circulating NK cells in patients with ALD cirrhosis was significantly higher compared to MASLD cirrhosis, but significance was lost when comparing patients with HCC on a background of ALD cirrhosis to patients with HCC on a background of MASLD cirrhosis (Figure 23).

NKp30 surface expression on circulating NK cells and underlying disease aetiology

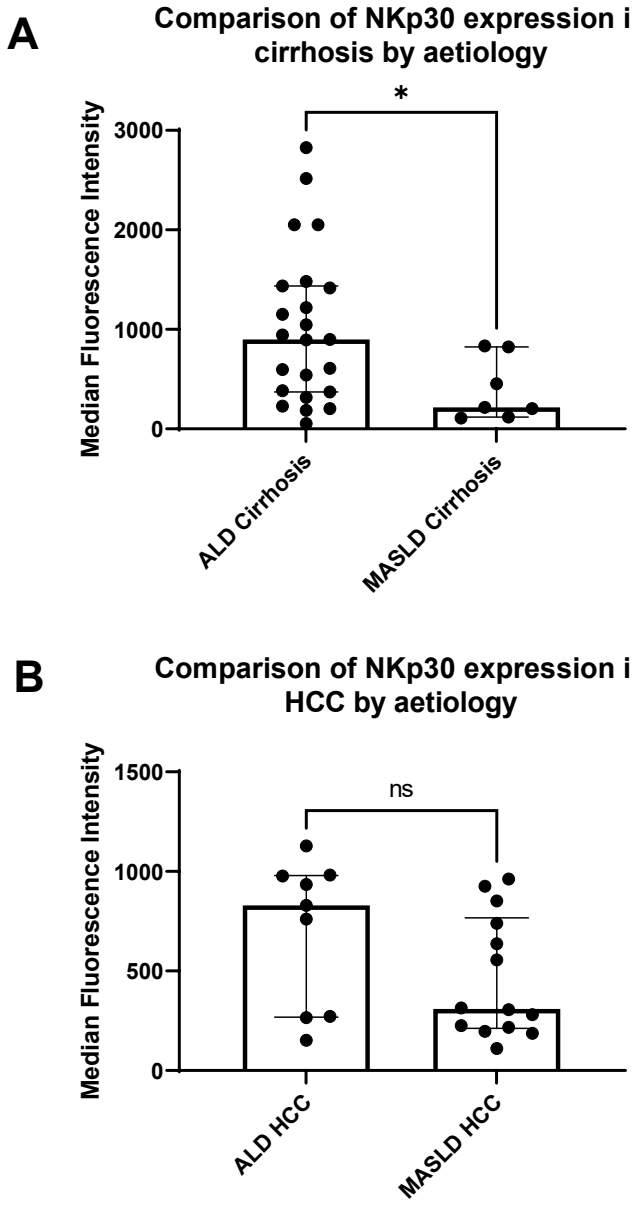


Figure 23 Comparisons of NKp30 expression in cirrhosis and HCC delineated by underlying aetiology. A) The median fluorescence intensity (MFI) of NKp30 on circulating NK cells was compared between patients with cirrhosis secondary to ALD (ALD cirrhosis) and patients with cirrhosis and MASLD (MASLD cirrhosis). Expression of NKp30 on circulating NK cells was reduced in patients with MASLD cirrhosis compared to ALD cirrhosis. B) The MFI of NKp30 on circulating NK cells was compared between patients with HCC secondary to ALD cirrhosis (ALD HCC) and patients with cirrhosis and HCC secondary to MASLD cirrhosis (MASLD HCC). Again, there was a reduced expression of NKp30 on circulating NK cells in the MASLD HCC group

*compared to the ALD HCC group. (MASLD = metabolic dysfunction-associated steatotic liver disease; ALD= Alcohol related fatty liver disease; HCC= Hepatocellular carcinoma). (Graphs display individual values and the median value. Comparisons between groups have been made using the Mann-Whitney test. Error bars represent the interquartile range. P values are denoted on the figures as follows: * p<0.05, ** p<0.01, *** p<0.001, **** p<0.0001).*

NKp30 expression on circulating NK cells did not correlate with the MELD-Na score or Child-Pugh status in patients with cirrhosis (Figure 24). NKp30 expression did not correlate with BCLC staging in patients with HCC (Figure 25).

NKp30 expression on circulating NK cells and underlying cirrhosis status

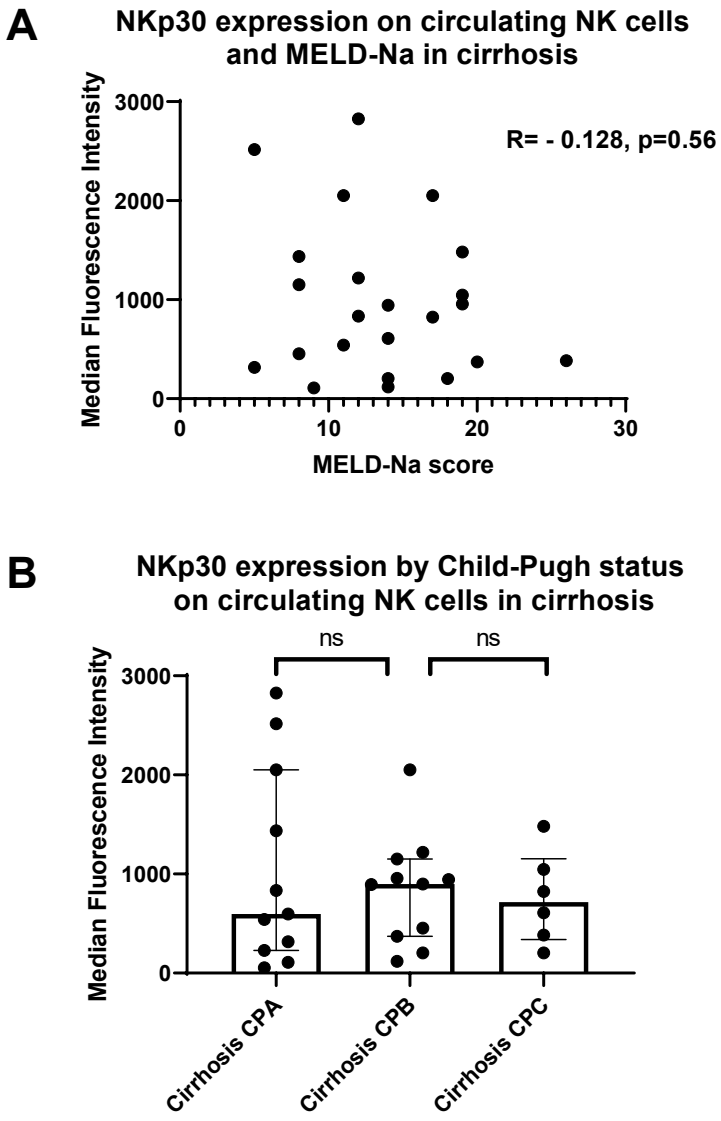


Figure 24 NKp30 expression on circulating NK cells in cirrhosis and underlying MELD-Na score and Child-Pugh classification. NKp30 expression (median fluorescence intensity) on circulating NK cells was determined in patients with cirrhosis. A) NKp30 expression did not correlate with MELD-Na score in patients with cirrhosis without HCC (spearman rank correlation). B) There were no differences in NKp30 expression on circulating NK cells in patients with cirrhosis categorised by Child-Pugh status (CPA= Child-Pugh A, CPB = Child-Pugh B, CPC = Child-Pugh C). (Graphs display individual values, and the median value is also displayed on the bar graph. Comparisons between groups have been made using the Mann-Whitney test. Error bars represent the interquartile range). Analyses were repeated for patients with MASLD cirrhosis

and for ALD cirrhosis but did not demonstrate correlation with MELD-Na or significance between Child-Pugh status.

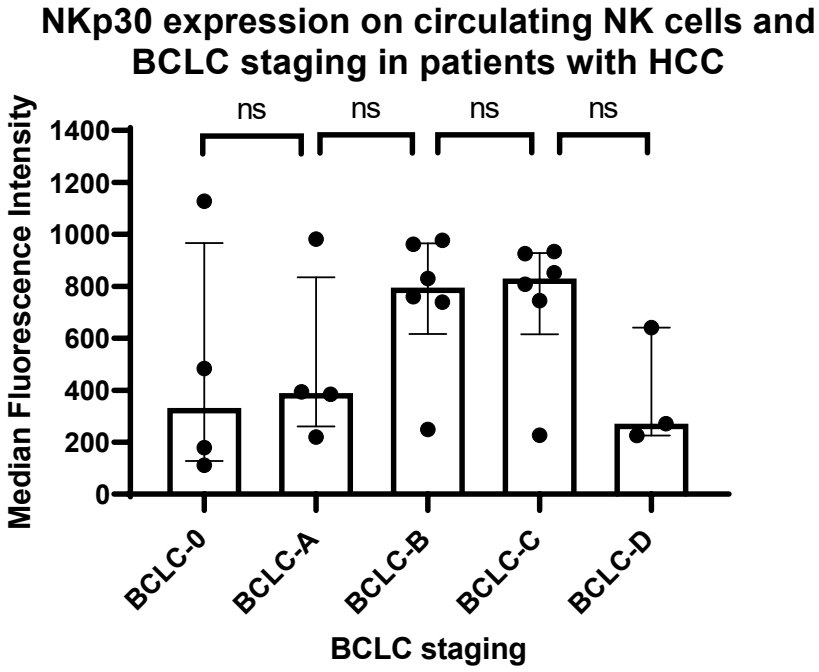


Figure 25 NKp30 expression on circulating NK cells in individuals with HCC analysed by Barcelona Clinic Liver Cancer (BCLC) classification. Comparisons between groups with different stages did not reveal a difference in NKp30 expression (Kruskal-Wallis test with Dunn's multiple comparisons). (Graphs display individual values and the median value. Error bars represent the interquartile range).

NKp30 expression has been demonstrated to have a reduced expression in older people (Almeida-Oliveira et al., 2011) and this negative correlation with age was seen here in the cirrhosis group (R= -0.5243, p=0.0042) (Figure 26), but the correlation was lost in the HCC group. Correlation was also lost when the cirrhosis group was split by underlying aetiology. The MASLD cirrhosis patient group was significantly older than the ALD cirrhosis patient group (55 years (ALD group) vs. 67years (MASLD group), p=0.013) and this may, to some extent explain, the reduced NKp30 expression seen in patients with cirrhosis secondary to MASLD in comparison to patients with ALD cirrhosis (Figure 23). Furthermore, the healthy volunteer group was significantly younger in comparison to patients with HCC secondary to MASLD related cirrhosis and patients with MASLD cirrhosis without HCC. However, the healthy volunteer group

was also significantly younger than the ALD cirrhosis group, but no significant differences were seen in NKp30 expression between these two groups, indicating a possible association between MASLD and a reduction in the surface expression of NKp30 on circulating NK cells.

NKp30 expression on circulating NK cells did not correlate with any other individual clinical parameters (Appendix 8.3, table 8.3).

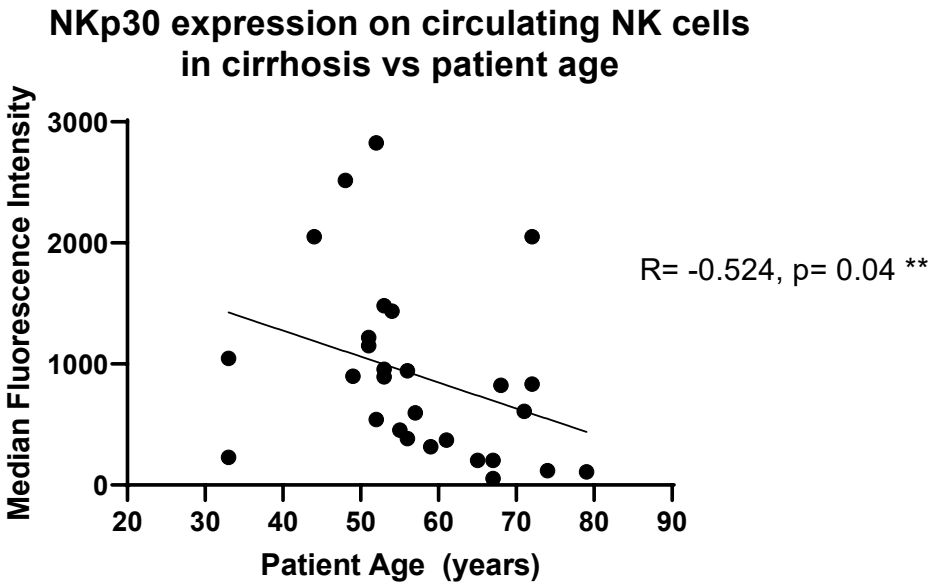
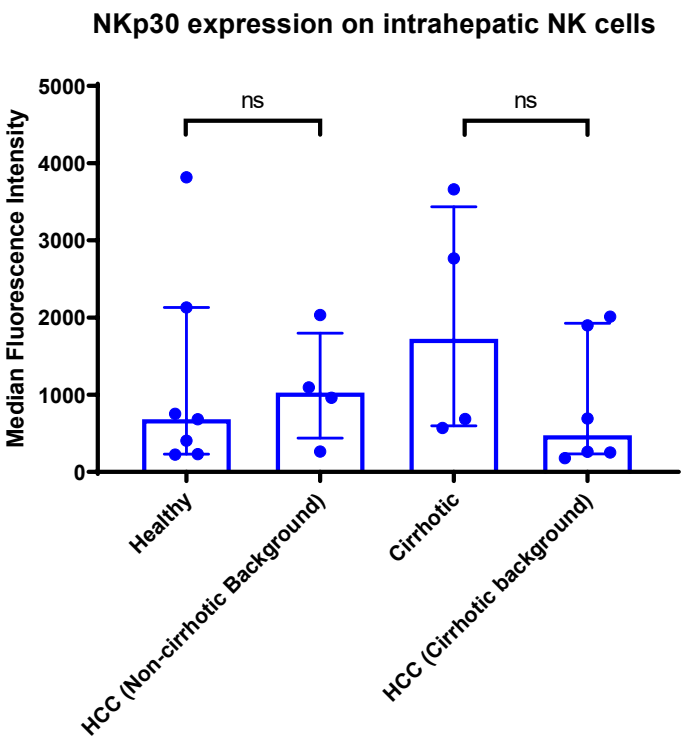


Figure 26 NKp30 expression (median fluorescence intensity) on circulating NK cells in cirrhosis correlated negatively with patient age (spearman rank correlation). However, the negative correlation of NKp30 expression and age lost significance when the cirrhosis group was subdivided by underlying aetiology (MASLD cirrhosis group: R= -0.49, p=0.38; ALD cirrhosis group R= -0.36, p=0.10).

NKp30 expression in intrahepatic NK cells is demonstrated in Figure 27. Again sample sizes were too small to determine differences between healthy and disease states. Comparison with circulating NK cells did not reveal differences in expression.

Surface expression of NKp30 on intrahepatic NK cells

A



B

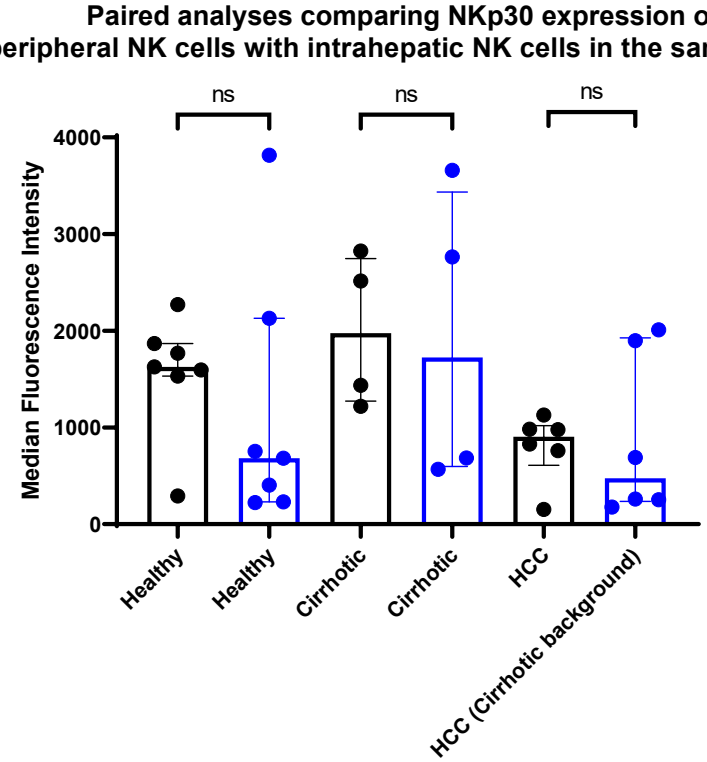


*Figure 27 NKp30 expression on intrahepatic NK cells. A) Intrahepatic NK cell expression of NKp30 (median fluorescence intensity). Comparisons between groups have been made using the Mann-Whitney test. B) Comparison of NKp30 expression in circulating NK cells (data in black) compared to intrahepatic NK cells (data in blue) from the same donor. Comparisons were made using the non-parametric Wilcoxon matched-pairs signed rank test. Graphs display individual values and the median value. Error bars represent the interquartile range. P values are denoted on the figures as follows: * p<0.05, ** p<0.01, *** p<0.001, **** p<0.0001).*

NKp46 expression on circulating and intrahepatic NK cells was determined using the gating strategy demonstrated in Figure 21 following staining with Phenotyping Panel 1 (Table 3). NKp46 demonstrated a significantly reduced expression on circulating NK cells in HCC when compared to healthy volunteers (Figure 28A). The reduced expression of NKp46 on circulating NK cells in HCC was seen in patients with an underlying MASLD aetiology in comparison to healthy patients, but significance was lost when comparing NKp46 expression in MASLD cirrhosis to healthy volunteers (Figure 28B). There was no significant difference in expression of NKp46 in ALD compared to healthy volunteers, however there was wide variation of expression in patients with ALD HCC with a downward trend (Figure 28C).

Surface expression of NKp46 on circulating NK cells

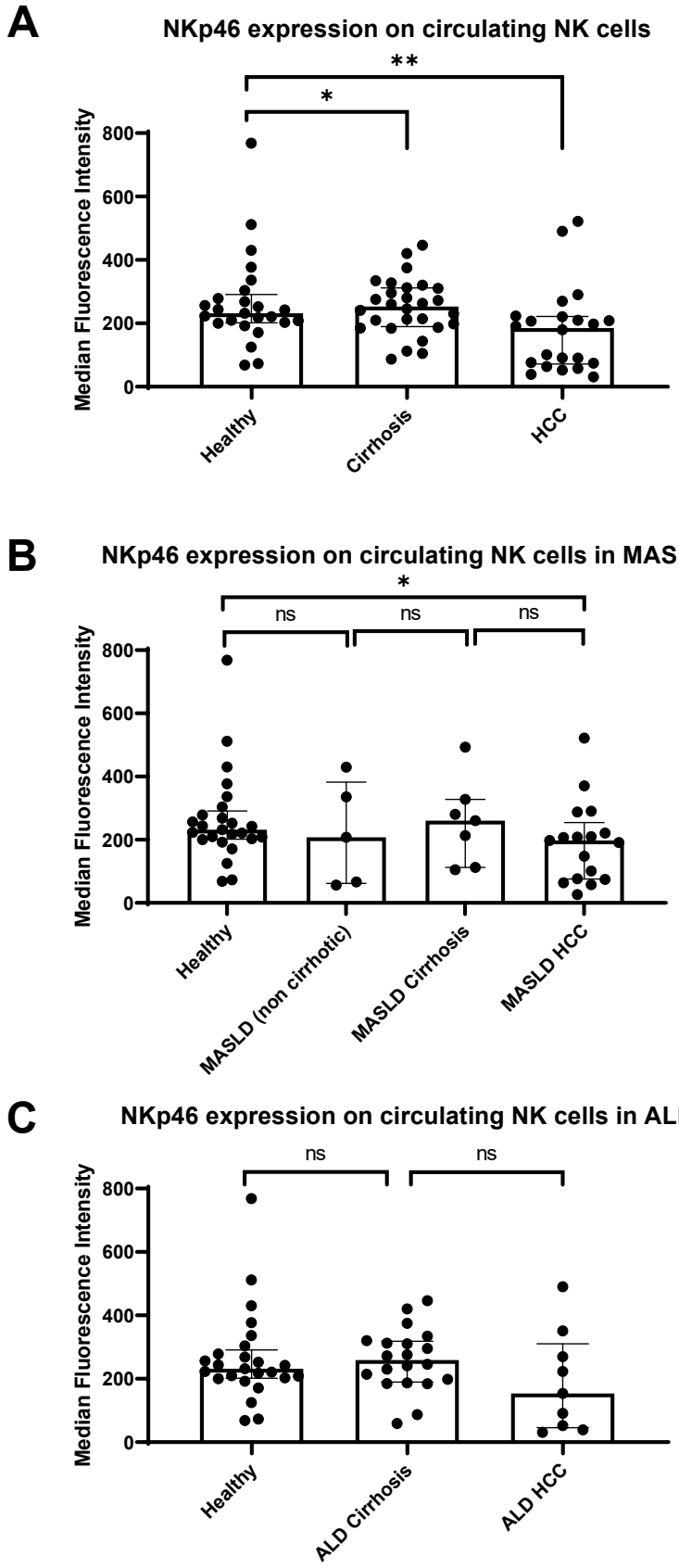


*Figure 28 NKp46 expression on circulating NK cells. A) The median fluorescence intensity (MFI) of NKp46 on all circulating NK cells in healthy volunteers, patients with cirrhosis and patients with HCC on a background of cirrhosis. There was reduced expression of NKp46 on circulating NK cells in cirrhosis and HCC when compared to NK cells from healthy individuals. B) The MFI of NKp46 expression on NK cells from healthy volunteers in comparison to patients with MASLD without cirrhosis (MASLD (non-cirrhotic)), MASLD with cirrhosis (MASLD cirrhosis) and MASLD cirrhosis with HCC (MASLD HCC). There was a reduced expression of NKp46 on circulating NK cells in patients with MASLD HCC compared to healthy volunteers, but no significant differences in expression when comparing the MASLD (non-cirrhotic) and MASLD cirrhosis group with the MASLD HCC. C) The MFI of NKp46 expression on NK cells from healthy volunteers in comparison to patients with ALD cirrhosis and patients HCC secondary to ALD cirrhosis (ALD HCC). There were no significant differences in NKp46 expression when comparing healthy individuals with patient groups with ALD. (MASLD = metabolic dysfunction-associated steatotic liver disease; ALD= Alcohol related fatty liver disease; HCC= Hepatocellular carcinoma). Graphs display individual values and the median value. Comparisons between groups have been made using the Mann-Whitney test. Error bars represent the interquartile range. P values are denoted on the figures as follows: * p<0.05, ** p<0.01, *** p<0.001, **** p<0.0001.*

On direct comparison of cirrhosis groups separated by aetiology (ALD compared to MASLD), there was no significant difference in NKp46 expression (Figure 29A). The same was true for direct comparison of expression in patients with ALD HCC compared to MASLD HCC (Figure 29B).

NKp46 surface expression on circulating NK cells and underlying disease aetiology

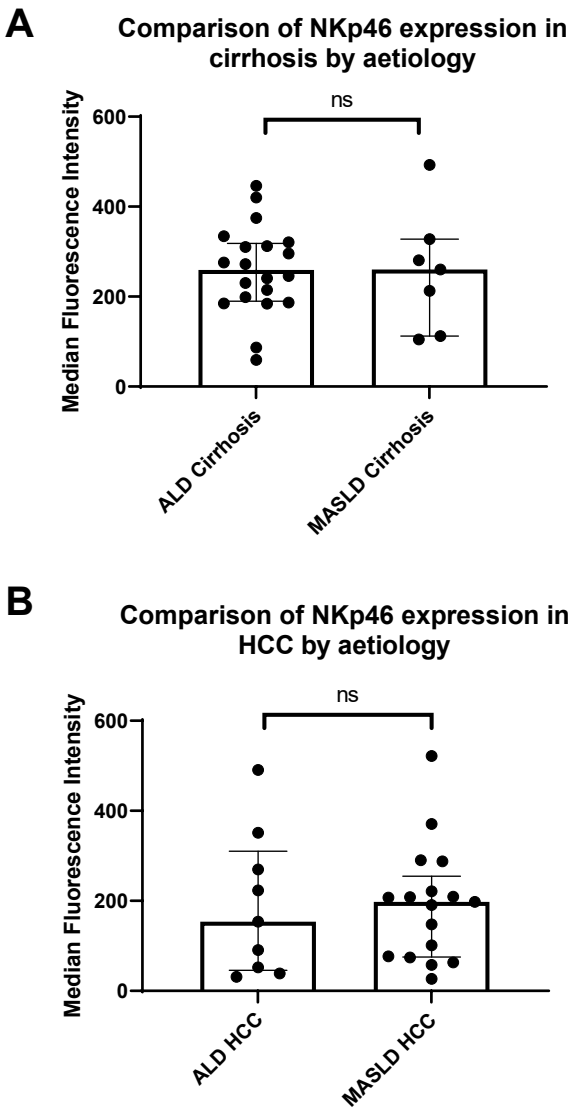


Figure 29 Comparisons of NKp46 expression in cirrhosis and HCC delineated by underlying aetiology. A) The median fluorescence intensity (MFI) of NKp46 on circulating NK cells was compared between patients with cirrhosis secondary to ALD (ALD cirrhosis) with patients with cirrhosis secondary to MASLD (MASLD cirrhosis). There was no significant difference in the circulating NK cell expression of NKp46 between patients with ALD cirrhosis and patients with MASLD cirrhosis. B) The MFI of NKp46 on circulating NK cells was compared between patients with HCC secondary to ALD cirrhosis (ALD HCC) and patients with HCC secondary to MASLD cirrhosis (MASLD HCC). There was no significant difference in NKp46 expression on circulating NK cells between both patient groups. (MASLD = metabolic dysfunction-associated steatotic liver disease; ALD= Alcohol related fatty liver disease; HCC= Hepatocellular carcinoma).

(Graphs display individual values and the median value. Comparisons between groups have been made using the Mann-Whitney test. Error bars represent the interquartile range).

NKp46 expression did not correlate with Child-Pugh or MELD-Na composite scores (Figure 30) and there were no differences seen in NKp46 expression in HCC when split by BCLC staging (Figure 31).

NKp46 expression on circulating NK cells and underlying cirrhosis status

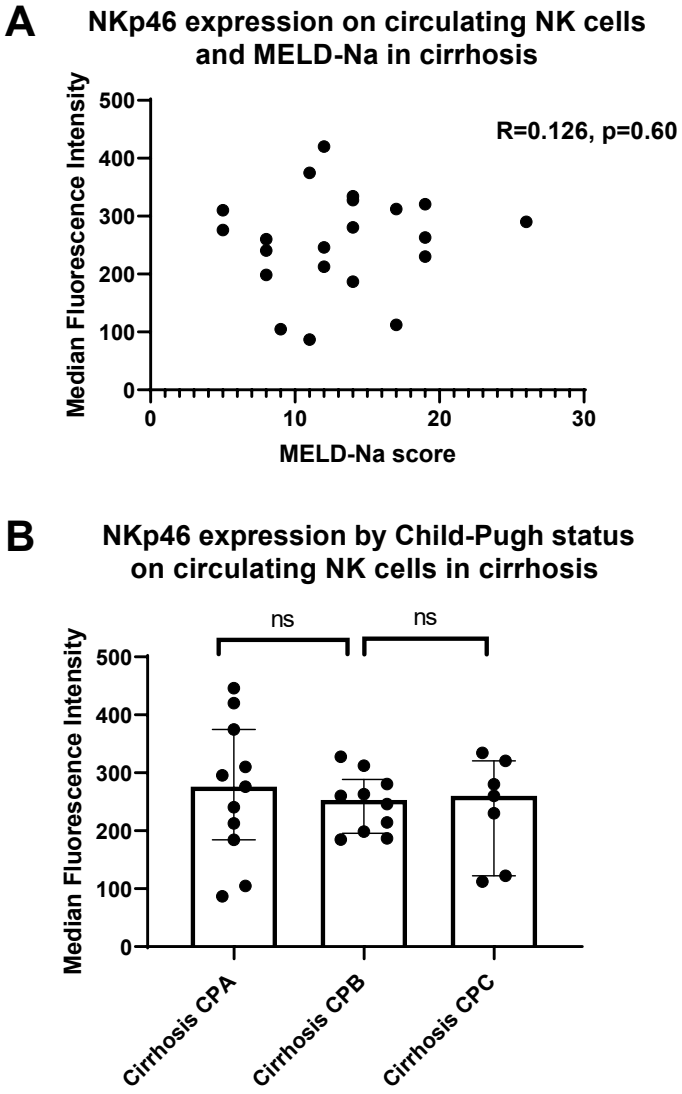


Figure 30 NKp46 expression on circulating NK cells in cirrhosis and underlying MELD-Na score and Child-Pugh classification. NKp46 expression (median fluorescence intensity) on circulating NK cells was determined in patients with cirrhosis. A) NKp46 expression did not correlate with MELD-Na score in patients with cirrhosis without HCC (spearman rank correlation). B) There were no differences in NKp46 expression on circulating NK cells in patients with cirrhosis categorised by Child-Pugh status (CPA= Child-Pugh A, CPB = Child-Pugh B, CPC = Child-Pugh C). (Graphs display individual values, and the median value is displayed by the bar. Comparisons between groups have been made using the Mann-Whitney test. Error bars represent the interquartile range). Analyses were repeated for patients with MASLD cirrhosis and for ALD cirrhosis but did not demonstrate correlation with MELD-Na or significance between Child-Pugh status.

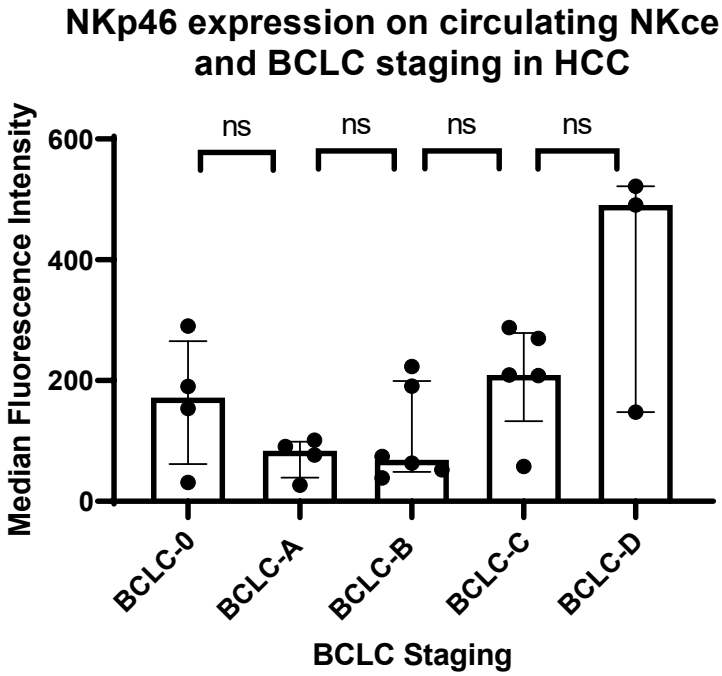


Figure 31 NKp46 expression (median fluorescence intensity) on circulating NK cells in individuals with HCC analysed by Barcelona Clinic Liver Cancer (BCLC) classification. Comparisons between groups with different stages did not reveal a difference in NKp46 expression (Kruskal-Wallis test with Dunn's multiple comparisons). (Graphs display individual values and the median value. Error bars represent the interquartile range).

Finally, no differences were seen between disease groups in NKp46 expression on intrahepatic NK cells and no significant differences were detected in expression of NKp46 on intrahepatic NK cells in comparison to circulating NK cells from the same donors, although patient numbers may not have been large enough to detect differences (Figure 32 B).

Surface expression of NKp46 on intrahepatic NK cells

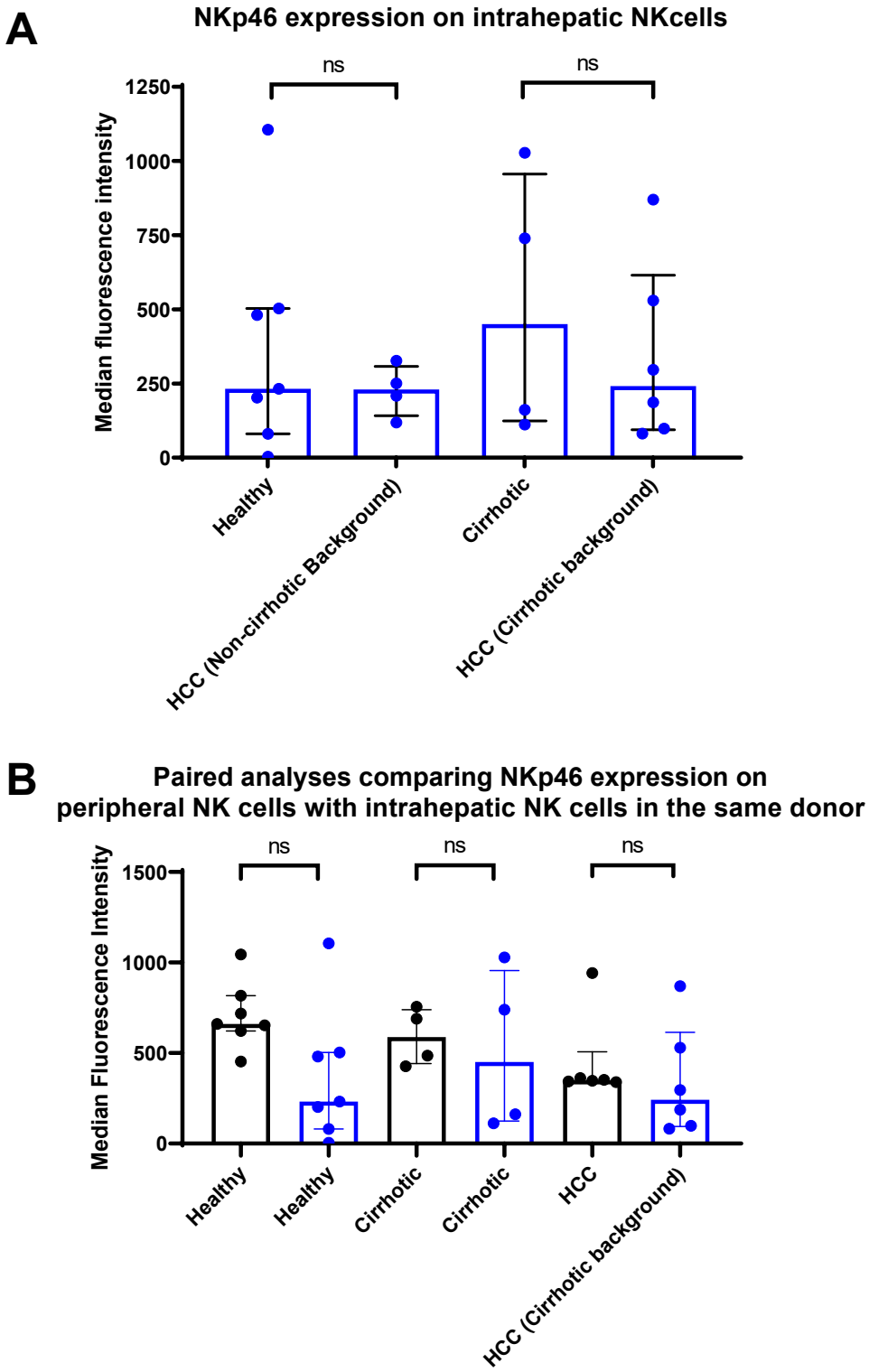


Figure 32 NKp46 expression on intrahepatic NK cells. A) Intrahepatic NK cell expression of NKp46 (median fluorescence intensity). Comparisons between groups have been made using

*the Mann-Whitney test. B) Comparison of NKp46 expression in circulating NK cells (data in black) compared to intrahepatic NK cells (data in blue) from the same donor. Comparisons were made using the non-parametric Wilcoxon matched-pairs signed rank test. Graphs display individual values and the median value. Error bars represent the interquartile range .P values are denoted on the figures as follows: * p<0.05, ** p<0.01, *** p<0.001, **** p<0.0001).*

3.1.3 Inhibitory receptor - CD161 expression

CD161 is an inhibitory receptor, expressed by the majority of NK cells. Interaction with the ligand for CD161, LLT1, results in impaired NK cell cytotoxicity and interferon gamma release. In order to determine if NK cells in disease may have impaired function secondary to an increase in inhibitory cell signalling, CD161 expression was determined using flow cytometry techniques after staining with Phenotyping Panel 1 (Table 3). (Figure 33).

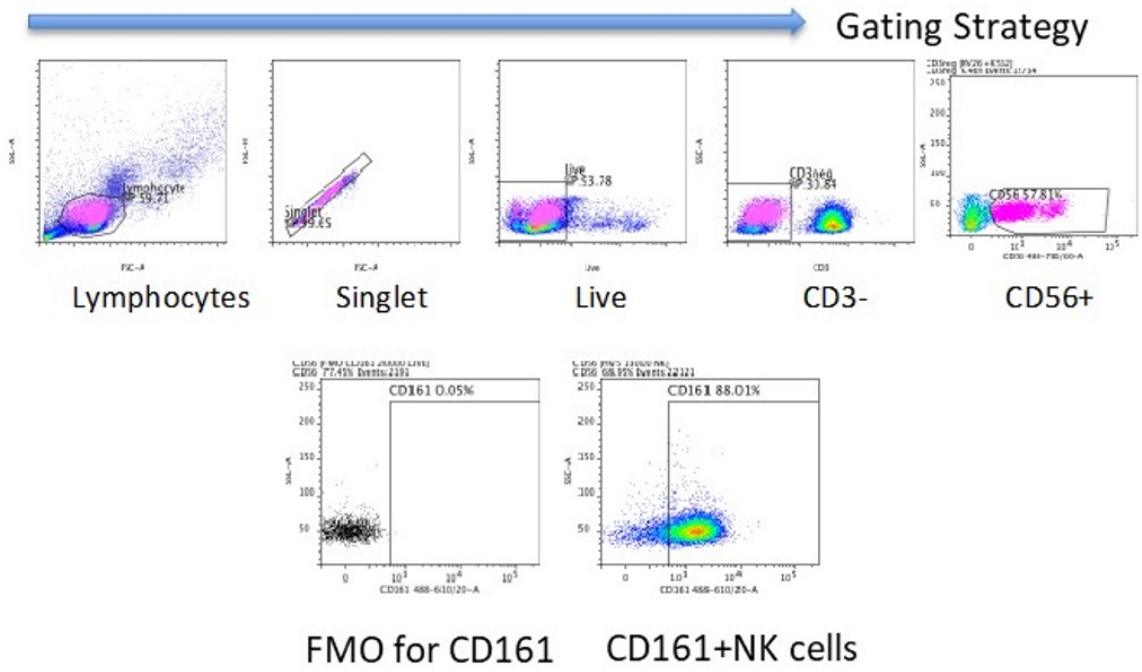


Figure 33 Gating strategy for circulating and intrahepatic CD161+NK cells using flow cytometry. Following gating for lymphocytes, singlet gating and live cells, CD3-CD56+ NK cells were selected. The percentage of NK cells expressing CD161 was determined using a fluorescence minus one (FMO) control.

Surface expression of CD161 on circulating NK cells

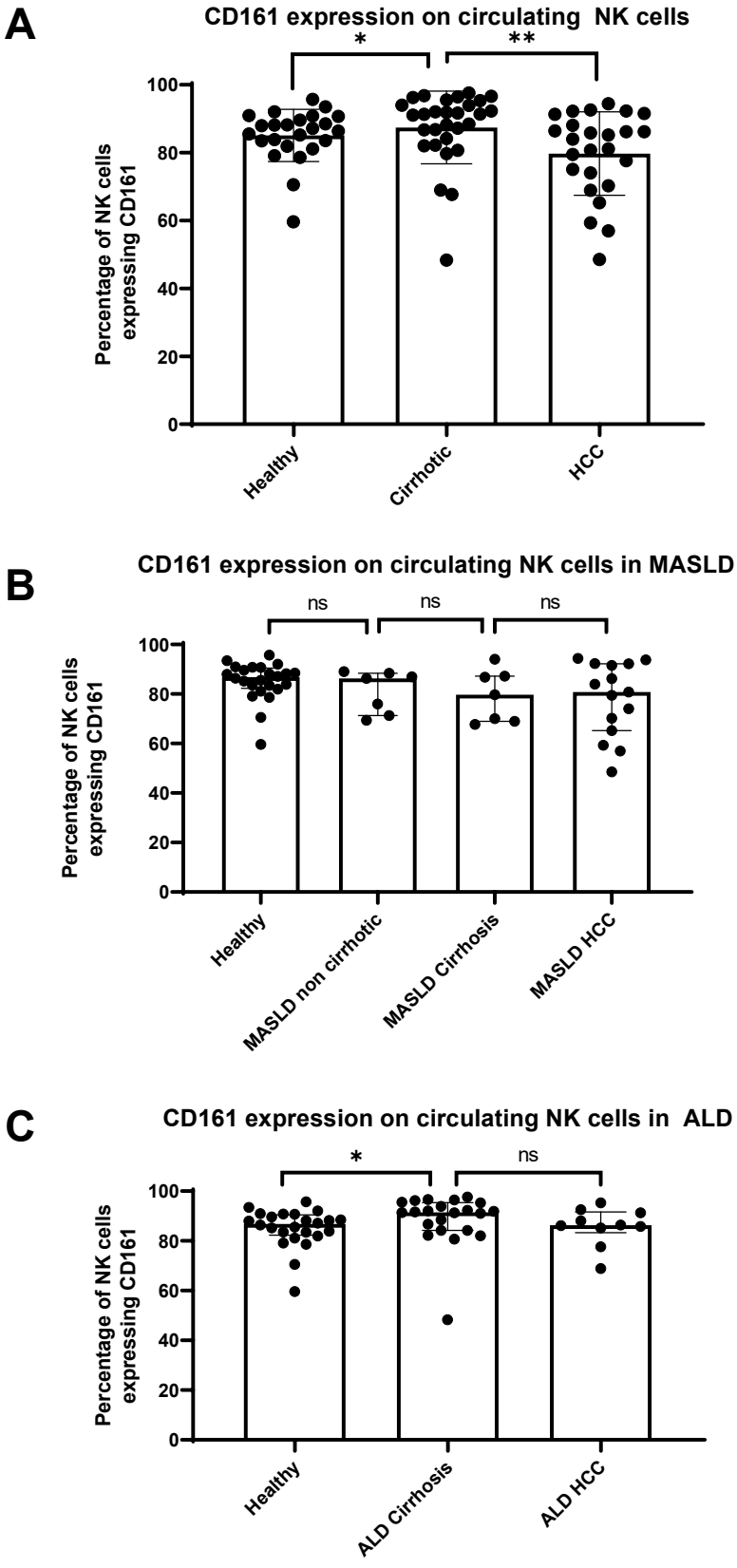


*Figure 34 CD161 expression on circulating NK cells. Graphs demonstrate the percentage of all circulating NK cells that express CD161. A) CD161+NK cells as a proportion of all circulating NK cells in healthy volunteers, patients with cirrhosis and patients with HCC. There is a significantly increased proportion of circulating CD161+NK cells in patients with cirrhosis compared to healthy individuals, and patients with HCC on a background of cirrhosis (B) CD161+NK cells as a proportion of all NK cells from healthy volunteers in comparison to patients with MASLD without cirrhosis (MASLD (non-cirrhotic)), MASLD with cirrhosis (MASLD cirrhosis) and MASLD cirrhosis with HCC (MASLD HCC). There were no significant differences in the proportion of circulating CD161+NK cells between population groups. C) CD161+NK cells as a proportion of all NK cells from healthy volunteers in comparison to patients with ALD cirrhosis and patients with ALD cirrhosis and HCC (ALD HCC). Again there was a significantly higher circulating proportion of CD161+ NK cells in patients with ALD cirrhosis compared to healthy individuals (median values 91.5% vs 86.7%, p=0.01) (MASLD= metabolic dysfunction-associated steatotic liver disease; ALD= Alcohol related fatty liver disease; HCC= Hepatocellular carcinoma). (Graphs display individual values with the median value displayed by the bar. Comparisons between groups have been made using the Mann-Whitney test. Error bars represent the interquartile range. P values are denoted on the figures as follows: * p<0.05, ** p<0.01, *** p<0.001, **** p<0.0001).*

CD161 expression was increased in cirrhosis, circulating CD161+NK cells in comparison to healthy volunteers (Figure 34A), though significance was lost in the MASLD groups (Figure 34B). There was an increased proportion of CD161+NK cells in ALD related cirrhosis compared with MASLD related cirrhosis (Figure 35).

CD161 surface expression on circulating NK cells and underlying disease aetiology

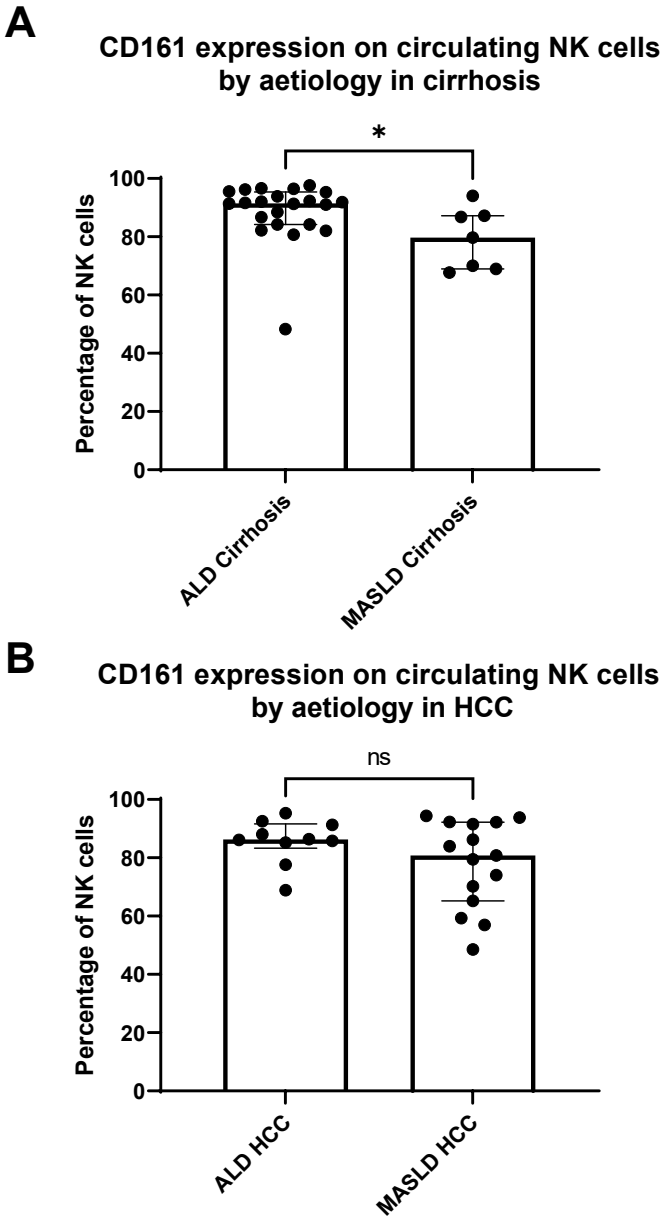


Figure 35 Comparing the proportion of circulating CD161+NK cells in cirrhosis and in HCC delineated by underlying aetiology. Graphs demonstrated the percentage of NK cells expressing CD161. A) The proportion of circulating CD161+NK cells in patients with cirrhosis secondary to ALD (ALD cirrhosis) was compared to patients with cirrhosis secondary to MASLD (MASLD cirrhosis). There was a significantly increased proportion of circulating CD161+ NK cells in ALD cirrhosis compared to MASLD cirrhosis (median values 91.3% vs 79.7%, p=0.02) B) The proportion of circulating CD161+NK cells in patients with HCC secondary to ALD cirrhosis (ALD HCC) was compared to patients with HCC secondary to MASLD cirrhosis (MASLD HCC).

*Comparisons between these two groups of patients with HCC did not reveal a significant difference. (MASLD= metabolic dysfunction-associated steatotic liver disease; ALD= Alcohol related fatty liver disease; HCC= Hepatocellular carcinoma). (Graphs display individual values and the median value. Comparisons between groups are made using the Mann-Whitney test. Error bars represent the interquartile range. P values are denoted on the figures as follows: * p<0.05, ** p<0.01, *** p<0.001, **** p<0.0001).*

CD161 expression did not correlate with the MELD-Na score in cirrhosis and there were no significant differences in expression in cirrhosis between Child-Pugh score categories (Figure 36). CD161 expression did not show any significant differences between BCLC staging in patients with HCC (Figure 37).

CD161 expression on circulating NK cells and underlying cirrhosis status

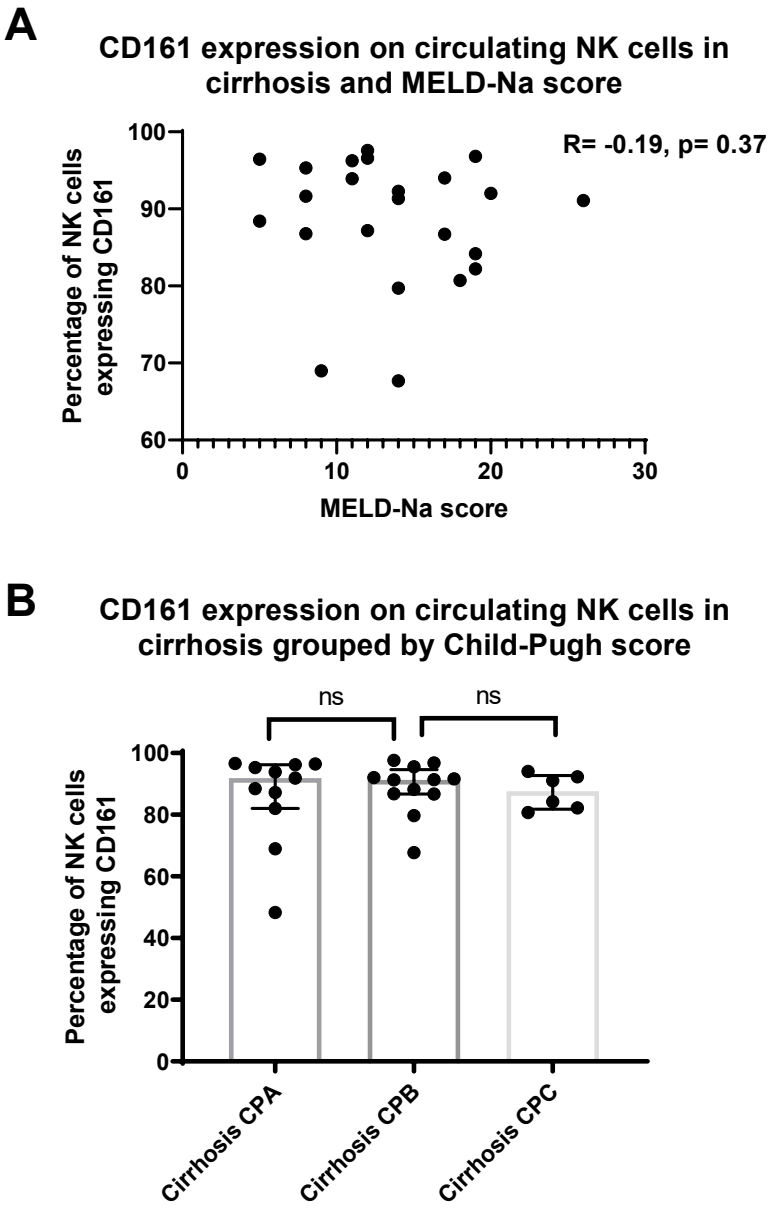


Figure 36 *CD161 expression on circulating NK cells in cirrhosis and underlying MELD-Na score and Child-Pugh classification. CD161+NK cells were determined in patients with cirrhosis using flow cytometry. Graphs display the percentage of circulating NK cells that expressed CD161. A) CD161+NK cell proportion did not correlate with MELD-Na score in patients with cirrhosis without HCC (spearman rank correlation). B) The circulating CD161+NK cell proportion in patients with cirrhosis did not differ by underlying Child-Pugh status (CPA= Child-Pugh A, CPB = Child-Pugh B, CPC = Child-Pugh C). (Graphs display individual values, and the median value is also displayed on the bar graph. Comparisons between groups have been made using the*

*Mann-Whitney test. Error bars represent the interquartile range. P values are denoted on the figures as follows: * p<0.05, ** p<0.01, *** p<0.001, **** p<0.0001). Analyses were repeated for patients with MASLD cirrhosis and for ALD cirrhosis but did not demonstrate correlation with MELD-Na or significance between Child-Pugh status.*

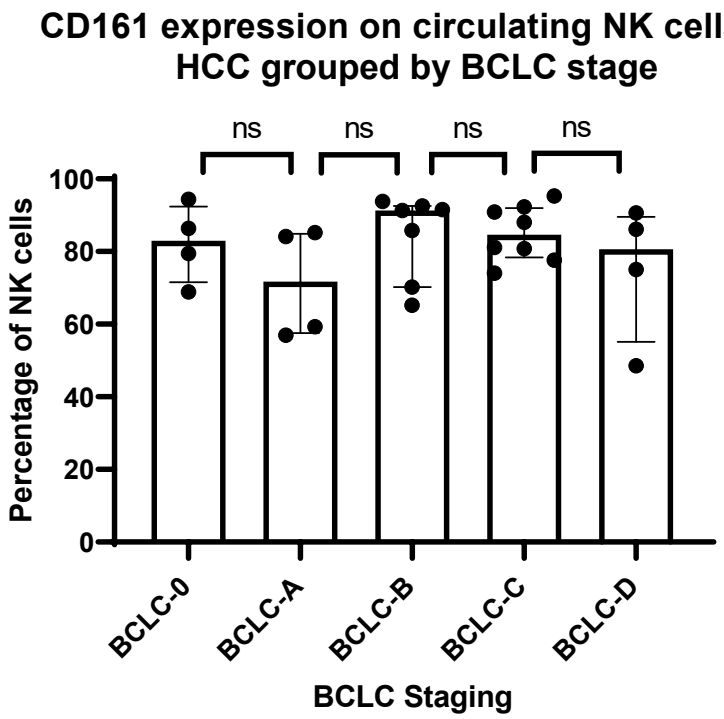


Figure 37 The proportion of CD161+NK cells in the circulation in patients with HCC on a background of cirrhosis categorised by BCLC staging. Graph displays the percentage of circulating CD161+NK cells. Comparisons between groups with different stages did not reveal a difference in the circulating proportion of CD161+NK cells. (Kruskal-Wallis test with Dunn's multiple comparisons). (Graphs display individual values and the median value. Error bars represent the interquartile range).

Overall, there was a greater proportion of CD161+ intrahepatic NK cells compared to circulating NK cells, however this did not reach significance (Figure 38B). There were no significant differences in intrahepatic CD161 expression on NK cells between different disease groups, although sample sizes were small (Figure 38A).

Surface expression of CD161 on intrahepatic NK cells

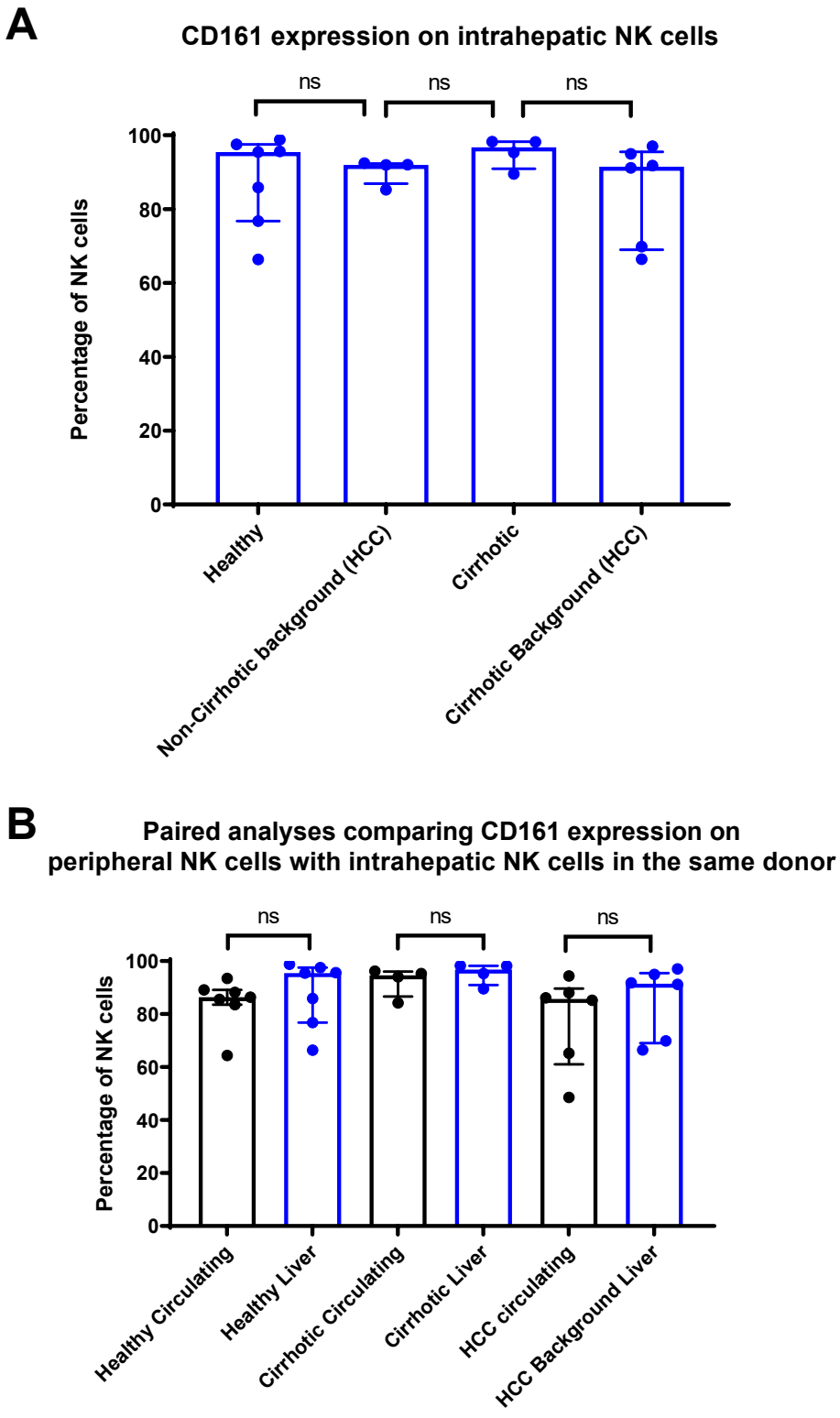


Figure 38 CD161 expression on intrahepatic NK cells. Graph displays the percentage of CD161+NK cells. A) CD161 expression on intrahepatic NK cells, expressed as a proportion of

*total intrahepatic NK cells. Comparisons between groups have been made using the Mann-Whitney test. B) Comparison of CD161 expression in circulating NK cells (data in black) compared to intrahepatic NK cells (data in blue) from the same donor. Comparisons were made using the non-parametric Wilcoxon matched-pairs signed rank test. Graphs display individual values and the median value. Error bars represent the interquartile range. P values are denoted on the figures as follows: * p<0.05, ** p<0.01, *** p<0.001, **** p<0.0001).*

3.1.5 NK subpopulations as characterised by CD16 expression

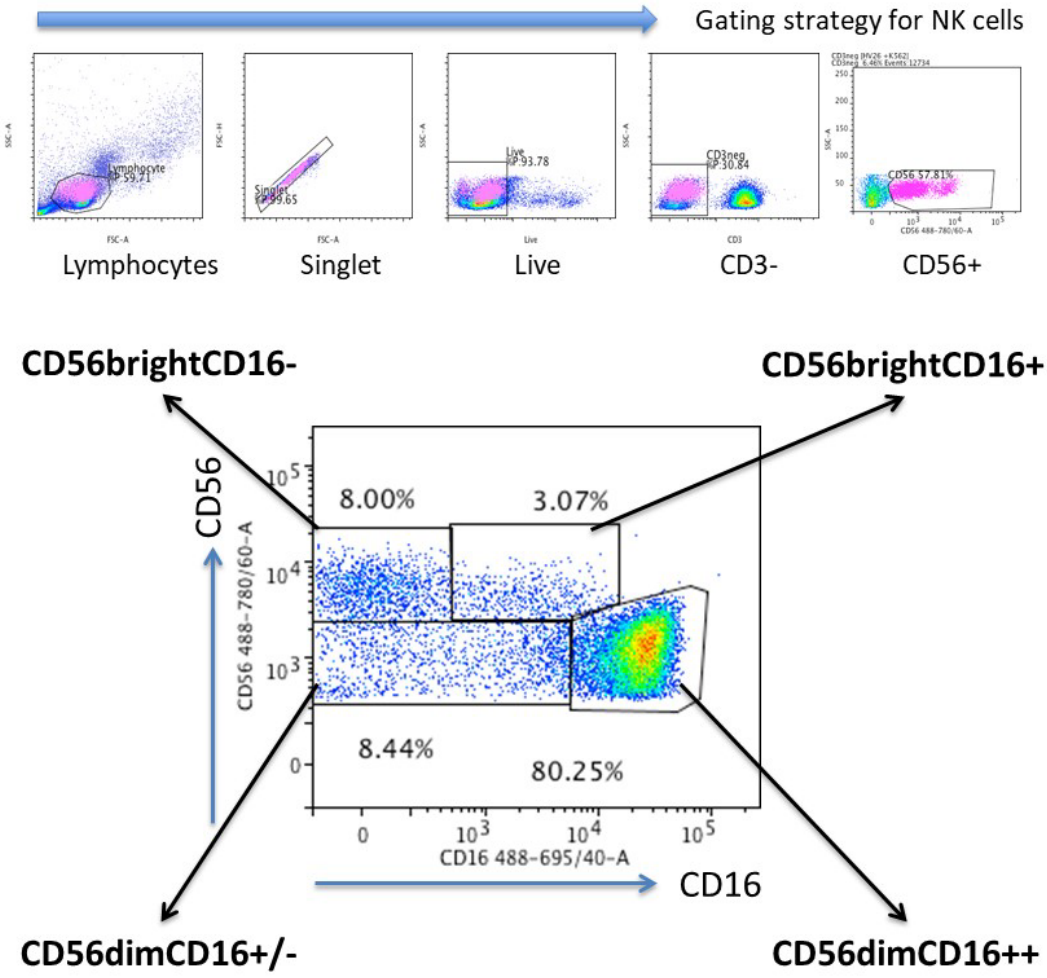


Figure 39 Gating strategy for CD3-CD56+ NK cell subpopulations based on CD16 expression. Following gating on lymphocytes, singlet cells and live cells, NK cells were selected by gating on CD3-CD56+ cells. NK cell subpopulations were then gated based on CD56 and CD16 expression.

Circulating NK cells are classically comprised of two populations based on CD16 expression. The majority are mature CD56dimCD16++ NK cells, and the remained 5-10% of circulating NK cells are CD56brightCD16- NK cells (Abel et al., 2018). NK cells were placed into four groups based on CD56 and CD16 expression (Figure 39). Figure 40 demonstrates the gating applied to peripheral blood samples from healthy donors, patients with cirrhosis and patients with cirrhosis and HCC an example of intrahepatic NK cell gating following staining of NK cells with Phenotyping Panel 1 (Table 3).

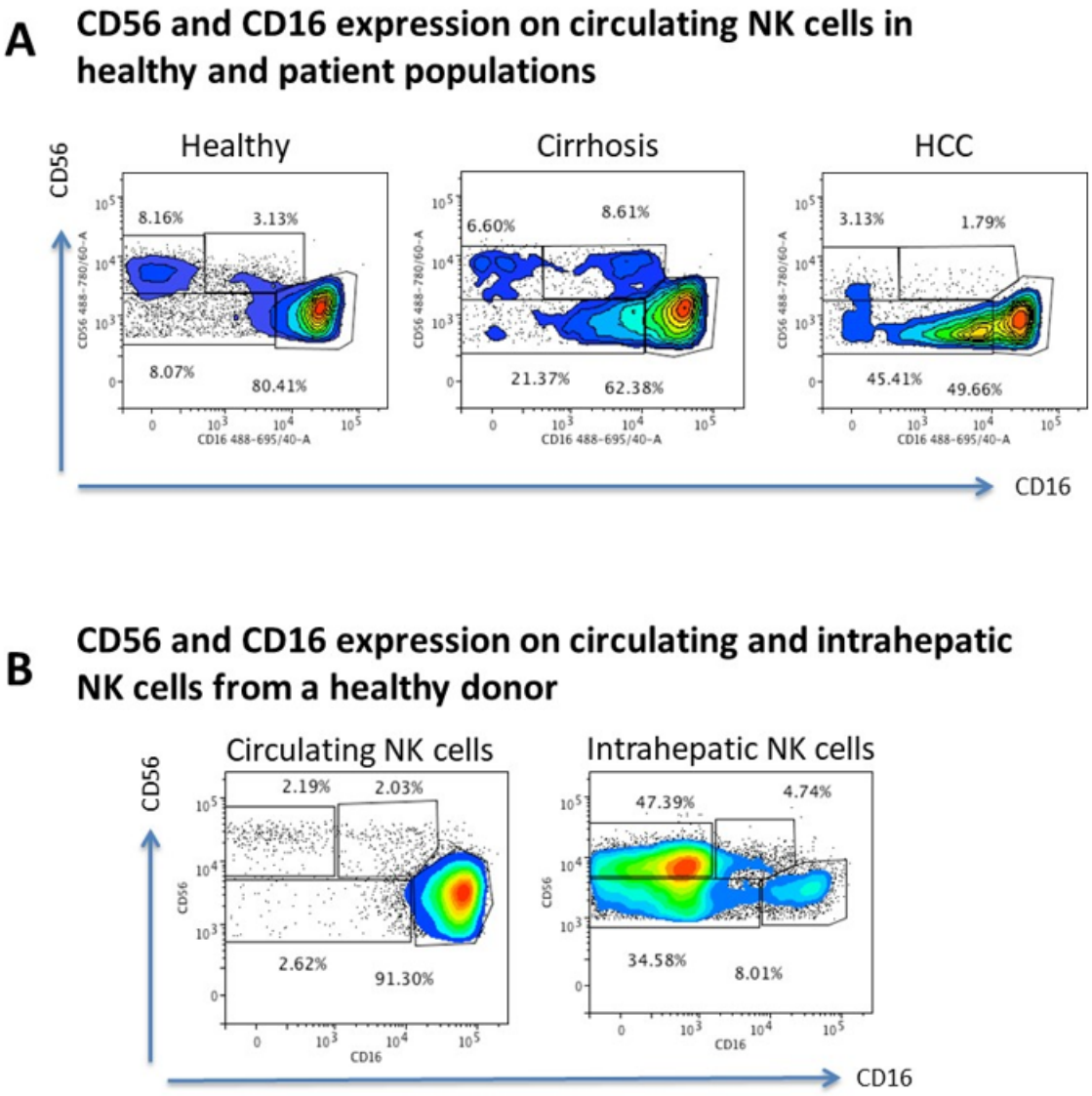


Figure 40 CD56 and CD16 gating applied to peripheral blood and intrahepatic samples. A) Representative flow cytometry plots demonstrating circulating NK cell subsets as determined by CD56 and CD16 expression in healthy, cirrhosis and HCC patient groups. B) NK cell subsets as determined by CD56 and CD16 expression on circulating NK cells from a healthy individual compared to intrahepatic NK cells from healthy liver tissue (representative flow cytometry plots from a matched paired sample from the same donor).

There was a significant increase in the proportion of circulating CD56dim NK cells with low or intermediate CD16 expression (CD56dimCD16+/-) in cirrhosis and HCC in comparison to healthy volunteers (16.57% vs. 9.66%, cirrhosis vs. healthy, p= 0.004; 18.65% vs. 9.66%, HCC vs. healthy p=0.003) with a corresponding relative decrease in the circulating proportions of CD56dimCD16++ NK cells (65.14% vs. 80.04%, cirrhosis vs. healthy, p=0.02; 52.84% vs. 80.04%, HCC vs. healthy, p=0.0004) (Figure 41).

Circulating CD56dim NK cell subpopulations determined by CD16 expression

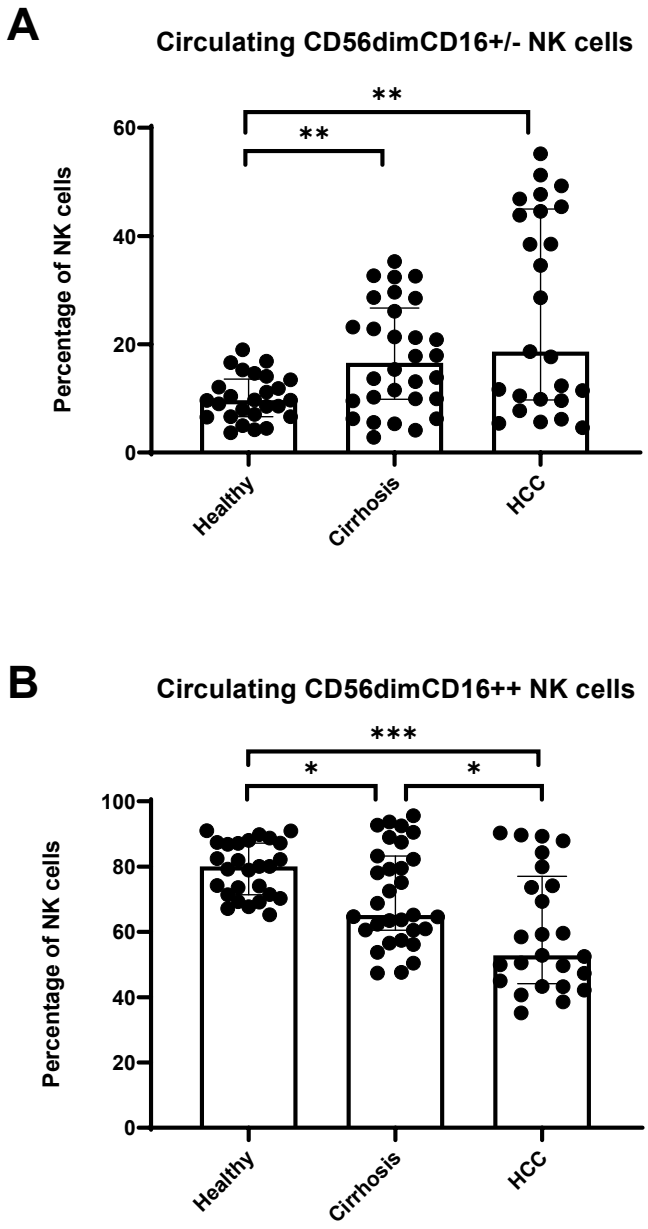


Figure 41 CD16 expression on circulating CD56dim NK cells. A) The proportion of circulating NK cells that are CD56dim NK cells with intermediate/low expression of CD16 (CD56dimCD16+/- NK cells) was increased in cirrhosis and hepatocellular carcinoma (HCC) patient groups in comparison to healthy individuals. B) The proportion of circulating NK cells that are CD56dim

*NK cells with high expression of CD16 (CD56dimCD16++ NK cells) was reduced in patients with cirrhosis and patients with HCC in comparison to healthy individuals (all data points shown; bar demonstrating median value; error bars demonstrating the interquartile range). Statistical analyses performed using the non-parametric Mann-Whitney test. P values are denoted on the figures as follows: * p<0.05, ** p<0.01, *** p<0.001, **** p<0.0001.*

There were no significant differences in the circulating CD56bright NK cell subpopulation between patient groups (Figure 42).

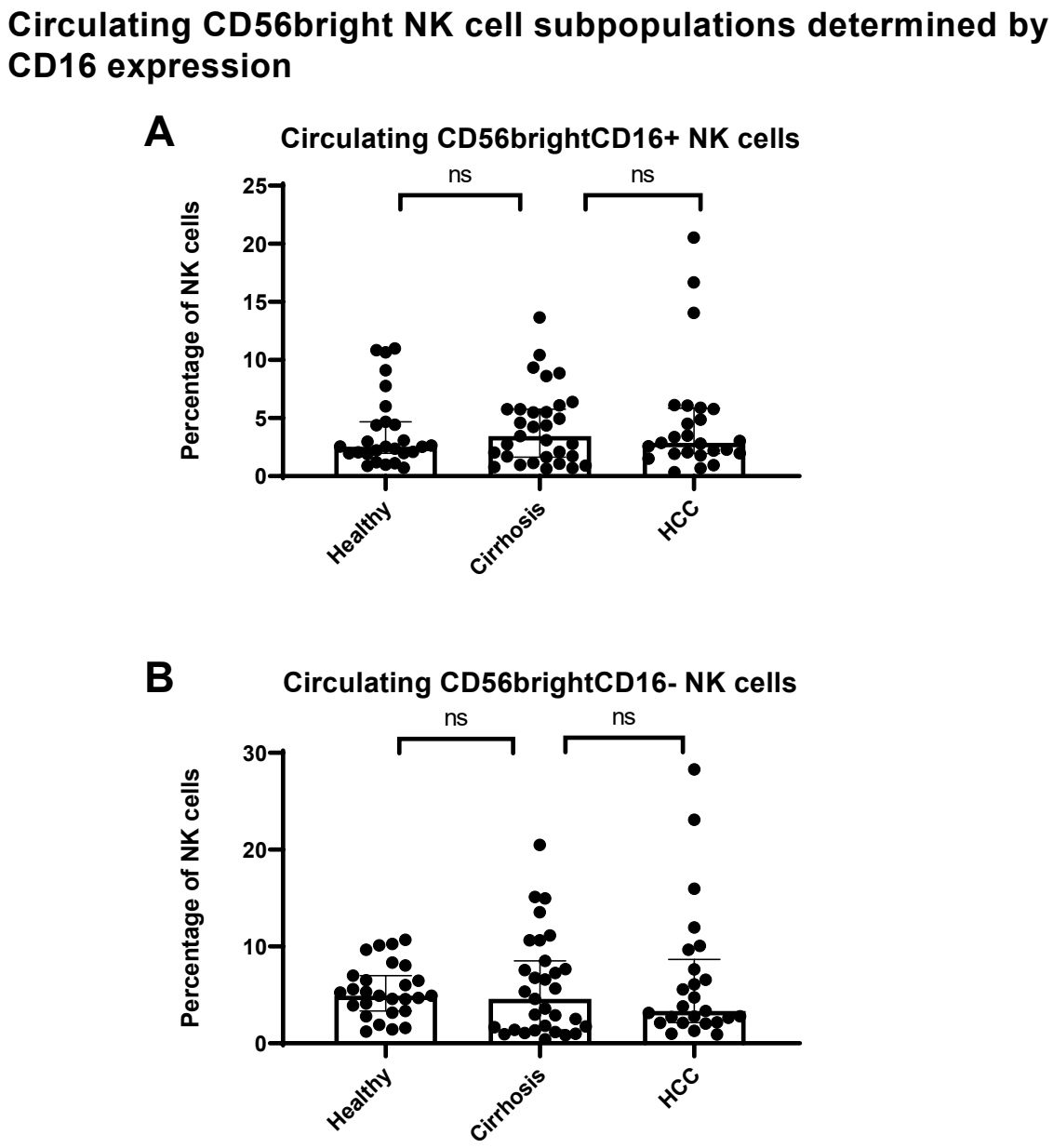


Figure 42 CD16 expression on circulating CD56bright NK cells. A) There were no significant differences in the proportion of circulating NK cells that were CD56brightCD16+ NK cells when

comparing healthy individuals, patients with cirrhosis and patients with HCC. B) There were no significant differences in the proportion of circulating NK cells that were CD56brightCD16- NK cells when comparing healthy individuals, patients with cirrhosis and patients with HCC. (all data points shown; bar demonstrating median value; error bars demonstrating the interquartile range). Statistical analyses performed using the non-parametric Mann-Whitney test.

Circulating CD56dimCD16+/- NK cells as a proportion of all circulating NK cells

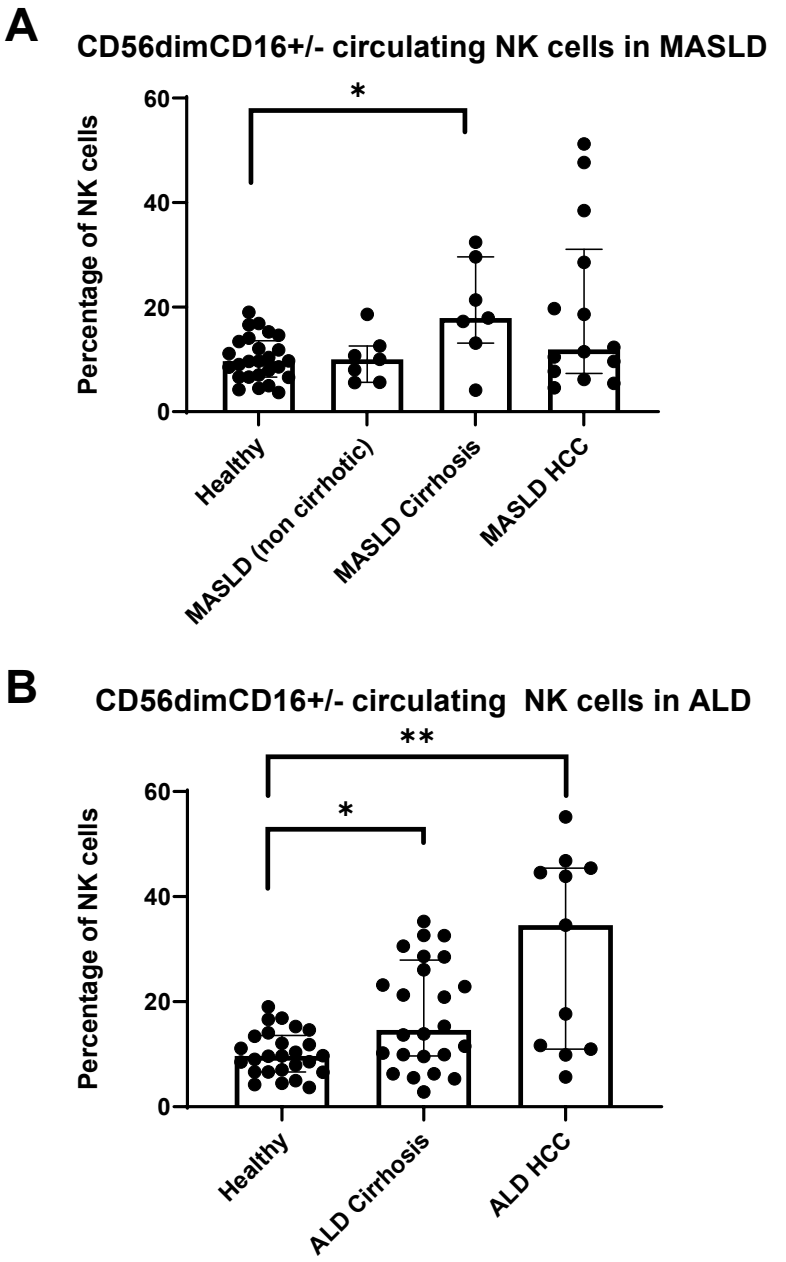


Figure 43 Circulating proportions of CD56dimCD16+/- NK cells. Graphs demonstrate the percentage of all circulating NK cells that are CD56dimCD16+/- NK cells. A) CD56dimCD16+/- NK cells as a proportion of all NK cells from healthy volunteers in comparison to patients with MASLD without cirrhosis (MASLD (non-cirrhotic), MASLD with cirrhosis (MASLD cirrhosis) and MASLD cirrhosis with HCC (MASLD HCC). There was a significantly increased proportion of CD56dimCD16+/- NK cells in patients with MASLD cirrhosis in comparison to healthy individuals. There was an increased proportion of CD56dimCD16+/- NK cells in some donors

*with MASLD HCC but this did not reach significance when compared to the other patient groups. B) CD56dimCD16+/- NK cells as a proportion of all NK cells from healthy volunteers in comparison to patients with ALD with cirrhosis (ALD cirrhosis) and ALD cirrhosis with HCC (ALD HCC). Again there was a significantly higher circulating proportion of CD56dimCD16+/- NK cells in patients with ALD cirrhosis compared to healthy individuals. There was a significantly increased proportion of CD56dimCD16+/- NK cells in patients with ALD HCC in comparison to healthy donors. (MASLD = metabolic dysfunction-associated steatotic liver disease; ALD= Alcohol related fatty liver disease; HCC= Hepatocellular carcinoma). (Graphs display individual values with the median value displayed by the bar. Comparisons between groups have been made using the Mann-Whitney test. Error bars represent the interquartile range. P values are denoted on the figures as follows: * p<0.05, ** p<0.01, *** p<0.001, **** p<0.0001).*

Patients with ALD cirrhosis and MASLD cirrhosis had an increased proportion of circulating CD56dimCD16+/- NK cells in comparison to healthy individuals (Figure 43). There were no significant differences in the proportion of circulating CD56dimCD16+/- NK cells when comparing patients with cirrhosis or HCC of differing aetiologies (ALD or MASLD) (Figure 44).

Circulating CD56dimCD16+/- NK cells, as a proportion of all NK cells, and underlying disease aetiology

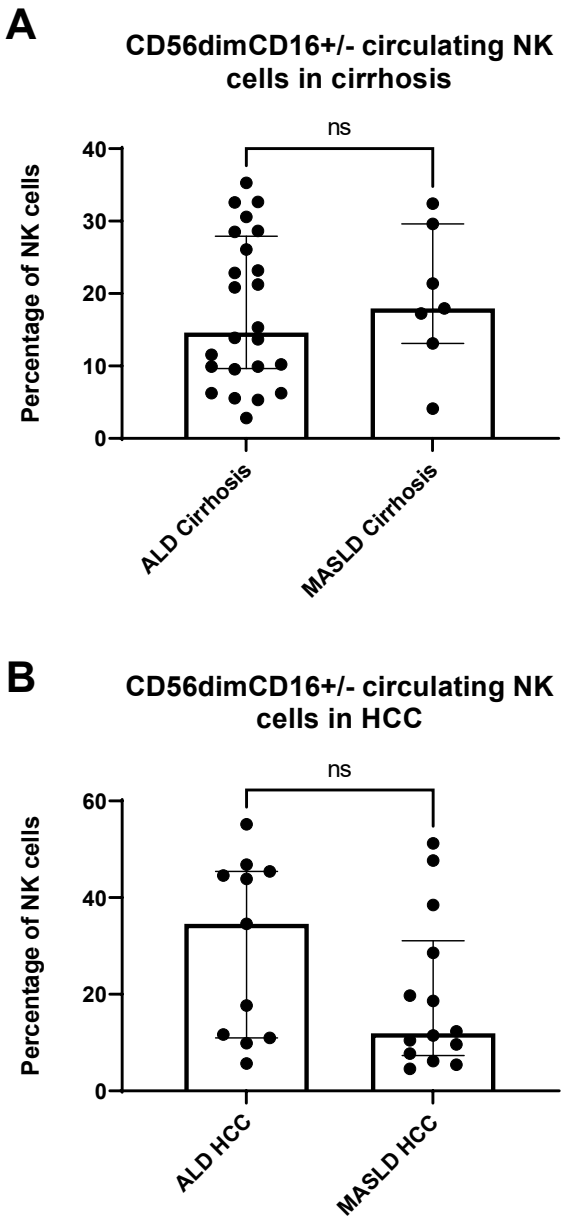


Figure 44 A comparison of the proportion of circulating CD56dimCD16+/- NK cells in cirrhosis and HCC of differing aetiologies. Graphs display the percentage of all circulating NK cells that are CD56dimCD16+/-NK cells. A) The proportion of circulating CD56dimCD16+/-NK cells was compared between patients with cirrhosis secondary to ALD (ALD cirrhosis) and patients with cirrhosis secondary to MASLD (MASLD cirrhosis). There were no significant differences in the proportion of circulating NK cells that were CD56dimCD16+/- NK cells between these two patient groups. B) The proportion of circulating NK cells that are CD56dimCD16+/- NK cells was compared between patients with HCC secondary to ALD cirrhosis (ALD HCC) and patients with

HCC secondary to MASLD cirrhosis (MASLD HCC). There were no significant differences in the proportion of circulating CD56dimCD16+/- NK cells when comparing these two patient groups (all data points shown, bar demonstrating median value, error bar demonstrating the interquartile range. Statistical analyses performed using non-parametric Mann-Whitney tests). (MASLD = metabolic dysfunction-associated steatotic liver disease; ALD= Alcohol related fatty liver disease; HCC= Hepatocellular carcinoma).

The proportion of circulating CD56dimCD16+/- NK cells did not correlate with the MELD-Na score or differ in patients with cirrhosis separated by underlying Child-Pugh status (Figure 45). The proportion of circulating CD56dimCD16+/- NK cells did not differ in patients with HCC when grouped by underlying BCLC staging (Figure 46).

The circulating proportion of NK cells that are CD56dimCD16+/- and underlying cirrhosis status

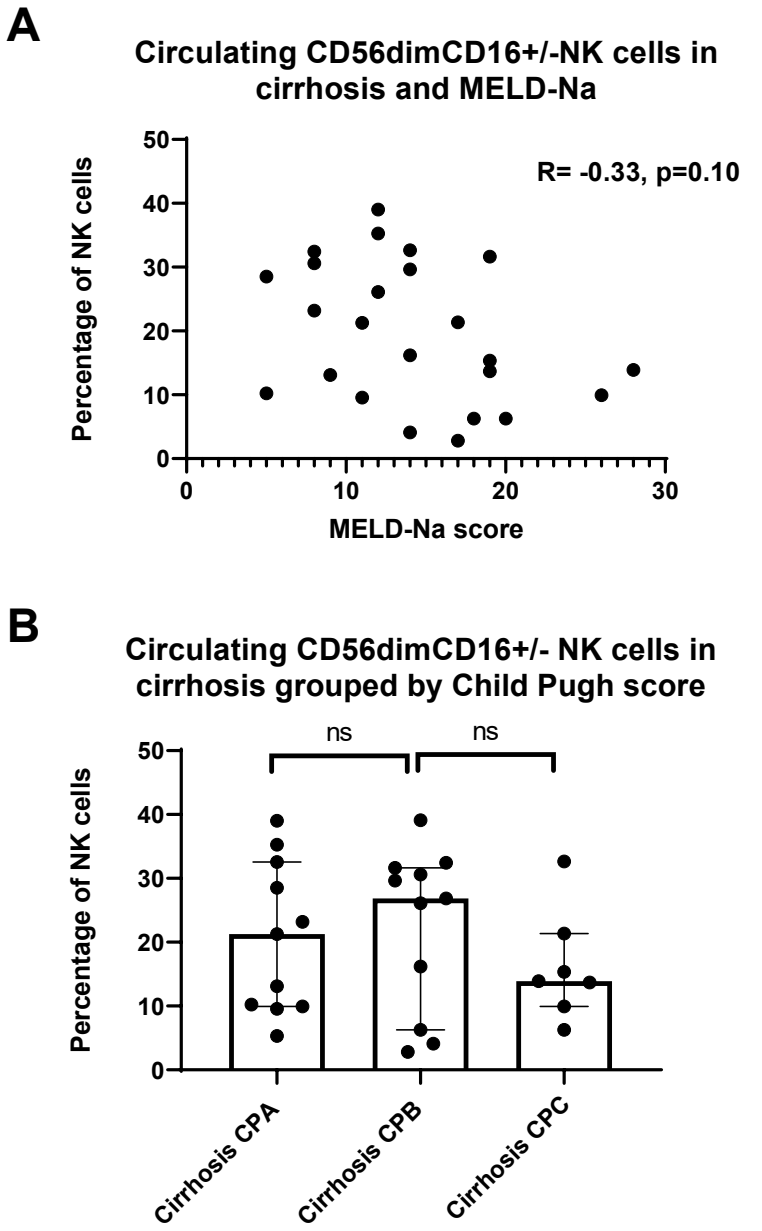


Figure 45 *Circulating CD56dimCD16+/-NK cells in cirrhosis and underlying MELD-Na score and Child-Pugh classification. The proportion of CD56dimCD16+/- circulating NK cells were determined in patients with cirrhosis. Graphs display the percentage of circulating NK cells that were CD56dimCD16+/- NK cells. A) The CD56dimCD16+/NK cell proportion did not correlate with MELD-Na score in patients with cirrhosis without HCC (spearman rank correlation). B) The circulating CD56dimCD16+/-NK cell proportion in patients with cirrhosis did not differ by underlying Child-Pugh status (CPA= Child-Pugh A, CPB = Child-Pugh B, CPC = Child-Pugh C). (Graphs display individual values, and the median value is displayed with the*

*bar. Comparisons between groups have been made using the Mann-Whitney test. Error bars represent the interquartile range. P values are denoted on the figures as follows: * p<0.05, ** p<0.01, *** p<0.001, **** p<0.0001). Analyses were repeated for patients with MASLD cirrhosis and for ALD cirrhosis but did not demonstrate correlation with MELD-Na or significance between Child-Pugh status.*

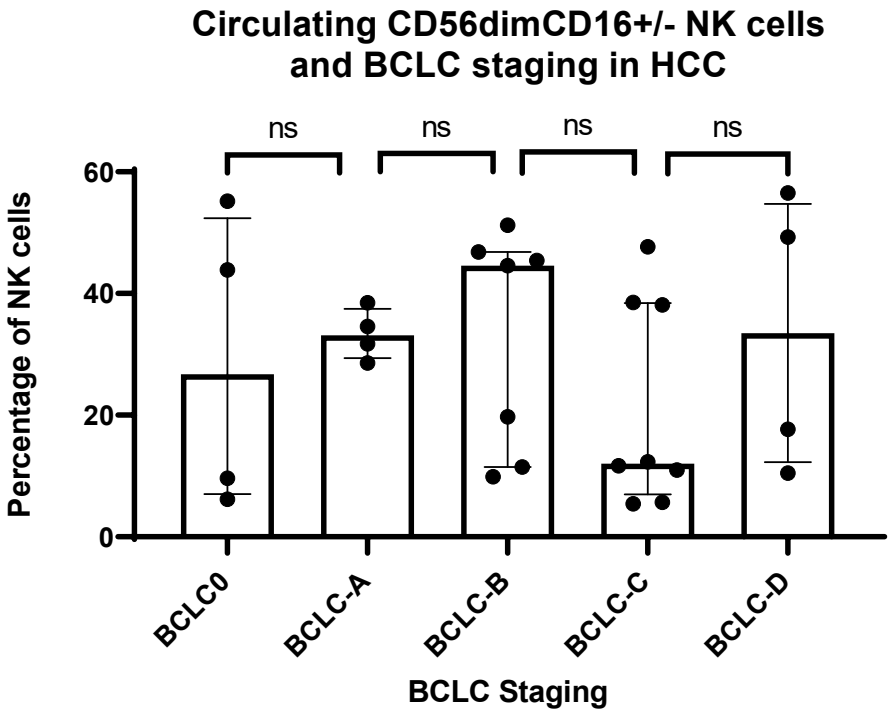


Figure 46 The proportion of CD56dimCD16+/-NK cells in the circulation in patients with HCC on a background of cirrhosis categorised by BCLC staging. Graph displays the percentage of circulating NK cells that are CD56dimCD16+/-NK cells. Comparisons between groups with different stages did not reveal a difference in the circulating proportion of CD56dimCD16+/-NK cells (Kruskal-Wallis test with Dunn's multiple comparisons). (Graphs display individual values and the median value is displayed by the bar. Error bars represent the interquartile range).

The proportion of CD56dimCD16+/-NK cells did not correlate with any other clinical parameters, tumour number, size or vascular invasion in HCC.

CD56dimCD16+/-NK cells formed a large portion of intrahepatic NK cells (median 35.8% in healthy livers). Paired analyses of circulating and intrahepatic NK cells from the same donor revealed that there was a significantly larger intrahepatic proportion

of CD56dimCD16+/-NK cells but significance was lost in the cirrhosis and HCC patient groups (Figure 47).

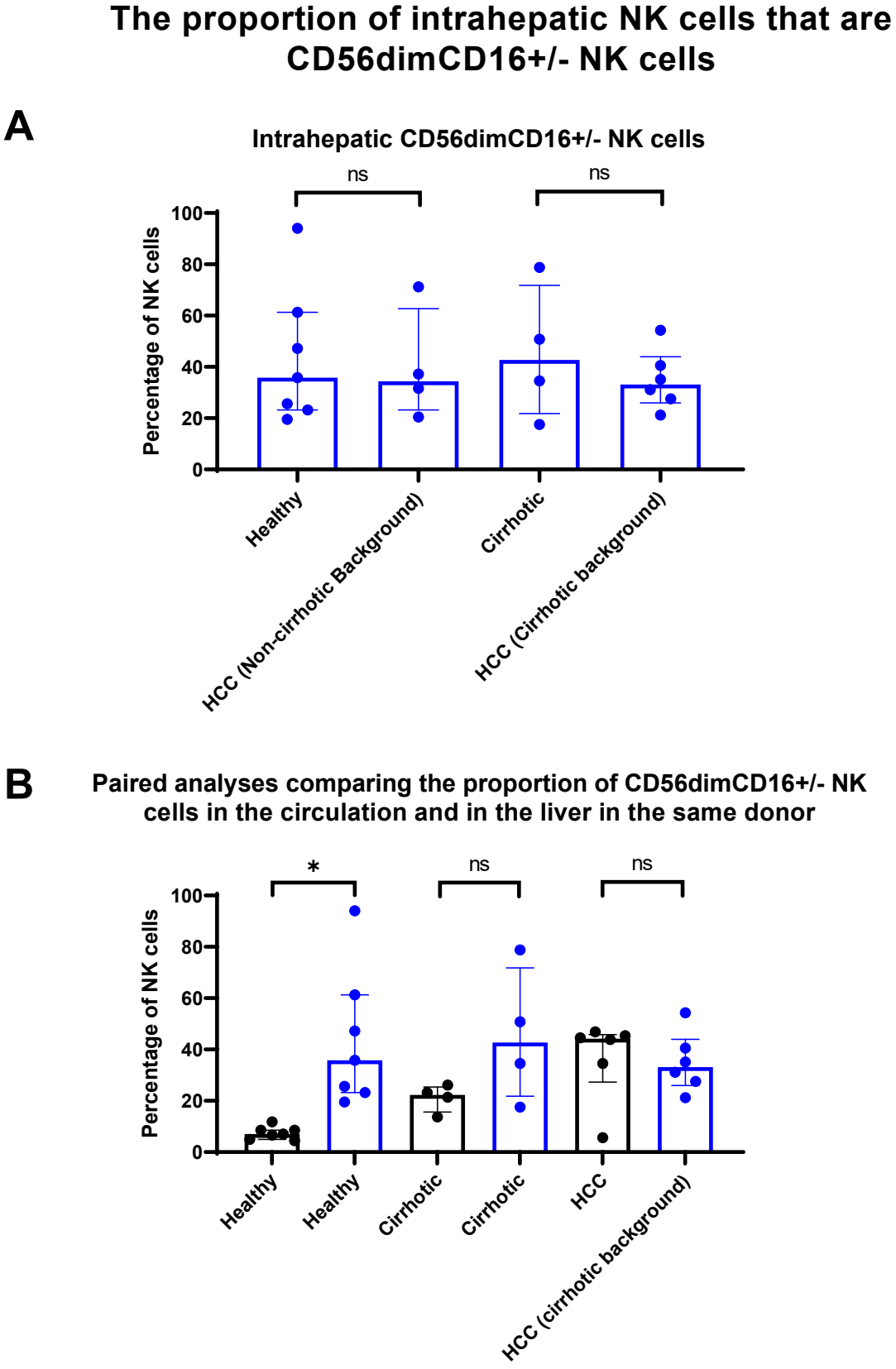


Figure 47 The proportion of intrahepatic CD56dimCD16+/-NK cells and comparison with circulating proportions of CD56dimCD16+/-NK cells. A) Graph displays the proportion of

*intrahepatic NK cells that are CD56dimCD16+/-NK cells. While CD56dimCD16+/-NK cells form a moderate proportion of total intrahepatic NK cells (median in healthy volunteers is 35.82%) there were no significant differences in the proportion of intrahepatic NK cells that are CD56dimCD16+/- when comparing healthy individuals and patient groups. Comparisons between groups have been made using the Mann-Whitney test. B) Comparison of CD56dimCD16+/-NK cells as a proportion of circulating NK cells (data in black) to intrahepatic NK cells (data in blue) from the same donor. Comparisons were made using the non-parametric Wilcoxon matched-pairs signed rank test. Graphs display individual values and the median value. Error bars represent the interquartile range. P values are denoted on the figures as follows: * p<0.05, ** p<0.01, *** p<0.001, **** p<0.0001).*

3.1.6 CXCR6 expression

Healthy intrahepatic NK cells classically express the liver homing CXCR6 and are thought not to re-enter the circulation, while circulating NK cells do not express CXCR6. In order to determine if this may be altered in liver disease and whether there may be an increased proportion of CXCR6+NK cells in the circulation, CXCR6 expression was determined in the circulation of patients with liver disease, and on intrahepatic NK cells in patients with liver disease (Phenotyping Panel 1 used (Table 3)) (Figure 48).

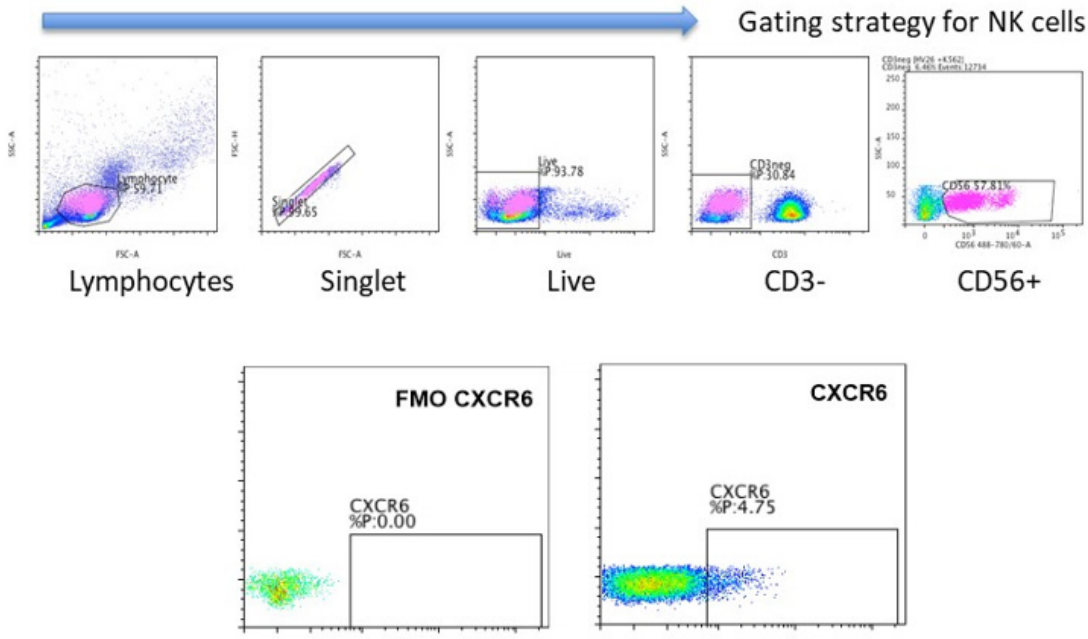
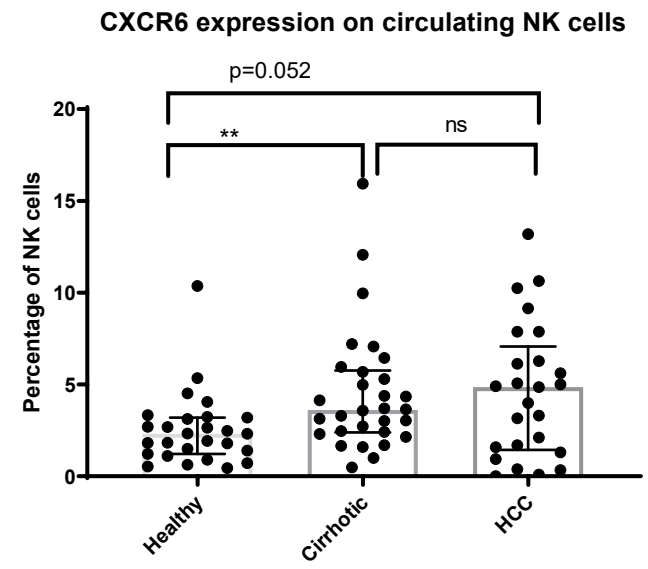


Figure 48 Gating strategy for circulating and intrahepatic CXCR6+NK cells using flow cytometry. Following gating for lymphocytes, singlet gating and live cells, CD3-CD56+ NK cells were selected as demonstrated on the density plots. The percentage of NK cells expressing CXCR6 was determined using a fluorescence minus one (FMO) control.

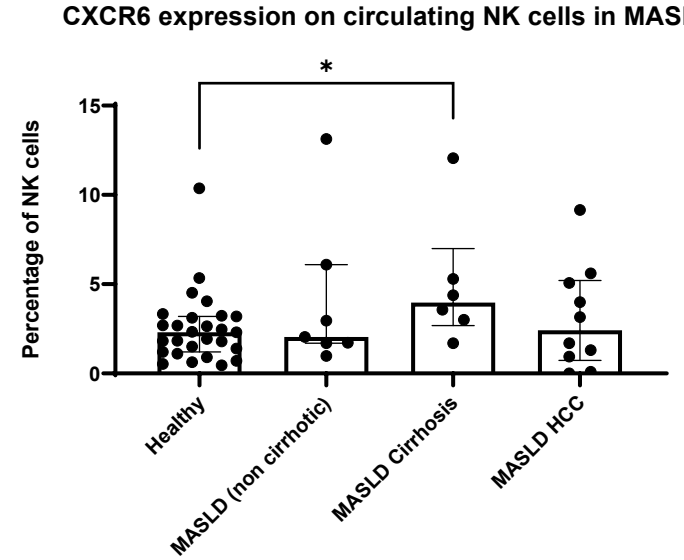
CXCR6 expression demonstrated a subtle but significant increase on circulating NK cells in cirrhosis and approached significance in patients with HCC, despite overall expression of CXCR6 remaining below 20% of all circulating NK cells (Figure 49).

Surface expression of CXCR6 on circulating NK cells

A



B



C

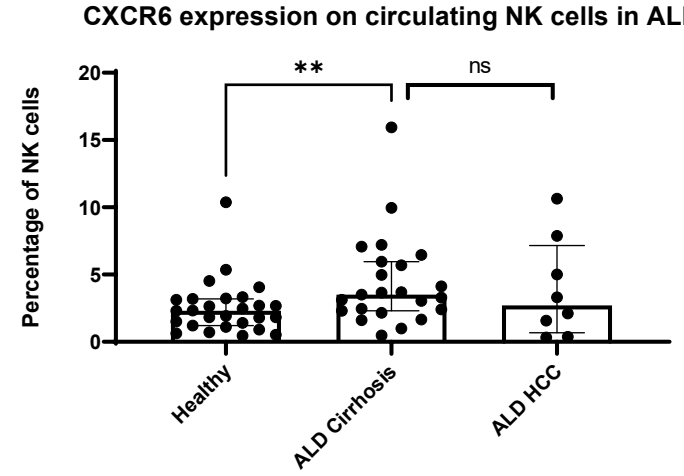


*Figure 49 CXCR6 expression on circulating NK cells. Graphs demonstrate the percentage of all circulating NK cells that express CXCR6. A) CXCR6+NK cells as a proportion of all circulating NK cells in healthy volunteers, patients with cirrhosis and patients with HCC on a background of cirrhosis. (B) CXCR6+NK cells as a proportion of all NK cells from healthy volunteers in comparison to patients with MASLD without cirrhosis (MASLD (non-cirrhotic)), MASLD with cirrhosis (MASLD cirrhosis) and MASLD cirrhosis with HCC (MASLD HCC). There was a significant increase in the proportion of CXCR6+NK cells in MASLD cirrhosis compared to healthy individuals, but significance was lost when comparing patients with MASLD cirrhosis and MASLD without cirrhosis. C) CXCR6+NK cells as a proportion of all NK cells from healthy volunteers in comparison to patients with ALD cirrhosis and patients with ALD cirrhosis and HCC (ALD HCC). Again there was a significantly higher circulating proportion of CXCR6+NK cells in patients with ALD cirrhosis compared to healthy individuals. (MASLD = metabolic dysfunction-associated steatotic liver disease; ALD= Alcohol related fatty liver disease; HCC= Hepatocellular carcinoma). (Graphs display individual values and the median value is displayed by the bar. Comparisons between groups have been made using the Mann-Whitney test. Error bars represent the interquartile range. P values are denoted on the figures as follows: * p<0.05, ** p<0.01, *** p<0.001, **** p<0.0001).*

There was no significant difference in the proportion of circulating CXCR6+ NK cells when comparing patients with cirrhosis or with HCC and different aetiologies (ALD vs MASLD) (Figure 50).

CXCR6 surface expression on circulating NK cells and underlying disease aetiology

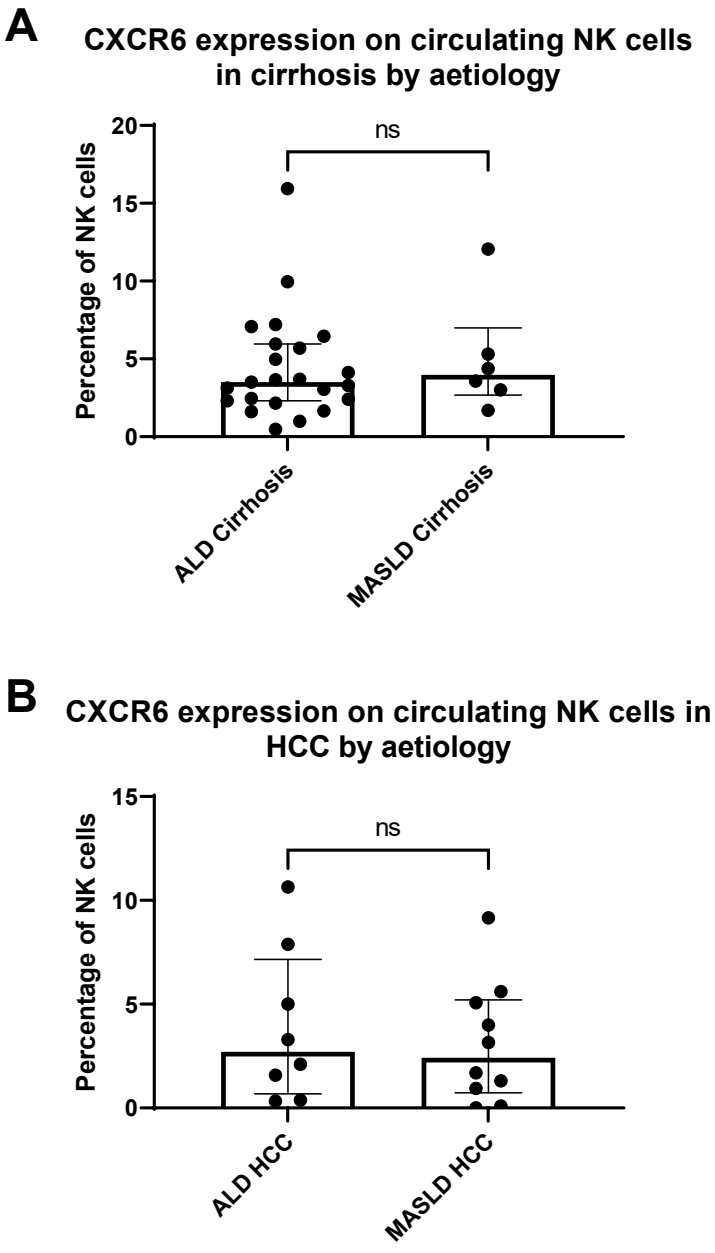


Figure 50 Comparing the proportion of circulating CXCR6+NK cells in cirrhosis and in HCC delineated by underlying aetiology. Graphs demonstrated the percentage of NK cells expressing CXCR6. A) The proportion of circulating CXCR6+NK cells in patients with cirrhosis secondary to ALD (ALD cirrhosis) was compared to patients with cirrhosis secondary to MASLD (MASLD cirrhosis). Comparisons did not reveal a significant difference in the circulating proportion of CXCR6+NK cells. B) The proportion of circulating CXCR6+NK cells in patients with HCC secondary to ALD cirrhosis (ALD HCC) was compared to patients with HCC secondary to

MASLD cirrhosis (MASLD HCC). Comparison did not reveal a significant difference in the circulating proportion of circulating CXCR6+NK cells. (MASLD = metabolic dysfunction-associated steatotic liver disease; ALD= Alcohol related fatty liver disease; HCC= Hepatocellular carcinoma). (Graphs display individual values with the median values displayed by the bars. Comparisons between groups are made using the Mann-Whitney test. Error bars represent the interquartile range).

CXCR6 expression on circulating NK cells did not correlate with MELD-Na score (spearman rank correlation) but there was a trend towards an increased proportion of circulating CXCR6+NK cells in patients with Child Pugh C cirrhosis compared to Child Pugh A cirrhosis (Figure 51B).

CXCR6 expression on circulating NK cells and underlying cirrhosis status

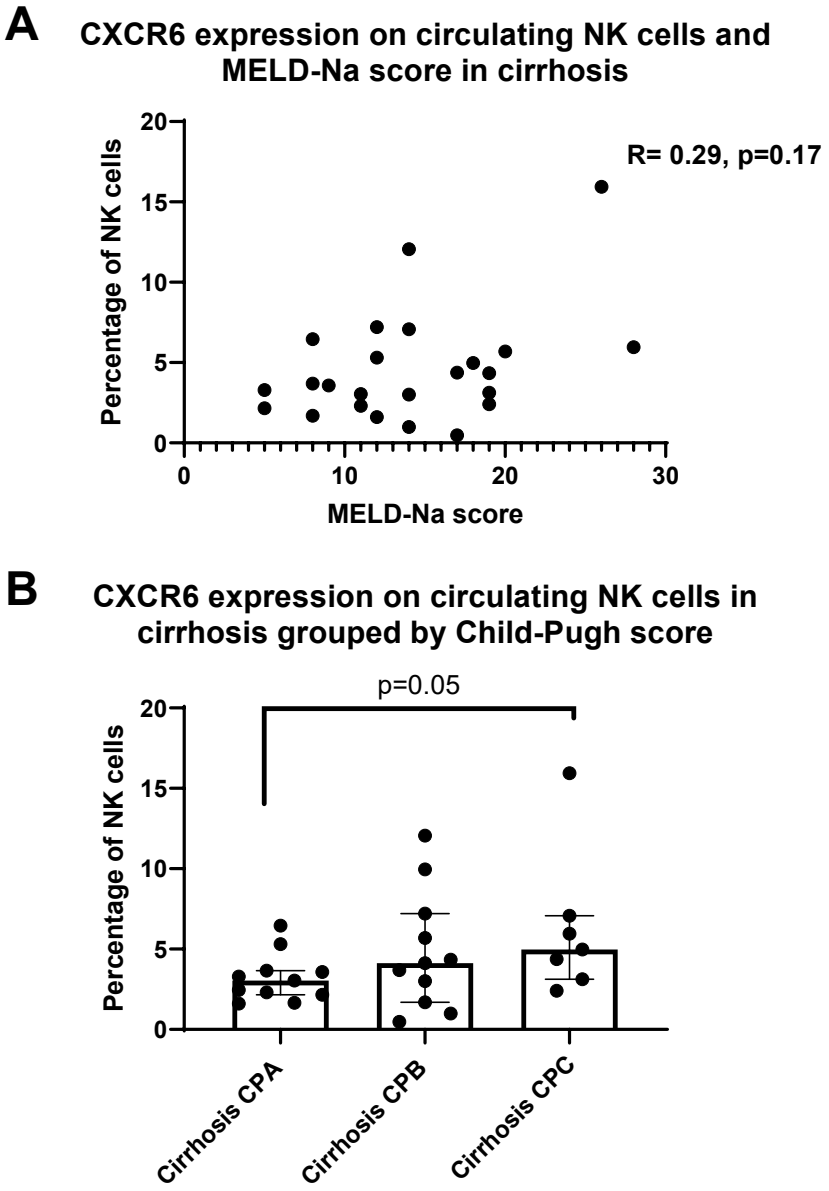


Figure 51 CXCR6 expression on circulating NK cells in cirrhosis and underlying MELD-Na score and Child-Pugh classification. CXCR6+ circulating NK cells were determined in patients with cirrhosis. Graphs display the percentage of circulating NK cells that expressed CXCR6. A) CXCR6+NK cell proportion did not correlate with MELD-Na score in patients with cirrhosis without HCC (spearman rank correlation). B) The circulating CXCR6+ NK cell proportion in patients with cirrhosis did not differ significantly by underlying Child-Pugh status (CPA= Child-Pugh A, CPB = Child-Pugh B, CPC = Child-Pugh C). (Graphs display individual values with the median value displayed by the bar. Comparisons between groups have been made using the

*Mann-Whitney test. Error bars represent the interquartile range. P values are denoted on the figures as follows: * p<0.05, ** p<0.01, *** p<0.001, **** p<0.0001). Analyses were repeated for patients with MASLD cirrhosis and for ALD cirrhosis but did not demonstrate correlation with MELD-Na or significance between Child-Pugh status.*

CXCR6 expression did not vary significantly with underlying BCLC (Barcelona Clinic Liver Cancer) staging in patients with HCC (Figure 52).

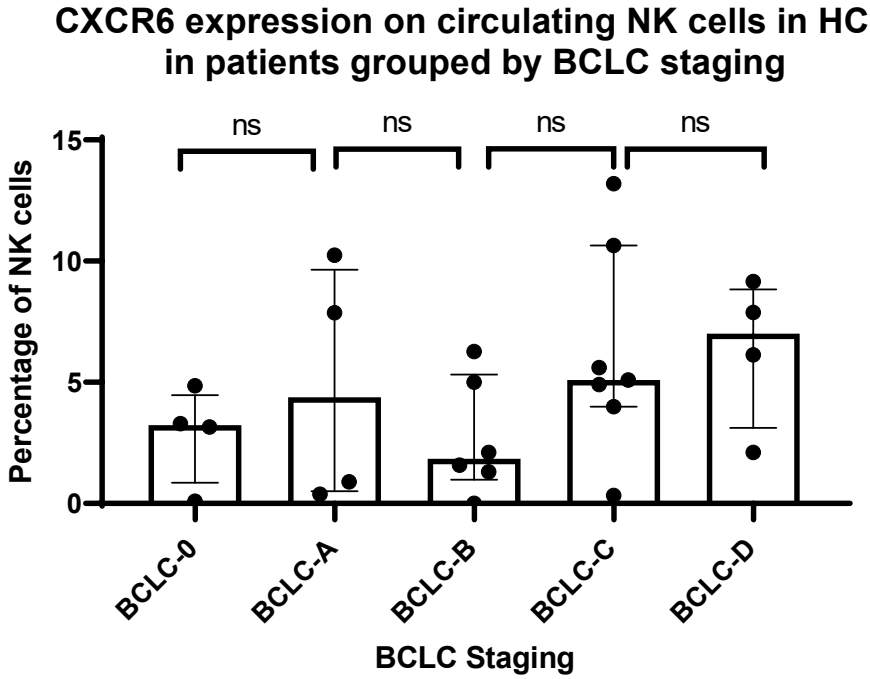


Figure 52 The proportion of CXCR6+NK cells in the circulation in patients with HCC on a background of cirrhosis categorised by BCLC staging. Graph displays the percentage of circulating NK cells expressing CXCR6. Comparisons between groups with different stages did not reveal a difference in the circulating proportion of NK cells that express CXCR6 (Kruskal-Wallis test with Dunn's multiple comparisons). (Graphs display individual values and the median value. Error bars represent the interquartile range).

Finally, CXCR6 expression on intrahepatic NK cells did not show significant differences between patient groups, but limitations on sample size do not allow further

conclusions to be drawn here (Figure 53A). However, the majority of intrahepatic NK cells expressed CXCR6 in keeping with published data (Figure 53B).

Surface expression of CXCR6 on intrahepatic NK cells

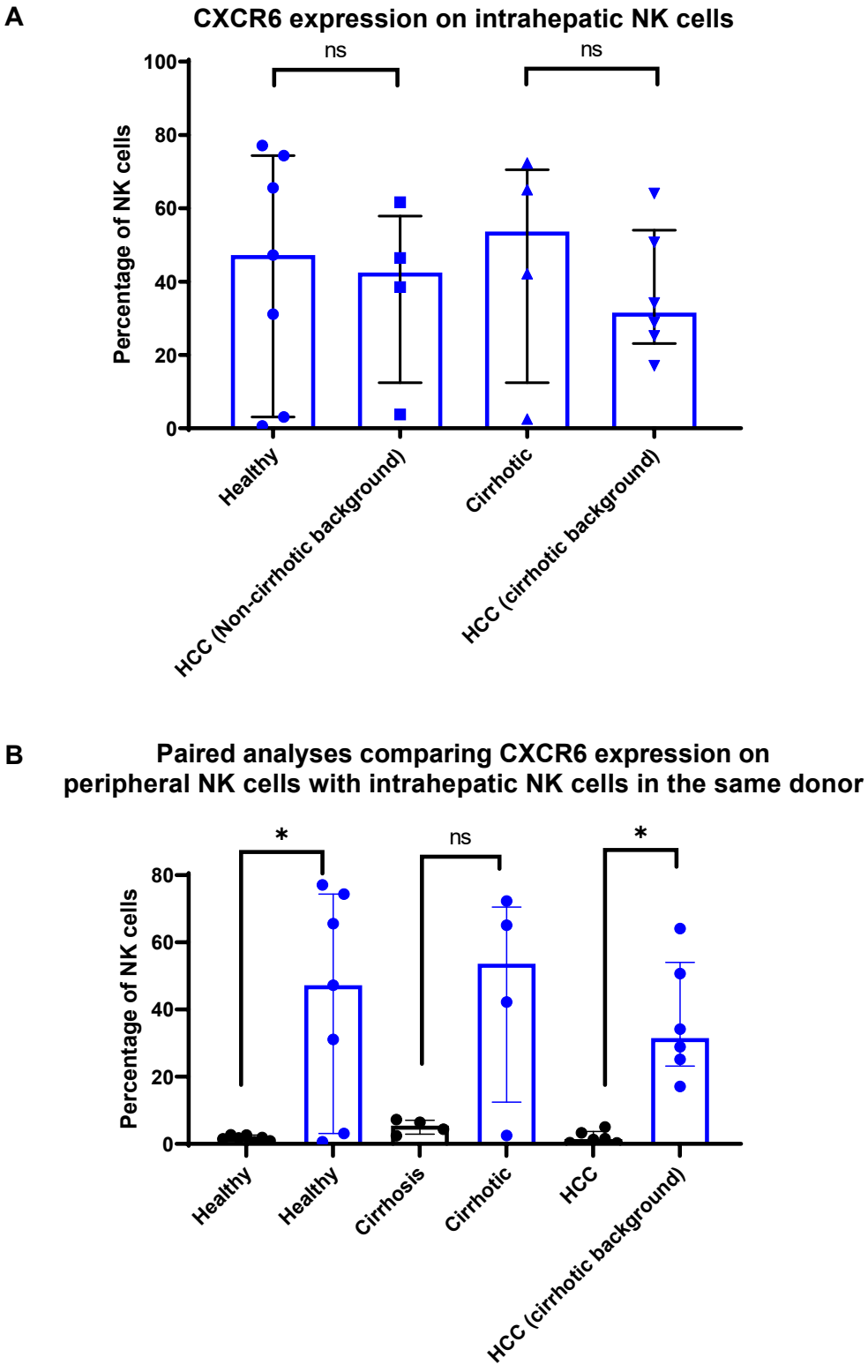


Figure 53 *CXCR6 expression on intrahepatic NK cells. A) CXCR6 expression on intrahepatic NK cells, expressed as a proportion of total intrahepatic NK cells. Comparisons between groups*

*have been made using the Mann-Whitney test. B) Comparison of CXCR6 expression in circulating NK cells (data in black) compared to intrahepatic NK cells (data in blue from the same donor. Comparisons were made using the non-parametric Wilcoxon matched-pairs signed rank test. Graphs display individual values and the median value. Error bars represent the interquartile range .P values are denoted on the figures as follows: * p<0.05, ** p<0.01, *** p<0.001, **** p<0.0001).*

3.1.7 Surface receptor co-expression

As individual activating and inhibitory receptors demonstrated a wide variation in expression in patients with HCC, individual receptor expression was correlated with other receptors on circulating NK cells from the same donor with HCC to determine if NK cells in some donors demonstrated a lower expression of all receptors or combinations of receptors in HCC. Correlations were calculated using Spearman rank correlations in patients with HCC and underlying MASLD cirrhosis, and in patients with HCC and underlying ALD cirrhosis. Correlations were also calculated for receptor expression in patients with MASLD or ALD cirrhosis without HCC, to see if correlations seen in HCC were as a consequence of variation in expression in underlying cirrhosis.

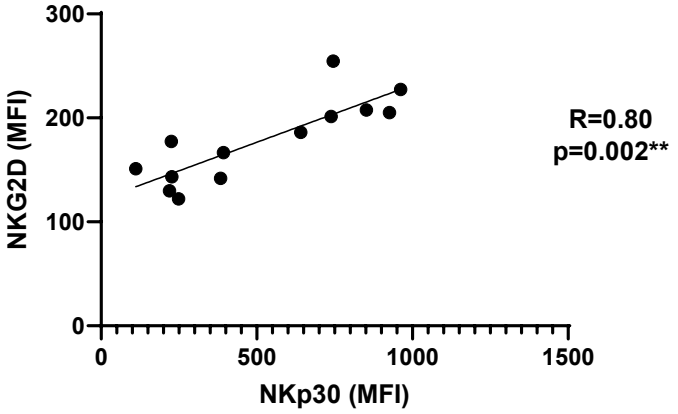
Activating receptor co-expression in HCC

NKG2D expression correlated positively with NKp30 and DNAM-1 expression in both ALD related and MASLD related HCC (Figures 54A, 54C, 55A, 55C). NKp30 expression correlated positively with DNAM-1 expression in MASLD related HCC but not in ALD related HCC (Figures 54B and 55B respectively). Interestingly, this positive correlation between the expression of activating receptors NKp30, NKG2D and DNAM-1 in ALD HCC was also seen in patients with ALD cirrhosis without HCC. However, the positive correlations in activating receptor expression seen in MASLD HCC was not seen in patients with MASLD cirrhosis without HCC.

Activating receptor co-expression on circulating NK cells in patients with MASLD HCC

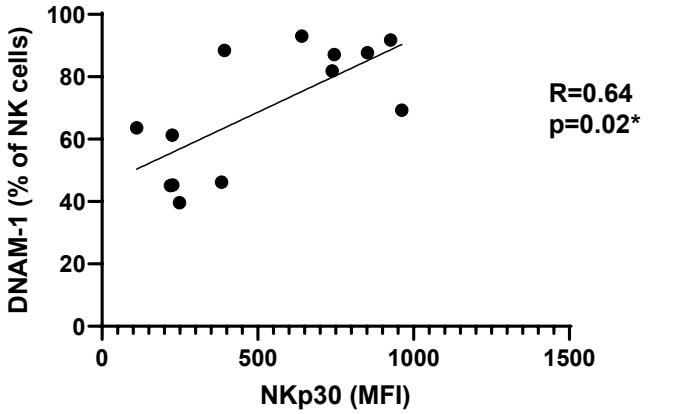
A

NKp30 expression correlates with NKG2D expression



B

NKp30 expression correlates with DNAM-1 expression



C

DNAM-1 expression correlates with NKG2D expression

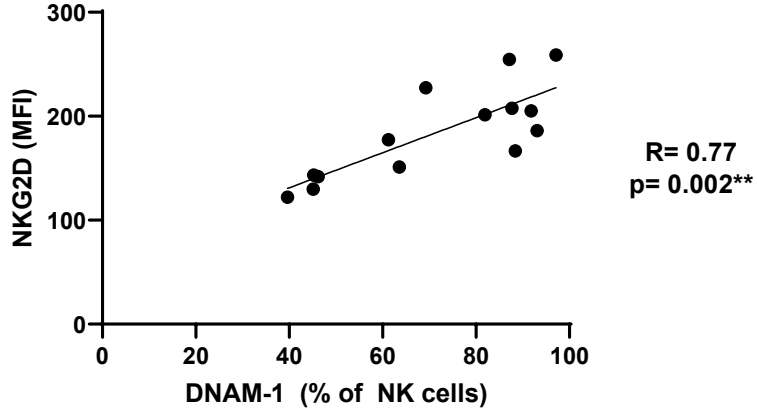


Figure 54 Activating receptor co-expression on circulating NK cells in patients with hepatocellular carcinoma with cirrhosis secondary to underlying metabolic dysfunction-associated steatotic liver disease (MASLD HCC). A) NKp30 expression (median fluorescent intensity, MFI) correlates positively with NKG2D expression (MFI). B) NKp30 expression (MFI) correlates positively with DNAM-1 expression (measured as the percentage of total circulating NK cells expressing DNAM-1). C) DNAM-1 expression (measured as the percentage of total circulating NK cells expressing DNAM-1) correlates positively with NKG2D expression (MFI). Spearman rank correlation R values were calculated to determine the correlation between receptor expression on the same circulating NK cells from the same donor. All individual values displayed on each graph with Spearman Rank Correlation R values shown along with p values for significance (p<0.05, ** p<0.01, *** p<0.001, **** p<0.0001).*

Activating receptor co-expression on circulating NK cells in patients with ALD HCC

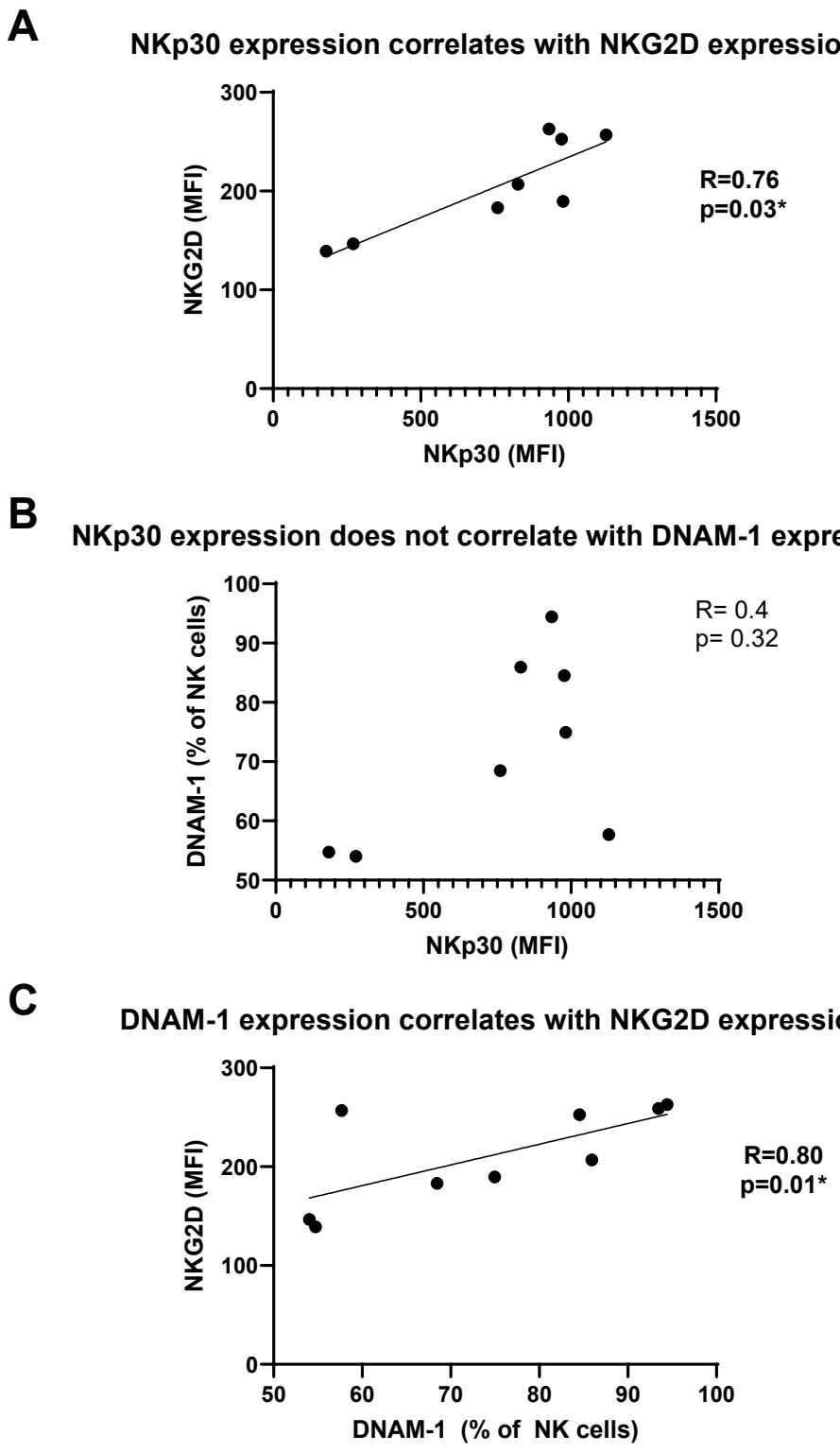


Figure 55 Activating receptor co-expression on circulating NK cells in patients with hepatocellular carcinoma and underlying cirrhosis secondary to alcohol related liver disease

(ALD HCC). A) NKp30 expression (median fluorescent intensity, MFI) correlates positively with NKG2D expression (MFI). B) NKp30 expression (MFI) does not correlate with DNAM-1 expression (measured as the percentage of total circulating NK cells expressing DNAM-1). C) DNAM-1 expression (measured as the percentage of total circulating NK cells expressing DNAM-1) correlates positively with NKG2D expression (MFI). Spearman rank correlation R values were calculated to determine the correlation between receptor expression on the same circulating NK cells from the same donor. All individual values displayed on each graph with Spearman Rank Correlation R values shown along with p values for significance (p<0.05, ** p<0.01, *** p<0.001, **** p<0.0001).*

While NKp46 is an activating receptor, NKp46 expression did not correlate with the other activating receptors in patients with HCC. However, NKp46 did correlate negatively with the proportion of circulating CD56dimCD16+/- NK cells in patients with HCC regardless of the aetiology (Figure 56). NKp46 however did not correlate with the CD56dimCD16+/- NK subpopulation in patients with cirrhosis without HCC of either aetiology. The CD56dimCD16+/- NK cell subpopulation did not correlate with any other receptors.

NKp46 expression on circulating NK cells correlated negatively with the proportion of CD56dimCD16+/-NK cells

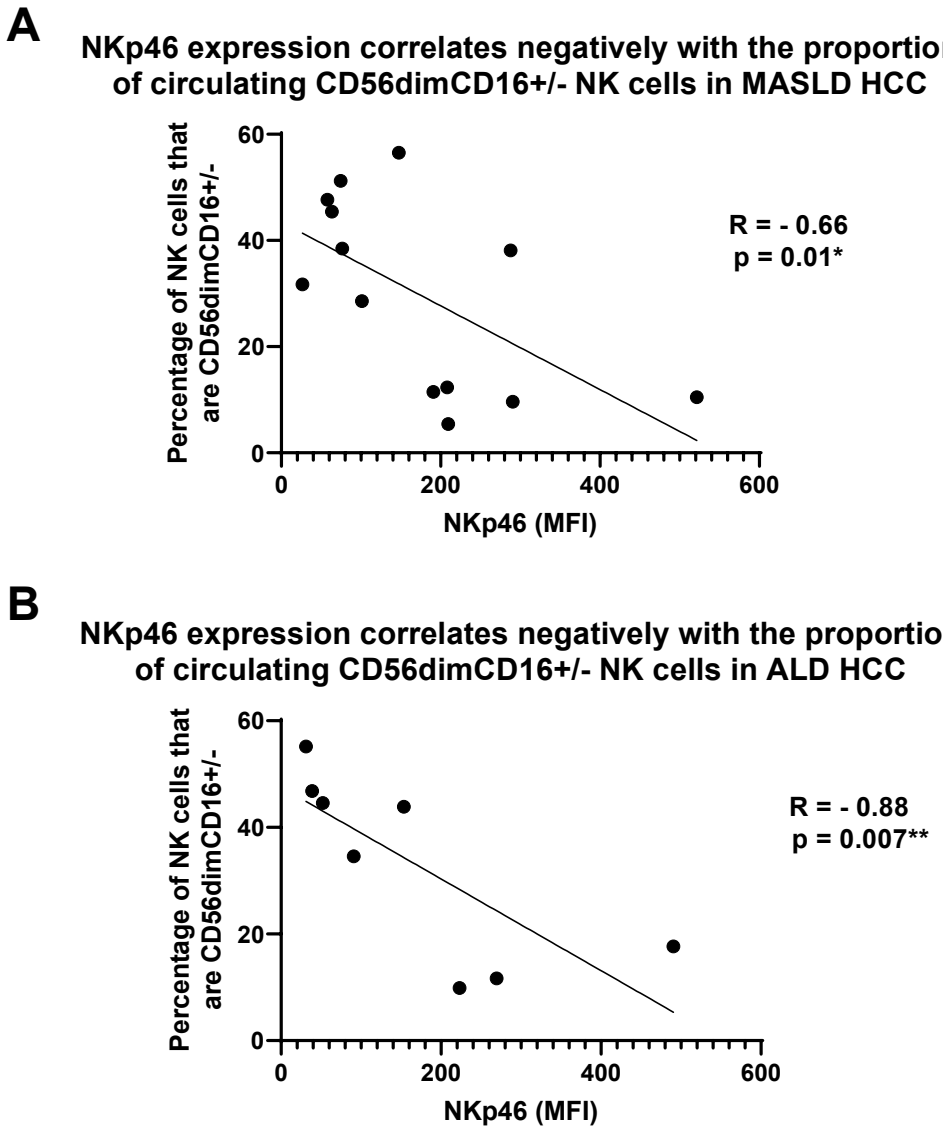


Figure 56 NKp46 expression on circulating NK cells correlated negatively with the proportion of circulating NK cells that were CD56dimCD16+/- in patients with hepatocellular carcinoma (HCC). Spearman rank correlation R values were calculated for NKp46 expression (measured as median fluorescence intensity (MFI) on circulating NK cells and the percentage of NK cells that are CD56dimCD16+/-NK cells in patients with HCC secondary to A) metabolic dysfunction-associated steatotic liver disease (MASLD) cirrhosis and B) alcohol related liver disease (ALD) cirrhosis. All individual values displayed on each graph with Spearman Rank Correlation R values shown along with p values for significance (p<0.05, ** p<0.01, *** p<0.001, **** p<0.0001). The analysis was repeated in patients with MASLD cirrhosis without HCC and ALD*

cirrhosis without HCC, but there were no significant correlations between NKp46 and the proportion of circulating NK cells that are CD56dimCD16+/- NK cells in cirrhosis without HCC.

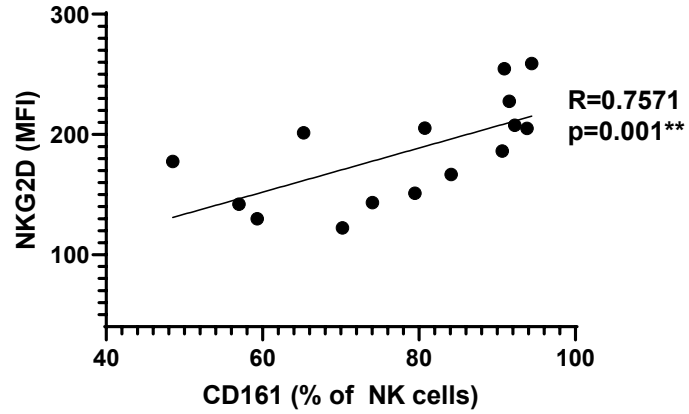
Inhibitory receptor co-expression in HCC

Interestingly, although CD161 is an inhibitory receptor, CD161 expression also correlated positively with the surface expression of activating receptors NKp30, DNAM-1 and NKG2D on circulating NK cells in patients with HCC and underlying MASLD cirrhosis (Figure 57). This positive correlation was not seen in patients with ALD related HCC, MASLD cirrhosis or ALD cirrhosis without HCC.

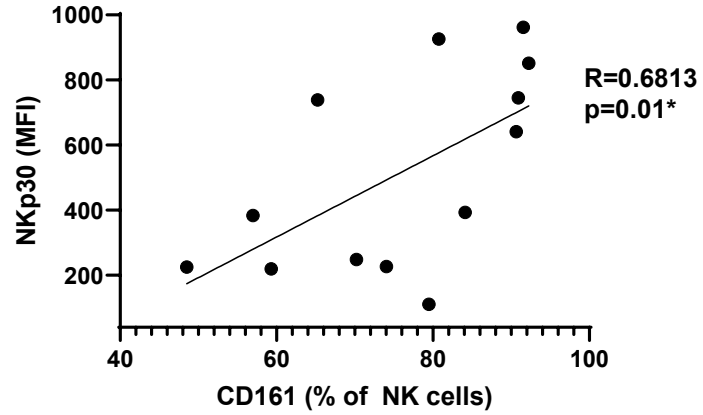
CD161 did not correlate with the proportion of circulating CD56dimCD16+/- NK cells.

CD161 co-expression with Activating receptors on circulating NK cells in patients with MASLD HCC

A NKG2D expression correlates with CD161 expression



B NKp30 expression correlates with CD161 expression



C DNAM-1 expression correlates with CD161 expression

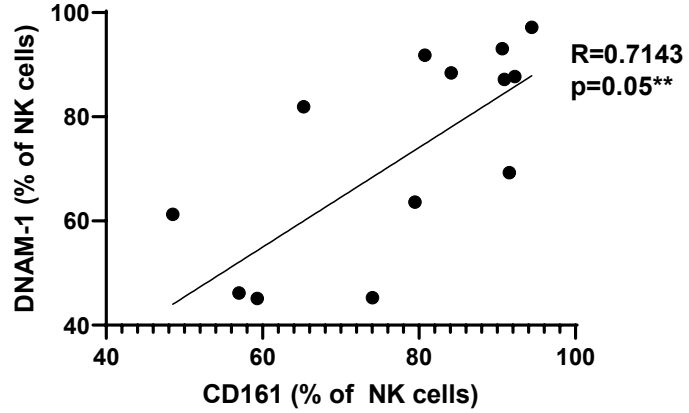


Figure 57 CD161 expression correlates with activating receptors NKp30, NKG2D and DNAM-1 on circulating NK cells in patients with hepatocellular carcinoma (HCC) and underlying cirrhosis secondary to metabolic dysfunction-associated steatotic liver disease (MASLD). A) NKG2D expression (median fluorescent intensity, MFI) correlates positively with CD161 expression (measured as the percentage of total circulating NK cells expressing CD161). B) NKp30 expression (MFI) correlates positively with CD161 expression (measured as the percentage of total circulating NK cells expressing CD161). C) DNAM-1 expression (measured as the percentage of total circulating NK cells expressing DNAM-1) correlates positively with CD161 expression (measured as the percentage of total circulating NK cells expressing CD161). Spearman rank correlation R values were calculated to determine the correlation between receptor expression on the same circulating NK cells from the same donor. All individual values displayed on each graph with Spearman Rank Correlation R values shown along with p values for significance (p<0.05, ** p<0.01, *** p<0.001, **** p<0.0001).*

CXCR6 co-expression in HCC

Finally, the liver homing receptor CXCR6 correlated negatively with CD161 and DNAM-1 expression in patients with HCC on a background of MASLD cirrhosis, but did not correlate with any other receptors in MASLD cirrhosis, ALD cirrhosis or HCC with underlying ALD cirrhosis (Figure 58).

CXCR6 surface receptor expression correlation in MASLD HCC

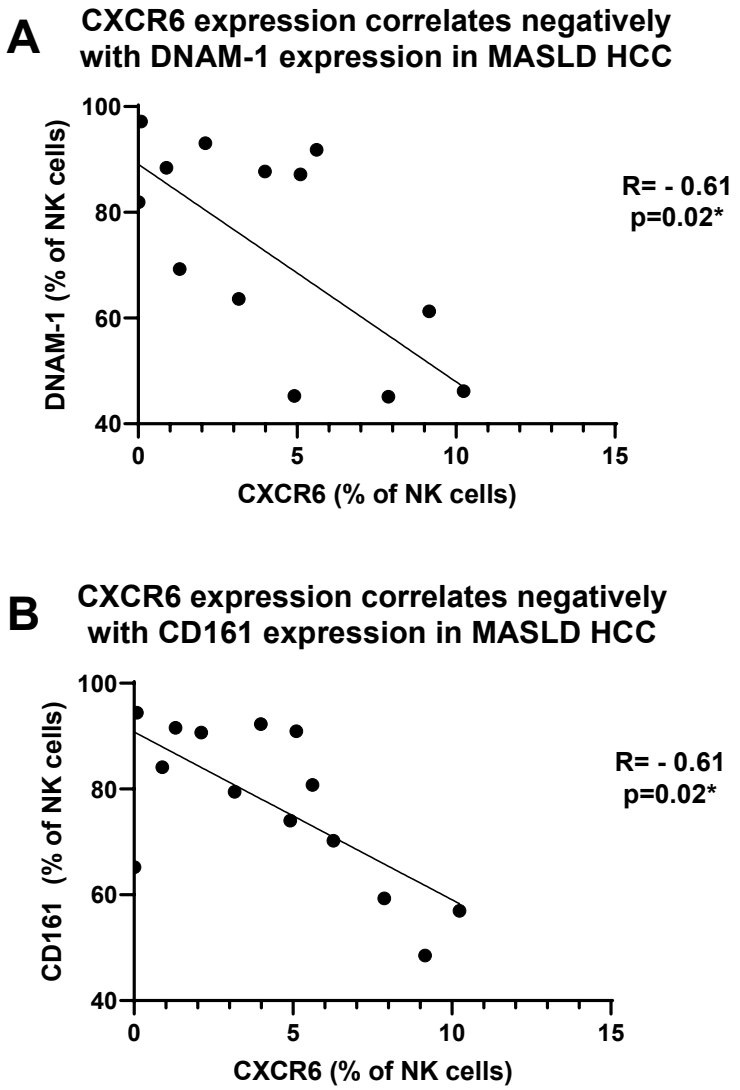


Figure 58 CXCR6 expression negatively correlated with DNAM-1 expression and CD161 expression on circulating NK cells in patients with Hepatocellular carcinoma (HCC) on a background of cirrhosis secondary to metabolic dysfunction-associated steatotic liver disease (MASLD). Spearman Rank correlation R values were calculated for CXCR6 expression (measured as the percentage of circulating NK cells expressing CXCR6) and A) DNAM-1 expression (measured as the percentage of circulating NK cells expressing DNAM-1) and B) CD161 expression (measured as the percentage of circulating NK cells expressing CD161) in patients with HCC secondary to MASLD cirrhosis. All individual values displayed on each graph with Spearman Rank Correlation R values shown along with p values for significance (p<0.05,*

*** p<0.01, *** p<0.001, **** p<0.0001). The analysis was repeated in patients with MASLD cirrhosis without HCC, ALD (alcohol related liver disease) cirrhosis without HCC and patients with HCC on a background of ALD cirrhosis, but there were no significant correlations between CXCR6 expression and other receptors in those patient groups.*

In summary, there is a positive correlation in the expression NKp30, NKG2D, DNAM-1 and CD161 on circulating NK cells in HCC, suggesting that NK cells in HCC may have a globally low expression of surface receptors in HCC. This correlation in expression of these surface receptors was seen in patients with HCC on a background of cirrhosis but not seen in patients with cirrhosis without HCC, and may explain the wide variation of receptor expression seen in the HCC patient group. Interestingly, NK cells with an upregulation of surface CXCR6 had lower expression of CD161 and DNAM-1 in patients with MASLD HCC.

Receptor expression in HCC did not correlate with any clinical parameters (cirrhosis composite scores, tumour burden, vascular invasion, metastases).

3.2 NK cell function

NK cell phenotyping demonstrated differences in surface receptor expression, with an increase in a CD56dimCD16+/- NK cell subset, inhibitory CD161 and liver-homing CXCR6 expression in cirrhosis, with a further reduction in the proportion of circulating NK cells expressing activating receptors NKp46 and DNAM-1 in HCC. To determine if these changes were accompanied with functional deficits in cirrhosis and HCC, functional analyses were undertaken on circulating NK cells.

NK cells have the capacity for both cytotoxicity and as well as cytokine secretion, predominantly interferon gamma (IFNγ) and tumour necrosis factor alpha (TNFα). NK cell degranulation, in response to activation following encounters with target cells, results in the release of perforin and granzyme and direct target cell death (R. Wang et al., 2012). Granules containing perforin and granzyme are lined with CD107a, and these granule membranes fuse with the NK cell surface membranes upon degranulation resulting in a measurable increase in CD107a surface expression. Therefore, the measurement of CD107a surface expression following the incubation of NK cells with target cells, has been described and established as method of measuring NK cell cytotoxic capacity (Alter et al., 2004).

3.2.1 Singular NK cell responses to target cells

To determine NK cell functional capacity, K562 and HepG2 cell line targets were used. K562 cells do not express MHC class I and hence act as potent activators of NK cells. HepG2 cells, derived from a hepatocellular carcinoma, were used to elucidate NK cell responses to HCC target cells. PBMCs were incubated for a four-hour period with target cells (K562 cells or HepG2 cells) at a 5:1 ratio (PBMCs:Target cells). PBMCs were then stained for functional outputs, (antibodies as described by Functional Panel 1, Chapter 2, Table 4). CD107a surface expression was then measured as a marker for degranulation and NK cell cytotoxicity, in addition to measuring intracellular interferon gamma (IFNγ) and tumour necrosis factor alpha (TNFα) production (Figure 59). The proportion of PBMCs that are NK cells did not differ between disease groups

(Figure 60 A), and optimal ratios of PBMCs to targets were determined by performing degranulation assays at different PBMC:Target ratios (Figure 60B). Based on these data I performed subsequent experiments at a 5:1 ratio. Table 10 below describes the demographics of the patient samples used in these functional experiments.

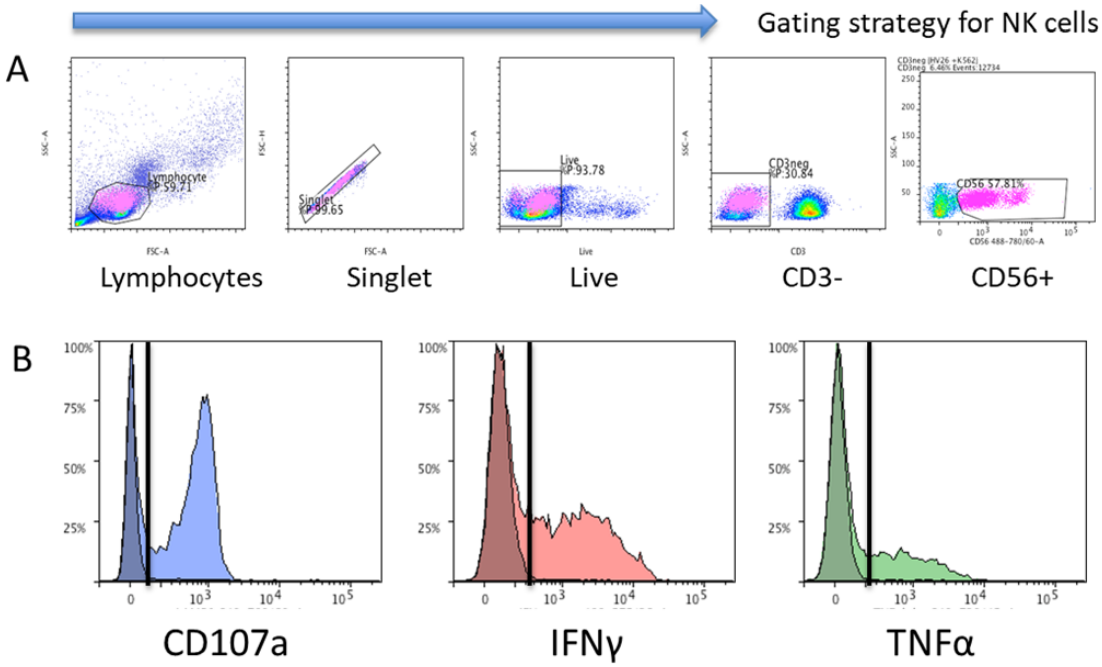


Figure 59 Gating strategy for NK cells and functional experiments. A) Peripheral blood mononuclear cells (PBMCs) were surface stained as described in the methods with fluorescently labelled anti-CD3, anti-CD56 antibodies and a cell viability dye (Functional Panel 1, Table 4). Lymphocytes were gated on the forward and side scatter plot, followed by singlet live cells and then CD53-CD56+ NK cells selected. B) Following incubation with target cells in the presence of a fluorescently labelled anti-CD107a antibody (used as a marker for NK cell degranulation), PBMCs were surface stained for CD3 and CD56 expression and intracellularly stained for interferon gamma (IFNγ) and tumour necrosis factor alpha (TNFα). Baseline background spontaneous degranulation and IFNγ/TNFα production was determined by incubating pbmcs from each donor without target cells and subtracting the baseline rate from the measured total percentage of NK cells degranulating and producing cytokine when incubated with target cells. Plots in B) demonstrate the functional outputs of CD107a, IFNγ and TNFα production from one donor against target cells, with gating set by the baseline background spontaneous functional output measured from that donor in the absence of target cells.

Table 10 Population characteristics of peripheral blood samples used for functional experiments. All patients had liver disease of a non-viral aetiology. (HCC= patient group with treatment naïve, non-viral cirrhosis with hepatocellular carcinoma; ALD= alcohol related liver disease; MASLD= metabolic dysfunction associated-steatotic liver disease; BCLC staging= Barcelona clinic Liver Cancer staging; p values calculated using non-parametric Mann Whitney analyses).

	Healthy	Cirrhosis	HCC	Healthy vs. Cirrhosis (p value)	Healthy vs. HCC (p value)	Cirrhosis vs. HCC (p value)
Total number	22	22	16			
Age, years mean, (range)	41 (23-62)	54 (26-79)	73 (57-84)	**p<0.0001** ****	**p<0.0001** ****	**p<0.0001** ****
Male n, (%)	21, (70.0%)	16, (72.7%)	15 (93.8%)			
Child-Pugh (CP) Score:						
CPA n, (%)		8 (36.4%)	14 (87.5%)			
CPB n, (%)		9 (40.9%)	1 (6.3%)			
CPC n, (%)		5 (22.7%)	1 (6.3%)			p=0.38
MELD-Na score mean, (range)		13 (8-19)	10 (6-18)			
Aetiology:						
ALD n, (%)		14 (77.3%)	8 (50.0%)			
MASLD n, (%)		8 (22.7%)	8 (50.0%)			
BCLC staging:						
BCLC 0 n, (%)			2 (12.5%)			
BCLC A n, (%)			4 (25.0%)			
BCLC B n, (%)			4 (25.0%)			
BCLC C n, (%)			4 (25.0%)			
BCLC D n. (%)			2 (12.5%)			
Lymphocyte count (10^9/L) mean, (range)		1.6 (0.2-3.5)	1.2 (0.2-2.1)			p=0.71

	Healthy	Cirrhosis	HCC	Healthy vs. Cirrhosis (p value)	Healthy vs. HCC (p value)	Cirrhosis vs. HCC (p value)
Bilirubin (total) (µmol/L) mean, (range)		24.8 (5-97)	19.5 (4-64)			p=0.09
Platelets (10^9/L) mean, (range)		168 (35-313)	156 (33-337)			p=0.94
INR mean, (range)		1.24 (1.0-2.2)	1.14 (1.0-1.4)			p=0.12
Albumin (g/L) mean, (range)		33.6 (18-42)	36.4 (27-44)			p=0.09
ALT (IU/L) mean, (range)		32.6 (6-114)	44.1 (10-202)			p=0.14
Creatinine (µmol/L) mean, (range)		76.8 (43-160)	101 (44-171)			p=0.28
AFP (µg/L) mean, (range)			2939 (3-3556)			

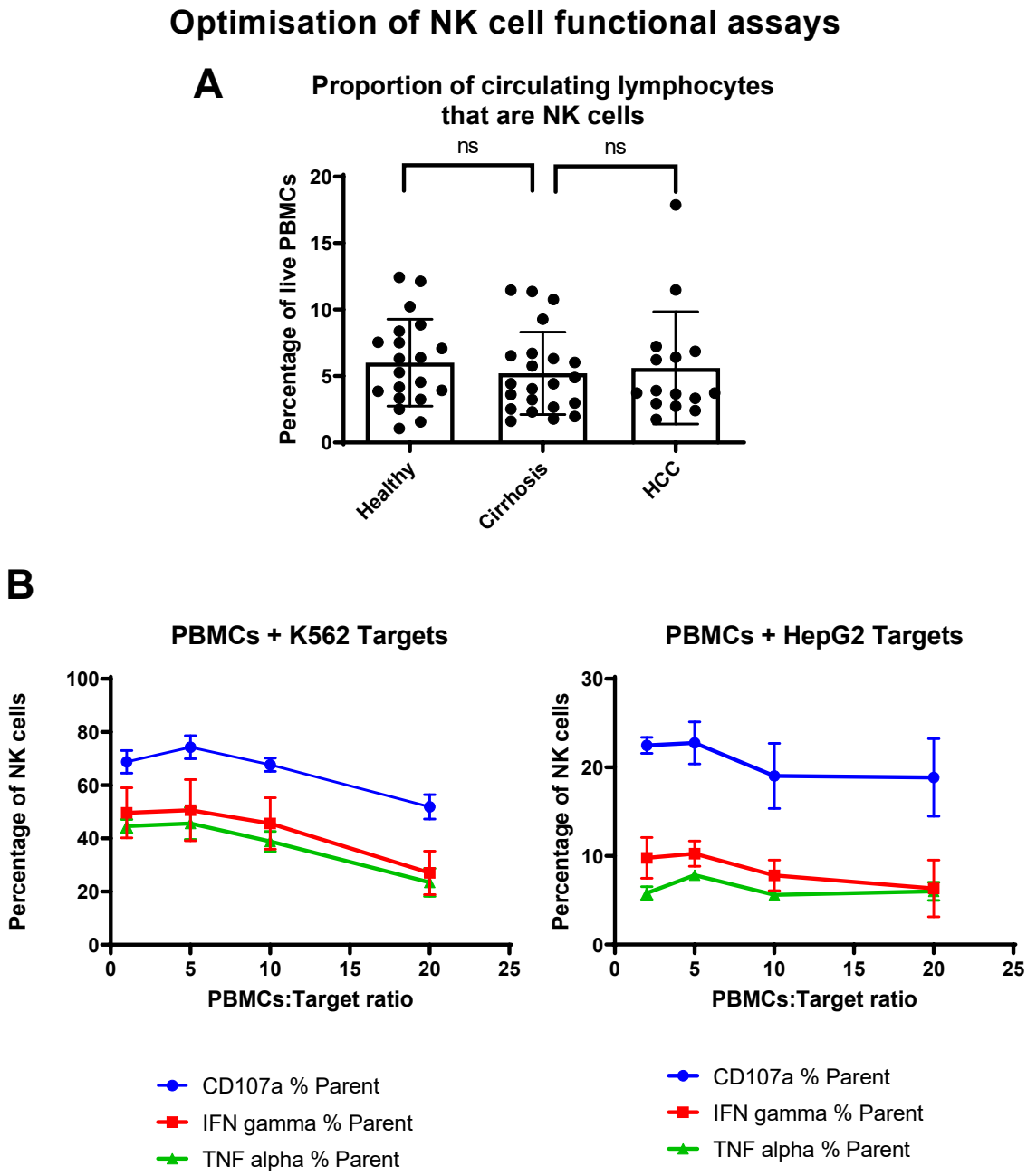


Figure 60 Optimisation for functional NK cell experiments. A) NK cells were selected using flow cytometry, gating on lymphocytes on the forward and side scatter plots, selecting live singlet cells and gating on CD3-CD56+NK cells. There were no significant differences in the proportion of circulating live lymphocytes that were NK cells between healthy individuals and patient groups. B) Peripheral blood mononuclear cells (PBMCs) were incubated for 4 hours in the presence of a fluorescently labelled anti-CD107a antibody with K562 target cells or HepG2 target cells at different ratios (PBMCs:Target cells at ratios of 2:1, 5:1, 10:1 and 20:1). Following the incubation period, PBMCs were washed, stained with fluorescently labelled CD3

and CD56 and intracellular staining was undertaken for interferon (IFN) gamma and tumour necrosis factor (TNF) alpha as described in the methods. CD107a expression, IFN gamma and TNF alpha production was determined using flow cytometry (all data values plotted on graphs; graphs show functional outputs from 3 different donors and error bars demonstrate the mean and standard deviation). Subsequently, a target ratio of 5:1 (PBMCs:target cells) was selected as the optimal ratio for the functional experiments.

CD107a expression in peripheral blood NK cells in response to target cells

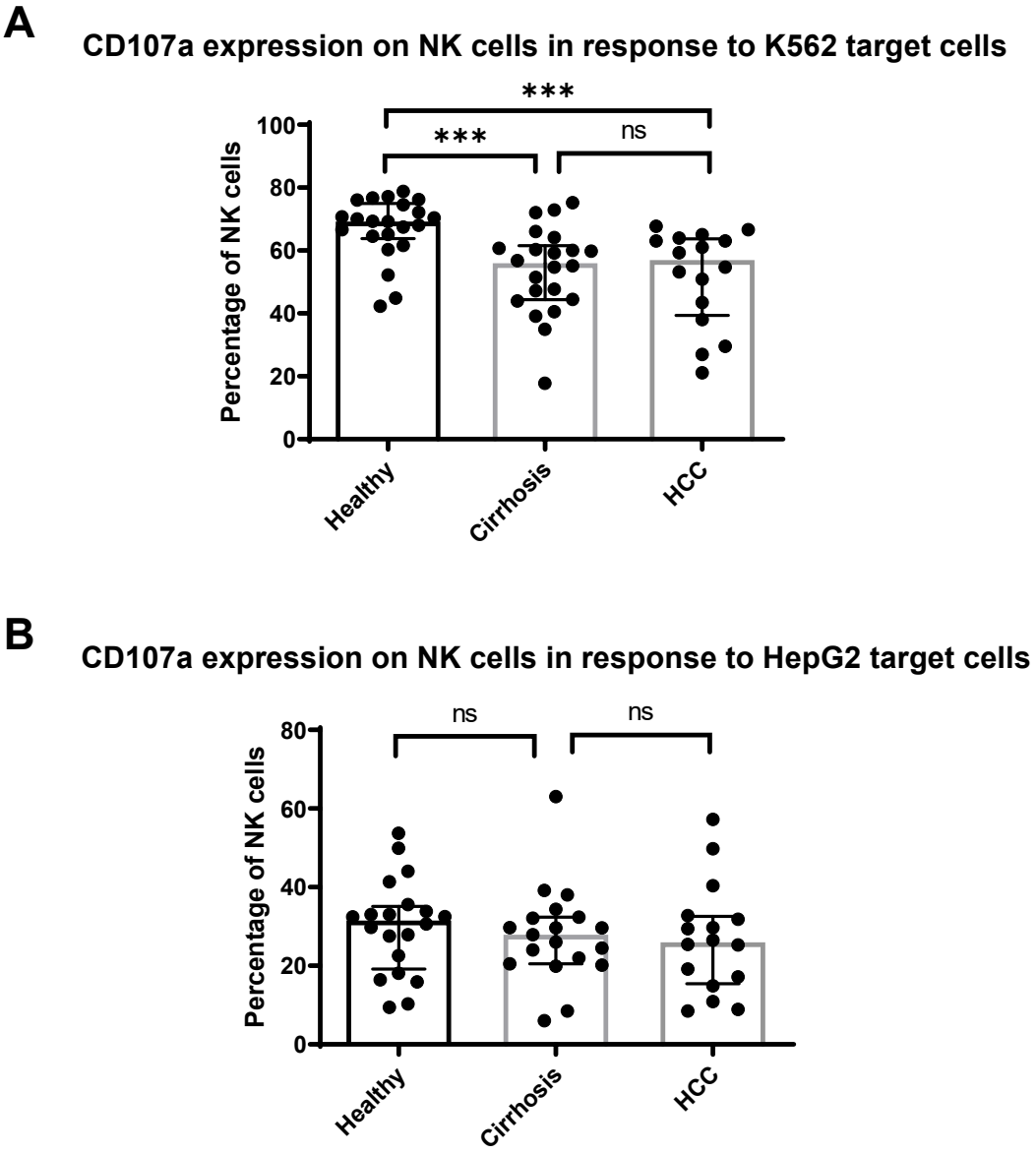


Figure 61 Degranulation (CD107a expression) in circulating NK cells in response to K562 and HepG2 target cells. Peripheral blood mononuclear cells (PBMCs) from healthy individuals (n=22), patients with cirrhosis (n=22) and patients with Hepatocellular carcinoma (HCC) with underlying cirrhosis (n=16) were incubated in a 5:1 ratio for 4 hours with target cells (K562 or HepG2 cells) in the presence of fluorescently labelled anti-CD107a antibody. Following this, surface staining for CD3 and CD56 with fluorescently labelled antibodies was undertaken. Using flow cytometry, NK cells were selected by gating on live CD3-CD56+ lymphocytes and CD107a expression, using PBMC's incubated without target cells as a control baseline. Graph

*A demonstrates functional outputs for NK cells when PBMCs were incubated with K562 target cells. Graph B demonstrates functional outputs for NK cells when PBMCs were incubated with HepG2 target cells. Graphs display individual values with the bar representing the median value. Error bars display the interquartile range. P values for significance are displayed on the graphs as follows: * p<0.05, ** p<0.01, *** p<0.001, **** p<0.0001.*

Deficits in NK cell effector functions were seen against K562 target cells in the cirrhosis group and in the HCC group. CD107a and IFNγ expression was reduced in response to K562 targets in cirrhosis, and further attenuated in HCC (Figures 61A and 62A). TNFα production against K562 target cells was reduced in patients with HCC compared to healthy individuals, with a downward trend in patients with cirrhosis that did not reach significance (Figure 63A). Interestingly, no significant functional deficits were seen in NK cells against HepG2 target cells (Figures 61B, 62B, 63B). The experiment was repeated using another HCC cell line (Huh7 cells), but high variability was seen in degranulation responses to this cell line with the same donors, and hence results were not reliable.

IFNγ production in peripheral blood NK cells in response to target cells

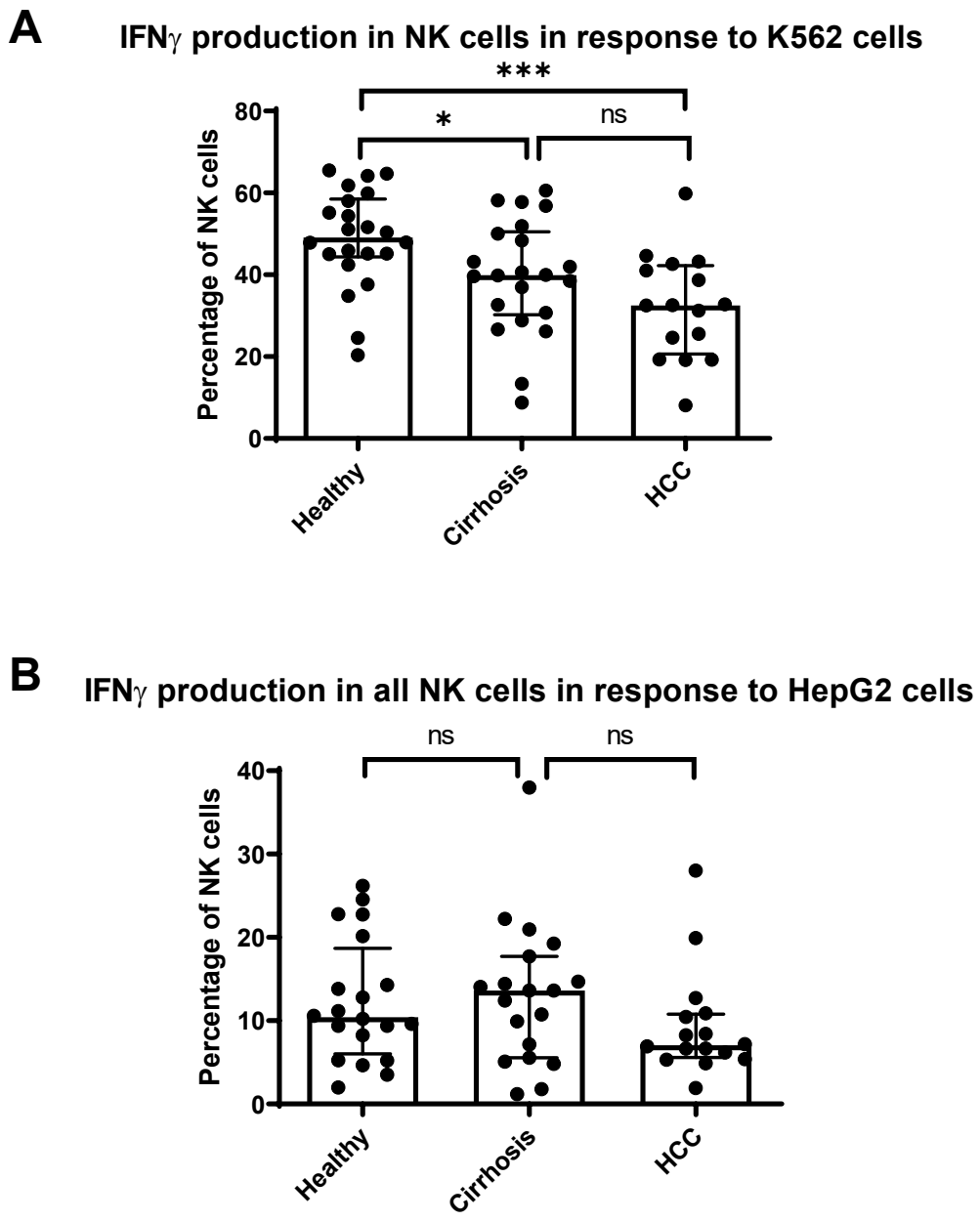


Figure 62 Interferon gamma (IFNγ) production in circulating NK cells in response to K562 and HepG2 target cells. Peripheral blood mononuclear cells (PBMCs) from healthy individuals (n=22), patients with cirrhosis (n=22) and patients with Hepatocellular carcinoma (HCC) with underlying cirrhosis (n=16) were incubated in a 5:1 ratio for 4 hours with target cells (K562 or HepG2 cells). Following this, surface staining for CD3 and CD56 with fluorescently labelled antibodies was undertaken, and intracellular staining was undertaken for interferon gamma

*(IFNγ). Using flow cytometry, NK cells were selected by gating on live CD3-CD56+ lymphocytes, and IFNγ production measured, using PBMC's incubated without target cells as a control baseline. Graph A demonstrates functional outputs for NK cells when PBMCs were incubated with K562 target cells. Graph B demonstrates functional outputs for NK cells when PBMCs were incubated with HepG2 target cells. Graphs display individual values with the bar representing the median value. Error bars display the interquartile range. P values for significance are displayed on the graphs as follows: * p<0.05, ** p<0.01, *** p<0.001, **** p<0.0001.*

TNFα production in peripheral blood NK cells in response to target cells

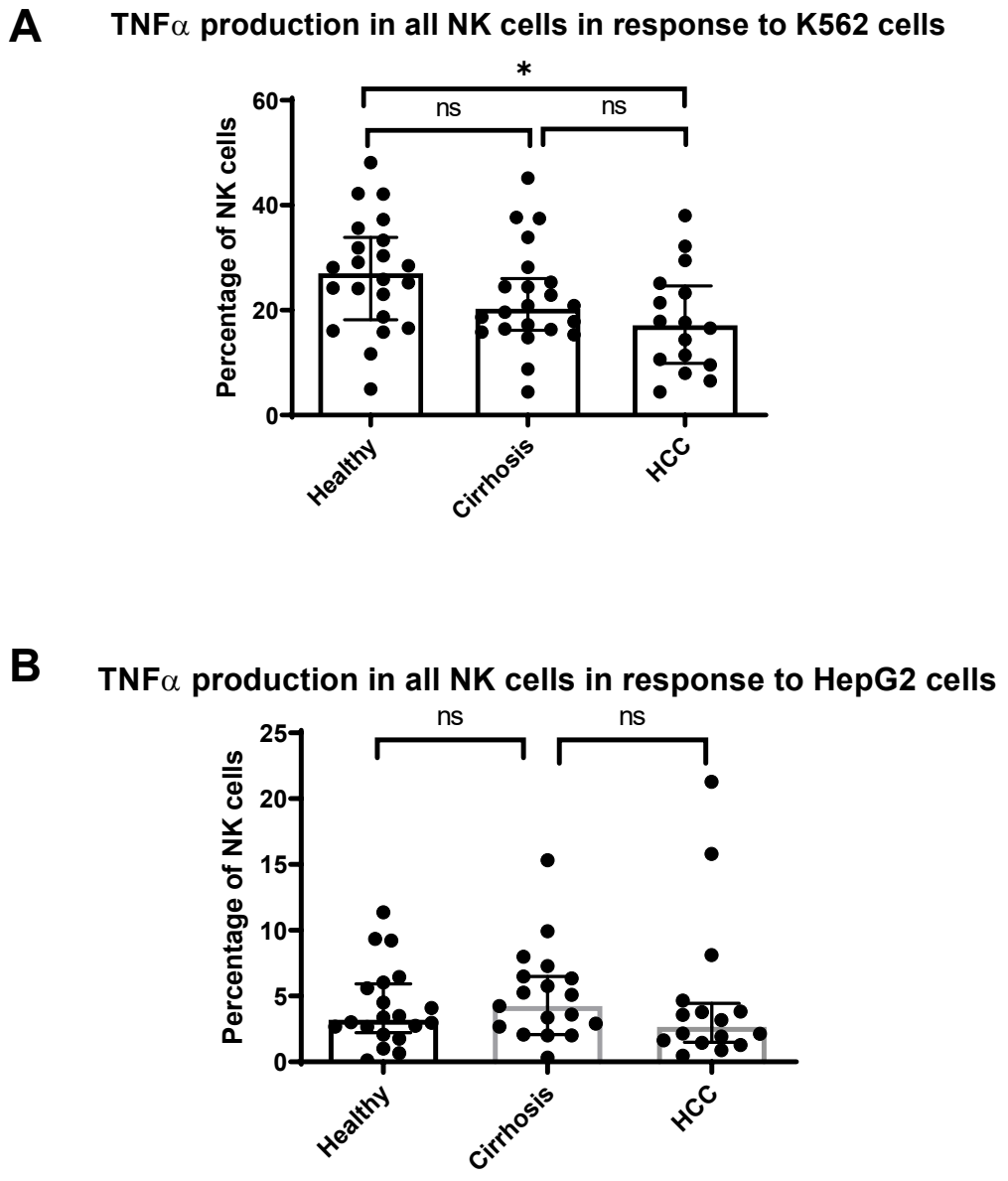


Figure 63 Tumour necrosis alpha (TNFα) production in circulating NK cells in response to K562 and HepG2 target cells. Peripheral blood mononuclear cells (PBMCs) from healthy individuals (n=22), patients with cirrhosis (n=22) and patients with Hepatocellular carcinoma (HCC) with underlying cirrhosis (n=16) were incubated in a 5:1 ratio for 4 hours with target cells (K562 or HepG2 cells). Following this, surface staining for CD3 and CD56 with fluorescently labelled antibodies was undertaken, and intracellular staining was undertaken for tumour necrosis

*factor (TNFα). Using flow cytometry, NK cells were selected by gating on live CD3-CD56+ lymphocytes and TNFα production measured, using PBMC's incubated without target cells as a control baseline. Graph A demonstrates functional outputs for NK cells when PBMCs were incubated with K562 target cells. Graph B demonstrates functional outputs for NK cells when PBMCs were incubated with HepG2 target cells. Graphs display individual values with the bar representing the median value. Error bars display the interquartile range. P values for significance are displayed on the graphs as follows: * p<0.05, ** p<0.01, *** p<0.001, **** p<0.0001.*

3.2.2 Polyfunctional NK cell responses to target cells

The polyfunctionality of NK cells was assessed by looking at the proportion of NK cells that were capable of both direct cytotoxicity by degranulation (indirectly measured by assessing CD107a expression) and cytokine (IFNγ and TNFα) production in response to target cells (Figure 64).

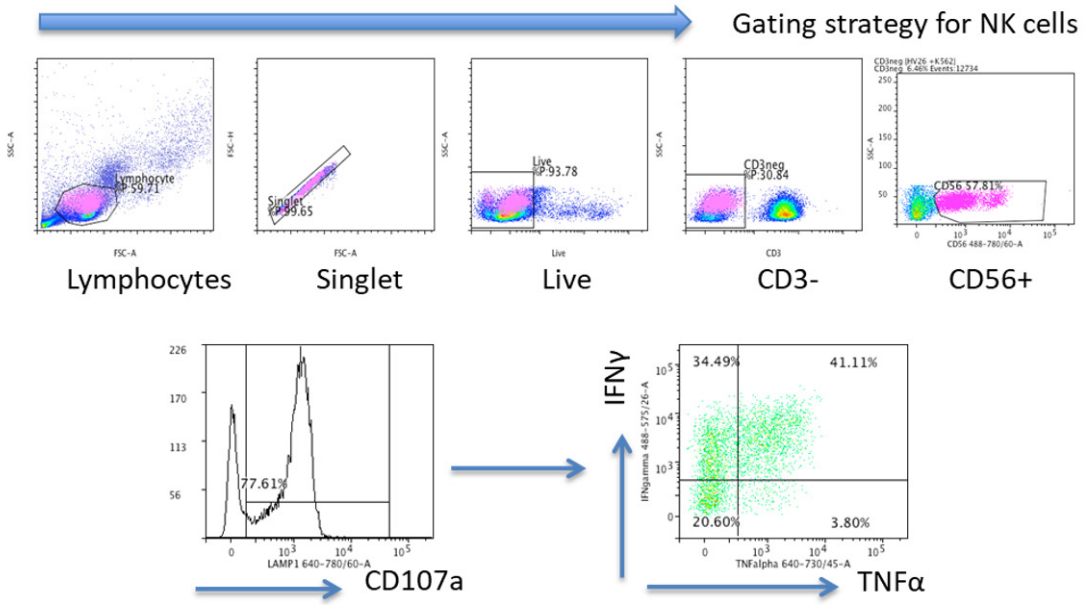


Figure 64 Gating strategy to identify polyfunctional NK cells with the capacity to produce a cytotoxic and cytokine response to target cells. Peripheral blood mononuclear cells (PBMCs) were incubated for 4 hours with target cells (5:1 ratio PBMC:Target) in the presence of fluorescently labelled anti-CD107a antibody. Following this, PBMCs were surface stained with CD3, CD56 and viability dye, and stained for interferon gamma (IFNγ) and tumour necrosis

alpha (TNFα) production via intracellular staining (Functional Panel 1, Table 4). NK cells were gated for as demonstrated on the figure above, by selecting live CD3-CD56+ lymphocytes, and the proportion of NK cells expressing CD107a (expressed in NK cells that have degranulated in keeping with a cytotoxic NK cell response to the target cell) was selected. The proportion of NK cells simultaneously producing a cytokine response (IFNγ production +/- TNFα production) in addition to the cytotoxic response (CD107a expression) was determined as demonstrated with the flow cytometry plots.

There were no significant differences in the proportion of NK cells with the capacity to produce all three functional responses to target cells (degranulation (CD107a expression), IFNγ and TNFα) (Figure 65). There was a significant reduction however in the proportion of circulating NK with dual functionality of degranulation and IFNγ production against K562 target cells in patients with HCC compared to healthy (Figure 66A). There was also a downward trend in the proportion of these NK cells with dual functionality in patients with cirrhosis compared with healthy, but it did not reach significance (p=0.06, Figure 66A).

Polyfunctional peripheral blood NK cells expressing CD107a in addition to producing TNFα and IFNγ in response to target cells

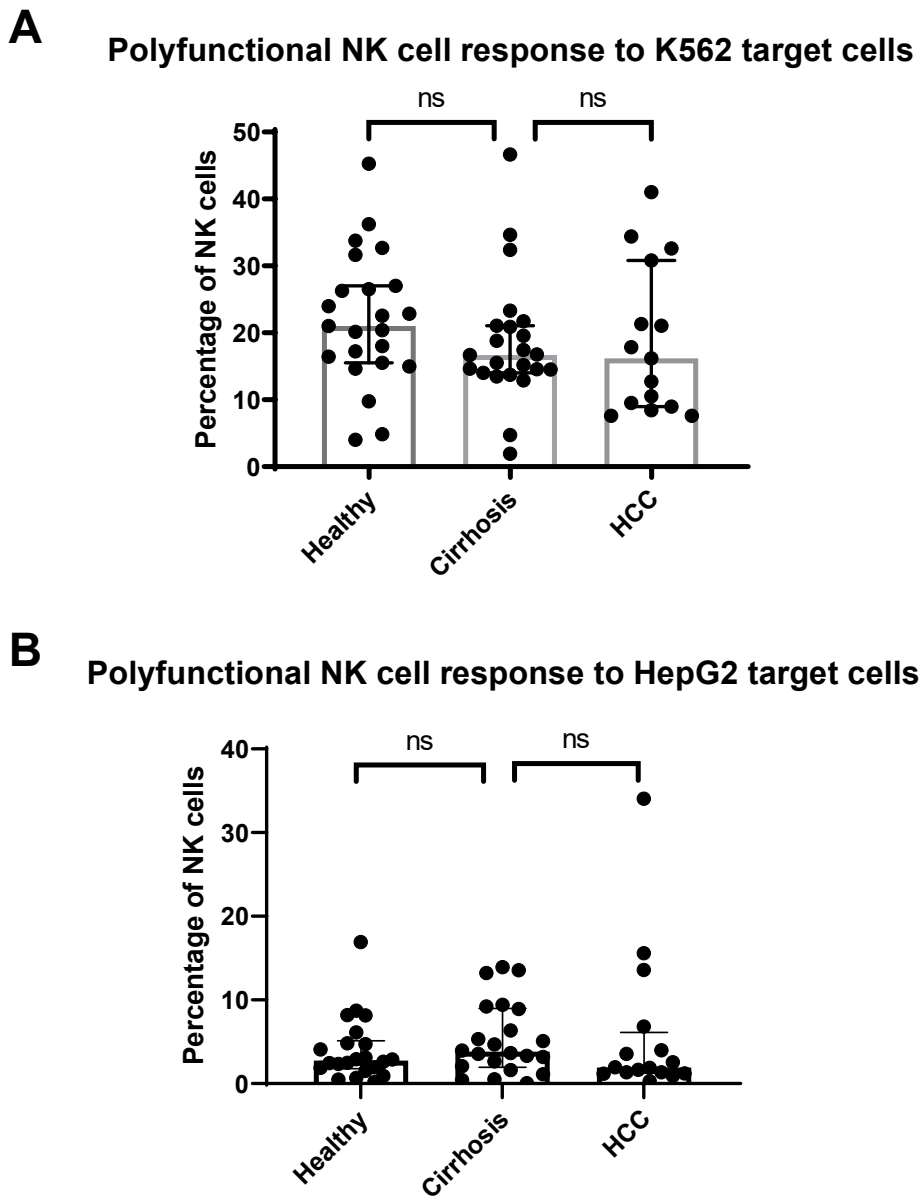


Figure 65 Polyfunctional circulating NK cell responses to target cells. Following a 4 hour incubation with either K562 target cells or HepG2 cells, peripheral blood NK cells were fluorescently labelled for CD107a, interferon gamma (IFNγ) and tumour necrosis alpha (TNFα), and NK cells producing all three functional responses were identified using flow cytometry. Graph A displays functional responses to K562 target cells. Graph B displays functional responses to HepG2 target cells. There were no significant differences between the proportion

of polyfunctional NK cells in healthy individuals and patients. Healthy=healthy individuals; cirrhosis = patients with cirrhosis; HCC = patients with hepatocellular carcinoma (HCC) on a background of cirrhosis. Graphs display individual values with the bar representing the median value. Error bars display the interquartile range.

Polyfunctional peripheral blood NK cells expressing CD107a and IFNγ in response to target cells

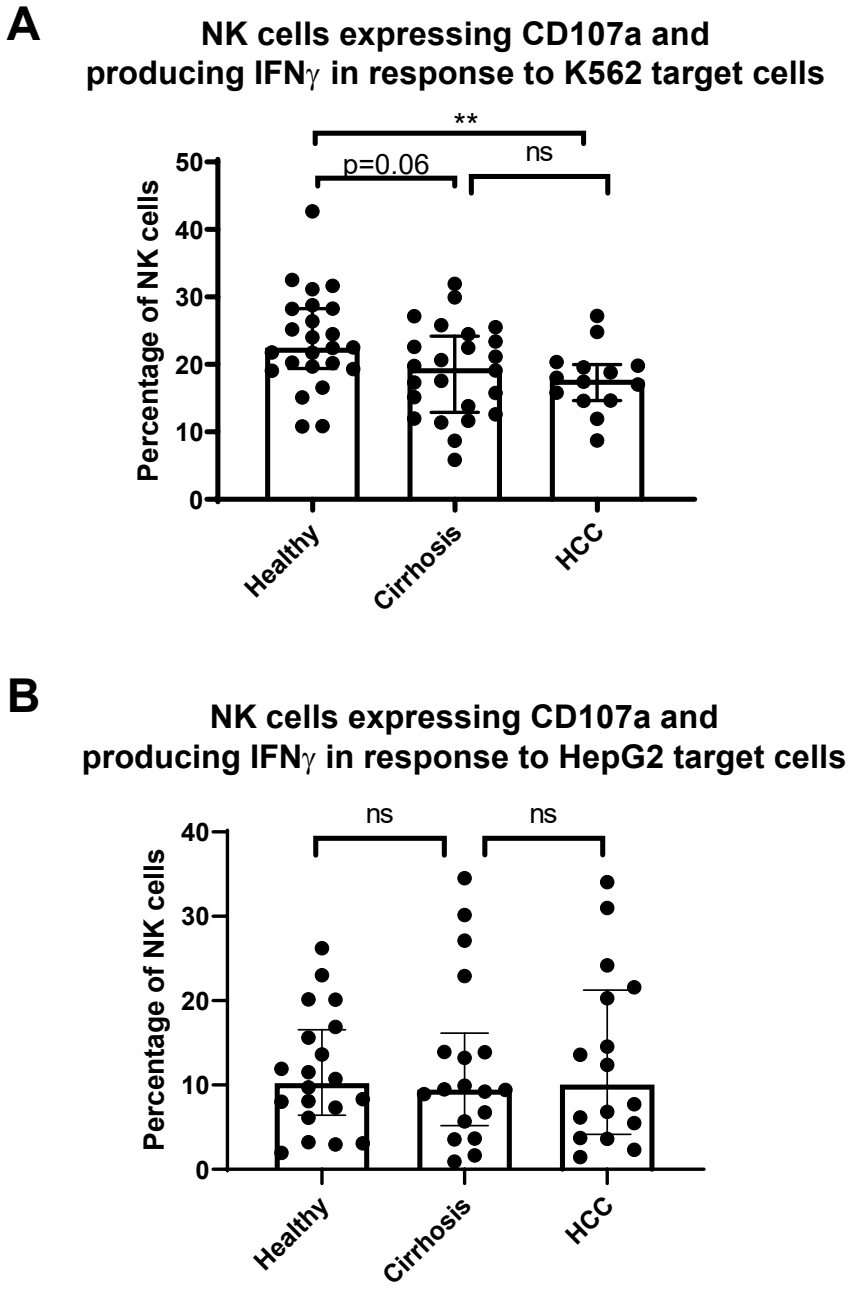


Figure 66 *Combined peripheral blood NK cell cytotoxic and interferon gamma responses to target cells. Following a 4 hour incubation with either K562 target cells or HepG2 cells, peripheral blood NK cells were fluorescently labelled for CD107a and interferon gamma (IFNγ), and NK cells producing both functional responses were identified using flow cytometry. Graph A displays functional responses to K562 target cells. Graph B displays functional responses to*

*HepG2 target cells. There was a reduction in the proportion of circulating NK cells with dual functionality (producing IFNγ and a cytotoxic response (CD107a expression) to K562 target cells) in patients with HCC compared to healthy. Healthy=healthy individuals; cirrhosis = patients with cirrhosis; HCC = patients with hepatocellular carcinoma (HCC) on a background of cirrhosis. Graphs display individual values with the bar representing the median value. Error bars display the interquartile range. P values for significance are displayed on the graphs as follows: * p<0.05, ** p<0.01, *** p<0.001, **** p<0.0001.*

Polyfunctional peripheral blood NK cells expressing CD107a and TNFα in response to target cells

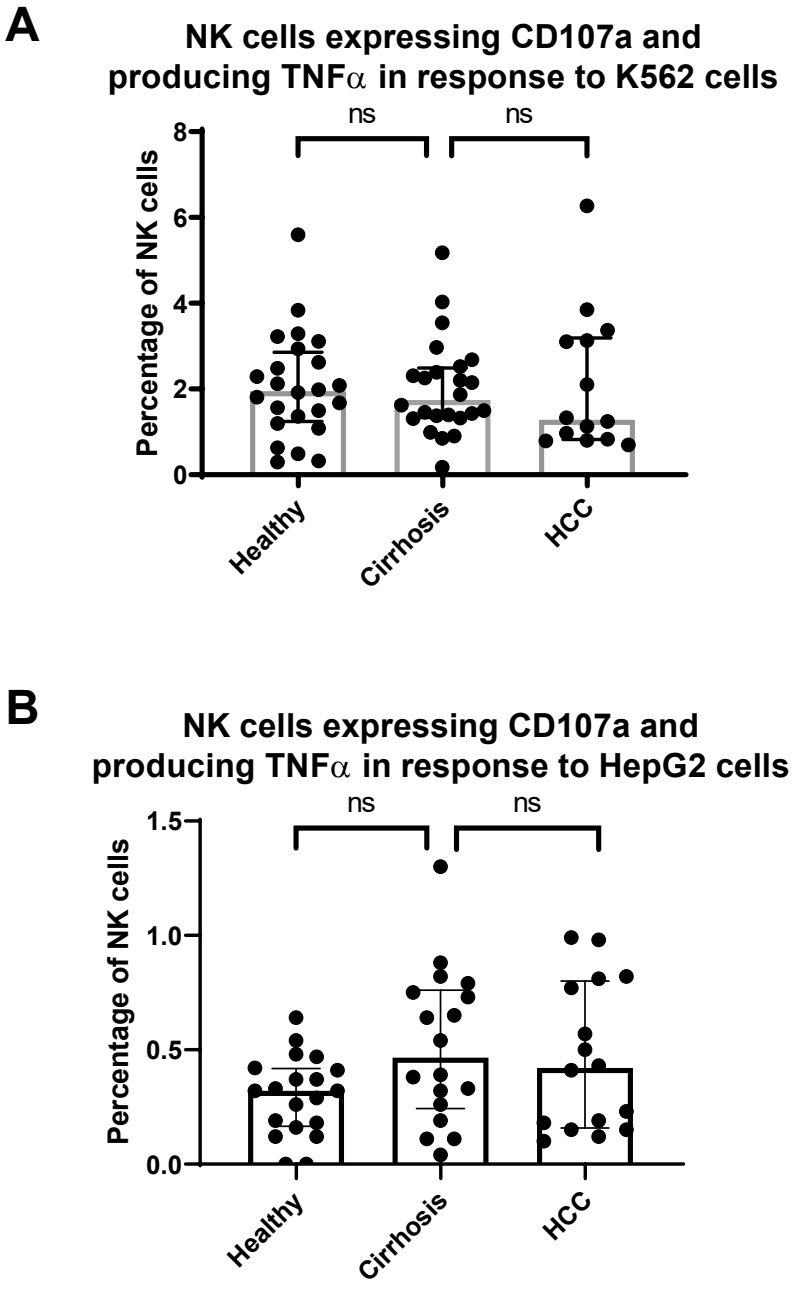


Figure 67 Combined peripheral blood NK cell cytotoxic and tumour necrosis alpha responses to target cells. Following a 4 hour incubation with either K562 target cells or HepG2 cells, peripheral blood NK cells were fluorescently labelled for CD107a and tumour necrosis alpha

(TNFα), and NK cells producing both functional responses were identified using flow cytometry. Graph A displays functional responses to K562 target cells. Graph B displays functional responses to HepG2 target cells. There were no significant differences in NK cell responses between healthy and patient groups. Healthy=healthy individuals; cirrhosis = patients with cirrhosis; HCC = patients with hepatocellular carcinoma (HCC) on a background of cirrhosis. Graphs display individual values with the bar representing the median value. Error bars display the interquartile range.

3.2.3 CD56bright and CD56dim NK cell responses to target cells

Circulating CD56bright NK cells are classically associated with an increased capacity for producing cytokines compared with CD56dim NK cells, and in turn peripheral blood CD56dim NK cells have a greater direct cytotoxic capacity (Cooper et al., 2001). To determine whether the functional deficit was attributed to the CD56bright or the CD56dim NK cell subset, effector functions for each NK cell subset were compared between patient groups and healthy volunteers against K562 cells.

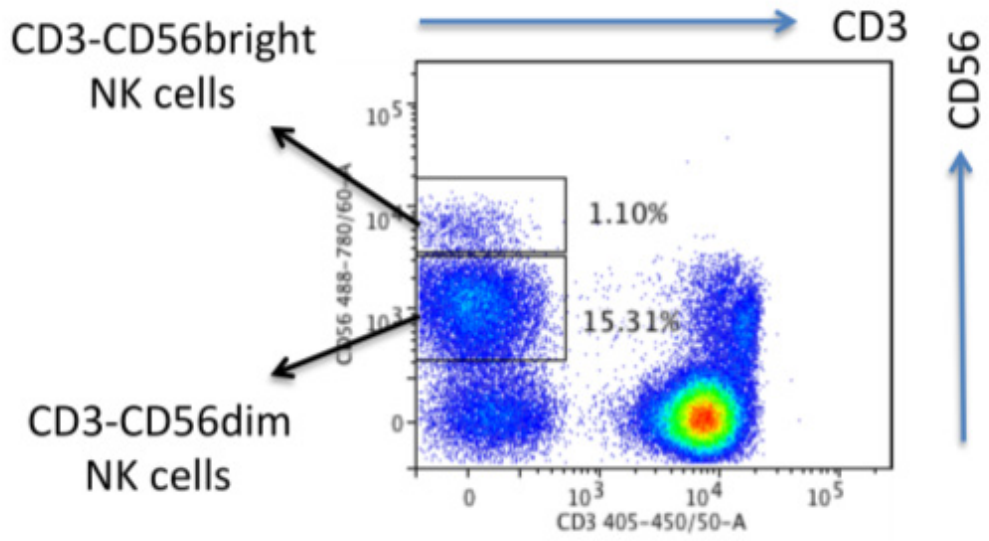


Figure 68 Gating strategy for CD56bright and CD56dim NK cells. NK cells were identified by gating on live lymphocytes that are CD3 negative and CD56positive. CD56bright NK cells and CD56dim NK cells were identified using the gating strategy demonstrated.

CD56dim NK cells displayed significant dysfunction in the HCC group in all modalities (degranulation and cytokine production) and had a significantly reduced proportion of circulating cells with a polyfunctional capacity (11.6% vs. 21.2%; HCC vs. Healthy, median values, p=0.03) (Figures 69A, 70A, 71A, 72A). CD56dim NK cells in the cirrhosis group were also significantly dysfunctional, with reduced CD107a expression and IFNγ production, and a reduced proportion of polyfunctional CD56dim NK cells producing cytotoxic responses and cytokine secretion (Figures 69A, 70A, 71A, 72A).

CD56bright NK cells did demonstrate capacity for degranulation following contact with K562 target cells. However, there were no significant differences in CD56bright NK cell function in the cirrhosis and HCC groups in comparison to healthy NK cells (Figures 69B, 70B, 71B, 72B)).

Comparing CD107a expression in CD56dim NK cells and CD56bright NK cells in response to K562 target cells

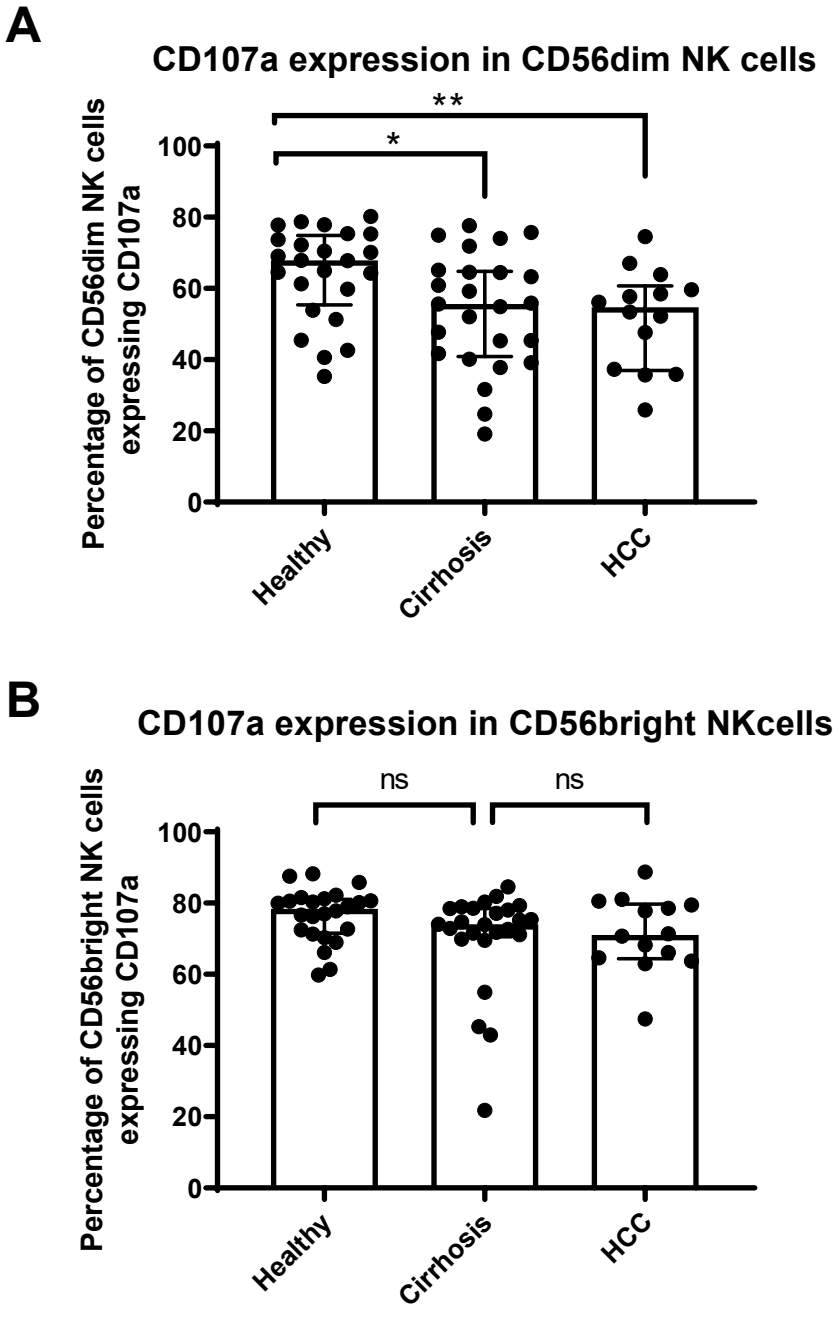


Figure 69 Comparing the NK cell cytotoxicity response (by measuring CD107a expression) in CD56dim and CD56bright NK cells in healthy volunteers and patient groups against K562 target cells. Peripheral blood mononuclear cells (PBMCs) were co-cultured with K562 target cells in a 5:1 ratio respectively. Degranulation of NK cells were measured by measuring CD107a

*expression using flow cytometry techniques. A) Graph displays the percentage of CD56dim NK cells expressing CD107a against K562 target cells. CD56dim NK cells from patients with cirrhosis or HCC had a reduced cytotoxic response to K562 cells in comparison to CD56dim NK cells from healthy volunteers. B) Graph displays the percentage of CD56bright NK cells expressing CD107a against K562 target cells. There were no significant functional deficits with regards to cytotoxicity in patient groups compared to healthy volunteers. This analysis was also undertaken for PBMCs against HepG2 target cells but there were no significant differences in functional outputs in the CD56dim or CD56bright subset in either healthy or disease states (data not shown). Healthy=healthy individuals; cirrhosis = patients with cirrhosis; HCC = patients with hepatocellular carcinoma (HCC) on a background of cirrhosis. Graphs display individual values with the bar representing the median value. Error bars display the interquartile range. P values for significance are displayed on the graphs as follows: * p<0.05, ** p<0.01, *** p<0.001, **** p<0.0001.*

Comparing interferon gamma (IFNγ) production in CD56dim NK cells and CD56bright NK cells in response to K562 target cells

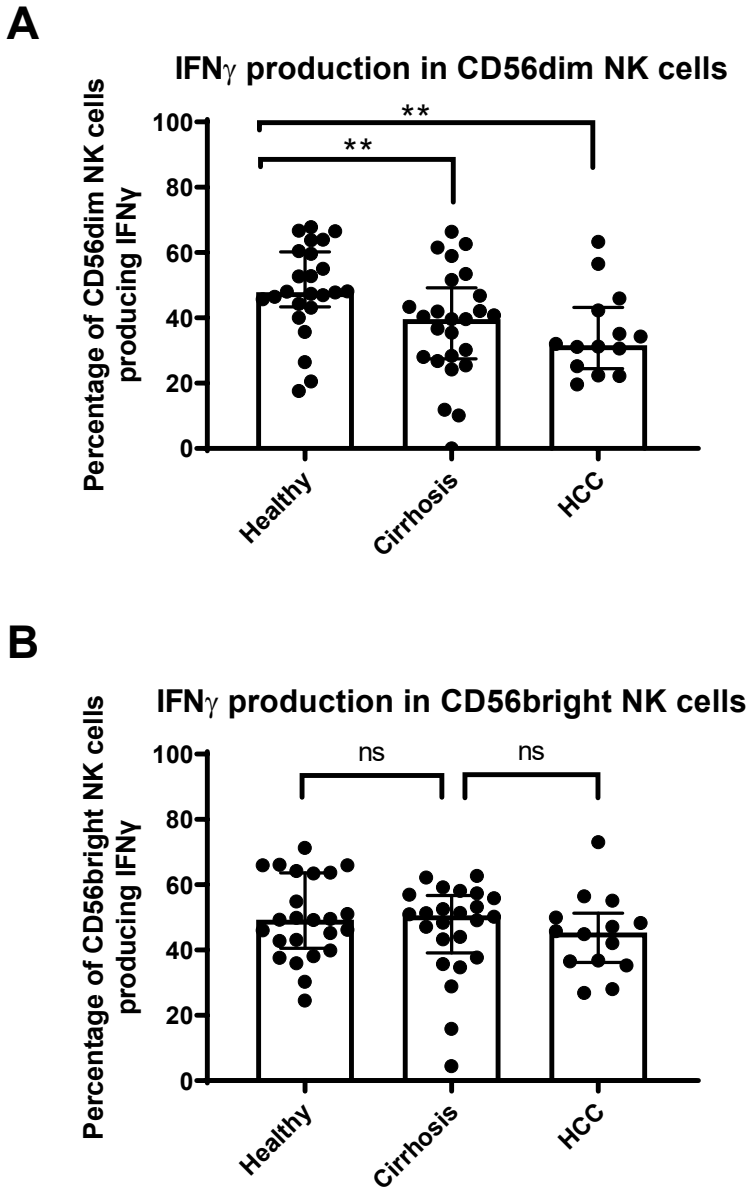


Figure 70 Comparing interferon gamma (IFNγ) response in CD56dim and CD56bright NK cells in healthy volunteers and patient groups against K562 target cells. Peripheral blood mononuclear cells (PBMCs) were co-cultured with K562 target cells in a 5:1 ratio respectively. Intracellular staining followed by flow cytometry was undertaken to determine IFNγ production. A) Graph displays the percentage of CD56dim NK cells producing IFNγ against K562 target cells. CD56dim NK cells from patients with cirrhosis or HCC had a reduced IFNγ response to K562 cells in comparison to CD56dim NK cells from healthy volunteers. B) Graph displays the percentage of CD56bright NK cells producing IFNγ against K562 target cells. There

*were no significant functional deficits with regards to IFNγ production in patient groups compared to healthy volunteers. This analysis was also undertaken for PBMCs against HepG2 target cells but there were no significant differences in functional outputs in the CD56dim or CD56bright subset in either healthy or disease states (data not shown). Healthy=healthy individuals; cirrhosis = patients with cirrhosis; HCC = patients with hepatocellular carcinoma (HCC) on a background of cirrhosis. Graphs display individual values with the bar representing the median value. Error bars display the interquartile range. P values for significance are displayed on the graphs as follows: * p<0.05, ** p<0.01, *** p<0.001, **** p<0.0001.*

Comparing tumour necrosis factor alpha (TNFα) production in CD56dim NK cells and CD56bright NK cells in response to K562 target cells

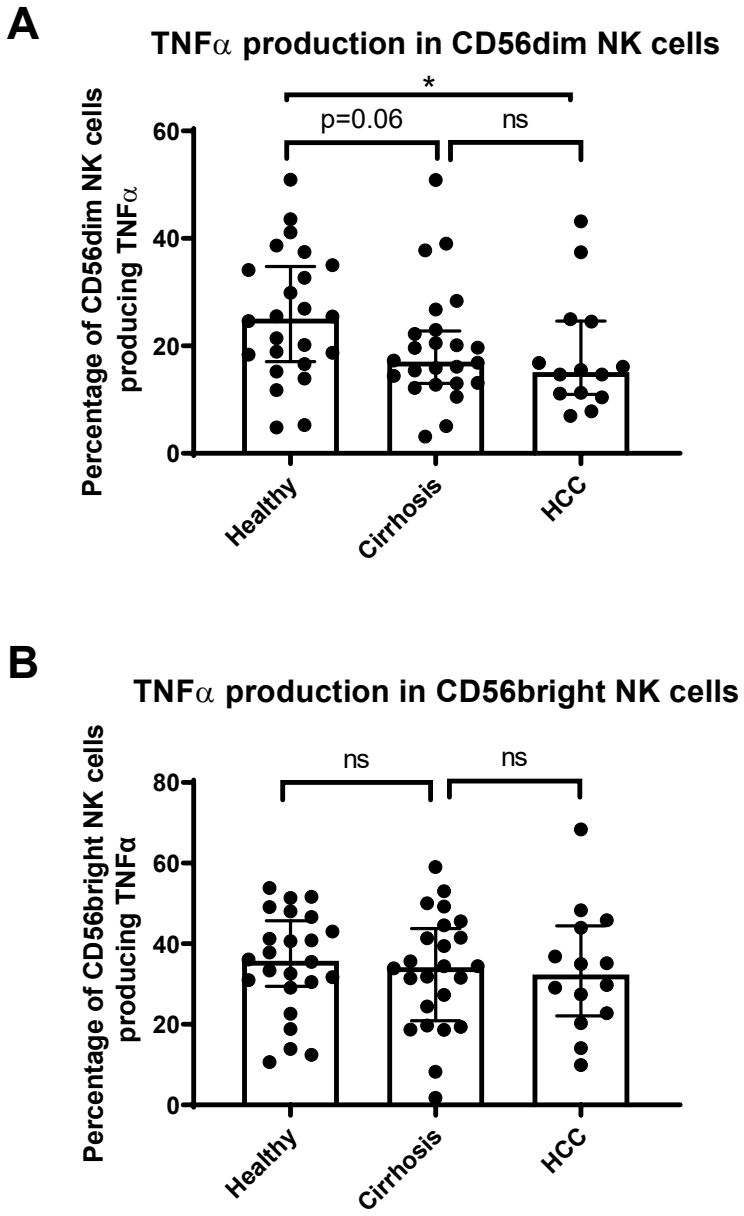


Figure 71 Comparing tumour necrosis factor alpha (TNFα) response in CD56dim and CD56bright NK cells in healthy volunteers and patient groups against K562 target cells. Peripheral blood mononuclear cells (PBMCs) were co-cultured with K562 target cells in a 5:1 ratio respectively. Intracellular staining followed by flow cytometry was undertaken to determine TNFα production. A) Graph displays the percentage of CD56dim NK cells producing TNFα against K562 target cells. CD56dim NK cells from patients with HCC had a reduced TNFα

*response to K562 cells in comparison to CD56dim NK cells from healthy volunteers. CD56dim NK cells from patient with cirrhosis also had a reduced TNFα response in comparison to healthy NK cells, but the difference did not reach significance (p=006). B) Graph displays the percentage of CD56bright NK cells producing TNFα against K562 target cells. There were no significant functional deficits with regards to TNFα production in patient groups compared to healthy volunteers. This analysis was also undertaken for PBMCs against HepG2 target cells but there were no significant differences in functional outputs in the CD56dim or CD56bright subset in either healthy or disease states (data not shown). Healthy=healthy individuals; cirrhosis = patients with cirrhosis; HCC = patients with hepatocellular carcinoma (HCC) on a background of cirrhosis. Graphs display individual values with the bar representing the median value. Error bars display the interquartile range. P values for significance are displayed on the graphs as follows: * p<0.05, ** p<0.01, *** p<0.001, **** p<0.0001.*

Comparing the capacity of CD56dim and CD56bright NK cells in producing a polyfunctional response (expressing CD107a, TNFα and IFNγ) to K562 target cells

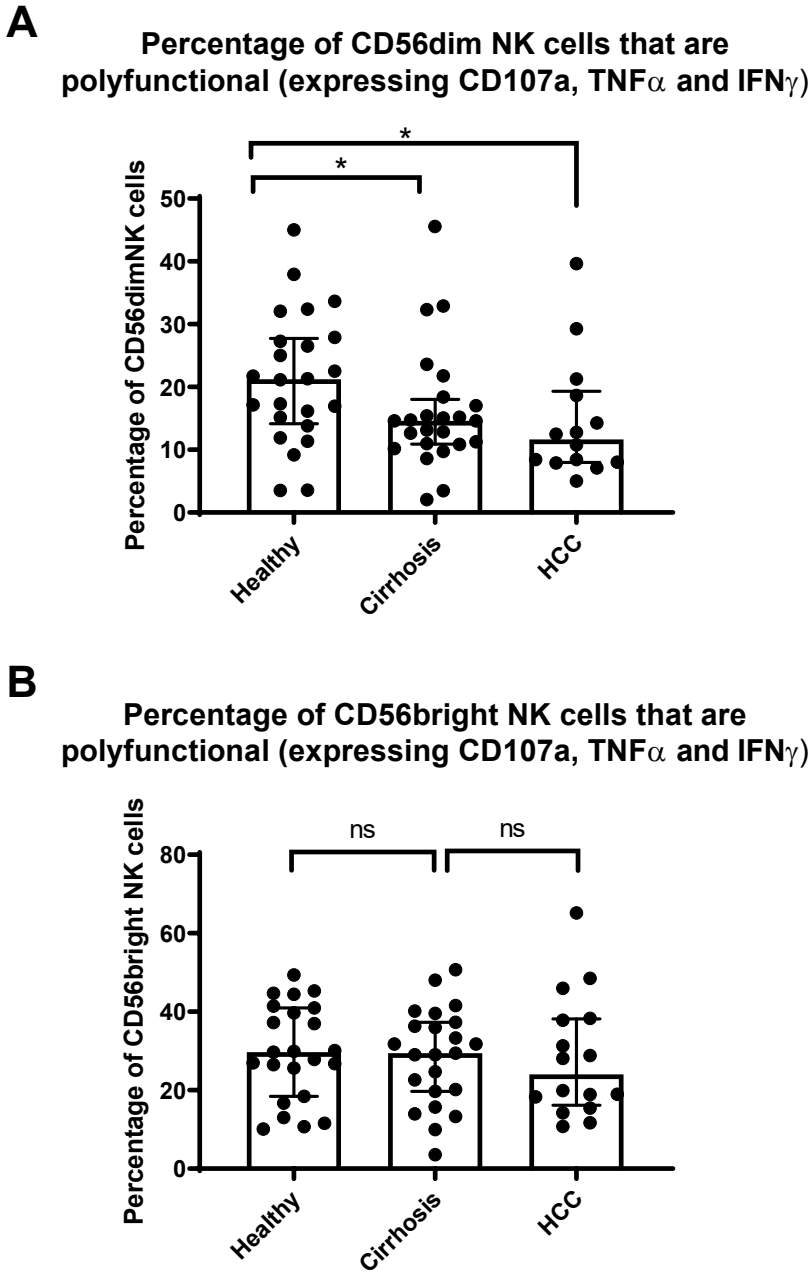


Figure 72 Comparing the capacity for a polyfunctional response in CD56dim and CD56bright NK cells in healthy volunteers and patient groups against K562 target cells. Peripheral blood mononuclear cells (PBMCs) were co-cultured with K562 target cells in a 5:1 ratio respectively. Intracellular staining followed by flow cytometry was undertaken to determine cytotoxicity (CD107a expression), interferon gamma (IFNγ) production and tumour necrosis factor alpha

*(TNFα) production. A) Graph displays the percentage of CD56dim NK cells producing a polyfunctional response to K562 cells i.e. expressing CD107a and producing IFNγ, and TNFα in response to K562 target cells. CD56dim NK cells from patients with cirrhosis and HCC had a significantly reduced proportion of CD56dim NK cells producing a polyfunctional response to K562 cells. B) Graph displays the percentage of CD56bright NK cells producing a polyfunctional response to K562 target cells. There were no significant differences in the proportion of CD56bright NK cells that produce a polyfunctional response in patient groups compared to healthy volunteers. This analysis was also undertaken for PBMCs against HepG2 target cells but there were no significant differences in functional outputs in the CD56dim or CD56bright subset in either healthy or disease states (data not shown). Healthy=healthy individuals; cirrhosis = patients with cirrhosis; HCC = patients with hepatocellular carcinoma (HCC) on a background of cirrhosis. Graphs display individual values with the bar representing the median value. Error bars display the interquartile range. P values for significance are displayed on the graphs as follows: * p<0.05, ** p<0.01, *** p<0.001, **** p<0.0001.*

3.2.4 Correlation of NK cell functional responses with cirrhosis status and cirrhosis aetiology

Functional responses (CD107a expression, IFNγ and TNFα production) for circulating NK cells from patients with cirrhosis against K562 targets did not correlate with the cirrhosis status as measured by MELD-Na score and Child-Pugh status (Figures 73-75). The analysis was repeated for functional responses to HepG2 cells, but this also did not yield significant correlations with underlying MELD-Na or Child-Pugh score (data not shown). The analysis was repeated separating the cirrhosis group further by underlying aetiology (ALD compared to MASLD) but this did not yield any significant correlations with MELD-Na or any significant differences with underlying Child-Pugh score (data not shown).

CD107a expression in NK cells from patients with cirrhosis in response to K562 target cells did not correlate with underlying cirrhosis status

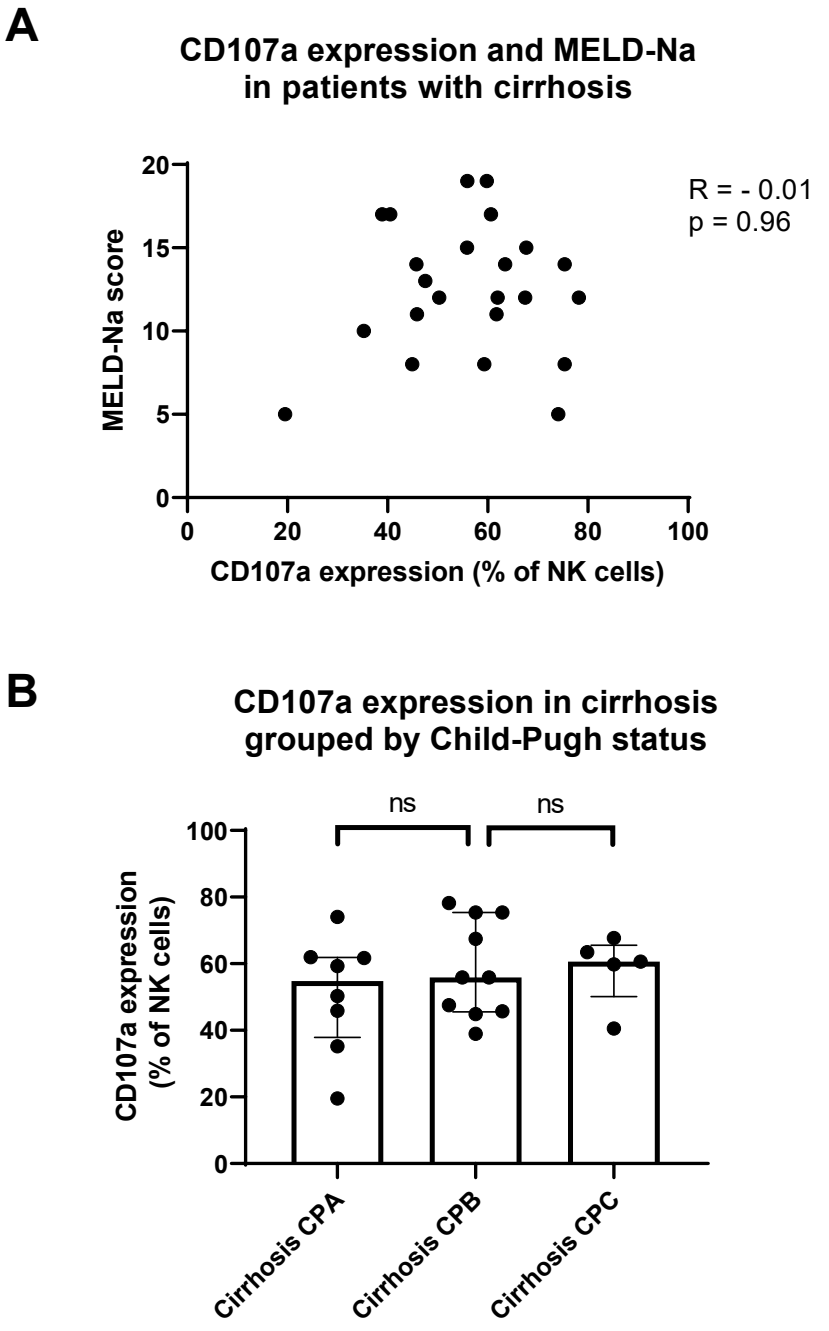


Figure 73 CD107a expression in NK cells from patients with cirrhosis does not correlate with underlying cirrhosis status. Peripheral blood mononuclear cells (PBMCs) from patients with cirrhosis were incubated for 4 hours with K562 target cells in the presence of fluorescently labelled CD107a antibody. PBMCs then underwent surface staining with fluorescently labelled

antibodies to CD3 and CD56, and CD107a expression in NK cells within the PBMCs was assessed using flow cytometry. Spearman Rank correlation coefficients were calculated for CD107a expression and the underlying MELD-Na score for each patient (graph A). Patients were also grouped by their underlying Child-Pugh score, and comparisons in CD107a expression between groups made using the Mann-Whitney test (graph B). Graphs display individual values with the bar representing the median value on the bar graphs. Error bars display the interquartile range. A) Graph showing the lack of correlation in CD107a expression in NK cells from patients with cirrhosis and their underlying MELD-NA score. B) There were no significant differences in CD107a expression and Child-Pugh status (CPA= Child-Pugh A, CP-B = Child-Pugh B, CPC = Child-Pugh C). The analysis was repeated for functional responses to HepG2 cells, but this also did not yield significant correlations with underlying MELD-Na or Child-Pugh score (data not shown). The analysis was repeated separating the cirrhosis group further by underlying aetiology (alcohol related liver disease or metabolic dysfunction-associated steatotic liver disease) but this did not yield any significant correlations with MELD-Na or any significant differences with underlying Child-Pugh score (data not shown).

IFNγ production in NK cells from patients with cirrhosis in response to K562 target cells did not correlate with underlying cirrhosis status

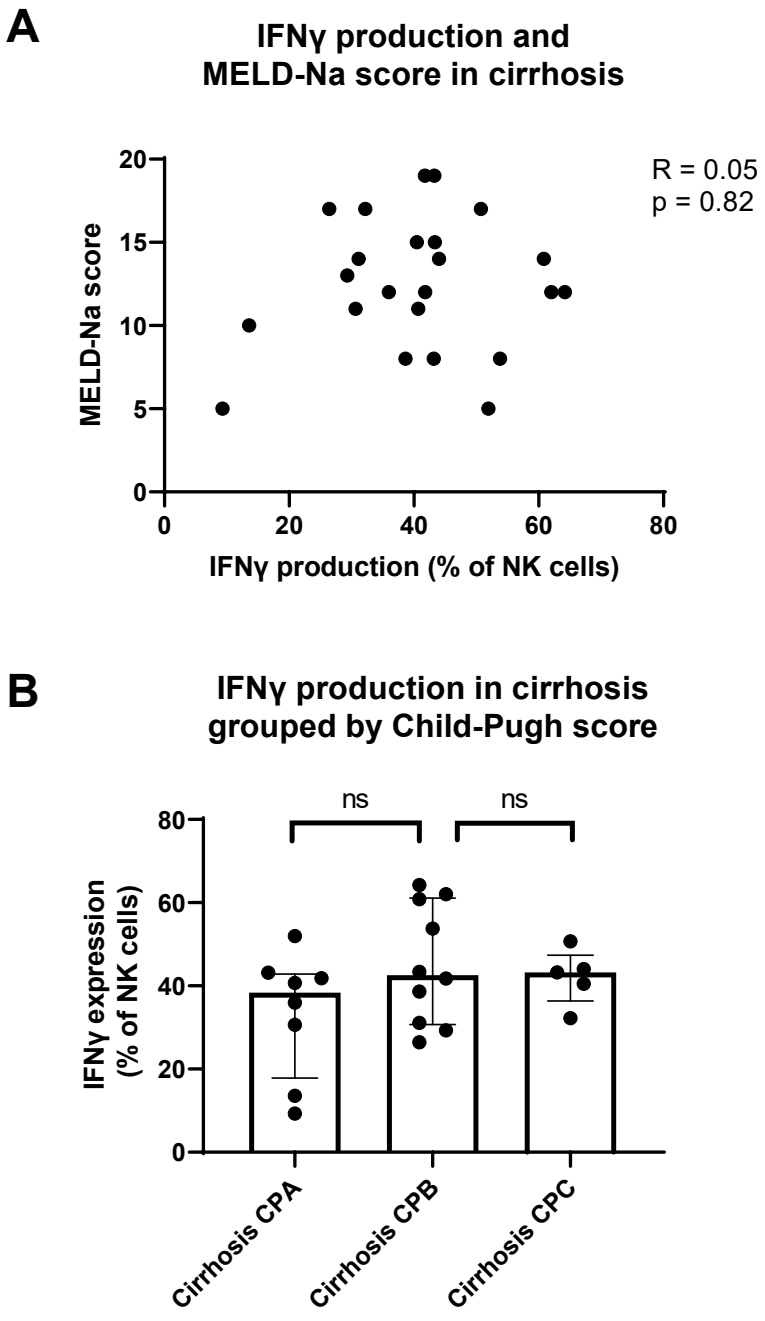


Figure 74 Interferon gamma (IFNγ) production in NK cells from patients with cirrhosis does not correlate with underlying cirrhosis status. Peripheral blood mononuclear cells (PBMCs) from patients with cirrhosis were incubated for 4 hours with K562 target cells. PBMCs then underwent surface staining with fluorescently labelled antibodies to CD3 and CD56, and IFNγ

production in NK cells within the PBMCs was assessed using intracellular staining followed by flow cytometry. Spearman Rank correlation coefficients were calculated for IFNγ production and the underlying MELD-Na score for each patient (graph A). Patients were also grouped by their underlying Child-Pugh score, and comparisons in IFNγ production between groups made using the Mann-Whitney test (graph B). Graphs display individual values with the bar representing the median value on the bar graphs. Error bars display the interquartile range. A) Graph showing the lack of correlation in IFNγ production in NK cells from patients with cirrhosis and their underlying MELD-NA score. B) There were no significant differences in IFNγ production and Child-Pugh status (CPA= Child-Pugh A, CP-B = Child-Pugh B, CPC = Child-Pugh C). The analysis was repeated for functional responses to HepG2 cells, but this also did not yield significant correlations with underlying MELD-Na or Child-Pugh score (data not shown). The analysis was repeated separating the cirrhosis group further by underlying aetiology (alcohol related liver disease or metabolic dysfunction-associated steatotic liver disease) but this did not yield any significant correlations with MELD-Na or any significant differences with underlying Child-Pugh score (data not shown).

TNFα production in NK cells from patients with cirrhosis in response to K562 target cells did not correlate with underlying cirrhosis status

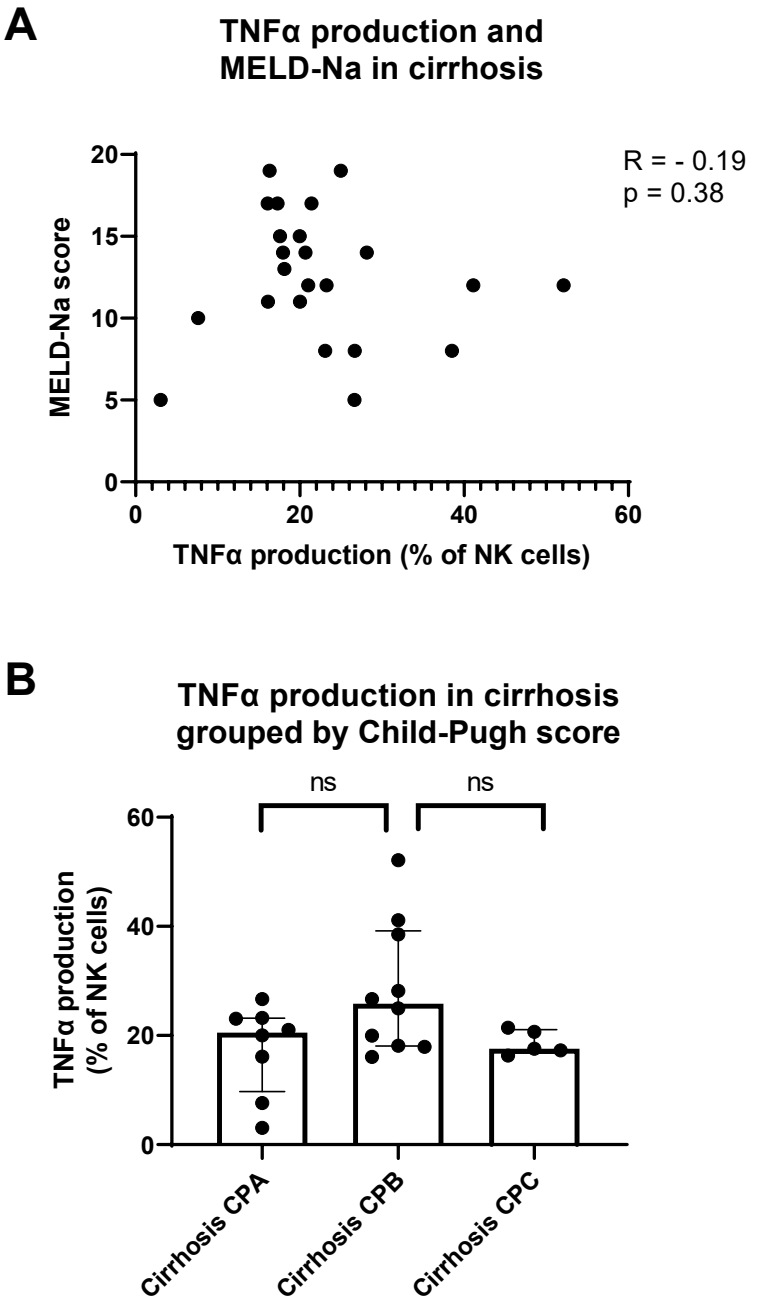


Figure 75 Tumour necrosis factor alpha (TNFα) production in NK cells from patients with cirrhosis does not correlate with underlying cirrhosis status. Peripheral blood mononuclear cells (PBMCs) from patients with cirrhosis were incubated for 4 hours with K562 target cells. PBMCs then underwent surface staining with fluorescently labelled antibodies to CD3 and

CD56, and TNFα production in NK cells within the PBMCs was assessed using intracellular staining followed by flow cytometry. Spearman Rank correlation coefficients were calculated for TNFα production and the underlying MELD-Na score for each patient (graph A). Patients were also grouped by their underlying Child-Pugh score, and comparisons in TNFα production between groups made using the Mann-Whitney test (graph B). Graphs display individual values with the bar representing the median value on the bar graphs. Error bars display the interquartile range. A) Graph showing the lack of correlation in TNFα production in NK cells from patients with cirrhosis and their underlying MELD-NA score. B) There were no significant differences in TNFα production and Child-Pugh status (CPA= Child-Pugh A, CP-B = Child-Pugh B, CPC = Child-Pugh C). The analysis was repeated for functional responses to HepG2 cells, but this also did not yield significant correlations with underlying MELD-Na or Child-Pugh score (data not shown). The analysis was repeated separating the cirrhosis group further by underlying aetiology (alcohol related liver disease or metabolic dysfunction-associated steatotic liver disease) but this did not yield any significant correlations with MELD-Na or any significant differences with underlying Child-Pugh score (data not shown).

No statistically significant differences were seen in NK cell functional responses to K562 cells when comparing patients with cirrhosis secondary to ALD with patients with cirrhosis secondary to MASLD (Figures 76-78). Similarly, there were no differences in NK cell responses in patients with HCC with underlying ALD cirrhosis compared to patients with underlying MASLD cirrhosis (Figures 76-78). There were not enough samples to determine functional variation and underlying BCLC staging.

CD107a expression in NK cells in response to K562 targets is not significantly different in patients with ALD compared to patients with MASLD

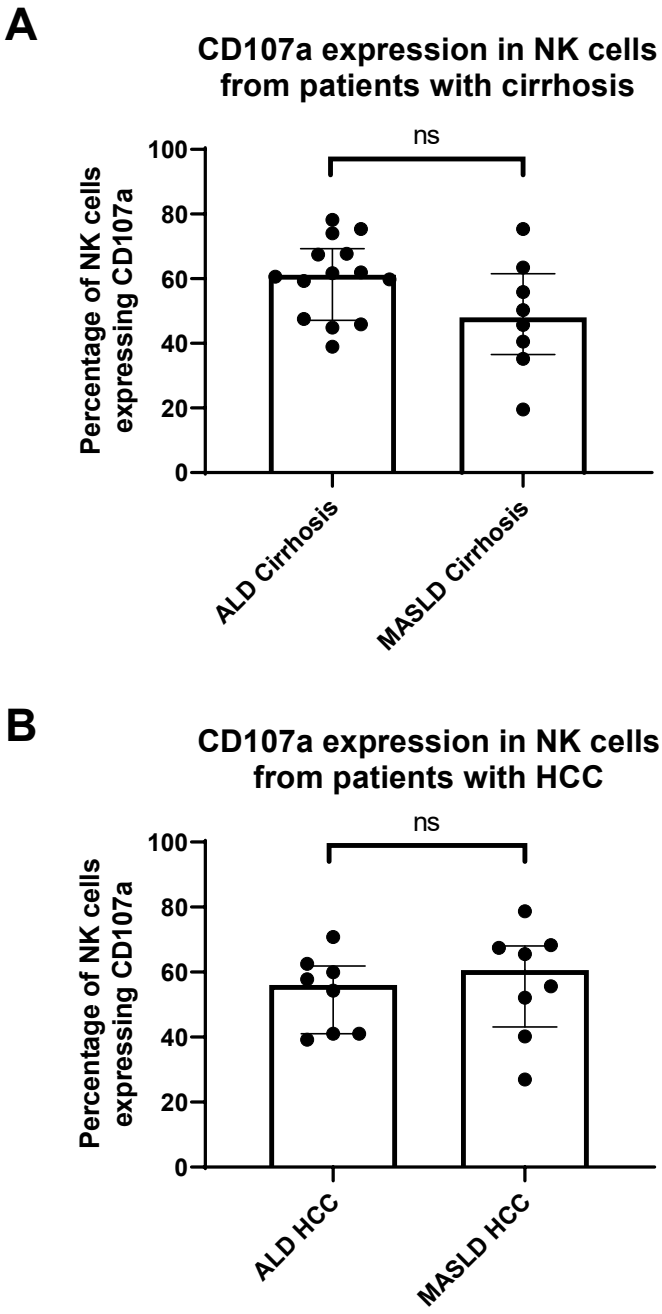


Figure 76 Comparison of CD107a expression in NK cells in patients with alcohol related liver disease (ALD) and metabolic dysfunction-associated steatotic liver disease (MASLD). Peripheral blood mononuclear cells (PBMCs) from patients were incubated with K562 target cells for four hours at a 5:1 PBMC:K562 ratio in the presence of CD107a antibody. Subsequent

surface staining and flow cytometry allowed measurement of the NK cell proportion expressing CD107a. Graph A demonstrates CD107a expression in NK cells from patients with cirrhosis. Graph B demonstrates CD107a expression in patients with hepatocellular carcinoma (HCC) on a background of cirrhosis. Graphs display individual values with the bar representing the median value on the bar graphs. Error bars display the interquartile range. Comparisons were made using Mann-Whitney tests. There were no significant differences between patients with cirrhosis or HCC with underlying ALD or MASLD. The analysis was repeated for functional responses to HepG2 cells, but this also did not yield significant differences (data not shown).

IFNγ production in NK cells in response to K562 targets is not significantly different in patients with ALD compared to patients with MASLD

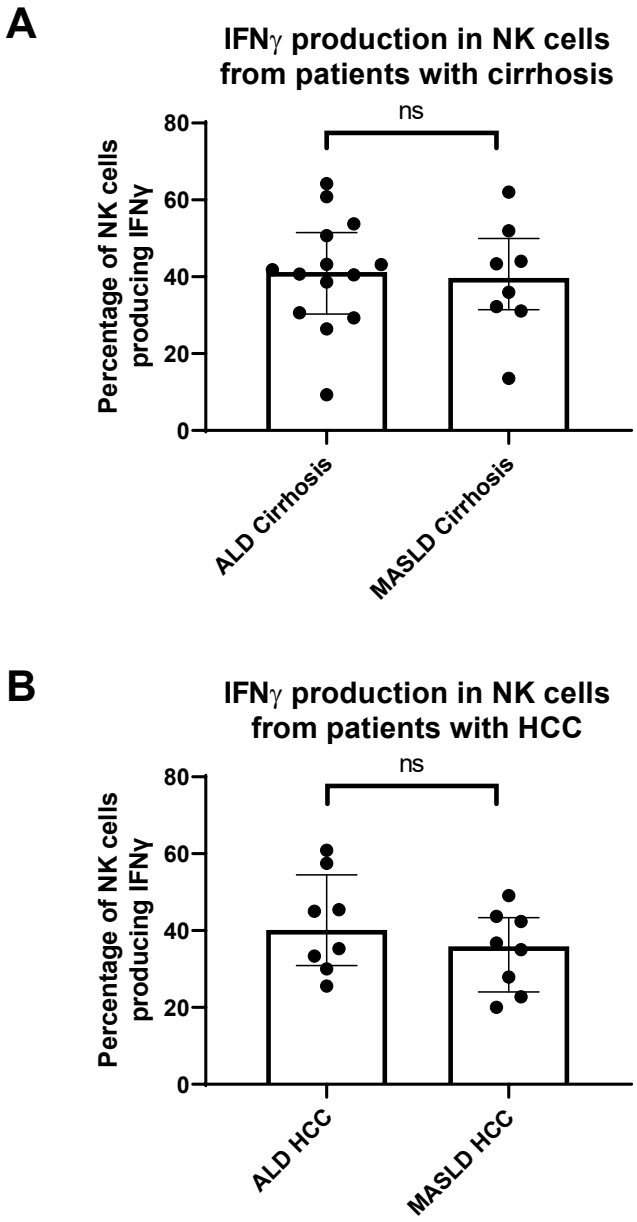


Figure 77 Comparison of interferon gamma(IFNγ) production in NK cells in patients with alcohol related liver disease (ALD) and metabolic dysfunction-associated steatotic liver disease (MASLD). Peripheral blood mononuclear cells (PBMCs) from patients were incubated with K562 target cells for four hours at a 5:1 PBMC:K562 ratio. Subsequent intracellular staining and flow cytometry allowed measurement of the NK cell proportion expressing IFNγ. Graph A demonstrates IFNγ production in NK cells from patients with cirrhosis. Graph B demonstrates

IFNγ production in patients with hepatocellular carcinoma (HCC) on a background of cirrhosis. Graphs display individual values with the bar representing the median value on the bar graphs. Error bars display the interquartile range. Comparisons were made using Mann-Whitney tests. There were no significant differences between patients with cirrhosis or HCC with underlying ALD or MASLD. The analysis was repeated for functional responses to HepG2 cells, but this also did not yield significant differences (data not shown).

TNFα production in NK cells in response to K562 targets is not significantly different in patients with ALD compared to patients with MASLD

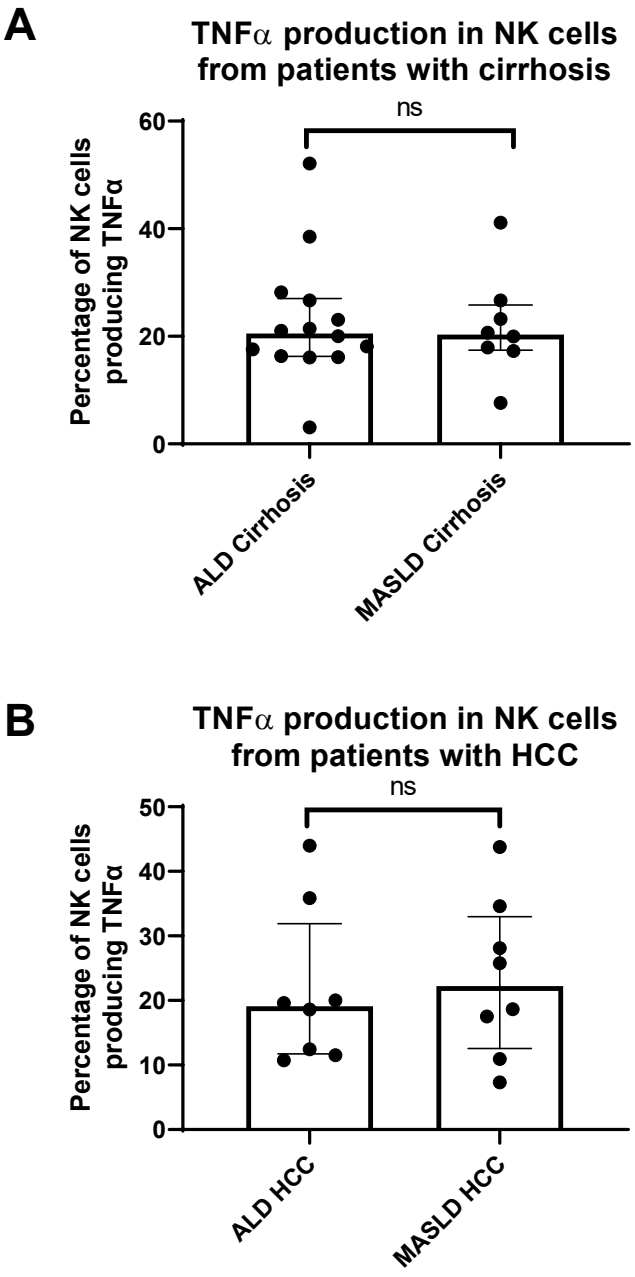


Figure 78 Comparison of tumour necrosis factor alpha(TNFα) production in NK cells in patients with alcohol related liver disease (ALD) and metabolic dysfunction-associated steatotic liver disease (MASLD). Peripheral blood mononuclear cells (PBMCs) from patients were incubated with K562 target cells for four hours at a 5:1 PBMC:K562 ratio. Subsequent intracellular

staining and flow cytometry allowed measurement of the NK cell proportion expressing TNFα. Graph A demonstrates TNFα production in NK cells from patients with cirrhosis. Graph B demonstrates TNFα production in patients with hepatocellular carcinoma (HCC) on a background of cirrhosis. Graphs display individual values with the bar representing the median value on the bar graphs. Error bars display the interquartile range. Comparisons were made using Mann-Whitney tests. There were no significant differences between patients with cirrhosis or HCC with underlying ALD or MASLD. The analysis was repeated for functional responses to HepG2 cells, but this also did not yield significant differences (data not shown).

3.2.5 NK cell surface receptor correlation with functional responses

NK cell functional responses (CD107a expression, IFNγ and TNFα production) against K562 and HepG2 target cells were correlated with NK cell receptor expression from the same patients with cirrhosis or HCC with underlying MASLD or ALD cirrhosis.

The only receptor that demonstrated any correlation with functional NK cell responses against K562 cells was NKp30. Correlations were not seen however with functional responses against HepG2 cells and NKp30.

The expression of NKp30 correlated negatively with CD107a expression, IFNγ and TNFα production in patients with MASLD HCC (Figure 79). A negative correlation between all functional responses and NKp30 was also seen in MASLD cirrhosis without HCC but did not reach significance. NKp30 expression on NK cells in ALD cirrhosis however correlated positively with CD107a expression and IFNγ expression (Figure 80). There was also positive correlation of NKp30 expression with all functional responses in patients with ALD HCC but did not reach significance.

NK cell functional responses to K562 targets correlate negatively with NKp30 receptor expression in patients with MASLD HCC

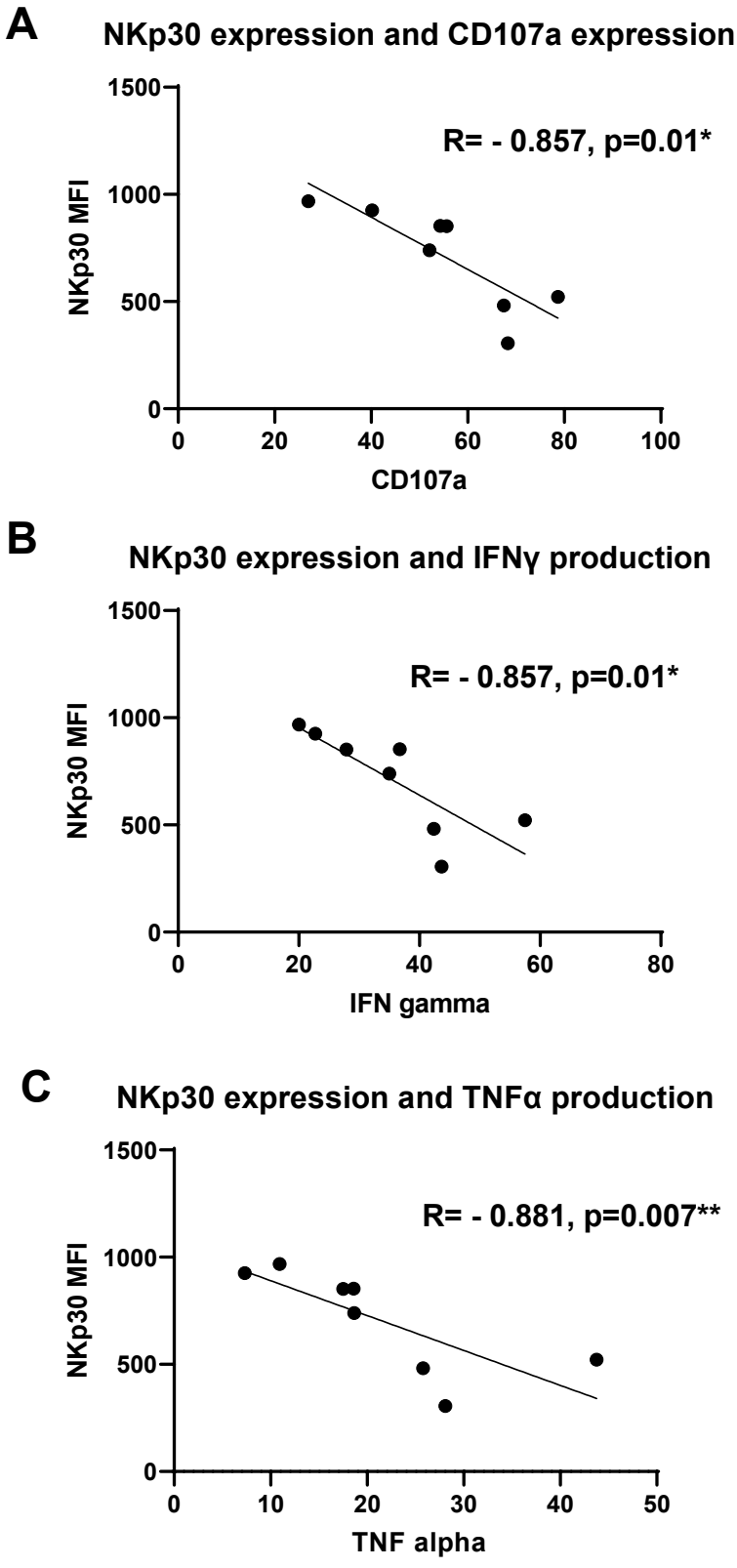


*Figure 79 NKp30 expression inversely correlated with NK cell functional responses in patients with hepatocellular carcinoma (HCC) on a background of cirrhosis secondary to metabolic dysfunction-associated steatotic liver disease (MASLD). Peripheral blood mononuclear cells (PBMCs) from patients with HCC on a background of MASLD cirrhosis (MASLD HCC) were incubated for four hours with K562 target cells in a 5:1 ratio (PBMC:K562) in the presence of CD107a antibody. Following this, functional responses (degranulation (CD107a expression) (graph A), interferon gamma (IFNγ) (graph B) and tumour necrosis factor alpha (TNFα) production) (graph C) in the NK cells were measured in response to the K562 cells using flow cytometry following surface and intracellular staining. PBMCs from the same donors were also surface stained for NKp30 expression. The Spearman Rank correlation coefficient (R) was calculated for NKp30 expression and each functional response on circulating NK cells in the same donors. There was a significant negative correlation with each functional response and NKp30 expression. Graphs show individual values plotted as dots; P values for significance are displayed on the graphs as follows: * p<0.05, ** p<0.01, *** p<0.001, **** p<0.0001.*

NK cell functional responses to K562 targets correlate positively with NKp30 receptor expression in patients with ALD cirrhosis

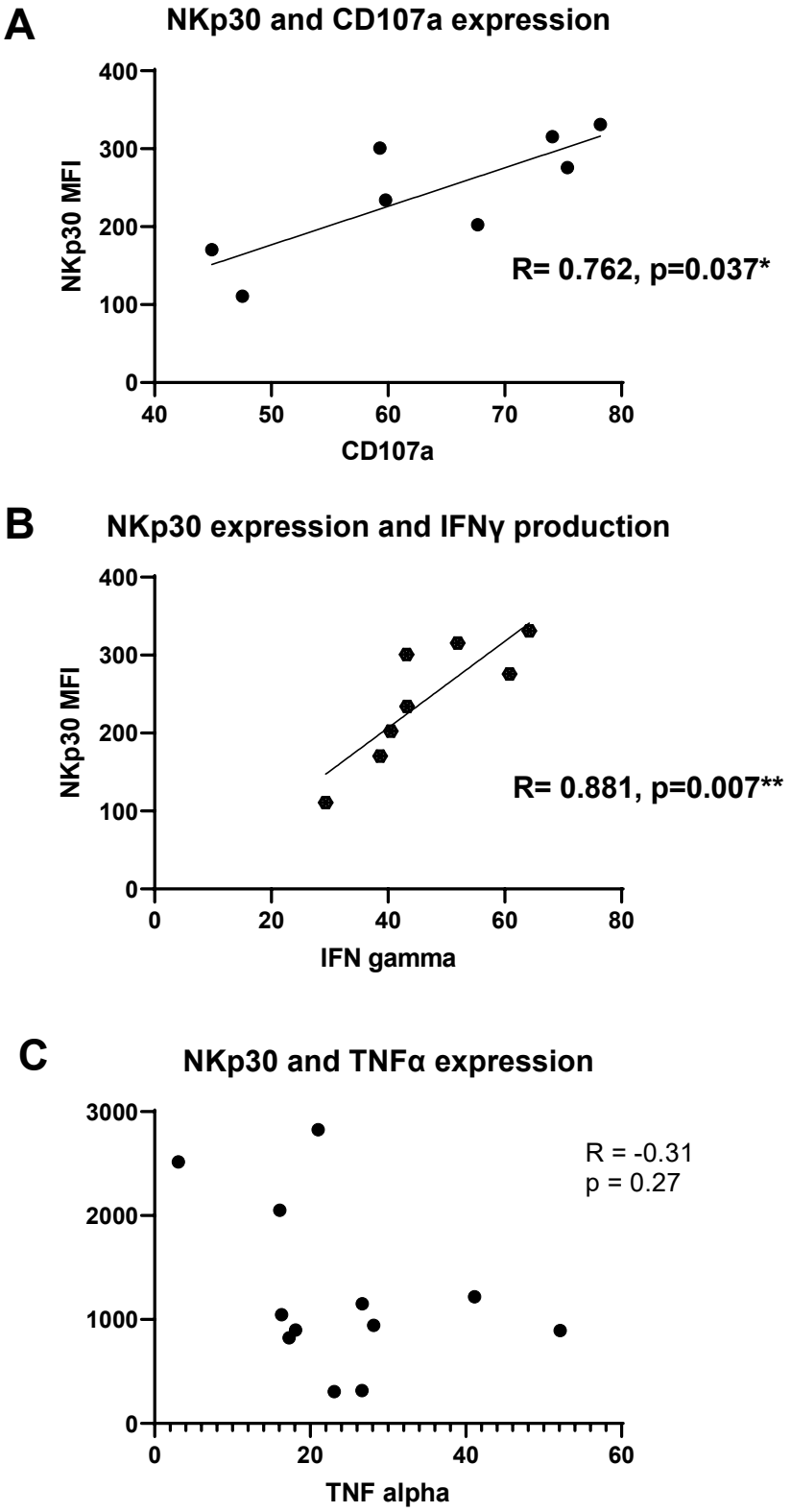


*Figure 80 NKp30 expression correlated with NK cell degranulation and interferon gamma (IFNγ) production in circulating NK cells from patients with cirrhosis secondary to alcohol related liver disease (ALD). Peripheral blood mononuclear cells (PBMCs) from patients with ALD cirrhosis were incubated for four hours with K562 target cells in a 5:1 ratio (PBMC:K562) in the presence of CD107a antibody. Following this, functional responses (degranulation (CD107a expression) (graph A), IFNγ (graph B) and tumour necrosis factor alpha (TNFα) production) (graph C) in the NK cells were measured in response to the K562 cells using flow cytometry following surface and intracellular staining. PBMCs from the same donors were also surface stained for NKp30 expression. The Spearman Rank correlation coefficient (R) was calculated for NKp30 expression and each functional response on circulating NK cells in the same donors. There was a significant positive correlation with CD107a expression and IFNγ production and NKp30 expression. Graphs show individual values plotted as dots; P values for significance are displayed on the graphs as follows: * p<0.05, ** p<0.01, *** p<0.001, **** p<0.0001.*

3.3 Gene expression

In order to understand the processes involved resulting in these phenotypic and functional differences seen in cirrhosis and HCC, gene expression was evaluated using NanoString technology, and comparisons made between the classical circulating NK cell populations (CD56dimCD16++ and CD56brightCD16- NK cells) in health and disease. Peripheral blood mononuclear cells were extracted from healthy volunteers (n=3), patients with Child-Pugh B cirrhosis with underlying ALD (n=3) or MASLD (n=4) and patients with hepatocellular carcinoma (HCC) complicating Child-Pugh B cirrhosis secondary to MASLD (n=3). NK cells were sorted into CD56dimcD16++ and CD56brightCD16- NK subpopulations, lysed as described in methods and gene expression evaluated using a customised NanoString panel. Full differential expression analyses can be found in Appendix D.

Mononuclear cells extracted from explanted livers with MASLD cirrhosis were sorted using the same strategy as for peripheral blood mononuclear cells as described above. Gene expression on these intrahepatic NK cells from patients with MASLD cirrhosis (n=3) was compared to circulating NK cells from patients with MASLD cirrhosis (n=4; non-paired samples). Genes with significant differential expression are demonstrated on the heat maps below. Full differential expression analyses can be found in Appendix D.

The significance of the differential gene expression profile seen in disease was analysed using web-based platforms Reactome and Ingenuity Pathway Analysis software (IPA, Ingenuity Systems, Qiagen).

Table 11 Characteristics of patients from whom samples were utilised for gene expression profiling using Nansostring technology. MASLD= metabolic dysfunction-associated steatotic liver disease; ALD= Alcohol related liver disease; HCC= Hepatocellular carcinoma. Samples were wither peripheral blood samples (circulating) or extracted from within the liver (intrahepatic). All patients had Child-Pugh B cirrhosis.

	MASLD Cirrhosis (circulating)	ALD Cirrhosis (circulating)	MASLD HCC (circulating)	MASLD Cirrhosis (intrahepatic)
Total number of patients	4	3	3	3
Age, years mean, (range)	64 (55-74)	57 (53-62)	72 (60-84)	61 (56-64)
Male, n	2	2	3	3
Child-Pugh Score B, n	4	3	3	3
MELD-Na score mean, (range)	14 (12– 14)	14 (12 – 15)	14 (11 – 18)	19 (18-20)

3.3.1 Comparison of gene expression in CD56dimCD16++ NK cells in the circulation in health and in disease

Comparison of the gene expression profile of the circulating CD56dimCD16++ NK cell subpopulation between healthy states and disease, demonstrated a downregulation of the transcription factor *EGR1* in cirrhosis of either aetiology (ALD or MASLD related cirrhosis) and in MASLD HCC (Figures 81-82). *EGR1* has been demonstrated to be upregulated in activated NK cells and responsible for limiting TRAIL expression (Balzarolo et al., 2013; Fu et al., 2003). However, despite a downregulation in *EGR1*, there was no significant differential expression in TRAIL at the gene expression level in this experiment.

Furthermore, CD56dimCD16++ NK cells in both cirrhosis and HCC groups demonstrated a reduced expression of interferon gamma (*IFNG*) compared to healthy CD56dimCD16++ NK cells. CD56dimCD16++ NK cells in ALD related cirrhosis and MASLD HCC also demonstrated reduced expression of Tumour necrosis factor (*TNF*) compared to healthy CD56dimCD16++NK cells. Transcription factors *STAT1* and *IRF4* were upregulated in CD56dimCD16++NK cells in MASLD HCC compared to healthy NK

cells, but not significantly upregulated in cirrhosis. *STAT1* and *IRF4* have been described as upregulated in NK cells that are activated (Costanzo et al., 2018).

Kir activating subgroup 2 was downregulated on CD56dimCD16++ NK cells in patients with alcohol related cirrhosis compared to healthy controls. KIR activating subgroup 2 was also downregulated significantly in patients with MASLD cirrhosis, though at less than a 2 fold difference (1.86 fold).

There were no significant differences in gene expression in circulating NK cell subpopulations in MASLD related cirrhosis compared to NK cell subpopulations in ALD related cirrhosis. There were no significant differences in circulating CD56dimCD++NK cells when comparing CD56dimCD16++NK cells in patients with MASLD HCC to CD56dimCD16++NK cells from patients with MASLD cirrhosis.

Differential gene expression in MASLD cirrhosis CD56dimCD16++ NK cells compared to CD56dimCD16++ NK cells from healthy volunteers

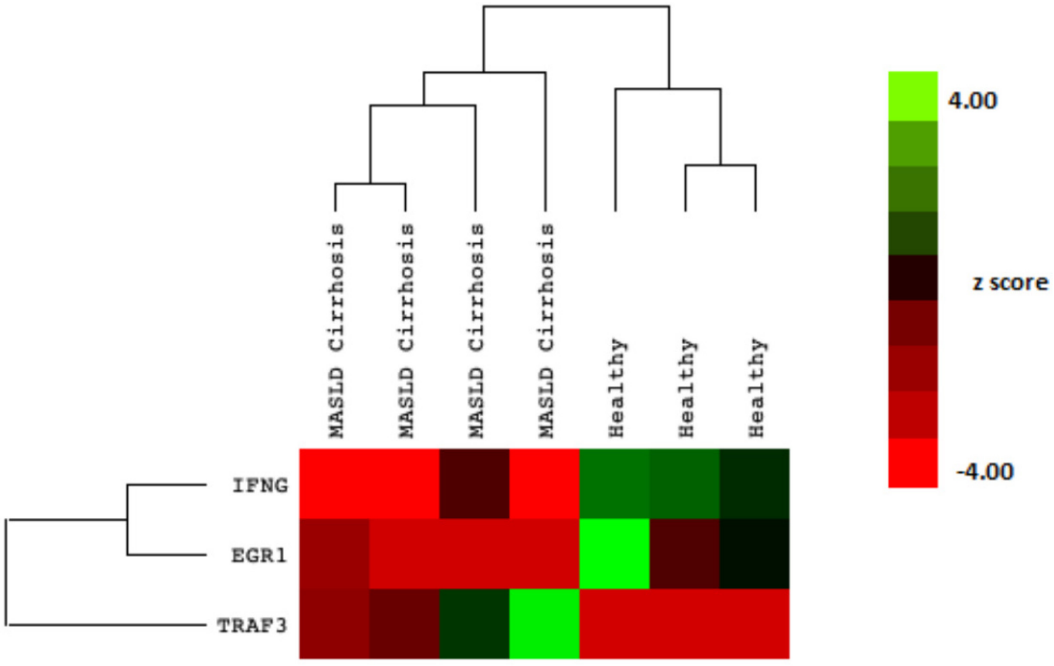


Figure 81 Differential gene expression in circulating CD56dimCD16++NK cells in MASLD cirrhosis when compared to CD56dimCD16++NK cells from healthy donors. Red corresponds to lower gene expression and green corresponds to higher gene expression. There was a significantly reduced expression of IFNG, EGR1 and TRAF3 in MASLD cirrhosis compared to healthy. The z score was calculated as follows: (gene expression value in the sample of interest) – (mean expression value across healthy samples)/standard deviation. (Genes displayed are expressed at >20 copies, demonstrate more than a 2 fold difference in expression with p<0.05 and FDR value of <0.05; MASLD = metabolic dysfunction-associated steatotic liver disease) .

Differential gene expression in ALD cirrhosis CD56dimCD16++ NK cells compared to CD56dimCD16++ NK cells from healthy volunteers

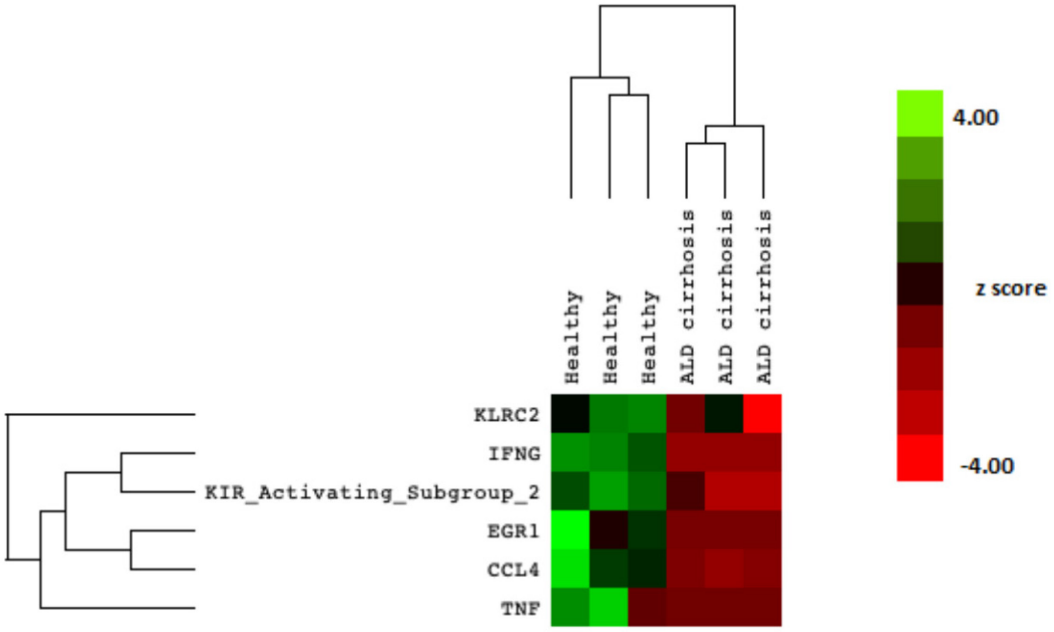


Figure 82 Differential gene expression in circulating CD56dimCD16++ NK cells in ALD cirrhosis when compared to CD56dimCD16++NK cells from healthy donors. Red corresponds to lower gene expression and green corresponds to higher gene expression. The z score was calculated as follows: (gene expression value in the sample of interest) – (mean expression value across healthy samples)/standard deviation. (Genes displayed are expressed at >20 copies, demonstrate more than a 2 fold difference in expression with p<0.05 and FDR value of <0.05; ALD = alcohol related liver disease liver disease).

Differential gene expression in MASLD HCC CD56dimCD16++ NK cells compared to CD56dimCD16++ NK cells from healthy volunteers

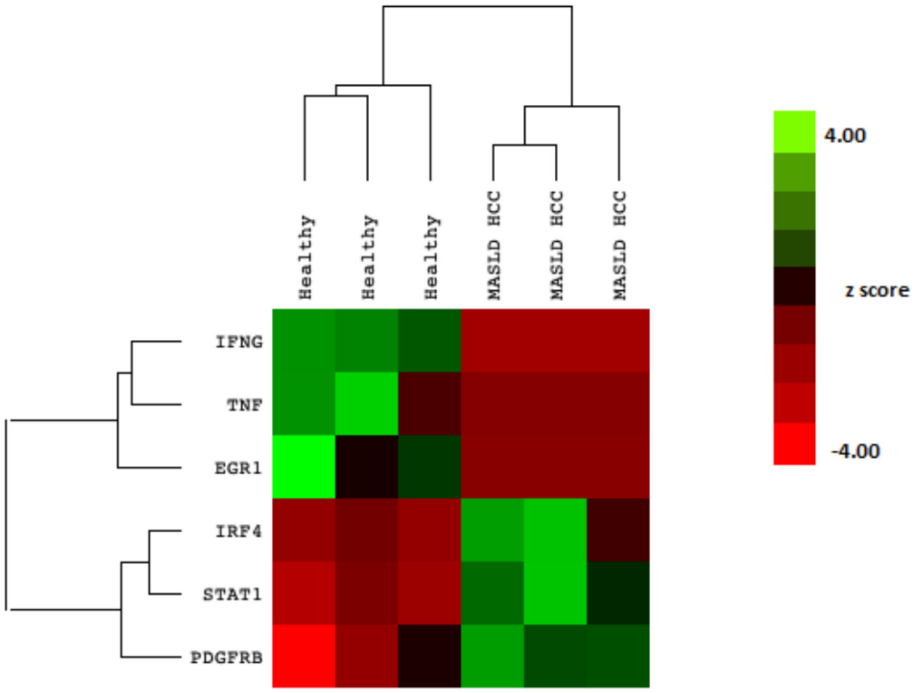


Figure 83 Differential gene expression in circulating CD56dimCD16++NK cells in MASLD HCC when compared to CD56dimCD16++NK cells from healthy donors. Red corresponds to lower gene expression and green corresponds to higher gene expression. There was a significantly reduced expression of IFNG, EGR1 and TNF in MASLD HCC compared to healthy state, but also an increased expression of IRF4, STAT1 and PDGFRB. The z score was calculated as follows: (gene expression value in the sample of interest) – (mean expression value across healthy samples)/standard deviation. (Genes displayed are expressed at >20 copies, demonstrate more than a 2 fold difference in expression with p<0.05 and FDR value of <0.05; MASLD HCC= hepatocellular carcinoma and underlying cirrhosis related to metabolic dysfunction-associated steatotic liver disease). ***There were no significant differences when comparing gene expression in CD56dimCD16++NK cells in MASLD HCC to MASLD cirrhosis.***

3.3.2 Comparison of gene expression in CD56brightCD16- NK cells in the circulation in health and in disease

Circulating CD56brightCD16-NK cells demonstrated an increased expression of CCL5 in MASLD cirrhosis in comparison to healthy CD56brightCD16-NK cells (Figure 84).

When comparing circulating CD56brightCD16-NK cell subpopulations in MASLD cirrhosis with or without HCC, there was a significant reduction in expression of the following genes in patients with MASLD HCC: cell signalling genes *S100A8*, *S100A9* and *LYN*, the inhibitory receptor *CD74,* and *HLA-DRA* (associated with NK cell activation) (Figure 86).

Differential gene expression in MASLD cirrhosis CD56brightCD16- NK cells compared to CD56brightCD16- NK cells from healthy volunteers

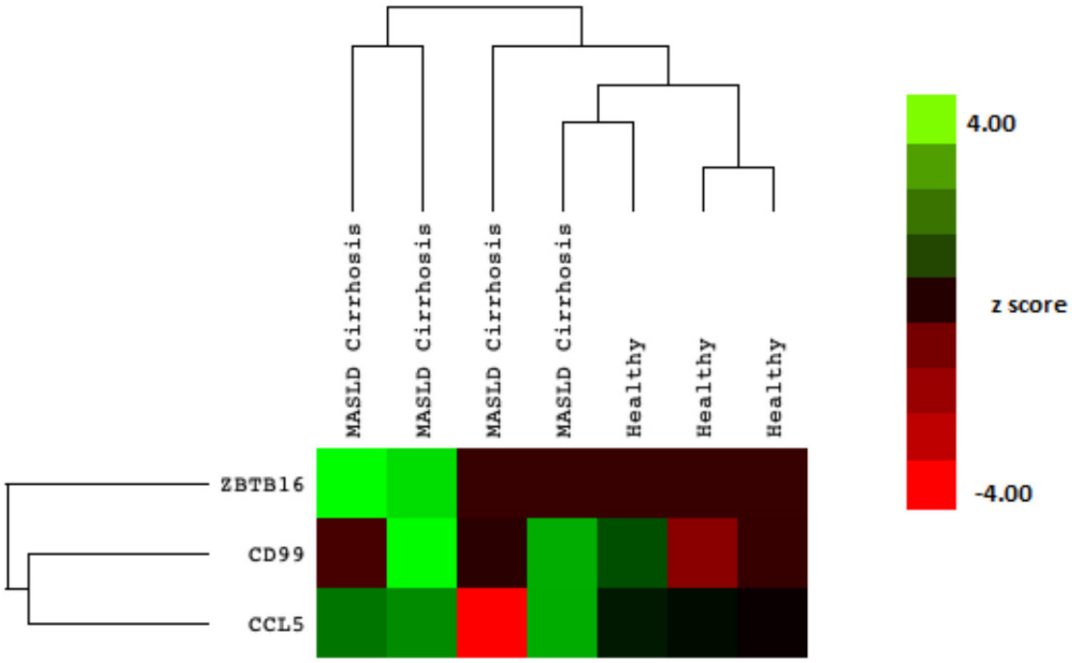


Figure 84 Differential gene expression in circulating CD56brightCD16-NK cells in MASLD cirrhosis when compared to CD56brightCD16-NK cells from healthy donors. Red corresponds to lower gene expression and green corresponds to higher gene expression. The z score was calculated as follows: (gene expression value in the sample of interest) – (mean expression value across healthy samples)/standard deviation. (Genes displayed are expressed at >20 copies, demonstrate more than a 2 fold difference in expression with p<0.05 and FDR value of <0.05; MASLD= metabolic dysfunction-associated steatotic liver disease).

Differential gene expression in ALD cirrhosis CD56brightCD16- NK cells compared to CD56brightCD16- NK cells from healthy volunteers

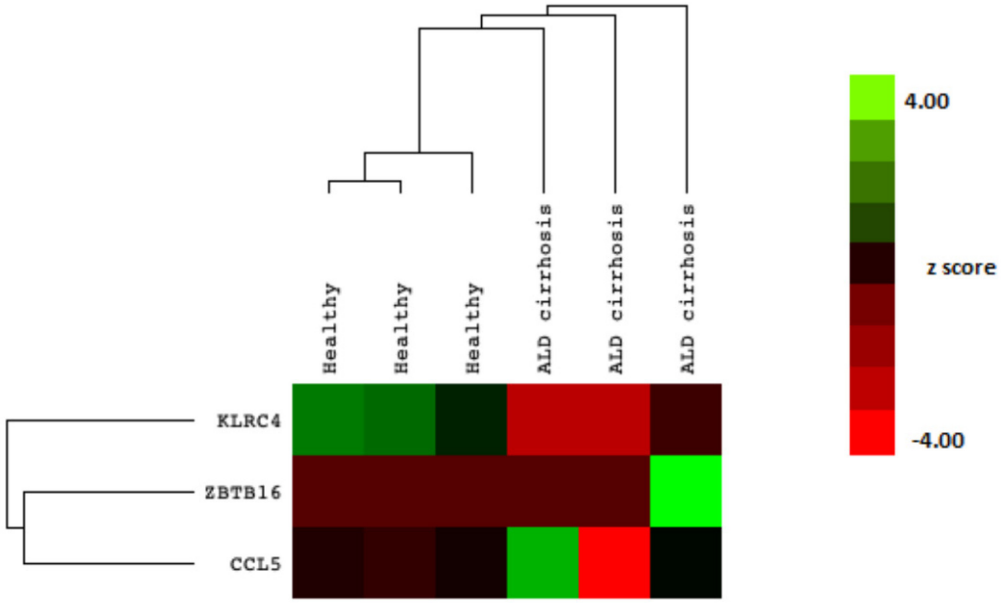


Figure 85 Differential gene expression in circulating CD56brightCD16-NK cells in ALD cirrhosis when compared to CD56brightCD16-NK cells from healthy donors. Red corresponds to lower gene expression and green corresponds to higher gene expression. The z score was calculated as follows: (gene expression value in the sample of interest) – (mean expression value across healthy samples)/standard deviation. (Genes displayed are expressed at >20 copies, demonstrate more than a 2 fold difference in expression with p<0.05 and FDR value of <0.05; ALD= alcohol related liver disease liver disease).

Differential gene expression in MASLD HCC CD56brightCD16- NK cells compared to CD56brightCD16- NK cells from MASLD cirrhosis

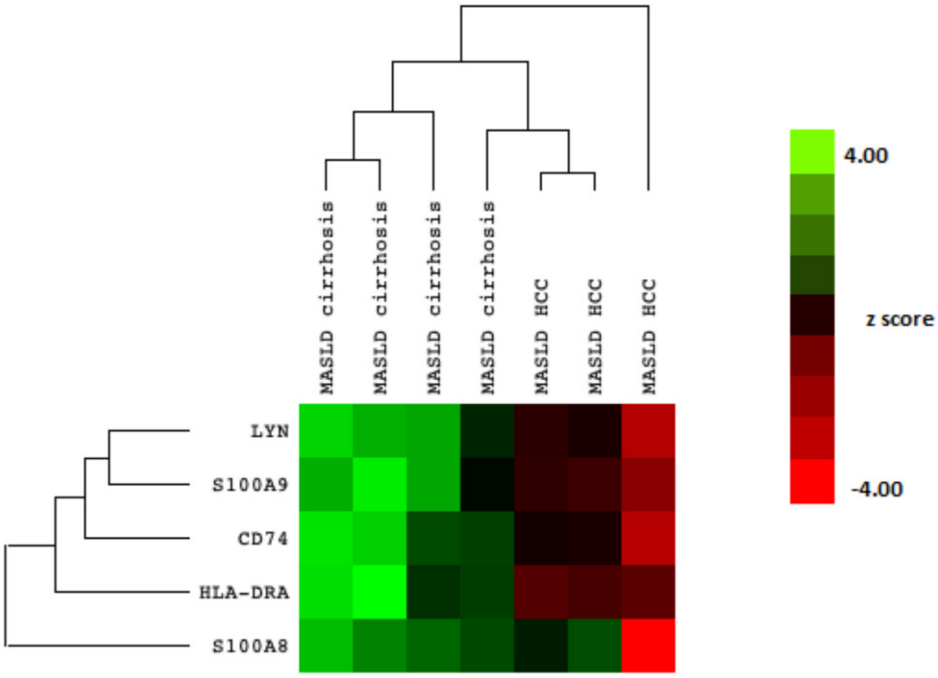


Figure 86 Differential gene expression in circulating CD56brightCD16-NK cells in MASLD HCC when compared to CD56brightCD16-NK cells from patients with MASLD cirrhosis. Gene expression profiles from circulating CD56brightCD16-NK cells from patients with hepatocellular carcinoma and underlying cirrhosis related to metabolic dysfunction-associated steatotic liver disease (MASLD HCC) were compared with circulating CD56brightCD16-NK cells from patients with MASLD related cirrhosis without HCC (MASLD cirrhosis). Red corresponds to lower gene expression and green corresponds to higher gene expression. There was a reduced expression of LYN, S100A9, S100A8, CD74 and HLA-DRA in patients with MASLD HCC. The z score was calculated as follows: (gene expression value in the sample of interest) – (mean expression value across healthy samples)/standard deviation. (Genes displayed are expressed at >20 copies, demonstrate more than a 2 fold difference in expression with p<0.05 and FDR value of <0.05).

3.3.3 Gene-set enrichment analysis

As CD56dimCD16++NK cells form the majority of circulating NK cells, and functional deficits in disease states were seen in the CD56dim NK cell fraction, gene-set enrichment analysis was undertaken to determine if there were particular pathways affected in cirrhosis and HCC in comparison to healthy states in CD56dimCD16++ NK cells. Gene-enrichment analysis was undertaken using two different platforms: ReactomeGSA and Ingenuity Pathway Analysis (Qiagen). CD56dimCD16++ NK cells from patients with MASLD cirrhosis (n=4) and ALD cirrhosis (n=3) was initially compared to CD56dimCD16++ NK cells from healthy volunteers (see Figures 87 and 88 respectively).

The top 10 most enriched pathways with the largest number of differentially expressed genes were determined in patients compared to healthy volunteers. The displayed pathways were all significantly altered in patients compared to healthy states ($p<0.05$) but the calculated False Discovery Rate (FDR), calculated using the Benjamini-Hochberg approach, was >0.05. This may be due to the paucity of samples in each group.

DAP12 signalling and TNF signalling were enriched pathways in both ALD cirrhosis and MASLD cirrhosis compared to healthy, and both with reduced activity, suggesting a reduced capacity for activation, cytotoxic responses and TNFα production in cirrhosis. Furthermore, 'PIP3 activates AKT signalling' was also a pathway with reduced activity in both ALD and MASLD cirrhosis compared to healthy, and also a pathway involved in downstream signalling from activating receptors.

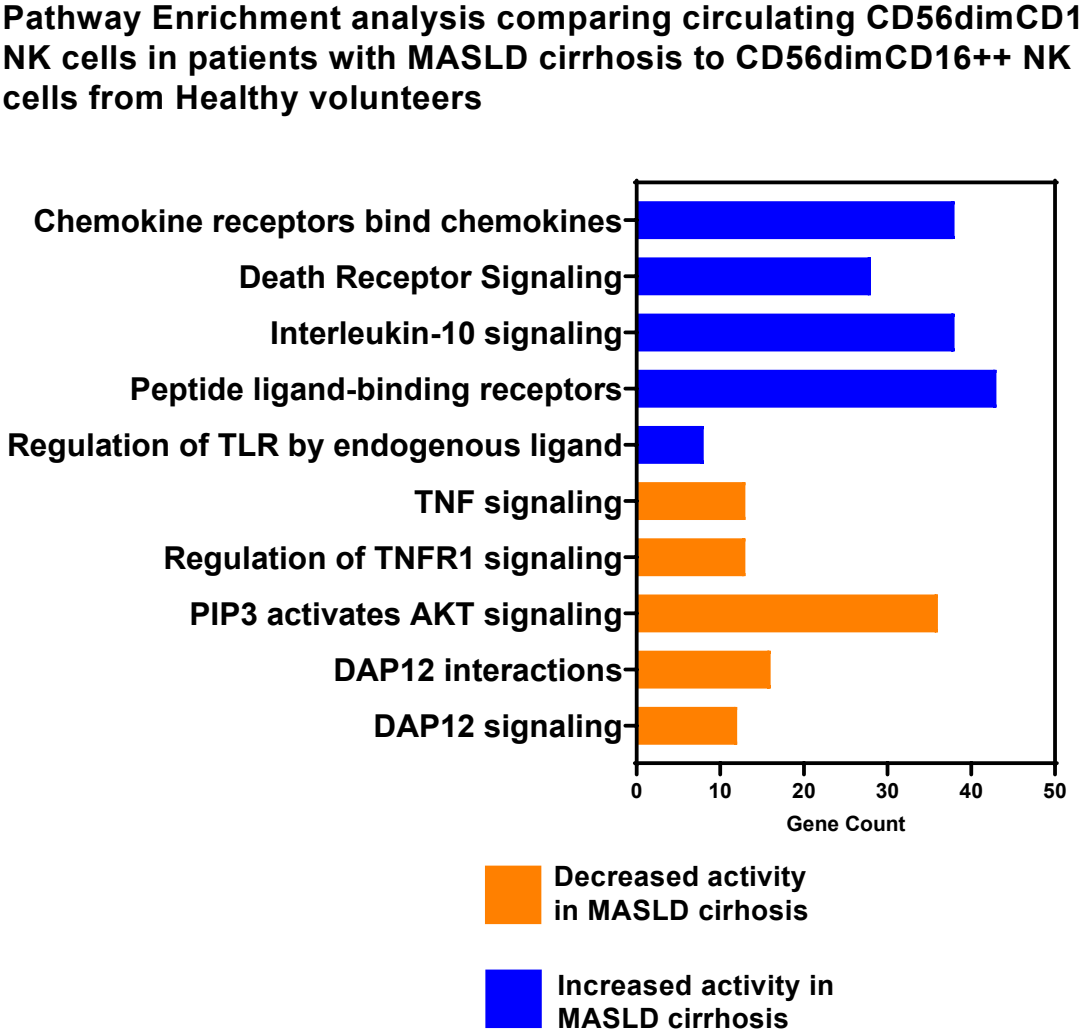


Figure 87 Gene enrichment pathway analysis, comparing circulating CD56dimCD16++NK cells in patients with MASLD cirrhosis (n=4) with CD56dimCD16++NK cells from healthy volunteers (n=3). Normalised gene expression data was uploaded to the web-based platform ReactomeGSA for CD56dimCD16++NK cells from patients with MASLD cirrhosis and healthy volunteers. The ReactomeGSA platform calculated pathway enrichment based on differential gene expression when comparing MASLD cirrhosis with the healthy state. The top 10 most enriched pathways are displayed, involving the largest number of differentially expressed genes in patients with MASLD cirrhosis compared to healthy volunteers. The displayed pathways were all significantly altered in MASLD cirrhosis compared to healthy states ($p<0.05$) but the calculated FDR was not significant (FDR>0.05). Orange bars demonstrate overall downregulated pathways in MASLD cirrhosis and blue bars represent upregulated pathways in MASLD cirrhosis compared to healthy.

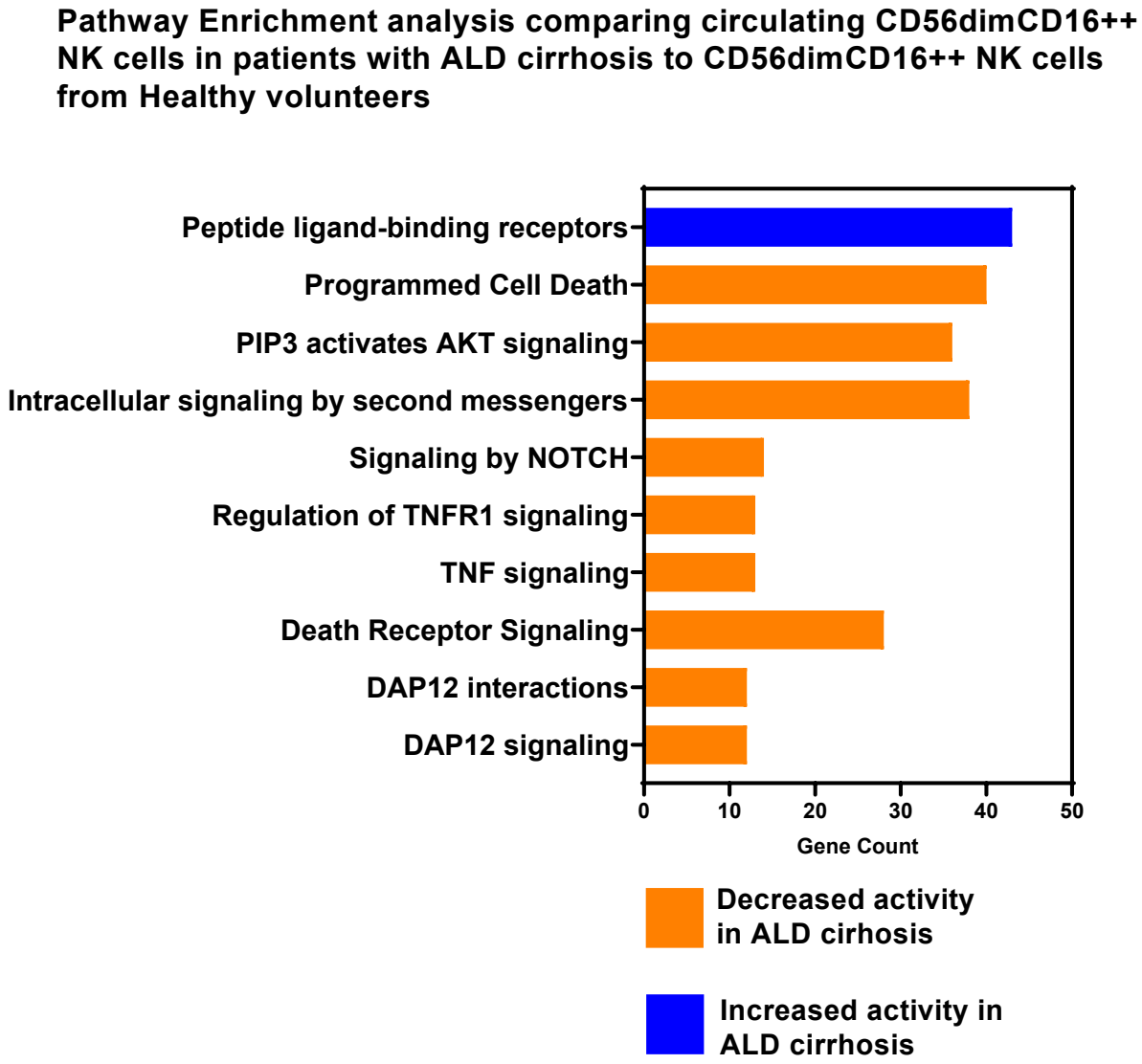


Figure 88 Gene enrichment pathway analysis, comparing circulating CD56dimCD16++NK cells in patients with ALD cirrhosis (n=3) with CD56dimCD16++NK cells from healthy volunteers (n=3). Normalised gene expression data was uploaded to the web-based platform ReactomeGSA for CD56dimCD16++NK cells from patients with ALD cirrhosis and healthy volunteers. The ReactomeGSA platform calculated pathway enrichment based on differential gene expression when comparing ALD cirrhosis with the healthy state. The top 10 most enriched pathways are displayed, involving the largest number of differentially expressed genes in patients with ALD cirrhosis compared to healthy volunteers. The displayed pathways were all significantly altered in ALD cirrhosis compared to healthy states ($p<0.05$) but the calculated FDR was not significant (FDR>0.05). Orange bars demonstrate overall downregulated pathways in ALD cirrhosis and blue bars represent upregulated pathways in ALD cirrhosis compared to healthy.

CD56dimCD16++ NK cells from patients with MASLD cirrhosis and HCC (n=3) was then compared to patients with MASLD cirrhosis without HCC (n=4) (Figure 89). The top 10 most enriched pathways with the largest number of differentially expressed genes were determined in patients compared to healthy volunteers. The displayed pathways were all significantly altered in patients with HCC compared to patients with cirrhosis ($p<0.05$) but the calculated False Discovery Rate (FDR), calculated using the Benjamini-Hochberg approach, was >0.05. This may be due to the paucity of samples in each group.

In MASLD HCC, there was enrichment of the DAP 12 signalling pathways and IL2 signalling with upregulated activity in comparison to MASLD cirrhosis. Furthermore there was a downregulation in IL10 signalling in CD56dimCD16++ NK cells in MASLD HCC. The 'immunoregulatory interactions (lymphoid with non-lymphoid) pathway demonstrated increased activity however. Genes involved in this pathway include NK surface receptors (NKG2D, NKG2A, CD160, KLRG1, CD94, CD96) as well as cell-adhesion molecules (LFA-1).

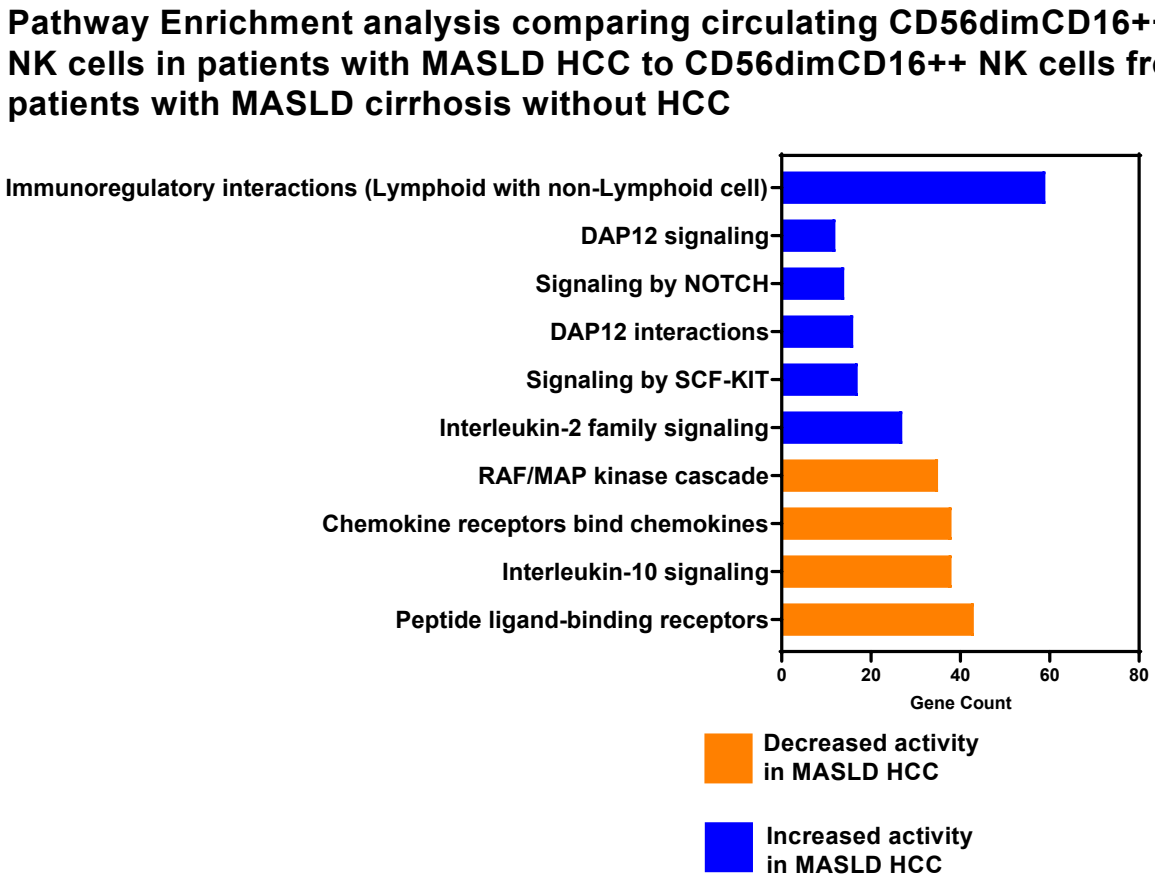


Figure 89 Gene enrichment pathway analysis, comparing circulating CD56dimCD16++NK cells in patients with MASLD HCC (n=3) with CD56dimCD16++NK cells from patients with MASLD cirrhosis (n=4). Normalised gene expression data was uploaded to the web-based platform ReactomeGSA for CD56dimCD16++NK cells from patients with HCC on a background of cirrhosis secondary to MASLD (MASLD HCC) and patients with MASLD related cirrhosis without HCC (MASLD cirrhosis). The ReactomeGSA platform calculated pathway enrichment based on differential gene expression when comparing MASLD HCC with the MASLD cirrhosis. The top 10 most enriched pathways are displayed, involving the largest number of differentially expressed genes in patients with MASLD HCC compared to MASLD cirrhosis. The displayed pathways were all significantly altered in MASLD HCC compared to MASLD cirrhosis ($p<0.05$) but the calculated FDR was not significant (FDR>0.05). Orange bars demonstrate overall downregulated pathways in MASLD HCC and blue bars represent upregulated pathways in MASLD HCC compared to MASLD cirrhosis.

To analyse the predicted downstream effects of differential gene expression, Ingenuity pathway analysis software (Qiagen) was used to map differential gene expression in CD56dimCD16++NK cells from patients with MASLD cirrhosis compared to healthy volunteers on to NK cell signalling pathways (Figure 90). This predicted overall attenuated NK cell functions, with predicted inhibition of TNFSF10 (encoding Tumour necrosis factor related apoptosis-inducing ligand (TRAIL)) and Fas ligand mediated apoptosis, cytotoxic granule release and NK cell mediated antibody dependent cell mediated cytotoxicity (Figure 90).

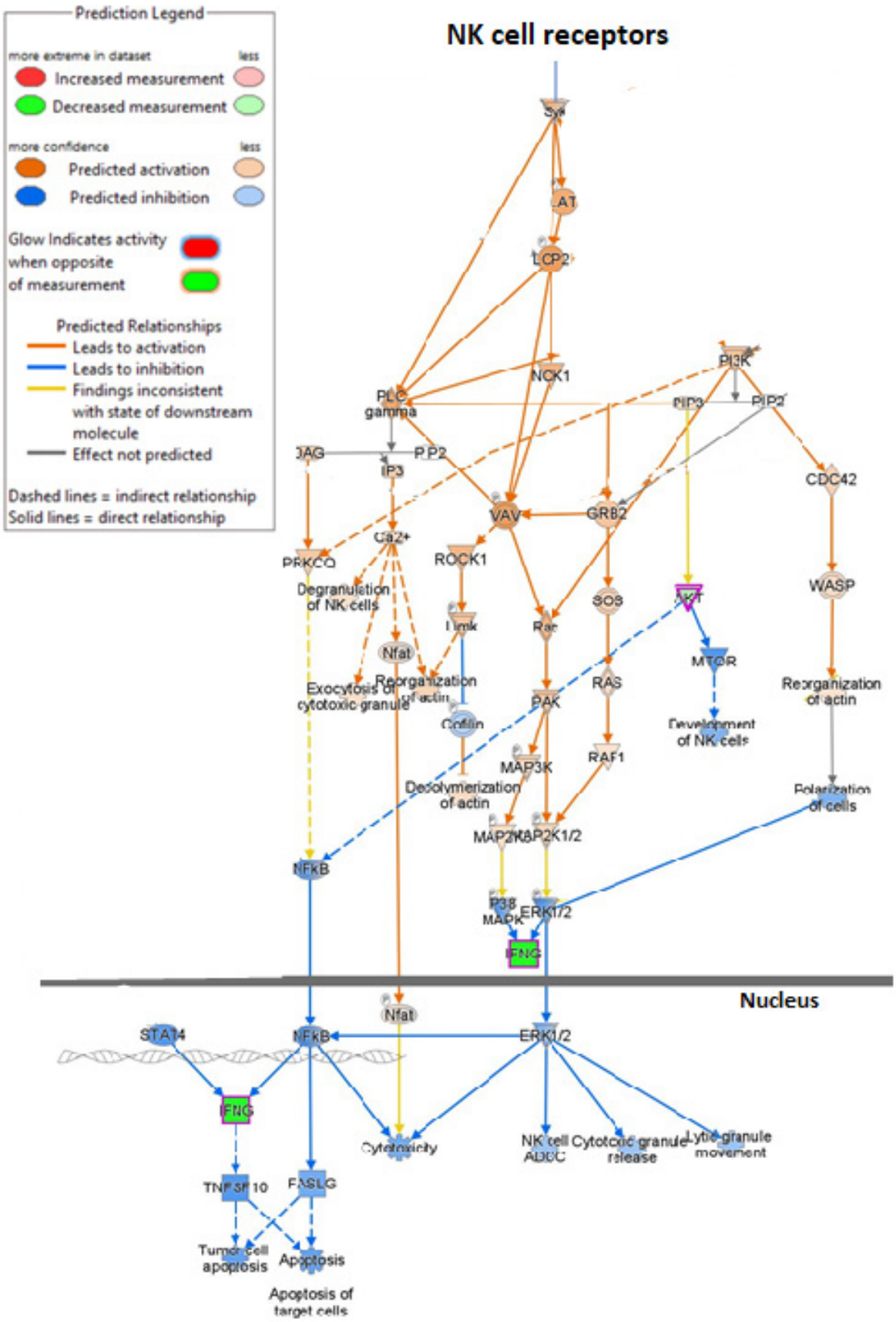

Prediction Legend
more extreme in dataset
less
Increased measurement
Decreased measurement
more confidence
less
Predicted activation
Predicted inhibition
Glow Indicates activity when opposite of measurement
Predicted Relationships
Leads to activation
Leads to inhibition
Findings inconsistent with state of downstream molecule
Effect not predicted
Dashed lines = indirect relationship
Solid lines = direct relationship
NK cell receptors
Syk
LAT
LCP2
NCK1
PI3K
PLC gamma
PIP3
PIP2
DAG
PP2
IP3
CDC42
VAV
GRB2
Ca2+
PRKCQ
ROCK1
WASP
Degranulation of NK cells
SOS
AKT
Rac
Nfat
MTOR
Reorganization of actin
Exocytosis of cytotoxic granule
RAS
PAK
Cofilin
Development of NK cells
RAF1
MAP3K
Depolymerization of actin
Polarization of cells
MAP2K1/2
NFkB
P38 MAPK
ERK1/2
IFNG
Nucleus
Nfat
STAT4
NFkB
ERK1/2
IFNG
Cytotoxicity
NK cell ADCC
Cytotoxic granule release
Lytic granule movement
TNFSF10
FASLG
Tumor cell apoptosis
Apoptosis
Apoptosis of target cells

Figure 90 Predicted effects of differential gene expression on NK cell signalling in circulating CD56dimCD16++ NK cells in MASLD cirrhosis when compared to healthy NK cells. Differential gene expression in circulating CD56dimCD16++NK cells in MASLD cirrhosis in comparison to healthy volunteers was overlaid on to NK cell intracellular signalling pathways using Ingenuity Pathway Analysis (IPA, Qiagen). Genes in green have a reduced measurement in MASLD cirrhosis in comparison to healthy controls. Genes in blue are predicted to be inhibited in MASLD cirrhosis while genes in orange are predicted to be activated based on the reduced expression seen of the genes in green. There is predicted inhibition of NK cell cytotoxicity and degranulation in addition to the measured reduced interferon gamma (IFNG) expression in CD56dimcD16++NK cells in MASLD cirrhosis compared to healthy cells.

The Ingenuity pathway analysis software was also utilised to identify potential genes that may be modulated upstream of the affected genes, resulting in the differential expression seen in these affected genes in disease. These genes are termed 'upstream regulators'. The NFκB complex and IRF8 were identified as potentially suppressed upstream regulators in MASLD cirrhosis, resulting in the differential gene expression seen in CD56dimCD16++ NK cells in MASLD cirrhosis in comparison to healthy NK cells (Figure 91). NFκB complex has been shown to be important in NK cell activation (Pandey et al., 2007) while IRF8 is important for NK cell maturation, proliferation and anti-viral responses (N. M. Adams et al., 2018; Mace et al., 2016).

The IRF8 transcription factor was also predicted to be suppressed in patients with cirrhosis secondary to ALD and in patients with HCC and cirrhosis secondary to MASLD (MASLD HCC).

Predicted inhibition of genes upstream of the genes demonstrating reduced expression in circulating CD56dimCD16++ NK cells in MASLD cirrhosis

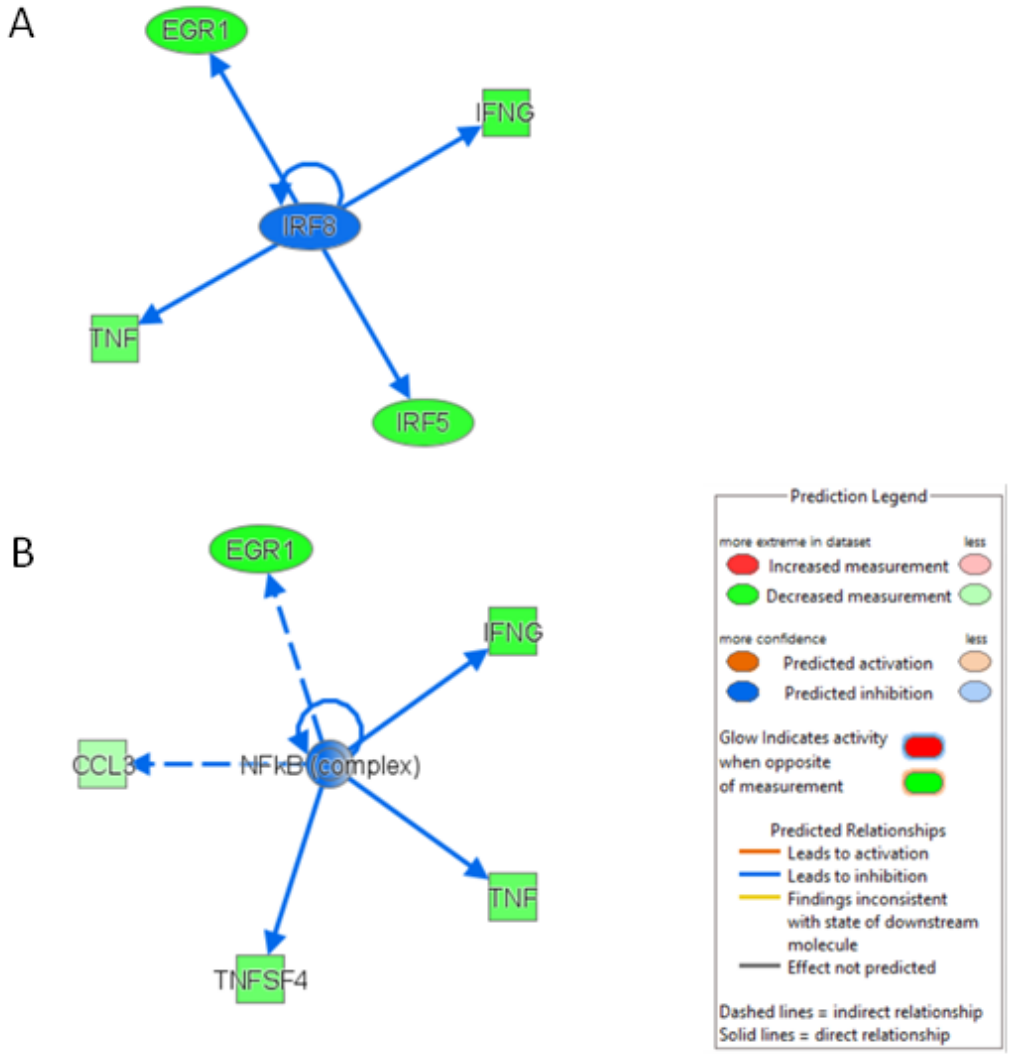


Figure 91 Upstream regulators in circulating CD56dimCD16++ NK cells in cirrhosis secondary to metabolic dysfunction-associated steatotic liver disease (MASLD cirrhosis). Gene expression in CD56dimCD16++ NK cells in patients with MASLD cirrhosis (n=4) was compared to CD56dimCD16++ NK cells from healthy individuals (n=3). Ingenuity Pathway Analysis (IPA, Qiagen) was utilised to predict regulatory genes that were activated or suppressed, thus resulting in the differential gene expression seen (upstream regulators). IPA predicted an inhibition of the IRF8 transcription factor (A) and the NFκB complex (B) thus resulting in the differential expression seen in CD56dimCD16++NK cells in MASLD cirrhosis compared to healthy NK cells. The figure demonstrates the predicted inhibition of IRF8 and NFκB complex (in blue) and the resulting measured reduced expression (in green) of EGR1, IFNG and TNF in MASLD cirrhosis.

3.3.2 Comparison of gene expression of intrahepatic NK cell subpopulations and circulating NK cell subpopulations

3.3.2.1 Liver residency markers

Intrahepatic CD56dimCD16++ NK cells demonstrated multiple genes that were upregulated in comparison to circulating CD56dimCD16++ NK cells in cirrhosis. These included *EOMES, CXCR6, CXCR31* and *CD69* which have been characterised as markers of liver resident NK cells (Cuff et al., 2016; Hudspeth et al., 2016a; Stegmann et al., 2016) (Figure 92).

Intrahepatic CD56brightCD16- NK cells also revealed a gene expression profile consistent with published literature for liver resident NK cells, with an upregulation of *EOMES, ZBTB16, CXCR6* and *CCR5* in comparison to circulating CD56brightCD16- NK cells (Figure 94).

3.3.2.2 Inhibitory and Activating NK cell receptors

KLRB1 (encoding CD161) was upregulated at gene expression level on intrahepatic CD56dimCD16++ NK cells and CD56brightCD16- NK cells, supporting flow cytometry data presented earlier in this chapter demonstrating an increased surface expression of CD161 on intrahepatic NK cells (Figures 92 and 94). *LAIR1*, encoding another inhibitory receptor, was also upregulated on intrahepatic CD56dimCD16++ NK cells (Figure 92).

3.3.2.3 Gene expression associated with effector function

Interestingly, there was also an upregulation in genes in intrahepatic CD56dimCD16++ NK cells associated with cytotoxic and proinflammatory responses such as *TNF, GZMB, GZMA, KLRK1* (Figure 92). There was also an upregulation in *FASLG* and *TNSF10* (encoding TRAIL) (Figure 92). However, *EGR1* was also upregulated in intrahepatic CD56dimCD16++ and CD56brightCD16- NK cells (Figures 92 and 94). As overexpression of EGR1 is associated with a reduced protein expression of TRAIL (Fu et al., 2003), the increased EGR1 expression seen here may limit the protein expression of TRAIL.

There was also an upregulation in *TNF* and *IFNG* in intrahepatic CD56brightCD16- NK cells compared to circulating CD56brightCD16- NK cells in cirrhosis (Figure 94).

3.3.2.4 Maturity status

Interestingly, there was a downregulation of the transcription factor *TCF7* in intrahepatic CD56brightCD16- NK cells compared to circulating CD56brightCD16- NK cells, indicating that intrahepatic CD56brightCD16- NK cells may in a different stage of maturity to circulating CD56brightCD16- NK cells (Figure 93).

Differential gene expression in CD56dimCD16++ NK cells

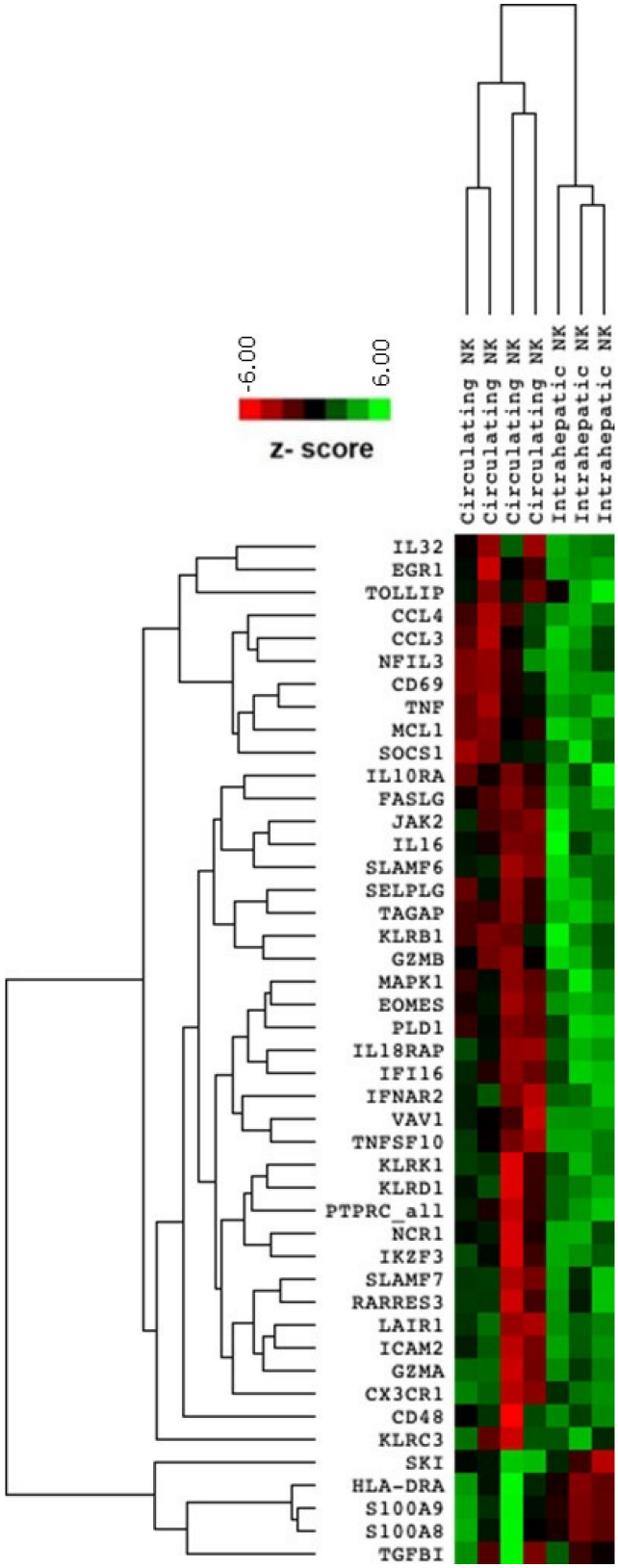


Figure 92 Gene expression in intrahepatic CD56dimCD16++ NK cells from patients MASLD cirrhosis compared to circulating CD56dimCD16++ NK cells from patients with MASLD

cirrhosis. Gene expression profiles from intrahepatic CD56dimCD16++ NK cells from patients with MASLD cirrhosis (n=3) was compared with circulating CD56dimCD16++ NK cells from patients with MASLD cirrhosis (n=4; non=paired samples, genes demonstrating significant differential expression only demonstrated). Red corresponds to lower gene expression and green corresponds to higher gene expression. The z score was calculated as follows: (gene expression value in intrahepatic samples) – (mean expression value across circulating samples)/standard deviation. (Genes displayed are expressed at >20 copies, demonstrate more than a 2 fold difference in expression and p<0.05 and FDR value of <0.05).

Downregulated genes in intrahepatic CD56brightCD16- NK cells compared to circulating CD56brightCD16- NK cells

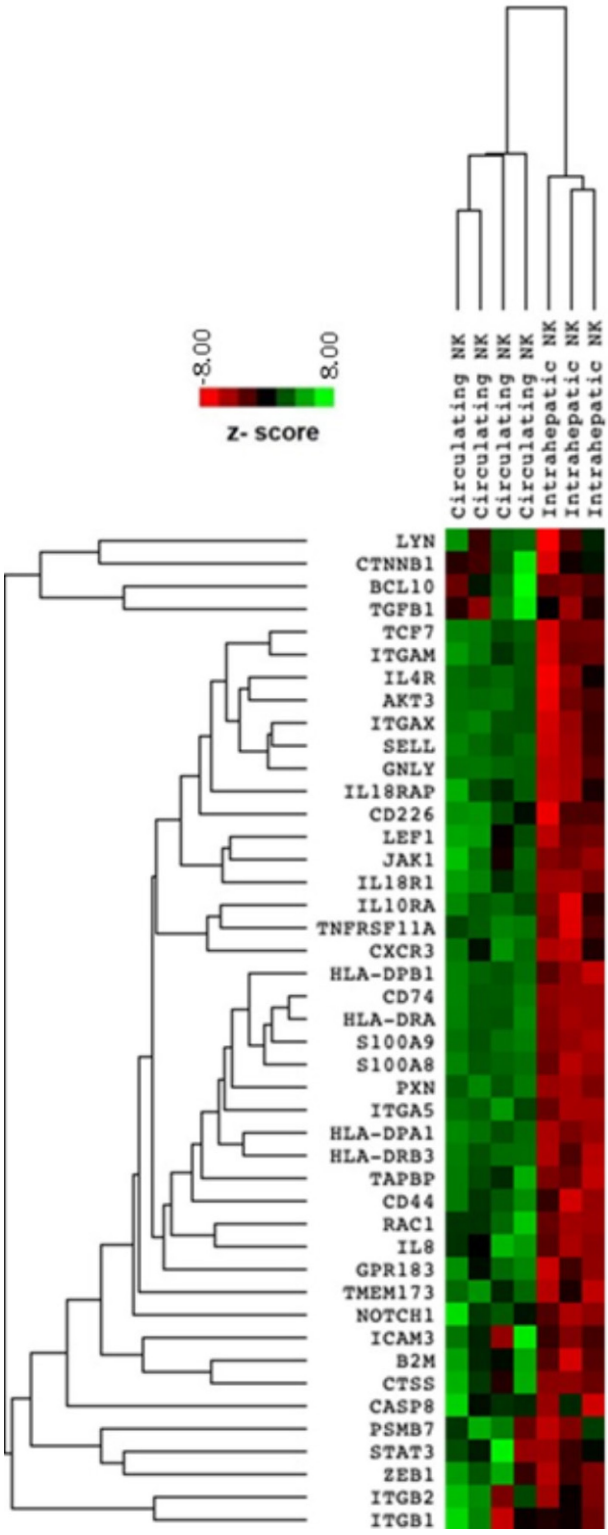


Figure 93 *Downregulated genes in intrahepatic CD56brightCD16- NK cells when compared to circulating CD56brightCD16- NK cells. Gene expression in intrahepatic CD56brightCD16- NK cells from patients with MASLD cirrhosis compared to circulating CD56brightCD16- NK cells from patients with MASLD cirrhosis. Gene expression profiles from intrahepatic CD56brightCD16- NK cells from patients with MASLD cirrhosis (n=3) was compared with circulating CD56brightCD16- NK cells from patients MASLD cirrhosis (n=4; non=paired samples, genes demonstrating significant differential expression only demonstrated). Red corresponds to lower gene expression and green corresponds to higher gene expression. The z score was calculated as follows: (gene expression value in intrahepatic NK cells) – (mean expression value across circulating NK cells)/standard deviation. (Genes displayed are expressed at >20 copies, demonstrate more than a 2 fold difference in expression and p<0.05 and FDR value of <0.05).*

Upregulated genes in intrahepatic CD56brightCD16- NK cells compared to circulating CD56brightCD16- NK cells

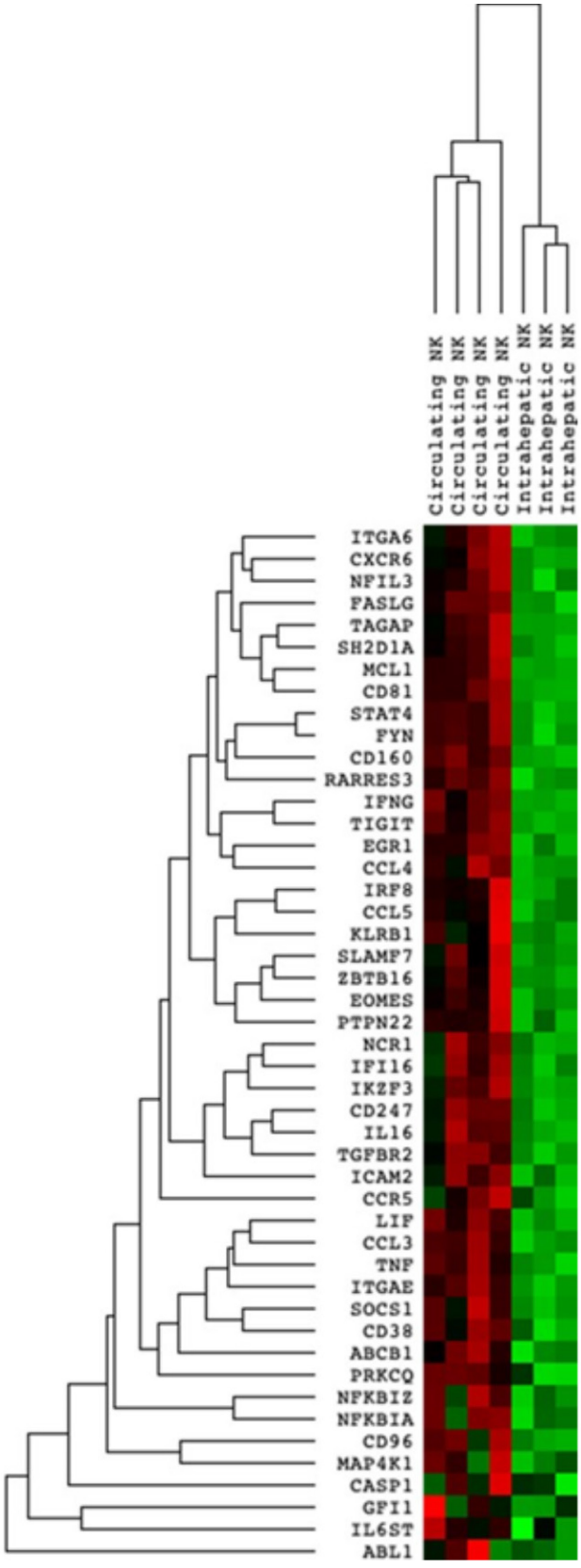


Figure 94 Upregulated genes in intrahepatic CD56brightCD16- NK cells when compared to circulating CD56brightCD16- NK cells. Gene expression in intrahepatic CD56brightCD16- NK cells from patients with MASLD cirrhosis compared to circulating CD56brightCD16- NK cells from patients with MASLD cirrhosis. Gene expression profiles from intrahepatic CD56brightCD16- NK cells from patients with MASLD cirrhosis (n=3) was compared with circulating CD56brightCD16- NK cells from patients MASLD cirrhosis (n=4; non=paired samples, genes demonstrating significant differential expression only demonstrated). Red corresponds to lower gene expression and green corresponds to higher gene expression. The z score was calculated as follows: (gene expression value in intrahepatic NK cells) – (mean expression value across circulating NK cells)/standard deviation. (Genes displayed are expressed at >20 copies, demonstrate more than a 2 fold difference in expression and p<0.05 and FDR value of <0.05).

To further understand the differential gene expression seen here, gene-set enrichment analysis using ReactomeGSA was undertaken to determine if there were particular pathways affected when comparing intrahepatic NK cells with circulating NK cells. Intrahepatic CD56dimCD16++ NK cells from patients with MASLD cirrhosis (n=3) was compared with circulating CD56dimCD16++ NK cells from patients with MASLD cirrhosis (n=4; non-matched donors) (Figure 95). The same was undertaken when comparing intrahepatic CD56brightCD16- NK cells with circulating CD56brightCD16- NK cells in MASLD cirrhosis (Figure 96).

The top 10 most enriched pathways with the largest number of differentially expressed genes were determined. The displayed pathways were all significantly altered in patients compared to healthy states ($p<0.05$) but the calculated False Discovery Rate (FDR), calculated using the Benjamini-Hochberg approach, was >0.05. This again may be due to the paucity of samples in each group.

Overall, most of the enriched pathways demonstrated reduced activity in intrahepatic NK cells (Figures 95 and 96). There was a reduction in interferon signalling, cellular responses to chemical stress and viral response pathways in intrahepatic CD56dimCD16++ NK cells. There was a reduction in the PD-1 signalling pathway and in increased activity in the regulation of interferon gamma signalling pathways in intrahepatic CD56brightCD16-NK cells.

Pathway Enrichment analysis of differentially expressed genes when comparing intrahepatic CD56dimCD16++ NK cells to circulating CD56dimCD16++ NK cells in patients with MASLD cirrhosis

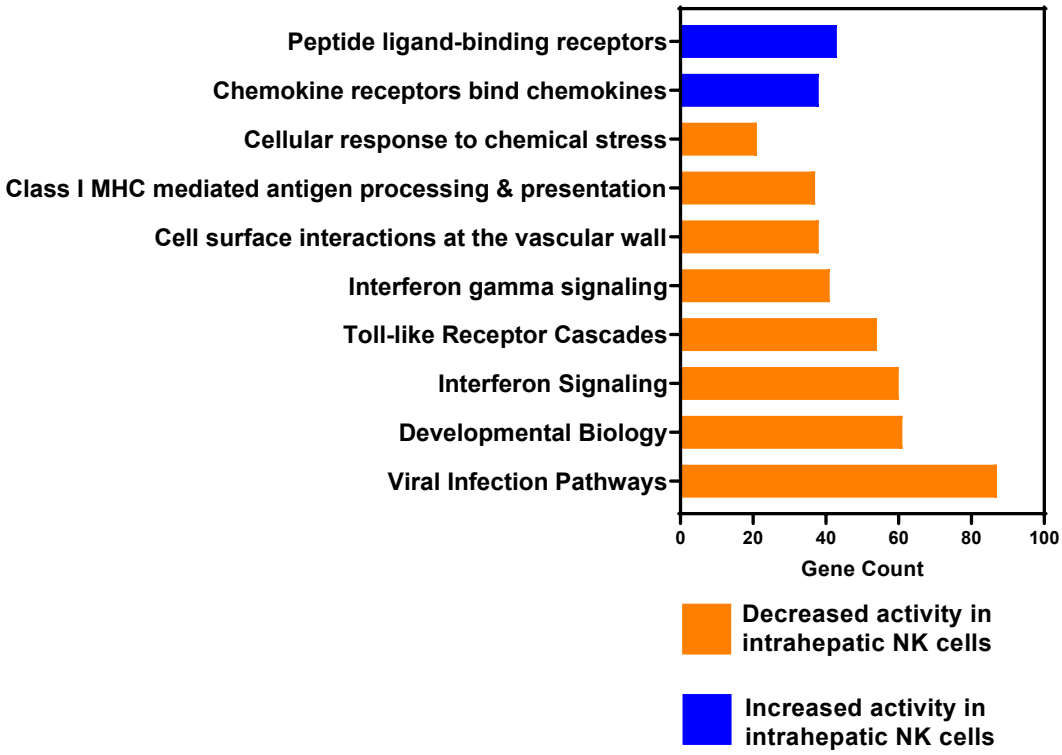


Figure 95 Gene enrichment pathway analysis, comparing intrahepatic CD56dimCD16++NK cells in patients with MASLD cirrhosis (n=3) with circulating CD56dimCD16++NK cells from patients with MASLD cirrhosis (n=3; non-paired samples). Normalised gene expression data was uploaded to the web-based platform ReactomeGSA for intrahepatic and circulating CD56dimCD16++NK cells from patients with MASLD cirrhosis. The ReactomeGSA platform calculated pathway enrichment based on differential gene expression when comparing intrahepatic NK cells with circulating NK cells in MASLD cirrhosis. The top 10 most enriched pathways are displayed, involving the largest number of differentially expressed genes in patients with MASLD cirrhosis compared to healthy volunteers. The displayed pathways were all significantly altered in intrahepatic NK cells compared to circulating NK cells ($p<0.05$) but the calculated FDR was >0.05. Orange bars demonstrate overall downregulated pathways in intrahepatic CD56dimCD16++NK cells in MASLD cirrhosis and blue bars represent upregulated pathways in intrahepatic CD56dimCD16++ NK cells MASLD cirrhosis compared to circulating CD56dimCD16++ NK cells in MASLD cirrhosis.

Pathway Enrichment analysis of differentially expressed genes when comparing intrahepatic CD56brightCD16- NK cells to circulating CD56brightCD15- NK cells in patients with MASLD cirrhosis

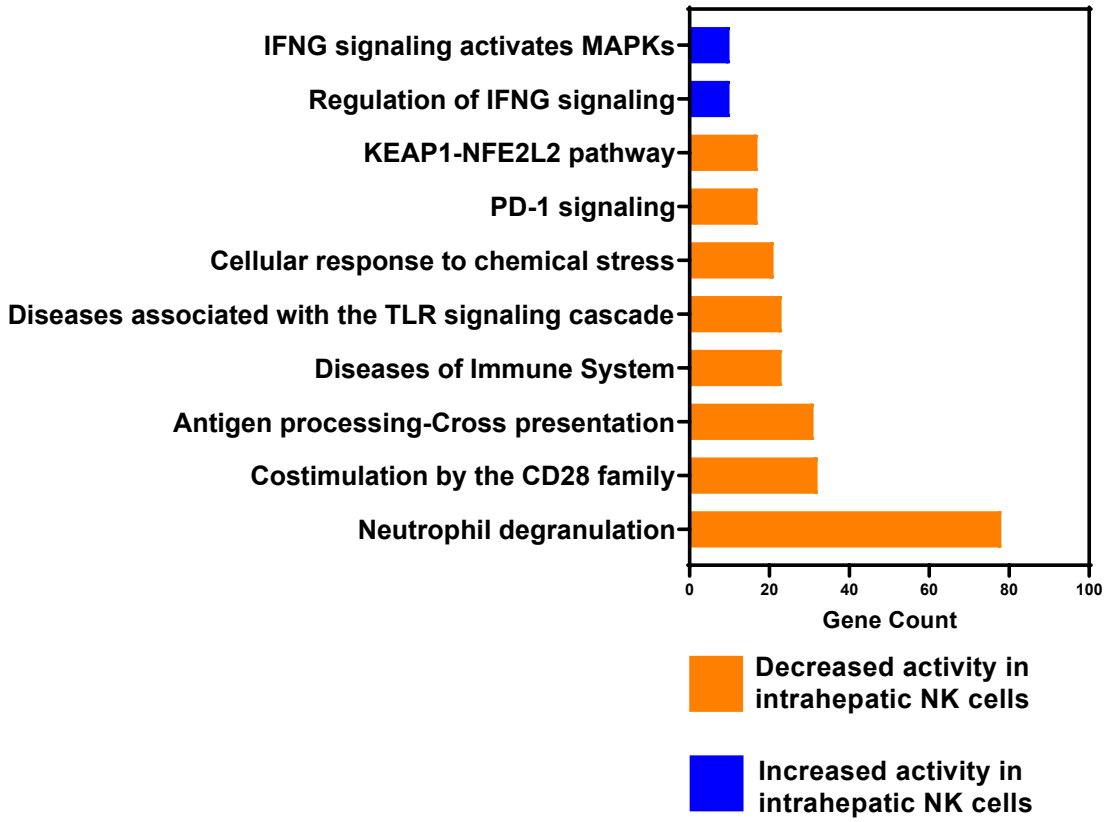


Figure 96 Gene enrichment pathway analysis, comparing intrahepatic CD56brightCD16-NK cells in patients with MASLD cirrhosis (n=3) with circulating CD56brightCD16-NK cells from patients with MASLD cirrhosis (n=3; non-paired samples). Normalised gene expression data was uploaded to the web-based platform ReactomeGSA for intrahepatic and circulating CD56brightCD16-NK cells from patients MASLD cirrhosis. The ReactomeGSA platform calculated pathway enrichment based on differential gene expression when comparing intrahepatic NK cells with circulating NK cells in MASLD cirrhosis. The top 10 most enriched pathways are displayed, involving the largest number of differentially expressed genes in patients with MASLD cirrhosis compared to healthy volunteers. The displayed pathways were all significantly altered in intrahepatic NK cells compared to circulating NK cells ($p<0.05$) but the calculated FDR was >0.05. Orange bars demonstrate overall downregulated pathways in intrahepatic CD56brightCD16- NK cells in MASLD cirrhosis and blue bars represent upregulated pathways in intrahepatic CD56brightCD16- NK cells MASLD cirrhosis compared to circulating CD56brightCD16- NK cells in MASLD cirrhosis.

3.4 Discussion

Circulating peripheral NK cells are dysfunctional in cirrhosis and HCC of a non-viral aetiology. NK cells from patients with cirrhosis demonstrated a reduced capacity for degranulation and direct cytotoxicity with reduced interferon gamma production against K562 target cells. NK cells from patients with HCC and underlying cirrhosis also display attenuated cytotoxicity against K562 target cells, with impaired interferon gamma production (IFNγ) and impaired tumour necrosis factor alpha (TNFα) production in the CD56dimNK cell subset that accounts for approximately 90% of circulating NK cells. Moreover, there is a reduction in circulating CD56dim polyfunctional NK cells with the capacity to produce a cytotoxic response and a cytokine response (IFNγ and TNFα) in patients with cirrhosis and in patients with HCC.

Although clear and significant functional deficits were elicited against MHC class I deficient K562 cells, no functional differences were seen between healthy volunteers and patient groups against HepG2 cells, an HCC cell line. HepG2 cells express MHC class I molecules and hence need to overcome this inhibition to elicit effector responses. In addition, HepG2 express other inhibitory molecules, such as CD155, on the cell surface which may engage with the inhibitory CD96 on NK cells (H. Sun, Huang, et al., 2019), and lacks the expression for ligands for the activating NKG2D (Zhuang et al., 2019). Exposure to secreted factors was minimised by exchanging the cell culture media for fresh media when setting up the co-culture for NK cells with HepG2 cells, but nevertheless, there may be soluble factors released from HepG2 cells that further suppressed NK cell activity. Lastly, as peripheral blood mononuclear cells were incubated together in the functional assay in order to mimic physiological conditions, cross-talk between other immune cells and NK cells may have contributed to suppressing NK cell function. Monocytes have been found to interact with NK cells through the co-receptor 2B4 and thus inhibit NK cell activity (Y. Wu et al., 2013).

This chapter focussed on key, non-MHC class I restricted NK cell receptors, in a bid to characterise any variations which may result in additional NK cell dysfunction when interacting with transformed cells that may downregulate MHC class I. Circulating NK cells from patients with HCC and underlying cirrhosis expressed significantly reduced levels of the activating receptors DNAM-1 and NKp46 in comparison to healthy volunteers. Furthermore,

NKp46 also correlated positively with degranulation against MHC class I deficient K562 target cells in this patient group, and hence the reduced surface expression of NKp46 on circulating NK cells may account in part for the reduced activity of NK cells in individuals with HCC. However, although dysfunction was also clearly demonstrated in patients with cirrhosis only, NKp46 expression did not correlate with CD107a expression in this patient group, indicating other mechanisms may play a more important role here.

NKp46 (NCR1), an activating natural cytotoxicity receptor, is expressed on all NK cells (Sivori et al., 1997). Multiple ligands have been identified as interacting with this receptor, including heparin sulphate proteoglycans expressed on tumour tissue, resulting in IFNγ secretion and NK cell cytotoxicity towards tumour cells (Barrow et al., 2019). NKp30 however, another natural cytotoxicity receptor, has been described as a key receptor in activating NK cell cytotoxicity against the K562 cell line. NKp30 expression was specifically altered in MASLD. NKp30 was down-regulated in MASLD related cirrhosis and MASLD related HCC, as well as non-cirrhotic MASLD and correlated negatively with patient age. However, NKp30 expression negatively correlated with degranulation in the MASLD HCC group against K562 targets. The NKp30 receptor has the capacity to induce an inhibitory environment, promoting IL10 secretion from NK cells and inhibiting NK cell cytotoxicity depending on which isomer of NKp30 is expressed on NK cells (Delahaye et al., 2011; Mantovani et al., 2019). An inhibitory NKp30 isomer has been described in gastrointestinal stromal tumours and in HCC (Delahaye et al., 2011; Mantovani et al., 2019). Galectin-3 has been well described as being expressed in the cirrhotic liver and in HCC regardless of aetiology (Hsu et al., 1999; Song et al., 2020), and has been demonstrated to inhibit NK cell cytotoxicity via interaction with NKp30 (Barrow et al., 2019; Delahaye et al., 2011). Despite the overall reduced expression of NKp30 on the MASLD HCC subgroup compared to healthy volunteers, cytotoxicity was impaired in the MASLD HCC group and this may be attributed to the reduced expression of NKp46.

Whilst differences in NKG2D expression have been described in HCC in the literature, I did not find differences in NKG2D expression in the cirrhosis or the HCC patient groups. This may be in part related to the underlying aetiology, as NKG2D has been demonstrated to be down-regulated on NK cells in hepatitis B infection (Koumbi et al., 2016). However, DNAX Accessory Molecule-1 (DNAM-1) did display reduced expression on peripheral circulating NK cells in patients with HCC. Engagement of DNAM-1 has been described to promote NK cell

cytotoxicity by directing granule release towards target cells (Z. Zhang et al., 2015), and plays an important role in tumour surveillance and the elimination of transformed cells (Iguchi-Manaka et al., 2008). CD155 (poliovirus receptor, PVR) was identified as a ligand for DNAM-1 (Bottino et al., 2003). However prolonged exposure of DNAM-1+NK cells to CD155 expressing ovarian tumour epithelia resulting in downregulation of DNAM-1, and NK cells in these patients were hypofunctional against K562 target cells (Carlsten et al., 2009). Reduced tumour expression of CD155 has been associated with a poor prognosis in HCC (Qu et al., 2015). Moreover, CD155 can engage CD96 and TIGIT, with both receptors capable of inhibiting NK cell function, further complicating the role of CD155 in HCC (H. Sun, Huang, et al., 2019; Q. Zheng et al., 2020). Sun et al have recently described an increase in CD96+ intratumoural NK cells that are exhausted in HCC, and demonstrate a restoration of NK cell function on blocking the CD155-CD96 interaction (H. Sun, Huang, et al., 2019).

Sun et al associated elevated plasma levels of transforming growth factor beta-one (TGF-β1) with elevated CD96 expression and demonstrated that blocking TGF-β1 also restored NK cell function (H. Sun, Huang, et al., 2019). Elevated plasma levels of TGF-β1 has also been associated with the altered expression of NKp46, NKp30, DNAM-1 and NKG2D in gastric cancer (Han et al., 2018). TGF-β1 is a key player in the progression of liver disease and cirrhosis (Dooley & Ten Dijke, 2012), and though serum levels of TGF-β1 are elevated in cirrhosis, they are elevated to a greater extent in HCC (Flisiak et al., 2000; Kohla et al., 2017). This combination of possible secreted soluble factors from HCC, increased tumour expression of stress-induced ligands and elevated levels of TGF-β1 may explain why alterations in NKp46 and DNAM-1 are seen in patients with HCC but not in patients with cirrhosis only.

Circulating NK cells from patients with cirrhosis demonstrate an inhibitory phenotypic profile, with an increase in the inhibitory CD161 surface receptor expression and with reduced CD16 expression indicating a reduced capacity for indirect cytotoxicity. The reduction in CD16 expression on circulating CD56dimNK cells persists in HCC, but CD161 levels are not significantly different in the HCC patient group in comparison to healthy volunteers. CD161 is a C-type lectin expressed on the surface of the majority of NK cells (Lanier et al., 1994). Engagement with LLT1, another C-type lectin expressed on activated lymphocytes and granulocytes, has been demonstrated to inhibit NK cytotoxicity and interferon gamma production (Aldemir et al., 2005; Germain et al., 2011; D. B. Rosen et al., 2005). LLT1 expression has been demonstrated also in cancer (prostate, breast, glioblastoma) and in viral infection (respiratory syncytial viral infections of the lung, hepatitis B infection) (Koumbi et al.,

2016; Marrufo et al., 2018; S. O. Mathew et al., 2016; Roth et al., 2007; Satkunanathan et al., 2014).

CD16 (FcγRIIIa is a potent activator of NK cells, allowing antibody dependent cell mediated cytotoxicity (O Mandelboim et al., 1999). CD16 exerts it effector functions by engaging with the Fc portion of antibodies coating infected or transformed cells and triggering NK cell cytotoxicity. CD16 is expressed on mature circulating CD56dimNK cells that make up the majority of circulating NK cells (Abel et al., 2018). However, patients with cirrhosis had a reduced expression of surface CD16, with a significantly increased portion of CD56dimCD16+/- NK cells and a correspondingly reduced circulating proportion of CD56dimCD16++ NK cells.

CD16 and CD161 expression did not directly correlate with the effector functions measured here, but there was significant NK cell dysfunction, indicating that the effector functions measured (CD107a expression, IFNγ production) may be impaired due to other mechanisms.

CXCR6, a liver homing receptor, is highly expressed on intrahepatic NK cells in comparison to circulating NK cells, and engages with CXCL16, resulting in the retention of NK cells within liver sinusoids of the healthy liver (Hudspeth et al., 2016a; Stegmann et al., 2016). It is important to consider that NK cell subpopulations within the liver differ significantly from NK cells within the circulation, with a greater proportion of liver resident CD56brightCD16- NK cells expressing CXCR6, CCR5 and CD69, and a smaller subpopulation expressing CD49a (Marquardt et al., 2015; Mikulak et al., 2019). Incubation of peripheral blood NK cells with cytokines can induce NK cells to express CXCR6 (T. Hydes et al., 2017; T. J. Hydes et al., 2019), and there is evidence that peripheral NK cells can be induced to express transcription factor Eomes typical of liver resident NK cells (Cuff et al., 2016).

There was wide variation in receptor expression in HCC, with some individuals with very low expression of receptors and some individuals with increased receptor expression. While individual receptors did not correlate with clinical parameters to explain the variation seen here, receptor co-expression was seen for activating receptors NKp30, DNAM-1, NKG2D and

the inhibitory CD161 in patients with HCC, implying that individuals with low expression of one receptor also demonstrated a low expression of these other receptors. Furthermore, CXCR6 negatively correlated with CD161 and DNAM-1, suggesting the NK cells with reduced surface expression of these receptors may be liver homing or have traversed through the liver.

Deeper phenotyping using Nanostring technology allowed differences at gene expression to be detected between patient groups. Gene expression profiles of the classical circulating cytotoxic subset, CD56dimCD16++ NK cells, demonstrated a reduced expression of *IFNG* and *TNF*, as well as the transcription factor *EGR1* in cirrhosis and HCC on a background of cirrhosis in comparison to healthy CD56dimCD16++ NK cells. *EGR1* regulates multiple genes and has interestingly been implicated in the reduced expression of TRAIL (Balzarolo et al., 2013; Fu et al., 2003). TRAIL however was not upregulated at the gene expression level in cirrhosis or HCC despite the downregulation of *EGR1*, although protein expression would need to be characterised. Although K562 cells are resistant to TRAIL mediated apoptosis (M. J. Kim et al., 2009), TRAIL mediated apoptosis remains an important mechanism for killing transformed cells.

Both the downregulation of *EGR1*, and the upregulation of *STAT1* should result in an increased TRAIL mediated cytotoxic responses to transformed cells, and increased interferon gamma responses respectively in CD56dimCD16++ NK cells. However, no significant differences were demonstrated with regards to cytotoxic responses of peripheral CD56dim NK cells against HepG2 cells in health and disease. In fact, the overall cytotoxic response to HepG2 cells is low across all CD56dim NK cells in comparison to K562 cells. This implies that other factors may play a more important role in inhibiting NK cells responses to HepG2 cells, such as the expression of receptors on HepG2 cells to inhibitory ligands expressed on NK cells. There was however, a clear functional deficit in cytotoxic and cytokine responses to K562 cells in CD56dim NK cells from patients with cirrhosis or HCC compared to healthy volunteers. Whether EGR1 mediates other inhibitory measures on effector NK cell functions remains yet to be determined.

Pathway enrichment analysis was very interesting and again demonstrated key pathways that were downregulated regardless of the underlying aetiology of cirrhosis. DAP12 signalling/interactions and TNF signalling was reduced in both ALD and MASLD cirrhosis compared to healthy. DAP 12 is involved in signal transduction from multiple activating

receptors on NK cells and triggers cytotoxic responses (Campbell & Colonna, 1999). PI3K signalling was also downregulated in both ALD and MASLD cirrhosis. This is again an important pathway in downstream signalling from activating receptors (Mace, 2018).

Intrahepatic NK cell gene expression in cirrhosis was similar to that described in the literature for healthy intrahepatic NK cells, with increased CXCR6 and EOMES denoting liver resident NK cells. On comparison with circulating NK cells from patients with cirrhosis, intrahepatic NK cells surprisingly demonstrated an increase at gene expression level of genes associated with effector functions (*IFNG, TNF, PRF, FASLG, TNFSF10*). However, *PRDM1*, encoding Blimp1 which is expressed in mature NK cells and negatively regulates the expression of interferon and TNF α (Luevano et al., 2012), is increased at gene expression levels in intrahepatic CD56brightCD16- NK cells in comparison to circulating CD56brightCD16-NK cells. Furthermore, inhibitory receptors such as KLRB1 encoding CD161, are upregulated in intrahepatic NK cells extracted from cirrhotic livers, supporting the flow cytometry data and may be contributing to modulating effector functions.

This chapter has identified functional deficits in both the cirrhosis and HCC patient groups in circulating CD56dim NK cells, a downregulation of several activating receptors in NK cells in patients with HCC, and an up-regulation of an inhibitory phenotype in cirrhosis with the increased expression of CD161 and a novel circulating population of CD56dimCD16+/- NK cells. NKp30 was the only surface receptor to demonstrate a differential expression and correlation with function when comparing MASLD with ALD cirrhosis. Otherwise, no significant differences in receptor expression, function and pathway analyses were seen when comparing cirrhosis of differing aetiologies. Cirrhosis composite scores did not demonstrate a correlation with receptor expression or function also. There were not enough individuals in each BCLC category to understand if BCLC staging may impact on the receptor expression and NK cell function seen here.

The identification of this novel circulating CD56dimCD16+/- NK cell subpopulation, with increased CXCR6 expression and CD161 expression in hypofunctional CD56dimNK cells, needs further characterisation. A significant proportion of the intrahepatic NK cells were also identified here as CD56dimCD16+/- NK cells, and hence it is imperative to see if the circulating CD56dimCD16+/- subpopulation shares any further traits with intrahepatic cells. Furthermore, the up-regulation of CD161 in cirrhosis on peripheral NK cells is intriguing given

that CD161 expression is also increased on intrahepatic NK cells. Evidence for the expression of and the interaction with LLT1, the ligand for CD161, either within the liver or in soluble form in the circulation, and the significance of this interaction needs to be determined to understand the mechanisms of immune dysfunction in cirrhosis. The following two chapters explore these findings further.

4. Results: Characterising the circulating CD56dimCD16+/- NK cell subpopulation in cirrhosis

4.1 Introduction

CD16 (FcγRIIIa) is a potent activating NK cell receptor. Engagement of CD16 by the Fc portion of antibodies opsonising an infected or transformed cell triggers the release of cytokines such as interferon gamma and tumour necrosis factor (TNF) alpha, as well as triggering antibody dependent cell mediated cytotoxicity (ADCC) via degranulation, releasing cytotoxic granules containing perforin and granzyme towards the target cell (Capuano et al., 2021; De Maria et al., 2011; Ofer Mandelboim et al., 1999). CD16 is acquired during NK cell maturation, with the mature circulating NK cells demonstrating a CD56dimCD16++ phenotype (Abel et al., 2018). This subpopulation composes the majority of the circulating NK cells, with CD56brightCD16- NK cells forming approximately 5-10% of circulating NK cells, with a reduced capacity for cytotoxicity but preserved cytokine secretion (Abel et al., 2018). CD16 is also expressed by a subset of monocytes with the capacity for ADCC (Yeap et al., 2016).

In the previous chapter, I demonstrated an increase in the circulating proportion of CD56dimCD16+/- NK cells in patients with cirrhosis, with a functional deficit in CD56dim NK cells against the MHC class I deficient K562 cell line. In patients with HCC and underlying cirrhosis, the increased proportion of circulating CD56dimCD16+/- NK cells persisted in some patients and correlated negatively with the expression of activating the receptor NKp46 in patients with HCC.

With emerging anti-cancer immunotherapies based on tumour specific antibodies and relying on CD16 engagement with subsequent NK cell mediated ADCC (Capuano et al., 2021), and with the established risk of HCC in patients with cirrhosis, it is imperative to understand the role of this NK cell subpopulation with intermediate levels of CD16 in cirrhosis.

In this chapter therefore, I aim to characterise the phenotype and function of these CD56dimCD16+/- NK cells in cirrhosis:

1. Determine the phenotype and function of CD56dimCD16+/- NK cells, and compare them to CD56dimCD16++ NK cells and CD56brightCD16- NK cells in cirrhosis, specifically to decipher:
    a. The activating and inhibitory receptor expression profile
    b. Whether CD56dimCD16+/- NK cells are in a different phase of maturity
    c. Whether CD56dimCD16+/- NK cells are akin to intrahepatic NK cells
2. To see if these cells can be induced in vitro and understand the mechanism by which they arise in the circulation.

4.2 CD56dimCD16+/- NK cell phenotype and function

In order to understand how the CD56dimCD16+/- NK cell subpopulation may differ in phenotype and function to the classical CD56dimCD16++ NK cells and CD56brightCD16- NK cells, surface expression of activating and inhibitory NK receptors was determined using flow cytometry. Functional differences between this subpopulation and the classical subpopulations were assessed with regards to degranulation against K562 cells, cytokine production differential gene expression and pathway analysis. Lastly, the expression of maturity markers and liver homing markers was determined in CD56dimCD16+/- NK cells in order to understand if this population represents a subset of NK cells in a different stage of maturity or possess liver homing capacity.

4.2.1 Surface expression of activating receptors on NK cell subpopulations

Surface expression of activating NK cell receptors (DNAM-1, NKp46, NKp30, NKG2D) was determined using flow cytometry, comparing expression between the CD56dimCD16+/- subset and the classical subpopulation (CD56dimCD16++ and CD56brightCD16- NK cells) within the same donors in the circulation and in intrahepatic NK cells in cirrhosis. Population characteristics of patient samples used can be found in results chapter 3, (peripheral blood samples: cirrhosis n=35, (Table 8); intrahepatic samples: cirrhosis n=4; (Table 9).

NK cells were selected into 3 subpopulations based on CD56 and CD16 expression: CD56dimCD16++ NK cells, CD56brightCD16- NK cells and CD56dimCD16+/- NK cells (see Chapter 2 Methods, Figure 3 for the gating strategy; Phenotyping Panel 1 used (Table 3)). Gating strategies used for each receptor are demonstrated in the phenotyping section of Chapter 3 (Figure 9 for NKG2D gating strategy, Figure 15 for DNAM-1 gating strategy, Figure 21 for NKp30 and NKp46 gating strategies). Receptor expression was compared between CD56dimCD16+/- NK cells and the classical subsets in the circulation and in the liver in cirrhosis. Further comparisons for receptor expression in NK cell subsets were also undertaken in healthy patients (peripheral

blood n=32; intrahepatic n=7) and patients with HCC on a background of cirrhosis (peripheral blood n=29; intrahepatic n=6) (results shown in Appendix 8.5).

DNAM-1 expression on NK cell subsets in cirrhosis

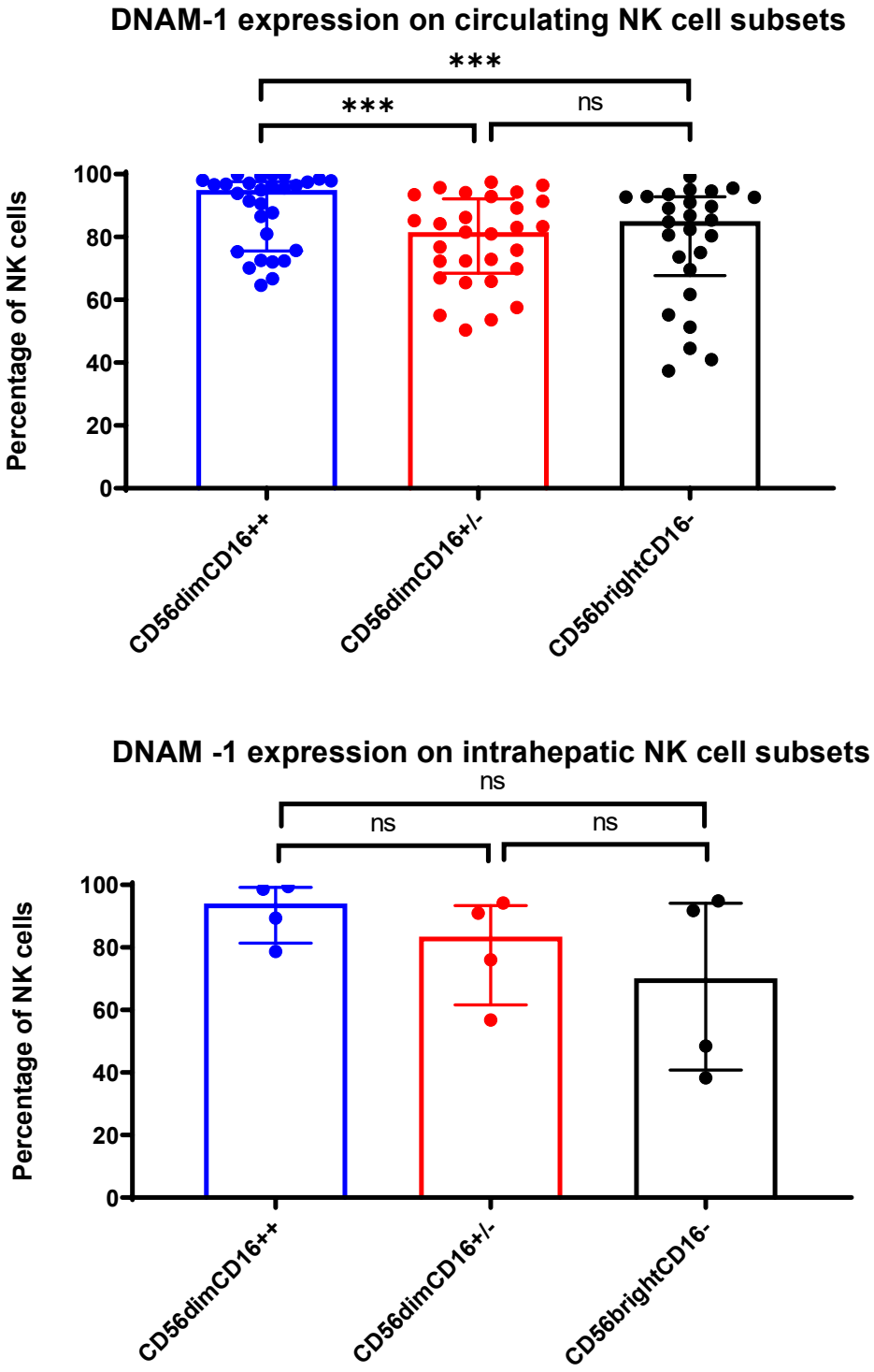


Figure 97 DNAM-1 expression in NK cell subsets defined by CD56 and CD16 expression in the circulation and in the liver in cirrhosis. The top graph demonstrates DNAM-1 expression in circulating NK cells in cirrhosis. The bottom graph demonstrates DNAM-1 expression on

*intrahepatic NK cells from patients with cirrhosis. (Graphs display individual values with the median value displayed by the bar. Comparisons between groups have been made using the paired Wilcoxon test between the same donors. Error bars represent the interquartile range. P values are denoted on the figures as follows: * p<0.05, ** p<0.01, *** p<0.001, **** p<0.0001). A reduced proportion of circulating CD56dimCD16+/- NK cells and CD56brightCD16- NK cells expressed DNAM-1 in comparison to the CD56dimCD16++ NK cell subset (top graph). There were no significant differences in DNAM-1 expression between intrahepatic NK cell subpopulations (bottom graph).*

A reduced proportion of circulating CD56dimCD16+/- NK cells and CD56brightCD16- NK cells expressed DNAM-1 in comparison to the CD56dimCD16++ NK cell subset. This expression pattern was maintained in CD56dimCD16+/- NK cells when the cirrhosis subpopulations were separated by underlying aetiology (ALD or MASLD) *(data not shown)*. A similar trend was seen in intrahepatic NK cells, with lower DNAM-1 expression in CD56brightCD16- and CD56dimCD16+/- NK cells compared to CD56dimCD16++ NK cells, but this did not reach significance (Figure 97). There was no significant difference in the proportion of DNAM-1+ CD56dimCD16+/-NK cells in ALD cirrhosis compared to MASLD cirrhosis (Figure 98).

Comparing DNAM-1 expression on circulating CD56dimCD16+/- NK cells in ALD cirrhosis with MASLD cirrhosis

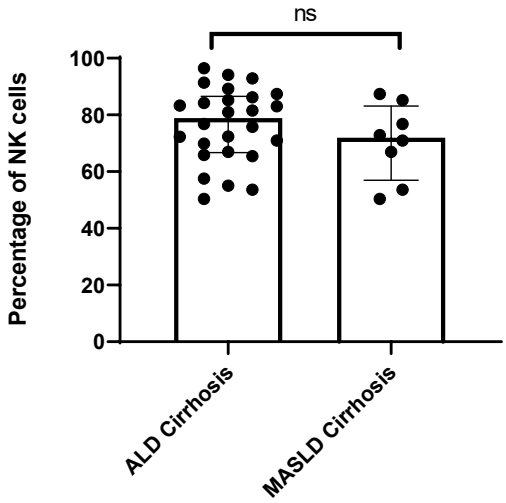


Figure 98 A comparison of DNAM-1 expression on CD56dimCD16+/- NK cells in patients with cirrhosis secondary to alcohol related liver disease (ALD) and metabolic dysfunction-associated steatotic liver disease (MASLD). (Graphs display individual values with the median value displayed by the bar. Comparisons between groups have been made using the Mann-Whitney test. Error bars represent the interquartile range).

NKG2D expression on NK cell subsets in cirrhosis

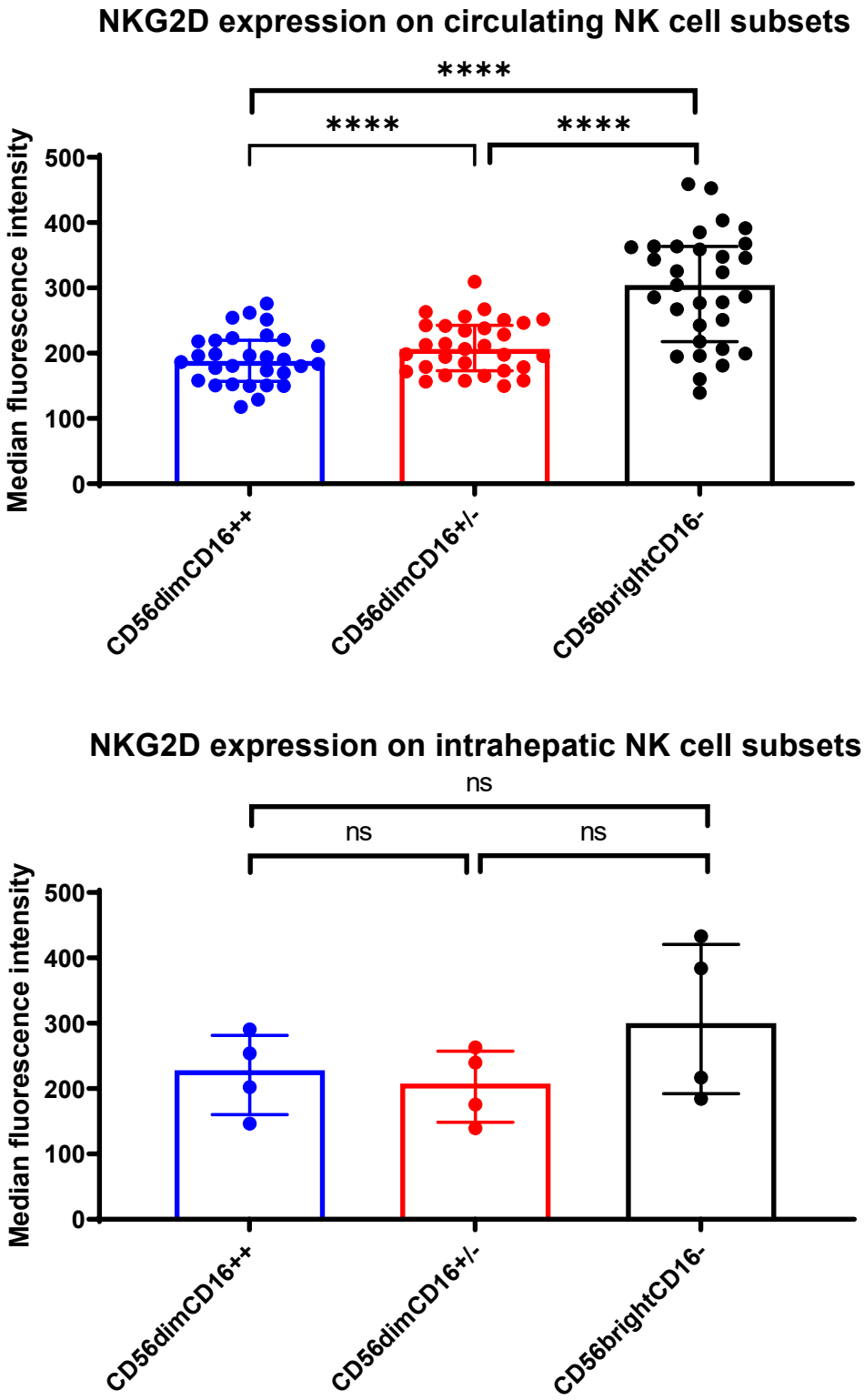


Figure 99 NKG2D expression in NK cell subsets defined by CD56 and CD16 expression in the circulation and in the liver in cirrhosis. The top graph demonstrates NKG2D expression in

*circulating NK cells in cirrhosis. The bottom graph demonstrates NKG2D expression on intrahepatic NK cells. (Graphs display individual values with the median value displayed by the bar. Comparisons between groups have been made using the paired Wilcoxon test between the same donors. Error bars represent the interquartile range. P values are denoted on the figures as follows: * p<0.05, ** p<0.01, *** p<0.001, **** p<0.0001). There was in increased proportion of NKG2D expressing CD56dimCD16+/- NK cells in comparison to CD56dimCD16++ NK cells (top graph). There were no significant differences in NKG2D expression between intrahepatic NK cell subpopulations (bottom graph).*

NKG2D demonstrated an increased expression on circulating CD56brightCD16- NK cells, in comparison to circulating CD56dim NK cell subsets. This expression pattern was maintained in CD56dimCD16+/- NK cells when the cirrhosis subpopulations were separated by underlying aetiology (ALD or MASLD) *(data not shown)*. This expression pattern was also seen in intrahepatic NK cell subsets, with intrahepatic CD56brightCD16- NK cells expressing more NKG2D than CD56dim NK cell subsets (Figure 99). There were no significant differences in NKG2D expression on circulating CD56dimCD16+/- NK cells in patients with ALD cirrhosis compared to patients with MASLD cirrhosis (Figure 100).

Comparing NKG2D expression on circulating CD56dimCD16+/- NK cells in ALD cirrhosis with MASLD cirrhosis

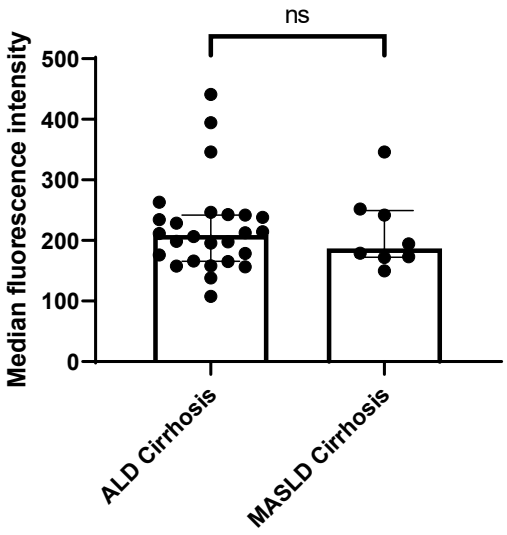


Figure 100 A comparison of NKG2D expression on CD56dimCD16+/- NK cells in patients with cirrhosis secondary to alcohol related liver disease (ALD) and metabolic dysfunction-associated steatotic liver disease (MASLD). (Graphs display individual values with the median value displayed by the bar. Comparisons between groups have been made using the Mann-Whitney test. Error bars represent the interquartile range).

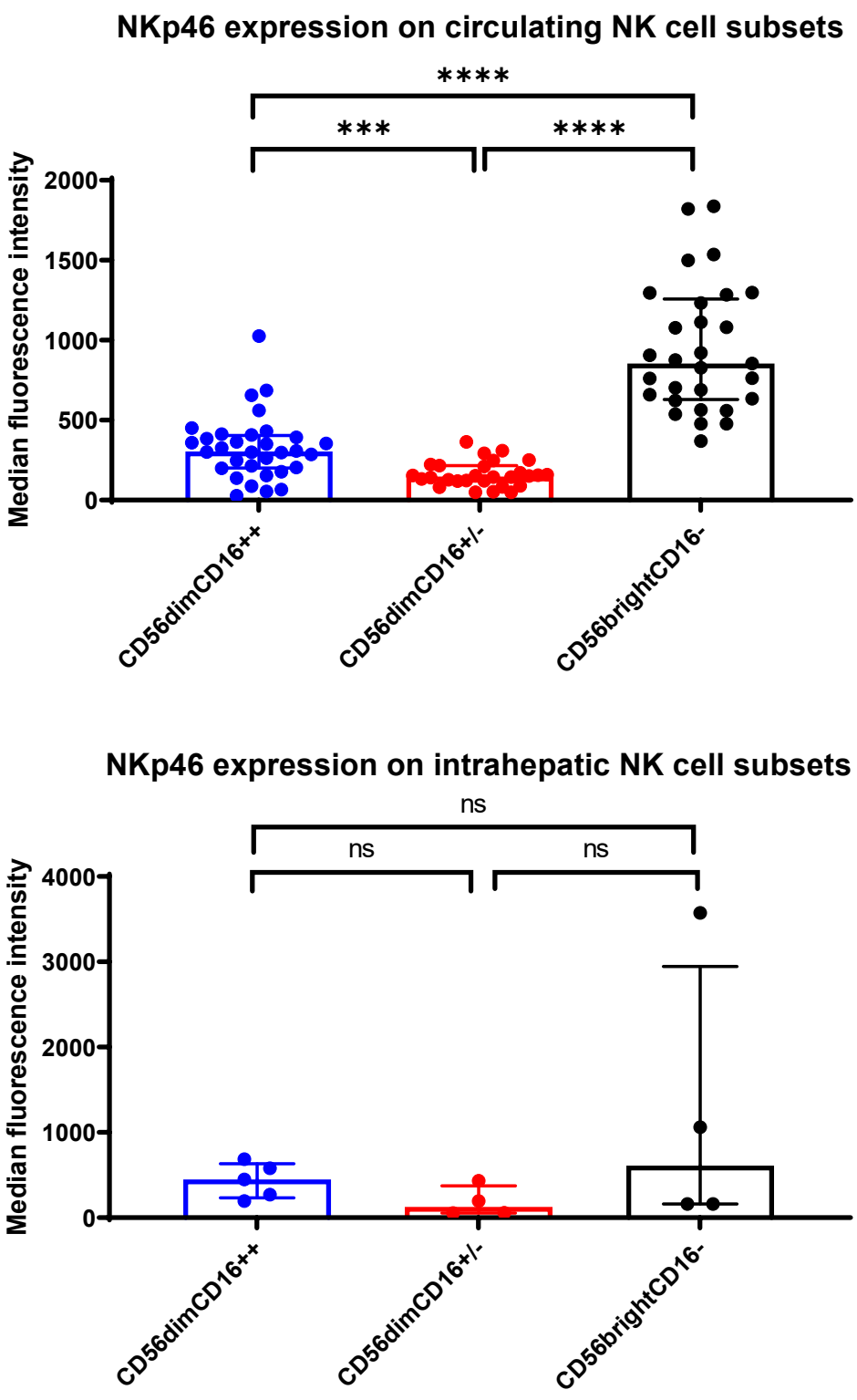


Figure 101 NKp46 expression in NK cell subsets defined by CD56 and CD16 expression in the circulation and in the liver in cirrhosis. The top graph demonstrates NKp46 expression in

*circulating NK cells in cirrhosis. The bottom graph demonstrates NKp46 expression on intrahepatic NK cells. (Graphs display individual values with the median value displayed by the bar. Comparisons between groups have been made using the paired Wilcoxon test between the same donors. P values are denoted on the figures as follows: * p<0.05, ** p<0.01, *** p<0.001, **** p<0.0001). There was a reduced expression of NKp46 in circulating NK cell CD56dimCD16+/- NK cells in patients in comparison to both CD56dimCD16++ NK cells and CD56brightCD16- NK cells (top graph). There were no significant differences in NKp46 expression between intrahepatic NK cell subpopulations (bottom graph).*

NKp46 expression was significantly lower on CD56dimCD16+/- NK cells compared to CD56dimCD16++ NK cells in cirrhosis in the circulation (Figure 101). This expression pattern was maintained in CD56dimCD16+/- NK cells when the cirrhosis subpopulations were separated by underlying aetiology (ALD or MASLD) *(data not shown)*. Again, comparison of NKp46 expression on CD56dimCD16+/- NK cells between patients with ALD cirrhosis and MASLD cirrhosis, with or without HCC, did not show significant differences (Figure 102).

Comparison of NKp46 expression on circulating CD56dimCD16+/- NK cells in ALD cirrhosis with MASLD cirrhosis

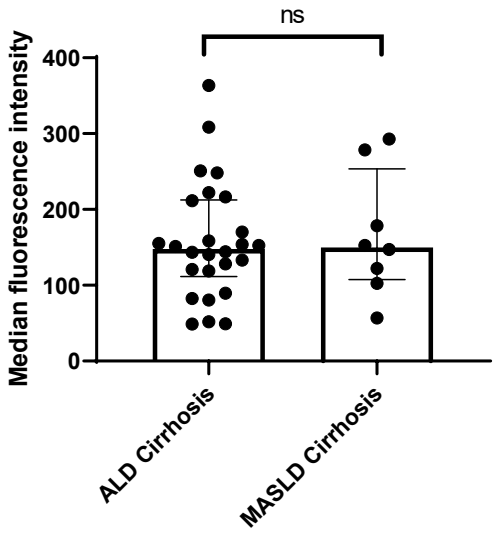


Figure 102 A comparison of NKp46 expression on CD56dimCD16+/- NK cells in patients with cirrhosis secondary to alcohol related liver disease (ALD) and metabolic dysfunction-associated

steatotic liver disease (MASLD). (Graphs display individual values with the median value displayed by the bar. Comparisons between groups have been made using the Mann-Whitney test. Error bars represent the interquartile range).

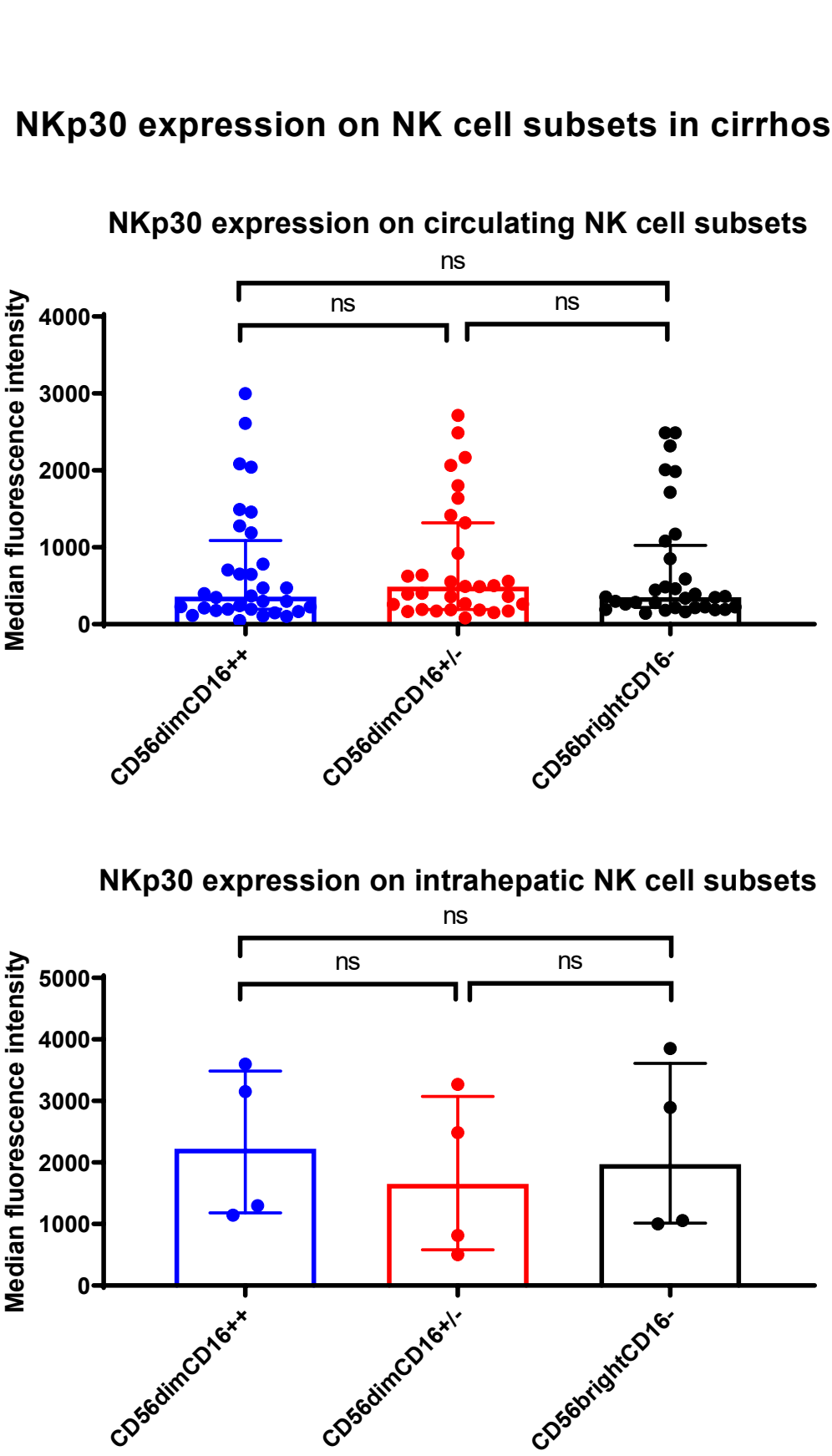


Figure 103 NKp30 expression in NK cell subsets defined by CD56 and CD16 expression in the circulation and in the liver in cirrhosis. The top graph demonstrates NKp30 expression in

*circulating NK cells in cirrhosis. The bottom graph demonstrates NKp30 expression on intrahepatic NK cells in cirrhosis. (Graphs display individual values with the median value displayed by the bar. Comparisons between groups have been made using the paired Wilcoxon test between the same donors. Error bars represent the interquartile range. P values are denoted on the figures as follows: * p<0.05, ** p<0.01, *** p<0.001, **** p<0.0001). There were no significant differences in NKp30 expression when comparing NK cells subpopulations in the circulation or in the liver.*

NKp30 expression did not show any differences between the NK cells subsets in the circulation or on intrahepatic NK cells in health or disease (Figure 103). There were still no differences in NKp30 expression when the cirrhosis subpopulations were separated by underlying aetiology (ALD or MASLD) *(data not shown)*. Again comparison of NKp30 expression on CD56dimCD16+/- NK cells between patients with ALD cirrhosis and MASLD cirrhosis did not yield any differences (Figure 104).

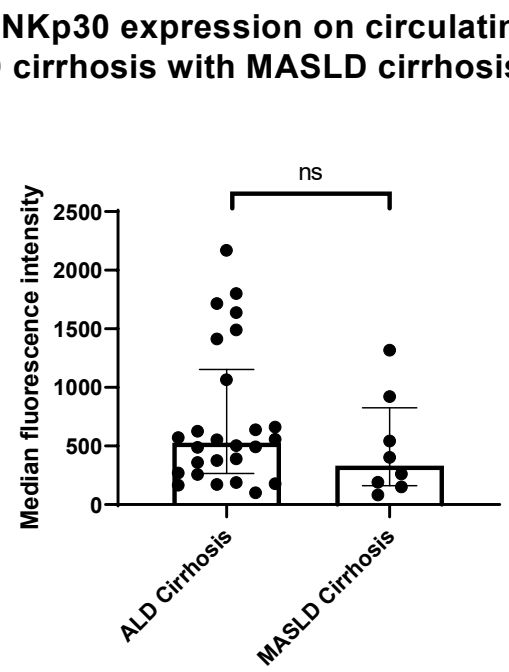


Figure 104 A comparison of NKp30 expression on CD56dimCD16+/- NK cells in patients with cirrhosis secondary to alcohol related liver disease (ALD) and metabolic dysfunction-associated steatotic liver disease (MASLD). (Graphs display individual values with the median value

displayed by the bar. Comparisons between groups have been made using the Mann-Whitney test. Error bars represent the interquartile range).

4.2.2 Surface expression of the inhibitory receptor CD161 on NK cell subpopulations

Protein expression determined using flow cytometry demonstrated an upregulation in CD161 expression on circulating NK cells in cirrhosis (see chapter 3). Again, NK cells for each individual donor were separated into 3 subpopulations: CD56dimCD16++, CD56brightCD16- and CD56dimCD16+/- NK cells (see Chapter 2, Figure 3 for gating strategy) and comparisons made within the same donor. CD161 surface expression was determined using flow cytometry in NK cell subpopulations (see Chapter 3, Figure 33 for the CD161 gating strategy; Phenotyping Panel 1, Table 3). CD161 expression in each subpopulation in cirrhosis was determined for circulating NK cells and intrahepatic NK cells (peripheral blood samples: cirrhosis n=35 (Table 8); intrahepatic: cirrhosis n=4; (Table 9). Further comparisons for receptor expression in NK cell subsets were also undertaken in healthy patients (peripheral blood n=32; intrahepatic n=7) and patients with HCC on a background of cirrhosis (peripheral blood n=29; intrahepatic n=6) (results shown in Appendix 8.5).

The proportion of circulating CD56dimCD16+/- NK cells expressing CD161 was significantly lower than CD56dimCD16++ NK cells in cirrhosis. Circulating CD56brightCD16- NK cells had the lowest proportion of CD161+ NK cells both in health and disease (Figure 105). This trend of a reduced CD161+ proportion in CD56dimCD16+/- NK cells was maintained when the cirrhosis subpopulations were separated by underlying aetiology (ALD or MASLD) (*data not shown*). The proportion of CD161+CD56dimCD16+/- NK cells in patients with ALD cirrhosis was not significantly different to the proportion in patients with MASLD cirrhosis (Figure 105).

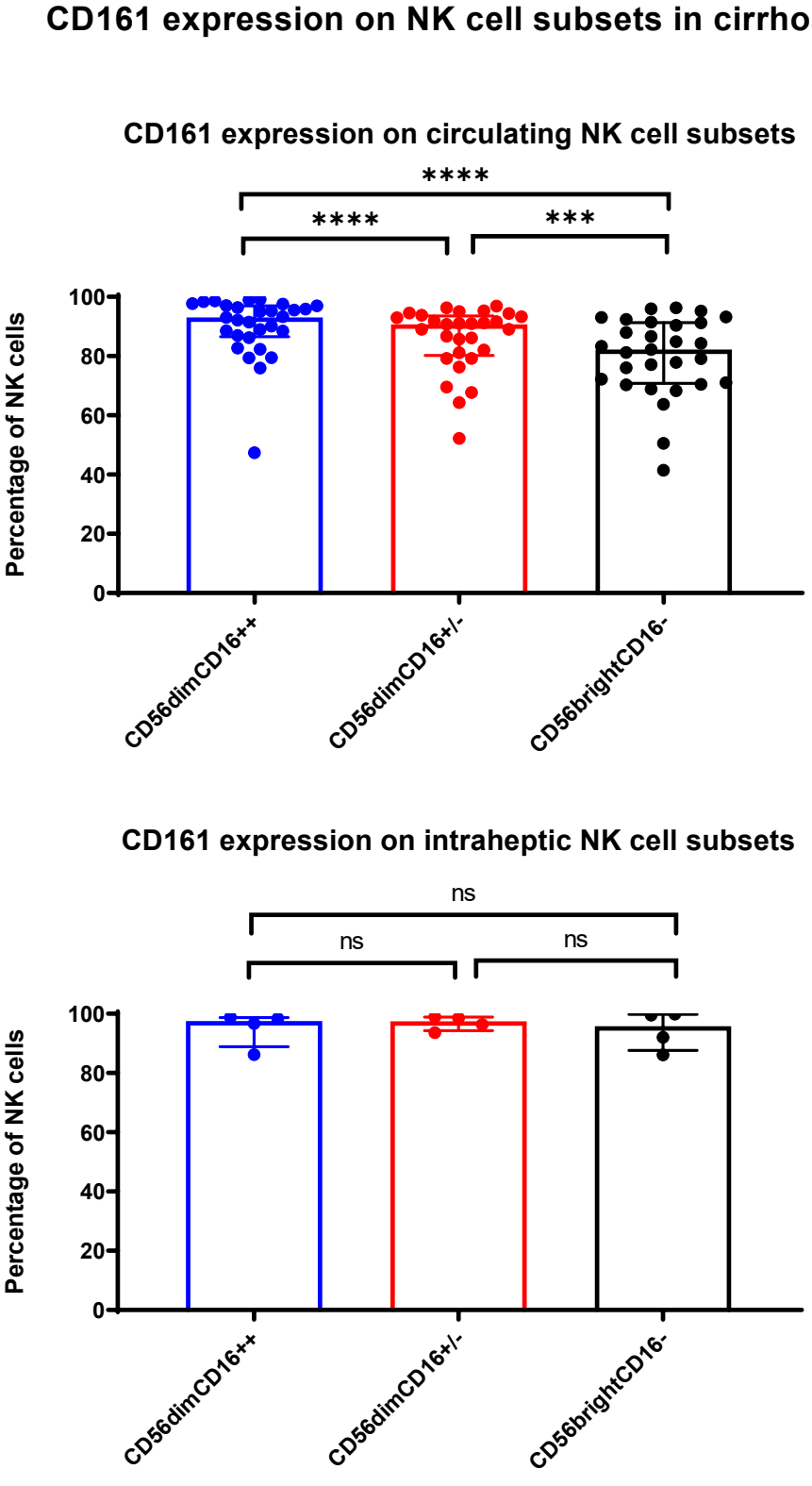


Figure 105 CD161 expression in NK cell subsets defined by CD56 and CD16 expression in the circulation and in the liver in cirrhosis. The top graph demonstrates CD161 expression in circulating NK cells in cirrhosis. The bottom graph demonstrates CD161 expression on intrahepatic NK cells in cirrhosis. (Graphs display individual values with the median value

*displayed by the bar. Comparisons between groups have been made using the paired Wilcoxon test between the same donors. Error bars represent the interquartile range. P values are denoted on the figures as follows: * p<0.05, ** p<0.01, *** p<0.001, **** p<0.0001). The proportion of circulating CD56+CD16+/- NK cells expressing CD161 was lower compared to CD56dimCD16++ NK cell. CD56brightCD16- NK cells had the lowest proportion of CD161+cells of the three NK subpopulations in the circulation (top graph). There were no significant differences between intrahepatic NK cell subpopulations (bottom graph).*

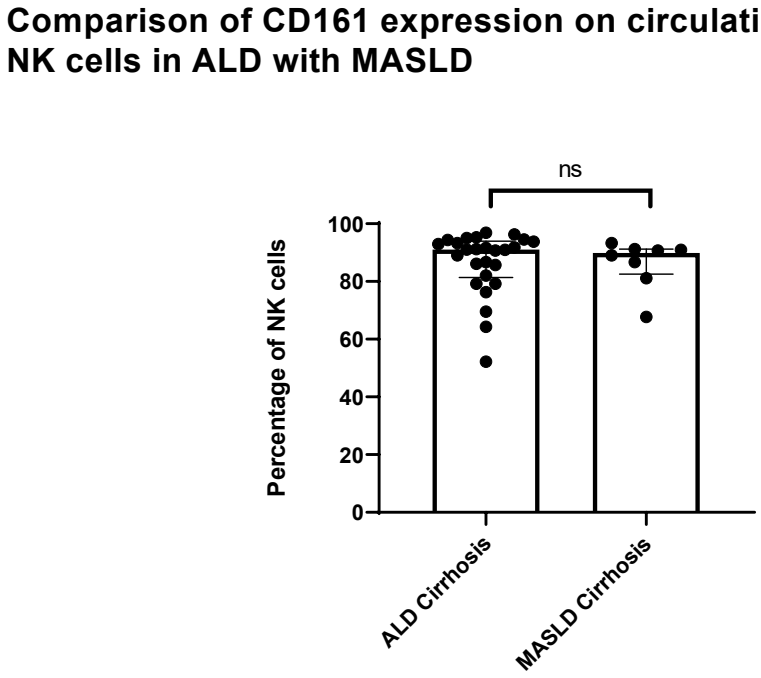


Figure 106 A comparison of CD161 expression on CD56dimCD16+/- NK cells in patients with cirrhosis secondary to alcohol related liver disease (ALD) and metabolic dysfunction-associated steatotic liver disease (MASLD). (Graphs display individual values with the median value displayed by the bar. Comparisons between groups have been made using the Mann-Whitney test. Error bars represent the interquartile range).

4.2.3 Surface expression of liver homing receptor CXCR6 and intrahepatic markers

Intrahepatic NK cells express the liver homing marker CXCR6 (Stegmann et al., 2016), and with increased expression of CCR5 (Hudspeth et al., 2016) and a subset expressing

CD49a (Marquardt et al., 2015). Intrahepatic NK cells express transcription factors Tbet and EOMES in inverse proportions to circulating NK cells, with intrahepatic NK cells being $Tbet^{lo}EOMES^{Hi}$ cells (Cuff et al., 2016; Stegmann et al., 2016).

Intrahepatic NK cells are thought to remain within liver sinusoidal spaces, due to engagement with CXCR6 and CCR5 (Hudspeth et al., 2016). However, the timeline for the acquisition of these liver homing markers is not clearly understood.

To determine if CD56dimCD16+/- NK cells are a transition population with features of intrahepatic NK cells, surface expression levels of CXCR6 were determined in patients with cirrhosis without HCC. NK cells were separated into 3 subpopulations: CD56dimCD16++, CD56brightCD16- and CD56dimCD16+/- NK cells (see Chapter 2, Figure 3 for gating strategy). CXCR6 surface expression was then determined using flow cytometry in NK cell subpopulations (see Chapter 3, Figure 48 for the CXCR6 gating strategy; Phenotyping Panel 1 used (Table 3)). CXCR6 expression was determined in each NK subpopulation in circulating and intrahepatic NK cells in cirrhosis (peripheral blood samples: cirrhosis n=35 (Table 8); intrahepatic samples: cirrhosis n=4 (Table 9). Further comparisons for receptor expression in NK cell subsets were also undertaken in healthy patients (peripheral blood n=32; intrahepatic n=7) and patients with HCC on a background of cirrhosis (peripheral blood n=29; intrahepatic n=6) (results shown in Appendix 8.5).

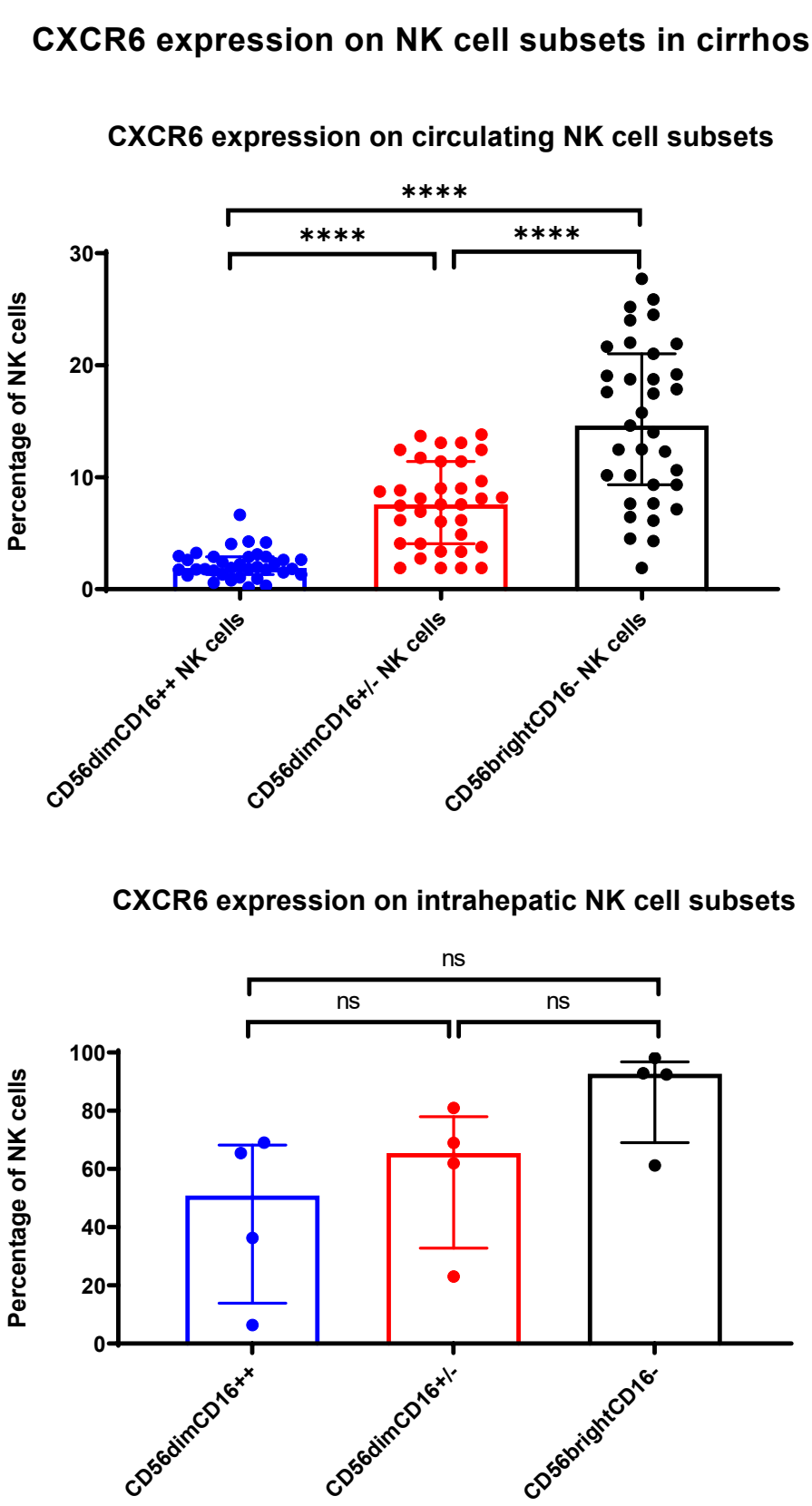


Figure 107 CXCR6 expression in NK cell subsets defined by CD56 and CD16 expression in the circulation and in the liver in cirrhosis. The top graph demonstrates CXCR6 expression in

*circulating NK cells in cirrhosis. The bottom graph demonstrates CXCR6 expression on intrahepatic NK cells. (Graphs display individual values with the median value displayed by the bar. Comparisons between groups have been made using the paired Wilcoxon test between the same donors. Error bars represent the interquartile range. P values are denoted on the figures as follows: * p<0.05, ** p<0.01, *** p<0.001, **** p<0.0001). There was a significantly increased proportion of CXCR6+ NK cells in the CD56dimCD16+/- subpopulation and CD56brightCD16- NK cell subpopulation compared to CD56dimCD16++ NK cells in the circulation (top graph). This trend was maintained in intrahepatic NK subpopulations (bottom graph).*

Overall CXCR6 expression on intrahepatic NK cells was greater than on circulating NK cells, in keeping with published literature. Circulating CD56dimCD16+/- NK cells demonstrated an intermediate level of expression of CXCR6 in cirrhosis, with the CD56dimCD16++ NK cell subset having the lowest proportion of CXCR6+ NK cells, and CD56brightCD16- NK cells having the greatest proportion of CXCR6+NK cells (Figure 107). This expression pattern was maintained in CD56dimCD16+/- NK cells when the cirrhosis subpopulations were separated by underlying aetiology (ALD or MASLD) *(data not shown)*. Direct comparison of the proportion of CXCR6+ CD56dimCD16+/- NK cells between patients with ALD cirrhosis and MASLD cirrhosis did not yield a significant difference (Figure 108).

Comparison of CXCR6 expression on circulating CD56dimCD16+/- NK cells in ALD cirrhosis with MASLD cirrhosis

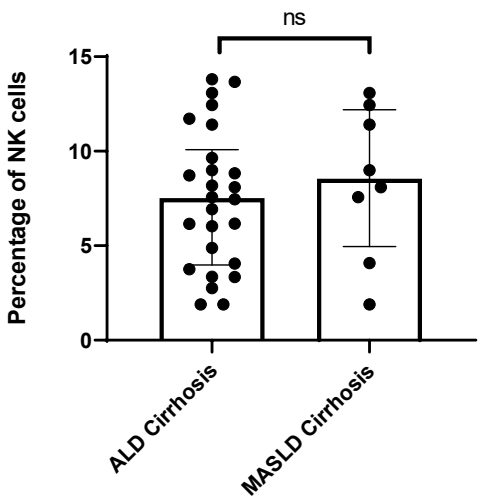


Figure 108 A comparison of CXCR6 expression on CD56dimCD16+/- NK cells in patients with cirrhosis secondary to alcohol related liver disease (ALD) with metabolic dysfunction-associated steatotic liver disease (MASLD). (Graphs display individual values with the median value displayed by the bar. Comparisons between groups have been made using the Mann-Whitney test. Error bars represent the interquartile range).

To determine if the CD56dimCD16+/-NK cell subset has potential liver-homing capacity, CCR5, CD49a and $Tbet^{lo}EOMES^{Hi}$ expression was also determined on circulating NK cells in patients with cirrhosis. To minimise variation in aetiology, all patients in this experiment had Child-Pugh score A cirrhosis and all patients had an underlying ALD (see Table 12 below). The expression of CCR5 and CD49a and the proportion of $Tbet^{lo}EOMES^{Hi}$ NK cells was also determined in intrahepatic NK cells (healthy n=7, cirrhosis n=4, HCC n=6; patient characteristics displayed in chapter 3, Table 9). NK cells were stained with the Liver phenotyping panel as described in methods (Table 3), separated by CD56 and CD16 expression as demonstrated in Chapter 2, Figure 3, and subsequently the proportions expressing CCR5, CD49a and $Tbet^{lo}EOMES^{Hi}$ determined using fluorescence minus one controls (FMOs, gating strategy demonstrated in Figure 109). Phenotyping was also undertaken for further comparisons in patients with healthy livers and HCC on a background of cirrhosis, both in the circulation and intrahepatic (from healthy individuals (n=7), patients with HCC and Child-Pugh score A ALD cirrhosis (n=5); see Table 12 for patient characteristics; data for healthy and HCC groups shown in Appendix 8.5).

Table 12 Characteristics of patients from whom peripheral blood samples were used to determine CCR5, CD49a, Tbet and EOMES expression on NK cell subsets. All patients had underlying cirrhosis from alcohol related liver disease (ALD).

	Healthy	Cirrhosis	HCC
Total number	7	12	5
Age, years mean, (range)	45 (34-54)	52 (33-72)	71 (57-76)
Male, n	5	9	4
Child-Pugh Score A, n		12	5
MELD-Na score mean, (range)		9 (7-15)	10 (7 – 12)
BCLC staging:			

BCLC 0, n	1
BCLC A, n	0
BCLC B, n	3
BCLC C, n	1
BCLC D, n	0

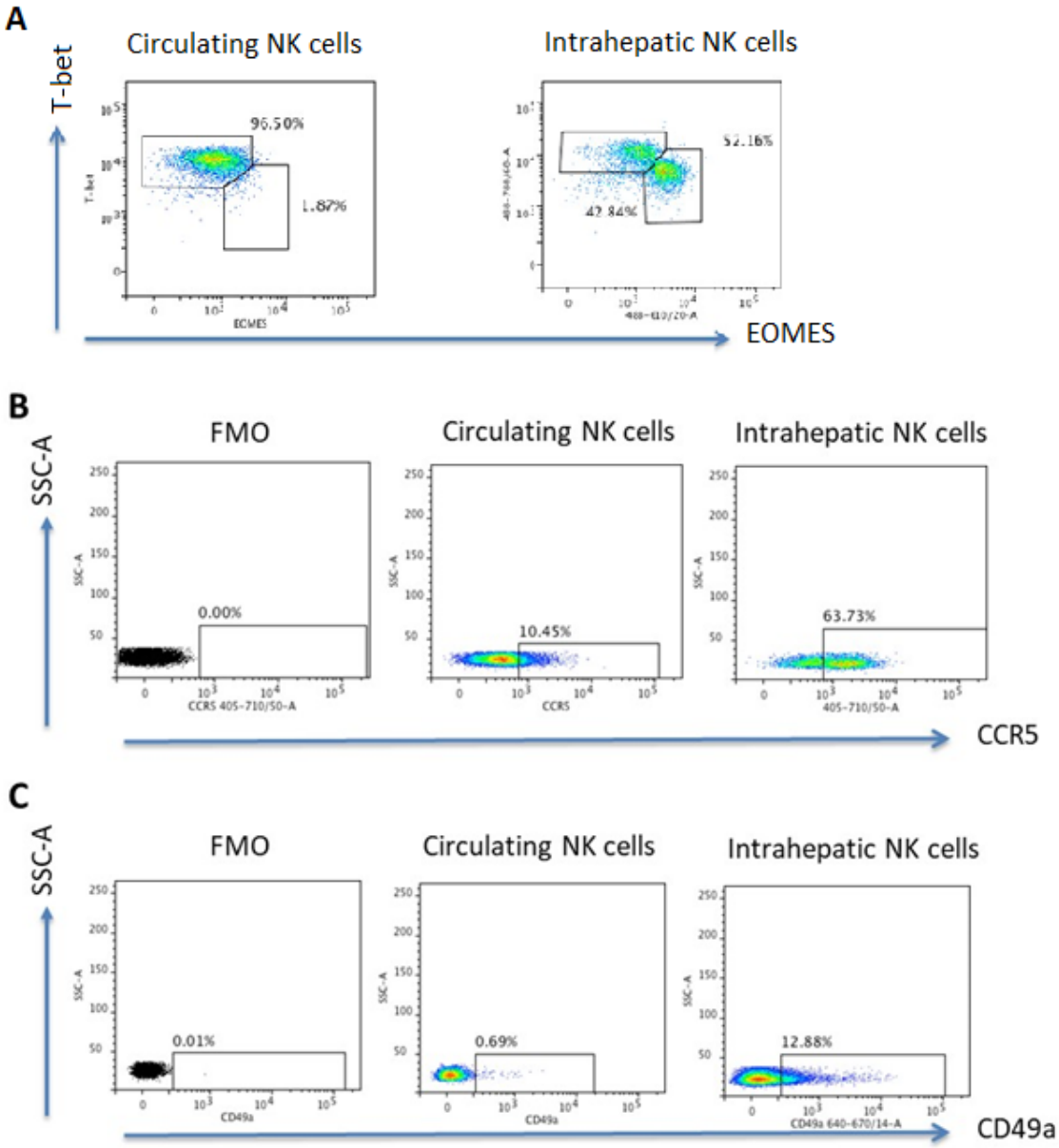


Figure 109 Gating strategies for surface receptors CXCR6, CCR5 and CD49a. Peripheral and intrahepatic mononuclear cells were surface stained with a viability dye, CD3, CD56, CD16, CCR5 and CD49a followed by intracellular staining for T-bet and EOMES (see methods Table 3, phenotyping panels – Liver Panel). NK cells were first identified by gating on live lymphocytes as determined by forward and side scatter area (SSC-A) and subsequently selecting CD3-CD56+ NK cells as described in chapter 3. NK cells were then separated into CD56dimCD16++ cells, CD56brightCD16- cells and CD56dimCD16+/- NK cells as described in Chapter 3. T-bet and EOMES (graph A) was determined using the gating strategy as demonstrated. CCR5 (graph B) and CD49a (graph C) expression was determined using a fluorescence minus one (FMO) method which was subtracted from the percentage of cells staining positively for each surface receptor.

Similar to CXCR6 expression, CD56dimCD16+/- NK cells and CD56brightCD16- NK cells demonstrated an increased proportion of CCR5+NK cells in comparison to CD56dimCD16++ NK cells, both in the circulation and within the liver (Figure 110).

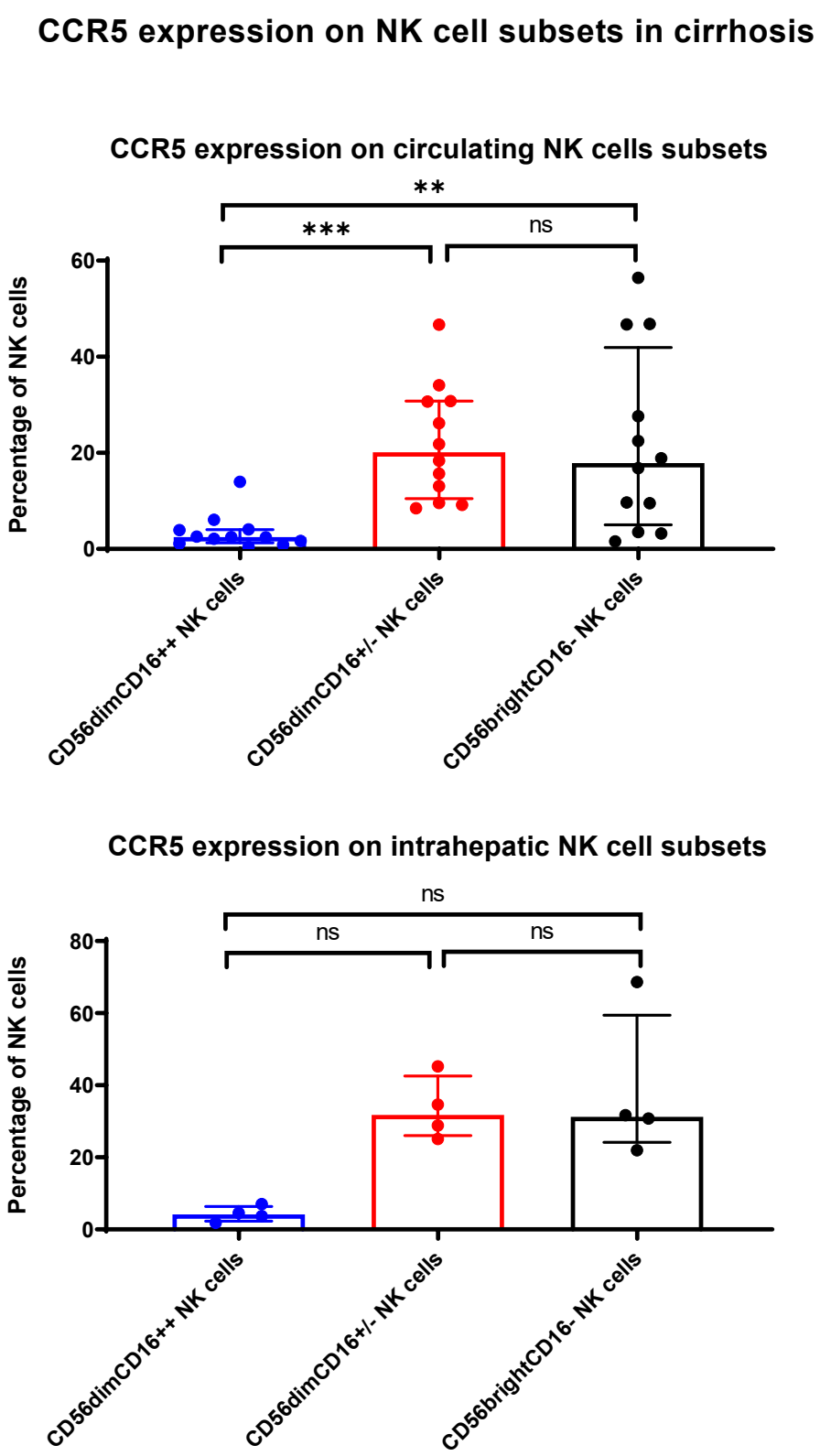


Figure 110 CCR5 expression in NK cell subsets defined by CD56 and CD16 expression in the circulation and in the liver in cirrhosis. The top graph demonstrates CCR5 expression in

*circulating NK cells in ALD cirrhosis. The bottom graph demonstrates CCR5 expression on intrahepatic NK cells in cirrhosis. (Graphs display individual values with the median value displayed by the bar. Comparisons between groups have been made using the paired Wilcoxon test between the same donors. Error bars represent the interquartile range. P values are denoted on the figures as follows: * p<0.05, ** p<0.01, *** p<0.001, **** p<0.0001). There was a significantly increased proportion of CCR5+ NK cells in the CD56dimCD16+/- subpopulation and CD56brightCD16- NK cell subpopulation compared to CD56dimCD16++ NK cells in the circulation (top graph). This trend was maintained in intrahepatic NK subpopulations (bottom graph).*

Differences in expression of CD49a was not detected on these samples on CD56dimCD16+/- NK cells compared to CD56dimCD16++ NK cells, but there was an overall increase in the proportion of CD56brightCD16-CD49a+ NK cells in the circulation in cirrhosis (Figure 111).

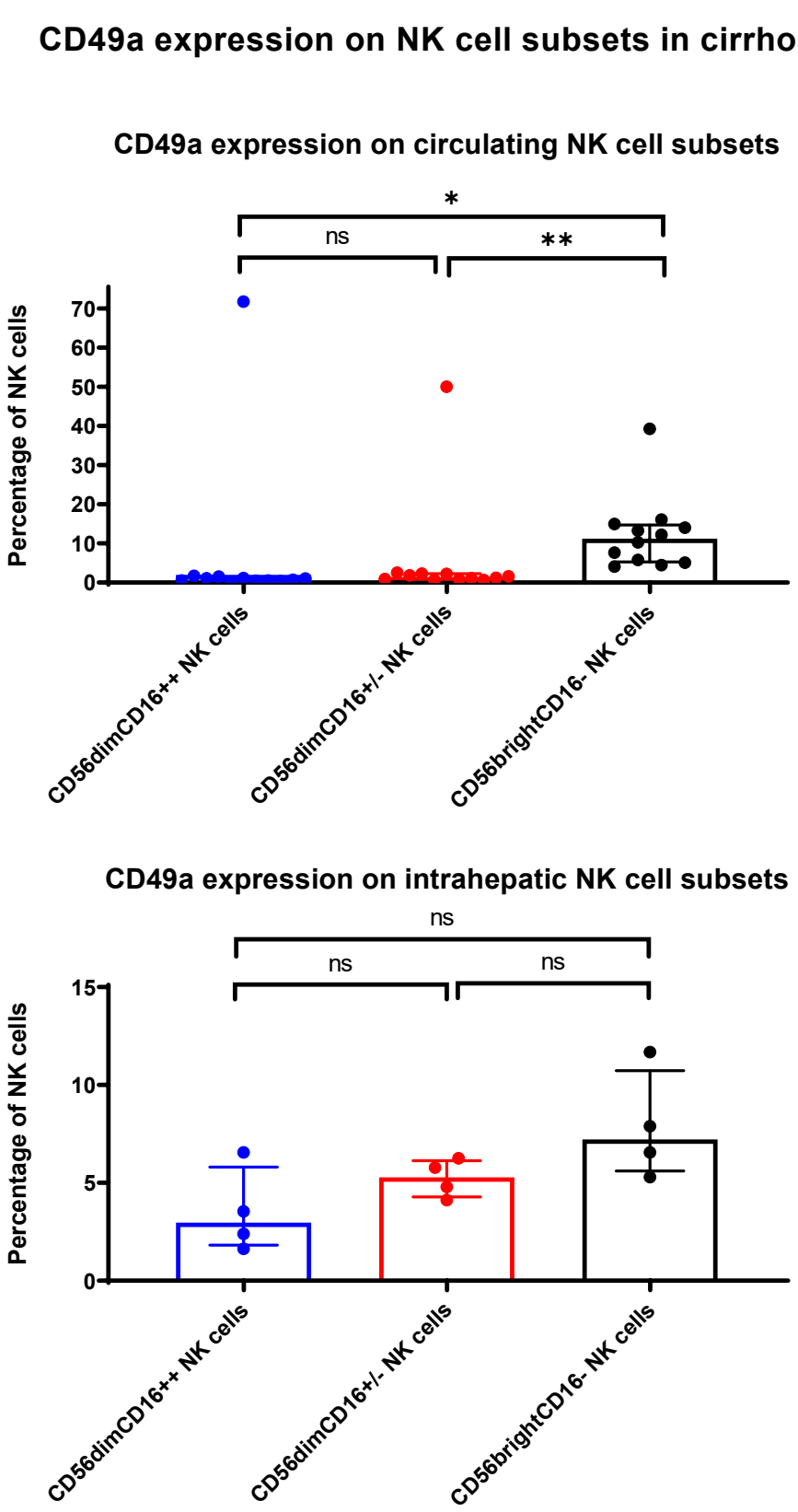


Figure 111 CD49a expression in NK cell subsets defined by CD56 and CD16 expression in the circulation and in the liver in cirrhosis. The top graph demonstrates CD49a expression in circulating NK cells in ALD cirrhosis. The bottom graph demonstrates CD49a expression on

*intrahepatic NK cells in cirrhosis. (Graphs display individual values with the median value displayed by the bar. Comparisons between groups have been made using the paired Wilcoxon test between the same donors. Error bars represent the interquartile range. P values are denoted on the figures as follows: * p<0.05, ** p<0.01, *** p<0.001, **** p<0.0001). There were no significant differences in CD49a expression in CD56dimCD16+/- NK cells in comparison to CD56dimCD16++ NK cells in the circulation (top graph).*

Over 80% of intrahepatic CD56brightCD16- NK cells were Tbet^{lo}EOMES^{Hi} in keeping with published literature, with intrahepatic CD56dimCD16+/- NK cells demonstrating an intermediate proportion, and intrahepatic CD56dimCD16++ NK cells demonstrating a similar Tbet and EOMES profile to circulatingCD56dimCD16++ NK cells (Figure 112). Interestingly, a greater proportion of circulating CD56dimCD16+/- NK cells were Tbet^{lo}EOMES^{Hi} in comparison to circulating CD56dimCD16++ NK cells, though these cells formed less than 10% of the circulating CD56dimCD16+/- NK cells. Circulating CD56brightCD16- NK cells had the greatest proportion of Tbet^{lo}EOMES^{Hi} NK cells (ranging up to 40% in cirrhosis, Figure 112).

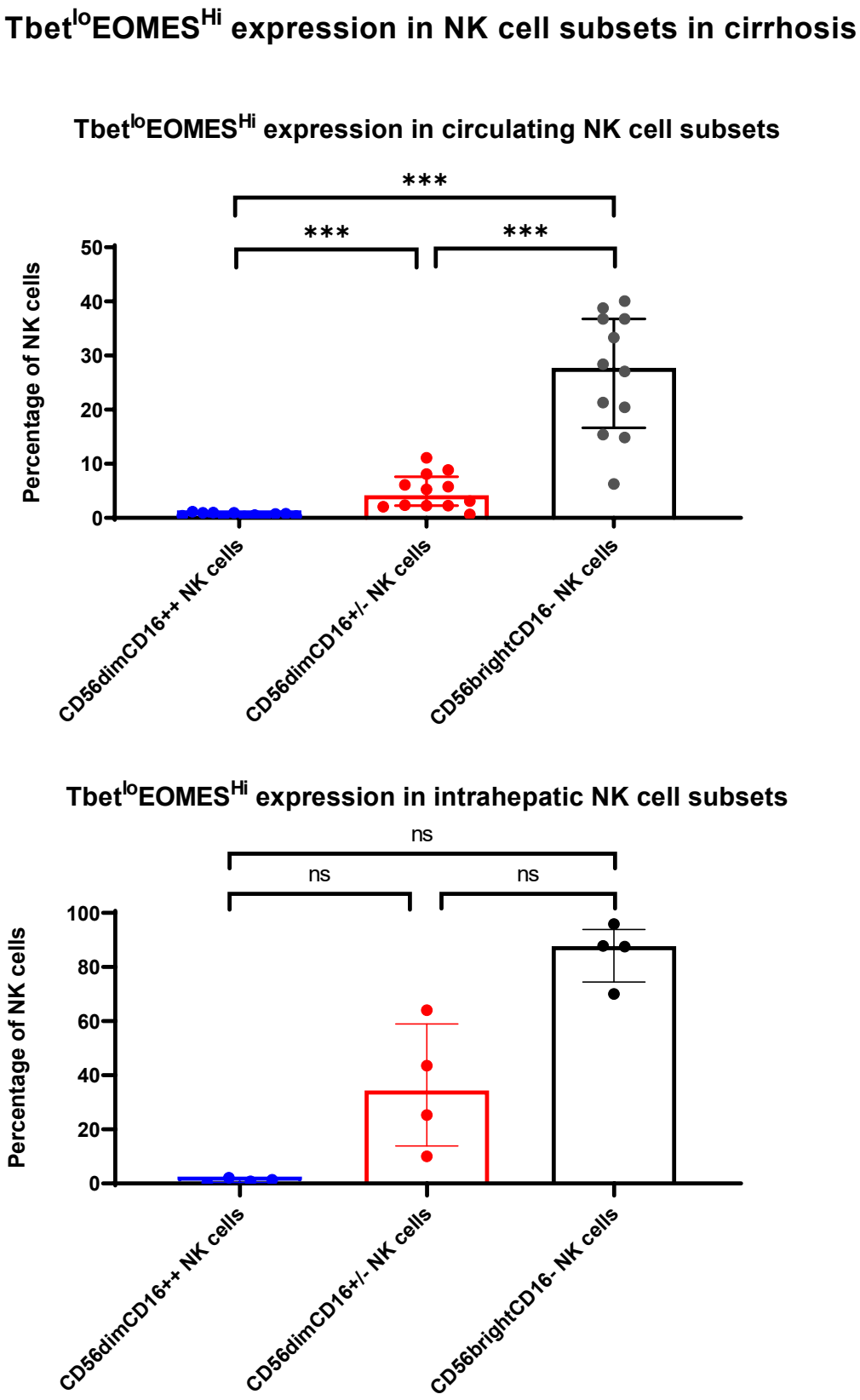


Figure 112 Tbet and EOMES expression in circulating and intrahepatic NK cells in cirrhosis. The top graph demonstrates the proportion of Tbet^{lo}EOMES^{Hi} circulating NK cells in ALD cirrhosis.

*The bottom graph demonstrates the proportion of Tbet^{lo}EOMES^{Hi} intrahepatic NK cells in cirrhosis. (Graphs display individual values with the median value displayed by the bar. Comparisons between groups have been made using the paired Wilcoxon test between the same donors. Error bars represent the interquartile range. P values are denoted on the figures as follows: * p<0.05, ** p<0.01, *** p<0.001, **** p<0.0001). Circulatory CD56brightCD16- NK cells had the highest proportion of Tbet^{lo}EOMES^{Hi} NK cells, with CD56dimCD16++ NK cells having the lowest proportion and CD56dimCD16+/- having an intermediate proportion (top graph). A similar trend was seen in intrahepatic NK cells (bottom graph).*

In summary, this phenotyping data demonstrates that CD56dimCD16+/- NK cells in the circulation in the circulation have a greater proportion of cells expressing CXCR6, CCR5 and a greater proportion of Tbet^{lo}EOMES^{Hi} NK cells in comparison to CD56dimCD16++ NK cells.

4.2.4 Gene expression analyses of circulating CD56dimCD16+/- cells in cirrhosis

NK cells were sorted based on CD56 and CD16 expression (sorting strategy demonstrated in methods Chapter 2, Figure 3). NK cell lysates were diluted to the same concentration (20000 cells per 1µl of buffer RLT) and Nanostring assays performed at the Nanostring facility at University College London as described in the methods. Gene expression in CD56dimCD16+/- NK cells were compared with CD56dimCD16++ NK cells and CD56brightCD16- NK cells from the same donors. Only patients with Child-Pugh B cirrhosis were selected in the cirrhosis groups (ALD (n=3) and MASLD (n=4)) and HCC group (MASLD related cirrhosis with treatment naïve HCC (n=3) (see Chapter 3, Table 11 for full patient characteristics for peripheral blood samples utilised in these gene expression analyses).

4.2.4.1. Gene expression in circulating CD56dimCD16+/- NK cells

The figures below demonstrate comparisons of gene expression between circulating CD56dimCD16+/- NK cells, CD56dimCD16++ NK cells and CD56brightCD16- NK cell subpopulations between the same donors. Only genes displaying a statistically

significant differential expression are demonstrated on the figures (background subtraction undertaken, threshold count of >20 copies, p and FDR value <0.05, fold change >2 or <-2). Comparisons are demonstrated below within disease aetiology and summarised with normalised values on heat maps. Fold change graphs demonstrating full differential expression can be located in Appendix 8.4.

Figure 113 displays significant differential gene expression across the 3 subpopulations in patients with MASLD cirrhosis. Figure 114 displays significant differential gene expression across the 3 subpopulations in patients with ALD cirrhosis. Finally figure 115 displays significant differential gene expression in patients with HCC on a background of MASLD cirrhosis.

There were no significant differences in gene expression when comparing the circulating CD56dimCD16+/- NK cell subpopulation between patients with MASLD cirrhosis to patients with ALD cirrhosis, and when comparing patients with MASLD cirrhosis to patients with HCC on a background of MASLD cirrhosis (*data not shown*).

Differential gene expression in circulating NK cell subpopulations in MASLD cirrhosis

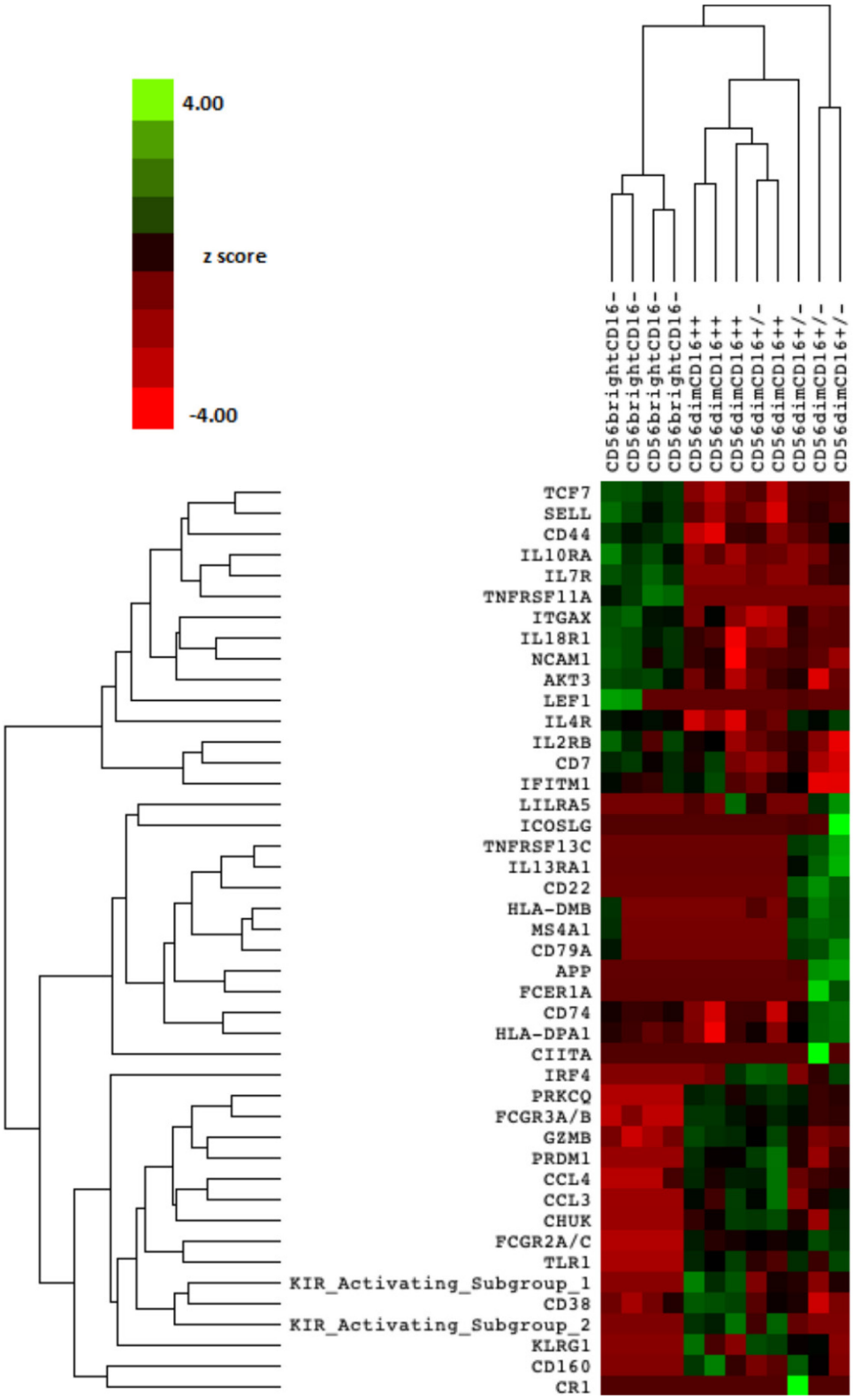


Figure 113 Differential gene expression in circulating NK cell subpopulations in patients with Metabolic dysfunction-associated liver dysfunction (MASLD) cirrhosis (normalised gene expression against housekeeping genes; green = higher expression, red = reduced expression, black = no difference in expression compared to baseline, n=4 patients). Only genes displaying a statistically significant differential expression are demonstrated (background subtraction undertaken, threshold count of >20, p and FDR value <0.05, fold change >2 or <-2).

Differential gene expression in circulating NK cell subpopulations in ALD cirrhosis

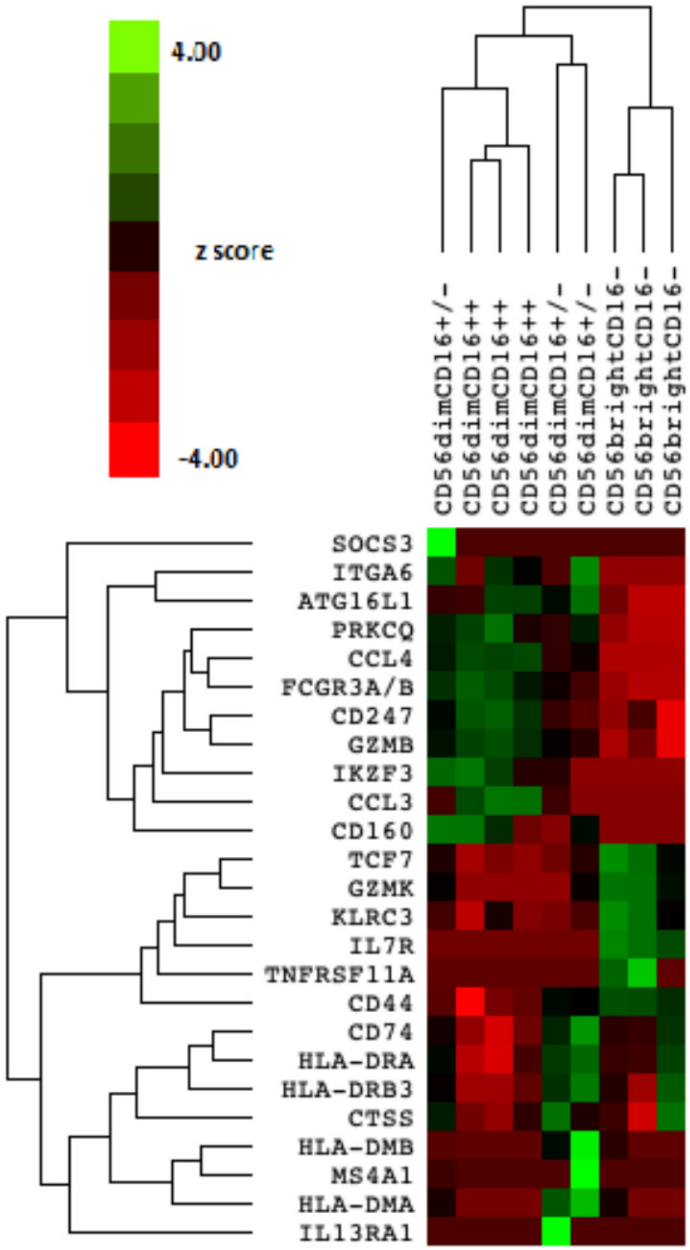


Figure 114 Differential gene expression in circulating NK cell subpopulations in patients with Alcohol related liver disease (ALD) cirrhosis (normalised gene expression against housekeeping genes; green = higher expression, red = reduced expression, black = no difference in expression compared to baseline, n=3 patients). Only genes displaying a statistically significant differential expression are demonstrated (background subtraction undertaken, threshold count of >20, p and FDR value <0.05, fold change >2 or <-2).

Differential gene expression in circulating NK cell subpopulations in HCC related to MASLD cirrhosis

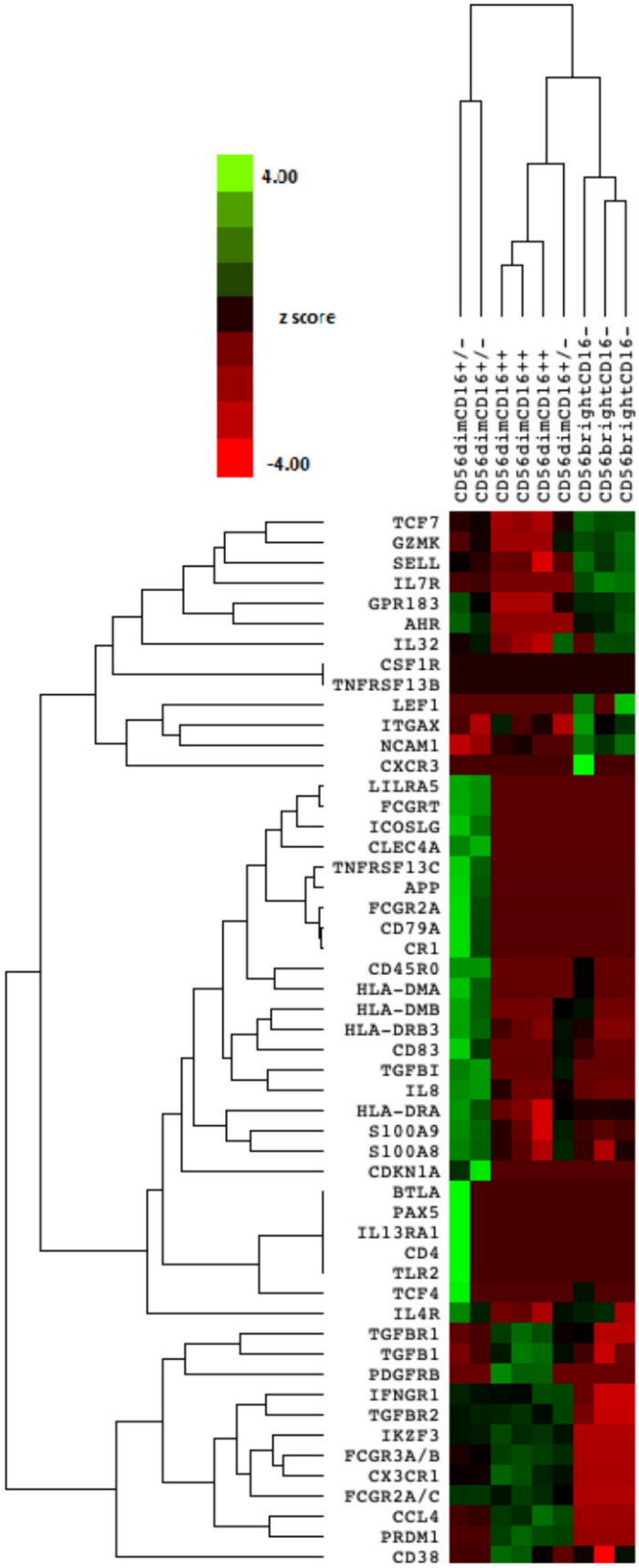


Figure 115 Differential gene expression in circulating NK cell subpopulations in patients with HCC on a background of MASLD cirrhosis (normalised gene expression against housekeeping genes; green = higher expression, red = reduced expression, black = no difference in expression compared to baseline, n=3 patients). Only genes displaying a statistically significant differential expression are demonstrated (background subtraction undertaken, threshold count of >20, p and FDR value <0.05, fold change >2 or <-2).

IL7R and the transcription factor TCF7, both associated with an immature phenotype, were upregulated on CD56brightCD16- cells as expected in comparison to the mature CD56dimCD16++ NK cells, but CD56dimCD16+/- demonstrated an intermediate expression of these across all aetiologies, suggesting that these cells may be in a phase of intermediate maturity.

Furthermore, circulating CD56dimCD16+/- cells demonstrated an intermediate expression of GZMK in ALD cirrhosis and MASLD HCC, with CD56bright NK cells expressing more GZMK and CD56dimCD16++ NK cells expressing the least GZMK. GZMB expression also showed intermediate expression in circulating CD56dimCD16+/- NK cells in ALD and MASLD cirrhosis. There was also an intermediate expression of KIR activating receptors on CD56dimCD16+/- cells (KIR Activating subgroup 1 including *KIR2DS1, KIR2DS2, KIR2DS4, KIR3DS1*; KIR Activating subgroup 2 including *KIR2DS1, KIR2DS2, KIR2DS3, KIR2DS4, KIR2DS5*) in patients with MASLD cirrhosis. In patients with MASLD HCC, *PRDM1* (encoding Blimp1 that negatively regulates secretion of IFNγ and TNFα [Smith et al., 2010]) demonstrated intermediate expression in CD56dimCD16+/- NK cells. There is also intermediate expression of *CD160,* an activating receptor (Tu et al., 2015), on CD56dimCD16+/- in cirrhosis regardless of aetiology.

However, there was a collection of genes that were upregulated on circulating CD56dimCD16+/- cells only in comparison to the two other subpopulations across all disease states: *LILRA5, TNFRSF13C, CD79A, MS4A1, ICOSLG, CR1, IL13RA1, HLA-DMB, HLA-DRA, HLA-DRB3, HLA-DMA, IL4R, APP, CLEC4A, PAK1.* HLA-DR expression has

been demonstrated on activated NK cells with enhanced degranulation (Evans et al., 2011).

4.2.4.2 Gene enrichment analysis in circulating CD56dimCD16+/- NK cells

ReactomeGSA was used to reveal if there were any particularly enriched pathways in the CD56dimCD16+/- circulating NK cell subpopulation. As there were no significant differences in gene expression in CD56dimCD16+/- NK cells between ALD and MASLD cirrhosis and between MASLD cirrhosis and MASLD HCC, gene enrichment analysis focussed on MASLD cirrhosis group only (n=4 patients).

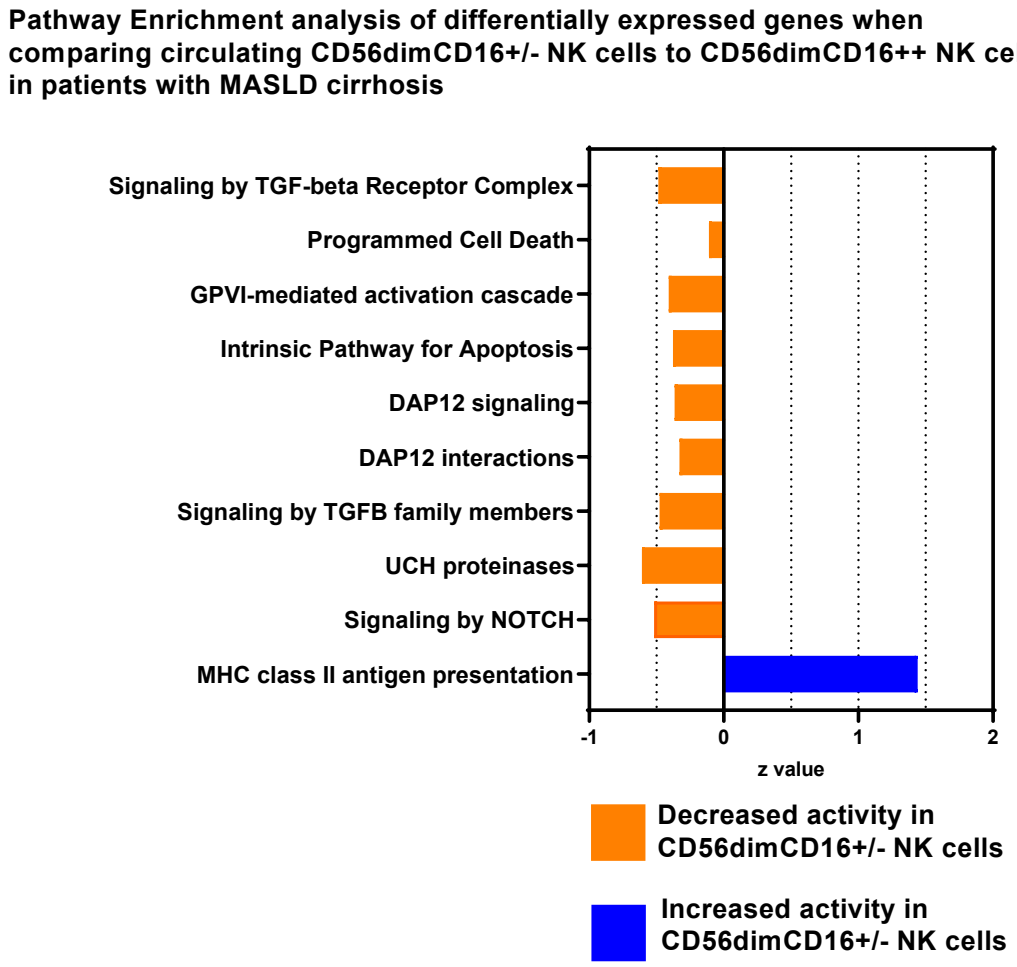


Figure 116 Gene enrichment pathway analysis, comparing circulating CD56dimCD16+/-NK cells with CD56dimCD16++ NK cells in patients with MASLD cirrhosis (n=4). Normalised gene expression data was uploaded to the web-based platform ReactomeGSA for CD56dimCD16+/- NK cells and CD56dimCD16++NK cells from patients with MASLD cirrhosis. The top 10 most enriched pathways are displayed, involving the largest number of differentially expressed genes. The displayed pathways were all significantly altered in CD56dimCD16+/-NK cells compared to CD56dimCD16++NK cells ($p<0.05$) but the calculated FDR was not significant (FDR>0.05). Orange bars demonstrate overall downregulated pathways in CD56dimCD16+/- NK cells and blue bars represent upregulated pathways in CD56dimCD16+/- NK cells compared to CD56dimCD16++NK cells.

In comparison to CD56dimCD16++ NK cells, the pathway enrichment analysis suggests that CD56dimCD16+/- NK cells have enriched pathways in DAP12 signalling and DAP12 interactions, with a reduced activity seen in CD56dimCD16+/- NK cells suggesting a reduced capacity for activation (Figure 116). NOTCH signalling was also enriched,

again with reduced activity in CD56dimCD16+/- NK cells (Figure 116). As NOTCH signalling is usually associated with NK cell maturity and the acquisition of CD16, reduced activity in CD56dimCD16+/- NK cells may suggest a more immature phenotype in these cells in comparison to CD56dimCD16++NK cells.

Interestingly, the pathway for MHC class II antigen presentation was positively enriched in CD56dimCD16+/-NK cells in comparison to both CD56dimCD16++NK cells and CD56brightCD16-NK cells (Figures 116 and 117 respectively). HLA-DR has been described in literature as induced in expression on activated NK cells, and the differential gene expression did demonstrate a significant upregulation of HLA-DR in CD56dimCD16+/-NK cells in all disease states.

As expected, comparison of CD56dimCD16++NK cells with CD56brightCD16-NK cells demonstrated increased NOTCH signalling in the mature CD56dimCD16++NK cells, increased activity in DAP12 interactions, TNF and interferon signalling (Figure 118).

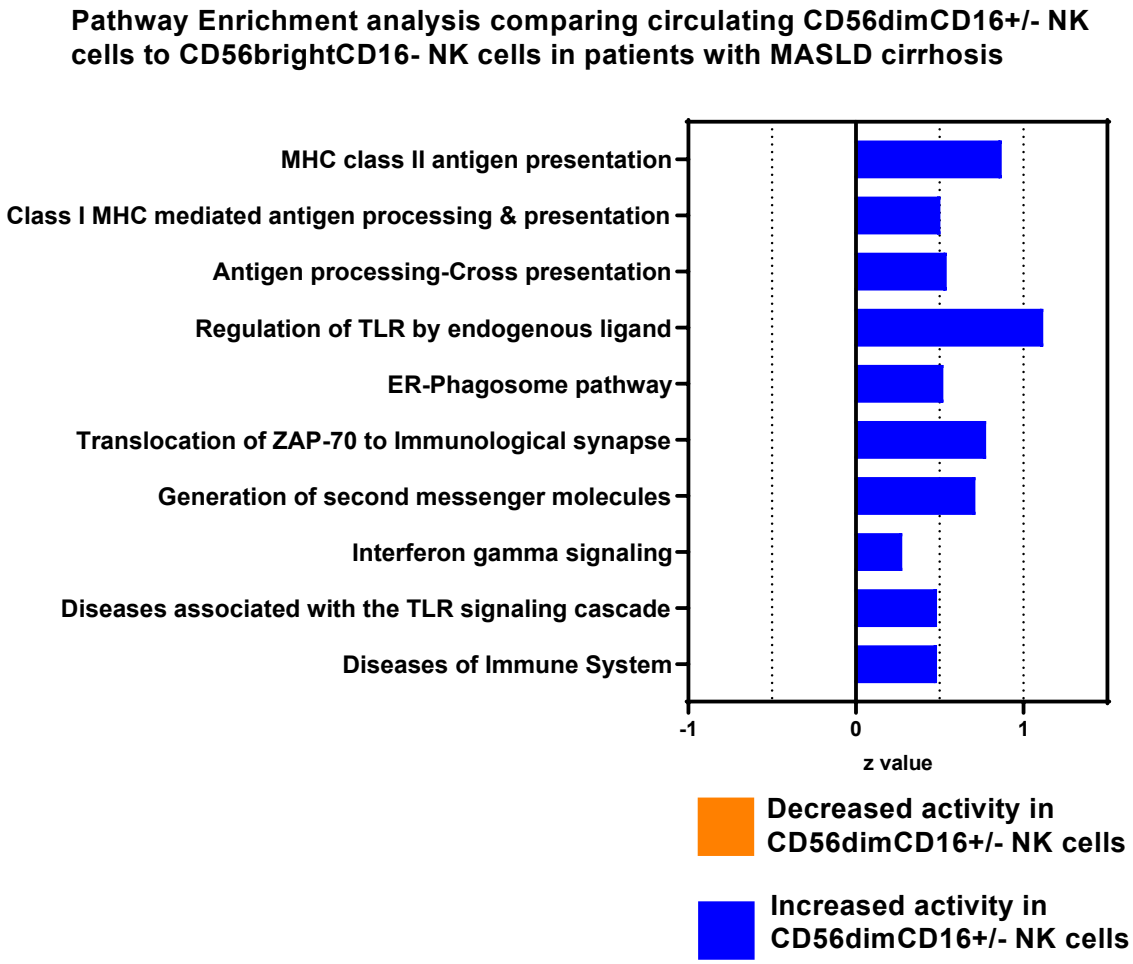


Figure 117 Gene enrichment pathway analysis, comparing circulating CD56dimCD16+/-NK cells with CD56brightCD16-NK cells in patients with MASLD cirrhosis (n=4). Normalised gene expression data was uploaded to the web-based platform ReactomeGSA for CD56dimCD16+/-NK cells and CD56brightCD16-NK cells from patients with MASLD cirrhosis. The top 10 most enriched pathways are displayed, involving the largest number of differentially expressed genes. The displayed pathways were all significantly altered in CD56dimCD16+/-NK cells compared to CD56dimCD16++NK cells ($p<0.05$) and the calculated FDR was significant for the top 7 pathways shown (FDR<0.05). Orange bars demonstrate overall downregulated pathways in CD56dimCD16+/-NK cells and blue bars represent upregulated pathways in CD56dimCD16+/- NK cells compared to CD56brightCD16-NK cells.

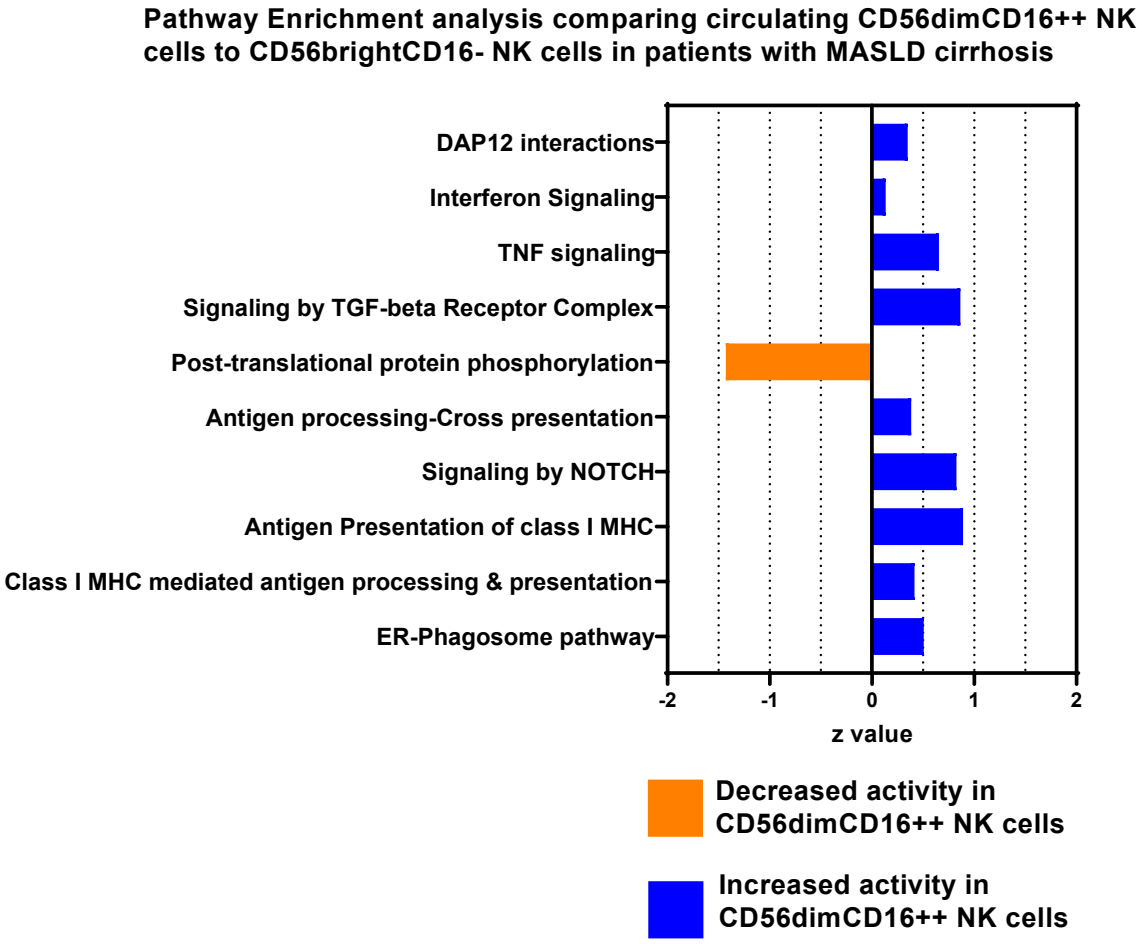


Figure 118 Gene enrichment pathway analysis, comparing circulating CD56dimCD16++NK cells with CD56brightCD16-NK cells in patients with MASLD cirrhosis (n=4). Normalised gene expression data was uploaded to the web-based platform ReactomeGSA for CD56dimCD16++NK cells and CD56brightCD16-NK cells from patients with MASLD cirrhosis. The top 10 most enriched pathways are displayed, involving the largest number of differentially expressed genes. The displayed pathways were all significantly altered in CD56dimCD16+/-NK cells compared to CD56dimCD16++NK cells ($p<0.05$) but the calculated FDR was not significant (FDR>0.05). Orange bars demonstrate overall downregulated pathways in CD56dimCD16++NK cells and blue bars represent upregulated pathways in CD56dimCD16++NK cells compared to CD56brightCD16-NK cells.

Ingenuity Pathway Analysis Software (IPA, Qiagen) was used to determine potentially activated upstream genes resulting in the gene expression profile and gene enrichment seen in CD56dimCD16+/-NK cells i.e. 'upstream regulators' of the CD56dimCD16+/- NK subpopulation (see Figure 119).

A

Upstream Regulator	Predicted activity of regulator	Activation z-score
CSF1	Inhibited	-2.000
PRDM1	Inhibited	-2.698
Ige	Activated	2.000
NFkB (complex)	Activated	2.194
IL5	Activated	2.236
LRRFIP2	Activated	2.000
MMP9	Activated	2.000
SPI1	Activated	2.230
CSF2	Activated	2.127
TP73	Activated	2.194
TGFB1	Activated	2.110
GATA1	Activated	2.186
POU2AF1	Activated	2.200
RBPJ	Activated	2.000

B

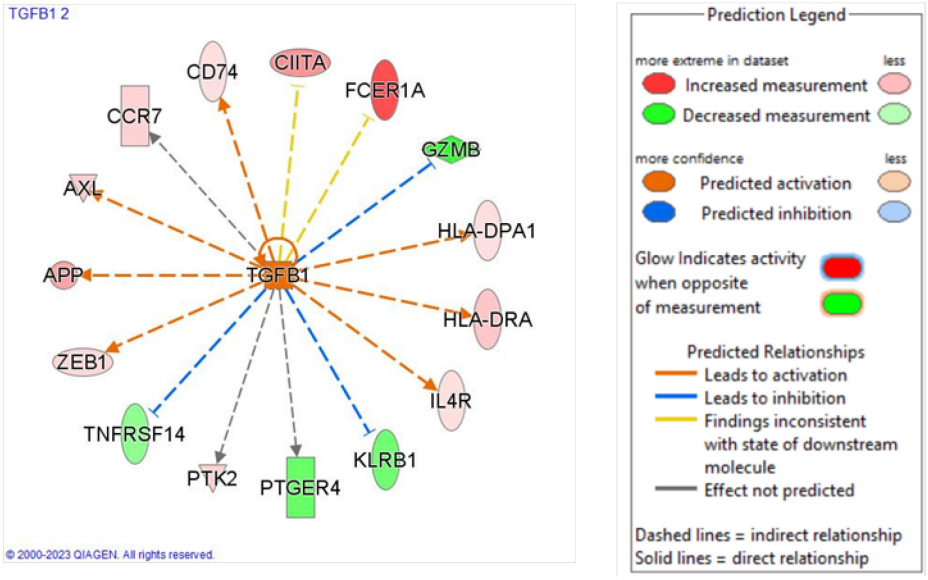


Figure 119 Predicted activation or inhibition of upstream transcriptional regulators and molecules that may result in the differential gene expression profile seen in CD56dimCD16+/- NK cells i.e. predicted 'upstream regulators' for the CD56dimCD16+/- NK cell subpopulation (using Ingenuity Pathway Analysis software, Qiagen). The circulating CD56dimCD16+/- NK cell subpopulation was compared to the circulating CD56dimCD16++ NK cell subpopulation in patients with MASLD cirrhosis (n=4 patients, subpopulations from the same donors compared (matched samples)). Differential gene expression and predicted upstream regulator analysis was performed using Ingenuity Pathway Analysis software (Qiagen). A) Table demonstrating

predicted potential upstream regulators based on differential gene expression measured in CD56dimCD16+/-NK cells compared to CD56dimCD16++NK cells. B) Network diagram demonstrating the effects of predicted activation of Tumour growth factor beta 1 (TGF B1) on gene expression in CD56dimCD16+/-NK cells.

The proteins encoded by identified upstream regulators may be derived from any source, including adjacent cells or within the circulation. In this case, gene expression in the circulating CD56dimCD16+/- NK cell subpopulation was compared with gene expression in the circulating CD56dimCD16++ NK cell subpopulations in the same patients with MASLD cirrhosis. Interestingly, TGFB1, amongst other regulators, was identified as a potential upstream regulator for the CD56dimCD16+/- NK cell subpopulation, potentially accounting for the differential gene expression seen in this subpopulation when compared with gene expression in CD56dimCD16++ NK cells. Given that TGFβ plays a major role in fibrosis and is found in abundance in cirrhosis (Dooley & Ten Dijke, 2012), exposure of NK cells to TGFβ may be one mechanism by which the CD56dimCD16+/- NK cell subpopulation may arise in liver disease.

4.2.5 CD56dimCD16+/- NK cell maturity

Differential gene expression analysis demonstrated the expression of several genes associated with a less mature phenotype in CD56dimCD16+/- NK cells in comparison to CD56dimCD16++ NK cells regardless of underlying disease aetiology. To ratify if this translates to differential protein expression, surface expression of CD57, NKG2C and KLRG1 (associated with mature NK cells) and IL7R and NKG2A (associated with an immature phenotype), as well as intracellular expression of TCF1 (encoded by *TCF7* associated with immature NK cells) was determined using flow cytometry in order to deduce the maturity status of CD56dimCD16+/- NK cells in comparison to CD56brightCD16- NK cells and CD56dimCD16++ NK cells. Due to sample availability, peripheral blood mononuclear cells from a subgroup of patients with cirrhosis only were compared (see Table 13 for patient characteristics for these experiments). Statistical comparisons were made using the non-parametric Wilcoxon paired tests as comparisons were made between NK cell subsets from the same donors.

Table 13 Characteristics of patients with cirrhosis from whom peripheral blood samples were used to determine if there was surface expression of CD57, NKG2C, NKG2A, IL7R, KLRG1 and TCF1.

	CD57	NKG2C	NKG2A	TCF1	IL7R	KLRG1
Total number of patients	15	10	10	10	5	5
Age, years mean, (range)	56 (33-74)	56 (33-74)	56 (33-74)	56 (33-74)	61 (49-65)	61 (49-65)
Male, n	13	8	8	8	5	5
Child-Pugh (CP) Score:						
CPA, n	6	4	4	4	1	1
CPB, n	5	3	3	3	4	4
CPC, n	4	3	3	3	0	0
MELD-Na score mean, (range)	11 (7–18)	11 (7–18)	11 (7–18)	11 (7–18)	10 (9-13)	10 (9-13)
Aetiology:						
ALD, n	12	7	7	7	3	3
MASLD, n	3	3	3	3	2	2

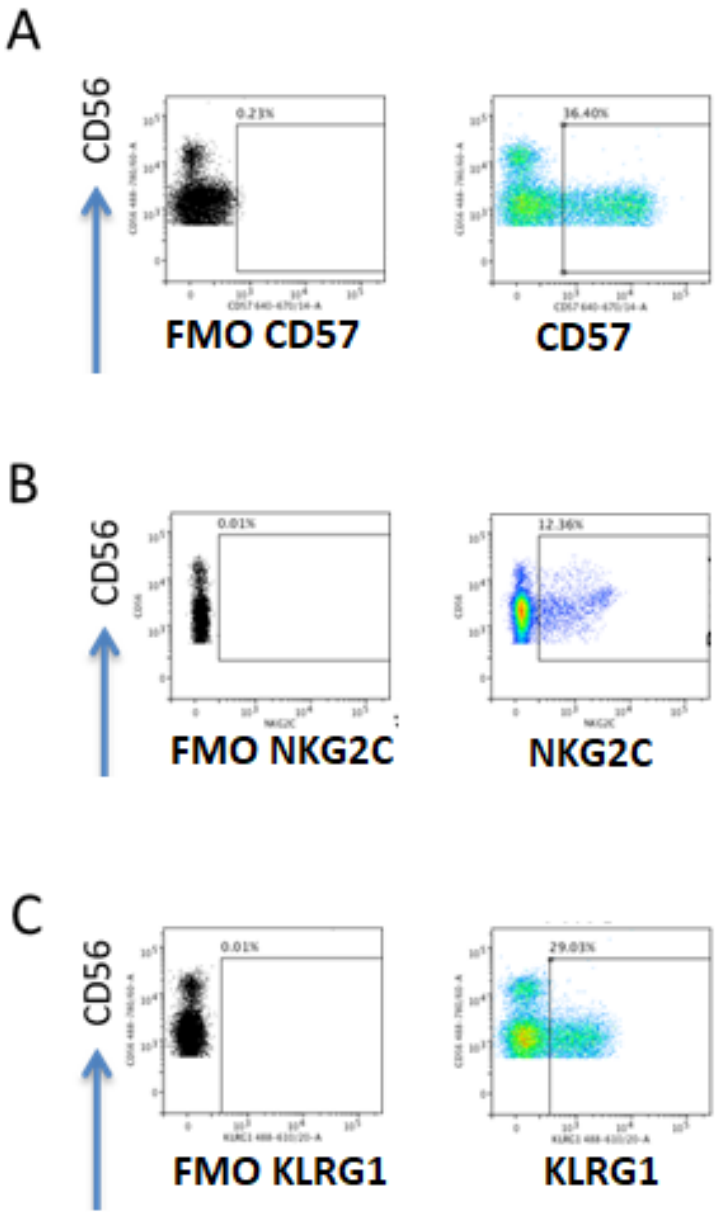


Figure 120 Gating strategy for CD57, NKG2C and KLRG1. NK cells were stained with phenotyping Maturity Panel 1 as described in methods (Table 3). Following gating for NK cells (lymphocyte gating, live singlet cells, CD3 negative cells, CD56positive cells), NK cell subsets (CD56dimCD16++, CD56dimCD16+/- and CD56brightCD16- cells) were identified as described in methods. Subsequent gating was applied as above, using fluorescence minus one (FMO) controls to subtract any background staining.

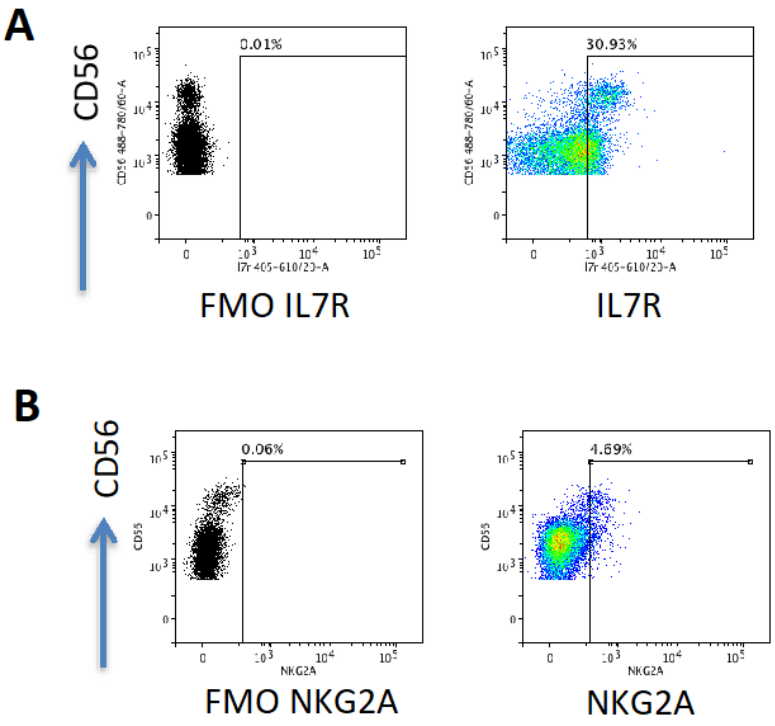


Figure 121 Gating strategy for IL7R and NKG2A. NK cells were stained with phenotyping Maturity Panel 1 as described in methods (Table 3). Following gating for NK cells (lymphocyte gating, live singlet cells, CD3 negative cells, CD56positive cells), NK cell subsets (CD56dimCD16++, CD56dimCD16+/- and CD56brightCD16- cells) were identified as described in methods. Subsequent gating was applied as above, using fluorescence minus one (FMO) controls to subtract any background staining.

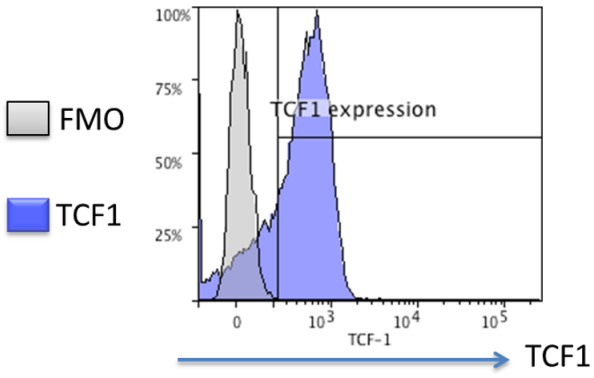


Figure 122 Gating strategy for TCF1. NK cells were stained with phenotyping Maturity Panel 2 as described in methods (Table 3). Following gating for NK cells (lymphocyte gating, live singlet

cells, CD3 negative cells, CD56positive cells), NK cell subsets (CD56dimCD16++, CD56dimCD16+/- and CD56brightCD16- cells) were identified as described in methods. Subsequent gating was applied as above, using fluorescence minus one (FMO) controls to subtract any background staining

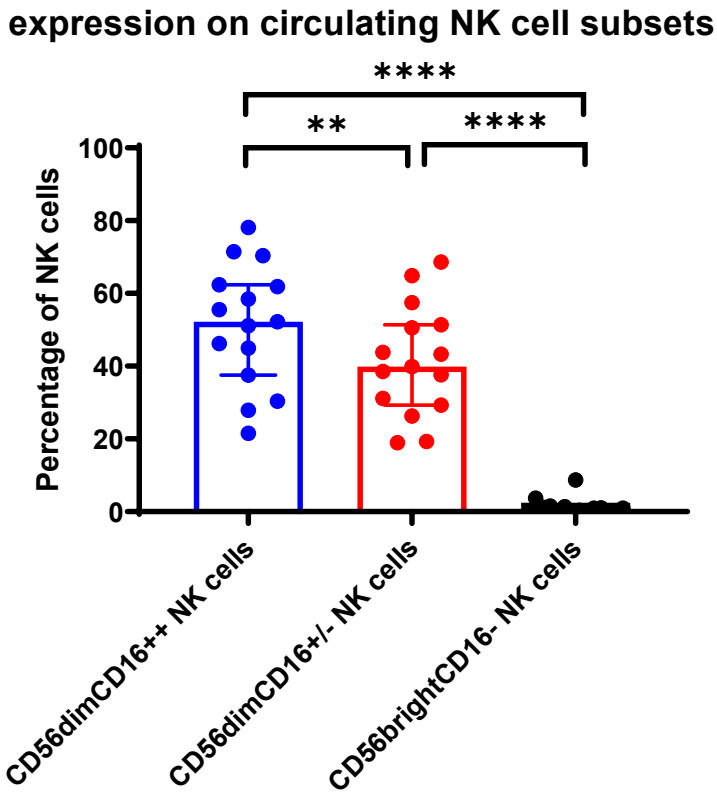


*Figure 123 CD57 expression in NK cell subsets defined by CD56 and CD16 expression in the circulation in cirrhosis. (Graphs display individual values with the median value displayed by the bar. Comparisons between groups have been made using the paired Wilcoxon test between the same donors. Error bars represent the interquartile range. P values are denoted on the figures as follows: * p<0.05, ** p<0.01, *** p<0.001, **** p<0.0001). There was a significant reduction in the proportion of CD56dimCD16+/- NK cells expressing CD57 in comparison to CD56dimCD16++ NK cells. CD57brightCD16- had the lowest proportion of CD57+ NK cells.*

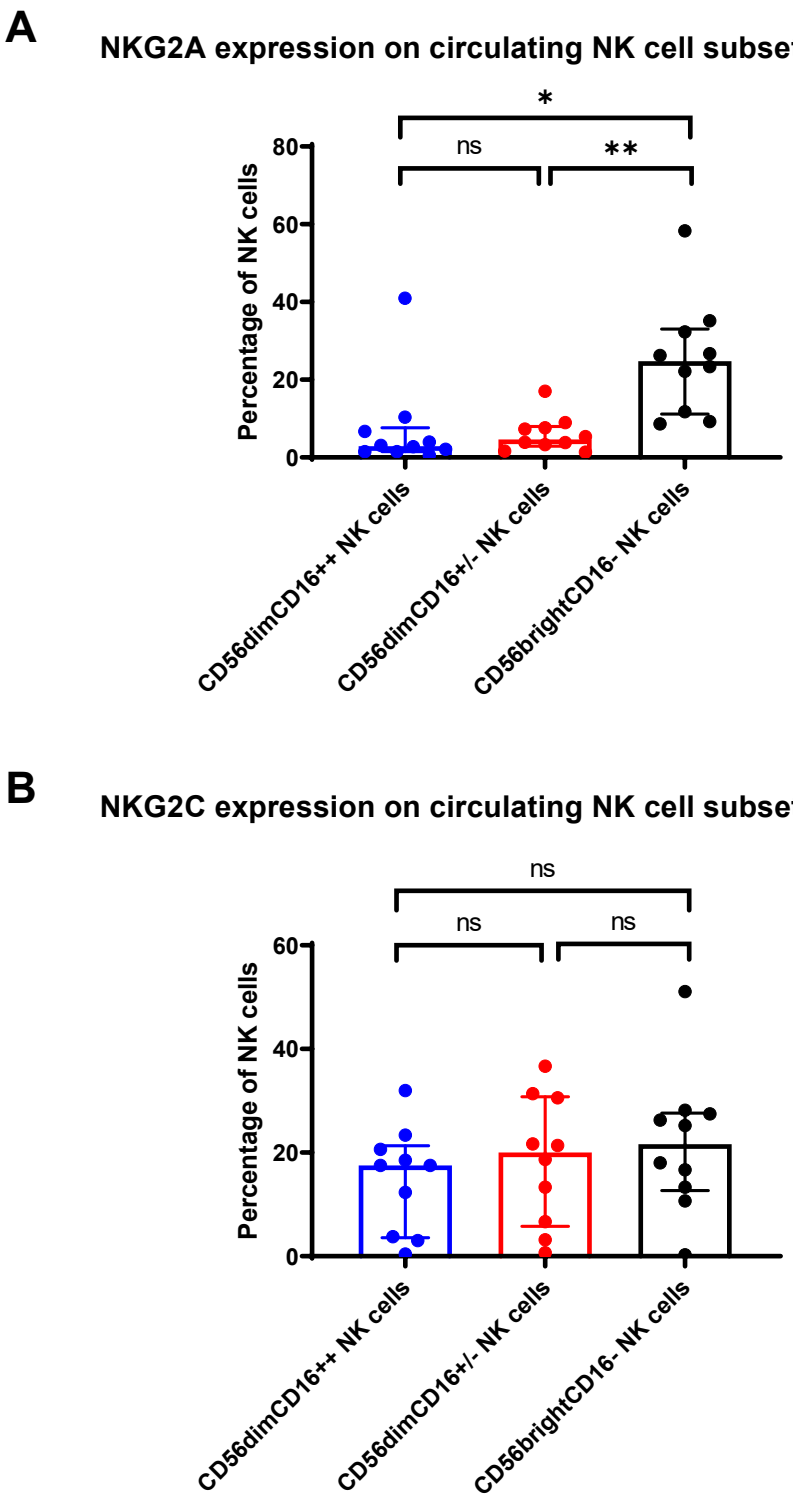


Figure 124 NKG2A and NKG2C expression in NK cell subsets defined by CD56 and CD16 expression in the circulation in cirrhosis. NKG2A (graph A) and NKG2C (graph B) expression in circulating NK cells in cirrhosis is demonstrated on NK cell subsets. (Graphs display individual values with the median value displayed by the bar. Comparisons between groups have been made using the paired Wilcoxon test between the same donors. Error bars represent the

*interquartile range. P values are denoted on the figures as follows: * p<0.05, ** p<0.01, *** p<0.001, **** p<0.0001).*

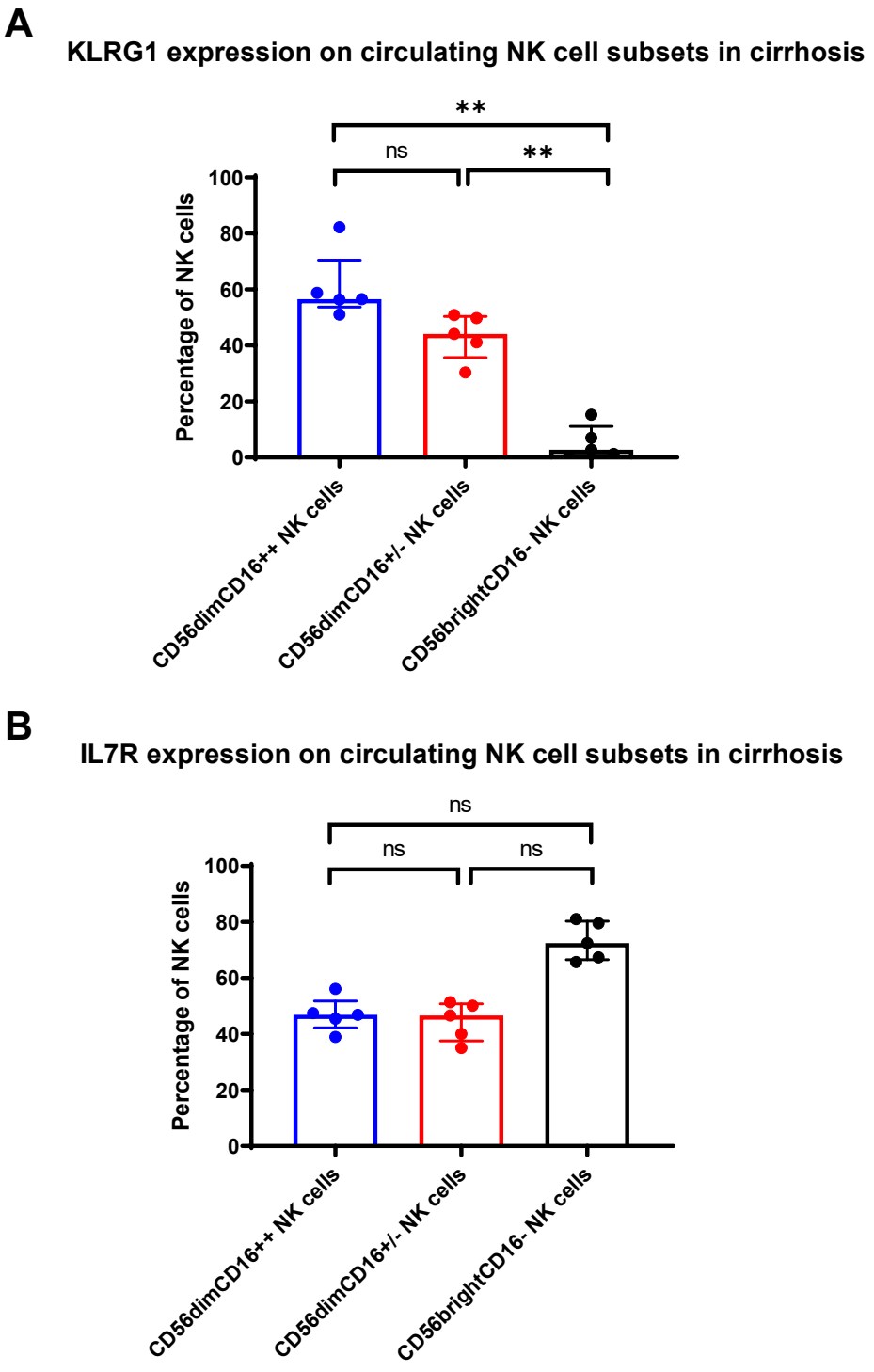


Figure 125 KLRG1 and IL7R expression in NK cell subsets defined by CD56 and CD16 expression in the circulation in cirrhosis. KLRG1 (graph A) and IL7R (graph B) expression in circulating NK cells in cirrhosis is demonstrated on NK cell subsets. (Graphs display individual values with the median value displayed by the bar. Comparisons between groups have been made using the paired Wilcoxon test between the same donors. Error bars represent the interquartile range.

*P values are denoted on the figures as follows: * p<0.05, ** p<0.01, *** p<0.001, **** p<0.0001).*

The proportion of CD56dimCD56+/- expressing CD57 was lower than CD56dimCD16++ NK cells, but not as low as CD56brightCD16- NK cells (Figure 122). However, the intermediate expression of IL7R seen at gene expression level, was not seen at protein expression level in cirrhosis (Figure 125). There may be a reduced proportion of CD56dimCD16+/- expressing KLRG1 (associated with terminal maturity), but this did not reach significance.

As expected, there was a significantly increased proportion of CD56brightCD16- NK cells expressing markers associated with less mature cells (IL7R, NKG2A, TCF1) and a reduced proportion expressing markers associated with terminal differentiation (CD57, KLRG1) (Figures 123-126).

The gene expression data suggested an intermediate expression of the *TCF7* gene (encoding the TCF1 transcription factor) in CD56dimCD16+/- NK cells in cirrhosis and HCC, with the highest expression in CD56brightCD16- NK cells and the lowest in CD56dimCD16++ NK cells. However, intracellular staining for TCF1 revealed that the CD56dimCD16+/- NK cells actually had lower levels of expression than CD56dimCD16++ NK cells (Figure 126).

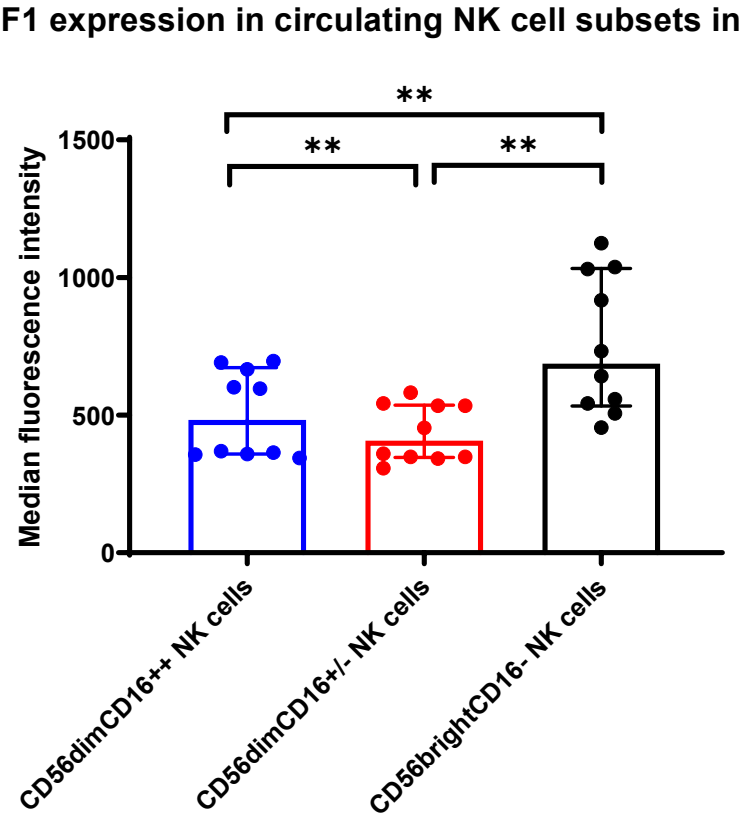


*Figure 126 TCF1 expression in NK cell subsets defined by CD56 and CD16 expression in the circulation in cirrhosis. (Graphs display individual values with the median value displayed by the bar. Comparisons between groups have been made using the paired Wilcoxon test between the same donors. Error bars represent the interquartile range. P values are denoted on the figures as follows: * p<0.05, ** p<0.01, *** p<0.001, **** p<0.0001).*

In summary, CD56dimCD16+/- NK cells did not have an intermediate immature phenotype as suggested by the gene expression data with regards to IL7R and TCF1 expression, but there was an intermediate expression of markers associated with terminal differentiation i.e. KLRG1 and CD57.

4.2.6 Effector function in circulating CD56dimCD16+/- NK cells in cirrhosis

4.2.6.1 Perforin and Granzyme B production

Ex-vivo intracellular staining for perforin and granzyme B was undertaken in patients with cirrhosis (n=10) using the Perforin and Granzyme B functional panel as described in methods (Chapter 2, Table 4 for panel details; Figure 127 for gating strategy; Table 14 for patient characteristics for samples used in this experiment). This demonstrated reduced perforin within and granzyme B in CD56dimCD16+/- NK cells compared to CD56dimCD16++ NK cells (Figure 128), supporting the gene expression data.

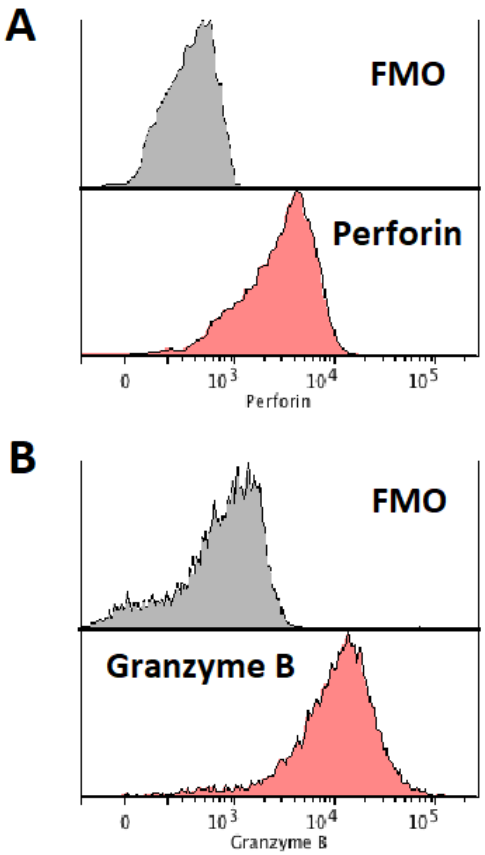


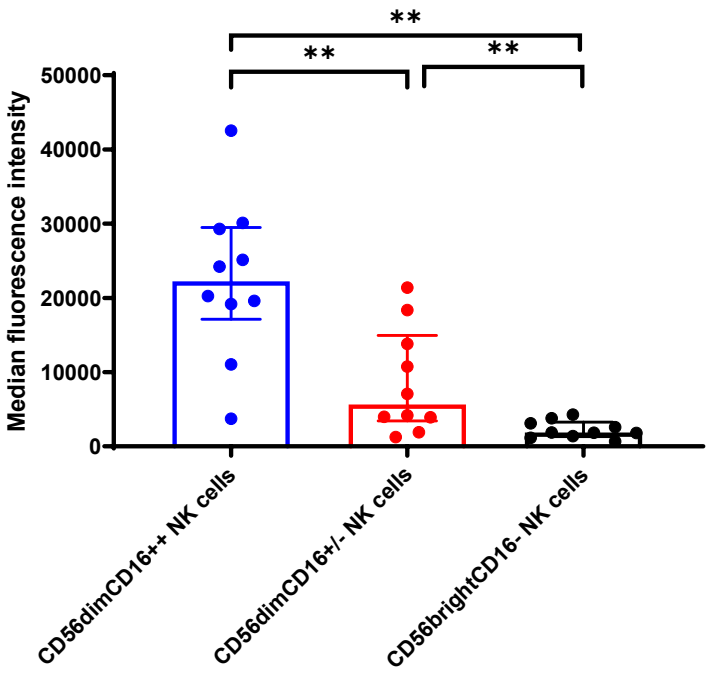
Figure 127 Gating strategy for Perforin and Granzyme B. NK cells were stained with functional Perforin and Granzyme B Panel as described in methods (Table 4). Following gating for NK cells (lymphocyte gating, live singlet cells, CD3 negative cells, CD56positive cells), NK cell subsets (CD56dimCD16++, CD56dimCD16+/- and CD56brightCD16- cells) were identified as described

in methods. Subsequent gating was applied as above, using fluorescence minus one (FMO) controls to subtract any background staining. Plot A demonstrates Perforin staining with a corresponding sample demonstrating the FMO control. Plot B demonstrates Granzyme B staining with the FMO control. The median fluorescence intensity was measured after subtracting the FMO control.

Table 14 Characteristics of patients with cirrhosis from whom peripheral blood samples were used to determine the ex-vivo perforin and granzyme B content.

	Perforin	**Granzyme B**
Total number of patients	10	10
Age, years mean, (range)	56 (33-74)	56 (33-74)
Male n	8	8
Child-Pugh (CP) Score:		
CPA, n	4	4
CPB, n	3	3
CPC, n	3	3
MELD-Na score mean, (range)	11 (7 – 18)	11 (7 – 18)
Aetiology:		
ALD, n	7	7
MASLD, n	3	3

A



B

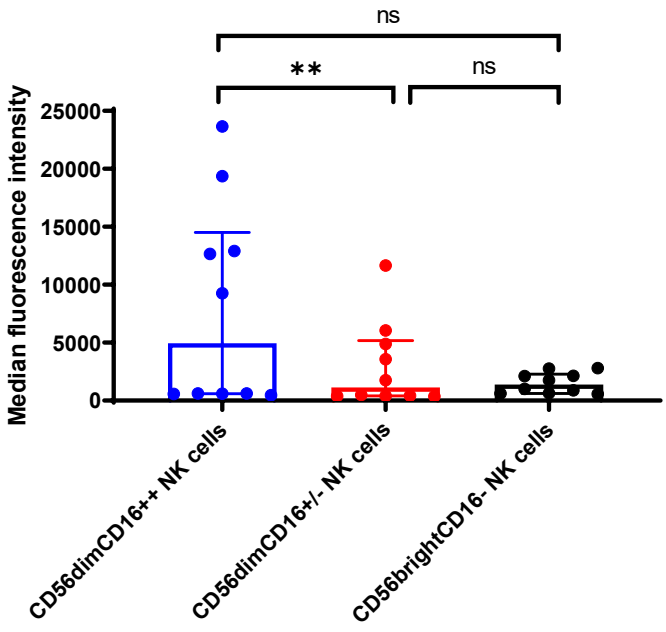


Figure 128 Perforin and Granzyme B within in NK cell subsets defined by CD56 and CD16 expression in the circulation in cirrhosis. Perforin (graph A) and Granzyme B (graph B) expression in circulating NK cells in cirrhosis. (Graphs display individual values with the median value displayed by the bar. Comparisons between groups have been made using the paired

*Wilcoxon test between the same donors. Error bars represent the interquartile range. P values are denoted on the figures as follows: * p<0.05, ** p<0.01, *** p<0.001, **** p<0.0001).*

4.2.6.2 Cytokine secretion

Peripheral blood mononuclear cells from patients with cirrhosis (n=3) were sorted into NK cell subpopulations based on CD56 and CD16 expression as demonstrated in Chapter 2, Figure 3. All patients had ALD cirrhosis with Child-Pugh A status. The isolated NK cell subpopulations were then stimulated with PMA and ionomycin in duplicates for four hours as described in the methods. The supernatants were then collected and cytokine secretion assessed using a multiplex cytokine detection system (V-plex Proinflammatory Panel 1 kit, MSD). Stimulation with PMA/ionomycin revealed a reduced capacity for CD56dimCD16+/- NK cells to produce interferon gamma and tumour necrosis factor alpha in comparison to CD56dimCD16++ NK cells and CD56brightCD16- NK cells (Figure 129 for interferon gamma and tumour necrosis factor alpha production; see Appendix 8.6 for full cytokine panel results).

Cytokine production following stimulation with PMA/Ionomycin in NK cell subsets

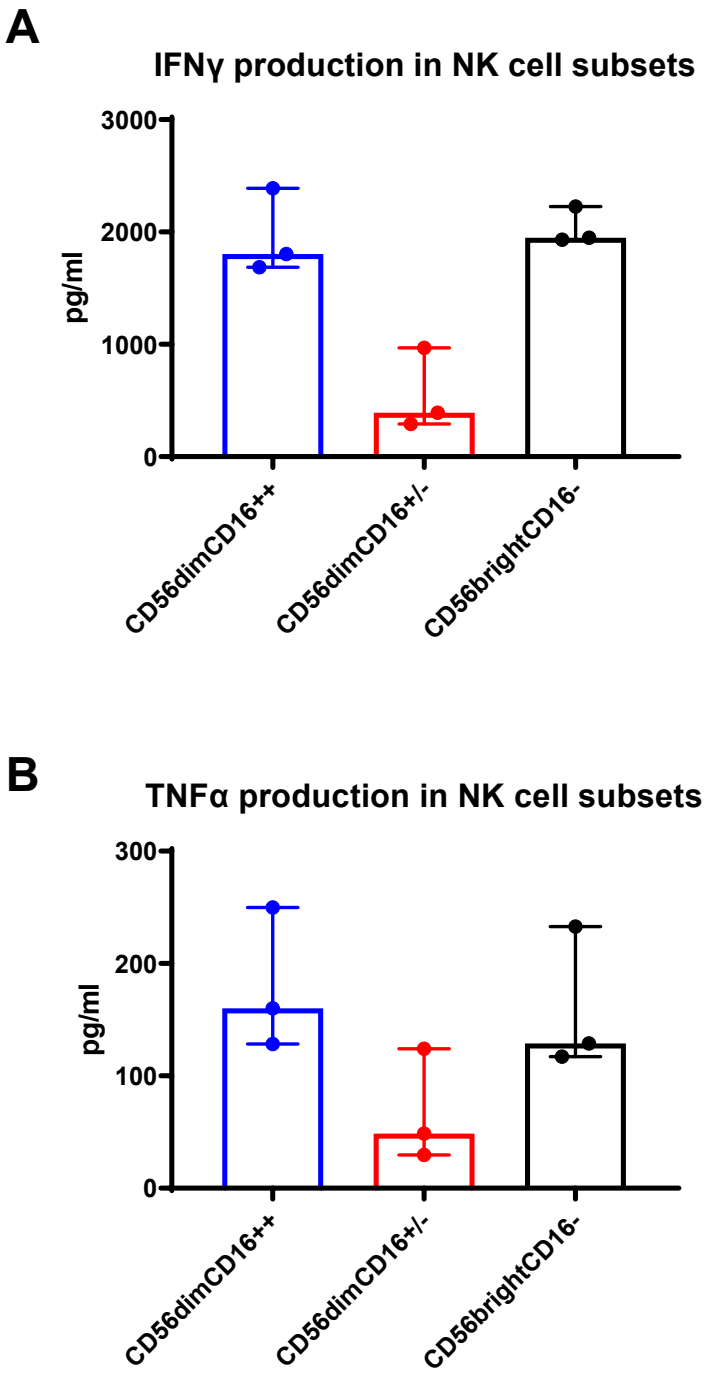


Figure 129 Cytokine expression in isolated sorted NK cells. Circulating NK cells from each donor with cirrhosis secondary to Alcohol related liver disease (ALD cirrhosis, Child-Pugh score A, n=3) were sorted into NK cell subsets by CD56 and CD16 expression following phenotyping (using Phenotyping Panel 1 described in Table 3) and using the gating strategy demonstrated in

Figure 3. These isolated NK cell subsets were stimulated with PMA (50ng/ml) and ionomycin (500ng/ml) in duplicates for four hours. Cytokine expression was read using a V-plex pro-inflammatory panel 1 MSD plate (n=3 samples run in duplicates, data points represent an average reading of the duplicates; IFN = interferon; TNF= tumour necrosis factor). Comparisons were made using the paired Wilcoxon test. Graphs display individual values with the median value displayed by the bar. Error bars represent the interquartile range

4.2.6.3 Degranulation against K562 target cells

Peripheral blood mononuclear cells from patients with ALD cirrhosis (n=3) (all with Child-Pugh A cirrhosis) were sorted into NK cell subpopulations based on CD56 and CD16 expression as demonstrated in Chapter 2, Figure 3. Isolated NK cell subpopulations were incubated for 12 hours with IL15 (1ng/ml) and then co-cultured for 4 hours in fresh complete media with K562 target cells in a 1:1 ratio. CD107a expression following this was determined using flow cytometry. Comparisons were made between CD56dimCD16+/- NK cells and CD56dimCD16++ NK cells as the functional deficits described in Chapter 3 in cirrhosis lay within the CD56dim subpopulation of NK cells. Interestingly, CD56dimCD16+/- NK cells demonstrated a preserved CD107a expression in response to K562 cells when compared to CD56dimCD16++ NK cells (Figure 130).

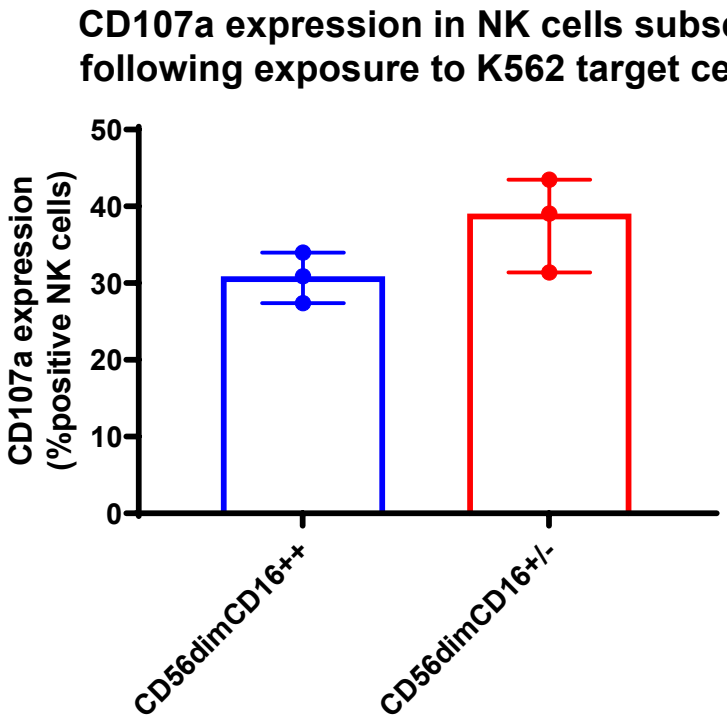


Figure 130 CD107a expression on pre-sorted NK cell subsets from patients with cirrhosis following incubation with K562 target cells. Circulating NK cells from each donor with ALD cirrhosis (Child-Pugh score A, n=3) were sorted into NK cell subsets by CD56 and CD16 expression following phenotyping (using Phenotyping Panel 1 described in Table 3) and using

the gating strategy demonstrated in Figure 3. These isolated NK cells were incubated for 12 hours with IL-15 (1ng/ml) and then co-cultured for 4 hours in fresh R10 media supplemented with 1µl APC-H7-CD107a antibody (eBioscience™, Thermofisher Scientific) per million cells with K562 target cells in a 1:1 ratio. CD107a expression was then measured using flow cytometry. Comparisons between subsets between the same donors was performed using the paired non-parametric Wilcoxon test. Graphs display individual values with the median value displayed by the bar. Error bars represent the interquartile range.

In summary, these functional experiments reveal a preserved cytotoxic capacity of CD56dimCD16+/- in terms of degranulation, but a reduced perforin content and hypofunctionality in terms of pro-inflammatory cytokine production.

4.3 Induction of the CD56dimCD16+/- NK cell subpopulation

To summarise, surface receptor expression in CD56dimCD16+/- NK cells demonstrated reduced DNAM-1 and NKp46 expression but increased CXCR6 and CCR5 expression compared to CD56dimCD16++ NK cells. Although CD161 was increased on circulating NK cells in cirrhosis compared to healthy volunteers, there was a reduced proportion of CD56dimCD16+/- CD161+ NK cells compared to CD56dimCD16++ NK cells. Gene enrichment analysis demonstrated an increase in the expression of HLA-DR, which can be seen in activated NK cells.

The following experiments were undertaken to determine the conditions that may cause an induction of this circulating CD56dimCD16+/- NK cell subset in patients with cirrhosis.

4.3.1 Culture of healthy PBMCs in media supplemented with sera

To determine if circulating CD56dimCD16+/- NK cells arise secondary to factors in the sera, PBMCs from a healthy donor was co-cultured for 24 and 48 hours with diluted sera (25% sera, 75% media supplemented with 1% penicillin/streptomycin) from patients with cirrhosis (n=6, Child-Pugh A cirrhosis with ALD) and other healthy

volunteers (n=4). Incubation in sera from patients with cirrhosis did not result in an increase in the CD56dimCD16+/- NK cell proportion (Figure 131).

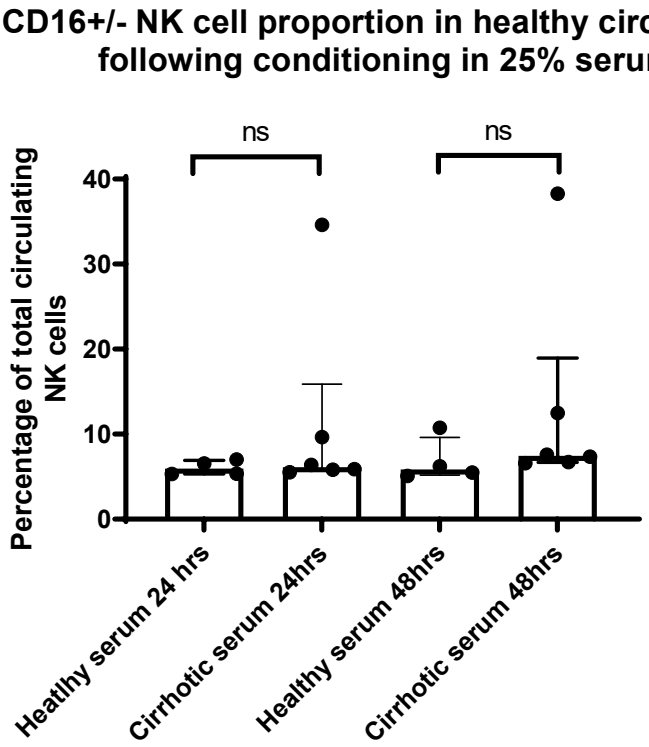


Figure 131 CD56dimCD16+/- NK cells as a proportion of all circulating NK cells following incubation with sera from healthy donors and patients. Peripheral blood mononuclear cells from a healthy donor were incubated in media supplemented with 25% healthy sera (n=4 healthy donors) or 25% sera from patients with cirrhosis secondary to alcohol related liver disease (n=6 patients). Comparisons between healthy and cirrhosis groups at 24hours of incubation and 48hours of incubation were made using Mann-Whitney tests. There were no significant differences. Further paired analyses using the Wilcoxon test were made for samples incubated in the same patient sera for 24hours and 48hours but again was not significant. Error bars represent the interquartile range. Graphs display individual values with the median value displayed by the bar.

4.3.2 Post-activation profile following incubation with K562 target cells

NK cell activation results in a reduced expression of surface CD16 on activated NK cells via a process known as ectodomain shedding (Romee et al., 2013). The following experiments were therefore undertaken to deduce if the expression profile of the resulting post-activation CD56dimCD16+/- population was similar to that seen in circulating NK cells in patients with cirrhosis.

Incubation of PBMCs with K562 target cells, for 4 hours resulted in an increase in CD56dimCD16+/- NK cells and a concomitant decrease in CD56dimCD16++ NK cells (Figures 132 and 133). However, the proportion of CD56dimCD16+/- NK cells following exposure to K562 target cells was lower in cirrhosis and HCC compared to healthy donors (Figure 134).

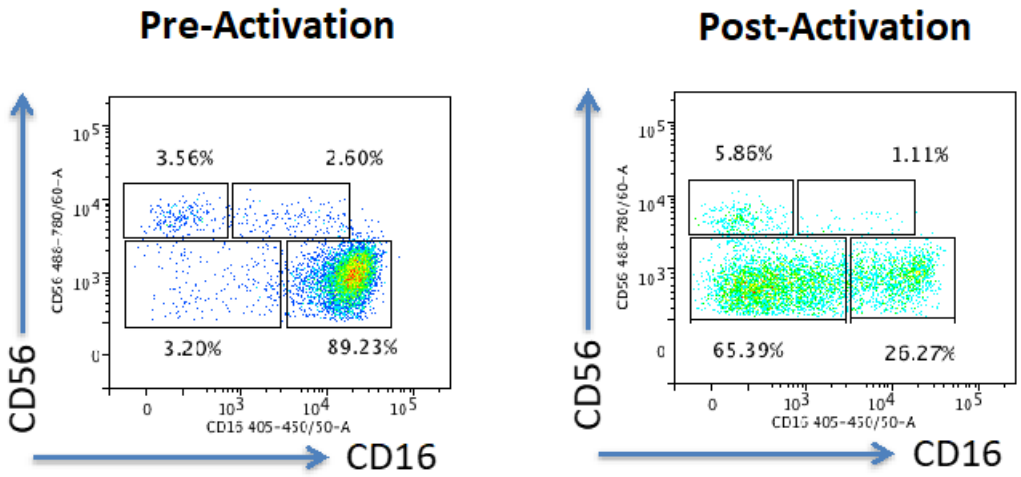


Figure 132 CD56 and CD16 expression on NK cells ex-vivo prior to incubation with K562 target cells (Pre-Activation profile, graph on left) and following incubation with K562 target cells (Post-Activation profile. Graph on right). Peripheral blood mononuclear cells from healthy donors were phenotyped using panel 1 (see Chapter 2 Methods, Table 3) prior to and following a 4 hour incubation with K562 target cells. Phenotyping revealed an increase in the CD56dimCD16+/- NK cell subset in the post-activation profile following the 4 hour incubation (graph on right).

CD56dimCD16+/- NK cells are increased in proportion following activation

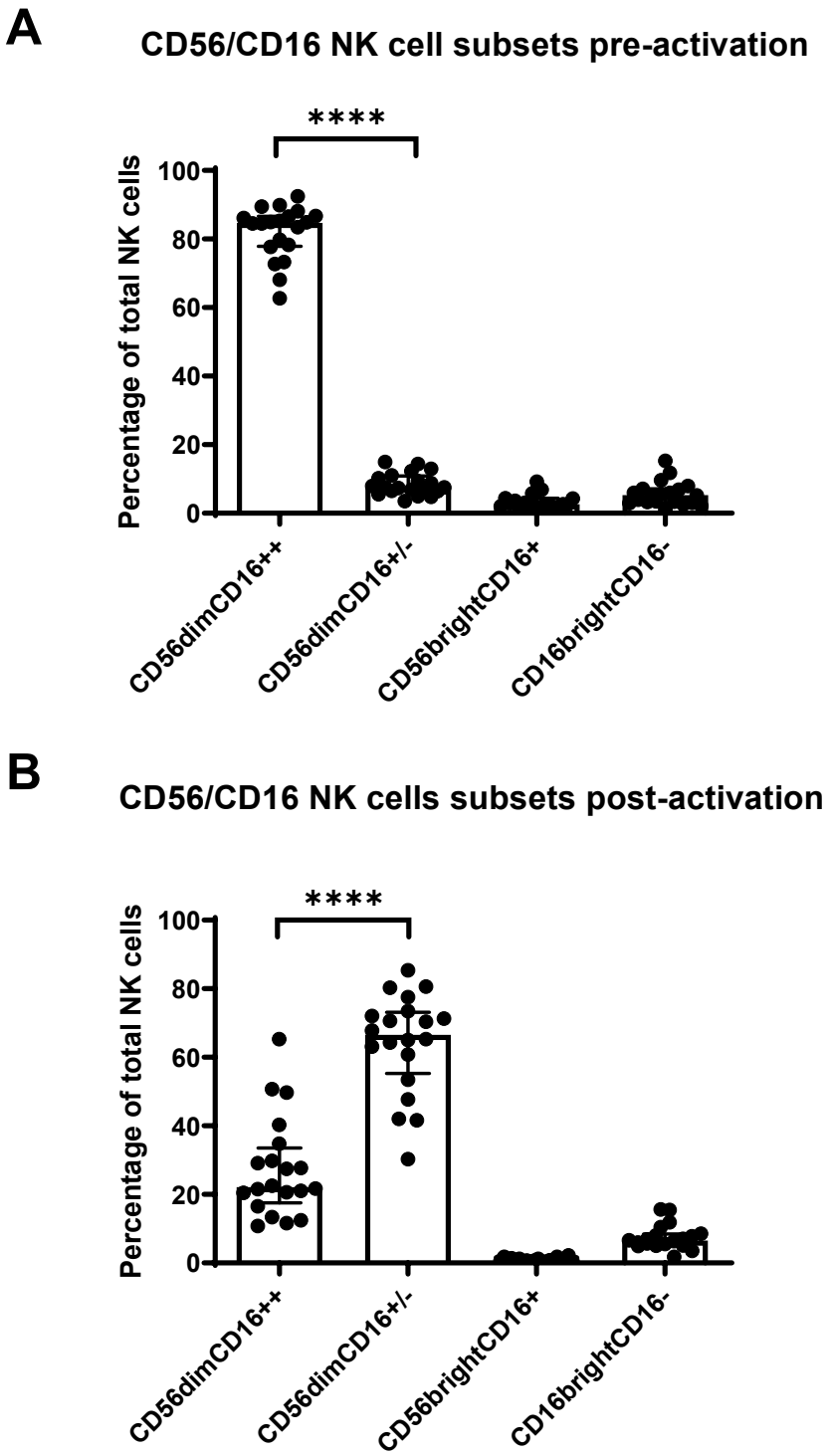


Figure 133 CD56dimCD16+/- NK cells are increased in proportion following activation. Peripheral blood mononuclear cells from healthy donors (n=20) were phenotyped using panel 1 (see Chapter 2 Methods, Table 3) prior to and following a 4 hour incubation with K562 target

*cells. Graph A demonstrated the NK cell subsets based on CD56 and CD16 expression (as described in Figure 3). Phenotyping following a 4 hour incubation revealed an increase in the CD56dimCD16+/- NK cell subset in the post-activation profile (Graph B). Comparisons between the same donors was undertaken using the Wilcoxon test. Graphs display individual values with the median value displayed by the bar. Error bars represent the interquartile range. P values are denoted on the figures as follows: * p<0.05, ** p<0.01, *** p<0.001, **** p<0.0001).*

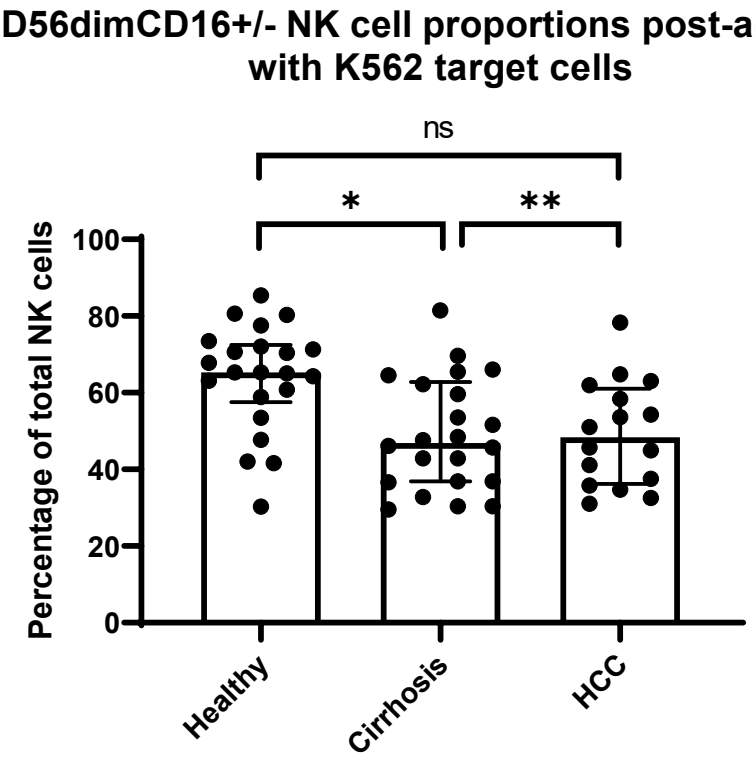


Figure 134 CD56dimCD16+/- NK cell proportions post-activation with K562 target cells. Peripheral blood mononuclear cells (PBMCs) from healthy donors (n=22), patients with cirrhosis (n=22) and patients with hepatocellular carcinoma (HCC, n=16) were co-cultured for 4 hours with K562 target cells as described in methods (all patient characteristics are described in Chapter 3, Table 10). Following this, the PBMCs were phenotyped using Phenotype Panel 1 (as described in Methods, Chapter 2, Table 3) to determine the post-activation NK cell CD56 and CD16 expression and the proportions of each CD56/CD16 NK cell subset as defined by the gating strategy described in Figure 3. The post-activation proportion of CD56dimCD16+/- NK cells in cirrhosis and HCC was lower than in healthy volunteers. Comparisons between groups was undertaken using the Mann-Whitney test. Graphs display individual values with the

*median value displayed by the bar. Error bars represent the interquartile range. P values are denoted on the figures as follows: * p<0.05, ** p<0.01, *** p<0.001, **** p<0.0001 (see Table 9 for patient demographics).*

Expression levels of DNAM-1, CXCR6 and CD161 were determined using flow cytometry on healthy NK cells following incubation with K562 cells for 4 hours. Comparisons were made between the ex vivo phenotyping profile and the post activation phenotyping profile following co-culture with K562 target cells (Figure 135).

Co-culture with K562 target cells for 4 hours resulted in a reduction in CXCR6 expression in CD56brightCD16- NK cells, but no significant difference or increase in CXCR6 in the resulting CD56dimCD16+/- NK cells compared to CD56dimCD16++ NK cells (Figure 135A).

The post activation phenotype of DNAM-1 on NK cell subsets did not demonstrate a significant difference (Figure 135C).

The post activation CD161 expression profile revealed a reduction of CD161 expression on the CD56dimCD16+/- NK cells in comparison to CD56dimCD16++ NK cells (Figure 135B).

In summary, though the 4 hour post activation phenotype does induce the CD56dimCD16+/- NK cell subpopulation, with similar expression profiles for CD161 as seen in cirrhosis, DNAM-1 expression was not significantly altered. However, it also resulted in a reduction of CXCR6 expression which was not in keeping with previous findings of CXCR6 expression on circulating CD56dimCD16+/- NK cells in cirrhosis.

To determine if the phenotypic changes seen in circulatory NK cells in cirrhosis are secondary to prolonged activation, NK cells were incubated for 48hours with K562 target cells and then phenotyped for the expression profiles of CXCR6, CD161 and DNAM-1 on NK cell subsets (Figure 136).

Receptor expression in the induced CD56dimCD16+/- NK cell subset following 4 hour co-culture with K562 cells

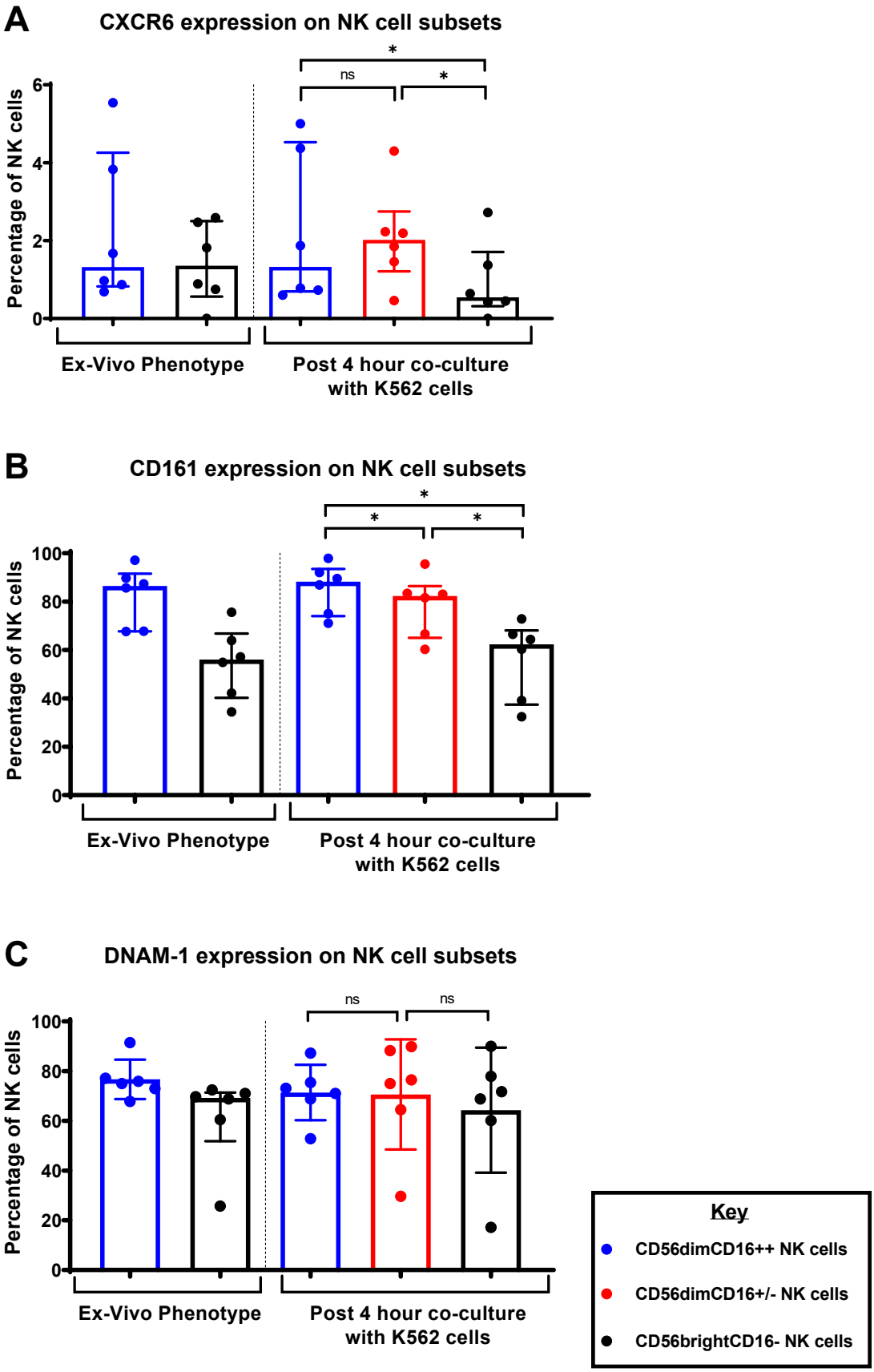


*Figure 135 Receptor expression on the induced CD56dimCD16+/- NK cell subset following a 4 hour co-culture with K562 target cells. Peripheral blood mononuclear cells (PBMCs) from healthy volunteers (n=6) were thawed from frozen. Baseline phenotyping using Phenotyping panel 1 (as described in methods, table 3) was undertaken on each sample to determine the ex-vivo phenotype. Remaining unstained PBMCs from each donor were cultured in complete R10 media supplemented with IL15 (1ng/ml) for 12 hours. Following this, PBMCs were washed, resuspended in fresh complete R10 media and co-cultured with K562 target cells for 4 hours as outlined in the methods. Surface expression of CXCR6 (Graph A), CD161 (Graph B), DNAM-1 (Graph C) was determined using flow cytometry following staining with Phenotyping Panel 1 (as described in methods, table 3).(Wilcoxon matched-pairs signed rank test used to make comparisons). Data in blue demonstrates the proportion of positive CD56dimCD16++ NK cells. Data in red demonstrates the proportion of positive CD56dimCD16+/- NK cells. Data in black demonstrates the proportion of positive CD56brightCD16- NK cells. (Graphs display individual values with the median value displayed by the bar. Comparisons between groups have been made using the paired Wilcoxon test between the same donors. Error bars represent the interquartile range. P values are denoted on the figures as follows: * p<0.05, ** p<0.01, *** p<0.001, **** p<0.0001).*

Following a 48hour incubation with K562 cells, CXCR6 expression was increased on the resulting CD56dimCD16+/- in comparison to CD56dimCD16++ NK cells, but this did not reach significance (Figure 136A). CD161 expression was also reduced in the CD56dimCD16+/- fraction (Figure 136B) but differences in DNAM-1 expression did not reach significance (Figure 136C).

Receptor expression in the induced CD56dimCD16+/- NK cell subset following 48 hour co-culture with K562 cells

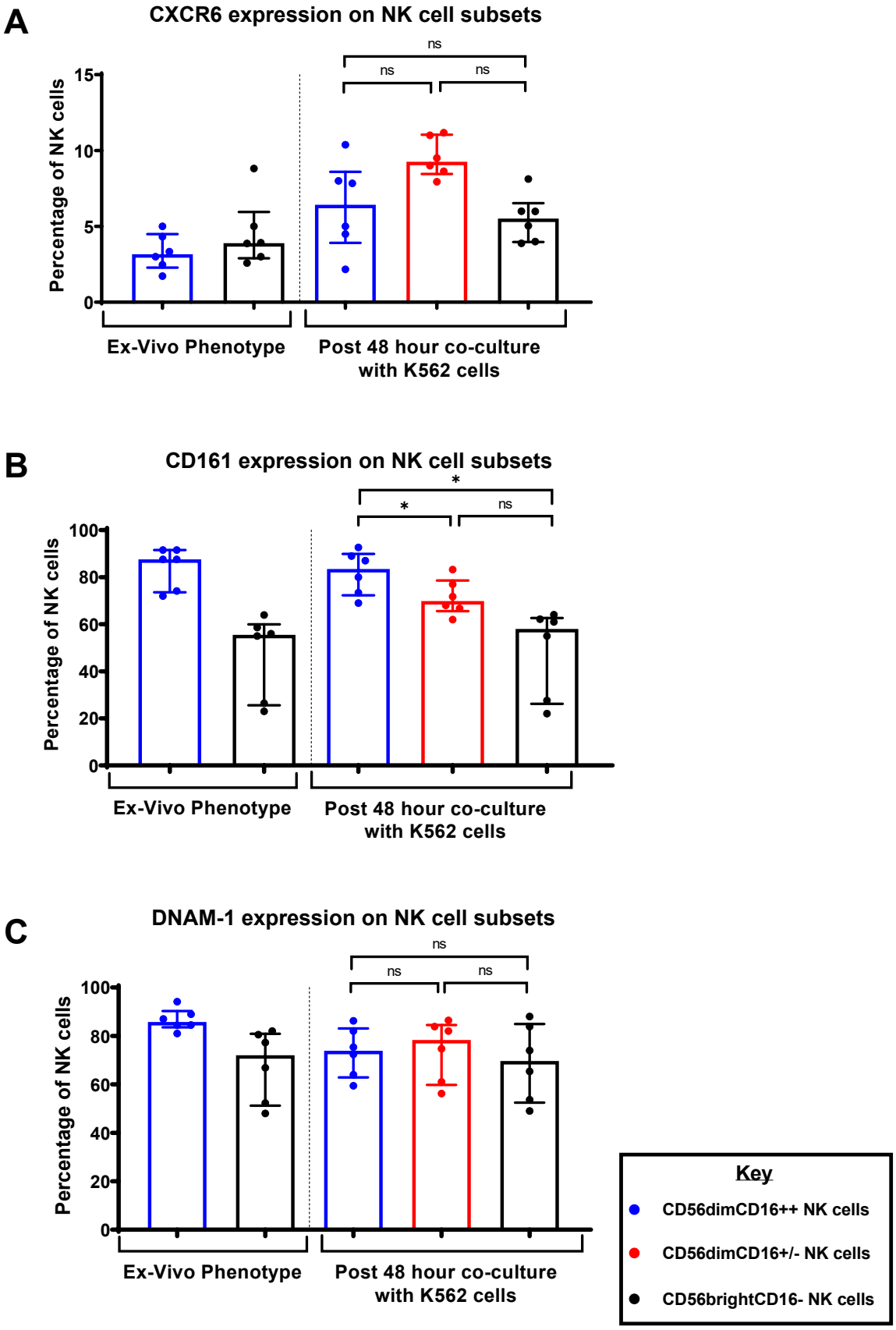


*Figure 136 Receptor expression on the induced CD56dimCD16+/- NK cell subset following a 48 hour co-culture with K562 target cells. Peripheral blood mononuclear cells (PBMCs) from healthy volunteers (n=6) were thawed from frozen. Baseline phenotyping using Phenotyping panel 1 (as described in methods, table 3) was undertaken on each sample to determine the ex-vivo phenotype. Remaining unstained PBMCs from each donor were cultured in complete R10 media supplemented with IL15 (1ng/ml) for 12 hours. Following this, PBMCs were washed, resuspended in fresh complete R10 media and co-cultured with K562 target cells for 48 hours as outlined in the methods. Surface expression of CXCR6 (Graph A), CD161 (Graph B), DNAM-1 (Graph C) was determined using flow cytometry following staining with Phenotyping Panel 1 (as described in methods, table 3).(Wilcoxon matched-pairs signed rank test used to make comparisons). Data in blue demonstrates the proportion of positive CD56dimCD16++ NK cells. Data in red demonstrates the proportion of positive CD56dimCD16+/- NK cells. Data in black demonstrates the proportion of positive CD56brightCD16- NK cells. (Graphs display individual values with the median value displayed by the bar. Comparisons between groups have been made using the paired Wilcoxon test between the same donors. Error bars represent the interquartile range. P values are denoted on the figures as follows: * p<0.05, ** p<0.01, *** p<0.001, **** p<0.0001).*

4.3.3 Post-activation phenotype following co-culture with Huh7 cells

To determine if the CD56dimCD16+/- NK cells profile seen in patients with cirrhosis could be induced following exposure to diseased hepatocytes, the following experiments were conducted using Huh7 cells as target cells.

Peripheral circulating mononuclear cells (PBMCs) from healthy donors (n=13) were incubated with Huh 7 cells under the following conditions for 48 hours, as described in the methods: direct incubation with Huh7 cells (PBMCs incubated within the same well as Huh7 cells); indirect incubation with Huh7 cells (PBMCs plated on top of a porous membrane placed above the Huh7 cells, allowing free flow of media within the well but prohibiting cell to cell contact); direct incubation with heat damaged Huh7 cells (Huh7 cells suspended in media and heated for 1 minute in a waterbath at 70°C and then plated in wells with the same media). All Huh7 cells were plated and left to rest overnight at 37°C, before adding PBMCs, in a 1:5 ratio (Huh7:PBMCs) as described in the methods.

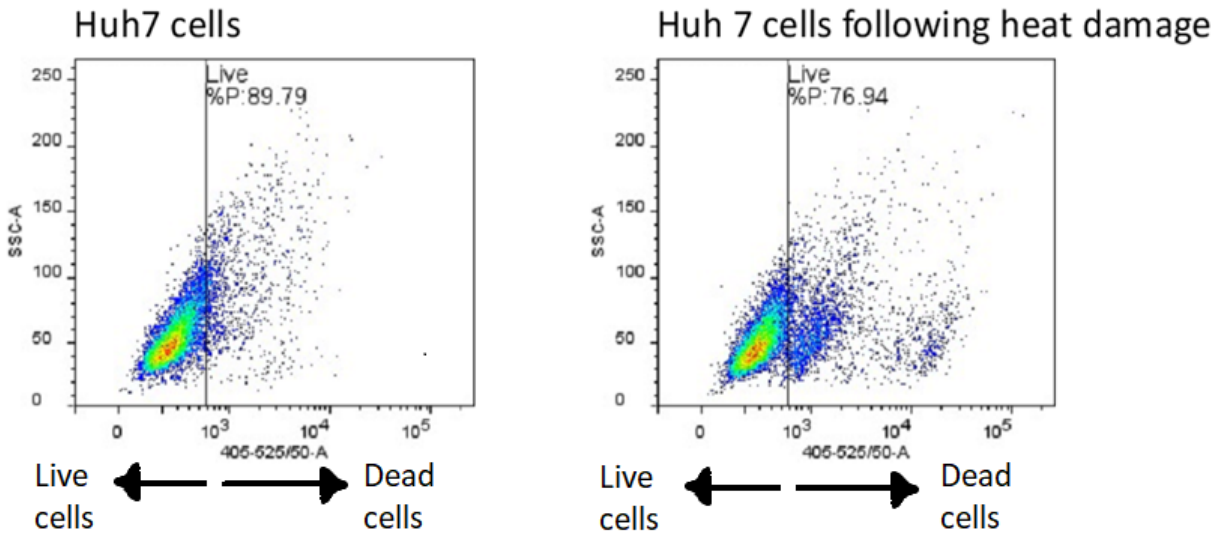


Figure 137 Huh7 cells with or without heat damage. Huh 7 cells were suspended in media and placed in a waterbath at 70℃ for 1 minute. They were then stained with a live/dead surface amine binding fluorescent dye and compared to Huh7 cells that had not undergone heat treatment. The above plots demonstrate a lower proportion of live Huh7 cells following heat damage. Heat damage Huh7 cells were resuspended in the same media within which they were exposed to the heat damage and plated into 24 well plates.

There was a significant increase in the CD56dimCD16+/- NK cell subpopulation following co-culture with heat damaged Huh7 cells (Figure 138). Incubation with Huh7 cells under all conditions resulted in a significant upregulation in CXCR6 (Figure 139) and a downregulation in CD161 as seen on circulating CD56dimCD16+/- NK cells in cirrhosis (Figure 140). However, only the co-culture with heat damaged Huh7 cells also resulted in a CD56dimCD16+/- NK cell subpopulation with a significant reduction in DNAM-1 expression in comparison to CD56dimCD16++ NK cells (Figure 141).

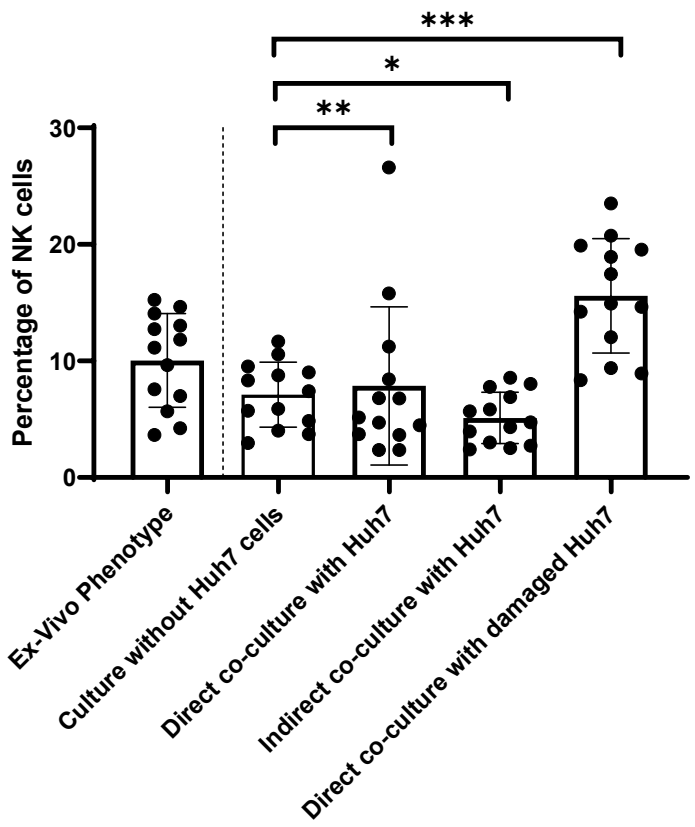


*Figure 138 Post activation phenotype in healthy peripheral blood NK cells incubated with Huh7 cells for 48 hours. Peripheral blood mononuclear cells (PBMCs) from healthy volunteers (n=13) were thawed from frozen. Baseline phenotyping using Phenotyping panel 1 (see methods, Table 3) was undertaken on each sample to determine the ex-vivo phenotype. Remaining unstained PBMCs from each donor were cultured in complete R10 media supplemented with IL15 (1ng/ml) for 12 hours. Following this, PBMCs were washed, resuspended in fresh complete R10 media and co-cultured with pre-plated Huh7 target cells for 48 hours as outlined in the methods, with one sample from each donor being cultured in complete R10 media without Huh7 target cells. Following 48hours of culture, PBMCs were stained with Phenotyping Panel 1 (Table 3) and the proportion of CD56dimCD16+/- NK cells was determined using flow cytometry. The CD56dimCD16+/- NK cell proportion within the PBMCs cultured without Huh7 cells was compared to the proportion of CD56dimCD16+/- NK cells after a 48 hour co-culture in direct contact with live or heat-damaged Huh7 cells, or co-cultured in the same well as Huh7 cells but separated by a barrier (indirect co-culture). Comparisons were made using the paired Wilcoxon test between the same donors. Graphs display individual values with the median value displayed by the bar. Error bars represent the interquartile range. P values are denoted on the figures as follows: * p<0.05, ** p<0.01, *** p<0.001, **** p<0.0001).*

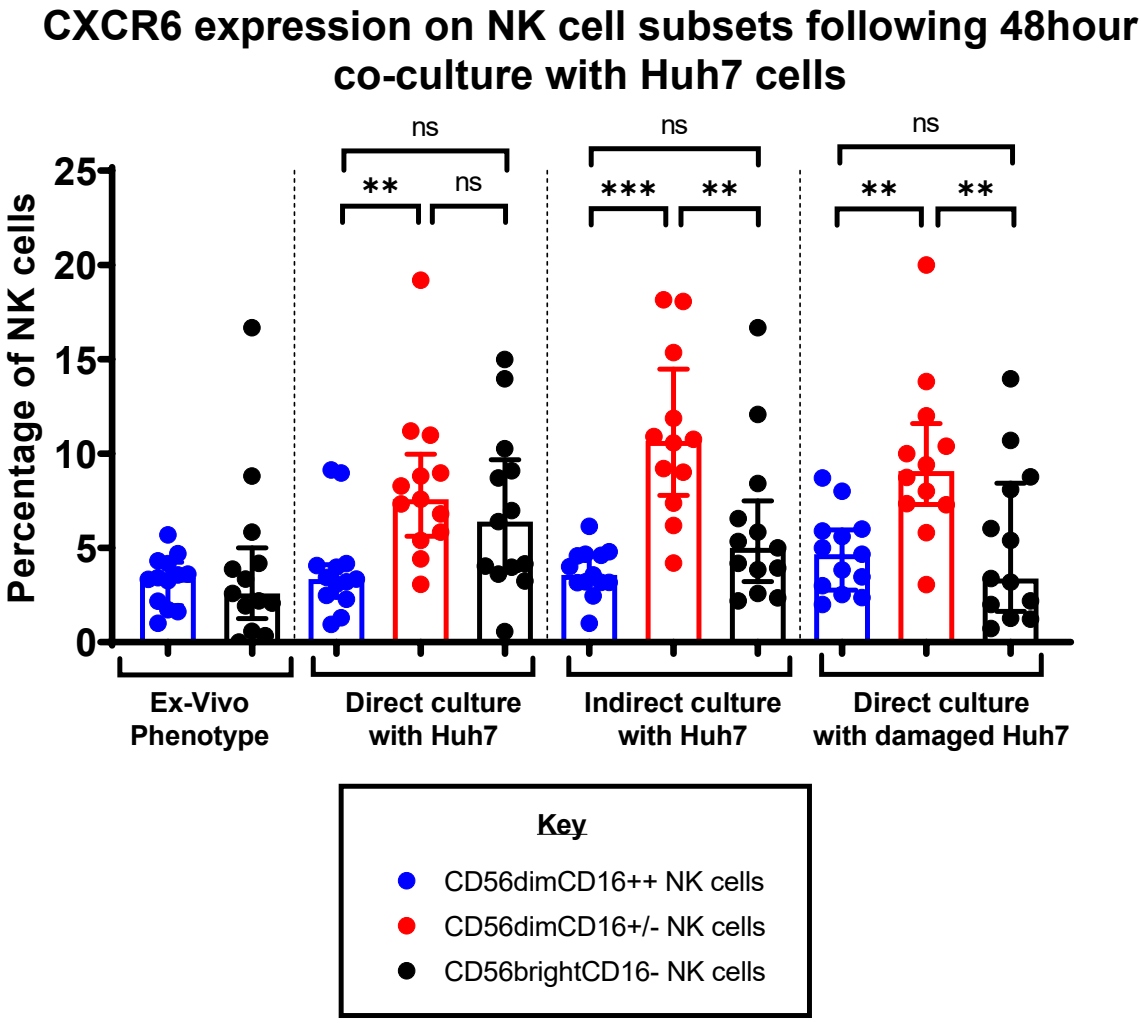


Figure 139 CXCR6 expression on NK cell subsets following 48hour co-culture with Huh7 cells. Peripheral blood mononuclear cells (PBMCs) from healthy volunteers (n=13) were thawed from frozen. Baseline phenotyping using Phenotyping panel 1 (as described in methods, table 3) was undertaken on each sample to determine the ex-vivo phenotype. Remaining unstained PBMCs from each donor were cultured in complete R10 media supplemented with IL15 (1ng/ml) for 12 hours. Following this, PBMCs were washed, resuspended in fresh complete R10 media and co-cultured with pre-plated Huh7 target cells in a 5:1 ratio for 48 hours as follows: Direct culture with Huh7 (PBMCs incubated within the same well as Huh7 cells); Indirect culture with Huh7 (PBMCs plated on top of a porous membrane placed above Huh7 cells, allowing free flow of media within the well but prohibiting cell to cell contact); Direct culture with damaged Huh7 (Huh7 cells suspended in media, heated for 1 minute in a waterbath at 70℃ and then plated in wells with the same media). Following 48hours, PBMCs were stained with Phenotyping panel 1 (as described in methods, table 3) and CXCR6 expression determined using flow

*cytometry. CXCR6 expression on each NK cell subset for each condition was compared using the paired Wilcoxon test between the same donors. Graphs display individual values with the median value displayed by the bar. Error bars represent the interquartile range. P values are denoted on the figures as follows: * p<0.05, ** p<0.01, *** p<0.001, **** p<0.0001).*

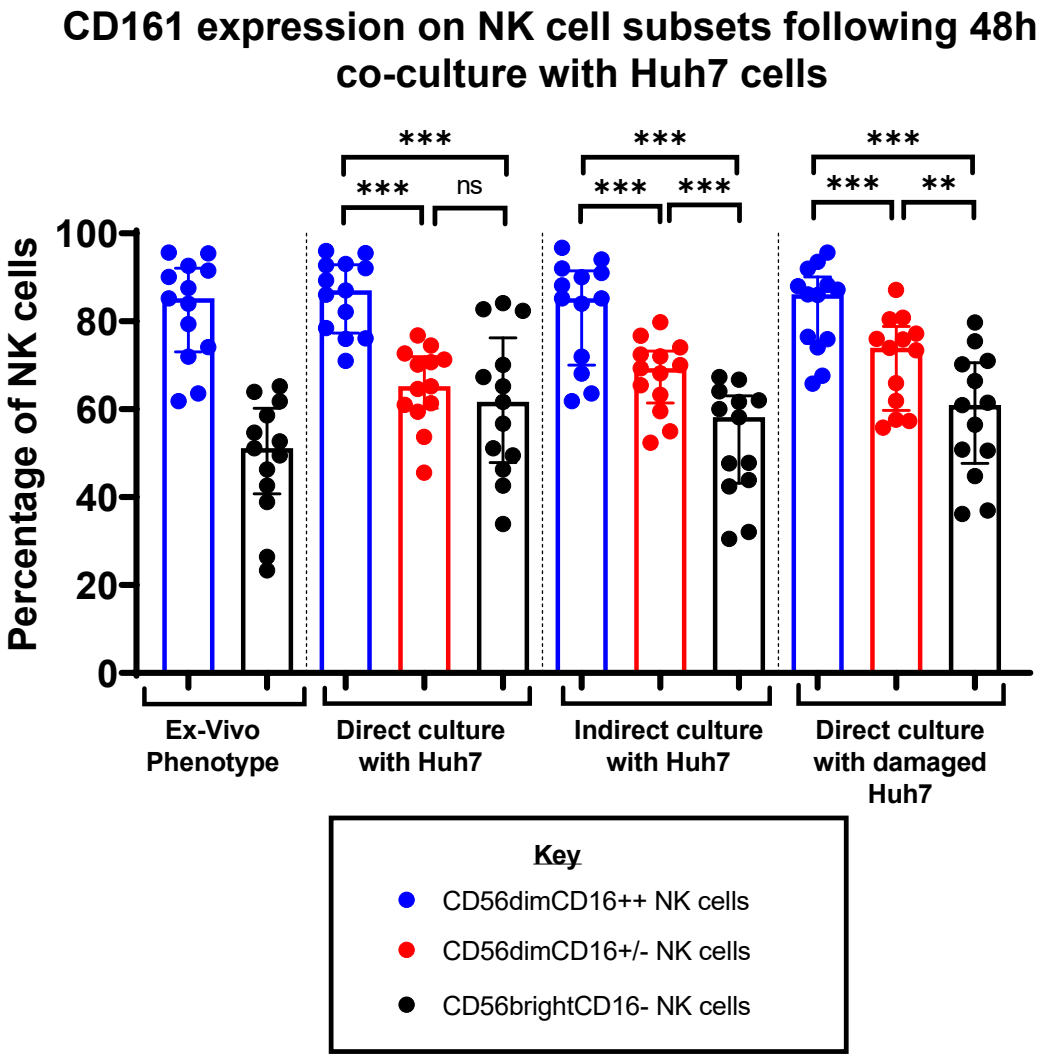


Figure 140 CD161 expression on NK cell subsets following 48hour co-culture with Huh7 cells. Peripheral blood mononuclear cells (PBMCs) from healthy volunteers (n=13) were thawed from frozen. Baseline phenotyping using Phenotyping panel 1 (as described in methods, table 3) was undertaken on each sample to determine the ex-vivo phenotype. Remaining unstained PBMCs from each donor were cultured in complete R10 media supplemented with IL15 (1ng/ml) for 12 hours. Following this, PBMCs were washed, resuspended in fresh complete R10 media and co-cultured with pre-plated Huh7 target cells in a 5:1 ratio for 48 hours as follows: Direct culture with Huh7 (PBMCs incubated within the same well as Huh7 cells); Indirect culture with Huh7 (PBMCs plated on top of a porous membrane placed above Huh7 cells, allowing free flow of media within the well but prohibiting cell to cell contact); Direct culture with damaged Huh7 (Huh7 cells suspended in media, heated for 1 minute in a waterbath at 70℃ and then plated in wells with the same media). Following 48hours, PBMCs were stained with Phenotyping panel 1 (as described in methods, table 3) and CD161 expression determined using flow

*cytometry. CXCR6 expression on each NK cell subset for each condition was compared using the paired Wilcoxon test between the same donors. Graphs display individual values with the median value displayed by the bar. Error bars represent the interquartile range. P values are denoted on the figures as follows: * p<0.05, ** p<0.01, *** p<0.001, **** p<0.0001).*

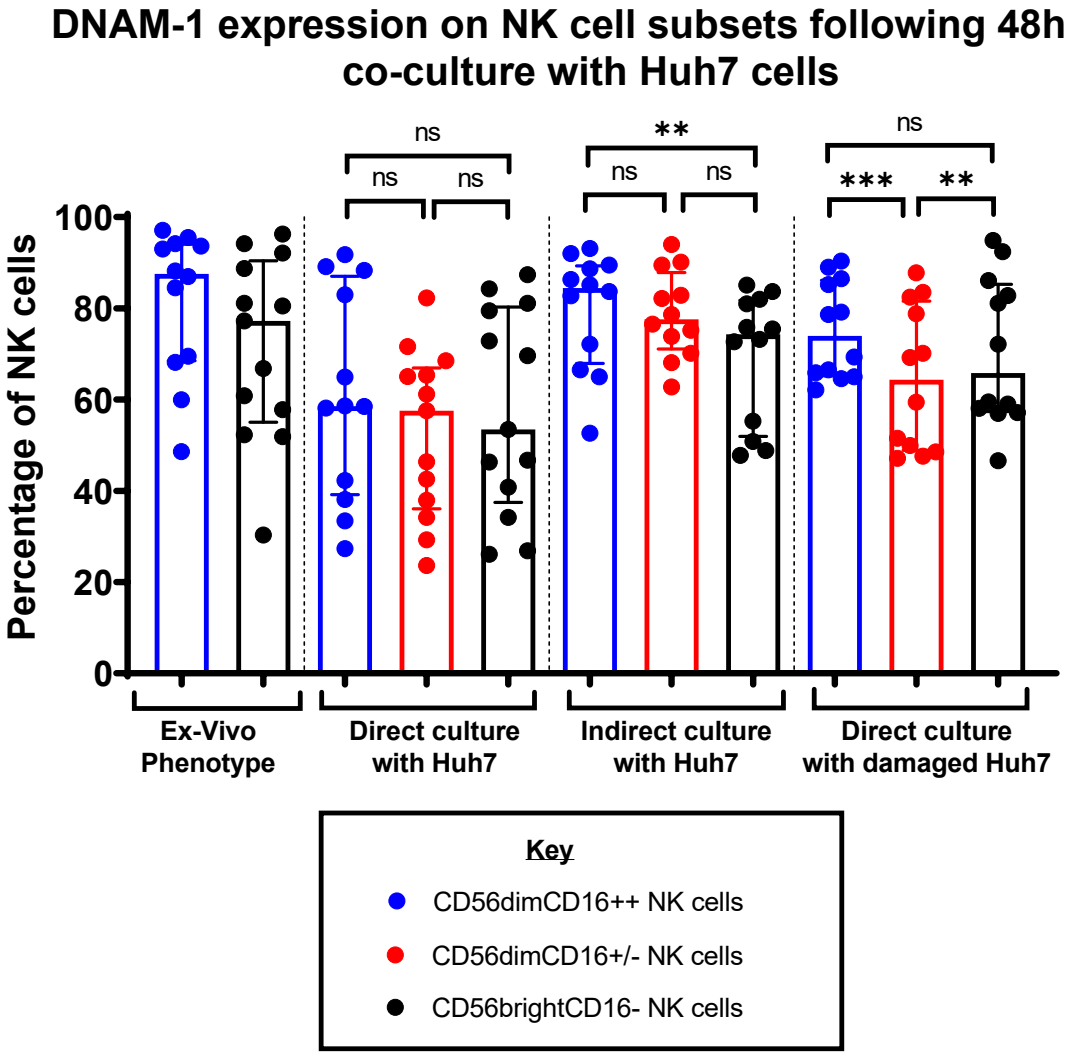


Figure 141 DNAM-1 expression on NK cell subsets following 48hour co-culture with Huh7 cells. Peripheral blood mononuclear cells (PBMCs) from healthy volunteers (n=13) were thawed from frozen. Baseline phenotyping using Phenotyping panel 1 (as described in methods, table 3) was undertaken on each sample to determine the ex-vivo phenotype. Remaining unstained PBMCs from each donor were cultured in complete R10 media supplemented with IL15 (1ng/ml) for 12 hours. Following this, PBMCs were washed, resuspended in fresh complete R10 media and co-cultured with pre-plated Huh7 target cells in a 5:1 ratio for 48 hours as follows: Direct culture with Huh7 (PBMCs incubated within the same well as Huh7 cells); Indirect culture with Huh7 (PBMCs plated on top of a porous membrane placed above Huh7 cells, allowing free flow of media within the well but prohibiting cell to cell contact); Direct culture with damaged Huh7 (Huh7 cells suspended in media, heated for 1 minute in a waterbath at 70℃ and then plated in wells with the same media). Following 48hours, PBMCs were stained with Phenotyping panel 1 (as described in methods, table 3) and CD161 expression determined using flow

*cytometry. DNAM-1 expression on each NK cell subset for each condition was compared using the paired Wilcoxon test between the same donors. Graphs display individual values with the median value displayed by the bar. Error bars represent the interquartile range. P values are denoted on the figures as follows: * p<0.05, ** p<0.01, *** p<0.001, **** p<0.0001).*

In summary, prolonged co-culture with damaged Huh7 cells reproduced the phenotype of the CD56dimCD16+/- NK cell subpopulation as seen in patients with cirrhosis: an increased CD56dimcD16+/- NK cell subset with reduced DNAM1 expression, reduced CD161 expression and increased CXCR6 expression.

4.4 Discussion

Using a number of different techniques, I have identified and characterised a CD56dimCD16+/- NK cell subpopulation that is expanded in patients with cirrhosis and persists in some patients with HCC.

Surface and gene expression profiles revealed a reduction in expression of some activating receptors, including DNAM-1, but an increase in CD160 (results summarised in Table 15 below). Furthermore, there was an altered inhibitory receptor profile, with reduced CD161 expression on CD56dimCD16+/- NK cells although there is an overall increased expression of CD161 on all subsets in cirrhosis in comparison to healthy controls. There was also an intermediate expression with regards to genes related to immaturity (*IL7R, TCF7*) but this was not supported by analysis of protein expression using flow cytometry. However, there was a lower protein expression of CD57 (associated with terminal maturation) in comparison to the mature CD56dimCD16++ NK cell subset.

KLRG1 has been described as a marker of terminal differentiation in T cells. KLRG1 has also been associated with murine NK cell exhaustion in association with a downregulation of NKG2D (Alvarez et al., 2019). Furthermore, Elpek et al describe mature NK cells with increased KLRG1 expression following prolonged activation with IL-15, that demonstrate a reduced functional capacity and reduced DNAM-1 expression (Elpek et al., 2010). Whilst KLRG1 is expressed on the CD56dimCD16+/- NK cell subset, with a downregulation in DNAM-1 expression, the CD56dimCD16++ NK cell subset also expresses KLRG1 expression in cirrhosis and does not demonstrate a downregulation in NKG2D. KLRG1 has also been described as an inhibitory receptor on NK cells upon interacting with the ligand E-cadherin that is expressed on K562 cells, and a potential checkpoint target for blockade in cancer therapy (Gründemann et al., 2010; Tata et al., 2021). Thus, expression of KLRG1 on CD56dim NK cells in cirrhosis may also explain some of the functional deficit seen against K562 cells in these experiments.

Table 15 Summary of phenotypic and functional characteristics of the CD56dimCD16+/- NK cell subpopulation in cirrhosis comparison to classical NK cell subpopulations (CD56dimCD16++ and CD56brightCD16- NK cells).

	CD56dimCD16++	*CD56dimCD16+/-*	*CD56brightCD16-*
Activating Receptors	↑ DNAM-1 ↑ NKp46 ↑↑ CD16	↓ DNAM-1 ↓ NKp46 ± CD16	↓ DNAM-1 ↑NKp46 - CD16
Inhibitory receptors	↑ CD161 ↑↑ KLRG1	↔ CD161 ↑ KLRG1 ↑ CD74 ↑ LAIR1	↓ CD161 ↓ KLRG1
Intrahepatic NK cell markers	↓ CXCR6 ↓ CCR5	↑ CXCR6 ↑ CCR5	↑ CXCR6 ↑ CCR5
Maturity markers	↓ IL7R ↑↑ CD57	↓ IL7R ↑ CD57	↑↑IL7R - CD57
Functional status	↑ Granzyme B ↑Perforin	↓ Granzyme B ↓ Perforin	↓ Granzyme B ↓ Perforin
Markers of Activation		↑↑ HLA-DR	

The CD56dimCD16+/- NK cell subpopulation demonstrates an altered functional capacity compared to other NK cell subsets, with reduced IFNγ and TNFα production but preserved degranulation as demonstrated by CD107a expression in comparison to CD56dimCD16++ NK cells in response to K562 target cells. However, perforin and granzyme B expression within

CD56dimCD16+/- NK cells is lower than CD56dimCD16++ NK cells, and a reduced expression of surface CD16 implies a reduced capacity for antibody dependent cell mediated cytotoxicity (ADCC).

NK cell polarisation towards cytotoxicity with reduced capacity for interferon production has been described in the context of chronic hepatitis C infection (Ahlenstiel et al., 2010). Ahlenstiel et al describe this NK cell subpopulation as expressing increased levels NKG2C, which is not seen in the CD56dimCD16+/- NK cell population described here. However, whilst the NK cell subpopulations may be different phenotypically, the functionally preserved cytotoxicity with reduce cytokine capacity is similar. Gene enrichment analysis further demonstrated reduced activity in DAP12 signalling in CD56dimCD16+/- NK cells in comparison to CD56dimCD16++ NK cells, indicating a reduced capacity for activation. This may explain the functional deficit seen in the CD56dim NK cells in cirrhosis. Furthermore, gene enrichment analysis demonstrated enrichment in the MHC class II presentation pathway, with HLA-DR genes upregulated on CD56dimCD16+/- NK cells. HLA-DR expression has been characterised following activation of NK cells, and hence further experiments were undertaken to see if the CD56dimCD16+/- NK cell subset may be a circulating activated NK cell subset.

Prolonged co-culture of peripheral blood mononuclear cells, from healthy donors, with Huh7 cells that had been damaged, releasing damage-associated molecular patterns (DAMPs), resulted in an increased proportion of CD56dimCD16+/- NK cells with a similar phenotypic profile to those found in the circulation of patients with cirrhosis. A higher proportion of circulating CD56dimCD16+/- NK cells also expressed CXCR6 and CCR5 in comparison to CD56dimCD16++ NK cells in cirrhosis, both surface receptors associated with liver homing and liver resident NK cells(Hudspeth et al., 2016; Stegmann et al., 2016). Furthermore, a small but significant proportion of circulating CD56dimCD16+/- NK cells were $Tbet^{lo}EOMES^{hi}$, characteristic of liver resident NK cells (Stegmann et al., 2016).

It is difficult to infer from this data whether the CD56dimCD16+/- subpopulation arises in the circulation after exposure to DAMPs released into the circulation following damage to the liver, or whether the subpopulation arises as a result of passage through the inflamed liver and activation following cell to cell contact. Along with apoptotic cell death, hepatocyte necrosis and the release of DAMPs has been described in ALD and MASLD (Albillos et al., 2014; Mihm, 2018). DAMPs released locally and may activate circulating NK cells via the hepatic lymph nodes but DAMPs have also been detected in the circulation, for example, keratin 18, expressed by hepatocytes, can be found in the circulation following hepatic necrosis in alcohol related liver disease (Albillos et al., 2014; Mihm, 2018). Therefore, exposure to DAMPs in the circulation could explain the CD56dimCD16+/- NK cell profile seen in patients with cirrhosis. Furthermore, NK cells have been postulated to be retained within sinusoids following engagement of CXCR6 and CCR5, and therefore do not re-enter the circulation (Hudspeth et al., 2016). However, this was determined using healthy liver tissue, and it is not clear if liver damage and disease progression would result in a release of NK sinusoidal cells into the circulation. Indeed, a combination of these processes may explain the heterogeneity of this NK cell subpopulation. It would be interesting to study NK cell subpopulations in patients with cirrhosis undergoing liver surgery to see if the release of DAMPs in that scenario does indeed increase the circulating CD56dimCD16+/- NK subpopulation. Furthermore, gene expression and pathway analysis predicted that exposure of NK cells to TGF beta, a cytokine found in abundance in cirrhosis and the pathogenesis of fibrosis, may account for the differential gene expression seen in CD56dimCD16+/- NK cells in comparison to CD56dimCD16++ NK cells.

The effect of pathogen associated molecular patterns (PAMPs) on NK cells was not evaluated here. PAMPs have been well documented in cirrhosis, due to an increased gut permeability (‘leaky gut’) resulting in increased pathogen exposure in the liver as well as in the circulation (Albillos et al., 2014). The ability of NK cells to alter immune responses after direct recognition of bacterial and viral PAMPs has been demonstrated (Oth et al., 2018), and it would be worth investigating if recurrent or persistent exposure of NK cells to PAMPs could also contribute to the NK cell phenotype documented here.

NK cell activation has been associated with a reduction in the surface expression of CD16. A disintegrin and metalloprotease-17 (ADAM17) expressed in NK cells results in shedding of CD16 following NK cell activation (Romee et al., 2013). However, inhibition of ADAM17 did not result in a reduction in the capacity of NK cells to produce cytokines but actually enhanced interferon gamma production when CD16 was crosslinked (Romee et al., 2013). Interestingly, IL-1beta stimulation results in an increase in EGR1 expression via ADAM17 (Sanchez-Guerrero et al., 2012). Furthermore, increased levels of ADAM17 and EGR1 expression were associated with an increased expression of proinflammatory cytokines (Junbing He et al., 2022). CD56dimCD16++ NK cells demonstrate a lower *EGR1* expression in cirrhosis at the gene level, as demonstrated in chapter 3. This reduction in *EGR1* expression may therefore account for the reduced *IFNG* and *TNF* gene expression in cirrhosis compared to healthy NK cells as demonstrated in Chapter 3. Furthermore, whilst loss of CD16 and hence an increase in the CD56dimCD16+/- NK cell proportion after exposure to K562 targets was found, there was a lower proportion of CD56dimCD16+/- NK cells following exposure to K562 target cells in cirrhosis and HCC in comparison to healthy volunteers, along with an attenuated degranulation and interferon gamma response. It would be interesting to evaluate ADAM17 protein expression in NK cells in cirrhosis, specifically in the CD56dimCD16++ and CD56dimCD16+/- NK cell subpopulations in cirrhosis and healthy volunteers to determine if ADAM17 is depleted in CD56dimCD16++ NK cells and if inhibition of ADAM17 could restore CD16 expression in the CD56dimCD16+/- NK cell subpopulation in cirrhosis.

Whether the CD56dimCD16+/- NK cell subpopulation is harmful or beneficial in cirrhosis and HCC remains to be determined. It is important to note that the CD56dimCD16+/- NK cell subpopulation was increased in the majority of patients with cirrhosis. However, there was a significant proportion of patients with HCC on a background of cirrhosis who had reduced levels of circulating CD56dimCD16+/- NK cells (Chapter 3, Figure 41A). The proportion of CD56dimCD16+/- NK cells in HCC did not appear to correlate with aetiology or composite scores or BCLC staging (though BCLC staging was underpowered to detect significant differences). Further longitudinal studies following patients with cirrhosis who go on to develop HCC would be useful to delineate the true function of the CD56dimCD16+/- NK cell subpopulation.

5. Chapter 5: LLT1 expression in the liver and interaction with CD161+ NK cells

5.1 Introduction

CD161+ NK cells are increased in proportion in the circulation in cirrhosis as demonstrated in chapter 3. CD161 is a C-type lectin receptor expressed on the majority of NK cells(Aldemir et al., 2005; Kamishikiryo et al., 2011; Lanier et al., 1994; D. B. Rosen et al., 2005). CD161+NK cells have been demonstrated to have an increased capacity to secrete IFNγ in response to IL-12 and IL-18 stimulation, an increased proliferative capacity and may play a pro-inflammatory role(Kurioka et al., 2018). However, engagement of CD161 results in inhibition of NK cell cytotoxicity and IFNγ production(D. B. Rosen et al., 2008). The CLEC2D gene produces several isoforms, but it is only the membrane bound C-type lectin receptor, Lectin-like Transcript 1 (LLT1), that is the ligand for CD161(Aldemir et al., 2005; Germain et al., 2010; Kamishikiryo et al., 2011; D. B. Rosen et al., 2005). Reduced CD161 expression on NK cells has been associated with an increased rate of clearance of acute hepatitis C infection(Alter et al., 2011). Engagement of CD161 on NK cells by LLT1 has been demonstrated to reduce cytotoxicity and IFNγ production by NK cells(Germain et al., 2011).

CD161 surface expression is not isolated to NK cells, but can also be found on CD4+ T cells and a subset of CD8+ T cells that home to the liver in disease(Billerbeck et al., 2010; Northfield et al., 2008). The greater proportion (90%) of the CD161++CD8+ T cells are Mucosal Associated Invariant T (MAIT) cells, which possess an invariant T cell receptor (TCR) that recognizes microbial vitamin B metabolites via MHC-like Receptor 1 (MR1)(Dusseaux et al., 2010; Walker et al., 2012). The CD161++CD8+ T cell population also contain the Tc17 cell population, which are enriched in the liver in chronic viral infection and expanded in HCC(Billerbeck et al., 2010; Kuang et al., 2010; Northfield et al., 2008). Though they do not have the Vα7.2 invariant TCR that MAIT cells have, they are phenotypically similar(Fergusson et al., 2014). The functional effects of CD161 engagement on these CD8+ T cells appears to be costimulatory, boosting IFNγ and tumour necrosis factor alpha (TNFα) production on activation via the TCR(Aldemir

et al., 2005; Fergusson et al., 2014; D. B. Rosen et al., 2008). CD4+ T cells have also been identified to express CD161+ and encompass a group termed TH17 cells. These cells are able to secrete IL-17, produce IFNγ in response to activation by IL-23 and have a role in autoimmune conditions(Kleinschek et al., 2009).

The LLT1 receptor is not usually found on circulating lymphocytes, but is expressed upon activation(Germain et al., 2011). Several mechanisms for the induction of LLT1 expression have been identified. Stimulation of dendritic cells with lipopolysaccharide, a toll- like receptor 4 agonist, induced LLT1 expression(Germain et al., 2011). LLT1, when expressed on activated NK cells, can induce IFNγ production, which subsequently further up-regulates LLT1 expression via the ERK signaling pathway(Bambard et al., 2010; P. a Mathew et al., 2004). We have described infection with respiratory syncytial virus induces LLT1 expression on lung epithelium, confirming viral pathogen infection as another mechanism resulting in LLT1 induction(Satkunanathan et al., 2014). Malignancy is another area that LLT1 up-regulation has been demonstrated. LLT1 has been demonstrated as being expressed on prostate and breast tumour tissue(Marrufo et al., 2018; S. O. Mathew et al., 2016). LLT1 expression has also been demonstrated on malignant glioblastoma tissue, and it is suggested that TGF beta may be another mechanism inducing LLT1 expression(Roth et al., 2007). An increase in CLEC2D gene expression has been demonstrated in a mouse liver cancer model(Coulouarn et al., 2011).

Given the increase in CD161 surface receptor expression on circulating NK cells in cirrhosis, as demonstrated in chapter 3, in this chapter I aim to explore the following:

1. Is LLT1, the ligand for CD161, expressed in the liver or in the circulation, and is expression different in healthy and disease states? If LLT1 expression is upregulated in the cirrhotic liver, is it present in non-viral aetiologies or limited to the virally infected liver? What are the underlying mechanisms causing an up regulation in LLT1 expression?
2. Is there an up regulation of T cell subsets expressing CD161 in cirrhosis?
3. What are the functional consequences of the LLT1-CD161 interaction on NK cells?

5.2 LLT1 expression is up-regulated on liver epithelium in cirrhosis and Hepatocellular carcinoma

LLT1 expression on liver tissue was determined by immunohistochemistry on formalin-fixed paraffin embedded liver tissue and findings corroborated utilising quantitative real-time PCR on snap frozen liver tissue.

As LLT1 has been demonstrated to be upregulated on respiratory epithelium in viral infection, liver tissue from patients with or without cirrhosis from underlying previously treated Hepatitis C infection was included as a comparison.

5.2.1 LLT1 expression on liver tissue determined by immunohistochemistry

Structurally normal liver margins from patients undergoing liver resection for indications other than primary liver cancer (i.e. colorectal cancer metastases) were taken as representative of normal liver (n=18). LLT1 expression in normal liver was compared with biopsies demonstrating cirrhosis (n=24), liver resection tumour tissue demonstrating hepatocellular carcinoma (HCC, n=20) and background non-tumour liver tissue taken from the margins of the same resection specimens undertaken for patients with treatment naïve hepatocellular carcinoma (HCC) (n=15 demonstrating background cirrhosis, n=5 not demonstrating background cirrhosis) (Table 16).

Table 16 Demographics and clinical data for patients from whom liver LLT1 expression was determined using immunohistochemistry. ALD = Alcohol related liver disease; MASLD – Metabolic dysfunction-associated steatotic liver disease; HCC = Hepatocellular carcinoma; HCV – Hepatitis C viral infection.

	Normal Liver	**Cirrhotic Liver**	**HCC**
Total	18	24	20
Age, years (range)	64.5 (53-78)	48.2 (29-64)	60.2 (37-72)
Sex (n male/total)	10/18	15/24	16/20
Cirrhosis (n/total)		24/24	15/20
Aetiology:			
Viral (n/total cirrhotic)		16/24	
HCV (n/total cirrhotic)		16/24	6/15
ALD (n/total cirrhotic)		5/24	3/15
MASLD (n/total cirrhotic)		3/24	4/15
ALD + Haemochromatosis (n/total cirrhotic)		0/24	2/15
Vascular invasion (n/total cirrhotic):			10/15
Tumour differentiation:			
Well differentiated (n/total cirrhotic)			0/15
Moderately differentiated (n/total cirrhotic)			11/15
Poorly differentiated (n/total cirrhotic)			4/15
Non-cirrhotic (n/total)		0/24	5/20
Aetiology:			
Viral (n/total non-cirrhotic)			5/5
HCV (n/total non-cirrhotic)			5/5

Normal liver hepatocytes demonstrated a weak homogenous expression of LLT1, with strongly positive staining non-hepatocyte sinusoidal and perisinusoidal cells (Figure 142). Immunohistochemistry for LLT1 expression demonstrated a uniform homogenous up-regulation in hepatocyte expression in cirrhosis in comparison to normal liver tissue, with both cytosolic and membranous staining present (Figure 143B). Immunohistochemistry for LLT1 expression in HCC specimens however, demonstrated variable expression, with some tumour tissue demonstrating up-regulation in comparison to background hepatocytes from

the same patient, and vice versa in other cases (Figure 143C). HCC tumour tissue demonstrated further variability: some tumours demonstrated random patchy expression across the same resection specimen and tissue slide; some demonstrated up-regulation of LLT1 in tumour cells along the invading edge of the tumour and/or within the surrounding background liver tissue; some tumours demonstrating random single positive cells within the tumour. LLT1 expression was also evaluated in cholangiocarcinoma resection specimens in order to determine whether LLT1 expression was up-regulated in other primary liver cancers, but cholangiocarcinoma was negative for LLT1 (Appendix 8.7).

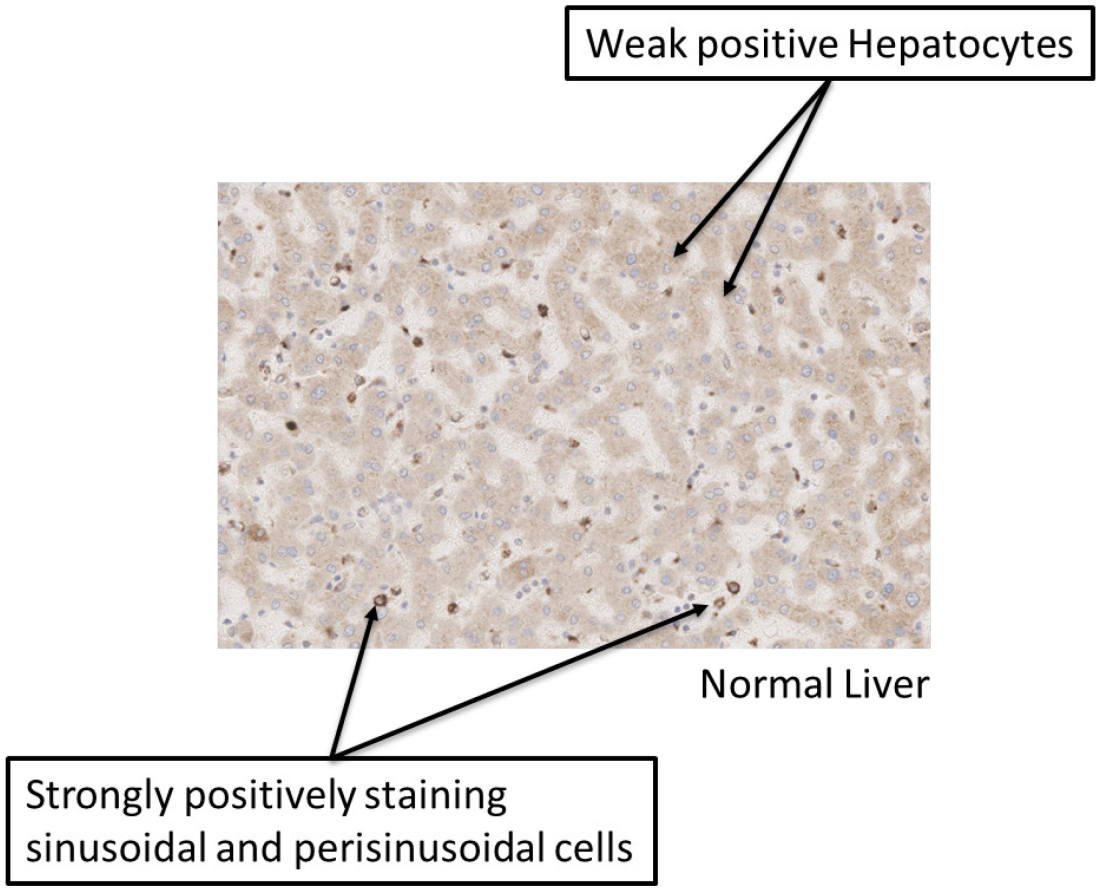


Figure 142 Immunohistochemistry demonstrating LLT1 expression in normal liver. Normal margins from liver resections conducted for non-HCC indications (i.e. liver resections for colorectal metastases) were stained for LLT1 (1:4000 dilution, anti-human CLEC2D mouse monoclonal antibody (Abnova, clone 4C7)). Hepatocytes demonstrate weak positive homogenous staining for LLT1 while sinusoidal and perisinusoidal cells demonstrate strongly positive staining (image displayed at x20 magnification).

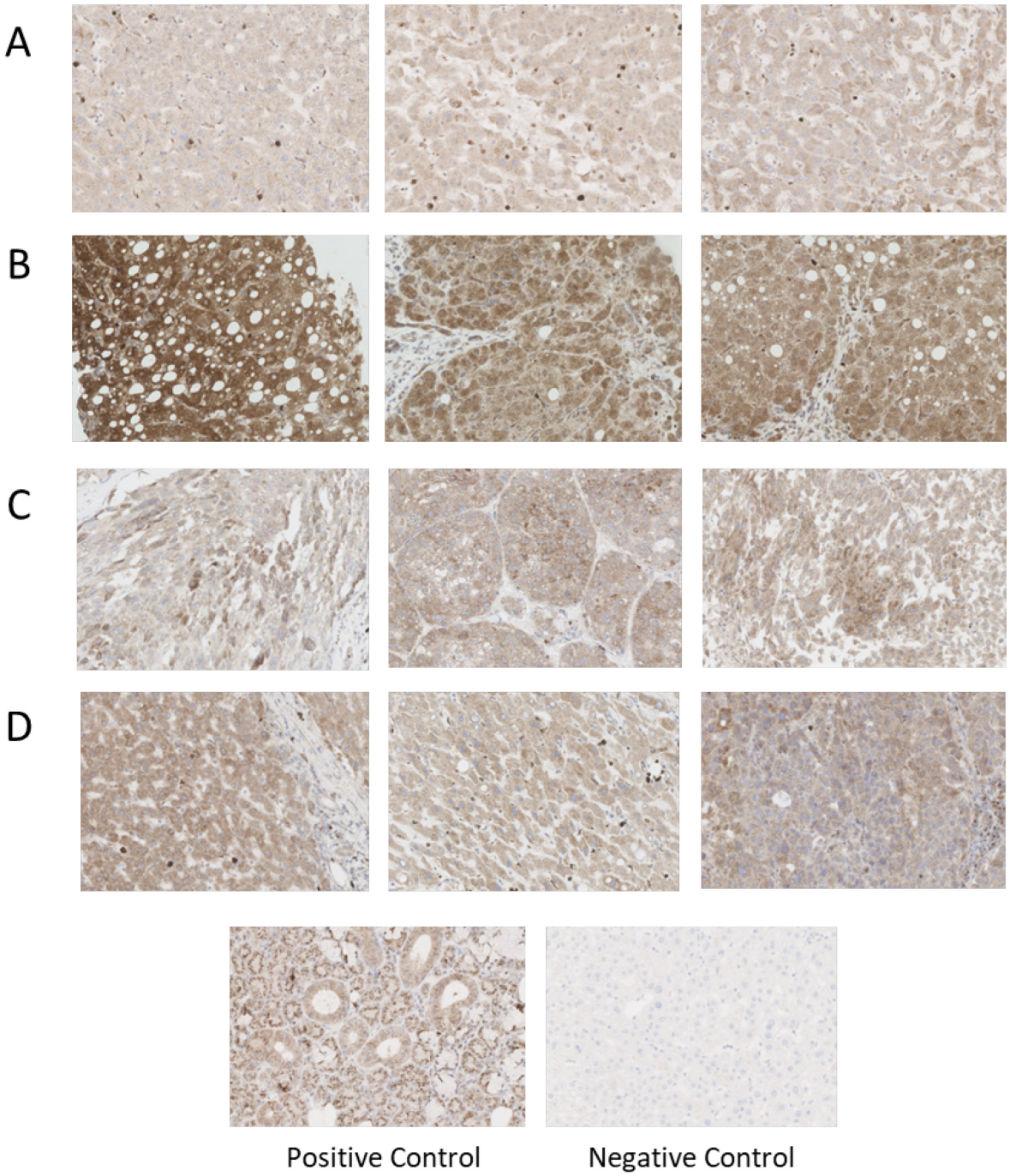


Figure 143 Immunohistochemistry demonstrating LLT1 expression on formalin fixed paraffin embedded (FFPE) liver tissue. Tissue slides at 3µm thickness were prepared from FFPE blocks of liver tissue demonstrating normal liver margins from liver resections undertaken for indications other than primary liver cancer (e.g. colorectal metastases), cirrhotic liver tissue from patients with cirrhosis and without HCC (any aetiology), HCC tumour tissue and HCC non-tumour background liver tissue from the same patients (any aetiology). Tissue slides were stained with LLT1 (1:4000 dilution, anti-human CLEC2D mouse monoclonal antibody (Abnova, clone 4C7)) and haematoxylin. 3 representative images

from different donors are demonstrated here for each tissue type. Images are displayed at x20 magnification. A) Microscopically normal liver tissue from liver resection margins from patients without HCC. B) Cirrhotic liver biopsy tissue from patients without HCC. C) Liver tissue from liver resections for treatment naïve patients with HCC demonstrating tumour tissue, and D) background (non-tumour) cirrhotic liver tissue from liver resections for patients with HCC. E) Positive control (salivary gland tissue). F) Negative control (unstained liver tissue).

To take into account the variability in expression across tumour samples, a weighted scoring system was devised to quantitate LLT1 expression as described in the methods, Chapter 2 (Figure 4 and Table 5). The staining intensity (negative, weak, moderate, strong) was determined against positive and negative control slides for each staining batch, and corresponding contrast levels set using ImageJ 1.48v software. Entire stained slides for each tissue type were scanned and images taken of the entire slide at the same magnification (0.45x) using NDPview v2.4.26. The total area of liver tissue (healthy, cirrhotic, background non-tumour tissue) was outlined and measured using ImageJ. For patients with HCC, the total area of HCC tumour tissue on the slide was outlined and measured using ImageJ. Contrast thresholds for each staining intensity were then applied to the image. The area of tissue corresponding to each staining intensity was measured and calculated as a percentage of the total tissue area on the slide (for healthy, cirrhotic, background non-tumour liver) or as a percentage of the total tumour area on the slide (hepatocytes only; fibrous, vascular and connective tissue areas were excluded; Figure 4). Each staining intensity was given a weighted score to reflect numerically the strength of the staining (0 for negative, 1 for weak, 2 for moderate, 3 for strong), and each percentage area of the slide corresponding to each staining intensity was multiplied by this weighted score (minimum score of 0 for an entirely negatively staining slide; maximum score of 300 for a slide with all of the hepatocytes staining strongly, Table 5). The total LLT1 Expression Score was the sum of each weighted score at each staining intensity for each tissue slide (Table 5). Statistical analyses were performed using Prism 9 software, using the Mann-Whitney test to compare different groups, and the Wilcoxon matched pairs test to compare matched HCC and background liver tissue expression scores.

Normal liver tissue was initially compared to all cirrhotic biopsy samples and HCC samples on a background of cirrhosis (tumour and non-tumour background tissue) LLT1 immunohistochemistry expression scores were significantly higher in all tissue types

compared normal liver. Normal liver samples were also compared to HCC samples arising within non-cirrhotic livers (tumour and non-tumour tissue) (Figure 144 B). LLT1 expression scores were higher in both HCC tumour tissue and non-cirrhotic background liver tissue compared to normal liver. Significance was maintained when separating out patients with cirrhosis and HCC secondary to a viral cause (hepatitis C infection) and patients with cirrhosis and HCC secondary to a non-viral cause (ALD and MASLD) (Figure 146).

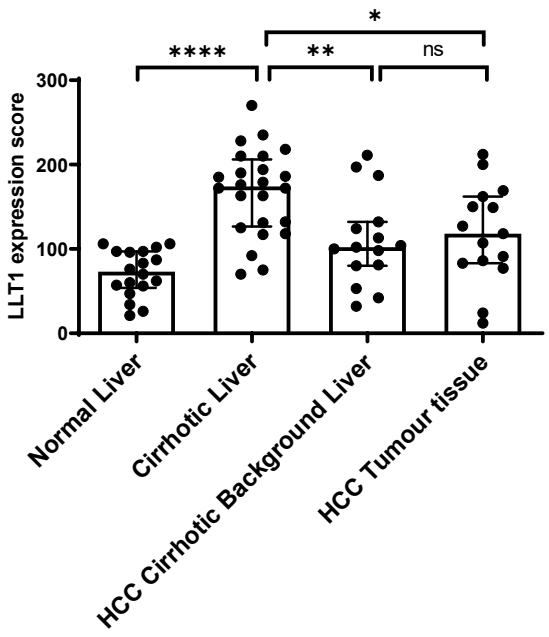
It is important to note that all non-cirrhotic samples with HCC in this group were patients with previously treated Hepatitis C virus. Comparison of LLT1 expression scores in the liver in patients with cirrhosis of a non-viral aetiology also demonstrated raised LLT1 expression scores in comparison to healthy livers (Figure 145).

HCC tumour tissue and background cirrhotic liver margins from HCC resections demonstrated a lower LLT1 expression score in comparison to cirrhotic biopsy liver tissue, however significance this did not reach significance. There was wide variability in LLT1 expression in HCC tumour tissue and background non-tumour tissue from patients with HCC.

LLT1 expression scores determined by immunohistochemistry on liver tissue in cirrhosis and in non-cirrhotic livers.

A

LLT1 expression is upregulated on liver tissue in cirrhosis and HCC (tumour and non-tumour tissue) on a background of cirrhosis



B

LLT1 expression is upregulated on liver tissue in HCC (tumour and non-tumour tissue) without cirrhosis

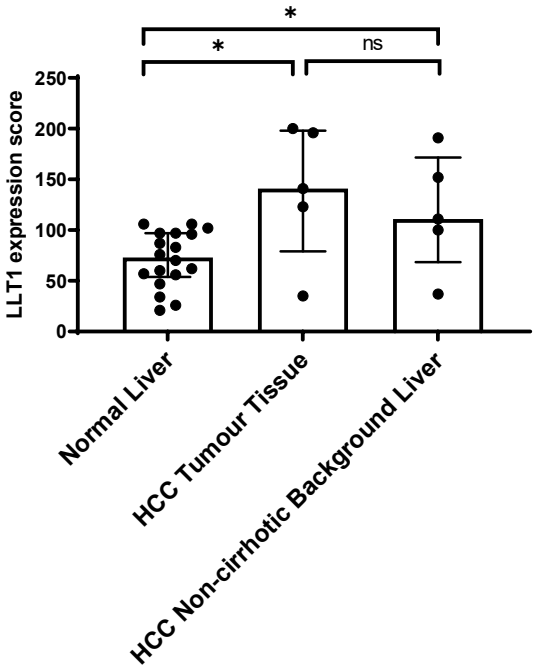


Figure 144 LLT1 is upregulated in the liver in disease. Immunohistochemistry on healthy liver tissue (normal liver margins from resections undertaken for indications other than primary liver cancer),

*cirrhotic liver tissue, tumour tissue and paired non-tumour background liver tissue from patients with HCC was undertaken for LLT1 expression (1:4000 dilution, clone 4C7, Abnova). The LLT1 expression score for each sample was calculated as described in the methods (Chapter 2 and in Figure 4 and Table 5). The higher the expression score, the greater the intensity of LLT1 staining was seen in the liver. Graph A) displays LLT1 expression scores in patients with cirrhosis or HCC on a background of cirrhosis. All groups had significantly higher LLT1 expression scores than in healthy livers as displayed (in addition healthy vs HCC cirrhotic background liver p<0.001**; healthy vs HCC tumour tissue p<0.05*). Graph B) displays LLT1 expression scores in patients with HCC with a non-cirrhotic background liver. Again all patients had an increase in LLT1 expression scores compared to the healthy group. It is important to note that all patients in this non-cirrhotic group had underlying treated Hepatitis C infection. Comparisons between groups were made using the non-parametric Mann-Whitney test, apart from when comparing the paired samples of HCC tumour tissue and HCC background liver tissue, where the Wilcoxon-paired test was used. Paired analyses between samples of HCC tumour tissue and samples of HCC background liver tissue did not show a significant relationship with or without underlying cirrhosis. Graphs display LLT1 expression scores for individual patient samples with the median value displayed by the bar. Error bars represent the interquartile range. P values are denoted on the figures as follows: * p<0.05, ** p<0.01, *** p<0.001, **** p<0.0001).*

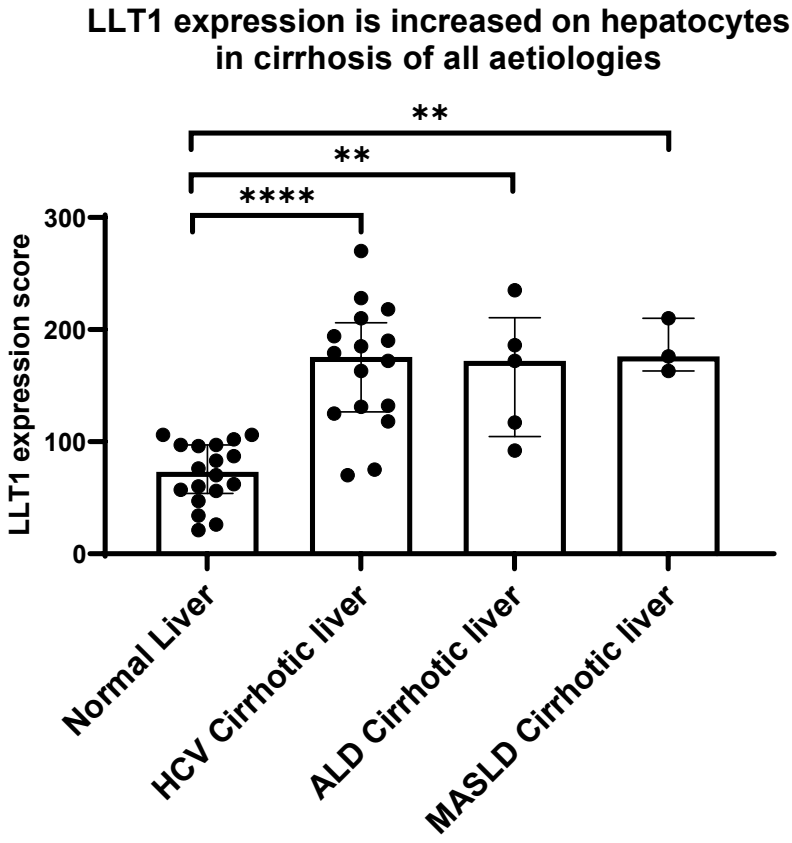


*Figure 145 LLT1 expression is increased on hepatocytes in cirrhosis of all aetiologies. Immunohistochemistry on healthy liver tissue (normal liver margins from resections undertaken for indications other than primary liver cancer) and cirrhotic liver tissue without HCC was undertaken for LLT1 expression (1:4000 dilution, clone 4C7, Abnova). The LLT1 expression score for each sample was calculated as described in the methods (Chapter 2 and in Figure 4 and Table 5). The higher the expression score, the greater the intensity of LLT1 staining was seen in the liver. Groups compared were patients with cirrhosis secondary to previous chronic Hepatitis C (HCV), Alcohol related liver disease (ALD) and Metabolic dysfunction-associated steatotic liver disease (MASLD). Comparisons between groups were made using the non-parametric Mann-Whitney test. Graphs display LLT1 expression scores for individual patient samples with the median value displayed by the bar. Error bars represent the interquartile range. P values are denoted on the figures as follows: * p<0.05, ** p<0.01, *** p<0.001, **** p<0.0001).*

LLT1 expression in cirrhosis and HCC separated by underlying aetiology (viral or non-viral aetiology)

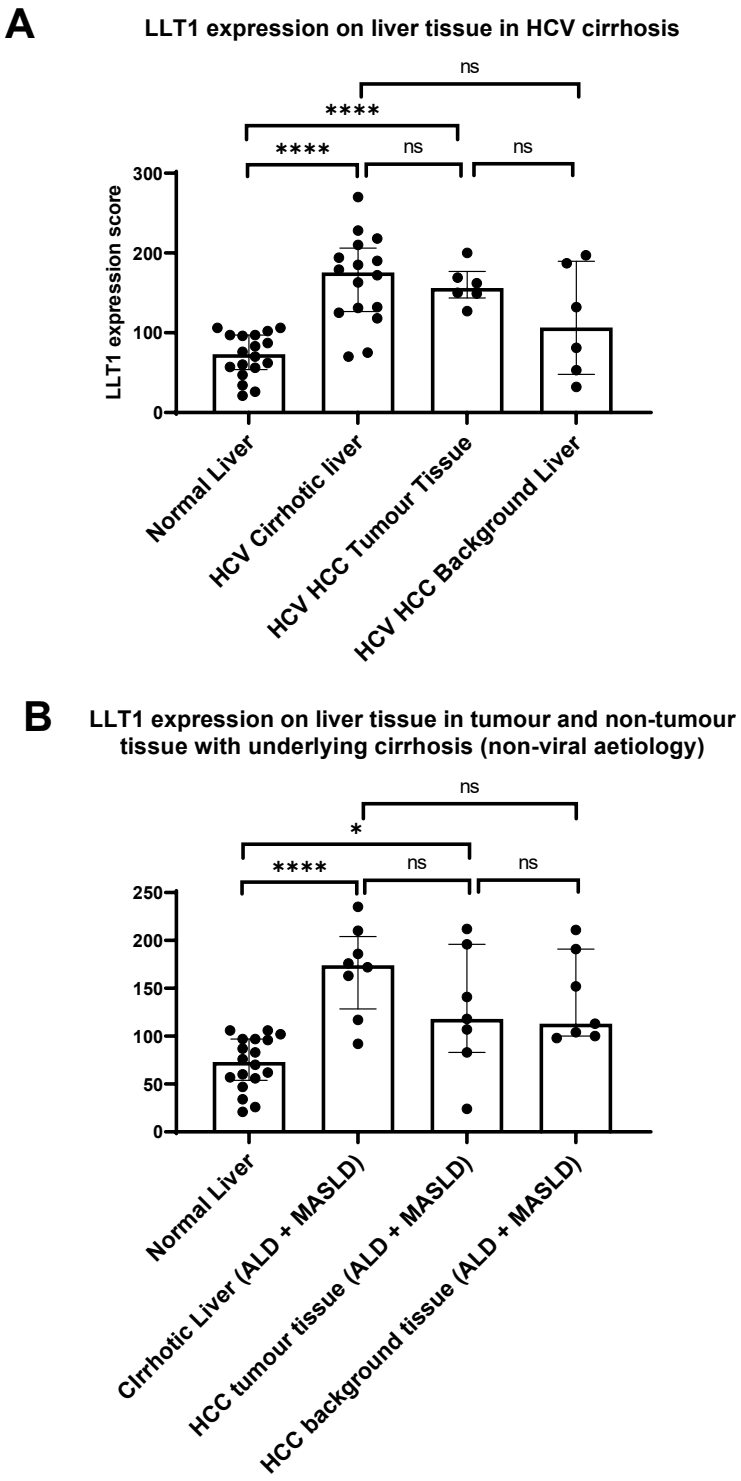


Figure 146 LLT1 expression in cirrhosis and Hepatocellular carcinoma (HCC) separated by underlying aetiology (viral or non-viral aetiology). Immunohistochemistry on healthy liver tissue (normal liver

margins from resections undertaken for indications other than primary liver cancer), cirrhotic liver tissue, tumour tissue and paired non-tumour background liver tissue from patients with HCC was undertaken for LLT1 expression (1:4000 dilution, clone 4C7, Abnova). The LLT1 expression score for each sample was calculated as described in the methods (Chapter 2 and in Figure 4 and Table 5). The higher the expression score, the greater the intensity of LLT1 staining was seen in the liver. Graph A) displays LLT1 expression scores in patients with cirrhosis or HCC on a background of cirrhosis secondary to treated Hepatitis C infection (HCV). All groups had significantly higher LLT1 expression scores than in healthy livers as displayed (in addition healthy vs HCC cirrhotic background liver p<0.05; healthy vs HCC tumour tissue p<0.001**). Graph B) displays LLT1 expression scores in patients with cirrhosis or HCC on a background of cirrhosis secondary to Alcohol related liver disease (ALD) or Metabolic dysfunction-associated steatosis of the liver (MASLD). Again all patients had an increase in LLT1 expression scores compared to the healthy group. Comparisons between groups were made using the non-parametric Mann-Whitney test, apart from when comparing the paired samples of HCC tumour tissue and HCC background liver tissue, where the Wilcoxon-paired test was used. Paired analyses between samples of HCC tumour tissue and samples of HCC background liver tissue did not show a significant relationship. Graphs display LLT1 expression scores for individual patient samples with the median value displayed by the bar. Error bars represent the interquartile range. P values are denoted on the figures as follows: * p<0.05, ** p<0.01, *** p<0.001, **** p<0.0001). Comparisons were further made between patients with ALD cirrhosis and MASLD cirrhosis, and comparing HCC and underlying ALD cirrhosis with patients with HCC and underlying MASLD cirrhosis but no significant differences were seen.*

Given the wide variation of LLT1 expression seen in HCC tissue, paired sample analysis was undertaken to see if there was a pattern in the geographical distribution of LLT1. LLT1 expression scores were determined for HCC tumour tissue, paired background liver tissue adjacent to the tumour and background liver tissue distal from the tumour from the same patient (if available)) (Figure 147). Comparisons were undertaken using the paired Wilcoxon test. There were no significant detectable patterns in LLT1 expression across tumour and background resection tissue with underlying cirrhosis, regardless of the underlying viral or non-viral aetiology.

LLT1 expression in HCC tumour tissue and paired background liver tissue, adjacent to and distal from the tumour, in patients with cirrhosis

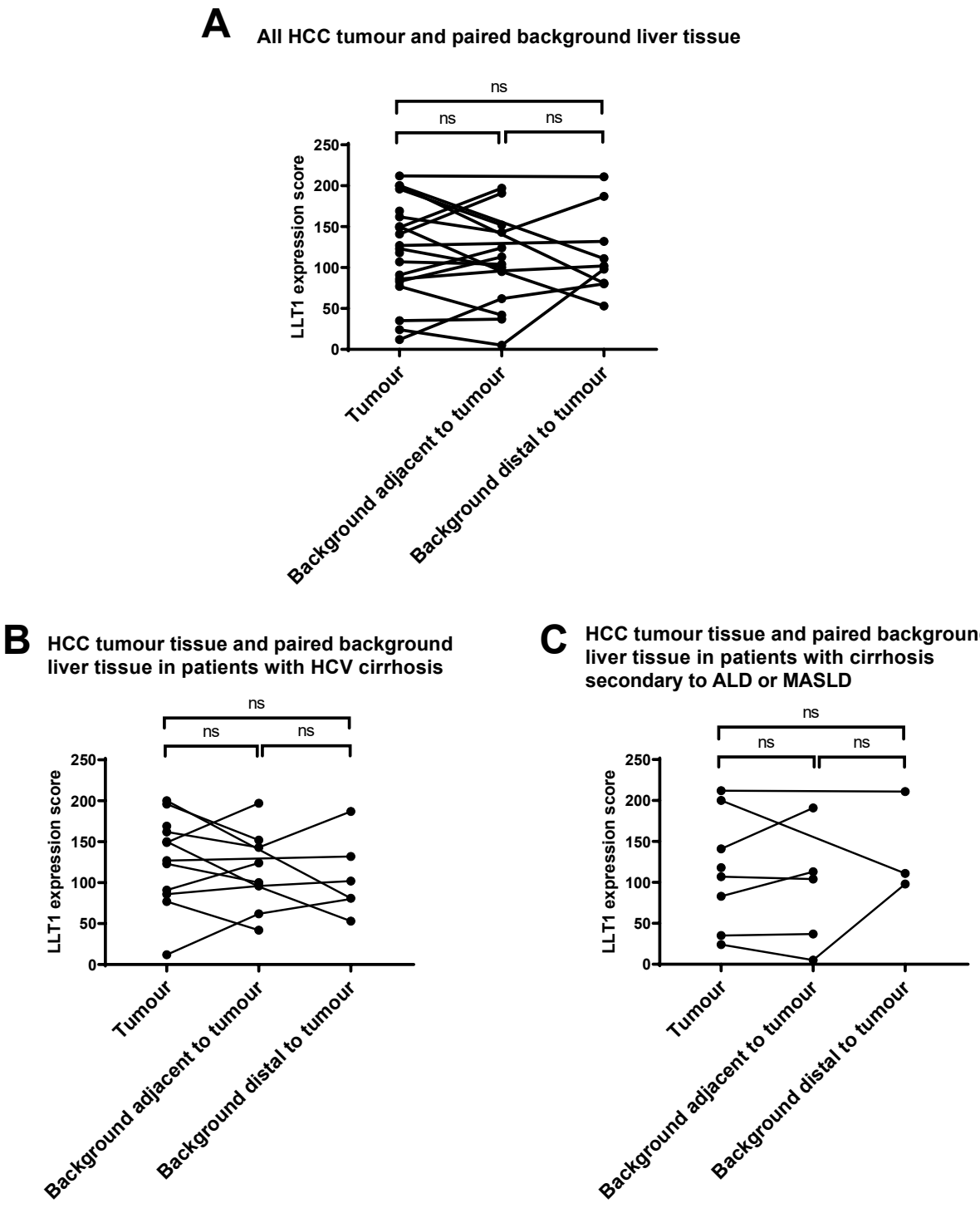


Figure 147 LLT1 expression in HCC tumour tissue and adjacent background liver tissue and distal background liver tissue in patients with underlying cirrhosis. Paired analyses looking at the LLT1

*expression distribution across tumour tissue, adjacent background liver tissue and liver tissue distal to the tumour in A) all samples, B) virally infected samples with previous hepatitis C infection (HCV) and C) non-infected samples (ALD and MASLD). Immunohistochemistry for LLT1 expression (1:4000 dilution, clone 4C7, Abnova) was undertaken on liver resection specimens undertaken for HCC. The LLT1 expression score for each sample was calculated as described in the methods (Chapter 2 and in Figure 4 and Table 5). The higher the expression score, the greater the intensity of LLT1 staining was seen in the liver. Comparisons between groups were made with the Wilcoxon matched pairs test. Graphs display LLT1 expression scores for individual patient samples with the median value displayed by the bar. Error bars represent the interquartile range. P values are denoted on the figures as follows: * p<0.05, ** p<0.01, *** p<0.001, **** p<0.0001). There were no significant consistent patterns in the geographical expression of LLT1 across the tumour and adjacent background non-tumour liver.*

Furthermore, HCC tumour LLT1 expression reach significance when separated by the presence of underlying vascular invasion or with degree of tumour differentiation (Figure 148).

LLT1 expression scores in HCC tumour tissue and underlying tumour differentiation and vascular invasion

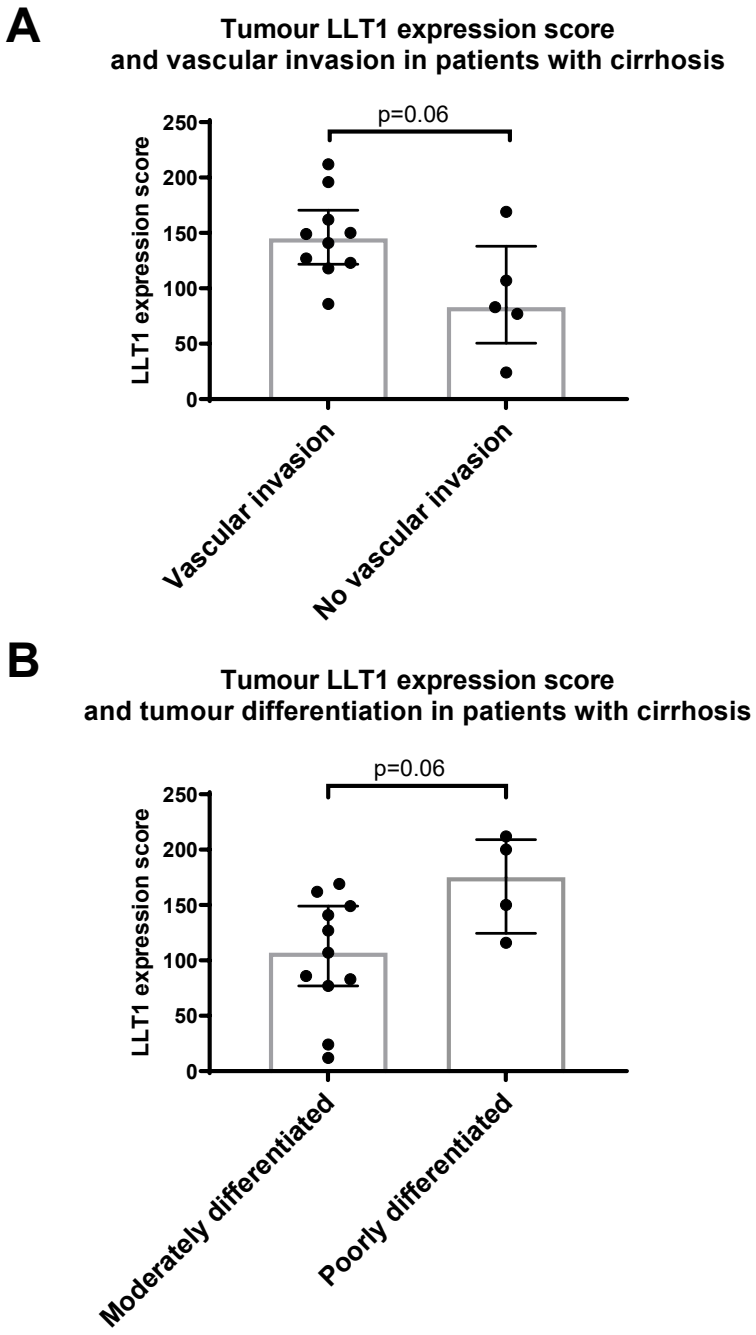


Figure 148 Immunohistochemistry LLT1 expression scores in HCC tumour tissue in patients with underlying cirrhosis depending on the presence of vascular invasion and tumour differentiation. Immunohistochemistry for LLT1 expression (1:4000 dilution, clone 4C7, Abnova) was undertaken on liver resection specimens undertaken for HCC. The LLT1 expression score for each sample was calculated as described in the methods (Chapter 2 and in Figure 4 and Table 5). The higher the expression score, the greater the intensity of LLT1 staining was seen in the liver. Graph A demonstrates

LLT1 expression scores within HCC tumour tissue in patients with cirrhosis of any underlying aetiology and the presence or absence of vascular invasion histologically. Graph B demonstrates the LLT1 expression scores within HCC tumour tissue in patients with cirrhosis of any underlying aetiology and the underlying tumour differentiation. Comparisons between groups were made using the non-parametric Mann-Whitney test. Graphs display LLT1 expression scores for individual patient samples with the median value displayed by the bar. Error bars represent the interquartile range.

In order to determine the nature of the sinusoidal and perisinusoidal cells that were strongly positive for LLT1 in normal liver tissue, immunohistochemistry double staining for LLT1 with either CD68(Tomita et al., 1994) (monocyte/macrophage/Kupffer cells), vimentin(Shang et al., 2018) (hepatic stellate cells), CD20(Huang et al., 2016) (B cells) or CD3(Dimitropoulou et al., 2011) (T cells) was undertaken in three different normal liver samples. Co-localisation was subsequently analysed using Nuance technology (Figure 149). LLT1 positive cells were found to co-localise to different extents with the other markers (Figure 150). Cells expressing vimentin, CD68, CD20 and CD3, all expressed LLT1 to varying degrees, with a minimal number of vimentin positive cells co-expressing LLT1 (range 0.13%-17.27%), and with larger proportions of CD20 expressing cells co-expressing LLT1 (range 29.1%-50.2%), CD68 positive cells co-expressing LLT1 (1.00%-25.0%) and CD3 positive cells co-expressing LLT1 (12.1%-44.1%). The differences in LLT1 positive cells co-expressing different cell surface markers did not reach significance. LLT1 is known to be up-regulated and expressed on activated haematopoietic cells(Germain et al., 2011) but surface expression has not been described on vimentin-positive stellate cells. In fact, Hou et al state that activated stellate cells did not up-regulate CLEC2D(Hou et al., 2012).

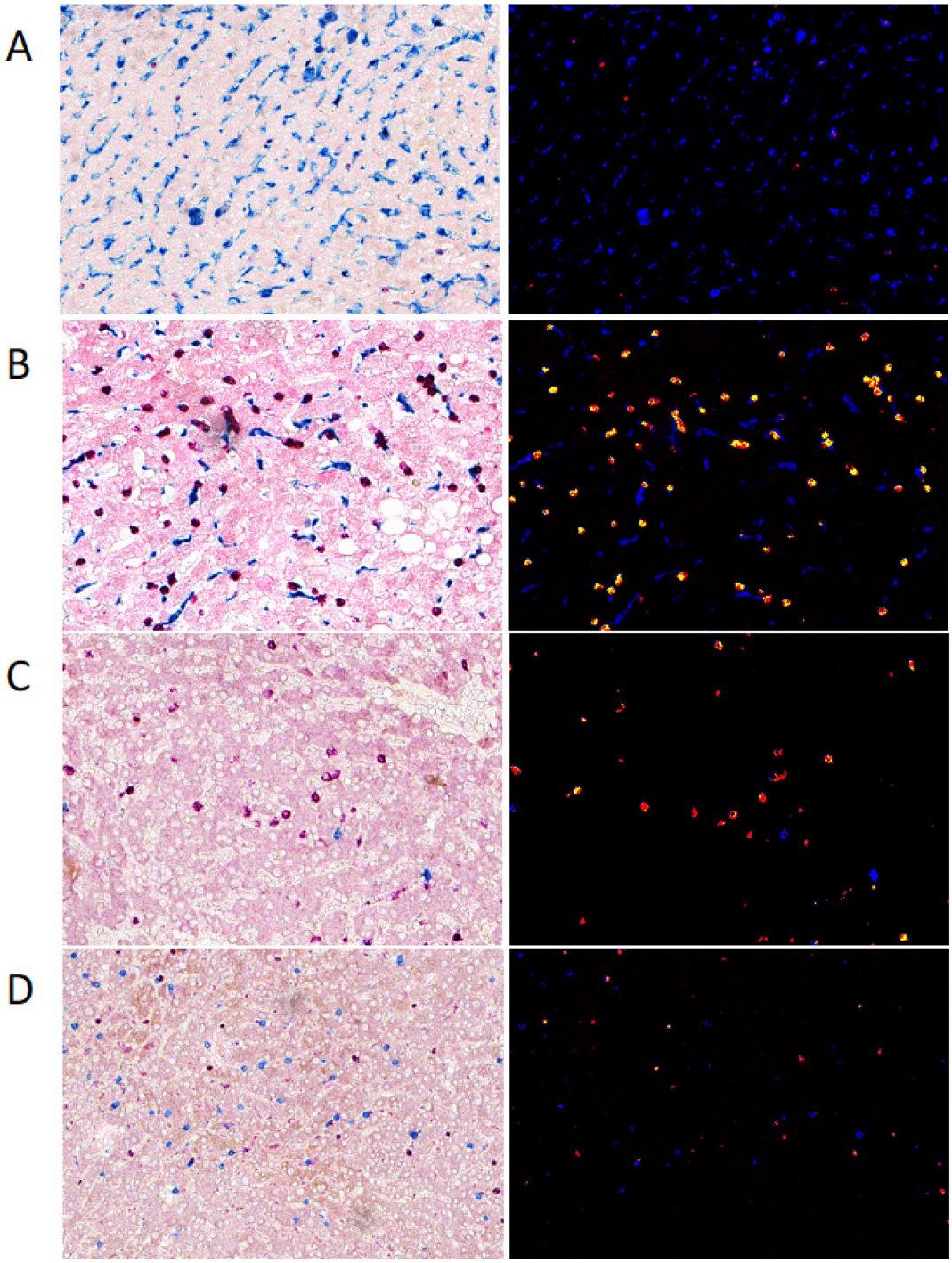


Figure 149 Characterisation of LLT1 expressing cells in normal liver. Formalin fixed paraffin embedded normal liver tissue taken from the margins of liver resections undertaken for indications other than primary liver cancer (n=3) was double stained for LLT1 (Fast red chromagen) and either Vimentin (A), CD68 (B). CD20 (C) or CD3 (D) (vector blue chromagen) (left panel of A-D, at x40 magnification). Nuance technology was utilised to capture five images from each normal liver sample and demonstrate colocalisation of LLT1 with the other markers (corresponding images on right panel: red areas signify LLT1 positive cells, blue areas signify positive staining for either Vimentin (A), CD68 (B), CD20 (C), or

CD3 (D), yellow areas mark colocalisation). 5 measurements from each normal liver sample were taken, measuring the percentage of cells that are positive for the marker of interest that are also expressing LLT1 and vice versa.

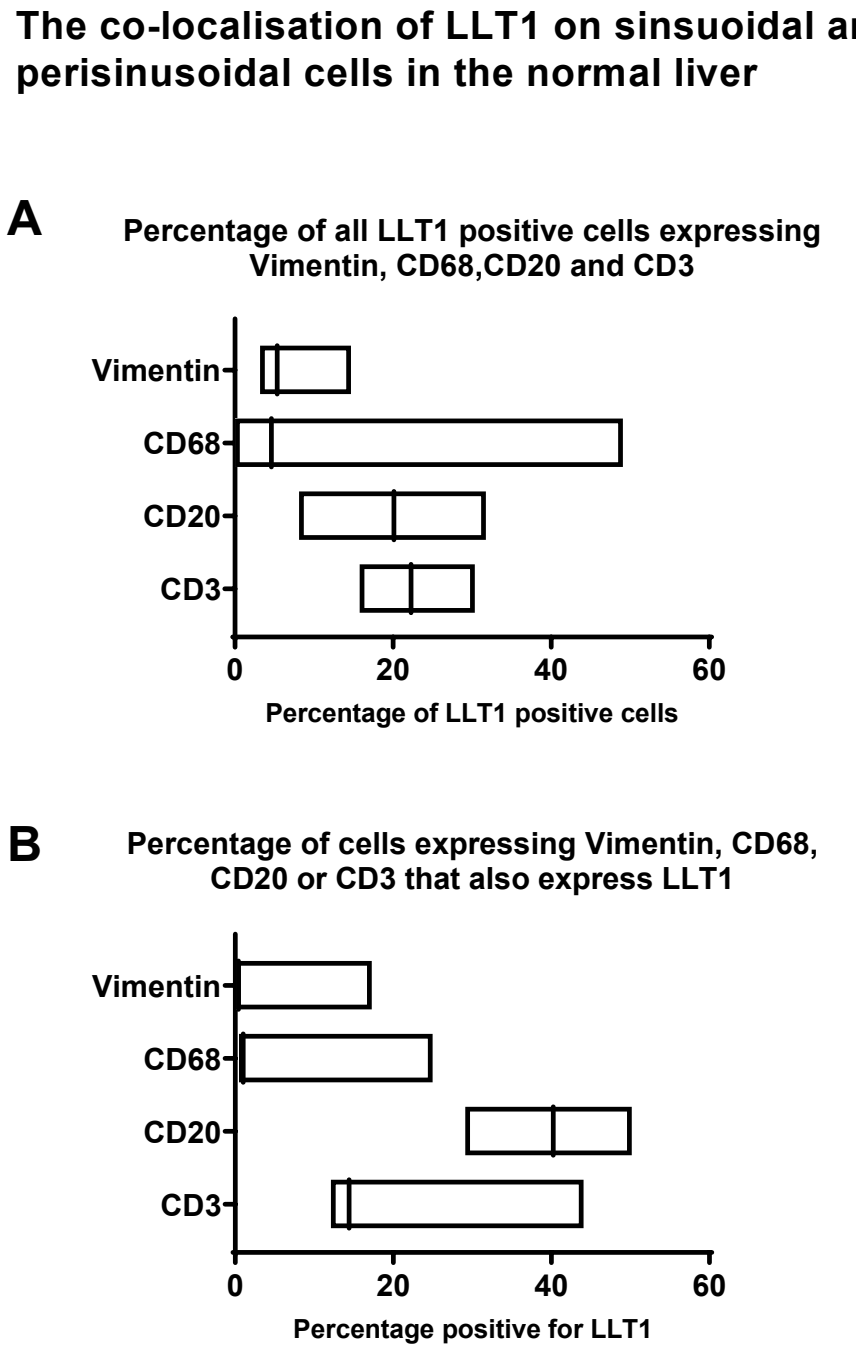


Figure 150 The co-localisation of LLT1 on sinusoidal and perisinusoidal cells with other markers. Following double staining for LLT1 (Fast red chromagen) and markers Vimentin, CD68, CD20 or CD3 (Vector blue chromagen) as described in methods and in Figure 149, Nuance technology was utilised

to identify and quantitate co-expression of LLT1 and these markers. 5 images at x40 magnification were taken across each normal liver tissue sample (n=3). Nuance technology identified the number of LLT1 positive cells in each image, the number of cells expressing a marker of interest (Vimentin/CD68/CD20/CD3) within the same image, and the number of cells expressing both LLT1 and the marker of interest (co-localisation). Measurements were taken from each of the five images of each normal liver tissue sample (n=3), measuring the proportion of LLT1 expressing cells in each sample that are also positive for each of the markers of interest (Graph A) and total proportion of cells expressing the marker of interest (Vimentin, CD68, CD20 or CD) and LLT1 (Graph B).

5.2.2 LLT1 expression on liver tissue as determined by quantitative real-time PCR

In order to ratify the increased expression of LLT1 seen in cirrhosis, LLT1 expression was relatively quantified using real-time PCR. RNA was extracted from snap frozen liver tissue (normal liver margins from liver resections for indications other than primary liver cancer (n=6), cirrhotic liver samples from explant tissue (n=5), HCC tumour tissue and paired background tissue from explant/resection tissue with cirrhosis (n=6) or without cirrhosis (n=6)) and converted to cDNA as described in the methods in chapter 2 (see Table 17 below for patient characteristics). Each cDNA sample was run in duplicates, with duplexing for LLT1 with GAPDH as the endogenous control. Reactions were run for 40 cycles, C_t values averaged across replicates, $\Delta\Delta C_t$ values calculated and $2^{\Delta\Delta Ct}$ plotted to determine the relative expression of LLT1 in each tissue sample.

Table 17 Demographics and clinical data for patients from whom liver tissue samples were used for quantitative PCR for LLT1 expression. Fresh liver tissue samples taken within 12hours of resection or from a liver explant were snap frozen in liquid nitrogen and stored in liquid nitrogen at –190°C. For patients with Hepatocellular carcinoma (HCC), HCC tumour tissue, adjacent liver non-tumour tissue and background liver tissue distal to the tumour was stored where available. ALD = Alcohol related liver disease. MASLD = Metabolic dysfunction-associated steatotic liver disease.

	Normal Liver	**Cirrhotic Liver**	**HCC**
Total	6	5	12
Age, years (range)	66 (53-78)	58 (50-64)	68 (52-72)
Sex (n male/total)	6/6	2/5	9/12
Cirrhosis (n/total)		5/5	6/12
Aetiology:			
ALD (n/total cirrhotic)		5/5	5/6
MASLD (n/total cirrhotic)		0/5	1/6
Non-cirrhotic (n/total)		0/5	6/12
Aetiology:			
ALD (n/total non-cirrhotic)			5/6
MASLD (n/total non-cirrhotic)			1/6

LLT1 expression was significantly raised in cirrhotic liver and HCC on a background of cirrhosis compared to normal liver (Figure 151). All cirrhotic liver tissue samples demonstrated an increased expression of LLT1 compared to normal tissue (Figure 151). Although HCC tumour tissue demonstrated an overall increased expression of LLT1 compared to normal liver regardless of whether there was underlying cirrhosis, the expression of LLT1 was hugely variable within the tumour tissue (range $2^{\Delta\Delta Ct}$ values 0.53 – 76432), with some tumour tissue demonstrating high expression of LLT1 and some tumour samples demonstrating very little LLT1. Analysis of HCC tumour tissue and paired background liver tissue (with the Wilcoxon matched-pairs signed rank test) did not demonstrate a significant pattern in samples with underlying cirrhosis or non-cirrhotic samples respectively.

LLT1 expression is increased in cirrhosis and shows wide variation in HCC (tumour and non-tumour tissue) with underlying cirrhosis

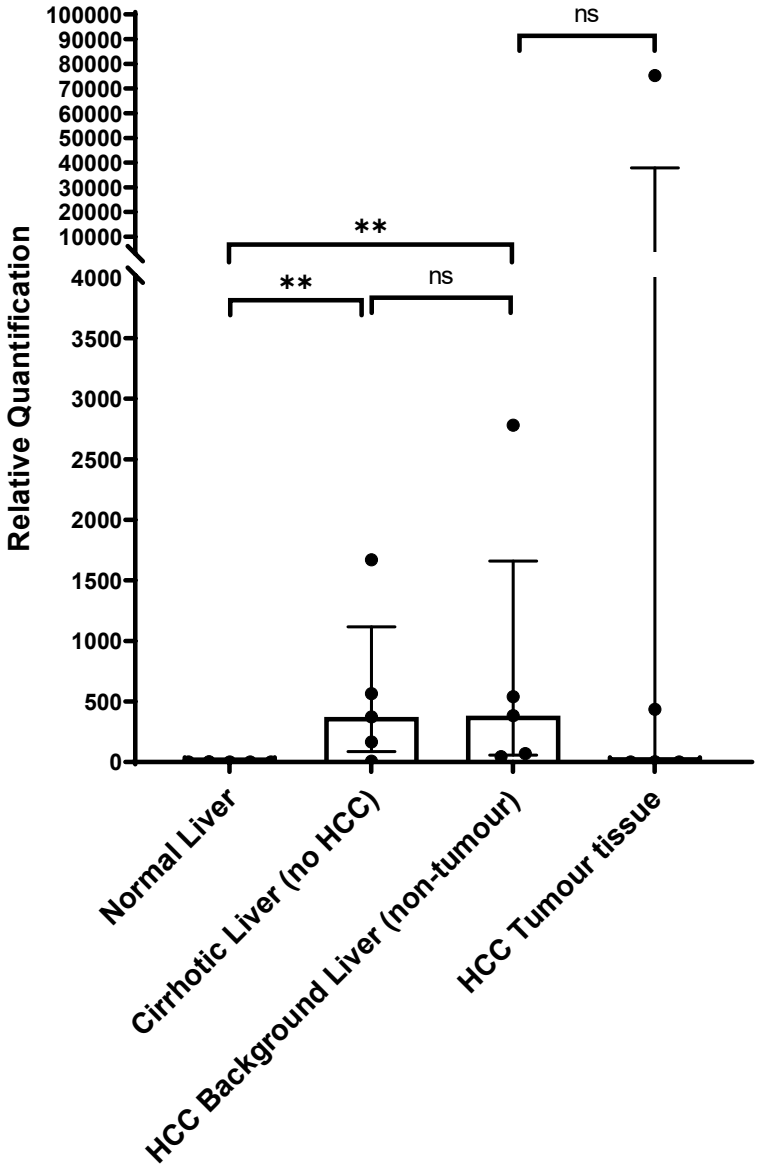


Figure 151 LLT1 expression is increased in patients with cirrhosis and variable in patients with HCC on a background of cirrhosis. Liver tissue taken within 12 hours of liver resection or explant was snap frozen and stored in liquid nitrogen. RNA was extracted from tissue samples and cDNA formed (Qiagen, Germany). Real time reverse transcription (RT)-PCR for LLT1 expression (CLEC2D gene) was performed using a TaqMan gene expression assay, multiplexing FAM dye-labelled LLT1 probe with VIC dye-labelled GAPDH probe (GAPDH used as an endogenous control). Each sample was run in duplicate with the difference in threshold cycles for LLT1 and GAPDH calculated for each sample (ΔC_T) and the difference in ΔC_T between normal liver, cirrhotic liver and HCC tumour tissue samples ($\Delta\Delta C_T$). Reactions

*were run for 40 cycles, C_T values averaged across replicates. The fold change in LLT1 expression was expressed as $2^{\Delta\Delta CT}$. Statistical comparisons were made using Mann-Whitney tests (with Wilcoxon matched-pairs signed rank test when comparing HCC tumour samples with the HCC background liver from the same donor). Graphs display the average LLT1 relative quantification for individual patient samples with the median value displayed by the bar. Error bars represent the interquartile range. P values are denoted on the figures as follows: * p<0.05, ** p<0.01, *** p<0.001, **** p<0.0001). LLT1 expression was increased in cirrhotic liver tissue in comparison to normal liver tissue. There was wide variability in LLT1 expression in HCC and background non-tumour cirrhotic liver tissue from patients with HCC.*

Quantitative PCR was also undertaken for liver tissue samples from patients with HCC but without underlying cirrhosis (Figure 152). While LLT1 expression was increased in HCC background non-tumour liver tissue in comparison to normal liver tissue, there was again wide variability seen in LLT1 expression in HCC and background non-tumour liver tissue.

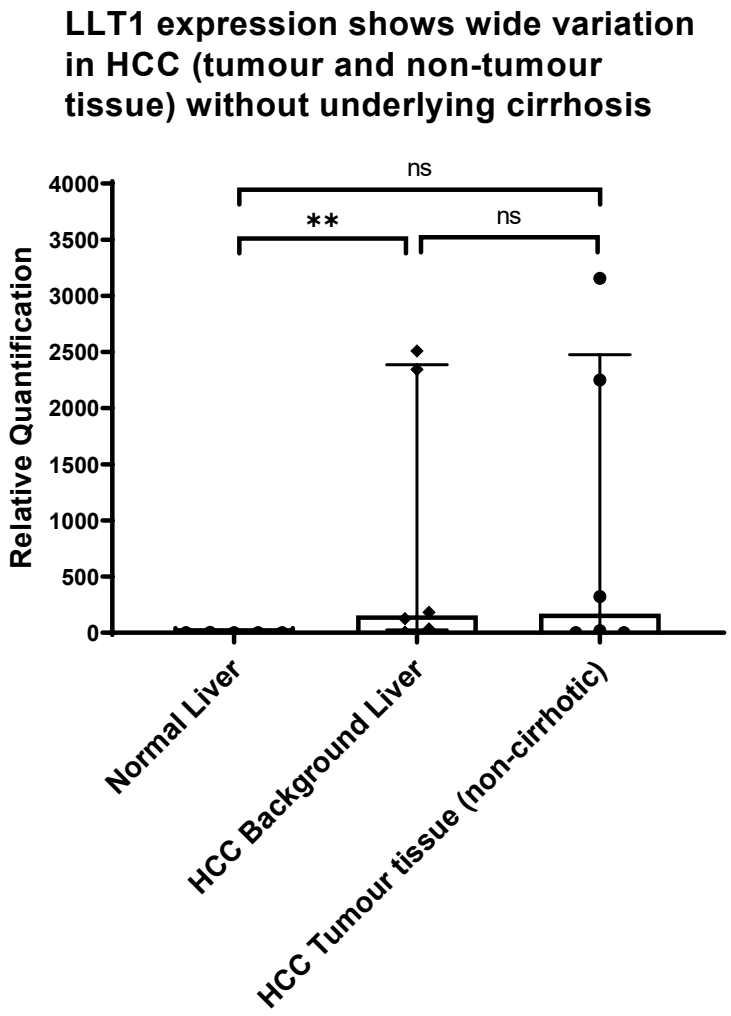


*Figure 152 LLT1 expression in patients with HCC without underlying cirrhosis. Liver tissue taken within 12 hours of liver resection or explant was snap frozen and stored in liquid nitrogen. RNA was extracted from tissue samples and cDNA formed (Qiagen, Germany). Real time reverse transcription (RT)-PCR for LLT1 expression (CLEC2D gene) was performed using a TaqMan gene expression assay, multiplexing FAM dye-labelled LLT1 probe with VIC dye-labelled GAPDH probe (GAPDH used as an endogenous control). Each sample was run in duplicate with the difference in threshold cycles for LLT1 and GAPDH calculated for each sample (ΔC_T) and the difference in ΔC_T between normal liver, cirrhotic liver and HCC tumour tissue samples ($\Delta\Delta C_T$). Reactions were run for 40 cycles, C_T values averaged across replicates. The fold change in LLT1 expression was expressed as $2^{\Delta\Delta CT}$. Statistical comparisons were made using Mann-Whitney tests, (with Wilcoxon matched-pairs signed rank test when comparing HCC tumour samples with the HCC background liver from the same donor). Graphs display the average LLT1 relative quantification for individual patient samples with the median value displayed by the bar. Error bars represent the interquartile range. P values are denoted on the figures as follows: * p<0.05, ** p<0.01,*

**** p<0.001, **** p<0.0001). While LLT1 expression was increased in HCC background non-tumour liver tissue in comparison to normal liver tissue, there was wide variability in LLT1 expression in HCC and background non-tumour liver tissue.*

In summary, increased expression of LLT1 in cirrhotic liver tissue seen using immunohistochemistry is supported by the qPCR data. The qPCR data also supports the variability seen in the LLT1 expression data within HCC tumour tissue and background non-tumour liver tissue, both with or without cirrhosis.

5.2.3 Soluble LLT1 expression

Serum samples from healthy volunteers (n=10), patients with cirrhosis with an underlying non-viral aetiology (n=17) or HCC on a background of cirrhosis (treatment naïve, n=13) were run in duplicate on an ELISA to determine if there was any significant soluble circulating LLT1 (see Table 18 below for patient characteristics). There was no significant difference in soluble LLT1 levels between healthy volunteers, patients with cirrhosis and patients with HCC (Figure 153).

Table 18 Demographics and clinical data of patients and healthy donors from whom serum samples were taken to detect circulating soluble LLT1. ALD = Alcohol related liver disease; MASLD – Metabolic dysfunction-associated steatotic liver disease; HCC = Hepatocellular carcinoma.

	Healthy	**Cirrhosis**	**HCC**
Total	10	17	13
Age, years (range)	43 (31-54)	53 (33-72)	74 (64-84)
Sex (n male/total)		12/17	13/13
Cirrhosis (n/total)		17/17	17/17
Aetiology:			
ALD (n/total cirrhotic)		9/17	6/13
MASLD (n/total cirrhotic)		8/17	7/13

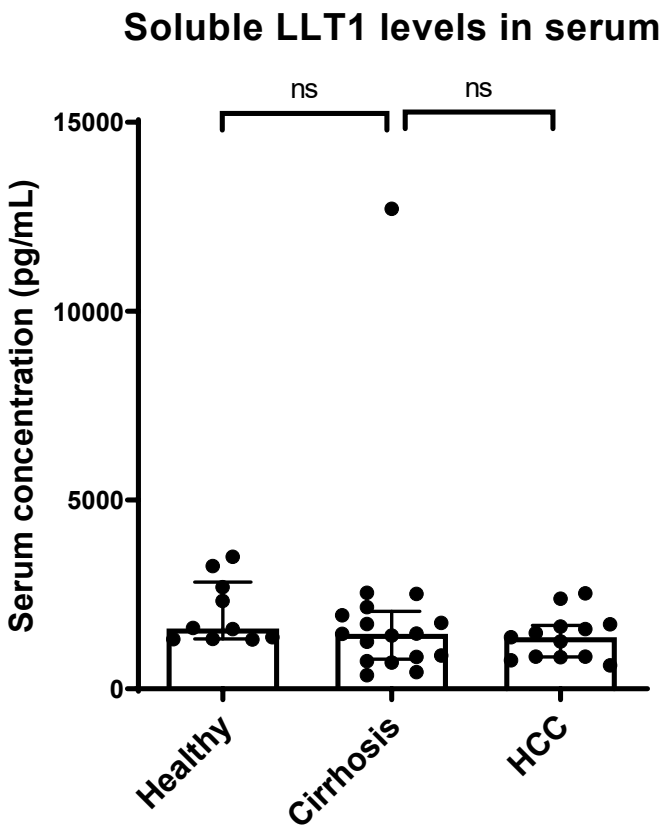


Figure 153 ELISA to detect soluble LLT1 expression in serum from healthy donors (n=10), patients with cirrhosis (n=17), and patients with hepatocellular carcinoma (HCC) with underlying cirrhosis (n=13). All patients had either alcohol related liver disease (ALD) or metabolic dysfunction-associated steatotic liver disease as their underlying cause of cirrhosis. Serum samples from healthy donors and patients was diluted 1:2 and plated in duplicate on to the assay plate as per manufacturer's instructions (C type lectin domain family 2 member D (CLEC2D) ELISA kit (Mybiosource, San Diego, US, MBS7213167)). The average serum concentration was measured for each sample. Statistical comparisons were made using Mann-Whitney tests. Graphs display the average serum concentration for soluble LLT1 for individual patient samples with the median value displayed by the bar. Error bars represent the interquartile range.

5.3 CD161 expression on immune cells

5.3.1 CD161 expression on circulating and liver infiltrating NK cells

CD161 expression has been demonstrated in full in chapter 3. Circulating NK cells had a significantly greater proportion of CD161+ NK cells in cirrhosis compared to NK cells from healthy donors (91.3% vs 87.1%, p=0.04) (Figure 34). In fact, circulating NK cells from patients with cirrhosis had a significantly greater proportion of CD161+ NK cells compared to all other patient groups (see Chapter 3, Figure 34). Analysis by underlying aetiology demonstrated an increased CD161+NK cell proportion in patients with ALD related cirrhosis compared to MASLD cirrhosis (Figure 35).

CD161+NK cells were then further phenotyped to determine the expression of other checkpoint molecules including PD-1, CTLA-4, B- and T- lymphocyte attenuator (BTLA) and CD25 (Phenotyping panel 2, detailed in Chapter 2, Table 3; gating strategy as per Figure 154). Expression of these checkpoint inhibitors on circulating NK cells was analysed within the ALD patient group in order to remove underlying aetiology as a possible confounding factor and as the circulating CD161+NK cell proportion was significantly increased in cirrhosis in the ALD group. Due to sample limitations, a subset of patient samples and healthy volunteer samples were used in these experiments (patient demographics in Table 19 below of samples used in these experiments).

Intrahepatic samples were also phenotyped (Phenotyping Panel 2, Chapter 2, Table 3): Healthy livers (n=7) (normal liver margins from patients undergoing liver resection for indications other than primary cancer); patients with cirrhosis (n=4) or HCC with a background of cirrhosis (n=6) (full demographics in Chapter 3, Table 9), with paired samples from the circulation for each donor.

Table 19 Demographics of patients and healthy volunteers from whom peripheral blood samples were used for NK cell and T cell phenotyping. All patients had alcohol related liver disease (ALD) with underlying cirrhosis, with or without hepatocellular carcinoma (HCC).

	Healthy	Cirrhosis	HCC
Total number	21	18	11
Age, years mean, (range)	43 (26-60)	52 (26-62)	70 (57-75)
Male n	11	15	11
Child-Pugh (CP) Score: CPA n		9	8
CPB n		4	1
CPC n		5	2
MELD-Na score mean, (range)		10 (6-20)	9 (6-16)
Aetiology:			
ALD n		18	11
BCLC staging:			
BCLC 0 n, (%)			1
BCLC A n, (%)			1
BCLC B n, (%)			4
BCLC C n, (%)			2
BCLC D n. (%)			3

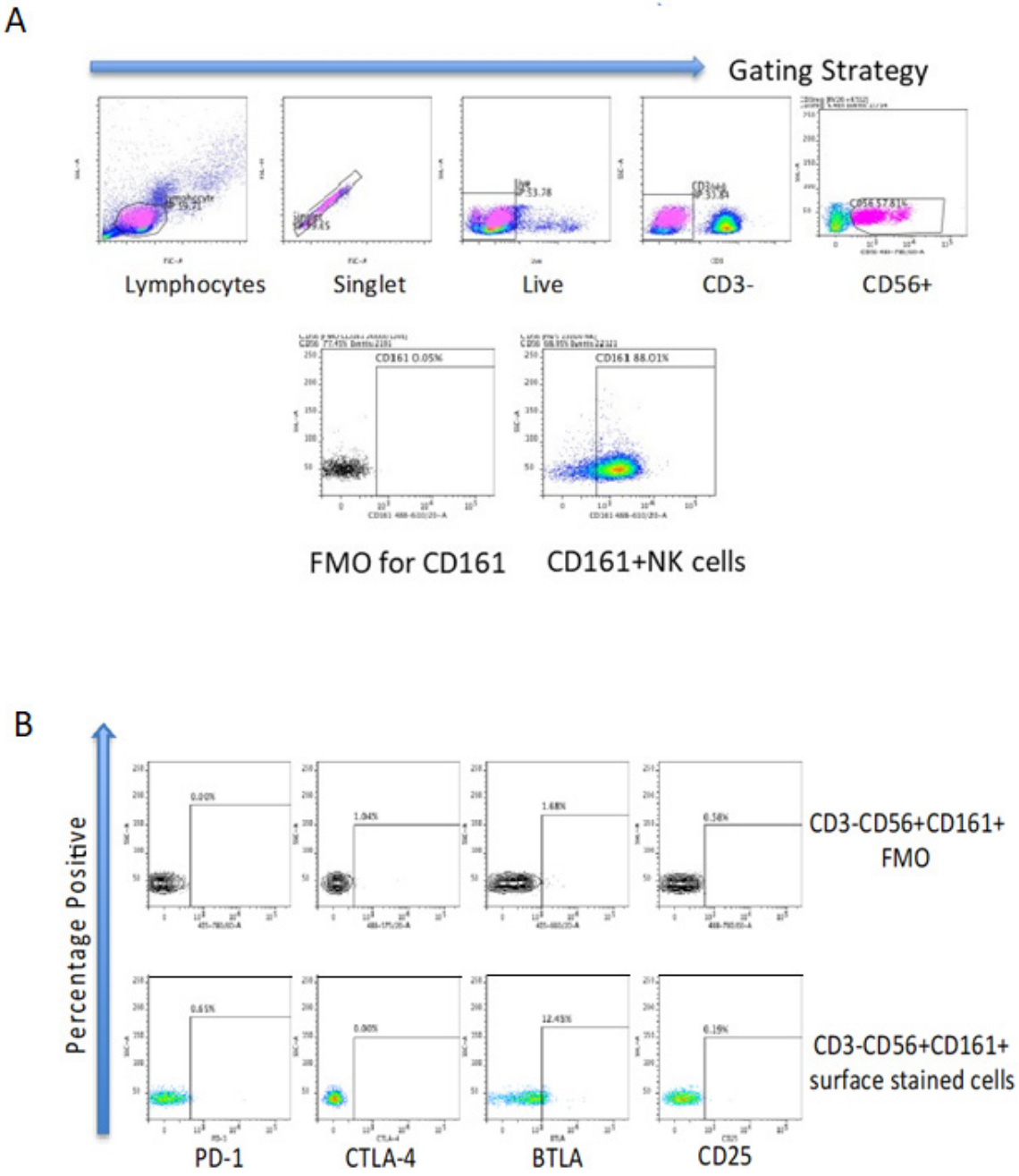


Figure 154 Gating strategy for checkpoint inhibitors on CD161+ NK cells. Peripheral blood mononuclear cells (PBMCs) and intrahepatic mononuclear cells (IMNCs) were phenotyped following surface staining using antibodies as described in Phenotyping panel 2 in the methods (Chapter 2, Table 3) and data acquired using flow cytometry as per the gating strategy demonstrated in this figure. A) CD161+ NK cells were gated as per the gating strategy shown following on gating for NK cells by selecting liver CD3-CD56+ liver lymphocytes. B) Gates for PD-1, CTLA-4, BTLA and CD25 were set using cells surface stained with all antibodies apart from the antibody of interest (fluorescence minus one,

FMO). Percentage positive NK cells were determined for circulating and intrahepatic NK cells using this gating strategy.

The proportion of circulating NK cells expressing PD-1 was significantly increased in patients with ALD cirrhosis with HCC on a background of ALD cirrhosis, compared to patients with cirrhosis without HCC, though CD161+PD-1+NK cells made up less than 10% of circulating NK cells in patients with HCC (Figure 155A). A greater proportion of CD161+ NK cells within healthy livers expressed PD-1 (Figure 155B). Conversely the proportion of intrahepatic NK cells expressing PD-1 varied widely and was reduced in patients with HCC on a background of cirrhosis in comparison to intrahepatic NK cells found in healthy and cirrhotic livers (Figure 155B).

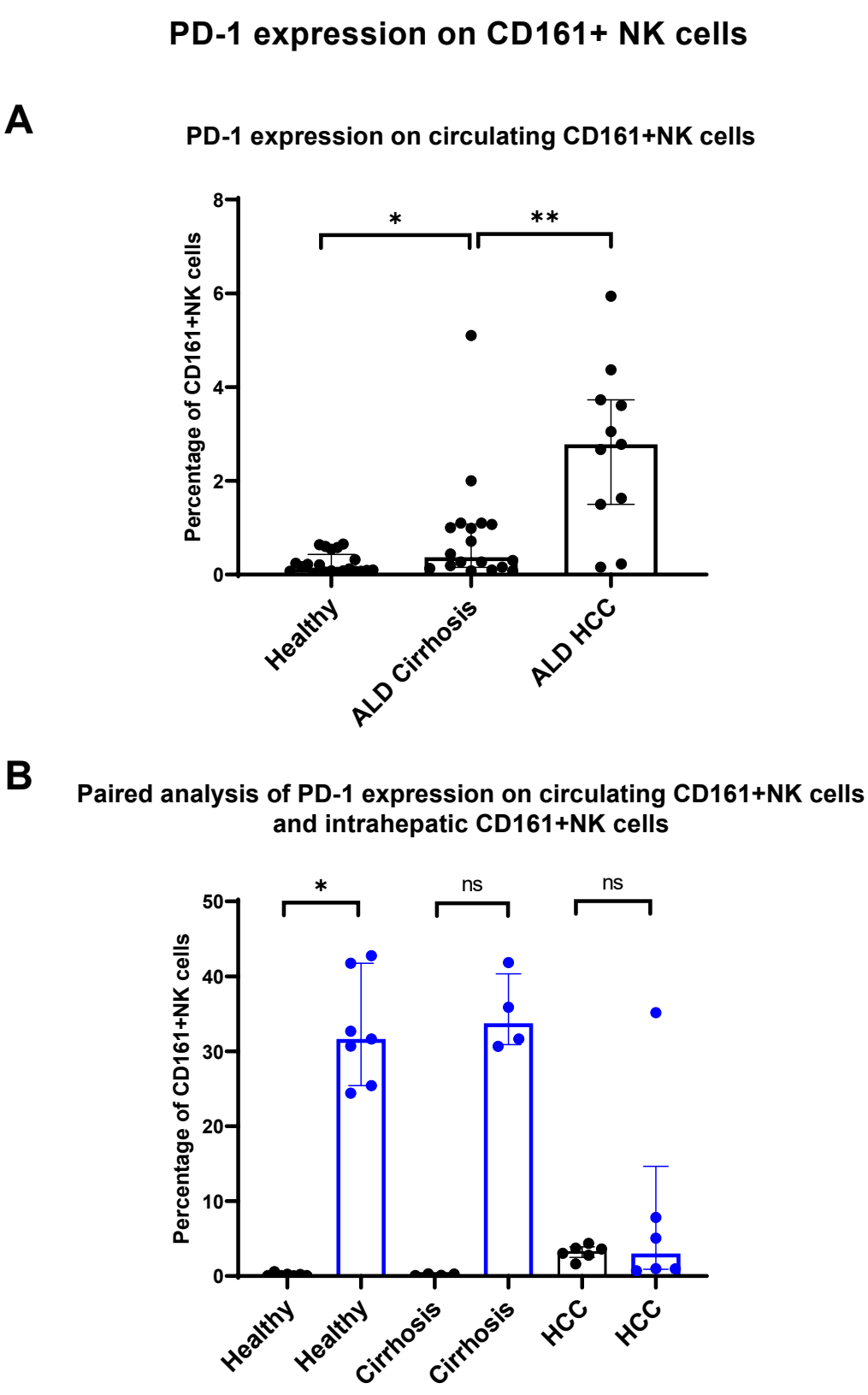


Figure 155 PD-1 expression on CD161+ NK cells. Graph A demonstrates the percentage of CD161+ NK cells in the circulation that express PD-1 in healthy volunteers (n=21), patients with cirrhosis from alcohol related liver disease (ALD Cirrhosis); n=18) and patients with HCC on a background of ALD

*cirrhosis (ALD HCC; n=11; patient demographics in Table 19). Comparisons were made using Mann-Whitney tests. Graph B demonstrates the percentage of CD161+ NK cells that express PD-1 in the liver (data in blue) compared to in the circulation from the same donor (data in black). Healthy livers were normal liver margins from patients undergoing liver resection for indications other than primary cancer (n=7). Patients with cirrhosis or HCC had an underlying non-viral aetiology, and all patients with HCC had underlying cirrhosis (Cirrhosis n=4, HCC n=6). Comparisons between paired samples were made using the Wilcoxon Match-pairs test. Graphs display individual values with the median value displayed by the bar. Error bars represent the interquartile range. P values are denoted on the figures as follows: * p<0.05, ** p<0.01, *** p<0.001, **** p<0.0001).*

BTLA expression followed a similar pattern as PD-1, with a significantly increased proportion of circulating CD161+BTLA+ NK cells in patients with HCC on a background of ALD cirrhosis compared to patients with ALD cirrhosis (18.0% vs 7.56%; p=0.02, median values respectively; Figure 156A). Similar to PD-1 expression, there was an increase also in the proportions of circulating CD161+BTLA+ NK cells in patients with cirrhosis. Intrahepatic NK cells demonstrated an increased CD161+BTLA+NK cell proportion in healthy livers and this pattern was maintained in cirrhosis (Figure 156B). Again, intrahepatic NK cells extracted from livers with HCC on a background of cirrhosis demonstrated wide variation in expression and a reduced proportion of CD161+BTLA+NK cells compared to healthy and cirrhotic intrahepatic NK cells. However, interpretation of the intrahepatic data is limited by small numbers in each patient group.

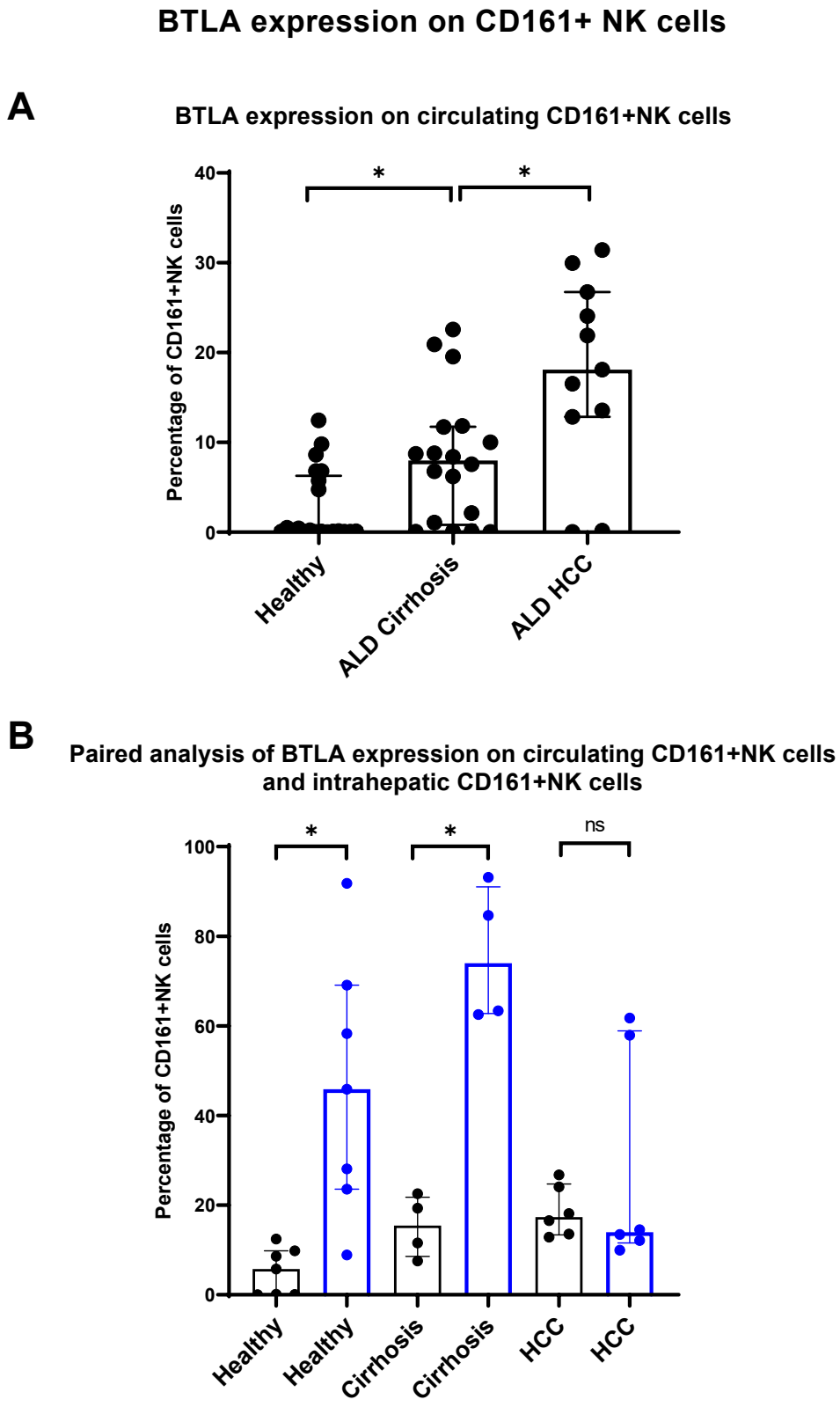


Figure 156 BTLA expression on CD161+ NK cells. Peripheral blood mononuclear cells (PBMCs) and intrahepatic mononuclear cells (IMNCs) were phenotyped following surface staining using antibodies as described in Phenotyping panel 2 in the methods (Chapter 2, Table 3). Graph A demonstrates the

*percentage of CD161+ NK cells in the circulation that express BTLA in healthy volunteers (n=21), patients with cirrhosis from alcohol related liver disease (ALD Cirrhosis; n=18) and patients with Hepatocellular carcinoma (HCC) on a background of ALD cirrhosis (ALD HCC; n=11; patient demographics in Table 19). Comparisons were made using Mann-Whitney tests. Graph B demonstrates the percentage of CD161+ NK cells that express BTLA in the liver (data in blue) compared to in the circulation from the same donor (data in black). Healthy livers were normal liver margins from patients undergoing liver resection for indications other than primary cancer (n=7). Patients with cirrhosis or HCC had an underlying non-viral aetiology, and all patients with HCC had underlying cirrhosis (Cirrhosis n=4, HCC n=6). Comparisons between paired samples were made using the Wilcoxon Match-pairs test. Graphs display individual values with the median value displayed by the bar. Error bars represent the interquartile range. P values are denoted on the figures as follows: * p<0.05, ** p<0.01, *** p<0.001, **** p<0.0001).*

Less than 2% of CD161+ NK cells expressed CD25 in the circulation (Figure 157A). CD25 expression in the liver was also very variable, with an increased proportion overall on paired analysis in the healthy liver compared to healthy circulating cells in the same donor (Figure 157B).

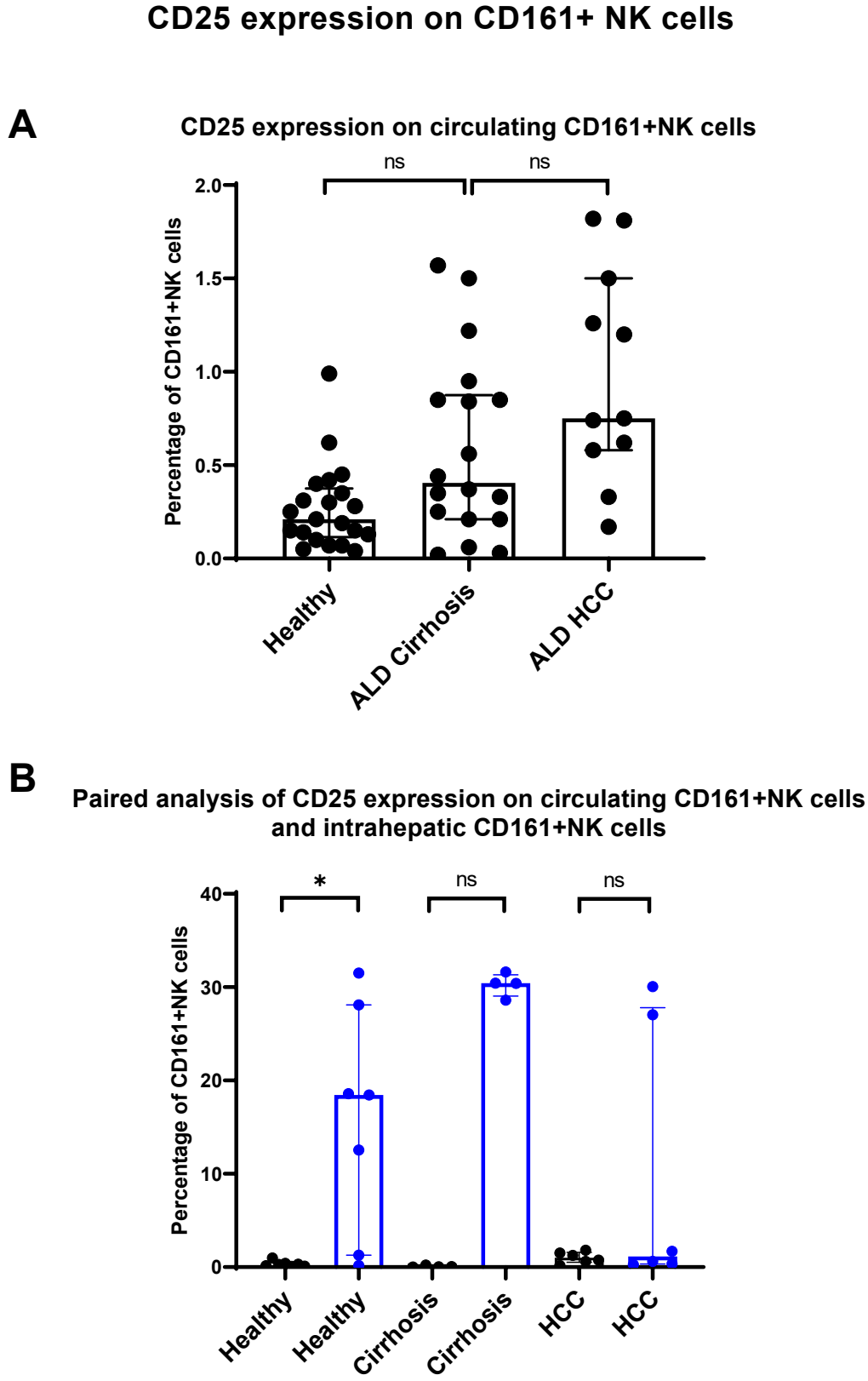


Figure 157 CD25 expression on CD161+ NK cells. Peripheral blood mononuclear cells (PBMCs) and intrahepatic mononuclear cells (IMNCs) were phenotyped following surface staining using antibodies as described in Phenotyping panel 2 in the methods (Chapter 2, Table 3). Graph A demonstrates the

*percentage of CD161+ NK cells in the circulation that express CD25 in healthy volunteers (n=21), patients with cirrhosis from alcohol related liver disease (ALD Cirrhosis; n=18) and patients with HCC on a background of ALD cirrhosis (ALD HCC; n=11; patient demographics in Table 19). Comparisons were made using Mann-Whitney tests. Graph B demonstrates the percentage of CD161+ NK cells that express CD25 in the liver (data in blue) compared to in the circulation from the same donor (data in black). Healthy livers were normal liver margins from patients undergoing liver resection for indications other than primary cancer (n=7). Patients with cirrhosis or HCC had an underlying non-viral aetiology, and all patients with HCC had underlying cirrhosis (Cirrhosis n=4, HCC n=6). Comparisons between paired samples were made using the Wilcoxon Match-pairs test. Graphs display individual values with the median value displayed by the bar. Error bars represent the interquartile range. P values are denoted on the figures as follows: * p<0.05, ** p<0.01, *** p<0.001, **** p<0.0001).*

There were no significant differences seen in CTLA-4 expression on NK cells, with less than 5% in circulating and intrahepatic CD161+ NK cells expressing CTLA-4 (Figure 158).

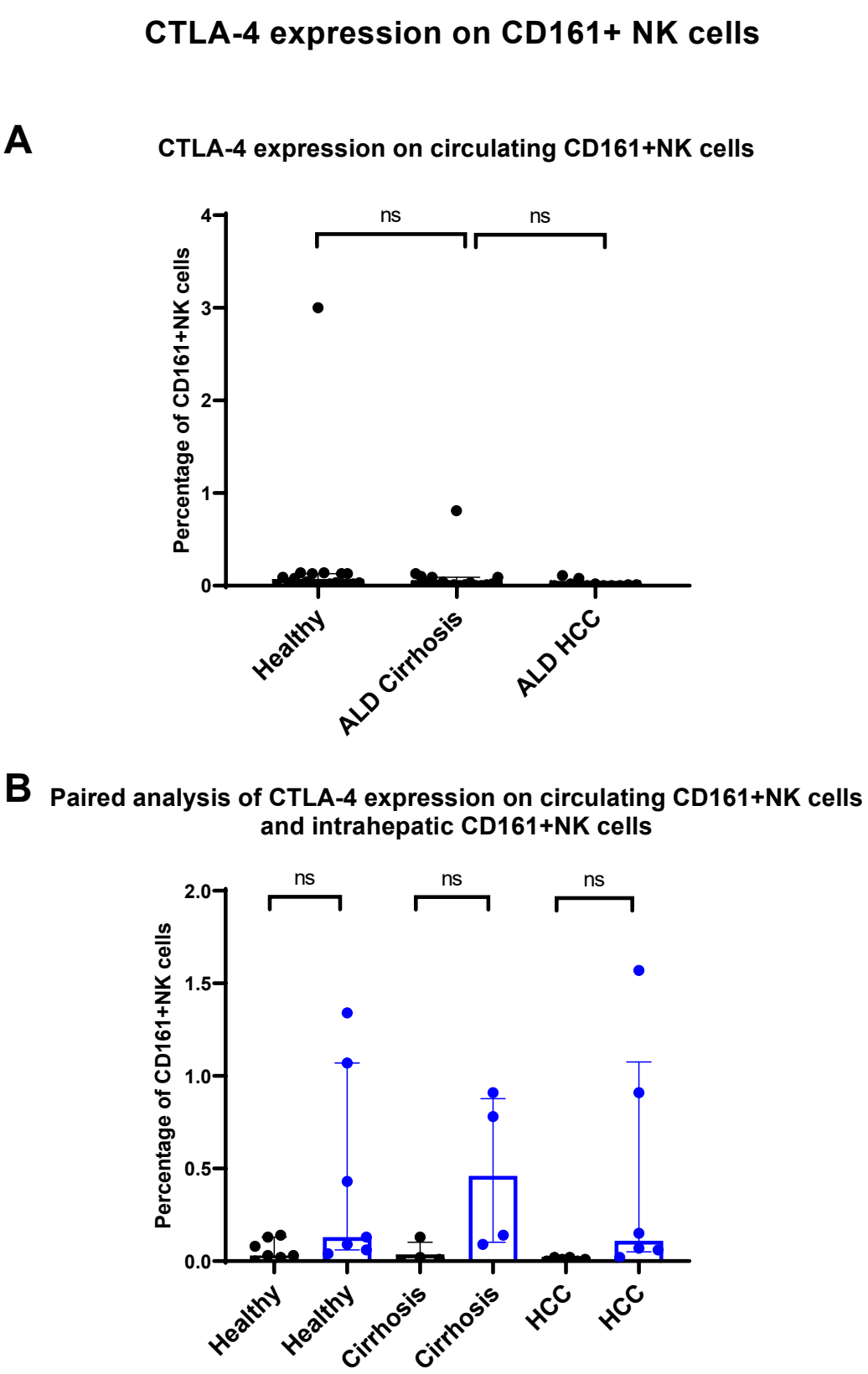


Figure 158 CTLA-4 expression on CD161+ NK cells. Peripheral blood mononuclear cells (PBMCs) and intrahepatic mononuclear cells (IMNCs) were phenotyped following surface staining using antibodies as described in Phenotyping panel 2 in the methods (Chapter 2, Table 3). Graph A demonstrates the

*percentage of CD161+ NK cells in the circulation that express CTLA-4 in healthy volunteers (n=21), patients with cirrhosis from alcohol related liver disease (ALD Cirrhosis; n=18) and patients with HCC on a background of ALD cirrhosis (ALD HCC; n=11; patient demographics in Table 19). Comparisons were made using Mann-Whitney tests. Graph B demonstrates the percentage of CD161+ NK cells that express CTLA-4 in the liver (data in blue) compared to in the circulation from the same donor (data in black). Healthy livers were normal liver margins from patients undergoing liver resection for indications other than primary cancer (n=7). Patients with cirrhosis or HCC had an underlying non-viral aetiology, and all patients with HCC had underlying cirrhosis (Cirrhosis n=4, HCC n=6). Comparisons between paired samples were made using the Wilcoxon Match-pairs test. Graphs display individual values with the median value displayed by the bar. Error bars represent the interquartile range. P values are denoted on the figures as follows: * p<0.05, ** p<0.01, *** p<0.001, **** p<0.0001).*

5.3.2 CD161 expression on circulating and liver infiltrating T cells

Phenotyping of circulating and intrahepatic T cells was undertaken to see if there is an increase in CD161 expressing T cells in cirrhosis and/or HCC.

Peripheral blood mononuclear cells and intrahepatic mononuclear cells were surface stained as described in methods using Phenotyping Panel 2 (Chapter 2, Table 3) and CD161+ cells were selected as demonstrated in the gating strategies below (see Table 19 for patient demographics and Figures 159 and 160).

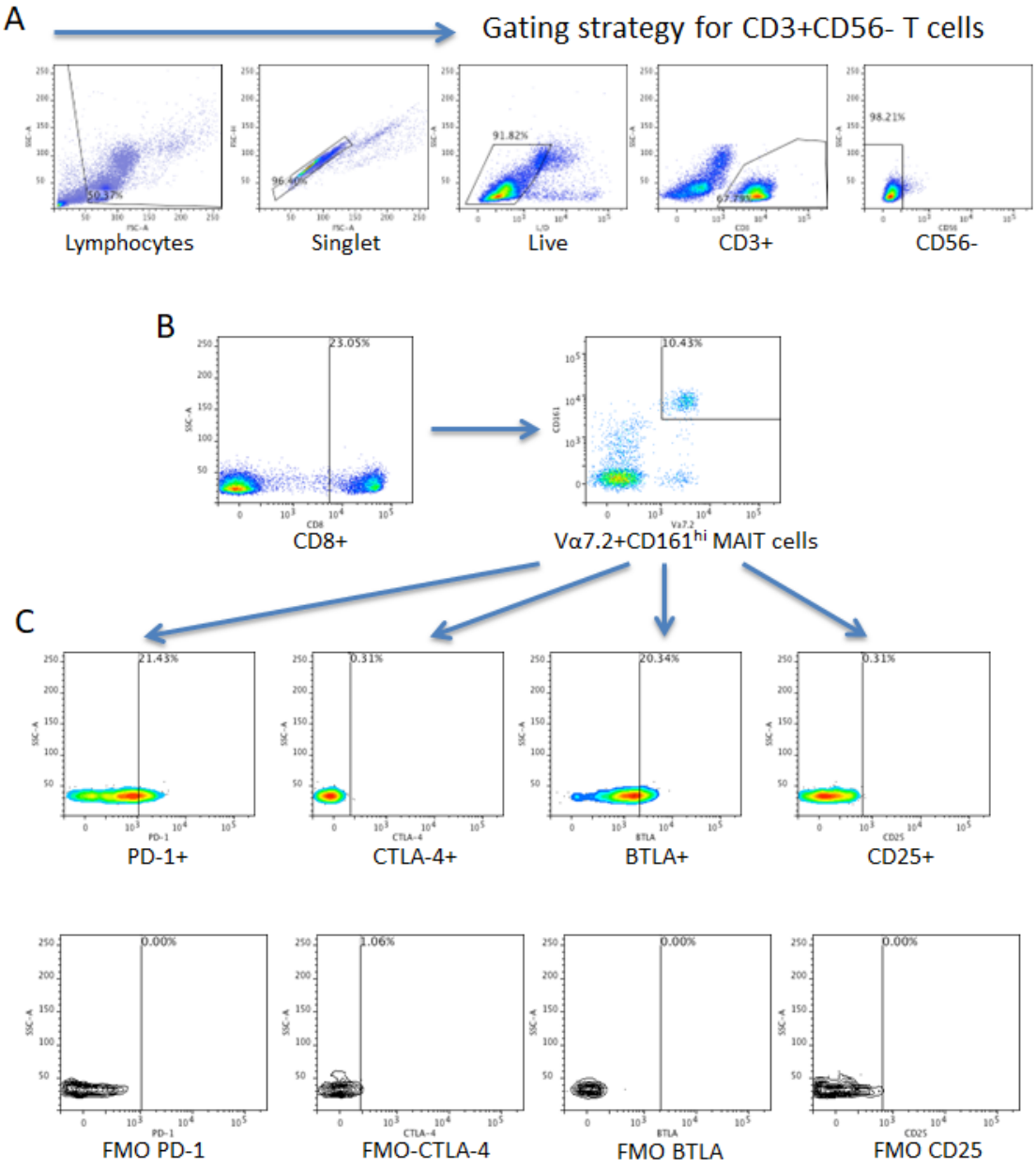


Figure 159 Gating strategy for identifying CD3+CD8+CD161^{hi}Vα7.2+ MAIT cells and the subsequent proportions of these cells that have PD-1, CTLA-4, BTLA and CD25 surface expression. Gating strategy demonstrated on peripheral blood mononuclear cells (PBMCs) extracted from a blood sample from a healthy volunteer. A) PBMCs and intrahepatic mononuclear cells (IMNCs) extracted from patients and healthy donors were phenotyped with Phenotyping Panel 2 as described in methods (Chapter 2, Table 3). T cells were identified using flow cytometry following the gating strategy displayed: gating on lymphocytes on a forward and side scatter plot, identifying singlet live cells, selecting CD3 positive cells that are CD56 negative. B) MAIT cells were identified by selecting CD8+ T cells and then selecting Vα7.2+CD161hi T cells (MAIT cells). C) PD-1, CTLA-4, BTLA and CD25 positivity on MAIT cells was

identified. Gates for PD-1, CTLA-4, BTLA and CD25 were set using cells surface stained with all antibodies apart from the antibody of interest (fluorescence minus one, FMO) as demonstrated.

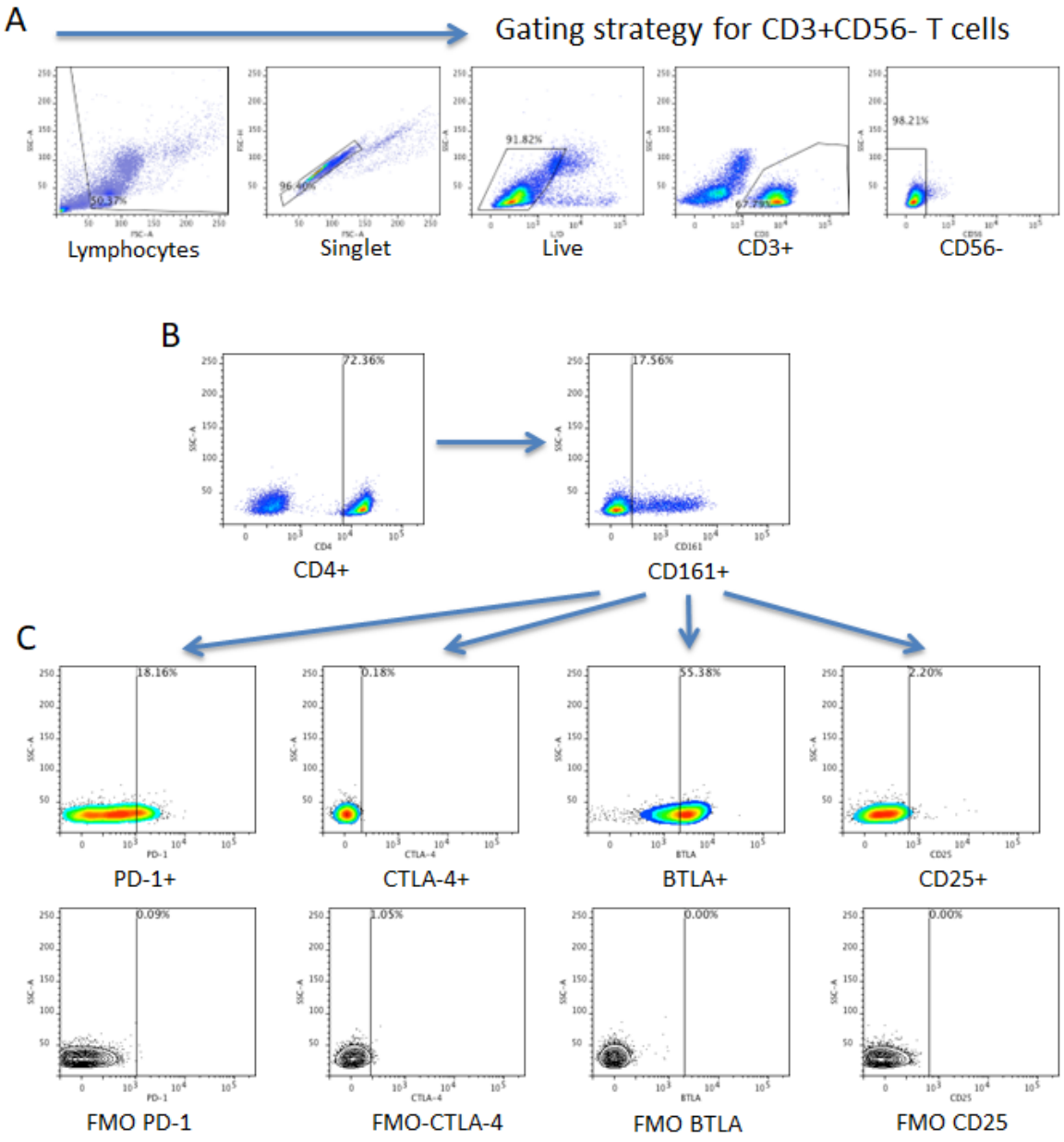


Figure 160 Gating strategy for identifying CD3+CD4+CD161+ T cells and the subsequent proportions of these cells that have PD-1, CTLA-4, BTLA and CD25 surface expression. Gating strategy demonstrated on peripheral blood mononuclear cells (PBMCs) extracted from a blood sample from a healthy volunteer. A) PBMCs and intrahepatic mononuclear cells (IMNCs) extracted from patients and healthy donors were phenotyped with Phenotyping Panel 2 as described in methods (Chapter 2, Table 3). T cells were identified using flow cytometry following the gating strategy displayed: gating on lymphocytes on a forward and side scatter plot, identifying singlet live cells, selecting CD3 positive cells

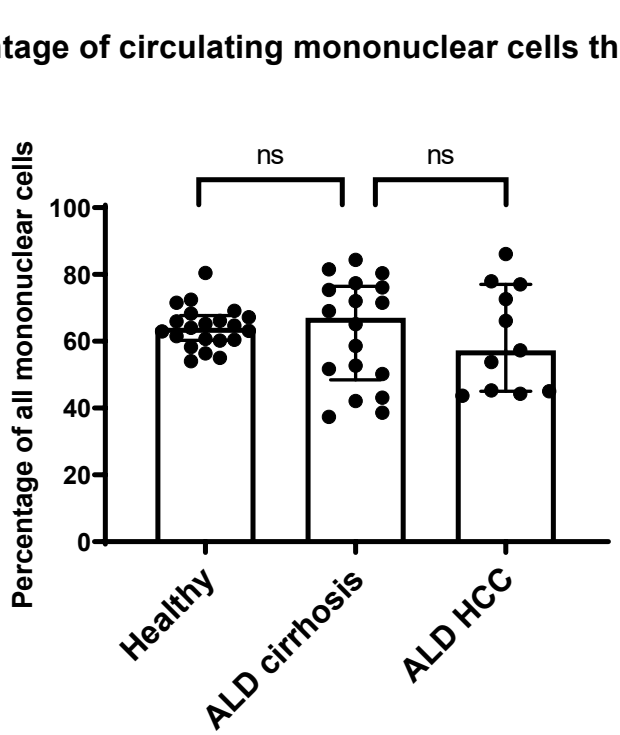
that are CD56 negative. B) CD4+ T cells were selected and then CD161+T cells were selected. C) PD-1, CTLA-4, BTLA and CD25 positivity on CD4+CD161+ was identified. Gates for PD-1, CTLA-4, BTLA and CD25 were set using cells surface stained with all antibodies apart from the antibody of interest (fluorescence minus one, FMO) as demonstrated.

There were no differences in the proportion of total circulating T cells or the proportion of intrahepatic T cells in these patient samples used (Figure 161).

The proportions of CD161 positive T cells, identified as mucosal associated invariant T (MAIT) cells (CD3+CD8+CD161hiVα7.2+ T cells) and CD4+CD161+ T cells, were determined (Figures 162 and 163). MAIT cells made up less than 10% of circulating T cells and less than 20% of intrahepatic T cells in health and in disease. However, there was a significant reduction in the circulating proportion of MAIT cells in both the cirrhosis group and the HCC group of patients in comparison to healthy volunteers (0.22% in cirrhosis (median percentage, n=21) vs 1.58% in healthy volunteers (median percentage, n=18),p=0.0002; 1.58% in healthy volunteers (median percentage, n=11) vs 0.09% in HCC (median percentage, n=15), p<0.0001). There were no significant differences in the proportion of intrahepatic MAIT cells but intrahepatic T cell data was limited due to limited numbers of samples.

Percentage of mononuclear cells that are CD3+CD56-T cells in the circulation and in the liver

A



B

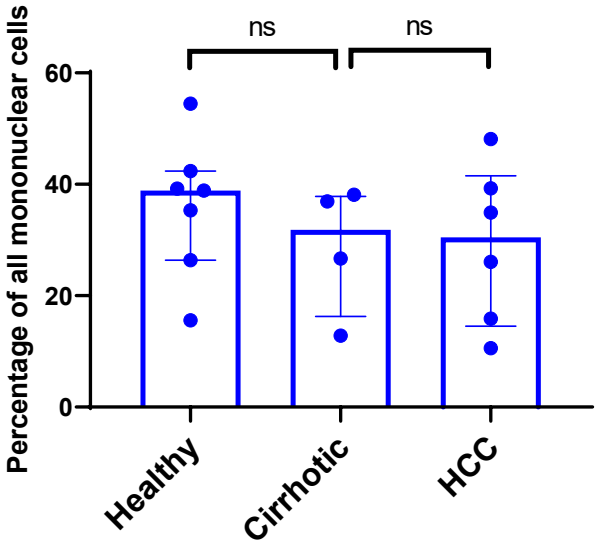


Figure 161 Percentage of mononuclear cells that are CD3+CD56-T cells in the circulation and in the liver. Peripheral blood samples were taken from healthy volunteers (n=21), patient with cirrhosis secondary to alcohol related liver disease (ALD cirrhosis, n=18) and patients with hepatocellular

*carcinoma (HCC) secondary to ALD cirrhosis (ALD HCC; n=11; see Table 19 for patient demographics). Intrahepatic mononuclear cells were extracted from the livers from patients undergoing resection for reasons other than primary liver cancer (n=7), liver explants with cirrhosis (n=4) and livers undergoing resection for HCC (n=6; demographics outlined in Table 9). Peripheral blood and intrahepatic mononuclear cells were isolate, stained using Phenotyping Panel 2 (as described in methods, Chapter 2, Table 3), and acquired using flow cytometry. CD3+CD56- lymphocytes (T cells) were identified and measured as a proportion of the total mononuclear cells. Graph A displays the percentage of peripheral blood mononuclear cells that are T cells. Graph B displays the percentage of intrahepatic mononuclear cells that are T cells. Comparisons were made using Mann-Whitney tests. Graphs display individual values with the median value displayed by the bar. Error bars represent the interquartile range. P values are denoted on the figures as follows: * p<0.05, ** p<0.01, *** p<0.001, **** p<0.0001).*

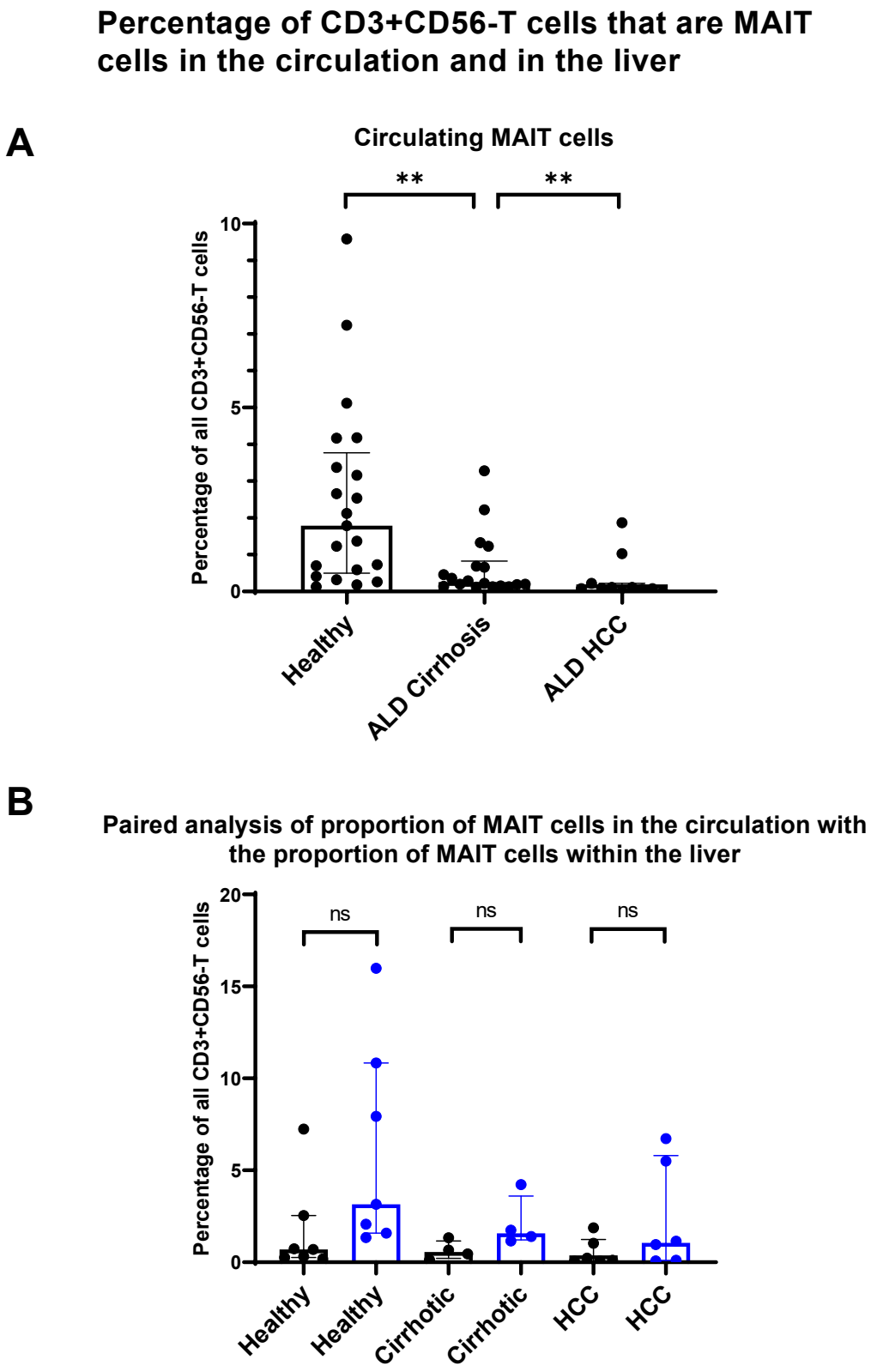


Figure 162 The percentage of CD3+CD56-T cells that are MAIT cells in the circulation and in the liver. Peripheral blood mononuclear cells (PBMCs) were isolated from healthy volunteers (n=21), patient with cirrhosis secondary to alcohol related liver disease (ALD cirrhosis, n=18) and patients with

*hepatocellular carcinoma (HCC) secondary to ALD cirrhosis (ALD HCC; n=11; see Table 19 for patient demographics). Intrahepatic mononuclear cells (IMNCs) were extracted from the livers from patients undergoing resection for reasons other than primary liver cancer (n=7), liver explants with cirrhosis (n=4) and livers undergoing resection for HCC (n=6; demographics outlined in Table 9). PBMCs and IMNCs were stained using Phenotyping Panel 2 (as described in methods, Chapter 2, Table 3), and acquired using flow cytometry. MAIT cells were identified and measured as a proportion of the total CD3+CD56-T cells in the circulation or in the liver. Graph A displays the percentage of CD3+CD56-T cells that are MAIT cells in the circulation. Comparisons were made using Mann-Whitney tests. Graph B displays a paired analysis of the percentage of intrahepatic CD3+CD56-T cells that are MAIT cells (data in blue) compared to the percentage of circulating CD3+CD56-T cells that are MAIT cells in the same patient. Comparisons were made using the matched-pairs Wilcoxon test. Graphs display individual values with the median value displayed by the bar. Error bars represent the interquartile range. P values are denoted on the figures as follows: * p<0.05, ** p<0.01, *** p<0.001, **** p<0.0001).*

CD4+CD161+T cells interestingly were increased in proportion in the circulation in patients with cirrhosis compared to healthy volunteers (27.5% vs 15.5%, p=0.008, median percentages respectively). There was also an increase in proportion in intrahepatic CD4+CD161+ T cells in cirrhotic livers in comparison to healthy livers.

In order to understand the state of these cells in health and disease, checkpoint inhibitor expression (PD-1, CTLA-4), BTLA expression and CD25 expression (as a marker of regulatory T cells) were assessed (Figures 164-167).

Percentage of CD3+CD56-T cells that are CD4+CD161+T cells in the circulation and in the liver

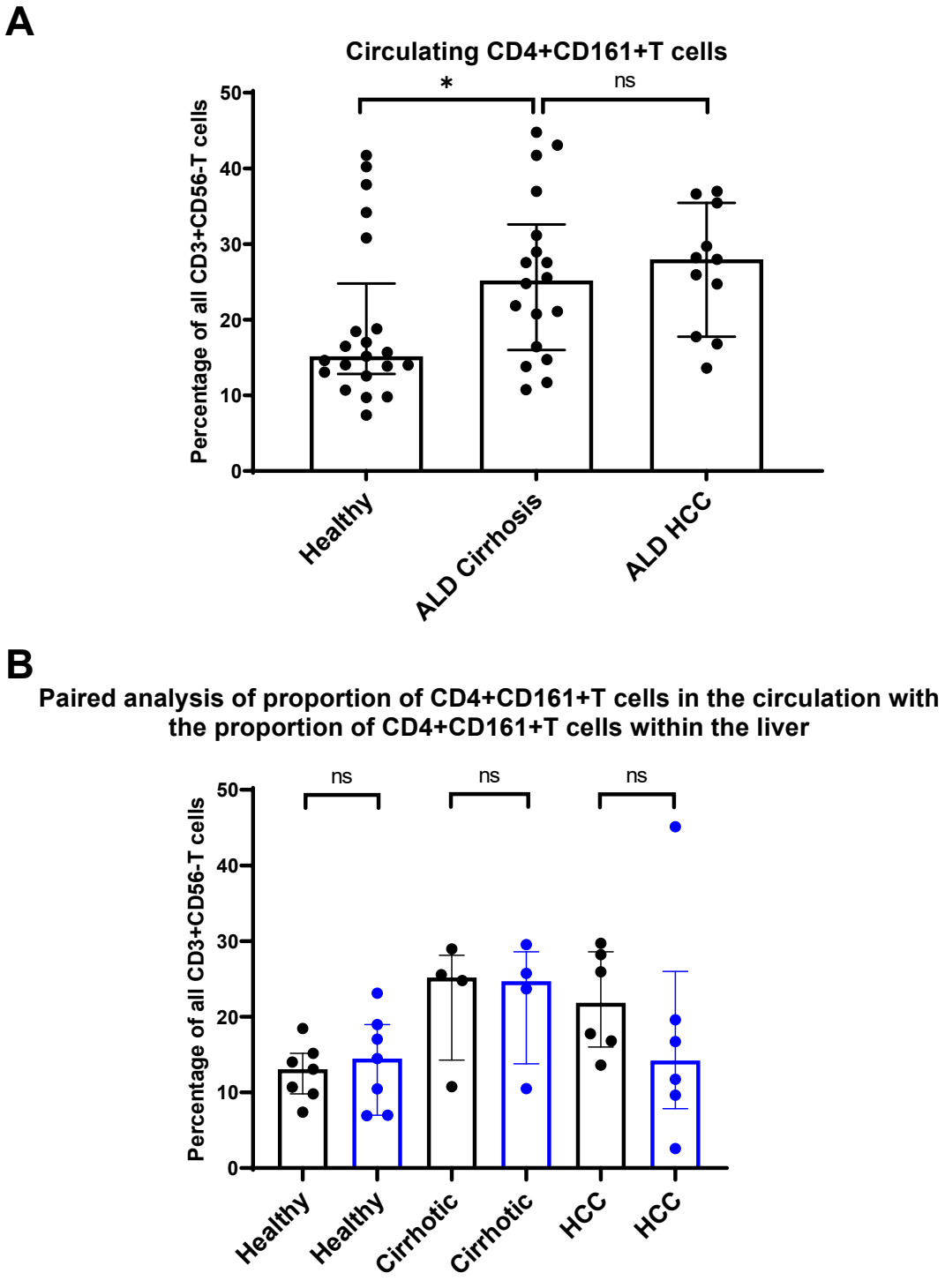


Figure 163 The percentage of CD3+CD56-T cells that are CD4+CD161+T cells in the circulation and in the liver. Peripheral blood mononuclear cells (PBMCs) were isolated from healthy volunteers (n=21), patient with cirrhosis secondary to alcohol related liver disease (ALD cirrhosis, n=18) and patients with

*hepatocellular carcinoma (HCC) secondary to ALD cirrhosis (ALD HCC; n=11; see Table 19 for patient demographics). Intrahepatic mononuclear cells (IMNCs) were extracted from the livers from patients undergoing resection for reasons other than primary liver cancer (n=7), liver explants with cirrhosis (n=4) and livers undergoing resection for HCC (n=6; demographics outlined in Table 9). PBMCs and IMNCs were stained using Phenotyping Panel 2 (as described in methods, Chapter 2, Table 3), and acquired using flow cytometry. CD4+CD161+T cells were identified and measured as a proportion of the total CD3+CD56-T cells in the circulation or in the liver. Graph A displays the percentage of CD3+CD56-T cells that are CD4+CD161+T cells in the circulation. Comparisons were made using Mann-Whitney tests. Graph B displays a paired analysis of the percentage of intrahepatic CD3+CD56-T cells that are CD4+CD161+T cells (data in blue) compared to the percentage of circulating CD3+CD56-T cells that are CD4+CD161+T cells in the same patient. Comparisons were made using the matched-pairs Wilcoxon test. Graphs display individual values with the median value displayed by the bar. Error bars represent the interquartile range. P values are denoted on the figures as follows: * p<0.05, ** p<0.01, *** p<0.001, **** p<0.0001).*

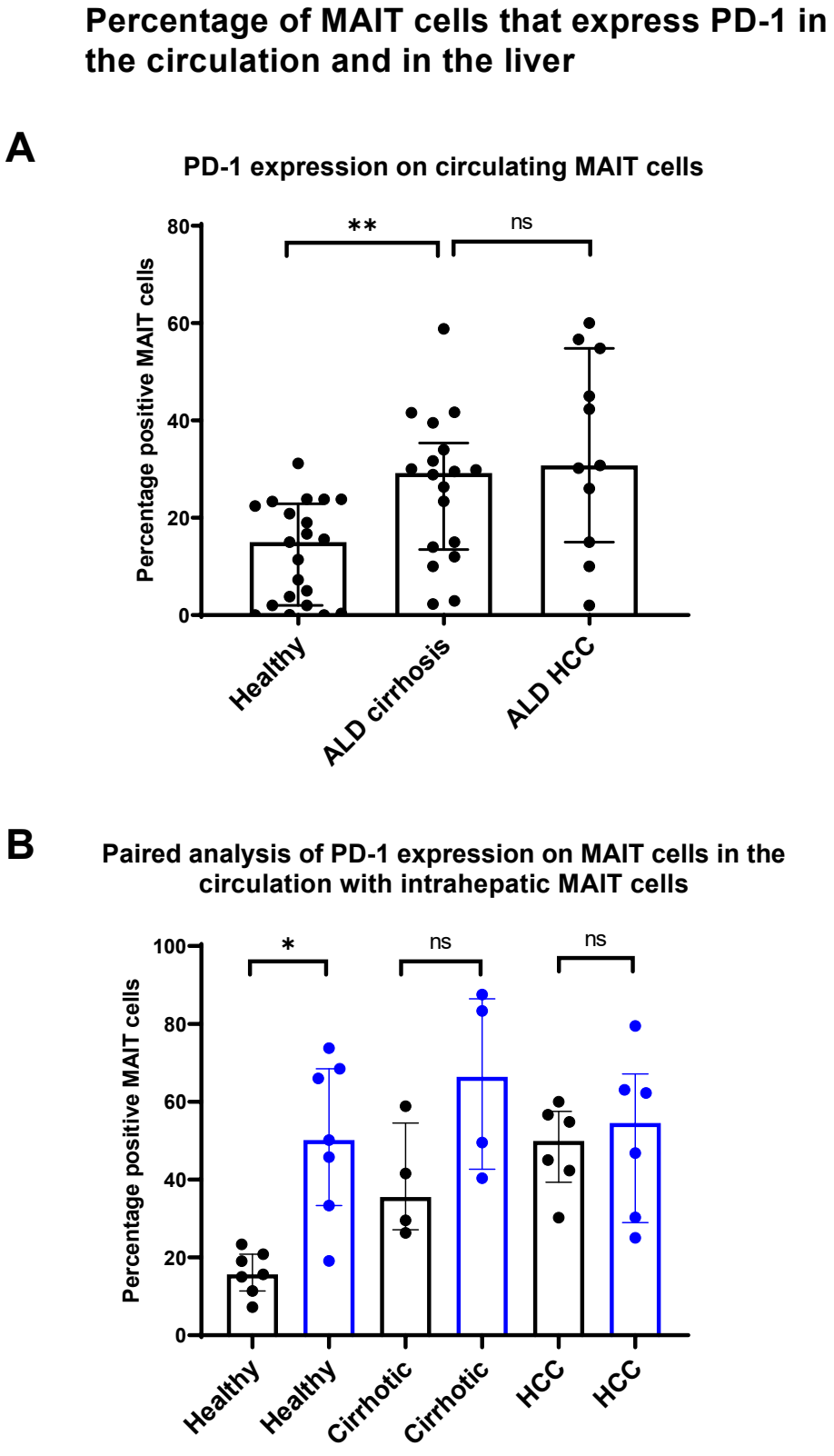


Figure 164 PD-1 expression on MAIT cells. Peripheral blood mononuclear cells (PBMCs) and intrahepatic mononuclear cells (IMNCs) were phenotyped following surface staining using antibodies

*as described in Phenotyping panel 2 in the methods (Chapter 2, Table 3). Graph A demonstrates the percentage of MAIT cells in the circulation that express PD-1 in healthy volunteers (n=21), patients with cirrhosis from alcohol related liver disease (ALD Cirrhosis; n=18) and patients with Hepatocellular carcinoma (HCC) on a background of ALD cirrhosis (ALD HCC; n=11; patient demographics in Table 19). Comparisons were made using Mann-Whitney tests. Graph B demonstrates the percentage of MAIT cells that express PD-1 in the liver (data in blue) compared to in the circulation from the same donor (data in black). Healthy livers were normal liver margins from patients undergoing liver resection for indications other than primary cancer (n-7). Patients with cirrhosis or HCC had an underlying non-viral aetiology, and all patients with HCC had underlying cirrhosis (full demographics in Chapter 3, Table 9; Cirrhosis n=4, HCC n=6). Comparisons between paired samples were made using the Wilcoxon Match-pairs test. Graphs display individual values with the median value displayed by the bar. Error bars represent the interquartile range. P values are denoted on the figures as follows: * p<0.05, ** p<0.01, *** p<0.001, **** p<0.0001).*

There was an increased expression of PD-1 on circulating MAIT cells in cirrhosis and HCC compared to the healthy group (Figure 164A). Overall there was an increased proportion of intrahepatic PD-1+MAIT cells compared to circulating MAIT cells in healthy states, but significance was lost in cirrhosis and HCC on a background of cirrhosis (Figure 164B).

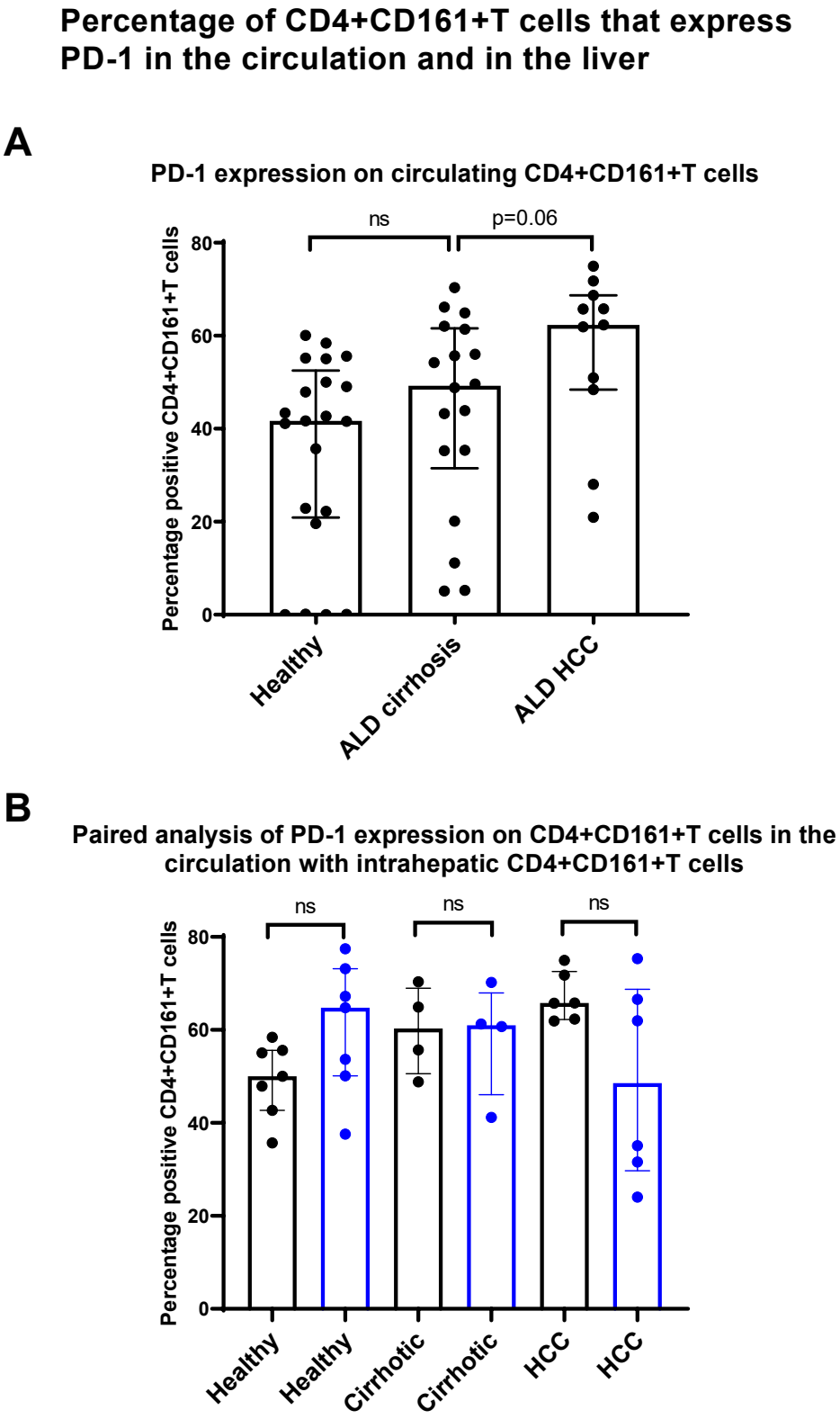


Figure 165 PD-1 expression on CD4+CD161+T cells. Peripheral blood mononuclear cells (PBMCs) and intrahepatic mononuclear cells (IMNCs) were phenotyped following surface staining using antibodies as described in Phenotyping panel 2 in the methods (Chapter 2, Table 3). Graph A demonstrates the

*percentage of CD4+CD161+T cells in the circulation that express PD-1 in healthy volunteers (n=21), patients with cirrhosis from alcohol related liver disease (ALD Cirrhosis; n=18) and patients with Hepatocellular carcinoma (HCC) on a background of ALD cirrhosis (ALD HCC; n=11; patient demographics in Table 19). Comparisons were made using Mann-Whitney tests. Graph B demonstrates the percentage of CD4+CD161+T cells that express PD-1 in the liver (data in blue) compared to in the circulation from the same donor (data in black). Healthy livers were normal liver margins from patients undergoing liver resection for indications other than primary cancer (n-7). Patients with cirrhosis or HCC had an underlying non-viral aetiology, and all patients with HCC had underlying cirrhosis (full demographics in Chapter 3, Table 9; Cirrhosis n=4, HCC n=6). Comparisons between paired samples were made using the Wilcoxon Match-pairs test. Graphs display individual values with the median value displayed by the bar. Error bars represent the interquartile range. P values are denoted on the figures as follows: * p<0.05, ** p<0.01, *** p<0.001, **** p<0.0001).*

There was an increasing proportion of PD-1+ CD4+CD161+T cells in the circulation in cirrhosis and HCC but it did not reach significance (Figure 165A). Paired analysis of circulating and intrahepatic CD4+CD161+T cells did not reveal a significant difference between the proportion of cells that are PD-1 positive (Figure 165B).

There were no significant differences in BTLA expression in health and disease states on MAIT or CD4+CD161+T cells in the circulation or on intrahepatic MAIT cells (Figures 166 and 167).

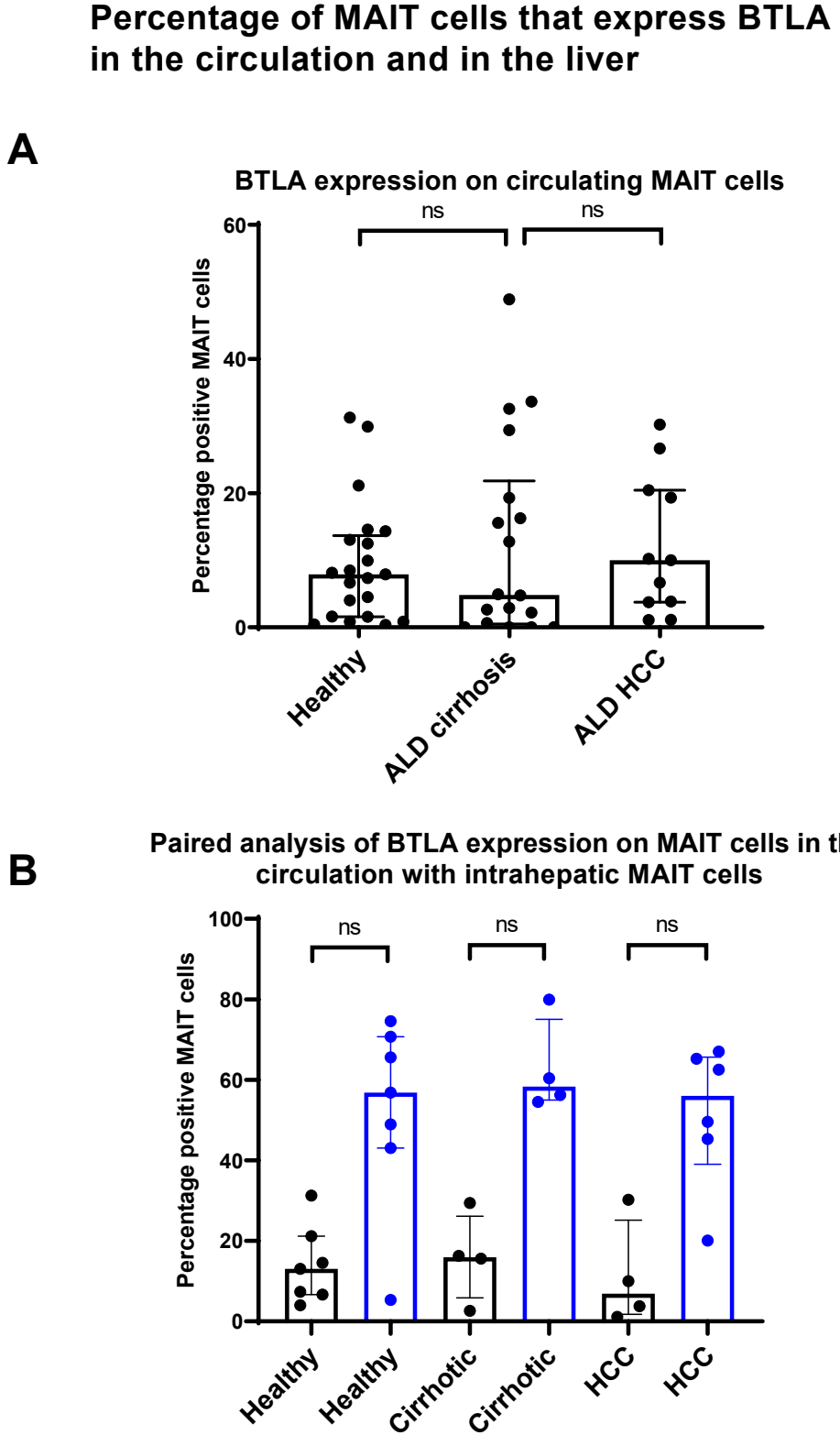


Figure 166 BTLA expression on MAIT cells. Peripheral blood mononuclear cells (PBMCs) and intrahepatic mononuclear cells (IMNCs) were phenotyped following surface staining using antibodies as described in Phenotyping panel 2 in the methods (Chapter 2, Table 3). Graph A demonstrates the

*percentage of MAIT cells in the circulation that express BTLA in healthy volunteers (n=21), patients with cirrhosis from alcohol related liver disease (ALD Cirrhosis; n=18) and patients with Hepatocellular carcinoma (HCC) on a background of ALD cirrhosis (ALD HCC; n=11; patient demographics in Table 19). Comparisons were made using Mann-Whitney tests. Graph B demonstrates the percentage of MAIT cells that express BTLA in the liver (data in blue) compared to in the circulation from the same donor (data in black). Healthy livers were normal liver margins from patients undergoing liver resection for indications other than primary cancer (n-7). Patients with cirrhosis or HCC had an underlying non-viral aetiology, and all patients with HCC had underlying cirrhosis (full demographics in Chapter 3, Table 9; Cirrhosis n=4, HCC n=6). Comparisons between paired samples were made using the Wilcoxon Match-pairs test. Graphs display individual values with the median value displayed by the bar. Error bars represent the interquartile range. P values are denoted on the figures as follows: * p<0.05, ** p<0.01, *** p<0.001, **** p<0.0001).*

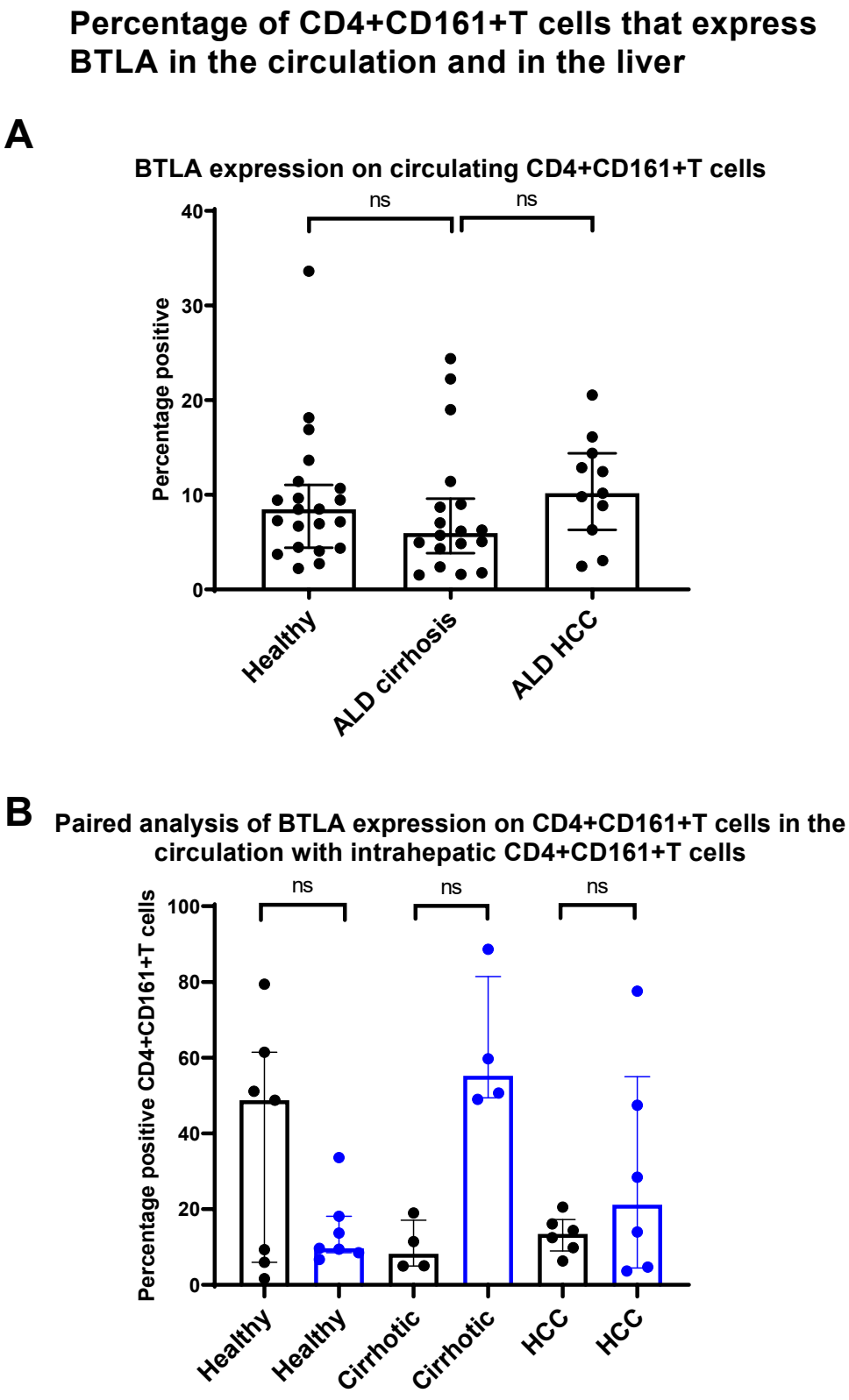


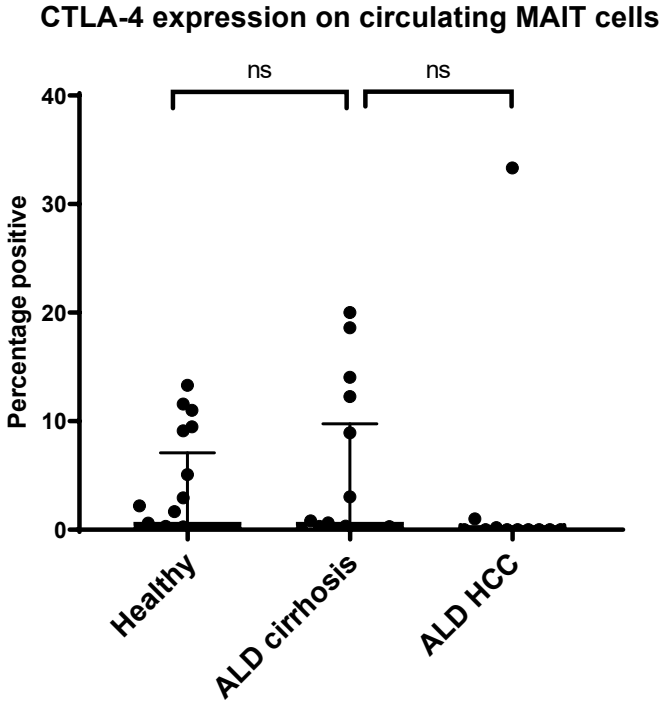
Figure 167 BTLA expression on CD4+CD161+T cells. Peripheral blood mononuclear cells (PBMCs) and intrahepatic mononuclear cells (IMNCs) were phenotyped following surface staining using antibodies as described in Phenotyping panel 2 in the methods (Chapter 2, Table 3). Graph A demonstrates the

*percentage of CD4+CD161+T cells in the circulation that express BTLA in healthy volunteers (n=21), patients with cirrhosis from alcohol related liver disease (ALD Cirrhosis; n=18) and patients with Hepatocellular carcinoma (HCC) on a background of ALD cirrhosis (ALD HCC; n=11; patient demographics in Table 19). Comparisons were made using Mann-Whitney tests. Graph B demonstrates the percentage of CD4+CD161+T cells that express BTLA in the liver (data in blue) compared to in the circulation from the same donor (data in black). Healthy livers were normal liver margins from patients undergoing liver resection for indications other than primary cancer (n-7). Patients with cirrhosis or HCC had an underlying non-viral aetiology, and all patients with HCC had underlying cirrhosis (full demographics in Chapter 3, Table 9; Cirrhosis n=4, HCC n=6). Comparisons between paired samples were made using the Wilcoxon Match-pairs test. Graphs display individual values with the median value displayed by the bar. Error bars represent the interquartile range. P values are denoted on the figures as follows: * p<0.05, ** p<0.01, *** p<0.001, **** p<0.0001).*

CTLA-4 expression was low on circulating MAIT cells and was expressed on less than 10% of the circulating CD4+CD161+T cells (Figures 168A and 169A). Paired analysis of circulating and intrahepatic T cells in the same donor however demonstrated a higher proportion of CTLA-4 expressing T cells in the liver (Figures 168B and 169B).

Percentage of MAIT cells that express CTLA-4 in the circulation and in the liver

A



B

Figure 168 CTLA-4 expression on MAIT cells. Peripheral blood mononuclear cells (PBMCs) and intrahepatic mononuclear cells (IMNCs) were phenotyped following surface staining using antibodies as described in Phenotyping panel 2 in the methods (Chapter 2, Table 3). Graph A demonstrates the

*percentage of MAIT cells in the circulation that express CTLA-4 in healthy volunteers (n=21), patients with cirrhosis from alcohol related liver disease (ALD Cirrhosis; n=18) and patients with Hepatocellular carcinoma (HCC) on a background of ALD cirrhosis (ALD HCC; n=11; patient demographics in Table 19). Comparisons were made using Mann-Whitney tests. Graph B demonstrates the percentage of MAIT cells that express CTLA-4 in the liver (data in blue) compared to in the circulation from the same donor (data in black). Healthy livers were normal liver margins from patients undergoing liver resection for indications other than primary cancer (n-7). Patients with cirrhosis or HCC had an underlying non-viral aetiology, and all patients with HCC had underlying cirrhosis (full demographics in Chapter 3, Table 9; Cirrhosis n=4, HCC n=6). Comparisons between paired samples were made using the Wilcoxon Match-pairs test. Graphs display individual values with the median value displayed by the bar. Error bars represent the interquartile range. P values are denoted on the figures as follows: * p<0.05, ** p<0.01, *** p<0.001, **** p<0.0001).*

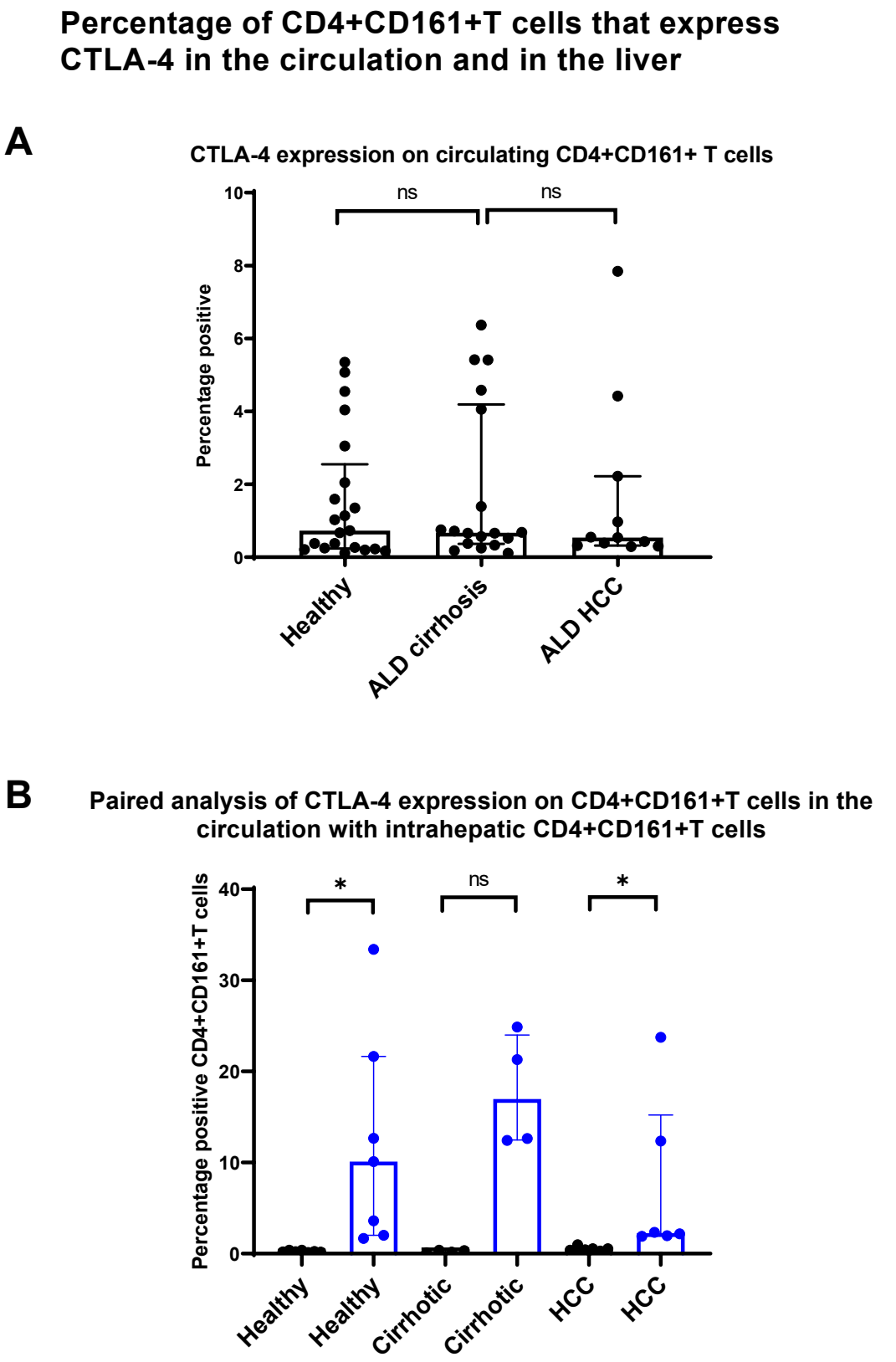


Figure 169 CTLA-4 expression on CD4+CD161+T cells. Peripheral blood mononuclear cells (PBMCs) and intrahepatic mononuclear cells (IMNCs) were phenotyped following surface staining using antibodies as described in Phenotyping panel 2 in the methods (Chapter 2, Table 3). Graph A demonstrates the

*percentage of CD4+CD161+T cells in the circulation that express CTLA-4 in healthy volunteers (n=21), patients with cirrhosis from alcohol related liver disease (ALD Cirrhosis; n=18) and patients with Hepatocellular carcinoma (HCC) on a background of ALD cirrhosis (ALD HCC; n=11; patient demographics in Table 19). Comparisons were made using Mann-Whitney tests. Graph B demonstrates the percentage of CD4+CD161+T cells that express CTLA-4 in the liver (data in blue) compared to in the circulation from the same donor (data in black). Healthy livers were normal liver margins from patients undergoing liver resection for indications other than primary cancer (n-7). Patients with cirrhosis or HCC had an underlying non-viral aetiology, and all patients with HCC had underlying cirrhosis (full demographics in Chapter 3, Table 9; Cirrhosis n=4, HCC n=6). Comparisons between paired samples were made using the Wilcoxon Match-pairs test. Graphs display individual values with the median value displayed by the bar. Error bars represent the interquartile range. P values are denoted on the figures as follows: * p<0.05, ** p<0.01, *** p<0.001, **** p<0.0001).*

CD25+MAIT cells formed less than 20% of circulating T cells and CD25+CD4+CD161+ T cells formed less than 10% of circulating T cells (Figures 170A and 171A). Again there were no significant differences between healthy and disease states in the proportions of CD25+ T cells.



Figure 170 CD25 expression on MAIT cells. Peripheral blood mononuclear cells (PBMCs) and intrahepatic mononuclear cells (IMNCs) were phenotyped following surface staining using antibodies as described in Phenotyping panel 2 in the methods (Chapter 2, Table 3). Graph A demonstrates the

*percentage of MAIT cells in the circulation that express CD25 in healthy volunteers (n=21), patients with cirrhosis from alcohol related liver disease (ALD Cirrhosis; n=18) and patients with Hepatocellular carcinoma (HCC) on a background of ALD cirrhosis (ALD HCC; n=11; patient demographics in Table 19). Comparisons were made using Mann-Whitney tests. Graph B demonstrates the percentage of MAIT cells that express CD25 in the liver (data in blue) compared to in the circulation from the same donor (data in black). Healthy livers were normal liver margins from patients undergoing liver resection for indications other than primary cancer (n-7). Patients with cirrhosis or HCC had an underlying non-viral aetiology, and all patients with HCC had underlying cirrhosis (full demographics in Chapter 3, Table 9; Cirrhosis n=4, HCC n=6). Comparisons between paired samples were made using the Wilcoxon Match-pairs test. Graphs display individual values with the median value displayed by the bar. Error bars represent the interquartile range. P values are denoted on the figures as follows: * p<0.05, ** p<0.01, *** p<0.001, **** p<0.0001).*

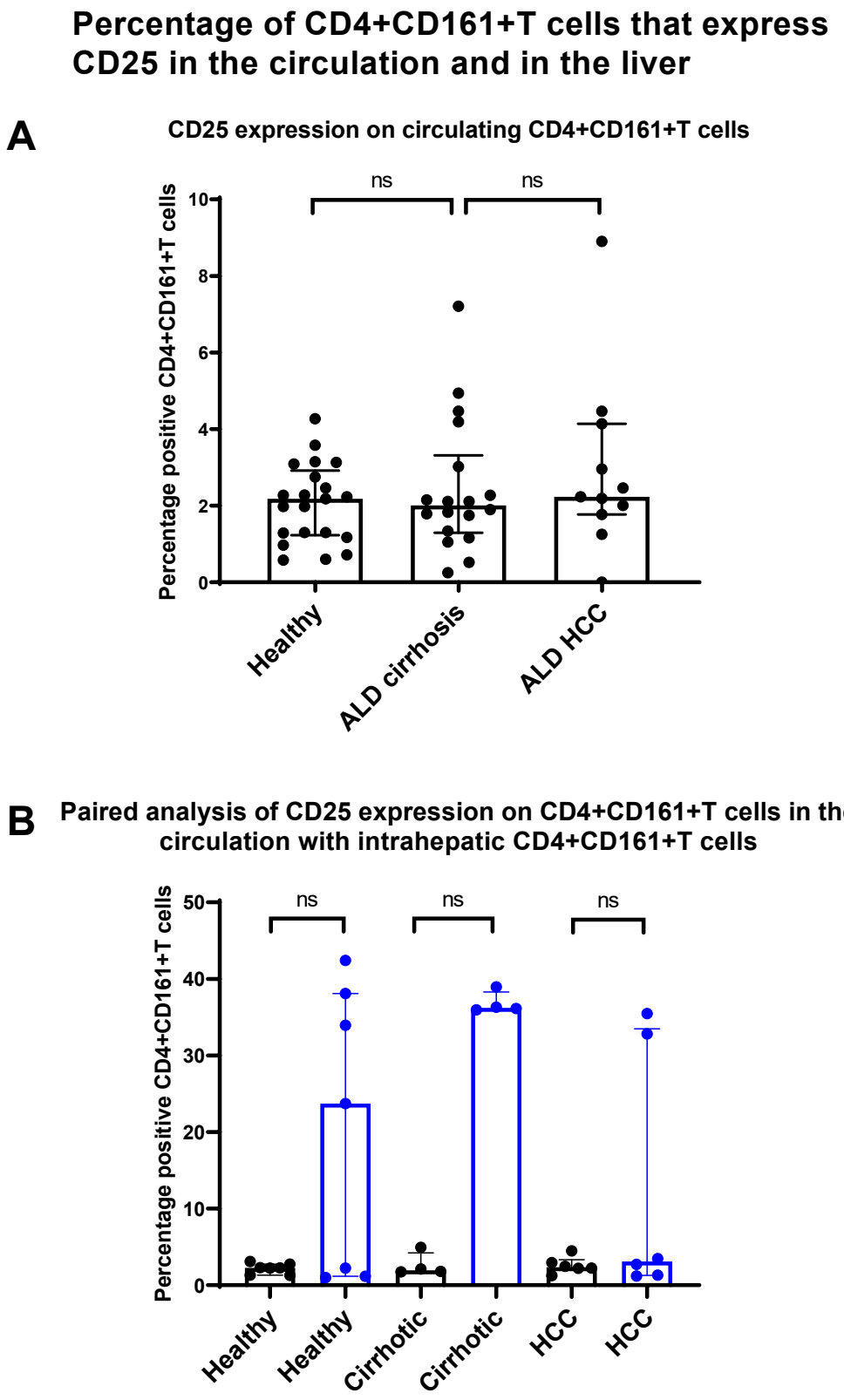


Figure 171 CD25 expression on CD4+CD161+T cells. Peripheral blood mononuclear cells (PBMCs) and intrahepatic mononuclear cells (IMNCs) were phenotyped following surface staining using antibodies as described in Phenotyping panel 2 in the methods (Chapter 2, Table 3). Graph A demonstrates the

*percentage of CD4+CD161+T cells in the circulation that express CD25 in healthy volunteers (n=21), patients with cirrhosis from alcohol related liver disease (ALD Cirrhosis; n=18) and patients with Hepatocellular carcinoma (HCC) on a background of ALD cirrhosis (ALD HCC; n=11; patient demographics in Table 19). Comparisons were made using Mann-Whitney tests. Graph B demonstrates the percentage of CD4+CD161+T cells that express CD25 in the liver (data in blue) compared to in the circulation from the same donor (data in black). Healthy livers were normal liver margins from patients undergoing liver resection for indications other than primary cancer (n-7). Patients with cirrhosis or HCC had an underlying non-viral aetiology, and all patients with HCC had underlying cirrhosis (full demographics in Chapter 3, Table 9; Cirrhosis n=4, HCC n=6). Comparisons between paired samples were made using the Wilcoxon matched-pairs test. Graphs display individual values with the median value displayed by the bar. Error bars represent the interquartile range. P values are denoted on the figures as follows: * p<0.05, ** p<0.01, *** p<0.001, **** p<0.0001).*

Overall, a significantly greater proportion of intrahepatic MAIT cells expressed PD-1 and CTLA-4 in comparison to circulating T cells. Circulating MAIT cells had a greater proportion expressing PD-1 in ALD cirrhosis and ALD HCC. Circulating CD4+CD161+T cells also did show an increased proportion expressing PD-1 in ALD cirrhosis and ALD HCC compared to healthy states, but this did not reach significance due to the wide variability seen in PD-1 expression in the patient groups. BTLA and CD25 expression was not significantly different in the circulation and there was wide variation in expression within the liver.

5.4 Functional consequences of the LLT1-CD161 interaction

5.4.1 LLT1 causes a reduction in the cytotoxic capacity of NK cells

In order to determine the effect of CD161 receptor engagement by LLT1 on NK cell function, Huh7 cells were stably transfected to overexpress LLT1 in an attempt to model the increased expression of LLT1 seen on hepatocytes in cirrhosis, and co-cultured with circulating NK cells as described below.

Surface staining for LLT1 revealed that naïve Huh7 cells constitutively express LLT1 at a low level (Figure 172). LLT1 was cloned by real-time PCR from Raji cells, tagged with a fluorescent protein (YFP) and Huh7 cells subsequently stably transfected using the Phoenix retroviral transfection system to overexpress LLT1 on the cell surface as described in methods, chapter 2 (Huh7-LLT1 YFP, Appendix 8.2 for LLT1 sequence). Flow cytometry demonstrated a transfection efficiency of 90% (Figure 172B).

PBMCs isolated from healthy donors (n=3) were incubated in triplicate for 4 hours in the presence of anti-CD107a antibody in a 5:1 ratio (PBMCs:target cell) (as described in Materials and Methods) with three target cell lines with different levels of LLT1 surface expression (naïve Huh7 cells with a low level of surface LLT1 expression, Huh7-LLT1 YFP transfectants with a high level of surface LLT1 expression and Jurkat cells with no demonstrable surface expression of LLT1 (Figure 172B)). Following the 4 hour incubation, the PBMCs were surface stained (antibodies described in Functional Panel 1, Table 4) and CD107a expression assessed as a marker of NK cell degranulation and cytotoxicity in CD161+ and CD161-NK cells (gating strategy demonstrated in Figure 173).

CD161+NK cells had lower expression levels of CD107a compared to CD161-NK cells when incubated with LLT1 expressing Huh7 cells. The difference in CD107a expression between CD161+ and CD161-NK cells was further exaggerated when the level of LLT1 expression was increased on the target cells (Figure 174). Increasing the expression of LLT1 on Huh7 cells resulted in an inhibition of NK cell cytotoxicity.

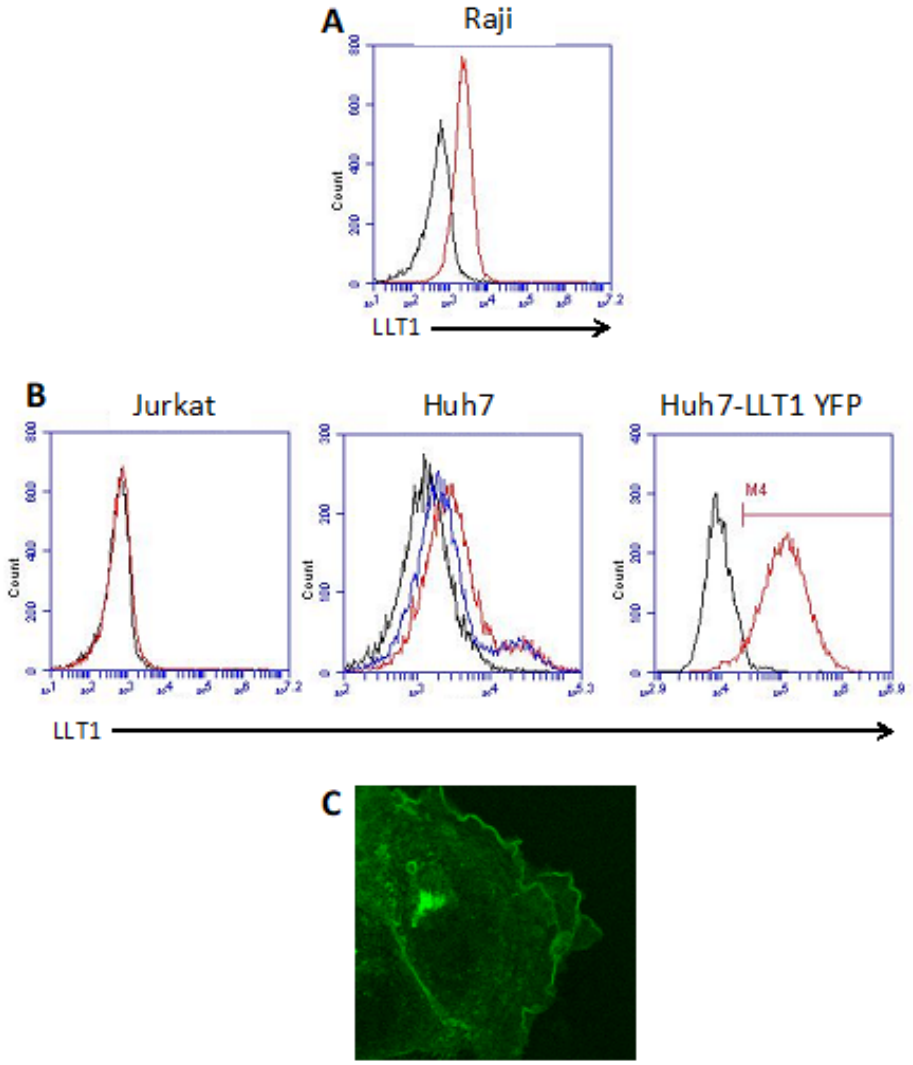


Figure 172 LLT1 expression in cell lines and transfection efficiency of Huh7 cells resulting in Huh7-LLT1 YFP transfectants.). Raji Cells, Jurkat cells, Huh7 cells and transfected Huh7-LLT1 cells were surface stained for LLT1 with anti-human LLT1 antibody (Clone 4C7, Abnova), and acquired with flow cytometry. Flow cytometry plots in A) and B) demonstrate positive LLT1 expression in red (black = unstained cells, blue = isotype control). A) Raji cells express LLT1. LLT1 was cloned using real-time PCR from cDNA produced from Raji cells (LLT1 sequence shown in Appendix B). B) Jurkat cells do not express LLT1. Huh7 cells constitutively express LLT1. Transfection of Huh7 cells with fluorescently tagged LLT1 resulted in increased surface expression of LLT1 (Huh7-LLT1 YFP). C) Confocal microscopy demonstrating the surface expression of LLT1 on Huh7-LLT1 YFP transfectants. Localisation of fluorescent YFP demonstrates the surface expression of LLT1-YFP on the transfected Huh7 cells.

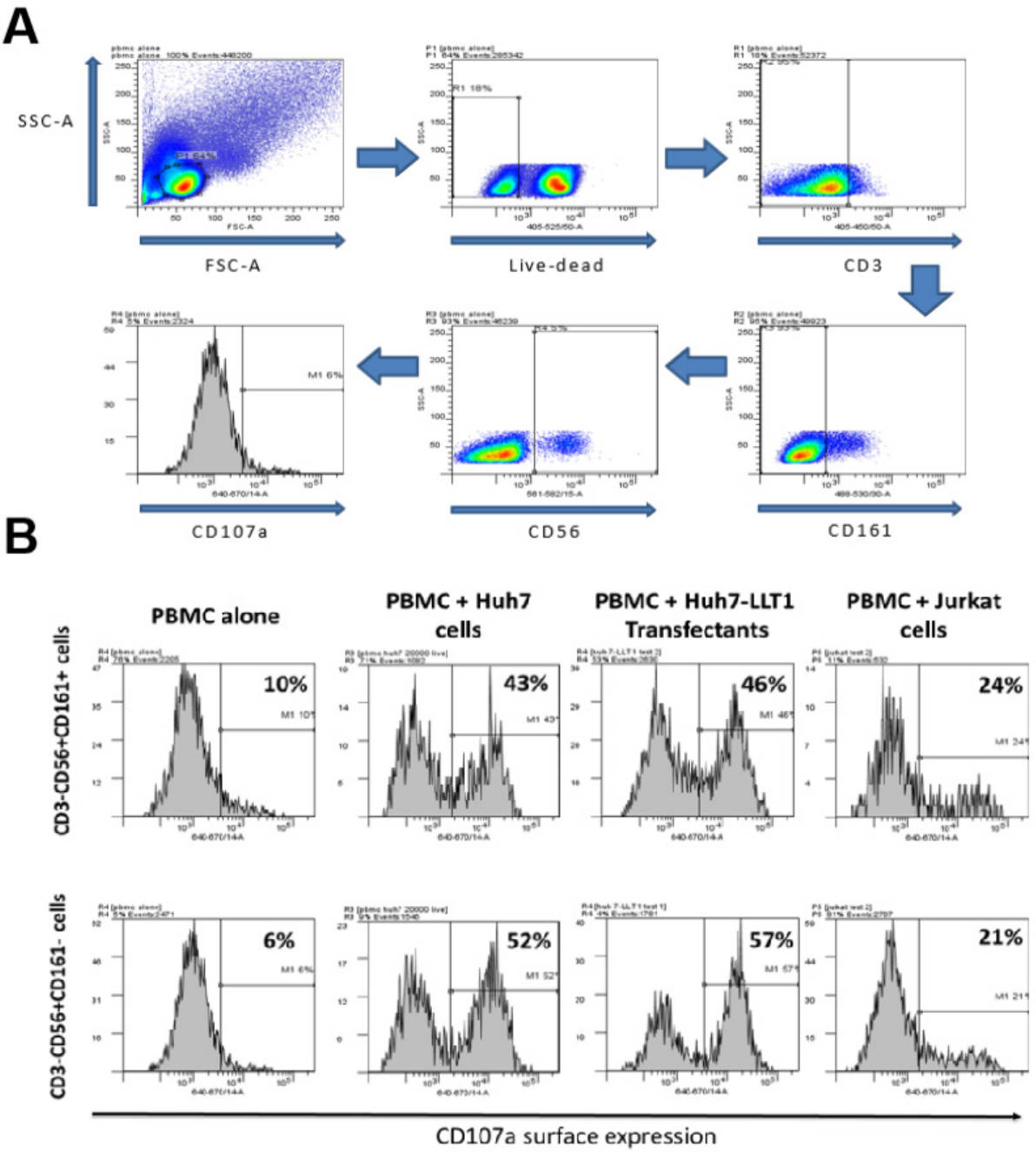


Figure 173 Gating strategy to assess CD107a expression in CD161+ and CD161- NK cells. PBMCs were co-cultured for 4hours in the presence of CD107a with cell line targets expressing LLT1 on the cell surface at varying levels (Jurkat cell with no expression of LLT1, Huh7 cells with low level LLT1 expression, Huh7-LLT1 YFP transfectants overexpressing LLT1; 5:1 PBMCs:Target ratio). Subsequent surface staining with CD3, CD56, CD161 (as described in the Functional Panel 1, Table 4) was conducted. A) Gating strategy utilised to identify CD161+ and CD161-NK cells. B) Gating strategy identifying CD107a expression on CD161+NK and CD161-NK cells as a measure of degranulation in response to target cells.

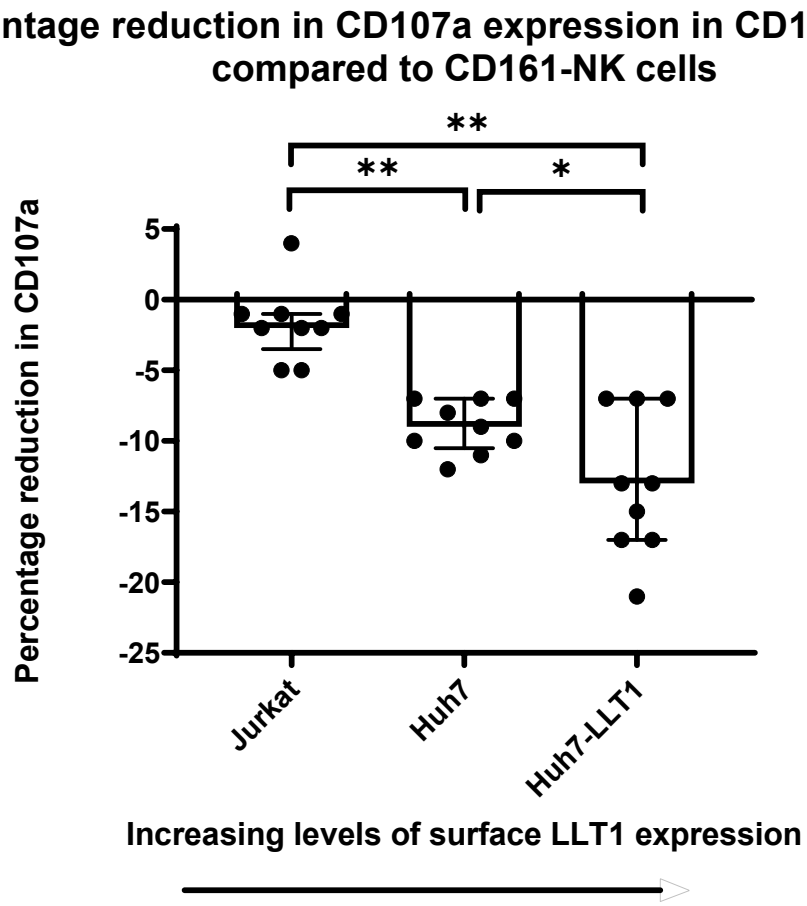


*Figure 174 LLT1 inhibits degranulation in CD161+NK cells. Peripheral blood mononuclear cells (PBMCs, n=3) from healthy donors were incubated in triplicate with target cells in a 5:1 ratio (PBMC: Target) in the presence of CD107a. Following 4 hours, PBMCs were surface stained with CD3, CD56 and CD161 and the percentage of CD161+NK cells and CD161-NK cells expressing CD107a measured. The difference in CD107a expression (percentage CD161+NK cells expressing CD107a – percentage CD161- cells expressing CD107a) was calculated for each target cell type. The difference in CD107a expression between CD161+ and CD161-NK cells increases with increased LLT1 levels on the target cell (as achieved by transfection). In contrast, the activity of CD161+ and CD161-NK cells is not significantly different when the target cell does not express LLT1 (Jurkat cells). Comparisons were made using the Wilcoxon matched-pairs test for the same donors. Graphs display individual values with the median value displayed by the bar. Error bars represent the interquartile range. P values are denoted on the figures as follows: * p<0.05, ** p<0.01, *** p<0.001, **** p<0.0001).*

5.5 Mechanism for LLT1 up-regulation on hepatocytes

Stimulation with toll-like receptor (TLR) ligands have been shown to up-regulate LLT1 on antigen presenting cells and activated haematopoietic cells(Germain et al., 2011; D. B. Rosen et al., 2008). The induction of LLT1 expression has also been demonstrated in viral infections(Koumbi et al., 2016; Satkunanathan et al., 2014). In cancer, TGF-β has been delineated as one possible mechanism of inducing LLT1 expression on glioblastoma tumours(Roth et al., 2007). Furthermore, TGF-β plays a significant role in multiple pathways for liver fibrosis and cirrhosis(Dooley & Ten Dijke, 2012).

To determine the mechanism of up-regulation of LLT1 in cirrhosis on hepatocytes, Huh7 cells were incubated in complete media supplemented with different cytokines or TLR ligands for 48 hours. Huh7 cells were then surface stained for LLT1 expression and compared control Huh7 cells incubated in complete media without any stimulation (Figures 175 and 176).

TGF-β significantly up-regulated LLT1 as demonstrated on Huh7 cells assessed after 48hours of stimulation (Figures 177 and 178). This increase in LLT1 expression following stimulation for 48hours with TGF-β stimulation was demonstrated on two different hepatocyte cell lines (Huh7 and Hep G2) and confirmed with two different surface staining secondary antibodies (mouse monoclonal anti-human CLEC2D (M01) clone 4C7, Abnova; goat polyclonal anti-human CLEC2D, R&D) (Figure 177).

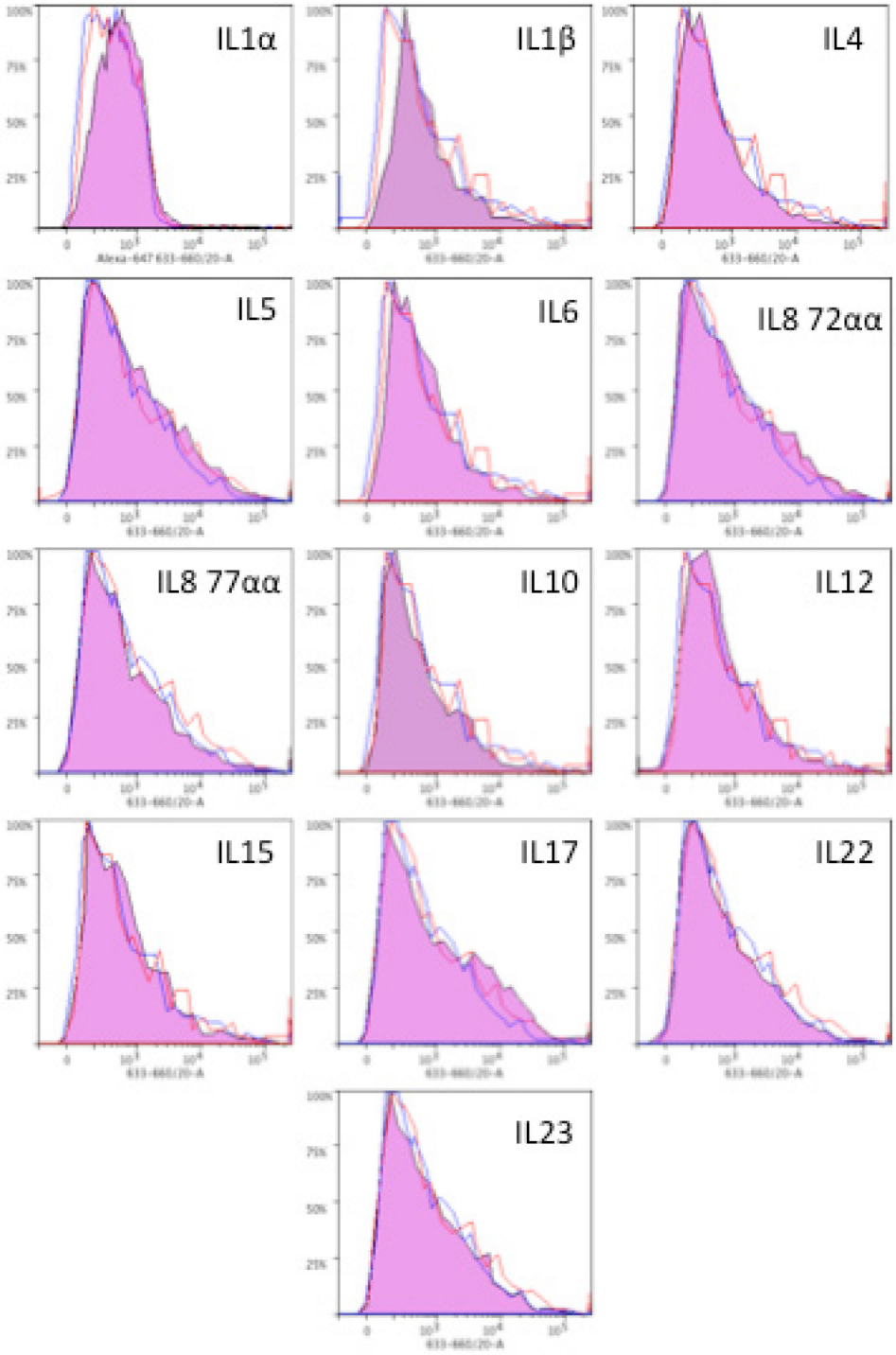


Figure 175 LLT1 surface expression on Huh7 cells post stimulation with Interleukins. LLT1 surface expression is demonstrated on Huh7 cells incubated for 24 hours with complete media (RPMI + 10% foetal calf serum + 1% penicillin-streptomycin) and supplemented with an interleukin as described in the methods (pink curve on flow cytometry plots show LLT1 expression, red curve demonstrated LLT1 expression in Huh7 cells in complete media alone for 24hours, blue curve demonstrates the negative control (Huh7 cells with the secondary antibody only), interleukin supplementing the media denoted in the top right hand corner of each plot).

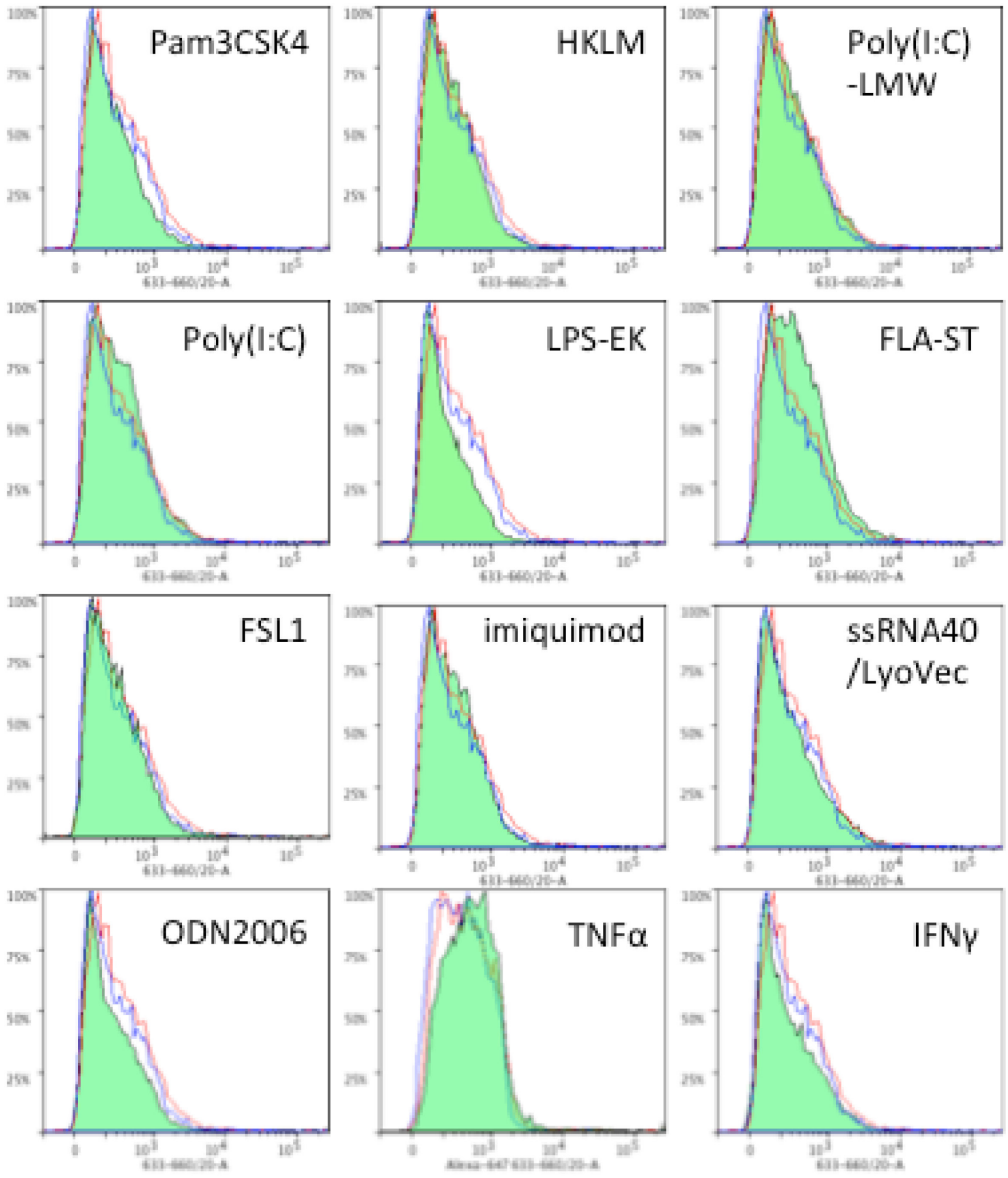


Figure 176 LLT1 surface expression on Huh7 cells post stimulation with TLR agonists. LLT1 surface expression was determined on Huh7 cells incubated for 24 hours with complete media (RPMI + 10% foetal calf serum + 1% penicillin-streptomycin) supplemented with at TLR ligand as described in the methods. LLT1 surface expression post incubation with TLR agonist supplemented complete media shown in green, with red for LLT1 surface expression on Huh7 cells in complete media alone for 24hours, and blue for control (Huh7 cells with the secondary antibody only; Invivogen Human TLR 1-9 agonist kit, TLR ligand supplementing the media is shown in the top right corner of each plot).

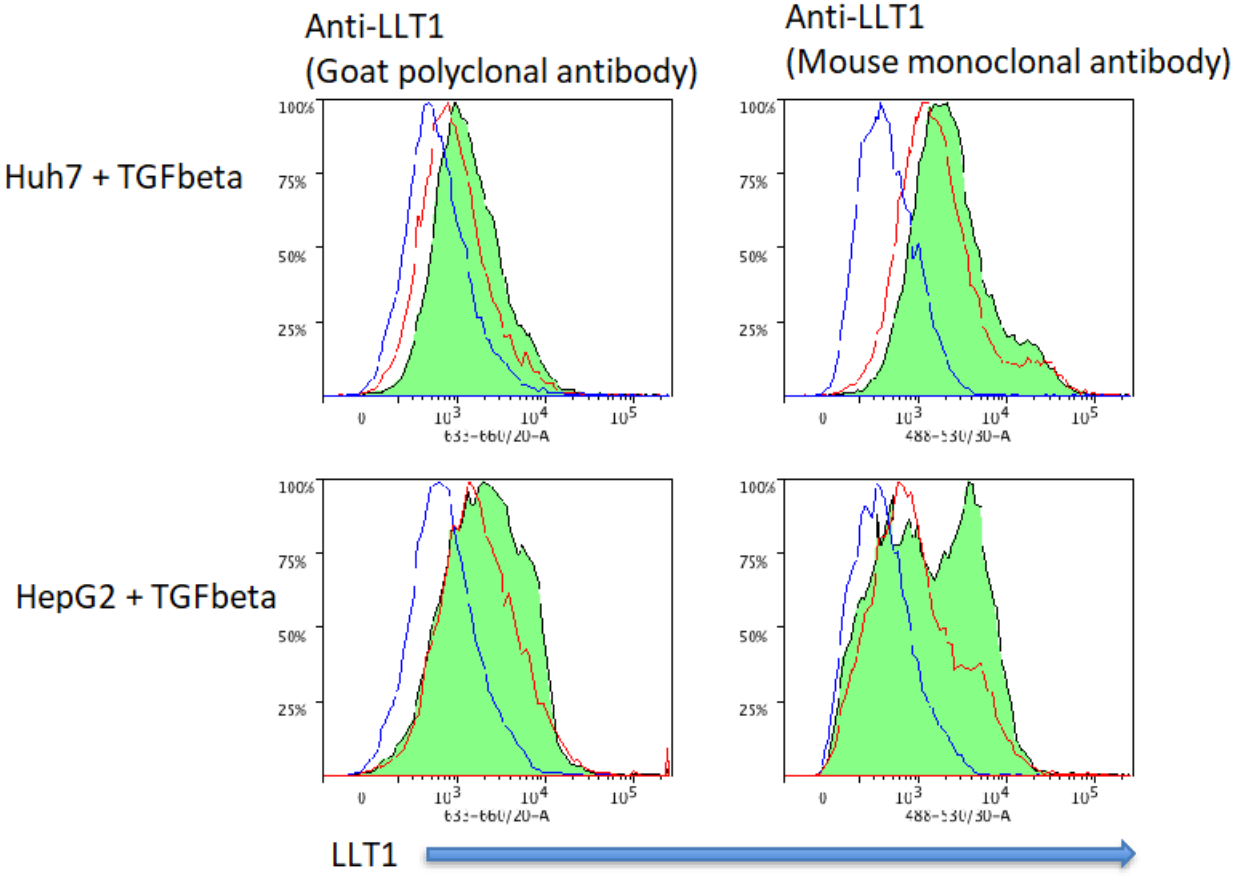


Figure 177 Tumour growth factor beta (TGF-β) upregulates LLT1 expression on liver cell lines. LLT1 expression was determined by surface staining for LLT1 with two different anti-LLT1 antibodies on Huh7 and HepG2 cell lines after incubation for 48 hours in complete media (RPMI + 10% foetal calf serum + 1% penicillin-streptomycin) supplemented with 10ng/ml TGF-β. Two different primary antibodies were tested: anti-human LLT1 goat polyclonal primary antibody (R and D) and anti-human LLT1 mouse monoclonal primary antibody (Abnova). Overlays demonstrate LLT1 expression post 48hours incubation in complete media supplemented with TGF-β (green), LLT1 expression post 48hours in complete media alone (red) and without the anti-LLT1 primary antibody (blue i.e. secondary antibody alone).

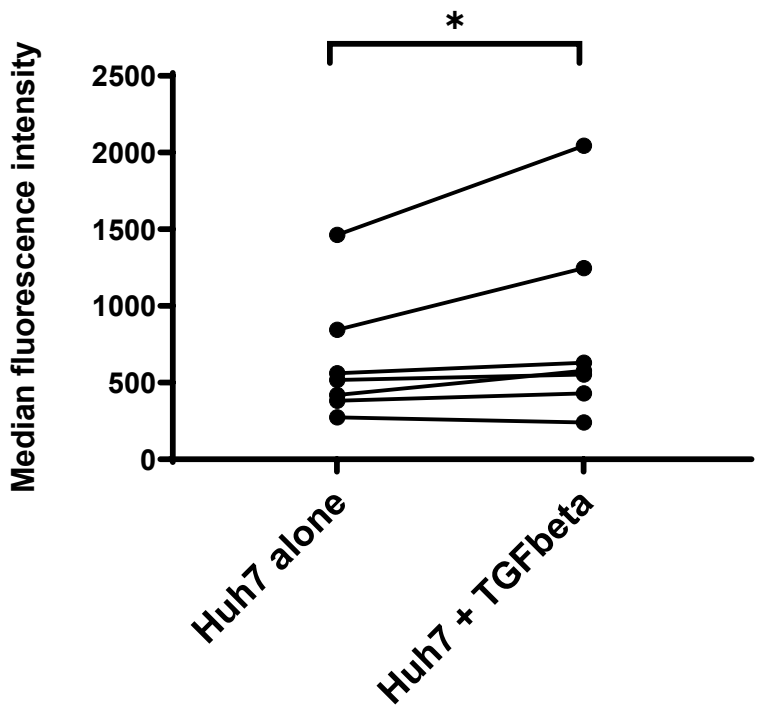


*Figure 178 Tumour growth factor beta (TGF-β) upregulates LLT1 expression on Huh7 cells. Huh7 cells were incubated for 48 hours in complete media (RPMI + 10% foetal calf serum + 1% penicillin-streptomycin) with or without supplementation with 10ng/ml TGF-β. Following this, the Huh7 cells were surface stained for LLT1 and the median fluorescence intensity of LLT1 was measured (n=7). Comparisons were made with the non-parametric Wilcoxon matched pairs signed-rank test. Graphs display individual values with the median value displayed by the bar. Error bars represent the interquartile range. P values are denoted on the figures as follows: * p<0.05, ** p<0.01, *** p<0.001, **** p<0.0001).*

5.6 Discussion

LLT1 expression is increased in the liver in cirrhosis, as demonstrated using immunohistochemistry and confirmed with relative quantification using real time PCR. Immunohistochemistry demonstrated a homogenous expression on hepatocytes in cirrhosis. However, expression in HCC tissue was variable, ranging from entirely negative expression in tumour tissue, patchy expression within the tumour or along the border of the tumour tissue or up-regulated on tumour tissue in relation to the background liver. Within the normal liver, hepatocytes did not express LLT1 but liver resident immune cells and sinusoidal cells were positive for LLT1, and accounted for a small proportion of CD68+ monocyte/Kupffer cells, vimentin positive hepatic stellate cells, CD20+ B cells and CD3+ T cells. LLT1 is not expressed on haematopoietic cells at rest but is induced following activation(Germain et al., 2011). Hence, the positively staining cells seen in these normal liver sections may represent activated cells, that have been activated on migrating through tumour tissue or in the liver resection process.

CD161+ NK cells comprise 70-90% of the healthy circulating NK cells and more than 90% of the intrahepatic NK cell population. The proportion of CD161+NK cells in the circulation was increased in cirrhosis, and significance persisted in patients with underlying ALD. In conjunction with the up-regulation of LLT1 on hepatocytes within the liver in cirrhosis, the CD161-LLT1 inhibitory interaction may be more meaningful in cirrhosis. Using the hepatocyte cell line Huh7, and stably transfecting these cells to overexpress LLT1 to model cirrhosis and a sub-group of HCC tumours, the CD161-LLT1 interaction is demonstrated to attenuate the cytotoxic response of CD161+NK cells to Huh7 cell targets. TGF-β significantly up-regulated LLT1 surface expression on Huh7 cells, and may explain the mechanism of induction of LLT1 expression on hepatocytes in cirrhosis. It would have been ideal to further ratify the data by adding a control group for the transfected Huh7 cells (i.e. Huh7 cells transfected with an empty vector) to ensure the effects of transfection seen are due to the LLT1-CD161 interaction rather than the transfection vector. However, the inhibition of NK cell cytotoxicity seen here is in keeping with published data (D. B. Rosen et al., 2005).

Inhibition of NK cell cytotoxicity via the LLT1-CD161 interaction may result in compromised tumour surveillance with impaired ability for NK cells to lyse and eliminate transformed cells, contributing to the pre-malignant state that characterises cirrhosis. Furthermore, Germain et al demonstrate that engagement of CD161 by LLT1 results in a reduction of IFNγ production(Germain et al., 2011). This in turn may impair monocyte/macrophage activation, potentially increasing susceptibility to infection.

Heterogeneity in HCC represents one of the key areas of difficulty in devising anti-cancer chemotherapy. Exciting progress in the field of immunotherapy provides more hope for tailoring therapies in heterogeneic cancers. The up-regulation of LLT1 in the liver in cirrhosis, coupled with the higher surface expression of CD161 on NK cells within the liver suggests direct inhibition of NK cell function within cirrhotic livers and may contribute to cirrhosis as a pre-malignant state and dysfunction of tumour surveillance due to attenuated NK cell responses. Wu et al demonstrated reduced NK cell numbers, exhausted and with impaired function secondary to inhibitory crosstalk with monocytes(Y. Wu et al., 2013). Whilst LLT1 expression in HCC tumour tissue is variable, in cases where LLT1 is expressed in tumour tissue and background cirrhotic liver epithelium, the CD161-LLT1 interaction may prove a useful therapy to block the inhibitory signal in NK cells as they traverse through the liver to the tumour tissue. Blockade of the LLT1-CD161 interaction has been shown to enhance tumour lysis in other cancers(Marrufo et al., 2018).

The use of checkpoint inhibitors has been an exciting advance in the field of immunotherapy for cancer. Indeed there are now approved therapies for PD-1 blockade in the treatment of HCC and evidence for CTLA-4 blockade. Whilst tumour tissue expression of these receptors was not assessed here, checkpoint inhibitor expression was determined on CD161+ NK and T cells in order to determine if checkpoint blockade may help further enhance the function of these cells.

PD-1 expression on circulating CD161+NK cells was minimal (<5%) but there was a significant increase, though small, in circulating CD161+PD-1+NK cells in HCC. Intrahepatic NK cells however had a significant PD-1+NK cells subset, with CD161+PD-1+NK cells comprising 25-

43% of intrahepatic NK cells within healthy livers. Similarly, an increased proportion of intrahepatic CD8+ and CD4+ CD161+ T cells expressed PD-1 compared to circulating T cells. The paucity of intrahepatic samples limited the ability to determine reliably variations in NK cell sub-populations in different disease groups.

PD-1 expression on tumour infiltrating T cells has been well described as an 'exhausted' phenotype, resulting in reduced CD8+ T cell cytotoxicity(Chang et al., 2017; Chemnitz et al., 2004; Pinato et al., 2020). There is emerging evidence for PD-1 being an important inhibitory receptor for NK cells in addition to the correlation of PD-1 expression on NK cells with worse outcomes in many cancers(Y. Liu et al., 2017; Siu et al., 2018). Niu et al have confirmed a similar level of expression of PD-1 expression on circulating NK cells and find a similar increase in circulating NK cells expressing PD-1 in lung cancer(Niu et al., 2020). They further demonstrate PD-1+NK cells have a reduced capacity for cytotoxicity and reduced intracellular perforin(Niu et al., 2020). Liu et al also confirm the presence of PD-1+NK cells within the tumour infiltrating lymphocytes extracted from tumours of the digestive tract and in HCC(Y. Liu et al., 2017). Furthermore, there is growing evidence for the restoration of NK cells function with the use of checkpoint inhibitor blockade(El-Khoueiry et al., 2017; Ohs et al., 2017; Pesce et al., 2019). Given the presence of a significant PD-1+NK cell subpopulation seen here in healthy livers, PD-1 expression is likely to add to the normal immune-tolerant phenotype of NK cells within the liver. However, with the up-regulation of other inhibitory receptor interactions within the pre-malignant cirrhotic liver, such as LLT1-CD161, combination immunotherapy blocking checkpoint inhibitors as well as these inhibitory receptor interactions within the cirrhotic liver is an exciting prospect that needs investigating.

Intrahepatic NK cells in the healthy and cirrhotic liver also demonstrated a significantly greater proportion of cells expressing CTLA-4, BTLA and CD25 in comparison to circulating NK cells. However, CTLA-4+NK cells contributed to a minimal proportion of NK cells (<5% of intrahepatic and circulating NK cells in health and in disease).

BTLA demonstrated a similar expression pattern on NK cells, with BTLA+NK cells were significantly expanded in HCC, and a trend towards an increased proportion of circulating BTLA+NK cells in cirrhosis. BTLA on T cells was initially described as purely inhibitory, induced on T cell activation, and inhibiting IL-2 production(Watanabe et al., 2003). There is some evidence now that BTLA on CD8+T cells can provide an inhibitory or a co-stimulatory signal, with the presence of CD8+BTLA+ tumour infiltrating lymphocytes correlating with positive outcomes in melanoma(Radvanyi et al., 2012; Ritthipichai et al., 2017). There is little literature on the role of BTLA on NK cells, but BTLA has been shown to be expressed on NK cells following activation via NKG2D(Šedý et al., 2013). Furthermore, Šedý et al demonstrate that the engagement of BTLA on NK cells by the ligand Herpesvirus entry mediator (HVEM) resulted in a reduced NK cell cytolytic ability(Šedý et al., 2013). BTLA has also been demonstrated as being expressed on tumour infiltrating lymphocytes(X. Li et al., 2020). Coupled with this data, BTLA blockade to enhance NK cell cytotoxicity as part of a combination immunotherapy is certainly an interesting area that needs to be explored.

CD25 (IL2RA) forms part of the IL-2 receptor complex. NK cells constitutively express the heterodimeric IL-2 receptor (IL-2Rβγ), but the induction of CD25 allows the formation of the heterotrimeric receptor IL-2Rαβγ which can stimulate NK cells in much lower concentrations of IL-2(Leong et al., 2014). Hence CD25 is deemed a marker of activation. IL-2 stimulation on NK cells promotes NK cells proliferation and modulation of surface NK receptors such as NKG2D(de Rham et al., 2007). Expression of CD25 is seen on activated NK cells and can be induced by IL-12, IL-15 and IL-18 and stimulation(Leong et al., 2014). Again, although there was a significant rise in the CD25+ NK cell proportion in the circulation, this still comprised less than 5% of circulating NK cells. Intrahepatic NK cells in health and disease expressed a significantly larger proportion of CD25+ NK cells, and this may be explained by the fact that the majority of intrahepatic NK cells are $CD56^{bright}$CD16- NK cells, that constitutively express CD25(Hudspeth et al., 2016c; Leong et al., 2014). CD25 expression on T cells indicates a more regulatory T cell phenotype and function(Rodríguez-Perea et al., 2016). However, FoxP3 staining was not undertaken here to differentiate these CD25+CD161+CD4+ T cells from true regulatory CD4+T cells or activated CD4+ T cells. The role for Il-2 infusions has been explored in many cancers but efficacy has been limited due to a narrow therapeutic window and

patient intolerance(Dutcher et al., 2014; C. Sun et al., 2015). However, there remains a potential role for pre-activation and expansion of NK cells with IL-2 prior to adoptive transfer(N. Kumar & Khakoo, 2018a). CD25 blockade is also being explored as an adjunct immunotherapy(Flynn & Hartley, 2017). However, in the case of HCC with a large proportion of intrahepatic CD25+NK cells, further work would be necessary to ensure the desired beneficial effect is achieved.

Interpretation of data presented here is limited for the following reasons. Normal liver samples used, both fresh and FFPE, were margins from liver resections undertaken for any other cause other than HCC. This included colorectal metastases. It is difficult to determine if the immune cells within these sections of liver are actually representative of normal healthy livers. Furthermore, LLT1 immunohistochemistry, and mononuclear cell extraction was all undertaken on liver tissue removed at resection or from liver explants. This does add a selection bias to the intrahepatic data, as these patients did not have advanced HCC. Lastly, there was a paucity of fresh liver samples.

However, this work highlights the importance in understanding the underlying inhibitory phenotype in cirrhosis in order to boost NK cell function. Future work would initially characterise further the potential consequences of LLT1-CD161 blockade on other immune cells. Determining whether LLT1 blockade works in synergy with PD-1 blockade to restore NK cell cytotoxicity in HCC, and if NK cells can be manipulated with these antibodies and expanded ex vivo, allowing individual tailoring of immunotherapy, would be an exciting avenue to explore.

6. Final Discussion and Conclusion

6.1 Novel Findings

NK cells play key roles in tumour surveillance and anti-pathogen responses. As an innate lymphocyte, NK cells do not need pre-sensitisation to elicit potent immune responses, allowing immediate potent immune responses. Licencing of NK cells allows NK cells to discriminate between self and non-self and promotes potent responses towards targets missing-self molecules.

The intrahepatic immune environment differs from the peripheral immune composition and is adapted to provide an immune tolerant environment with continuous exposure to pathogen and damage associated molecular patterns through the portal circulation. Immune responses are contained through a complex interplay between sinusoidal immune cells, liver sinusoidal endothelial cells and dendritic cells. Hepatocytes themselves are able to recognise and orchestrate immune responses though their expression of pattern recognition receptors.

However in cirrhosis, there are changes both within the liver and outside of the liver. An apparent cirrhosis associated immune dysfunction has been demonstrated in several immune cell types, including circulating monocytes and T cells, with an increase in activated and exhausted circulating immune cells with attenuated effector functions. Repeated liver injury from chemicals and pathogens result in repeated cycles of damage and repair with ultimate fibrosis. With the significant morbidity and mortality from alcohol and metabolic dysfunction-associated steatotic liver disease, cirrhosis and HCC, I determined the phenotype and function of circulating and intrahepatic NK cells in cirrhosis and HCC with these underlying aetiologies, and identified the following key novel differences:

1. Circulating NK cells in cirrhosis and HCC demonstrated reduced degranulation against K562 target cells, with a reduced capacity to produce IFNγ in cirrhosis, and a reduced capacity to produce both IFNγ and TNFα in HCC.
2. There was a reduction in the number of circulating NK cells with a polyfunctional capacity in cirrhosis and HCC (ie NK cells with the ability to produce a cytotoxic response and to produce both IFNγ and TNFα).
3. The expression of activating receptors DNAM-1 and NKp46 is reduced on circulating NK cells in patients with HCC.

4. NKp30 expression was reduced on circulating NK cells in patients with MASLD with or without cirrhosis and/or HCC. NKp30 expression correlated negatively with degranulation against K562 targets in patients with HCC on a background of MASLD cirrhosis.
5. There is an increased expression of the inhibitory receptor CD161 on circulating NK cells in cirrhosis.
6. Circulating CD161+NK cells had a subtle but significant increase in the surface expression of PD-1 and BTLA in cirrhosis and HCC.
7. There is a reduction in the cytotoxic circulating CD56dimCD16++ NK cell subpopulation in cirrhosis and HCC compared to healthy volunteers.
8. There is an expansion of a circulating CD56dimCD16+/- NK cell subpopulation in cirrhosis and HCC: using flow cytometry techniques and gene expression analysis of the CD56dimCD16+/- NK cell population revealed these cells to be a liver homing NK cell subpopulation with reduced expression of the activating receptor DNAM-1, preserved degranulation but with hypofunctional type 1 interferon responses. Furthermore, using tissue culture techniques, the circulating CD56dimCD16+/- NK cell phenotype seen in patients with cirrhosis was reproduced in healthy NK cells co-cultured with damaged Huh7 cells, suggesting exposure to damage associated molecular patterns (DAMPs) in the circulation of patients with cirrhosis and/or transient passage through damaged livers may explain the expansion of this CD56dimCD16+/- NK cell subpopulation in cirrhosis and HCC. Gene enrichment analysis suggested a key regulator resulting in the differential gene expression seen in CD56dimCD16+/- NK cells could be TGF-β.
9. There is an upregulation in LLT1 expression in the liver in cirrhosis: phenotyping circulating NK cells in patients with cirrhosis also demonstrated an increase in the proportion of NK cells expressing CD161 and an increase in the surface expression of CD161 on these NK cells. The ligand for CD161, LLT1, was expressed homogenously on hepatocytes in cirrhosis and an increased expression of LLT1 in cirrhosis was demonstrated using both immunohistochemistry techniques and real time PCR. Using the molecular biology techniques of cloning, I produced a stably transfected Huh-7 cell line overexpressing LLT1 and demonstrated that an increase in LLT1 expression reduced degranulation of CD161+NK cells, confirming the inhibitory effects of LLT1 on

NK cells. Furthermore, my data suggests that transforming growth factor beta (TGFβ), a cytokine found in abundance within the cirrhotic liver microenvironment, may result in the induction of expression of LLT1 on hepatocytes.

Cirrhosis associated immune dysfunction is well described in monocytes and T cells (Albillos et al., 2014, 2022) and the attenuated NK cell cytotoxic and cytokine responses seen here against target cells confirm that NK cells have dysfunctional responses in cirrhosis and HCC. Differential expression in surface receptors may account in part for functional discrepancies and attenuated NK cell responses. The reduction in the surface expression of the activating receptor NKp46 and the co-stimulatory molecule DNAM-1 in HCC may contribute to a reduced capacity for NK cell activation, and receptor expression was independent of the underlying aetiology of liver disease. However, reduced expression of the NKp30 receptor was seen specifically in MASLD, both in patients with and without cirrhosis and in patients with HCC and a background of MASLD related cirrhosis. NKp30 is classically deemed an activating receptor, however the expression of NKp30 in MASLD cirrhosis correlated negatively with NK cell cytotoxicity. Whilst another study has demonstrated a reduction in the expression of NKp30 in MASLD (Sakamoto et al., 2021), this negative association with NK cell cytotoxicity at the cirrhosis stage has not been described before. NKp30 has been shown to have different isoforms, including an inhibitory isoform which has been described on tumour infiltrating NK cells in HCC (Mantovani et al., 2019). By identifying this negative correlation with NK cell function at the cirrhosis stage, I demonstrate that inhibitory NKp30 expression on NK cells may precede HCC and, by attenuating NK cell cytotoxicity in cirrhosis, may contribute to the evolution of HCC. Interestingly, the ligand for NKp30, B7H6, belongs to the B7 family, other members of which are important ligands for the checkpoint inhibitor CTLA-4. It would be important to ascertain if blockade of the NKp30-B7H6 interaction would enhance NK cell function in MASLD.

Furthermore, I identified subtle but significant increases in the expression of regulatory checkpoint molecules PD-1 and BTLA on circulating NK cells in patients with cirrhosis and HCC, molecules associated with activation and exhaustion of NK cells (Quatrini et al., 2020). There is some in vitro evidence that PD-1 blockade may also improve NK cell function (Davis et al.,

2021), and hence immunotherapies for HCC containing PD-1 blockade may also improve NK cells function as well as relieving T cells inhibition.

In addition to the downregulation of activating receptors and the increased expression of checkpoint inhibitors, I demonstrated the upregulation of inhibitory receptor CD161 in circulating NK cells in cirrhosis. The engagement of CD161 by it's ligand, LLT1 results in reduced NK cell cytotoxicity and IFNγ production (Aldemir et al., 2005; Bambard et al., 2010; P. a Mathew et al., 2004).

I also demonstrated that LLT1 expression in the liver was only seen in disease, with a homogenous upregulation in expression on hepatocytes in cirrhosis. Thus the LLT1-CD161 mediated inhibition of intrahepatic NK cell function is a significant pathway in cirrhosis.

Whether NK cell inhibition via LLT1 receptor engagement is harmful or in fact beneficial in the context of cirrhosis and the evolution of HCC is yet to be determined. Indeed, a meta-analysis of thirty studies deemed that a reduced expression of E-cadherin, a ligand for the inhibitory KLRG1, in HCC is a poor prognostic indicator: reduced E-cadherin expression in the liver was associated with metastases, vascular invasion, advanced staging and poor survival (Chen et al., 2014). While LLT1 expression was demonstrated in cirrhosis, the expression in HCC appeared to be heterogenous, with upregulation in some samples, but a downregulation in other samples, and this did not correlate with clinical parameters. HCC has recently been re-classified as immunologically inflammatory and non-inflammatory (J. M. Llovet et al., 2022; Montironi et al., 2022). This may in part explain the differential expression of LLT1. Future work to establish the role of these inhibitory receptors on NK cells in cirrhosis and the evolution of HCC is essential to inform future NK cell mediated/targeted immunotherapies for HCC.

The role these inhibitory receptors play in the progression of liver disease and subsequent cirrhosis also needs further investigation. NK cells are essential for inhibition of fibrosis, with NK cells destroying activated stellate cells following an insult to the liver (Waggoner et al., 2016). The abundance of TGF-β however in chronic liver disease may induce the expression of LLT1 on hepatocytes, as demonstrated here in Huh7 cells stimulated with TGF-β, promoting the inhibition of NK cells in cirrhosis. Future work could determine at what point in the evolution of chronic liver disease LLT1 expression becomes significant within the liver in order

to see if it arises prior to cirrhosis, with the subsequent theoretical loss of deletion of activated stellate cells and resulting fibrosis.

The detection of an expanded liver homing CD56dimCD16+/- NK cells in cirrhosis and HCC is also an exciting aspect of this work. Whilst these cells appear to have preserved cytotoxicity, cytokine production appears to be dysfunctional. Patients with MASLD but without cirrhosis or significant fibrosis demonstrated similar proportions of NK cell subpopulations in comparison to healthy donor PBMCs. Co-culture experiments using damaged Huh7 cells induced this NK cell phenotype in healthy PBMCs, implying exposure to damaged hepatocytes and released DAMPs may result in the alteration of CD56dim NK cells to produce the CD56dimCD16+/- NK cells seen in the circulation in disease. The reduced expression of NKp46 on the CD56dimCD16+/- NK cell subpopulation may in part explain the impaired cytotoxicity against K562 cells demonstrated here in patients with cirrhosis and HCC as NKp46 mediated activation is integral to the NK cell response to K562 cells. However, there was no obvious impairment in comparison to healthy NK cells against Huh7 cells where the NKp46 mediated activation is less significant, and the expression of other receptors on Huh7 cells, such as LLT1, may impair NK cell function overall. The loss of CD16 expression on these CD56dim cells implies a reduced capacity for antibody dependent cell mediated cytotoxicity, and this coupled with the reduced production of IFNγ may have significant implications in anti-pathogen responses and contribute to the increased susceptibility of infection in patients with underlying cirrhosis.

6.2 Future directions

This study provides insight into the role of NK cells in cirrhosis, shedding light on inhibitory pathways modulating NK cell function coupled with an increased expression of markers of exhaustion and attenuated effector function. As the prospect for harnessing NK cells to deliver targeted immunotherapies grows, successful manipulation of NK cells to deliver immunotherapy relies on understanding the tumour microenvironment and systemic effects of underlying cirrhosis.

Whether the pre-existing CD56dimCD16+/- NK cells in patients could be harnessed to deliver therapy would be key to evaluate. The CXCR6 expression on these NK cells implies a capacity for these cells to be liver homing. NK cells can be pre-primed with IL12, IL15 and IL18 to

produce memory like cells with more potent responses when challenged again (Leong et al., 2014; Pahl et al., 2018; Romee et al., 2016). It would be worth assessing if IL12, IL15 and/or IL18 could restore the cytokine secretion capacity. Furthermore, coupling this with CD161 blockade could be explored to restore NK cell function against HCC cells where LLT1 expression is upregulated. However, NK cells from patients with obesity are dysfunctional, low in number and metabolic defects in NK cells from obese patients reduced the ability for NK cell training (Kedia-Mehta et al., 2021). Furthermore, as this work demonstrates, there are multiple different changes to NK cells at the gene expression and protein expression and hence it is likely that a combination of interventions may be required to restore NK cell function. In addition, given the heterogeneity of HCC, as demonstrated by other studies and seen here with regards to LLT1 expression, biopsies of tumour tissue and background liver tissue will be of increasing importance to tailoring combination immunotherapies.

This body of work provides multiple exciting novel avenues to explore with regards to targeting NK cells in patients and developing NK cell based immunotherapies for HCC in the context of cirrhosis.

7. References

Abel, A. M., Yang, C., Thakar, M. S., & Malarkannan, S. (2018). Natural killer cells: Development, maturation, and clinical utilization. *Frontiers in Immunology*, *9*(AUG), 1–23. https://doi.org/10.3389/fimmu.2018.01869

Adams, L. A., Anstee, Q. M., Tilg, H., & Targher, G. (2017). Non-alcoholic fatty liver disease and its relationship with cardiovascular disease and other extrahepatic diseases. *Gut*, *66*(6), 1138–1153. https://doi.org/10.1136/gutjnl-2017-313884

Adams, N. M., Lau, C. M., Fan, X., Rapp, M., Geary, C. D., Weizman, O.-E., Diaz-Salazar, C., & Sun, J. C. (2018). Transcription Factor IRF8 Orchestrates the Adaptive Natural Killer Cell Response. *Immunity*, *48*(6), 1172-1182.e6. https://doi.org/10.1016/j.immuni.2018.04.018

Aden, D. P., Fogel, A., Plotkin, S., Damjanov, I., & Knowles, B. B. (1979). Controlled synthesis of HBsAg in a differentiated human liver carcinoma-derived cell line. In *J. Trans. R. Soc. trap. Med. Hyg* (Vol. 282, Issue 9).

Agerberth, B., Charo, J., Werr, J., Olsson, B., Idali, F., Lindbom, L., Kiessling, R., Jö, H., Wigzell, H., & Gudmundsson, G. H. (2000). *The human antimicrobial and chemotactic peptides LL-37 and-defensins are expressed by specific lymphocyte and monocyte populations*.

Aggeletopoulou, I., Kalafateli, M., & Triantos, C. (2024). Chimeric Antigen Receptor T Cell Therapy for Hepatocellular Carcinoma: Where Do We Stand? *International Journal of Molecular Sciences*, *25*(5), 2631. https://doi.org/10.3390/ijms25052631

Ahlenstiel, G., Titerence, R. H., Koh, C., Edlich, B., Feld, J. J., Rotman, Y., Ghany, M. G., Hoofnagle, J. H., Liang, T. J., Heller, T., & Rehermann, B. (2010). Natural Killer Cells Are Polarized Toward Cytotoxicity in Chronic Hepatitis C in an Interferon-Alfa–Dependent Manner. *Gastroenterology*, *138*(1), 325-335.e2. https://doi.org/10.1053/j.gastro.2009.08.066

Albillos, A., Lario, M., & Alvarez-Mon, M. (2014). Cirrhosis-associated immune dysfunction: Distinctive features and clinical relevance. *Journal of Hepatology*, *61*(6), 1385–1396. https://doi.org/10.1016/j.jhep.2014.08.010

Albillos, A., Martin-Mateos, R., Van der Merwe, S., Wiest, R., Jalan, R., & Álvarez-Mon, M. (2022). Cirrhosis-associated immune dysfunction. In *Nature Reviews Gastroenterology and Hepatology* (Vol. 19, Issue 2, pp. 112–134). Nature Research. https://doi.org/10.1038/s41575-021-00520-7

Aldemir, H., Prod'homme, V., Dumaurier, M.-J., Retiere, C., Poupon, G., Cazareth, J., Bihl, F., & Braud, V. M. (2005). Cutting edge: lectin-like transcript 1 is a ligand for the CD161 receptor. *Journal of Immunology (Baltimore, Md. : 1950)*, *175*(12), 7791–7795. https://doi.org/10.4049/jimmunol.175.12.7791

Ali, A., Abdel-Hafiz, H., Suhail, M., Al-Mars, A., Zakaria, M. K., Fatima, K., Ahmad, S., Azhar, E., Chaudhary, A., & Qadri, I. (2014). Hepatitis B virus, HBx mutants and their role in hepatocellular carcinoma. *World Journal of Gastroenterology*, *20*(30), 10238–10248. https://doi.org/10.3748/wjg.v20.i30.10238

Almeida-Oliveira, A., Smith-Carvalho, M., Porto, L. C., Cardoso-Oliveira, J., Ribeiro, A. D. S.,

Falcão, R. R., Abdelhay, E., Bouzas, L. F., Thuler, L. C. S., Ornellas, M. H., & Diamond, H. R. (2011). Age-related changes in natural killer cell receptors from childhood through old age. *Human Immunology*, *72*(4), 319–329. https://doi.org/10.1016/j.humimm.2011.01.009

Alter, G., Jost, S., Rihn, S., Reyor, L., Nolan, B., Ghebremichael, M., Bosch, R., Alfield, M., & Lauer, G. (2011). Reduced frequencies of NKp30+ NKp46+, CD161+, and NKG2D+ NK cells in acute HCV infection may predict viral clearance. *Journal of Hepatology*, *55*(2), 278–288. https://doi.org/10.1016/j.jhep.2010.11.030

Alter, G., Malenfant, J. M., & Altfeld, M. (2004). CD107a as a functional marker for the identification of natural killer cell activity. *Journal of Immunological Methods*, *294*(1–2), 15–22. https://doi.org/10.1016/j.jim.2004.08.008

Amer, J., Salhab, A., Noureddin, M., Doron, S., Abu-Tair, L., Ghantous, R., Mahamid, M., & Safadi, R. (2018). Insulin signaling as a potential natural killer cell checkpoint in fatty liver disease. *Hepatology Communications*, *2*(3), 285–298. https://doi.org/10.1002/hep4.1146

Anton, O. M., Vielkind, S., Peterson, M. E., Tagaya, Y., & Long, E. O. (2015). NK Cell Proliferation Induced by IL-15 Transpresentation Is Negatively Regulated by Inhibitory Receptors. *The Journal of Immunology*, *195*(10), 4810–4821. https://doi.org/10.4049/jimmunol.1500414

Arase, H., Arase, N., & Saito, T. (1996). Interferon gamma production by natural killer (NK) cells and NK1.1+ T cells upon NKR-P1 cross-linking. *The Journal of Experimental Medicine*, *183*(5), 2391–2396. https://doi.org/10.1084/jem.183.5.2391

Ayoub, W. S., Steggerda, J., Yang, J. D., Kuo, A., Sundaram, V., & Lu, S. C. (2019). Current status of hepatocellular carcinoma detection: screening strategies and novel biomarkers. In *Therapeutic Advances in Medical Oncology* (Vol. 11). SAGE Publications Inc. https://doi.org/10.1177/1758835919869120

Baessler, T., Charton, J. E., Schmiedel, B. J., Gru, F., Krusch, M., Wacker, A., Rammensee, H., & Salih, H. R. (2010). CD137 ligand mediates opposite effects in human and mouse NK cells and impairs NK-cell reactivity against human acute myeloid leukemia cells. *Blood*, *115*(15), 3058–3069. https://doi.org/10.1182/blood-2009-06-227934.An

Balkwill, F. R., Capasso, M., & Hagemann, T. (2012). The tumor microenvironment at a glance. *Journal of Cell Science*, *125*(Pt 23), 5591–5596. https://doi.org/10.1242/jcs.116392

Balzarolo, M., Watzl, C., Medema, J. P., & Wolkers, M. C. (2013). NAB2 and EGR-1 exert opposite roles in regulating TRAIL expression in human Natural Killer cells. *Immunology Letters*, *151*(1–2), 61–67. https://doi.org/10.1016/j.imlet.2013.02.001

Bambard, N. D., Mathew, S. O., & Mathew, P. a. (2010). LLT1-mediated activation of IFN-gamma production in human natural killer cells involves ERK signalling pathway. *Scandinavian Journal of Immunology*, *71*(3), 210–219. https://doi.org/10.1111/j.1365-3083.2009.02367.x

Barrow, A. D., Martin, C. J., & Colonna, M. (2019). The natural cytotoxicity receptors in

health and disease. *Frontiers in Immunology*, *10*(MAY), 1–20. https://doi.org/10.3389/fimmu.2019.00909

Billerbeck, E., Kang, Y.-H., Walker, L., Lockstone, H., Grafmueller, S., Fleming, V., Flint, J., Willberg, C. B., Bengsch, B., Seigel, B., Ramamurthy, N., Zitzmann, N., Barnes, E. J., Thevanayagam, J., Bhagwanani, A., Leslie, A., Oo, Y. H., Kollnberger, S., Bowness, P., … Klenerman, P. (2010). Analysis of CD161 expression on human CD8+ T cells defines a distinct functional subset with tissue-homing properties. *Proceedings of the National Academy of Sciences of the United States of America*, *107*(7), 3006–3011. https://doi.org/10.1073/pnas.0914839107

Blach, S., Terrault, N. A., Tacke, F., Gamkrelidze, I., Craxi, A., Tanaka, J., Waked, I., Dore, G. J., Abbas, Z., Abdallah, A. R., Abdulla, M., Aghemo, A., Aho, I., Akarca, U. S., Alalwan, A. M., Alanko Blomé, M., Al-Busafi, S. A., Aleman, S., Alghamdi, A. S., … Razavi, H. A. (2022). Global change in hepatitis C virus prevalence and cascade of care between 2015 and 2020: a modelling study. *The Lancet Gastroenterology & Hepatology*, *7*(5), 396–415. https://doi.org/10.1016/S2468-1253(21)00472-6

Bloom, E. T., Furuke, K., Shiraishi, M., & Mostowski, H. S. (1999). *Cell-Dependent Pathway Calcineurin-Nuclear Factors of Activated T Regulated by Redox Through a Fas Ligand Induction in Human NK Cells Is*. http://www.jimmunol.org/content/162/4/1988

Bonorino, P., Ramzan, M., Camous, X., Dufeu-Duchesne, T., Thélu, M.-A., Sturm, N., Dariz, A., Guillermet, C., Pernollet, M., Zarski, J.-P., Marche, P. N., Leroy, V., & Jouvin-Marche, E. (2009). Fine characterization of intrahepatic NK cells expressing natural killer receptors in chronic hepatitis B and C. *Journal of Hepatology*, *51*(3), 458–467. https://doi.org/10.1016/j.jhep.2009.05.030

Bottino, C., Castriconi, R., Pende, D., Rivera, P., Nanni, M., Carnemolla, B., Cantoni, C., Grassi, J., Marcenaro, S., Reymond, N., Vitale, M., Moretta, L., Lopez, M., & Moretta, A. (2003). Identification of PVR (CD155) and Nectin-2 (CD112) as cell surface ligands for the human DNAM-1 (CD226) activating molecule. *Journal of Experimental Medicine*, *198*(4), 557–567. https://doi.org/10.1084/jem.20030788

Bowen, D. G., Zen, M., Holz, L., Davis, T., McCaughan, G. W., & Bertolino, P. (2004). The site of primary T cell activation is a determinant of the balance between intrahepatic tolerance and immunity. *Journal of Clinical Investigation*, *114*(5), 701–712. https://doi.org/10.1172/JCI200421593

Brodin, P., Kärre, K., & Höglund, P. (2009). NK cell education: not an on-off switch but a tunable rheostat. *Trends in Immunology*, *30*(4), 143–149. https://doi.org/10.1016/j.it.2009.01.006

Bryceson, Y. T., March, M. E., Ljunggren, H.-G., & Long, E. O. (2006a). Activation, coactivation, and costimulation of resting human natural killer cells. *Immunological Reviews*, *214*, 73–91. https://doi.org/10.1111/j.1600-065X.2006.00457.x

Bryceson, Y. T., March, M. E., Ljunggren, H.-G., & Long, E. O. (2006b). Synergy among receptors on resting NK cells for the activation of natural cytotoxicity and cytokine secretion. *Blood*, *107*(1), 159–166. https://doi.org/10.1182/blood-2005-04-1351

Cai, L., Zhang, Z., Zhou, L., Wang, H., Fu, J., Zhang, S., Shi, M., Zhang, H., Yang, Y., Wu, H.,

Tien, P., & Wang, F. S. (2008). Functional impairment in circulating and intrahepatic NK cells and relative mechanism in hepatocellular carcinoma patients. *Clinical Immunology*, *129*(3), 428–437. https://doi.org/10.1016/j.clim.2008.08.012

Campbell, K. S., & Colonna, M. (1999). DAP12: a key accessory protein for relaying signals by Natural Killer cell receptors. *The International Journal of Biochemistry & Cell Biology*, *31*(6), 631–636. https://doi.org/10.1016/S1357-2725(99)00022-9

Cao, W.-J., Zhang, X.-C., Wan, L.-Y., Li, Q.-Y., Mu, X.-Y., Guo, A.-L., Zhou, M.-J., Shen, L.-L., Zhang, C., Fan, X., Jiao, Y.-M., Xu, R.-N., Zhou, C.-B., Yuan, J.-H., Wang, S.-Q., Wang, F.-S., & Song, J.-W. (2022). Immune Dysfunctions of CD56neg NK Cells Are Associated With HIV-1 Disease Progression. *Frontiers in Immunology*, *12*. https://doi.org/10.3389/fimmu.2021.811091

Capuano, C., Pighi, C., Battella, S., De Federicis, D., Galandrini, R., & Palmieri, G. (2021). Harnessing cd16-mediated nk cell functions to enhance therapeutic efficacy of tumor-targeting mabs. *Cancers*, *13*(10), 1–24. https://doi.org/10.3390/cancers13102500

Cariani, E., Pilli, M., Barili, V., Porro, E., Biasini, E., Olivani, A., Dalla Valle, R., Trenti, T., Ferrari, C., & Missale, G. (2016). Natural killer cells phenotypic characterization as an outcome predictor of HCV-linked HCC after curative treatments. *OncoImmunology*, *5*(8). https://doi.org/10.1080/2162402X.2016.1154249

Carlsten, M., Norell, H., Bryceson, Y. T., Poschke, I., Schedvins, K., Ljunggren, H.-G., Kiessling, R., & Malmberg, K.-J. (2009). Primary Human Tumor Cells Expressing CD155 Impair Tumor Targeting by Down-Regulating DNAM-1 on NK Cells. *The Journal of Immunology*, *183*(8), 4921–4930. https://doi.org/10.4049/jimmunol.0901226

Cassetta, L., Bruderek, K., Skrzeczynska-Moncznik, J., Osiecka, O., Hu, X., Rundgren, I. M., Lin, A., Santegoets, K., Horzum, U., Godinho-Santos, A., Zelinskyy, G., Garcia-Tellez, T., Bjelica, S., Taciak, B., Kittang, A. O., Höing, B., Lang, S., Dixon, M., Müller, V., … Brandau, S. (2020). Differential expansion of circulating human MDSC subsets in patients with cancer, infection and inflammation. *Journal for ImmunoTherapy of Cancer*, *8*(2), e001223. https://doi.org/10.1136/jitc-2020-001223

Castriconi, R., Cantoni, C., Della Chiesa, M., Vitale, M., Marcenaro, E., Conte, R., Biassoni, R., Bottino, C., Moretta, L., & Moretta, A. (2003). Transforming growth factor 1 inhibits expression of NKp30 and NKG2D receptors: Consequences for the NK-mediated killing of dendritic cells. *Proceedings of the National Academy of Sciences of the United States of America*, *100*(7), 4120–4125. www.pnas.orgcgidoi10.1073pnas.0730640100

Chang, H., Jung, W., Kim, A., Kim, H. K., Kim, W. B., Kim, J. H., & Kim, B. H. (2017). Expression and prognostic significance of programmed death protein 1 and programmed death ligand-1, and cytotoxic T lymphocyte-associated molecule-4 in hepatocellular carcinoma. *Apmis*, *125*(8), 690–698. https://doi.org/10.1111/apm.12703

Cheent, K., & Khakoo, S. I. (2011). Natural killer cells and hepatitis C: action and reaction. *Gut*, *60*(2), 268–278. https://doi.org/10.1136/gut.2010.212555

Chemnitz, J. M., Riley, J. L., Frauwirth, K. a., Braunstein, I., Kobayashi, S. V., Linsley, P. S., Thompson, C. B., & Parry, R. V. (2004). CTLA-4 and PD-1 Receptors Inhibit T-Cell Activation by Distinct Mechanisms. *Blood*, *104*(11), 2657–2657.

https://doi.org/10.1182/blood.v104.11.2657.2657

Chen, J., Zhao, J., Ma, R., Lin, H., Liang, X., & Cai, X. (2014). Prognostic Significance of E-Cadherin Expression in Hepatocellular Carcinoma: A Meta-Analysis. *PLoS ONE*, *9*(8), e103952. https://doi.org/10.1371/journal.pone.0103952

Chew, V., Lai, L., Pan, L., Lim, C. J., Li, J., Ong, R., Chua, C., Leong, J. Y., Lim, K. H., Toh, H. C., Lee, S. Y., Chan, C. Y., Goh, B. K. P., Chung, A., Chow, P. K. H., & Albani, S. (2017). Delineation of an immunosuppressive gradient in hepatocellular carcinoma using high-dimensional proteomic and transcriptomic analyses. *Proceedings of the National Academy of Sciences*, *114*(29). https://doi.org/10.1073/pnas.1706559114

Childs, A., Aidoo-Micah, G., Maini, M. K., & Meyer, T. (2024). Immunotherapy for hepatocellular carcinoma. *JHEP Reports*, *6*(10), 101130. https://doi.org/10.1016/j.jhepr.2024.101130

Chong, W. P., Zhou, J., Law, H. K. W., Tu, W., & Lau, Y. L. (2010). Natural killer cells become tolerogenic after interaction with apoptotic cells. *European Journal of Immunology*, *40*(6), 1718–1727. https://doi.org/10.1002/eji.200939768

Chuang, W. L., Liu, H. W., & Chang, W. Y. (1990). Natural killer cell activity in patients with hepatocellular carcinoma relative to early development and tumor invasion. *Cancer*, *65*(4), 926–930.

Chuang, Y., Lian, Z., Tsuneyama, K., Chiang, B., Ansari, A., Coppel, R., & Ericgershwin, M. (2006). Increased killing activity and decreased cytokine production in NK cells in patients with primary biliary cirrhosis. *Journal of Autoimmunity*, *26*(4), 232–240. https://doi.org/10.1016/j.jaut.2006.04.001

Coffelt, S. B., Wellenstein, M. D., & de Visser, K. E. (2016). Neutrophils in cancer: neutral no more. *Nature Reviews Cancer*, *16*(7), 431–446. https://doi.org/10.1038/nrc.2016.52

Cooper, M. a., Fehniger, T. a., Turner, S. C., Chen, K. S., Ghaheri, B. a., Ghayur, T., Carson, W. E., & Caligiuri, M. a. (2001). Human natural killer cells: A unique innate immunoregulatory role for the CD56bright subset. *Blood*, *97*(10), 3146–3151. https://doi.org/10.1182/blood.V97.10.3146

Costanzo, M. C., Kim, D., Creegan, M., Lal, K. G., Ake, J. A., Currier, J. R., Streeck, H., Robb, M. L., Michael, N. L., Bolton, D. L., Steers, N. J., & Eller, M. A. (2018). Transcriptomic signatures of NK cells suggest impaired responsiveness in HIV-1 infection and increased activity post-vaccination. *Nature Communications*, *9*(1), 1212. https://doi.org/10.1038/s41467-018-03618-w

Coudert, J. D., Zimmer, J., Tomasello, E., Cebecauer, M., Colonna, M., Vivier, E., & Held, W. (2005). Altered NKG2D function in NK cells induced by chronic exposure to NKG2D ligand–expressing tumor cells. *Blood*, *106*(5), 1711–1717. https://doi.org/10.1182/blood-2005-03-0918

Coulouarn, C., Factor, V. M., Conner, E. a., & Thorgeirsson, S. S. (2011). Genomic modeling of tumor onset and progression in a mouse model of aggressive human liver cancer. *Carcinogenesis*, *32*(10), 1434–1440. https://doi.org/10.1093/carcin/bgr133

Cuff, A. O., Robertson, F. P., Stegmann, K. A., Pallett, L. J., Maini, M. K., Davidson, B. R., &

Male, V. (2016). Eomes ^{hi} NK Cells in Human Liver Are Long-Lived and Do Not Recirculate but Can Be Replenished from the Circulation. *The Journal of Immunology*, *197*(11), 4283–4291. https://doi.org/10.4049/jimmunol.1601424

Cuff, A. O., Sillito, F., Dertschnig, S., Hall, A., Luong, T. V., Chakraverty, R., & Male, V. (2019). The Obese Liver Environment Mediates Conversion of NK Cells to a Less Cytotoxic ILC1-Like Phenotype. *Frontiers in Immunology*, *10*. https://doi.org/10.3389/fimmu.2019.02180

Cui, K., Yan, G., Zheng, X., Bai, L., Wei, H., Sun, R., & Tian, Z. (2017). Suppression of Natural Killer Cell Activity by Regulatory NKT10 Cells Aggravates Alcoholic Hepatosteatosis. *Frontiers in Immunology*, *8*. https://doi.org/10.3389/fimmu.2017.01414

Davis, Z., Felices, M., Lenvik, T., Badal, S., Walker, J. T., Hinderlie, P., Riley, J. L., Vallera, D. A., Blazar, B. R., & Miller, J. S. (2021). Low-density PD-1 expression on resting human natural killer cells is functional and upregulated after transplantation. *Blood Advances*, *5*(4), 1069–1080. https://doi.org/10.1182/bloodadvances.2019001110

De Maria, A., Bozzano, F., Cantoni, C., & Moretta, L. (2011). Revisiting human natural killer cell subset function revealed cytolytic CD56dimCD16+ NK cells as rapid producers of abundant IFN-γ on activation. *Proceedings of the National Academy of Sciences of the United States of America*, *108*(2), 728–732. https://doi.org/10.1073/pnas.1012356108

De Re, V., Caggiari, L., De Zorzi, M., Repetto, O., Zignego, A. L., Izzo, F., Tornesello, M. L., Buonaguro, F. M., Mangia, A., Sansonno, D., Racanelli, V., De Vita, S., Pioltelli, P., Vaccher, E., Beretta, M., Mazzaro, C., Libra, M., Gini, A., Zucchetto, A., … De Paoli, P. (2015). Genetic diversity of the KIR/HLA system and susceptibility to hepatitis C virus-related diseases. *PLoS ONE*, *10*(2). https://doi.org/10.1371/journal.pone.0117420

de Rham, C., Ferrari-Lacraz, S., Jendly, S., Schneiter, G., Dayer, J. M., & Villard, J. (2007). The proinflammatory cytokines IL-2, IL-15 and IL-21 modulate the repertoire of mature human natural killer cell receptors. *Arthritis Research and Therapy*, *9*(6), 1–15. https://doi.org/10.1186/ar2336

Delahaye, N. F., Rusakiewicz, S., Martins, I., Ménard, C., Roux, S., Lyonnet, L., Paul, P., Sarabi, M., Chaput, N., Semeraro, M., Minard-Colin, V., Poirier-Colame, V., Chaba, K., Flament, C., Baud, V., Authier, H., Kerdine-Römer, S., Pallardy, M., Cremer, I., … Zitvogel, L. (2011). Alternatively spliced NKp30 isoforms affect the prognosis of gastrointestinal stromal tumors. *Nature Medicine*, *17*(6), 700–707. https://doi.org/10.1038/nm.2366

Desai, A., Sandhu, S., Lai, J. P., & Sandhu, D. S. (2019). Hepatocellular carcinoma in non-cirrhotic liver: A comprehensive review. In *World Journal of Hepatology* (Vol. 11, Issue 1, pp. 1–18). Baishideng Publishing Group Co. https://doi.org/10.4254/wjh.v11.i1.1

Devarbhavi, H., Asrani, S. K., Arab, J. P., Nartey, Y. A., Pose, E., & Kamath, P. S. (2023). Global burden of liver disease: 2023 update. *Journal of Hepatology*, *79*(2), 516–537. https://doi.org/10.1016/j.jhep.2023.03.017

Dhatchinamoorthy, K., Colbert, J. D., & Rock, K. L. (2021). Cancer Immune Evasion Through Loss of MHC Class I Antigen Presentation. *Frontiers in Immunology*, *12*(March). https://doi.org/10.3389/fimmu.2021.636568

Diedrich, T., Kummer, S., Galante, A., Drolz, A., Schlicker, V., Lohse, A. W., Kluwe, J., Eberhard, J. M., & Schulze zur Wiesch, J. (2020). Characterization of the immune cell landscape of patients with NAFLD. *PLOS ONE*, *15*(3), e0230307. https://doi.org/10.1371/journal.pone.0230307

Dimitropoulou, D., Karakantza, M., Tsamandas, A. C., Mouzaki, A., Theodorou, G., & Gogos, C. a. (2011). T-lymphocyte subsets in peripheral blood and liver tissue of patients with chronic hepatitis B and C. *In Vivo*, *25*(5), 833–840.

Ding, T., Xu, J., Wang, F., Shi, M., Zhang, Y., Li, S.-P., & Zheng, L. (2009). High tumor-infiltrating macrophage density predicts poor prognosis in patients with primary hepatocellular carcinoma after resection. *Human Pathology*, *40*(3), 381–389. https://doi.org/10.1016/j.humpath.2008.08.011

Dong, Z., Wei, H., Sun, R., Hu, Z., Gao, B., & Tian, Z. (2004). Involvement of natural killer cells in PolyI:C-induced liver injury. *Journal of Hepatology*, *41*(6), 966–973. https://doi.org/10.1016/j.jhep.2004.08.021

Dooley, S., & Ten Dijke, P. (2012). TGF-β in progression of liver disease. *Cell and Tissue Research*, *347*(1), 245–256. https://doi.org/10.1007/s00441-011-1246-y

Dring, M. M., Morrison, M. H., McSharry, B. P., Guinan, K. J., Hagan, R., O'Farrelly, C., & Gardiner, C. M. (2011). Innate immune genes synergize to predict increased risk of chronic disease in hepatitis C virus infection. *Proceedings of the National Academy of Sciences of the United States of America*, *108*(14), 5736–5741. https://doi.org/10.1073/pnas.1016358108

Duan, X., Liu, J., Cui, J., Ma, B., Zhou, Q., Yang, X., Lu, Z., Du, Y., & Su, C. (2019). Expression of TIGIT/CD155 and correlations with clinical pathological features in human hepatocellular carcinoma. *Molecular Medicine Reports*. https://doi.org/10.3892/mmr.2019.10641

Dufour, J. F., Greten, T. F., Raymond, E., Roskams, T., De, T., Ducreux, M., Mazzaferro, V., & Governing, E. (2012). Clinical Practice Guidelines EASL – EORTC Clinical Practice Guidelines : Management of hepatocellular carcinoma European Organisation for Research and Treatment of Cancer. *Journal of Hepatology*, *56*(4), 908–943. https://doi.org/10.1016/j.jhep.2011.12.001

Dunn, C., Brunetto, M., Reynolds, G., Christophides, T., Kennedy, P. T., Lampertico, P., Das, A., Lopes, A. R., Borrow, P., Williams, K., Humphreys, E., Afford, S., Adams, D. H., Bertoletti, A., & Maini, M. K. (2007). Cytokines induced during chronic hepatitis B virus infection promote a pathway for NK cell–mediated liver damage. *Journal of Experimental Medicine*, *204*(3), 667–680. https://doi.org/10.1084/jem.20061287

Dunn, G. P., Bruce, A. T., Ikeda, H., Old, L. J., & Schreiber, R. D. (2002). Cancer immunoediting: from immunosurveillance to tumor escape. *Nature Immunology*, *3*(11), 991–998. https://doi.org/10.1038/ni1102-991

Dusseaux, M., Martin, E., Serriari, N., Peguillet, I., Premel, V., Louis, D., Milder, M., Le Bourhis, L., Soudais, C., Treiner, E., & Lantz, O. (2010). Human MAIT cells are xenobiotic resistant, tissue-targeted, CD161hi IL-17 secreting T cells. *Blood*, *117*(4), 1250–1260. https://doi.org/10.1182/blood-2010-08-303339

Dutcher, J. P., Schwartzentruber, D. J., Kaufman, H. L., Agarwala, S. S., Tarhini, A. A., Lowder, J. N., & Atkins, M. B. (2014). High dose interleukin-2 (Aldesleukin) - expert consensus on best management practices-2014. *Journal for ImmunoTherapy of Cancer*, *2*(1), 26. https://doi.org/10.1186/s40425-014-0026-0

Easom, N. J. W., Marks, M., Jobe, D., Gillmore, R., Meyer, T., Maini, M. K., & Njie, R. (2020). ULBP1 Is Elevated in Human Hepatocellular Carcinoma and Predicts Outcome. *Frontiers in Oncology*, *10*. https://doi.org/10.3389/fonc.2020.00971

Eckl, J., Buchner, A., Prinz, P. U., Riesenberg, R., Siegert, S. I., Kammerer, R., Nelson, P. J., & Noessner, E. (2012). Transcript signature predicts tissue NK cell content and defines renal cell carcinoma subgroups independent of TNM staging. *Journal of Molecular Medicine*, *90*(1), 55–66. https://doi.org/10.1007/s00109-011-0806-7

El-Khoueiry, A. B., Sangro, B., Yau, T., Crocenzi, T. S., Kudo, M., Hsu, C., Kim, T. Y., Choo, S. P., Trojan, J., Welling, T. H., Meyer, T., Kang, Y. K., Yeo, W., Chopra, A., Anderson, J., dela Cruz, C., Lang, L., Neely, J., Tang, H., … Melero, I. (2017). Nivolumab in patients with advanced hepatocellular carcinoma (CheckMate 040): An open-label, non-comparative, phase 1/2 dose escalation and expansion trial. *The Lancet*. https://doi.org/10.1016/S0140-6736(17)31046-2

Eslam, M., Newsome, P. N., Sarin, S. K., Anstee, Q. M., Targher, G., Romero-Gomez, M., Zelber-Sagi, S., Wai-Sun Wong, V., Dufour, J.-F., Schattenberg, J. M., Kawaguchi, T., Arrese, M., Valenti, L., Shiha, G., Tiribelli, C., Yki-Järvinen, H., Fan, J.-G., Grønbæk, H., Yilmaz, Y., … George, J. (2020). A new definition for metabolic dysfunction-associated fatty liver disease: An international expert consensus statement. *Journal of Hepatology*, *73*(1), 202–209. https://doi.org/10.1016/j.jhep.2020.03.039

Evans, J. H., Horowitz, A., Mehrabi, M., Wise, E. L., Pease, J. E., Riley, E. M., & Davis, D. M. (2011). A distinct subset of human NK cells expressing HLA-DR expand in response to IL-2 and can aid immune responses to BCG. *European Journal of Immunology*, *41*(7), 1924–1933. https://doi.org/10.1002/eji.201041180

Ewen, E. M., Pahl, J. H. W., Miller, M., Watzl, C., & Cerwenka, A. (2018). KIR downregulation by IL-12/15/18 unleashes human NK cells from KIR/HLA-I inhibition and enhances killing of tumor cells. *European Journal of Immunology*, *48*(2), 355–365. https://doi.org/10.1002/eji.201747128

Faivre, S., Rimassa, L., & Finn, R. S. (2020). Molecular therapies for HCC : Looking outside the box. *Journal of Hepatology*, *72*(2), 342–352. https://doi.org/10.1016/j.jhep.2019.09.010

Farazi, P. A., & Depinho, R. A. (2006). *Hepatocellular carcinoma pathogenesis : from genes to environment*. *6*(September), 674–687. https://doi.org/10.1038/nrc1934

Fathy, A., Eldin, M. M., Metwally, L., Eida, M., & Abdel-Rehim, M. (2009). Diminished absolute counts of CD56dim and CD56bright natural killer cells in peripheral blood from Egyptian patients with hepatocellular carcinoma. *The Egyptian Journal of Immunology*, *16*(2), 17–25.

Faul, F., Erdfelder, E., Lang, A.-G., & Buchner, A. (2007). G*Power 3: A flexible statistical power analysis program for the social, behavioral, and biomedical sciences. *Behavior*

Research Methods, *39*(2), 175–191. https://doi.org/10.3758/BF03193146

Fauriat, C., Long, E., Ljunggren, H.-G., & Bryceson, Y. (2010). Regulation of human NK-cell cytokine and chemokine production by target cell recognition. *Blood*, *115*(11), 2167–2176.

Fergusson, J. R., Smith, K. E., Fleming, V. M., Rajoriya, N., Newell, E. W., Simmons, R., Marchi, E., Björkander, S., Kang, Y. H., Swadling, L., Kurioka, A., Sahgal, N., Lockstone, H., Baban, D., Freeman, G. J., Sverremark-Ekström, E., Davis, M. M., Davenport, M. P., Venturi, V., … Klenerman, P. (2014). CD161 defines a transcriptional and functional phenotype across distinct human T cell lineages. *Cell Reports*, *9*(3), 1075–1088. https://doi.org/10.1016/j.celrep.2014.09.045

Ferlazzo, G., & Morandi, B. (2014). Cross-talks between natural killer cells and distinct subsets of dendritic cells. In *Frontiers in Immunology* (Vol. 5, Issue APR). Frontiers Research Foundation. https://doi.org/10.3389/fimmu.2014.00159

Finn, R. S., Qin, S., Ikeda, M., Galle, P. R., Ducreux, M., Kim, T.-Y., Kudo, M., Breder, V., Merle, P., Kaseb, A. O., Li, D., Verret, W., Xu, D.-Z., Hernandez, S., Liu, J., Huang, C., Mulla, S., Wang, Y., Lim, H. Y., … Cheng, A.-L. (2020). Atezolizumab plus Bevacizumab in Unresectable Hepatocellular Carcinoma. *New England Journal of Medicine*, *382*(20), 1894–1905. https://doi.org/10.1056/nejmoa1915745

Finn, R. S., Ryoo, B.-Y., Merle, P., Kudo, M., Bouattour, M., Yeong Lim, H., Breder, V., Edeline, J., Chao, Y., Ogasawara, S., Yau, T., Garrido, M., Chan, S. L., Knox, J., Daniele, B., Ebbinghaus, S. W., Chen, E., Siegel, A. B., Zhu, A. X., & Cheng, A.-L. (2019). Pembrolizumab As Second-Line Therapy in Patients With Advanced Hepatocellular Carcinoma in KEYNOTE-240: A Randomized, Double-Blind, Phase III Trial. *J Clin Oncol*, *38*, 193–202. https://doi.org/10.1200/JCO.19

Fisicaro, P., Rossi, M., Vecchi, A., Acerbi, G., Barili, V., Laccabue, D., Montali, I., Zecca, A., Penna, A., Missale, G., Ferrari, C., & Boni, C. (2019). The good and the bad of natural killer cells in virus control: Perspective for anti-HBV therapy. *International Journal of Molecular Sciences*, *20*(20). https://doi.org/10.3390/ijms20205080

Flisiak, R., Pytel-Krolczuk, B., & Prokopowicz, D. (2000). Circulating transforming growth factor β1 as an indicator of hepatic function impairment in liver cirrhosis. *Cytokine*, *12*(6), 677–681. https://doi.org/10.1006/cyto.1999.0660

Flynn, M. J., & Hartley, J. a. (2017). The emerging role of anti-CD25 directed therapies as both immune modulators and targeted agents in cancer. *British Journal of Haematology*, *179*(1), 20–35. https://doi.org/10.1111/bjh.14770

Freitas-Lopes, M., Mafra, K., David, B., Carvalho-Gontijo, R., & Menezes, G. (2017). Differential Location and Distribution of Hepatic Immune Cells. *Cells*, *6*(4), 48. https://doi.org/10.3390/cells6040048

Fridman, W. H., Pagès, F., Sautès-Fridman, C., & Galon, J. (2012). The immune contexture in human tumours: impact on clinical outcome. *Nature Reviews Cancer*, *12*(4), 298–306. https://doi.org/10.1038/nrc3245

Fu, M., Zhu, X., Zhang, J., Liang, J., Lin, Y., Zhao, L., Ehrengruber, M. U., & Chen, Y. E. (2003).

Egr-1 target genes in human endothelial cells identified by microarray analysis. *Gene*, *315*(1–2), 33–41. https://doi.org/10.1016/S0378-1119(03)00730-3

Furumaya, C., Martinez-Sanz, P., Bouti, P., Kuijpers, T. W., & Matlung, H. L. (2020). Plasticity in Pro- and Anti-tumor Activity of Neutrophils: Shifting the Balance. *Frontiers in Immunology*, *11*. https://doi.org/10.3389/fimmu.2020.02100

Gabrilovich, D. I., & Nagaraj, S. (2009). Myeloid-derived suppressor cells as regulators of the immune system. *Nature Reviews Immunology*, *9*(3), 162–174. https://doi.org/10.1038/nri2506

Galle, P. R., Forner, A., Llovet, J. M., Mazzaferro, V., Piscaglia, F., Raoul, J. L., Schirmacher, P., & Vilgrain, V. (2018). EASL Clinical Practice Guidelines: Management of hepatocellular carcinoma. *Journal of Hepatology*, *69*(1), 182–236. https://doi.org/10.1016/j.jhep.2018.03.019

Ganne-Carrié, N., & Nahon, P. (2019). Hepatocellular carcinoma in the setting of alcohol-related liver disease. In *Journal of Hepatology* (Vol. 70, Issue 2, pp. 284–293). Elsevier B.V. https://doi.org/10.1016/j.jhep.2018.10.008

Gao, B., Jeong, W. Il, & Tian, Z. (2008). Liver: An organ with predominant innate immunity. *Hepatology*, *47*(2), 729–736. https://doi.org/10.1002/hep.22034

Gasteiger, G., Hemmers, S., Firth, M. A., Floc'h, A. Le, Huse, M., Sun, J. C., & Rudensky, A. Y. (2013). IL-2-dependent tuning of NK cell sensitivity for target cells is controlled by regulatory T cells. *Journal of Experimental Medicine*, *210*(6), 1065–1068. https://doi.org/10.1084/jem.20122462

Germain, C., Bihl, F., Zahn, S., Poupon, G., Dumaurier, M. J., Rampanarivo, H. H., Padkjær, S. B., Spee, P., & Braud, V. M. (2010). Characterization of alternatively spliced transcript variants of CLEC2D gene. *Journal of Biological Chemistry*, *285*(46), 36207–36215. https://doi.org/10.1074/jbc.M110.179622

Germain, C., Meier, A., Jensen, T., Knapnougel, P., Poupon, G., Lazzari, A., Neisig, A., Håkansson, K., Dong, T., Wagtmann, N., Galsgaard, E. D., Spee, P., & Braud, V. M. (2011). Induction of lectin-like transcript 1 (LLT1) protein cell surface expression by pathogens and interferon-γ contributes to modulate immune responses. *Journal of Biological Chemistry*, *286*(44), 37964–37975. https://doi.org/10.1074/jbc.M111.285312

Golden-Mason, L., Hahn, Y. S., Strong, M., Cheng, L., & Rosen, H. R. (2014). Extracellular HCV-core protein induces an immature regulatory phenotype in NK cells: Implications for outcome of acute infection. *PLoS ONE*, *9*(7). https://doi.org/10.1371/journal.pone.0103219

Goto, K., Andres Roca Suarez, A., Wrensch, F., Baumert, T. F., & Lupberger, J. (2020). Hepatitis c virus and hepatocellular carcinoma: When the host loses its grip. In *International Journal of Molecular Sciences* (Vol. 21, Issue 9). https://doi.org/10.3390/ijms21093057

Grgurevic, I., Bozin, T., Mikus, M., Kukla, M., & O'beirne, J. (2021). Hepatocellular carcinoma in non-alcoholic fatty liver disease: From epidemiology to diagnostic approach. In *Cancers* (Vol. 13, Issue 22). MDPI. https://doi.org/10.3390/cancers13225844

Guerra, N., Tan, Y. X., Joncker, N. T., Choy, A., Gallardo, F., Xiong, N., Knoblaugh, S., Cado, D., Greenberg, N. R., & Raulet, D. H. (2008). NKG2D-Deficient Mice Are Defective in Tumor Surveillance in Models of Spontaneous Malignancy. *Immunity*, *28*(4), 571–580. https://doi.org/10.1016/j.immuni.2008.02.016

Guo, C.-L., Yang, H.-C., Yang, X.-H., Cheng, W., Dong, T.-X., Zhu, W.-J., Xu, Z., & Zhao, L. (2012). Associations Between Infiltrating Lymphocyte Subsets and Hepatocellular Carcinoma. *Asian Pacific Journal of Cancer Prevention*, *13*(11), 5909–5913. https://doi.org/10.7314/APJCP.2012.13.11.5909

Habif, G., Crinier, A., André, P., Vivier, E., & Narni-Mancinelli, E. (2019). Targeting natural killer cells in solid tumors. *Cellular & Molecular Immunology*, *16*(5), 415–422. https://doi.org/10.1038/s41423-019-0224-2

Han, B., Mao, F. Y., Zhao, Y. L., Lv, Y. P., Teng, Y. S., Duan, M., Chen, W., Cheng, P., Wang, T. T., Liang, Z. Y., Zhang, J. Y., Liu, Y. G., Guo, G., Zou, Q. M., Zhuang, Y., & Peng, L. S. (2018). Altered NKp30, NKp46, NKG2D, and DNAM-1 Expression on Circulating NK Cells Is Associated with Tumor Progression in Human Gastric Cancer. *Journal of Immunology Research*, *2018*. https://doi.org/10.1155/2018/6248590

Hart, C. L., Morrison, D. S., Batty, G. D., Mitchell, R. J., & Davey Smith, G. (2010). Effect of body mass index and alcohol consumption on liver disease: analysis of data from two prospective cohort studies. *BMJ*, *340*(mar11 1), c1240–c1240. https://doi.org/10.1136/bmj.c1240

Hassan, M., Selimovic, D., Ghozlan, H., & Abdel-kader, O. (2009). Hepatitis C virus core protein triggers hepatic angiogenesis by a mechanism including multiple pathways. *Hepatology*, *49*(5), 1469–1482. https://doi.org/10.1002/hep.22849

He, G., Zhang, H., Zhou, J., Wang, B., Chen, Y., Kong, Y., Xie, X., Wang, X., Fei, R., Wei, L., Chen, H., & Zeng, H. (2015). Peritumoural neutrophils negatively regulate adaptive immunity via the PD-L1/PD-1 signalling pathway in hepatocellular carcinoma. *Journal of Experimental & Clinical Cancer Research*, *34*(1), 141. https://doi.org/10.1186/s13046-015-0256-0

He, Jinan, Miao, R., Chen, Y., Wang, H., & Liu, M. (2024). The dual role of regulatory <scp>T</scp> cells in hepatitis <scp>B</scp> virus infection and related hepatocellular carcinoma. *Immunology*, *171*(4), 445–463. https://doi.org/10.1111/imm.13738

He, Junbing, Zhao, T., Liu, L., Liao, S., Yang, S., Lu, F., Hong, Y., Wei, N., Cheng, H., Zhang, W., & Shao, Y. (2022). The −172 A-to-G variation in ADAM17 gene promoter region affects EGR1/ADAM17 pathway and confers susceptibility to septic mortality with sepsis-3.0 criteria. *International Immunopharmacology*, *102*, 108385. https://doi.org/10.1016/j.intimp.2021.108385

He, Y., & Tian, Z. (2017). NK cell education via nonclassical MHC and non-MHC ligands. *Cellular & Molecular Immunology*, *14*(4), 321–330. https://doi.org/10.1038/cmi.2016.26

He, Z., Yu, Y., Nong, Y., Du, L., Liu, C., Cao, Y., Bai, L., & Tang, H. (2017). Hepatitis B virus X protein promotes hepatocellular carcinoma invasion and metastasis via upregulating thioredoxin interacting protein. *Oncology Letters*, *14*(2), 1323–1332.

https://doi.org/10.3892/ol.2017.6296

Hoechst, B., Voigtlaender, T., Ormandy, L., Gamrekelashvili, J., Zhao, F., Wedemeyer, H., Lehner, F., Manns, M. P., Greten, T. F., & Korangy, F. (2009). Myeloid derived suppressor cells inhibit natural killer cells in patients with hepatocellular carcinoma via the NKp30 receptor. *Hepatology (Baltimore, Md.)*, *50*(3), 799–807. https://doi.org/10.1002/hep.23054

Hou, X., Yu, F., Man, S., Huang, D., Zhang, Y., Liu, M., Ren, C., & Shen, J. (2012). Negative regulation of Schistosoma japonicum egg-induced liver fibrosis by natural killer cells. *PLoS Neglected Tropical Diseases*, *6*(1), 1–10. https://doi.org/10.1371/journal.pntd.0001456

Hsu, D. K., Dowling, C. a., Jeng, K. C. G., Chen, J. T., Yang, R. Y., & Liu, F. T. (1999). Galectin-3 expression is induced in cirrhotic liver and hepatocellular carcinoma. *International Journal of Cancer*, *81*(4), 519–526. https://doi.org/10.1002/(SICI)1097-0215(19990517)81:4<519::AID-IJC3>3.0.CO;2-0

Huang, R., Wu, H., Liu, Y., Xiong, Y., Xia, J., Pan, Z., Wang, G., Sun, Z., Yan, X., Chen, J., Zhang, Z., & Wu, C. (2016). B cells may play a pathological role in hepatic inflammation in chronic liver diseases. *International Journal of Clinical and Experimental Pathology*, *9*(3), 3630–3635.

Hudspeth, K., Donadon, M., Cimino, M., Pontarini, E., Tentorio, P., Preti, M., Hong, M., Bertoletti, A., Bicciato, S., Invernizzi, P., Lugli, E., Torzilli, G., Gershwin, M. E., & Mavilio, D. (2016a). Human liver-resident CD56bright/CD16neg NK cells are retained within hepatic sinusoids via the engagement of CCR5 and CXCR6 pathways. *Journal of Autoimmunity*, *66*, 40–50. https://doi.org/10.1016/j.jaut.2015.08.011

Hudspeth, K., Donadon, M., Cimino, M., Pontarini, E., Tentorio, P., Preti, M., Hong, M., Bertoletti, A., Bicciato, S., Invernizzi, P., Lugli, E., Torzilli, G., Gershwin, M. E., & Mavilio, D. (2016b). Human liver-resident CD56bright/CD16negNK cells are retained within hepatic sinusoids via the engagement of CCR5 and CXCR6 pathways. *Journal of Autoimmunity*, *66*, 40–50. https://doi.org/10.1016/j.jaut.2015.08.011

Hudspeth, K., Donadon, M., Cimino, M., Pontarini, E., Tentorio, P., Preti, M., Hong, M., Bertoletti, A., Bicciato, S., Invernizzi, P., Lugli, E., Torzilli, G., Gershwin, M. E., & Mavilio, D. (2016c). Human liver-resident CD56bright/CD16neg NK cells are retained within hepatic sinusoids via the engagement of CCR5 and CXCR6 pathways. *Journal of Autoimmunity*, *66*, 40–50. https://doi.org/10.1016/j.jaut.2015.08.011

Hydes, T. J., Blunt, M. D., Naftel, J., Vallejo, A. F., Seumois, G., Wang, A., Vijayanand, P., Polak, M. E., & Khakoo, S. I. (2019). Constitutive Activation of Natural Killer Cells in Primary Biliary Cholangitis. *Frontiers in Immunology*, *10*(November), 1–12. https://doi.org/10.3389/fimmu.2019.02633

Hydes, T., Noll, A., Salinas-Riester, G., Abuhilal, M., Armstrong, T., Hamady, Z., Primrose, J., Takhar, A., Walter, L., & Khakoo, S. I. (2017). IL-12 and IL-15 induce the expression of CXCR6 and CD49a on peripheral natural killer cells. *Immunity, Inflammation and Disease*. https://doi.org/10.1002/iid3.190

Iguchi-Manaka, A., Kai, H., Yamashita, Y., Shibata, K., Tahara-Hanaoka, S., Honda, S. I., Yasui,

T., Kikutani, H., Shibuya, K., & Shibuya, A. (2008). Accelerated tumor growth in mice deficient in DNAM-1 receptor. *Journal of Experimental Medicine*, *205*(13), 2959–2964. https://doi.org/10.1084/jem.20081611

Imai, K., Matsuyama, S., Miyake, S., Suga, K., & Nakachi, K. (2000). Natural cytotoxic activity of peripheral-blood lymphocytes and cancer incidence: an 11-year follow-up study of a general population. *The Lancet*, *356*(9244), 1795–1799. https://doi.org/10.1016/S0140-6736(00)03231-1

Irvine, K. M., Ratnasekera, I., Powell, E. E., & Hume, D. A. (2019). Casuses and consequences of innate immune dysfucntion in cirrhosis. *Frontiers in Immunology*, *10*(FEB). https://doi.org/10.3389/fimmu.2019.00293

Jeffery, H. C., Braitch, M. K., Bagnall, C., Hodson, J., Jeffery, L. E., Wawman, R. E., Wong, L. L., Birtwistle, J., Bartlett, H., Lohse, A. W., Hirschfield, G. M., Dyson, J., Jones, D., Hubscher, S. G., Klenerman, P., Adams, D. H., & Oo, Y. H. (2018). Changes in natural killer cells and exhausted memory regulatory T Cells with corticosteroid therapy in acute autoimmune hepatitis. *Hepatology Communications*, *2*(4), 421–436. https://doi.org/10.1002/hep4.1163

Jeong, W., Park, O., & Gao, B. (2008). Abrogation of the Antifibrotic Effects of Natural Killer Cells/Interferon-γ Contributes to Alcohol Acceleration of Liver Fibrosis. *Gastroenterology*, *134*(1), 248–258. https://doi.org/10.1053/j.gastro.2007.09.034

Jinushi, M., Takehara, T., Tatsumi, T., Hiramatsu, N., Sakamori, R., Yamaguchi, S., & Hayashi, N. (2005). Impairment of natural killer cell and dendritic cell functions by the soluble form of MHC class I-related chain A in advanced human hepatocellular carcinomas. *Journal of Hepatology*, *43*(6), 1013–1020. https://doi.org/10.1016/j.jhep.2005.05.026

Jinushi, M., Takehara, T., Tatsumi, T., Yamaguchi, S., Sakamori, R., Hiramatsu, N., Kanto, T., Ohkawa, K., & Hayashi, N. (2007). Natural killer cell and hepatic cell interaction via NKG2A leads to dendritic cell-mediated induction of CD4+ CD25+ T cells with PD-1-dependent regulatory activities. *Immunology*, *120*(1), 73–82. https://doi.org/10.1111/j.1365-2567.2006.02479.x

Ju, Y., Hou, N., Meng, J., Wang, X., Zhang, X., Zhao, D., Liu, Y., Zhu, F., Zhang, L., Sun, W., Liang, X., Gao, L., & Ma, C. (2010). T cell immunoglobulin- and mucin-domain-containing molecule-3 (Tim-3) mediates natural killer cell suppression in chronic hepatitis B. *Journal of Hepatology*, *52*(3), 322–329. https://doi.org/10.1016/j.jhep.2009.12.005

Kahraman, A., Schlattjan, M., Kocabayoglu, P., Yildiz-Meziletoglu, S., Schlensak, M., Fingas, C. D., Wedemeyer, I., Marquitan, G., Gieseler, R. K., Baba, H. A., Gerken, G., & Canbay, A. (2010). Major histocompatibility complex class I-related chains A and B (MIC A/B): A novel role in nonalcoholic steatohepatitis. *Hepatology*, *51*(1), 92–102. https://doi.org/10.1002/hep.23253

Kamimura, H., Yamagiwa, S., Tsuchiya, A., Takamura, M., Matsuda, Y., Ohkoshi, S., Inoue, M., Wakai, T., Shirai, Y., Nomoto, M., & Aoyagi, Y. (2012). Reduced NKG2D ligand expression in hepatocellular carcinoma correlates with early recurrence. *Journal of Hepatology*, *56*(2), 381–388. https://doi.org/10.1016/j.jhep.2011.06.017

Kamishikiryo, J., Fukuhara, H., Okabe, Y., Kuroki, K., & Maenaka, K. (2011). Molecular basis for LLT1 protein recognition by human CD161 protein (NKRP1A/KLRB1). *Journal of Biological Chemistry*, *286*(27), 23823–23830. https://doi.org/10.1074/jbc.M110.214254

Kedia-Mehta, N., Tobin, L., Zaiatz-Bittencourt, V., Pisarska, M. M., De Barra, C., Choi, C., Elamin, E., O'Shea, D., Gardiner, C. M., Finlay, D. K., & Hogan, A. E. (2021). Cytokine-induced natural killer cell training is dependent on cellular metabolism and is defective in obesity. *Blood Advances*, *5*(21), 4447–4455. https://doi.org/10.1182/bloodadvances.2021005047

Khakoo, S. I., Thio, C. L., Martin, M. P., Brooks, C. R., Gao, X., Astemborski, J., Cheng, J., Goedert, J. J., Vlahov, D., Hilgartner, M., Cox, S., Little, A.-M., Alexander, G. J., Cramp, M. E., O'Brien, S. J., Rosenberg, W. M. C., Thomas, D. L., & Carrington, M. (2004). HLA and NK Cell Inhibitory Receptor Genes in Resolving Hepatitis C Virus Infection. *Science*, *305*(5685), 872–874. https://doi.org/10.1126/science.1097670

Kiessling, R., Klein, E., & Wigzell, H. (1975). „Natural" killer cells in the mouse. I. Cytotoxic cells with specificity for mouse Moloney leukemia cells. Specificity and distribution according to genotype. *European Journal of Immunology*, *5*(2), 112–117. https://doi.org/10.1002/eji.1830050208

Kim, M. J., Kim, H. B., Bae, J. H., Lee, J. W., Park, S. J., Kim, D. W., Park, S. I., Kang, C. D., & Kim, S. H. (2009). Sensitization of human K562 leukemic cells to TRAIL-induced apoptosis by inhibiting the DNA-PKcs/Akt-mediated cell survival pathway. *Biochemical Pharmacology*, *78*(6), 573–582. https://doi.org/10.1016/j.bcp.2009.05.016

Kim, S., Poursine-Laurent, J., Truscott, S. M., Lybarger, L., Song, Y.-J., Yang, L., French, A. R., Sunwoo, J. B., Lemieux, S., Hansen, T. H., & Yokoyama, W. M. (2005). Licensing of natural killer cells by host major histocompatibility complex class I molecules. *Nature*, *436*(7051), 709–713. https://doi.org/10.1038/nature03847

Kleinschek, M. a., Boniface, K., Sadekova, S., Grein, J., Murphy, E. E., Turner, S. P., Raskin, L., Desai, B., Faubion, W. a., De Malefyt, R. W., Pierce, R. H., McClanahan, T., & Kastelein, R. a. (2009). Circulating and gut-resident human Th17 cells express CD161 and promote intestinal inflammation. *Journal of Experimental Medicine*, *206*(3), 525–534. https://doi.org/10.1084/jem.20081712

Knapp, S., Usama Warshow, Hegazy, D., Brackenbury, L., Guha, I. N., Fowell, A., Little, A. M., Alexander, G. J., Rosenberg, W. M. C., Cramp, M. E., & Khakoo, S. I. (2010). Consistent beneficial effects of killer cell immunoglobulin-like receptor 2dl3 and group 1 human leukocyte antigen-c following exposure to hepatitis c virus. *Hepatology*, *51*(4), 1168–1175. https://doi.org/10.1002/hep.23477

Koeffler, H. P., & Golde, D. W. (1980). Human Myeloid Leukemia Cell Lines: A Review. In *Blood* (Vol. 56, Issue 3).

Kohga, K., Takehara, T., Tatsumi, T., Ishida, H., Miyagi, T., Hosui, A., & Hayashi, N. (2010). Sorafenib inhibits the shedding of major histocompatibility complex class i-related chain a on hepatocellular carcinoma cells by down-regulating a disintegrin and metalloproteinase 9. *Hepatology*, *51*(4), 1264–1273. https://doi.org/10.1002/hep.23456

Kohla, M. A. S., Attia, A., Darwesh, N., Obada, M., Taha, H., & Youssef, M. F. (2017). Association of serum levels of transforming growth factor b1 with disease severity in patients with hepatocellular carcinoma. *Hepatoma Research*, *3*(12), 294. https://doi.org/10.20517/2394-5079.2017.40

Kong, L.-Q., Zhu, X.-D., Xu, H.-X., Zhang, J.-B., Lu, L., Wang, W.-Q., Zhang, Q.-B., Wu, W.-Z., Wang, L., Fan, J., Tang, Z.-Y., & Sun, H.-C. (2013). The Clinical Significance of the CD163+ and CD68+ Macrophages in Patients with Hepatocellular Carcinoma. *PLoS ONE*, *8*(3), e59771. https://doi.org/10.1371/journal.pone.0059771

Kotsari, M., Dimopoulou, V., Koskinas, J., & Armakolas, A. (2023). Immune System and Hepatocellular Carcinoma (HCC): New Insights into HCC Progression. *International Journal of Molecular Sciences*, *24*(14), 11471. https://doi.org/10.3390/ijms241411471

Koumbi, L., Pollicino, T., Raimondo, G., Kumar, N., Karayiannis, P., & Khakoo, S. I. (2016). Hepatitis B viral replication influences the expression of natural killer cell ligands. *Annals of Gastroenterology*, *29*(3), 348–357. https://doi.org/10.20524/aog.2016.0036

Krensky, A. M., & Clayberger, C. (2009). Biology and clinical relevance of granulysin: REVIEW ARTICLE. In *Tissue Antigens* (Vol. 73, Issue 3, pp. 193–198). https://doi.org/10.1111/j.1399-0039.2008.01218.x

Krzewski, K., & Coligan, J. E. (2012). Human NK cell lytic granules and regulation of their exocytosis. In *Frontiers in Immunology* (Vol. 3, Issue NOV). https://doi.org/10.3389/fimmu.2012.00335

Kuang, D.-M., Peng, C., Zhao, Q., Wu, Y., Zhu, L.-Y., Wang, J., Yin, X.-Y., Li, L., & Zheng, L. (2010). Tumor-activated monocytes promote expansion of IL-17-producing CD8+ T cells in hepatocellular carcinoma patients. *Journal of Immunology (Baltimore, Md. : 1950)*, *185*(3), 1544–1549. https://doi.org/10.4049/jimmunol.0904094

Kumar, N., & Khakoo, S. I. (2018a). Hepatocellular carcinoma: Prospects for natural killer cell immunotherapy. *Hla*, *92*(1), 3–11. https://doi.org/10.1111/tan.13275

Kumar, N., & Khakoo, S. I. (2018b). Hepatocellular carcinoma: Prospects for natural killer cell immunotherapy. In *HLA* (Vol. 92, Issue 1, pp. 3–11). Blackwell Publishing Ltd. https://doi.org/10.1111/tan.13275

Kumar, V., Yi Lo, P. H., Sawai, H., Kato, N., Takahashi, A., Deng, Z., Urabe, Y., Mbarek, H., Tokunaga, K., Tanaka, Y., Sugiyama, M., Mizokami, M., Muroyama, R., Tateishi, R., Omata, M., Koike, K., Tanikawa, C., Kamatani, N., Kubo, M., … Matsuda, K. (2012). Soluble MICA and a MICA Variation as Possible Prognostic Biomarkers for HBV-Induced Hepatocellular Carcinoma. *PLoS ONE*, *7*(9), e44743. https://doi.org/10.1371/journal.pone.0044743

Kurioka, A., Cosgrove, C., Simoni, Y., van Wilgenburg, B., Geremia, a., Björkander, S., Sverremark-Ekström, E., Thurnheer, C., Günthard, H. F., Khanna, N., Walker, L. J., Arancibia-Cárcamo, C. V., Newell, E. W., Willberg, C. B., Klenerman, P., Aubert, V., Battegay, M., Bernasconi, E., Böni, J., … Uhlig, H. (2018). CD161 defines a functionally distinct subset of pro-inflammatory natural killer cells. *Frontiers in Immunology*, *9*(APR), 1–14. https://doi.org/10.3389/fimmu.2018.00486

Langhans, B., Alwan, A. W., Krämer, B., Glässner, A., Lutz, P., Strassburg, C. P., Nattermann, J., & Spengler, U. (2015). Regulatory CD4+ T cells modulate the interaction between NK cells and hepatic stellate cells by acting on either cell type. *Journal of Hepatology*, *62*(2), 398–404. https://doi.org/10.1016/j.jhep.2014.08.038

Lanier, L. L., Chang, C., & Phillips, J. H. (1994). Human NKR-P1A. A disulfide-linked homodimer of the C-type lectin superfamily expressed by a subset of NK and T lymphocytes. *Journal of Immunology (Baltimore, Md. : 1950)*, *153*(6), 2417–2428.

Laso, F J, Madruga, J. I., Giron, J. A., Lopez, A., Ciudad, J., San Miguel, J. F., Alvarez-Mon, M., & Orfao, A. (1997). Decreased natural killer cytotoxic activity in chronic alcoholism is associated with alcohol liver disease but not active ethanol consumption. *Hepatology*, *25*(5), 1096–1100. https://doi.org/10.1002/hep.510250508

Laso, Francisco Javier, Almeida, J., Torres, E., Vaquero, J. M., Marcos, M., & Orfao, A. (2010). Chronic Alcohol Consumption Is Associated With an Increased Cytotoxic Profile of Circulating Lymphocytes That May Be Related With the Development of Liver Injury. *Alcoholism: Clinical and Experimental Research*, *34*(5), 876–885. https://doi.org/10.1111/j.1530-0277.2010.01160.x

Lauer, G. M., & Walker, B. D. (2001). Hepatitis C Virus Infection. *New England Journal of Medicine*, *345*(1), 41–52. https://doi.org/10.1056/NEJM200107053450107

Lauzon, N. M., Mian, F., MacKenzie, R., & Ashkar, A. A. (2006). The direct effects of Toll-like receptor ligands on human NK cell cytokine production and cytotoxicity. *Cellular Immunology*, *241*(2), 102–112. https://doi.org/10.1016/j.cellimm.2006.08.004

Le Maux Chansac, B., Moretta, A., Vergnon, I., Opolon, P., Lecluse, Y., Grunenwald, D., Kubin, M., Soria, J.-C., Chouaib, S., & Mami-Chouaib, F. (2005). NK Cells Infiltrating a MHC Class I-Deficient Lung Adenocarcinoma Display Impaired Cytotoxic Activity toward Autologous Tumor Cells Associated with Altered NK Cell-Triggering Receptors. *The Journal of Immunology*, *175*(9), 5790–5798. https://doi.org/10.4049/jimmunol.175.9.5790

Lebossé, F., Gudd, C., Tunc, E., Singanayagam, A., Nathwani, R., Triantafyllou, E., Pop, O., Kumar, N., Mukherjee, S., Hou, T. Z., Quaglia, A., Zoulim, F., Wendon, J., Dhar, A., Thursz, M., Antoniades, C. G., & Khamri, W. (2019). CD8+ T cells from patients with cirrhosis display a phenotype that may contribute to cirrhosis-associated immune dysfunction. *EBioMedicine*, *49*, 258–268. https://doi.org/10.1016/j.ebiom.2019.10.011

Lee, H. A., Goh, H. G., Lee, Y.-S., Jung, Y. K., Kim, J. H., Yim, H. J., Lee, M.-G., An, H., Jeen, Y. T., Yeon, J. E., Byun, K. S., & Seo, Y. S. (2021). Natural killer cell activity is a risk factor for the recurrence risk after curative treatment of hepatocellular carcinoma. *BMC Gastroenterology*, *21*(1), 258. https://doi.org/10.1186/s12876-021-01833-2

Lee, M. H., Yang, H. I., Yuan, Y., L'Italien, G., & Chen, C. J. (2014). Epidemiology and natural history of hepatitis C virus infection. *World Journal of Gastroenterology*, *20*(28), 9270–9280. https://doi.org/10.3748/wjg.v20.i28.9270

Lencioni, R., Kudo, M., Erinjeri, J., Qin, S., Ren, Z., Chan, S., Arai, Y., Heo, J., Mai, A., Escobar, J., Lopez Chuken, Y. A., Yoon, J.-H., Tak, W. Y., Suttichaimongkol, T., Bouattour, M., Lin, S.-M., Żotkiewicz, M., Udoye, S., Cohen, G., & Sangro, B. (2024). EMERALD-1: A phase 3,

randomized, placebo-controlled study of transarterial chemoembolization combined with durvalumab with or without bevacizumab in participants with unresectable hepatocellular carcinoma eligible for embolization. *Journal of Clinical Oncology*, *42*(3_suppl), LBA432–LBA432. https://doi.org/10.1200/JCO.2024.42.3_suppl.LBA432

Leong, J. W., Chase, J. M., Romee, R., Schneider, S. E., Sullivan, R. P., Cooper, M. a., & Fehniger, T. a. (2014). Preactivation with IL-12, IL-15, and IL-18 induces cd25 and a functional high-affinity il-2 receptor on human cytokine-induced memory-like natural killer cells. *Biology of Blood and Marrow Transplantation*, *20*(4), 463–473. https://doi.org/10.1016/j.bbmt.2014.01.006

Levitt, L., Nagler, A., Lee, F., Abrams, J., Shatsky, M., & Thompson, D. (1991). Production of Granulocyte/Macrophage-Colony-stimulating Factorby Human Natural Killer Cells. *Journal of Clinical Investigation*, *88*, 67–75.

Li, F., Wei, H., Wei, H., Gao, Y., Xu, L., Yin, W., Sun, R., & Tian, Z. (2013). Blocking the Natural Killer Cell Inhibitory Receptor NKG2A Increases Activity of Human Natural Killer Cells and Clears Hepatitis B Virus Infection in Mice. *Gastroenterology*, *144*(2), 392–401. https://doi.org/10.1053/j.gastro.2012.10.039

Li, J., Zhao, Y. R., & Tian, Z. (2019). Roles of hepatic stellate cells in acute liver failure: From the perspective of inflammation and fibrosis. In *World Journal of Hepatology* (Vol. 11, Issue 5, pp. 412–420). Baishideng Publishing Group Co. https://doi.org/10.4254/wjh.v11.i5.412

Li, T., Yang, Y., Hua, X., Wang, G., Liu, W., Jia, C., Tai, Y., Zhang, Q., & Chen, G. (2012). Hepatocellular carcinoma-associated fibroblasts trigger NK cell dysfunction via PGE2 and IDO. *Cancer Letters*, *318*(2), 154–161. https://doi.org/10.1016/j.canlet.2011.12.020

Li, X., Xu, Z., Cui, G., Yu, L., & Zhang, X. (2020). BTLA expression in stage I–III non–small-cell lung cancer and its correlation with PD-1/PD-L1 and clinical outcomes. *OncoTargets and Therapy*, *13*, 215–224. https://doi.org/10.2147/OTT.S232234

Li, Y., & Sun, R. (2018). Tumor immunotherapy: New aspects of natural killer cells. *Chinese Journal of Cancer Research*, *30*(2), 173–196. https://doi.org/10.21147/j.issn.1000-9604.2018.02.02

Liu, M., Liang, S., & Zhang, C. (2021). NK Cells in Autoimmune Diseases: Protective or Pathogenic? *Frontiers in Immunology*, *12*. https://doi.org/10.3389/fimmu.2021.624687

Liu, Y., Cheng, Y., Xu, Y., Wang, Z., Du, X., Li, C., Peng, J., Gao, L., Liang, X., & Ma, C. (2017). Increased expression of programmed cell death protein 1 on NK cells inhibits NK-cell-mediated anti-tumor function and indicates poor prognosis in digestive cancers. *Oncogene*, *36*(44), 6143–6153. https://doi.org/10.1038/onc.2017.209

Llovet, J., Kelley, R. K., Villanueva, A., & Rossi, J. Z.-. (2021). Hepatocellular carcinoma. *Nature Reviews Disease Primers*, *0123456789*. https://doi.org/10.1038/s41572-020-00240-3

Llovet, J. M., Castet, F., Heikenwalder, M., Maini, M. K., Mazzaferro, V., Pinato, D. J., Pikarsky, E., Zhu, A. X., & Finn, R. S. (2022). Immunotherapies for hepatocellular carcinoma. *Nature Reviews Clinical Oncology*, *19*(3), 151–172.

https://doi.org/10.1038/s41571-021-00573-2

Llovet, J. M., Kelley, R. K., Villanueva, A., Singal, A. G., Pikarsky, E., Roayaie, S., Lencioni, R., Koike, K., Zucman-Rossi, J., & Finn, R. S. (2021). Hepatocellular carcinoma. In *Nature Reviews Disease Primers* (Vol. 7, Issue 1). Nature Research. https://doi.org/10.1038/s41572-020-00240-3

Lopez-Vergès, S., Milush, J. M., Schwartz, B. S., Pando, M. J., Jarjoura, J., York, V. A., Houchins, J. P., Miller, S., Kang, S. M., Norris, P. J., Nixon, D. F., & Lanier, L. L. (2011). Expansion of a unique CD57 +NKG2C hi natural killer cell subset during acute human cytomegalovirus infection. *Proceedings of the National Academy of Sciences of the United States of America*, *108*(36), 14725–14732. https://doi.org/10.1073/pnas.1110900108

Lu, L.-C., Chang, C.-J., & Hsu, C.-H. (2019). Targeting myeloid-derived suppressor cells in the treatment of hepatocellular carcinoma: current state and future perspectives . *Journal of Hepatocellular Carcinoma*, *Volume 6*, 71–84. https://doi.org/10.2147/jhc.s159693

Lucas, M., Schachterle, W., Oberle, K., Aichele, P., & Diefenbach, A. (2007). Natural Killer Cell-Mediated Control of Infections Requires Production of Interleukin 15 by Type I IFN-Triggered Dendritic Cells. *Immunity*, *26*(4), 503–517.

Luevano, M., Madrigal, A., & Saudemont, A. (2012). Transcription factors involved in the regulation of natural killer cell development and function: An update. *Frontiers in Immunology*, *3*(OCT), 1–6. https://doi.org/10.3389/fimmu.2012.00319

Mace, E. M. (2018). Phosphoinositide-3-Kinase Signaling in Human Natural Killer Cells: New Insights from Primary Immunodeficiency. *Frontiers in Immunology*, *9*. https://doi.org/10.3389/fimmu.2018.00445

Mace, E. M., Bigley, V., Gunesch, J. T., Chinn, I. K., Angelo, L. S., Care, M. A., Maisuria, S., Keller, M. D., Togi, S., Watkin, L. B., LaRosa, D. F., Jhangiani, S. N., Muzny, D. M., Stray-Pedersen, A., Coban Akdemir, Z., Smith, J. B., Hernández-Sanabria, M., Le, D. T., Hogg, G. D., … Orange, J. S. (2016). Biallelic mutations in IRF8 impair human NK cell maturation and function. *Journal of Clinical Investigation*, *127*(1), 306–320. https://doi.org/10.1172/JCI86276

Mackay, L. K., Minnich, M., Kragten, N. A. M., Liao, Y., Nota, B., Seillet, C., Zaid, A., Man, K., Preston, S., Freestone, D., Braun, A., Wynne-Jones, E., Behr, F. M., Stark, R., Pellicci, D. G., Godfrey, D. I., Belz, G. T., Pellegrini, M., Gebhardt, T., … van Gisbergen, K. P. J. M. (2016). Hobit and Blimp1 instruct a universal transcriptional program of tissue residency in lymphocytes. *Science*, *352*(6284), 459–463. https://doi.org/10.1126/science.aad2035

Maini, M. K., & Peppa, D. (2013). NK cells: A double-edged sword in chronic hepatitis B virus infection. In *Frontiers in Immunology* (Vol. 4, Issue MAR). https://doi.org/10.3389/fimmu.2013.00057

Mandelboim, O, Malik, P., Davis, D. M., Jo, C. H., Boyson, J. E., & Strominger, J. L. (1999). Human CD16 as a lysis receptor mediating direct natural killer cell cytotoxicity. *Proceedings of the National Academy of Sciences of the United States of America*,

96(10), 5640–5644. https://doi.org/10.1073/pnas.96.10.5640

Mandelboim, Ofer, Malik, P., Davis, D. M., Jo, C. H., Boyson, J. E., & Strominger, J. L. (1999). Human CD16 as a lysis receptor mediating direct natural killer cell cytotoxicity. *Proceedings of the National Academy of Sciences of the United States of America*, *96*(10), 5640–5644. https://doi.org/10.1073/pnas.96.10.5640

Mandlik, D. S., Mandlik, S. K., & Choudhary, H. B. (2023). Immunotherapy for hepatocellular carcinoma: Current status and future perspectives. *World Journal of Gastroenterology*, *29*(6), 1054–1075. https://doi.org/10.3748/wjg.v29.i6.1054

Mantovani, S., Oliviero, B., Lombardi, A., Varchetta, S., Mele, D., Sangiovanni, A., Rossi, G., Donadon, M., Torzilli, G., Soldani, C., Porta, C., Pedrazzoli, P., Chiellino, S., Santambrogio, R., Opocher, E., Maestri, M., Bernuzzi, S., Rossello, A., Clément, S., … Mondelli, M. U. (2019). Deficient Natural Killer Cell NKp30-Mediated Function and Altered NCR3 Splice Variants in Hepatocellular Carcinoma. *Hepatology*, *69*(3), 1165–1179. https://doi.org/10.1002/hep.30235

Marcus, A., Gowen, B. G., Thompson, T. W., Iannello, A., Ardolino, M., Deng, W., Wang, L., Shifrin, N., & Raulet, D. H. (2014). Recognition of tumors by the innate immune system and natural killer cells. *Advances in Immunology*, *122*, 91–128. https://doi.org/10.1016/B978-0-12-800267-4.00003-1

Markwick, L. J. L., Riva, A., Ryan, J. M., Cooksley, H., Palma, E., Tranah, T. H., Manakkat Vijay, G. K., Vergis, N., Thursz, M., Evans, A., Wright, G., Tarff, S., O'Grady, J., Williams, R., Shawcross, D. L., & Chokshi, S. (2015). Blockade of PD1 and TIM3 restores innate and adaptive immunity in patients with acute alcoholic hepatitis. *Gastroenterology*, *148*(3), 590-602.e10. https://doi.org/10.1053/j.gastro.2014.11.041

Marotel, M., Villard, M., Drouillard, A., Tout, I., Besson, L., Allatif, O., Pujol, M., Rocca, Y., Ainouze, M., Roblot, G., Viel, S., Gomez, M., Loustaud, V., Alain, S., Durantel, D., Walzer, T., Hasan, U., & Marçais, A. (2021). Peripheral natural killer cells in chronic hepatitis B patients display multiple molecular features of T cell exhaustion. *ELife*, *10*. https://doi.org/10.7554/eLife.60095

Marquardt, N., Béziat, V., Nyström, S., Hengst, J., Ivarsson, M. a, Kekäläinen, E., Johansson, H., Mjösberg, J., Westgren, M., Lankisch, T. O., Wedemeyer, H., Ellis, E. C., Ljunggren, H.-G., Michaëlsson, J., & Björkström, N. K. (2015). Cutting Edge: Identification and Characterization of Human Intrahepatic CD49a+ NK Cells. *Journal of Immunology (Baltimore, Md. : 1950)*, 0–2. https://doi.org/10.4049/jimmunol.1402756

Marrufo, A. M., Mathew, S. O., Chaudhary, P., Malaer, J. D., Vishwanatha, J. K., & Mathew, P. a. (2018). Blocking LLT1 (CLEC2D, OCIL)-NKRP1A (CD161) interaction enhances natural killer cell-mediated lysis of triple-negative breast cancer cells. *American Journal of Cancer Research*, *8*(6), 1050–1063. http://www.ncbi.nlm.nih.gov/pubmed/30034942

Martínez-Chantar, M. L., Delgado, T. C., & Beraza, N. (2021). Revisiting the Role of Natural Killer Cells in Non-Alcoholic Fatty Liver Disease. *Frontiers in Immunology*, *12*. https://doi.org/10.3389/fimmu.2021.640869

Martinez-Espinosa, I., Serrato, J. A., & Ortiz-Quintero, B. (2022). Role of il-10-producing natural killer cells in the regulatory mechanisms of inflammation during systemic

infection. *Biomolecules*, *12*(1). https://doi.org/10.3390/biom12010004

Mathew, P. a, Chuang, S. S., Vaidya, S. V, Kumaresan, P. R., Boles, K. S., & Pham, H.-T. K. (2004). The LLT1 receptor induces IFN-gamma production by human natural killer cells. *Molecular Immunology*, *40*(16), 1157–1163. https://doi.org/10.1016/j.molimm.2003.11.024

Mathew, S. O., Chaudhary, P., Powers, S. B., Vishwanatha, J. K., & Mathew, P. a. (2016). Overexpression of LLT1 (OCIL, CLEC2D) on prostate cancer cells inhibits NK cell-mediated killing through LLT1-NKRP1A (CD161) interaction. *Oncotarget*, *7*(42), 68650–68661. https://doi.org/10.18632/ONCOTARGET.11896

Matos, L. C., Batista, P., Monteiro, N., Ribeiro, J., Cipriano, M. A., Henriques, P., Girão, F., & Carvalho, A. (2013). Lymphocyte subsets in alcoholic liver disease. *World Journal of Hepatology*, *5*(2), 46–55. https://doi.org/10.4254/wjh.v5.i2.46

Mbeunkui, F., & Johann, D. J. (2009). Cancer and the tumor microenvironment: A review of an essential relationship. In *Cancer Chemotherapy and Pharmacology* (Vol. 63, Issue 4, pp. 571–582). https://doi.org/10.1007/s00280-008-0881-9

Meier, U.-C., Owen, R. E., Taylor, E., Worth, A., Naoumov, N., Willberg, C., Tang, K., Newton, P., Pellegrino, P., Williams, I., Klenerman, P., & Borrow, P. (2005). Shared Alterations in NK Cell Frequency, Phenotype, and Function in Chronic Human Immunodeficiency Virus and Hepatitis C Virus Infections. *Journal of Virology*, *79*(19), 12365–12374. https://doi.org/10.1128/JVI.79.19.12365-12374.2005

Michelet, X., Dyck, L., Hogan, A., Loftus, R. M., Duquette, D., Wei, K., Beyaz, S., Tavakkoli, A., Foley, C., Donnelly, R., O'Farrelly, C., Raverdeau, M., Vernon, A., Pettee, W., O'Shea, D., Nikolajczyk, B. S., Mills, K. H. G., Brenner, M. B., Finlay, D., & Lynch, L. (2018). Metabolic reprogramming of natural killer cells in obesity limits antitumor responses. *Nature Immunology*, *19*(12), 1330–1340. https://doi.org/10.1038/s41590-018-0251-7

Mikulak, J., Bruni, E., Oriolo, F., Di Vito, C., & Mavilio, D. (2019). Hepatic natural killer cells: Organ-specific sentinels of liver immune homeostasis and physiopathology. *Frontiers in Immunology*, *10*(APR), 1–12. https://doi.org/10.3389/fimmu.2019.00946

Montaldo, E., Vacca, P., Chiossone, L., Croxatto, D., Loiacono, F., Martini, S., Ferrero, S., Walzer, T., Moretta, L., & Mingari, M. C. (2016). Unique Eomes+ NK Cell Subsets Are Present in Uterus and Decidua During Early Pregnancy. *Frontiers in Immunology*, *6*. https://doi.org/10.3389/fimmu.2015.00646

Montironi, C., Castet, F., Haber, P. K., Pinyol, R., Torres-Martin, M., Torrens, L., Mesropian, A., Wang, H., Puigvehi, M., Maeda, M., Leow, W. Q., Harrod, E., Taik, P., Chinburen, J., Taivanbaatar, E., Chinbold, E., Solé Arqués, M., Donovan, M., Thung, S., … Llovet, J. M. (2022). Inflamed and non-inflamed classes of HCC: a revised immunogenomic classification. *Gut*, gutjnl-2021-325918. https://doi.org/10.1136/gutjnl-2021-325918

Moriya, K., Yotsuyanagi, H., Shintani, Y., Fujie, H., Ishibashi, K., Matsuura, Y., Miyamura, T., & Koike, K. (1997). Printed in Great Britain Hepatitis C virus core protein induces hepatic steatosis in transgenic mice. In *Journal of General Virology* (Vol. 78).

Muntasell, A., Ochoa, M. C., Cordeiro, L., Berraondo, P., López-Díaz de Cerio, A., Cabo, M.,

López-Botet, M., & Melero, I. (2017). Targeting NK-cell checkpoints for cancer immunotherapy. In *Current Opinion in Immunology* (Vol. 45, pp. 73–81). https://doi.org/10.1016/j.coi.2017.01.003

Nahon, P., & Zucman-Rossi, J. (2012). Single nucleotide polymorphisms and risk of hepatocellular carcinoma in cirrhosis. In *Journal of Hepatology* (Vol. 57, Issue 3, pp. 663–674). https://doi.org/10.1016/j.jhep.2012.02.035

Nakabayashi, H., Taketa, K., Miyano, K., Yamane, T., & Sato1, J. (1982). *Growth of Human Hepatoma Cell Lines with Differentiated Functions in Chemically Defined Medium*.

Nakamoto, N., & Kanai, T. (2014). Role of Toll-like receptors in immune activation and tolerance in the liver. In *Frontiers in Immunology* (Vol. 5, Issue MAY). Frontiers Media S.A. https://doi.org/10.3389/fimmu.2014.00221

Niu, C., Li, M., Zhu, S., Chen, Y., Zhou, L., Xu, D., Xu, J., Li, Z., Li, W., & Cui, J. (2020). Pd-1-positive natural killer cells have a weaker antitumor function than that of pd-1-negative natural killer cells in lung cancer. *International Journal of Medical Sciences*, *17*(13), 1964–1973. https://doi.org/10.7150/ijms.47701

Noh, J. Y., Yoon, S. R., Kim, T. D., Choi, I., & Jung, H. (2020). Toll-Like Receptors in Natural Killer Cells and Their Application for Immunotherapy. In *Journal of Immunology Research* (Vol. 2020). Hindawi Limited. https://doi.org/10.1155/2020/2045860

Northfield, J. W., Kasprowicz, V., Lucas, M., Kersting, N., Bengsh, B., Kim, A., Phillips, R. E., Walker, B. D., Thimme, R., Lauer, G., & Klenerman, P. (2008). CD161 expression on hepatitis C virus-specific CD8+ T cells suggests a distinct pathway of T cell differentiation. *Hepatology*, *47*(2), 396–406. https://doi.org/10.1002/hep.22040

Ohs, I., Ducimetière, L., Marinho, J., Kulig, P., Becher, B., & Tugues, S. (2017). Restoration of natural killer cell antimetastatic activity by IL12 and checkpoint blockade. *Cancer Research*, *77*(24), 7059–7071. https://doi.org/10.1158/0008-5472.CAN-17-1032

Okuda, M., Li, K., Beard, M. R., Showalter, L. A., Scholle, F., Lemon, S. M., & Weinman, S. A. (2002). Mitochondrial injury, oxidative stress, and antioxidant gene expression are induced by hepatitis C virus core protein. *Gastroenterology*, *122*(2), 366–375. https://doi.org/10.1053/gast.2002.30983

Oliviero, B, Varchetta, S., Paudice, E., Michelone, G., Zaramella, M., Mavilio, D., De Filippi, F., Bruno, S., & Mondelli, M. U. (2009). Natural killer cell functional dichotomy in chronic hepatitis B and chronic hepatitis C virus infections. *Gastroenterology*, *137*(3), 1151–1160, 1160 e1-7. https://doi.org/10.1053/j.gastro.2009.05.047

Oliviero, Barbara, Varchetta, S., Paudice, E., Michelone, G., Zaramella, M., Mavilio, D., De Filippi, F., Bruno, S., & Mondelli, M. U. (2009). Natural Killer Cell Functional Dichotomy in Chronic Hepatitis B and Chronic Hepatitis C Virus Infections. *Gastroenterology*, *137*(3), 1151-1160.e7. https://doi.org/10.1053/j.gastro.2009.05.047

Oppenheim, D. E., Roberts, S. J., Clarke, S. L., Filler, R., Lewis, J. M., Tigelaar, R. E., Girardi, M., & Hayday, A. C. (2005). Sustained localized expression of ligand for the activating NKG2D receptor impairs natural cytotoxicity in vivo and reduces tumor immunosurveillance. *Nature Immunology*, *6*(9), 928–937.

https://doi.org/10.1038/ni1239

Orange, J. S. (2008). Formation and function of the lytic NK-cell immunological synapse. In *Nature Reviews Immunology* (Vol. 8, Issue 9, pp. 713–725). https://doi.org/10.1038/nri2381

Oth, T., Habets, T. H. P. M., Germeraad, W. T. V., Zonneveld, M. I., Bos, G. M. J., & Vanderlocht, J. (2018). Pathogen recognition by NK cells amplifies the pro-inflammatory cytokine production of monocyte-derived DC via IFN-γ. *BMC Immunology*, *19*(1), 1–13. https://doi.org/10.1186/s12865-018-0247-y

Pahl, J. H. W., Cerwenka, A., & Ni, J. (2018). Memory-Like NK cells: Remembering a previous activation by cytokines and NK cell receptors. In *Frontiers in Immunology* (Vol. 9, Issue NOV). Frontiers Media S.A. https://doi.org/10.3389/fimmu.2018.02796

Pallett, L. J., Burton, A. R., Amin, O. E., Rodriguez-Tajes, S., Patel, A. A., Zakeri, N., Jeffery-Smith, A., Swadling, L., Schmidt, N. M., Baiges, A., Gander, A., Yu, D., Nasralla, D., Froghi, F., Iype, S., Davidson, B. R., Thorburn, D., Yona, S., Forns, X., & Maini, M. K. (2020). Longevity and replenishment of human liver-resident memory T cells and mononuclear phagocytes. *Journal of Experimental Medicine*, *217*(9). https://doi.org/10.1084/jem.20200050

Pallmer, K., & Oxenius, A. (2016). Recognition and regulation of T cells by NK cells. In *Frontiers in Immunology* (Vol. 7, Issue JUN). Frontiers Research Foundation. https://doi.org/10.3389/fimmu.2016.00251

Palmer, D. H. (2008). Sorafenib in advanced hepatocellular carcinoma. *The New England Journal of Medicine*, *359*(23), 2498; author reply 2498-2499. https://doi.org/10.1056/NEJMoa0708857

Palmer, D. H., Midgley, R. S., Mirza, N., Torr, E. E., Ahmed, F., Steele, J. C., Steven, N. M., Kerr, D. J., Young, L. S., & Adams, D. H. (2009). A phase II study of adoptive immunotherapy using dendritic cells pulsed with tumor lysate in patients with hepatocellular carcinoma. *Hepatology*, *49*(1), 124–132. https://doi.org/10.1002/hep.22626

Pan, H., Sun, R., Jaruga, B., Hong, F., Kim, W.-H., & Gao, B. (2006). Chronic Ethanol Consumption Inhibits Hepatic Natural Killer Cell Activity and Accelerates Murine Cytomegalovirus-Induced Hepatitis. *Alcoholism: Clinical and Experimental Research*, *30*(9), 1615–1623. https://doi.org/10.1111/j.1530-0277.2006.00194.x

Panasiuk, A., Prokopowicz, D., Zak, J., Panasiuk, B., & Wysocka, J. (2004). Lymphocyte subpopulations in peripheral blood in primary sclerosing cholangitis. *Hepato-Gastroenterology*, *51*(59), 1289–1291.

Panda, S. K., & Colonna, M. (2019). Innate Lymphoid Cells in Mucosal Immunity. *Frontiers in Immunology*, *10*. https://doi.org/10.3389/fimmu.2019.00861

Pandey, R., DeStephan, C. M., Madge, L. A., May, M. J., & Orange, J. S. (2007). NKp30 Ligation Induces Rapid Activation of the Canonical NF-κB Pathway in NK Cells. *The Journal of Immunology*, *179*(11), 7385–7396. https://doi.org/10.4049/jimmunol.179.11.7385

Pardee, A. D., & Butterfield, L. H. (2012). Immunotherapy of hepatocellular carcinoma: Unique challenges and clinical opportunities. *OncoImmunology*, *1*(1), 48–55. https://doi.org/10.4161/onci.1.1.18344

Paul, S., & Lal, G. (2017). The molecular mechanism of natural killer cells function and its importance in cancer immunotherapy. *Frontiers in Immunology*, *8*(SEP). https://doi.org/10.3389/fimmu.2017.01124

Paust, S., Gill, H. S., Wang, B. Z., Flynn, M. P., Moseman, E. A., Senman, B., Szczepanik, M., Telenti, A., Askenase, P. W., Compans, R. W., & Von Andrian, U. H. (2010). Critical role for the chemokine receptor CXCR6 in NK cell-mediated antigen-specific memory of haptens and viruses. *Nature Immunology*, *11*(12), 1127–1135. https://doi.org/10.1038/ni.1953

Paya, C. V, Kenmotsu, N., Schoon, R. A., & Leibson, P. J. (1988). Tumor necrosis factor and lymphotoxin secretion by human natural killer cells leads to antiviral cytotoxicity. *Journal of Immunology*, *141*(6), 1989–1995.

Pedroza-Pacheco, I., Madrigal, A., & Saudemont, A. (2013). Interaction between natural killer cells and regulatory T cells: Perspectives for immunotherapy. In *Cellular and Molecular Immunology* (Vol. 10, Issue 3, pp. 222–229). https://doi.org/10.1038/cmi.2013.2

Pembroke, T., Christian, A., Jones, E., Hills, R. K., Wang, E. C. Y., Gallimore, A. M., & Godkin, A. (2014). The paradox of NKp46+ natural killer cells: drivers of severe hepatitis C virus-induced pathology but in-vivo resistance to interferon α treatment. *Gut*, *63*(3), 515–524. https://doi.org/10.1136/gutjnl-2013-304472

Peppa, D., Gil, U. S., Reynolds, G., Easom, N. J. W., Pallett, L. J., Schurich, A., Micco, L., Nebbia, G., Singh, H. D., Adams, D. H., Kennedy, P. T. F., & Maini, M. K. (2013). Up-regulation of a death receptor renders antiviral T cells susceptible to NK cell-mediated deletion. *Journal of Experimental Medicine*, *210*(1), 99–114. https://doi.org/10.1084/jem.20121172

Peppa, D., Micco, L., Javaid, A., Kennedy, P. T. F., Schurich, A., Dunn, C., Pallant, C., Ellis, G., Khanna, P., Dusheiko, G., Gilson, R. J., & Maini, M. K. (2010). Blockade of Immunosuppressive Cytokines Restores NK Cell Antiviral Function in Chronic Hepatitis B Virus Infection. *PLoS Pathogens*, *6*(12), e1001227. https://doi.org/10.1371/journal.ppat.1001227

Perney, P., Portal??s, P., Corbeau, P., Roques, V., Blanc, F., & Clot, J. (2003). Specific Alteration of Peripheral Cytotoxic Cell Perforin Expression in Alcoholic Patients: A Possible Role in Alcohol-Related Diseases. *Alcoholism: Clinical & Experimental Research*, *27*(11), 1825–1830. https://doi.org/10.1097/01.ALC.0000093742.22787.30

Pesce, S., Greppi, M., Grossi, F., Del Zotto, G., Moretta, L., Sivori, S., Genova, C., & Marcenaro, E. (2019). PD/1-PD-Ls checkpoint: Insight on the potential role of NK cells. *Frontiers in Immunology*, *10*(JUN), 1–8. https://doi.org/10.3389/fimmu.2019.01242

Pijls, K. E., Koek, G. H., Elamin, E. E., De Vries, H., Masclee, A. A. M., & Jonkers, D. M. A. E. (2014). Large intestine permeability is increased in patients with compensated liver cirrhosis. *Am J Physiol Gastrointest Liver Physiol*, *306*, 147–153.

https://doi.org/10.1152/ajpgi.00330.2013.-Intestinal

Pinato, D. J., Guerra, N., Fessas, P., Murphy, R., Mineo, T., Mauri, F. a., Mukherjee, S. K., Thursz, M., Wong, C. N., Sharma, R., & Rimassa, L. (2020). Immune-based therapies for hepatocellular carcinoma. *Oncogene*, *39*(18), 3620–3637. https://doi.org/10.1038/s41388-020-1249-9

Pinyol, R., Montal, R., Bassaganyas, L., Sia, D., Takayama, T., Chau, G.-Y., Mazzaferro, V., Roayaie, S., Lee, H. C., Kokudo, N., Zhang, Z., Torrecilla, S., Moeini, A., Rodriguez-Carunchio, L., Gane, E., Verslype, C., Croitoru, A. E., Cillo, U., de la Mata, M., … Llovet, J. M. (2019). Molecular predictors of prevention of recurrence in HCC with sorafenib as adjuvant treatment and prognostic factors in the phase 3 STORM trial. *Gut*, *68*(6), 1065–1075. https://doi.org/10.1136/gutjnl-2018-316408

Platonova, S., Cherfils-Vicini, J., Damotte, D., Crozet, L., Vieillard, V., Validire, P., André, P., Dieu-Nosjean, M. C., Alifano, M., Régnard, J. F., Fridman, W. H., Sautès-Fridman, C., & Cremer, I. (2011). Profound coordinated alterations of intratumoral NK cell phenotype and function in lung carcinoma. *Cancer Research*, *71*(16), 5412–5422. https://doi.org/10.1158/0008-5472.CAN-10-4179

Porta, C., Rimoldi, M., Raes, G., Brys, L., Ghezzi, P., Di Liberto, D., Dieli, F., Ghisletti, S., Natoli, G., De Baetselier, P., Mantovani, A., & Sica, A. (2009). Tolerance and M2 (alternative) macrophage polarization are related processes orchestrated by p50 nuclear factor κB. *Proceedings of the National Academy of Sciences*, *106*(35), 14978–14983. https://doi.org/10.1073/pnas.0809784106

Portolani, N., Coniglio, A., Ghidoni, S., Giovanelli, M., Benetti, A., Tiberio, G. A. M., & Giulini, S. M. (2006). Early and late recurrence after liver resection for hepatocellular carcinoma: prognostic and therapeutic implications. *Annals of Surgery*, *243*(2), 229–235. https://doi.org/10.1097/01.sla.0000197706.21803.a1

Pulvertaft, R. J. V. (1965). A study of malignant tumours in Nigeria by short-term tissue culture. *Journal of Clinical Pathology*, *18*(3), 261–273. https://doi.org/10.1136/jcp.18.3.261

Qin, S., Chen, M., Cheng, A.-L., Kaseb, A. O., Kudo, M., Lee, H. C., Yopp, A. C., Zhou, J., Wang, L., Wen, X., Heo, J., Tak, W. Y., Nakamura, S., Numata, K., Uguen, T., Hsiehchen, D., Cha, E., Hack, S. P., Lian, Q., … Hsiehchen, D. (2023). Atezolizumab plus bevacizumab versus active surveillance in patients with resected or ablated high-risk hepatocellular carcinoma (IMbrave050): a randomised, open-label, multicentre, phase 3 trial. *The Lancet*, *402*(10415), 1835–1847. https://doi.org/10.1016/S0140-6736(23)01796-8

Qu, P., Huang, X., Zhou, X., Lü, Z., Liu, F., Shi, Z., Lü, L., Wu, Y., & Chen, Y. (2015). Loss of CD155 expression predicts poor prognosis in hepatocellular carcinoma. *Histopathology*, *66*(5), 706–714. https://doi.org/10.1111/his.12584

Quatrini, L., Mariotti, F. R., Munari, E., Tumino, N., Vacca, P., & Moretta, L. (2020). The Immune Checkpoint PD-1 in Natural Killer Cells: Expression, Function and Targeting in Tumour Immunotherapy. *Cancers*, *12*(11), 3285. https://doi.org/10.3390/cancers12113285

Radvanyi, L. G., Bernatchez, C., Zhang, M., Fox, P. S., Miller, P., Chacon, J., Wu, R., Lizee, G.,

Mahoney, S., Alvarado, G., Glass, M., Johnson, V. E., McMannis, J. D., Shpall, E., Prieto, V., Papadopoulos, N., Kim, K., Homsi, J., Bedikian, A., … Hwu, P. (2012). Specific lymphocyte subsets predict response to adoptive cell therapy using expanded autologous tumor-infiltrating lymphocytes in metastatic melanoma patients. *Clinical Cancer Research*, *18*(24), 6758–6770. https://doi.org/10.1158/1078-0432.CCR-12-1177

Ramakrishna, G., Rastogi, A., Trehanpati, N., Sen, B., Khosla, R., & Sarin, S. K. (2013a). *From Cirrhosis to Hepatocellular Carcinoma : New Molecular Insights on Inflammation and Cellular Senescence*. *110070*, 367–383. https://doi.org/10.1159/000343852

Ramakrishna, G., Rastogi, A., Trehanpati, N., Sen, B., Khosla, R., & Sarin, S. K. (2013b). From Cirrhosis to Hepatocellular Carcinoma: New Molecular Insights on Inflammation and Cellular Senescence. *Liver Cancer*, *2*(3–4), 367–383. https://doi.org/10.1159/000343852

Raulet, D. H., & Vance, R. E. (2006). Self-tolerance of natural killer cells. *Nature Reviews. Immunology*, *6*(7), 520–531. https://doi.org/10.1038/nri1863

Rawat, S., & Bouchard, M. J. (2015). The Hepatitis B Virus (HBV) HBx Protein Activates AKT To Simultaneously Regulate HBV Replication and Hepatocyte Survival. *Journal of Virology*, *89*(2), 999–1012. https://doi.org/10.1128/jvi.02440-14

Rinella, M. E., Lazarus, J. V., Ratziu, V., Francque, S. M., Sanyal, A. J., Kanwal, F., Romero, D., Abdelmalek, M. F., Anstee, Q. M., Arab, J. P., Arrese, M., Bataller, R., Beuers, U., Boursier, J., Bugianesi, E., Byrne, C. D., Castro Narro, G. E., Chowdhury, A., Cortez-Pinto, H., … Newsome, P. N. (2023). A multisociety Delphi consensus statement on new fatty liver disease nomenclature. *Journal of Hepatology*, *79*(6), 1542–1556. https://doi.org/10.1016/j.jhep.2023.06.003

Ringelhan, M., Pfister, D., O'Connor, T., Pikarsky, E., & Heikenwalder, M. (2018). The immunology of hepatocellular carcinoma review-article. In *Nature Immunology* (Vol. 19, Issue 3, pp. 222–232). Nature Publishing Group. https://doi.org/10.1038/s41590-018-0044-z

Riteau, B., Barber, D. F., & Long, E. O. (2003). Vav1 phosphorylation is induced by β2 integrin engagement on natural killer cells upstream of actin cytoskeleton and lipid raft reorganization. *Journal of Experimental Medicine*, *198*(3), 469–474. https://doi.org/10.1084/jem.20021995

Ritthipichai, K., Haymaker, C. L., Martinez, M., Aschenbrenner, A., Yi, X., Zhang, M., Kale, C., Vence, L. M., Roszik, J., Hailemichael, Y., Overwijk, W. W., Varadarajan, N., Nurieva, R., Radvanyi, L. G., Hwu, P., & Bernatchez, C. (2017). Multifaceted role of BTLA in the control of CD8+ T-cell fate after antigen encounter. *Clinical Cancer Research*, *23*(20), 6151–6165. https://doi.org/10.1158/1078-0432.CCR-16-1217

Roberto, A., Di Vito, C., Zaghi, E., Mazza, E. M. C., Capucetti, A., Calvi, M., Tentorio, P., Zanon, V., Sarina, B., Mariotti, J., Bramanti, S., Tenedini, E., Tagliafico, E., Bicciato, S., Santoro, A., Roederer, M., Marcenaro, E., Castagna, L., Lugli, E., & Mavilio, D. (2018). The early expansion of anergic NKG2A ^{pos} /CD56 ^{dim} /CD16 ^{neg} natural killer represents a therapeutic target in haploidentical hematopoietic stem cell transplantation. *Haematologica*, *103*(8), 1390–1402. https://doi.org/10.3324/haematol.2017.186619

Robinson, M. W., Harmon, C., & O'Farrelly, C. (2016). Liver immunology and its role in inflammation and homeostasis. *Cellular and Molecular Immunology*, *13*(3), 267–276. https://doi.org/10.1038/cmi.2016.3

Rocca, Y., Pouxvielh, K., Marotel, M., Benezech, S., Jaeger, B., Allatif, O., Bendriss-Vermare, N., Marçais, A., & Walzer, T. (2022). Combinatorial Expression of NK Cell Receptors Governs Cell Subset Reactivity and Effector Functions but Not Tumor Specificity. *The Journal of Immunology*, *208*(7), 1802–1812. https://doi.org/10.4049/jimmunol.2100874

Rodríguez-Perea, a. L., Arcia, E. D., Rueda, C. M., & Velilla, P. a. (2016). Phenotypical characterization of regulatory T cells in humans and rodents. *Clinical and Experimental Immunology*, *185*(3), 281–291. https://doi.org/10.1111/cei.12804

Roeb, E. (2018). Matrix metalloproteinases and liver fibrosis (translational aspects). In *Matrix Biology* (Vols. 68–69, pp. 463–473). Elsevier B.V. https://doi.org/10.1016/j.matbio.2017.12.012

Romee, R., Foley, B., Lenvik, T., Wang, Y., Zhang, B., Ankarlo, D., Luo, X., Cooley, S., Verneris, M., Walcheck, B., & Miller, J. (2013). NK cell CD16 surface expression and function is regulated by a disintegrin and metalloprotease-17 (ADAM17). *Blood*, *121*(18), 3599–3608. https://doi.org/10.1182/blood-2012-04-425397

Romee, R., Rosario, M., Berrien-Elliott, M. M., Wagner, J. A., Jewell, B. A., Schappe, T., Leong, J. W., Abdel-Latif, S., Schneider, S. E., Willey, S., Neal, C. C., Yu, L., Oh, S. T., Lee, Y.-S., Mulder, A., Claas, F., Cooper, M. A., & Fehniger, T. A. (2016). Cytokine-induced memory-like natural killer cells exhibit enhanced responses against myeloid leukemia. *Science Translational Medicine*, *8*(357), 357ra123. https://doi.org/10.1126/scitranslmed.aaf2341

Romeo, S., Kozlitina, J., Xing, C., Pertsemlidis, A., Cox, D., Pennacchio, L. A., Boerwinkle, E., Cohen, J. C., & Hobbs, H. H. (2008). Genetic variation in PNPLA3 confers susceptibility to nonalcoholic fatty liver disease. *Nature Genetics*, *40*(12), 1461–1465. https://doi.org/10.1038/ng.257

Rosen, D. B., Bettadapura, J., Alsharifi, M., Mathew, P. a, Warren, H. S., & Lanier, L. L. (2005). Cutting edge: lectin-like transcript-1 is a ligand for the inhibitory human NKR-P1A receptor. *Journal of Immunology (Baltimore, Md. : 1950)*, *175*(12), 7796–7799. https://doi.org/10.4049/jimmunol.175.12.7796

Rosen, D. B., Cao, W., Avery, D. T., Tangye, S. G., Liu, Y.-J., Houchins, J. P., & Lanier, L. L. (2008). Functional consequences of interactions between human NKR-P1A and its ligand LLT1 expressed on activated dendritic cells and B cells. *Journal of Immunology (Baltimore, Md. : 1950)*, *180*(10), 6508–6517. https://doi.org/180/10/6508 [pii]

Rosen, H. R., & Golden-Mason, L. (2020). Control of HCV infection by natural killer cells and macrophages. *Cold Spring Harbor Perspectives in Medicine*, *10*(9), 1–15. https://doi.org/10.1101/cshperspect.a037101

Roth, P., Mittelbronn, M., Wick, W., Meyermann, R., Tatagiba, M., & Weller, M. (2007). Malignant glioma cells counteract antitumor immune responses through expression of lectin-like transcript-1. *Cancer Research*, *67*(8), 3540–3544.

https://doi.org/10.1158/0008-5472.CAN-06-4783

Sakamoto, Y., Yoshio, S., Doi, H., Mori, T., Matsuda, M., Kawai, H., Shimagaki, T., Yoshikawa, S., Aoki, Y., Osawa, Y., Yoshida, Y., Arai, T., Itokawa, N., Atsukawa, M., Ito, T., Honda, T., Mise, Y., Ono, Y., Takahashi, Y., … Kanto, T. (2021). Increased Frequency of Dysfunctional Siglec-7−CD57+PD-1+ Natural Killer Cells in Patients With Non-alcoholic Fatty Liver Disease. *Frontiers in Immunology*, *12*. https://doi.org/10.3389/fimmu.2021.603133

Sanchez-Guerrero, E., Chen, E., Kockx, M., An, S. W., Chong, B. H., & Khachigian, L. M. (2012). Il-1beta signals through the egf receptor and activates egr-1 through mmp-adam. *PLoS ONE*, *7*(7), 1–9. https://doi.org/10.1371/journal.pone.0039811

Sangro, B., Chan, S. L., Kelley, R. K., Lau, G., Kudo, M., Sukeepaisarnjaroen, W., Yarchoan, M., De Toni, E. N., Furuse, J., Kang, Y. K., Galle, P. R., Rimassa, L., Heurgué, A., Tam, V. C., Van Dao, T., Thungappa, S. C., Breder, V., Ostapenko, Y., Reig, M., … Tuyet Phuong, L. T. (2024). Four-year overall survival update from the phase III HIMALAYA study of tremelimumab plus durvalumab in unresectable hepatocellular carcinoma. *Annals of Oncology*, *35*(5), 448–457. https://doi.org/10.1016/j.annonc.2024.02.005

Sangro, Bruno, Argemi, J., Ronot, M., Paradis, V., Meyer, T., Mazzaferro, V., Jepsen, P., Golfieri, R., Galle, P., Dawson, L., & Reig, M. (2024). EASL Clinical Practice Guidelines on the management of hepatocellular carcinoma. *Journal of Hepatology*. https://doi.org/10.1016/j.jhep.2024.08.028

Sangro, Bruno, Sarobe, P., Hervás-Stubbs, S., & Melero, I. (2021). Advances in immunotherapy for hepatocellular carcinoma. In *Nature Reviews Gastroenterology and Hepatology* (Vol. 18, Issue 8, pp. 525–543). Nature Research. https://doi.org/10.1038/s41575-021-00438-0

Satkunanathan, S., Kumar, N., Bajorek, M., Purbhoo, M. a, & Culley, F. J. (2014). Respiratory syncytial virus infection, TLR3 ligands, and proinflammatory cytokines induce CD161 ligand LLT1 expression on the respiratory epithelium. *Journal of Virology*, *88*(5), 2366–2373. https://doi.org/10.1128/JVI.02789-13

Sawada, Y., Ofuji, K., & Sakai, M. (2013). *Immunotherapy for Hepatocellular Carcinoma : Current Status and Future Perspectives*.

Schoenberg, M. B., Li, X., Li, X., Han, Y., Hao, J., Miksch, R. C., Koch, D., Börner, N., Beger, N. T., Bucher, J. N., Schiergens, T. S., Guba, M. O., Werner, J., & Bazhin, A. V. (2021). The predictive value of tumor infiltrating leukocytes in Hepatocellular Carcinoma: A systematic review and meta-analysis. *European Journal of Surgical Oncology*, *47*(10), 2561–2570. https://doi.org/10.1016/j.ejso.2021.04.042

Schwenk, H. U., & Schneider, U. (1975). Cell cycle dependency of a T-cell marker on lymphoblasts. *Blut*, *31*(5), 299–306. https://doi.org/10.1007/BF01634146

Scoville, S. D., Freud, A. G., & Caligiuri, M. A. (2017). Modeling Human Natural Killer Cell Development in the Era of Innate Lymphoid Cells. *Frontiers in Immunology*, *8*. https://doi.org/10.3389/fimmu.2017.00360

Šedý, J. R., Bjordahl, R. L., Bekiaris, V., Macauley, M. G., Ware, B. C., Norris, P. S., Lurain, N.

S., Benedict, C. A., & Ware, C. F. (2013). CD160 Activation by Herpesvirus Entry Mediator Augments Inflammatory Cytokine Production and Cytolytic Function by NK Cells. *The Journal of Immunology*, *191*(2), 828–836. https://doi.org/10.4049/jimmunol.1300894

Sehgal, R., Kaur, S., Shasthry, S. M., Agrawal, T., Dwivedi, V., Seth, D., Ramakrishna, G., Sarin, S. K., & Trehanpati, N. (2020). Natural Killer Cells Contribute to Pathogenesis of Severe Alcoholic Hepatitis by Inducing Lysis of Endothelial Progenitor Cells. *Alcoholism: Clinical and Experimental Research*, *44*(1), 78–86. https://doi.org/10.1111/acer.14242

Shang, L., Hosseini, M., Liu, X., Kisseleva, T., & Brenner, D. A. (2018). Human hepatic stellate cell isolation and characterization. *Journal of Gastroenterology*, *53*(1), 6–17. https://doi.org/10.1007/s00535-017-1404-4

Shen, C., Ge, Z., Dong, C., Wang, C., Shao, J., Cai, W., Huang, P., Fan, H., Li, J., Zhang, Y., & Yue, M. (2021). Genetic Variants in KIR/HLA-C Genes Are Associated With the Susceptibility to HCV Infection in a High-Risk Chinese Population. *Frontiers in Immunology*, *12*. https://doi.org/10.3389/fimmu.2021.632353

Sheppard, S., Guedes, J., Mroz, A., Zavitsanou, A. M., Kudo, H., Rothery, S. M., Angelopoulos, P., Goldin, R., & Guerra, N. (2017). The immunoreceptor NKG2D promotes tumour growth in a model of hepatocellular carcinoma. *Nature Communications*, *8*. https://doi.org/10.1038/ncomms13930

Shi, C., Yang, H., & Zhang, Z. (2020). Involvement of Nucleotide-Binding Oligomerization Domain-Like Receptor Family Pyrin Domain Containing 3 Inflammasome in the Pathogenesis of Liver Diseases. In *Frontiers in Cell and Developmental Biology* (Vol. 8). Frontiers Media S.A. https://doi.org/10.3389/fcell.2020.00139

Shi, F., Shi, M., Zeng, Z., Qi, R., Liu, Z., Zhang, J., Yang, Y., Tien, P., & Wang, F. (2011). PD-1 and PD-L1 upregulation promotes CD8 $^{+}$ T-cell apoptosis and postoperative recurrence in hepatocellular carcinoma patients. *International Journal of Cancer*, *128*(4), 887–896. https://doi.org/10.1002/ijc.25397

Shimoda, S., Harada, K., Niiro, H., Shirabe, K., Taketomi, A., Maehara, Y., Tsuneyama, K., Nakanuma, Y., Leung, P., Ansari, A. A., Gershwin, M. E., & Akashi, K. (2011). Interaction between Toll-like receptors and natural killer cells in the destruction of bile ducts in primary biliary cirrhosis. *Hepatology*, *53*(4), 1270–1281. https://doi.org/10.1002/hep.24194

Silva-Santos, B., & Strid, J. (2018). Working in "NK Mode": Natural Killer Group 2 Member D and Natural Cytotoxicity Receptors in Stress-Surveillance by γδ T Cells. *Frontiers in Immunology*, *9*. https://doi.org/10.3389/fimmu.2018.00851

Singal, A. G., Manjunath, H., Yopp, A. C., Beg, M. S., Marrero, J. A., Gopal, P., & Waljee, A. K. (2014). The effect of PNPLA3 on fibrosis progression and development of hepatocellular carcinoma: A meta-analysis. *American Journal of Gastroenterology*, *109*(3), 325–334. https://doi.org/10.1038/ajg.2013.476

Siu, E. H. L., Chan, A. W. H., Chong, C. C. N., Chan, S. L., Lo, K. W., & Cheung, S. T. (2018). Treatment of advanced hepatocellular carcinoma: Immunotherapy from checkpoint blockade to potential of cellular treatment. *Translational Gastroenterology and*

Hepatology, *3*(November), 1–15. https://doi.org/10.21037/tgh.2018.10.16

Sivori, S., Vacca, P., Del Zotto, G., Munari, E., Mingari, M. C., & Moretta, L. (2019). Human NK cells: surface receptors, inhibitory checkpoints, and translational applications. *Cellular and Molecular Immunology*, *16*(5), 430–441. https://doi.org/10.1038/s41423-019-0206-4

Sivori, S., Vitale, M., Morelli, L., Sanseverino, L., Augugliaro, R., Bottino, C., Moretta, L., & Moretta, A. (1997). P46, a Novel Natural Killer Cell-Specific Surface Molecule That Mediates Cell Activation. *Journal of Experimental Medicine*, *186*(7), 1129–1136. https://doi.org/10.1084/jem.186.7.1129

Song, M., Pan, Q., Yang, J., He, J., Zeng, J., Cheng, S., Huang, Y., Zhou, Z. Q., Zhu, Q., Yang, C., Han, Y., Tang, Y., Chen, H., Weng, D. S., & Xia, J. C. (2020). Galectin-3 favours tumour metastasis via the activation of β-catenin signalling in hepatocellular carcinoma. *British Journal of Cancer*, *123*(10), 1521–1534. https://doi.org/10.1038/s41416-020-1022-4

Souza-Fonseca-Guimaraes, F., Adib-Conquy, M., & Cavaillon, J. M. (2012). Natural killer (NK) cells in antibacterial innate immunity: angels or devils? In *Molecular medicine (Cambridge, Mass.)* (Vol. 18, Issue 1, pp. 270–285). https://doi.org/10.2119/molmed.2011.00201

Spallanzani, R. G., Torres, N. I., Avila, D. E., Ziblat, A., Iraolagoitia, X. L. R., Rossi, L. E., Domaica, C. I., Fuertes, M. B., Rabinovich, G. A., & Zwirner, N. W. (2015). Regulatory Dendritic Cells Restrain NK Cell IFN-γ Production through Mechanisms Involving NKp46, IL-10, and MHC Class I–Specific Inhibitory Receptors. *The Journal of Immunology*, *195*(5), 2141–2148. https://doi.org/10.4049/jimmunol.1403161

Stegmann, K. A., Robertson, F., Hansi, N., Gill, U., Pallant, C., Christophides, T., Pallett, L. J., Peppa, D., Dunn, C., Fusai, G., Male, V., Davidson, B. R., Kennedy, P., & Maini, M. K. (2016). CXCR6 marks a novel subset of T-bet lo Eomes hi natural killer cells residing in human liver. *Scientific Reports*, *6*. https://doi.org/10.1038/srep26157

Stiglund, N., Strand, K., Cornillet, M., Stål, P., Thorell, A., Zimmer, C. L., Näslund, E., Karlgren, S., Nilsson, H., Mellgren, G., Fernø, J., Hagström, H., & Björkström, N. K. (2019). Retained NK Cell Phenotype and Functionality in Non-alcoholic Fatty Liver Disease. *Frontiers in Immunology*, *10*. https://doi.org/10.3389/fimmu.2019.01255

Støy, S., Dige, A., Sandahl, T. D., Laursen, T. L., Buus, C., Hokland, M., & Vilstrup, H. (2015). Cytotoxic T lymphocytes and natural killer cells display impaired cytotoxic functions and reduced activation in patients with alcoholic hepatitis. *American Journal of Physiology-Gastrointestinal and Liver Physiology*, *308*(4), G269–G276. https://doi.org/10.1152/ajpgi.00200.2014

Strnad, P., Tacke, F., Koch, A., & Trautwein, C. (2017). Liver-guardian, modifier and target of sepsis. In *Nature Reviews Gastroenterology and Hepatology* (Vol. 14, Issue 1, pp. 55–66). Nature Publishing Group. https://doi.org/10.1038/nrgastro.2016.168

Strunz, B., Hengst, J., Deterding, K., Manns, M. P., Cornberg, M., Ljunggren, H. G., Wedemeyer, H., & Björkström, N. K. (2018). Chronic hepatitis C virus infection irreversibly impacts human natural killer cell repertoire diversity. *Nature Communications*, *9*(1). https://doi.org/10.1038/s41467-018-04685-9

Sugimoto, K., Abe, M., Yoshimasu, Y., Takeuchi, H., Kasai, Y., & Itoi, T. (2020). Irreversible electroporation of hepatocellular carcinoma: The role of ultrasonography. *Ultrasonography*, *39*(3), 229–237. https://doi.org/10.14366/usg.20023

Sun, C., Sun, H. Y., Xiao, W. H., Zhang, C., & Tian, Z. G. (2015). Natural killer cell dysfunction in hepatocellular carcinoma and NK cell-based immunotherapy. In *Acta Pharmacologica Sinica* (Vol. 36, Issue 10, pp. 1191–1199). https://doi.org/10.1038/aps.2015.41

Sun, H., Huang, Q., Huang, M., Wen, H., Lin, R., Zheng, M., Qu, K., Li, K., Wei, H., Xiao, W., Sun, R., Tian, Z., & Sun, C. (2019). Human CD96 Correlates to Natural Killer Cell Exhaustion and Predicts the Prognosis of Human Hepatocellular Carcinoma. *Hepatology*, *70*(1), 168–183. https://doi.org/10.1002/hep.30347

Sun, H., Liu, L., Huang, Q., Liu, H., Huang, M., Wang, J., Wen, H., Lin, R., Qu, K., Li, K., Wei, H., Xiao, W., Sun, R., Tian, Z., & Sun, C. (2019). Accumulation of Tumor-Infiltrating CD49a $^{+}$ NK Cells Correlates with Poor Prognosis for Human Hepatocellular Carcinoma. *Cancer Immunology Research*, *7*(9), 1535–1546. https://doi.org/10.1158/2326-6066.CIR-18-0757

Sun, J. C., Beilke, J. N., & Lanier, L. L. (2009). Adaptive immune features of natural killer cells. *Nature*, *457*(7229), 557–561. https://doi.org/10.1038/nature07665

Sun, Y.-F., Wu, L., Liu, S.-P., Jiang, M.-M., Hu, B., Zhou, K.-Q., Guo, W., Xu, Y., Zhong, Y., Zhou, X.-R., Zhang, Z.-F., Liu, G., Liu, S., Shi, Y.-H., Ji, Y., Du, M., Li, N.-N., Li, G.-B., Zhao, Z.-K., … Yang, X.-R. (2021). Dissecting spatial heterogeneity and the immune-evasion mechanism of CTCs by single-cell RNA-seq in hepatocellular carcinoma. *Nature Communications*, *12*(1), 4091. https://doi.org/10.1038/s41467-021-24386-0

Sung, H., Ferlay, J., Siegel, R. L., Laversanne, M., Soerjomataram, I., Jemal, A., & Bray, F. (2021). Global Cancer Statistics 2020: GLOBOCAN Estimates of Incidence and Mortality Worldwide for 36 Cancers in 185 Countries. *CA: A Cancer Journal for Clinicians*, *71*(3), 209–249. https://doi.org/10.3322/caac.21660

Swann, J. B., & Smyth, M. J. (2007). Review series Immune surveillance of tumors. *The Journal of Clinical Investigation*, *117*(5), 1137–1146. https://doi.org/10.1172/JCI31405.antigens

Tacke, F. (2012). Functional role of intrahepatic monocyte subsets for the progression of liver inflammation and liver fibrosis in vivo. *Fibrogenesis & Tissue Repair*, *5*(S1). https://doi.org/10.1186/1755-1536-5-s1-s27

Takeda, K., Kojima, Y., Ikejima, K., Harada, K., Yamashina, S., Okumura, K., Aoyama, T., Frese, S., Ikeda, H., Haynes, N. M., Cretney, E., Yagita, H., Sueyoshi, N., Sato, N., Nakanuma, Y., Smyth, M. J., & Okumura, K. (2008). Death receptor 5 mediated-apoptosis contributes to cholestatic liver disease. *Proceedings of the National Academy of Sciences*, *105*(31), 10895–10900. https://doi.org/10.1073/pnas.0802702105

Tang, L., Peng, H., Zhou, J., Chen, Y., Wei, H., Sun, R., Yokoyama, W. M., & Tian, Z. (2016). Differential phenotypic and functional properties of liver-resident NK cells and mucosal ILC1s. *Journal of Autoimmunity*, *67*, 29–35. https://doi.org/10.1016/j.jaut.2015.09.004

Tarannum, M., & Romee, R. (2021). Cytokine-induced memory-like natural killer cells for cancer immunotherapy. In *Stem Cell Research and Therapy* (Vol. 12, Issue 1). BioMed Central Ltd. https://doi.org/10.1186/s13287-021-02655-5

Tarao, K., Nozaki, A., Ikeda, T., Sato, A., Komatsu, H., Komatsu, T., Taguri, M., & Tanaka, K. (2019). Real impact of liver cirrhosis on the development of hepatocellular carcinoma in various liver diseases—meta-analytic assessment. *Cancer Medicine*, *8*(3), 1054–1065. https://doi.org/10.1002/cam4.1998

Targher, G., Byrne, C. D., & Tilg, H. (2024). MASLD: a systemic metabolic disorder with cardiovascular and malignant complications. *Gut*, gutjnl-2023-330595. https://doi.org/10.1136/gutjnl-2023-330595

Targher, G., Corey, K. E., Byrne, C. D., & Roden, M. (2021). The complex link between NAFLD and type 2 diabetes mellitus — mechanisms and treatments. *Nature Reviews Gastroenterology & Hepatology*, *18*(9), 599–612. https://doi.org/10.1038/s41575-021-00448-y

Tartter, P. I. (1987). The Prognostic Significance of Natural Killer Cytotoxicity in Patients With Colorectal Cancer. *Archives of Surgery*, *122*(11), 1264. https://doi.org/10.1001/archsurg.1987.01400230050009

Thoens, C., Berger, C., Trippler, M., Siemann, H., Lutterbeck, M., Broering, R., Schlaak, J., Heinemann, F. M., Heinold, A., Nattermann, J., Scherbaum, N., Alter, G., & Timm, J. (2014). KIR2DL3+NKG2A− natural killer cells are associated with protection from productive hepatitis C virus infection in people who inject drugs. *Journal of Hepatology*, *61*(3), 475–481. https://doi.org/10.1016/j.jhep.2014.04.020

Thomson, A. W., & Knolle, P. a. (2010). Antigen-presenting cell function in the tolerogenic liver environment. *Nature Reviews. Immunology*, *10*(11), 753–766. https://doi.org/10.1038/nri2858

Toh, T. B., Lim, J. J., & Chow, E. K. (2019). Epigenetics of hepatocellular carcinoma. *Clinical and Translational Medicine*, *8*(1). https://doi.org/10.1186/s40169-019-0230-0

Tomita, M., Yamamoto, K., Kobashi, H., Ohmoto, M., & Tsuji, T. (1994). Immunohistochemical phenotyping of liver macrophages in normal and diseased human liver. *Hepatology*, *20*(2), 317–325. https://doi.org/10.1002/hep.1840200208

Topham, N. J., & Hewitt, E. W. (2009). Natural killer cell cytotoxicity: How do they pull the trigger? *Immunology*, *128*(1), 7–15. https://doi.org/10.1111/j.1365-2567.2009.03123.x

Tuchendler, E., Tuchendler, P. K., & Madej, G. (2018). Immunodeficiency caused by cirrhosis. In *Clinical and Experimental Hepatology* (Vol. 4, Issue 3, pp. 158–164). Termedia Publishing House Ltd. https://doi.org/10.5114/ceh.2018.78119

Umemura, T., Joshita, S., Saito, H., Wakabayashi, S. I., Kobayashi, H., Yamashita, Y., Sugiura, A., Yamazaki, T., & Ota, M. (2021). Investigation of the effect of kir–hla pairs on hepatocellular carcinoma in hepatitis c virus cirrhotic patients. *Cancers*, *13*(13). https://doi.org/10.3390/cancers13133267

Van Erp, E. A., Van Kampen, M. R., Van Kasteren, P. B., & De Wit, J. (2019). Viral infection of human natural killer cells. In *Viruses* (Vol. 11, Issue 3). MDPI AG.

https://doi.org/10.3390/v11030243

Varchetta, S., Mele, D., Mantovani, S., Oliviero, B., Cremonesi, E., Ludovisi, S., Michelone, G., Alessiani, M., Rosati, R., Montorsi, M., & Mondelli, M. U. (2012). Impaired intrahepatic natural killer cell cytotoxic function in chronic hepatitis C virus infection. *Hepatology*, *56*(3), 841–849. https://doi.org/10.1002/hep.25723

Vidal-Castiñeira, J. R., López-Vázquez, A., Díaz-Peña, R., Alonso-Arias, R., Martínez-Borra, J., Pérez, R., Fernández-Suárez, J., Melón, S., Prieto, J., Rodrigo, L., & López-Larrea, C. (2010). Effect of Killer Immunoglobulin-Like Receptors in the Response to Combined Treatment in Patients with Chronic Hepatitis C Virus Infection. *Journal of Virology*, *84*(1), 475–481. https://doi.org/10.1128/jvi.01285-09

Viel, S., Besson, L., Charrier, E., Marçais, A., Disse, E., Bienvenu, J., Walzer, T., & Dumontet, C. (2017). Alteration of Natural Killer cell phenotype and function in obese individuals. *Clinical Immunology*, *177*, 12–17. https://doi.org/10.1016/j.clim.2016.01.007

Vitale, M., Della Chiesa, M., Carlomagno, S., Pende, D., Aricò, M., Moretta, L., & Moretta, A. (2005). NK-dependent DC maturation is mediated by TNFα and IFNγ released upon engagement of the NKp30 triggering receptor. *Blood*, *106*(2), 566–571. https://doi.org/10.1182/blood-2004-10-4035

Vogel, A., Cervantes, A., Chau, I., Daniele, B., Llovet, J., Meyer, T., Nault, J. C., Neumann, U., Ricke, J., Sangro, B., Schirmacher, P., Verslype, C., Zech, C. J., Arnold, D., & Martinelli, E. (2018). Hepatocellular carcinoma: ESMO Clinical Practice Guidelines for diagnosis, treatment and follow-up. *Annals of Oncology*, *29*, iv238–iv255. https://doi.org/10.1093/annonc/mdy308

Vogel, A., Martinelli, E., Cervantes, A., Chau, I., Daniele, B., Llovet, J. M., Meyer, T., Nault, J. C., Neumann, U., Ricke, J., Sangro, B., Schirmacher, P., Verslype, C., Zech, C. J., & Arnold, D. (2021). Updated treatment recommendations for hepatocellular carcinoma (HCC) from the ESMO Clinical Practice Guidelines. In *Annals of Oncology* (Vol. 32, Issue 6, pp. 801–805). Elsevier Ltd. https://doi.org/10.1016/j.annonc.2021.02.014

Vogt, A., Sievers, E., Lukacs-Kornek, V., Decker, G., Raskopf, E., Meumann, N., Büning, H., Sauerbruch, T., Strassburg, C. P., Schmidt-Wolf, I. G. H., & Gonzalez-Carmona, M. a. (2014). Improving immunotherapy of hepatocellular carcinoma (HCC) using dendritic cells (DC) engineered to express IL-12 in vivo. *Liver International*, *34*(3), 447–461. https://doi.org/10.1111/liv.12284

Waggoner, S. N., Reighard, S. D., Gyurova, I. E., Cranert, S. A., Mahl, S. E., Karmele, E. P., McNally, J. P., Moran, M. T., Brooks, T. R., Yaqoob, F., & Rydyznski, C. E. (2016). Roles of natural killer cells in antiviral immunity. In *Current Opinion in Virology* (Vol. 16, pp. 15–23). Elsevier B.V. https://doi.org/10.1016/j.coviro.2015.10.008

Walker, L. J., Kang, Y. H., Smith, M. O., Tharmalingham, H., Ramamurthy, N., Fleming, V. M., Sahgal, N., Leslie, A., Oo, Y., Geremia, A., Scriba, T. J., Hanekom, W. a., Lauer, G. M., Lantz, O., Adams, D. H., Powrie, F., Barnes, E., & Klenerman, P. (2012). Human MAIT and CD8???? cells develop from a pool of type-17 precommitted CD8 + T cells. *Blood*, *119*(2), 422–433. https://doi.org/10.1182/blood-2011-05-353789

Wan, S., Kuo, N., Kryczek, I., Zou, W., & Welling, T. H. (2015). Myeloid cells in hepatocellular

carcinoma. *Hepatology*, *62*(4), 1304–1312. https://doi.org/10.1002/hep.27867

Wang, D., Yang, L., Yue, D., Cao, L., Li, L., Wang, D., Ping, Y., Shen, Z., Zheng, Y., Wang, L., & Zhang, Y. (2019). Macrophage-derived CCL22 promotes an immunosuppressive tumor microenvironment via IL-8 in malignant pleural effusion. *Cancer Letters*, *452*, 244–253. https://doi.org/10.1016/j.canlet.2019.03.040

Wang, R., Jaw, J. J., Stutzman, N. C., Zou, Z., & Sun, P. D. (2012). Natural killer cell-produced IFN- and TNF- induce target cell cytolysis through up-regulation of ICAM-1. *Journal of Leukocyte Biology*, *91*(2), 299–309. https://doi.org/10.1189/jlb.0611308

Wang, S., & El-Deiry, W. S. (2003). TRAIL and apoptosis induction by TNF-family death receptors. In *Oncogene* (Vol. 22, Issue 53 REV. ISS. 7, pp. 8628–8633). https://doi.org/10.1038/sj.onc.1207232

Watanabe, N., Gavrieli, M., Sedy, J. R., Yang, J., Fallarino, F., Loftin, S. K., Hurchla, M. a., Zimmerman, N., Sim, J., Zang, X., Murphy, T. L., Russell, J. H., Allison, J. P., & Murphy, K. M. (2003). BTLA is a lymphocyte inhibitory receptor with similarities to CTLA-4 and PD-1. *Nature Immunology*, *4*(7), 670–679. https://doi.org/10.1038/ni944

Weston, C. J., Zimmermann, H. W., & Adams, D. H. (2019). The role of myeloid-derived cells in the progression of liver disease. In *Frontiers in Immunology* (Vol. 10, Issue APR). Frontiers Media S.A. https://doi.org/10.3389/fimmu.2019.00893

Wiencke, K. (2001). Primary sclerosing cholangitis is associated to an extended B8-DR3 haplotype including particular MICA and MICB alleles. *Hepatology*, *34*(4), 625–630. https://doi.org/10.1053/jhep.2001.27543

Wu, X., Dong, L., Lin, X., & Li, J. (2017). Relevance of the NLRP3 inflammasome in the pathogenesis of chronic liver disease. In *Frontiers in Immunology* (Vol. 8, Issue DEC). Frontiers Media S.A. https://doi.org/10.3389/fimmu.2017.01728

Wu, Y., Kuang, D. M., Pan, W. D., Wan, Y. Le, Lao, X. M., Wang, D., Li, X. F., & Zheng, L. (2013). Monocyte/macrophage-elicited natural killer cell dysfunction in hepatocellular carcinoma is mediated by CD48/2B4 interactions. *Hepatology*, *57*(3), 1107–1116. https://doi.org/10.1002/hep.26192

Yang, C. M., Yoon, J. C., Park, J. H., & Lee, J. M. (2017). Hepatitis C virus impairs natural killer cell activity via viral serine protease NS3. *PLoS ONE*, *12*(4). https://doi.org/10.1371/journal.pone.0175793

Yau, T., Park, J. W., Finn, R. S., Cheng, A. L., Mathurin, P., Edeline, J., Kudo, M., Harding, J. J., Merle, P., Rosmorduc, O., Wyrwicz, L., Schott, E., Choo, S. P., Kelley, R. K., Sieghart, W., Assenat, E., Zaucha, R., Furuse, J., Abou-Alfa, G. K., … Sangro, B. (2022). Nivolumab versus sorafenib in advanced hepatocellular carcinoma (CheckMate 459): a randomised, multicentre, open-label, phase 3 trial. *The Lancet Oncology*, *23*(1), 77–90. https://doi.org/10.1016/S1470-2045(21)00604-5

Yeap, W. H., Wong, K. L., Shimasaki, N., Teo, E. C. Y., Quek, J. K. S., Yong, H. X., Diong, C. P., Bertoletti, A., Linn, Y. C., & Wong, S. C. (2016). CD16 is indispensable for antibodydependent cellular cytotoxicity by human monocytes. *Scientific Reports*, *6*(March). https://doi.org/10.1038/srep34310

Yin, Y., Feng, W., Chen, J., Chen, X., Wang, G., Wang, S., Xu, X., Nie, Y., Fan, D., Wu, K., & Xia, L. (2024). Immunosuppressive tumor microenvironment in the progression, metastasis, and therapy of hepatocellular carcinoma: from bench to bedside. *Experimental Hematology & Oncology*, *13*(1), 72. https://doi.org/10.1186/s40164-024-00539-x

Yu, S., Wang, Y., Hou, J., Li, W., Wang, X., Xiang, L., Tan, D., Wang, W., Jiang, L., Claret, F. X., Jiao, M., & Guo, H. (2020). Tumor-infiltrating immune cells in hepatocellular carcinoma: Tregs is correlated with poor overall survival. *PLOS ONE*, *15*(4), e0231003. https://doi.org/10.1371/journal.pone.0231003

Zamai, L., Ahmad, M., Bennett, I. M., Azzoni, L., Alnemri, E. S., & Perussia, B. (1998). Natural Killer (NK) Cell-mediated Cytotoxicity: Differential Use of TRAIL and Fas Ligand by Immature and Mature Primary Human NK Cells. In *J. Exp. Med* (Vol. 188). http://www.jem.org

Zamora, A. E., Aguilar, E. G., Sungur, C. M., Khuat, L. T., Dunai, C., Lochhead, G. R., Du, J., Pomeroy, C., Blazar, B. R., Longo, D. L., Venstrom, J. M., Baumgarth, N., & Murphy, W. J. (2017). Licensing delineates helper and effector NK cell subsets during viral infection. *JCI Insight*, *2*(10). https://doi.org/10.1172/jci.insight.87032

Zea, A. H., Rodriguez, P. C., Atkins, M. B., Hernandez, C., Signoretti, S., Zabaleta, J., McDermott, D., Quiceno, D., Youmans, A., O'Neill, A., Mier, J., & Ochoa, A. C. (2005). Arginase-Producing Myeloid Suppressor Cells in Renal Cell Carcinoma Patients: A Mechanism of Tumor Evasion. *Cancer Research*, *65*(8), 3044–3048. https://doi.org/10.1158/0008-5472.CAN-04-4505

Zecca, A., Barili, V., Rizzo, D., Olivani, A., Biasini, E., Laccabue, D., Dalla Valle, R., Ferrari, C., Cariani, E., & Missale, G. (2021). Intratumor Regulatory Noncytotoxic NK Cells in Patients with Hepatocellular Carcinoma. *Cells*, *10*(3), 614. https://doi.org/10.3390/cells10030614

Zerbini, A., Pilli, M., Laccabue, D., Pelosi, G., Molinari, A., Negri, E., Cerioni, S., Fagnoni, F., Soliani, P., Ferrari, C., & Missale, G. (2010). Radiofrequency Thermal Ablation for Hepatocellular Carcinoma Stimulates Autologous NK-Cell Response. *Gastroenterology*, *138*(5), 1931-1942.e2. https://doi.org/10.1053/j.gastro.2009.12.051

Zhang, J., Gu, C., Song, Q., Zhu, M., Xu, Y., Xiao, M., & Zheng, W. (2020). Identifying cancer-associated fibroblasts as emerging targets for hepatocellular carcinoma. *Cell & Bioscience*, *10*(1), 127. https://doi.org/10.1186/s13578-020-00488-y

Zhang, L. H., Shin, J. H., Haggadone, M. D., & Sunwoo, J. B. (2016). The aryl hydrocarbon receptor is required for the maintenance of liver-resident natural killer cells. *Journal of Experimental Medicine*, *213*(11), 2249–2257. https://doi.org/10.1084/jem.20151998

Zhang, Q., Lou, Y., Bai, X., & Liang, T. (2020). *Intratumoral heterogeneity of hepatocellular carcinoma: From single-cell to population-based studies*. *26*(26), 3720–3736. https://doi.org/10.3748/wjg.v26.i26.3720

Zhang, Z., Wu, N., Lu, Y., Davidson, D., Colonna, M., & Veillette, A. (2015). DNAM-1 controls NK cell activation via an ITT-like motif. *Journal of Experimental Medicine*, *212*(12), 2165–2182. https://doi.org/10.1084/jem.20150792

Zheng, C., Zheng, L., Yoo, J.-K., Guo, H., Zhang, Y., Guo, X., Kang, B., Hu, R., Huang, J. Y., Zhang, Q., Liu, Z., Dong, M., Hu, X., Ouyang, W., Peng, J., & Zhang, Z. (2017). Landscape of Infiltrating T Cells in Liver Cancer Revealed by Single-Cell Sequencing. *Cell*, *169*(7), 1342-1356.e16. https://doi.org/10.1016/j.cell.2017.05.035

Zheng, Q., Xu, J., Gu, X., Wu, F., Deng, J., Cai, X., Wang, G., Li, G., & Chen, Z. (2020). Immune checkpoint targeting TIGIT in hepatocellular carcinoma. *American Journal of Translational Research*, *12*(7), 3212–3224.

Zhou, J., Wang, W., & Li, Q. (2021). Potential therapeutic targets in the tumor microenvironment of hepatocellular carcinoma: reversing the protumor effect of tumor-associated macrophages. In *Journal of Experimental and Clinical Cancer Research* (Vol. 40, Issue 1). BioMed Central Ltd. https://doi.org/10.1186/s13046-021-01873-2

Zhou, S.-L., Zhou, Z.-J., Hu, Z.-Q., Huang, X.-W., Wang, Z., Chen, E.-B., Fan, J., Cao, Y., Dai, Z., & Zhou, J. (2016). Tumor-Associated Neutrophils Recruit Macrophages and T-Regulatory Cells to Promote Progression of Hepatocellular Carcinoma and Resistance to Sorafenib. *Gastroenterology*, *150*(7), 1646-1658.e17. https://doi.org/10.1053/j.gastro.2016.02.040

Zhou, Z., Xu, M.-J., & Gao, B. (2016). *Hepatocytes: a key cell type for innate immunity*. https://doi.org/10.1038/cmi.2015.97;published

Zhuang, L., Fulton, R. J., Rettman, P., Sayan, A. E., Coad, J., Al-Shamkhani, A., & Khakoo, S. I. (2019). Activity of IL-12/15/18 primed natural killer cells against hepatocellular carcinoma. *Hepatology International*, *13*(1), 75–83. https://doi.org/10.1007/s12072-018-9909-3

8. Appendices

8.1 List of genes added to the Nanostring Immunology Panel

CD69
FASLG
CD226
PTK2B
VAV1
RAC1
NCR2
NKp30/NCR3
PTPN11
RAMP1
PIK3R2
MER
AXL
CCL25
ITGA1
PRKCE
AKT3
CD38
MAP2K1
CLEC2D
MAPK3
LYN
PXN
PAK1
MAP3K1
PRKCQ
PLD1
PPP3CA
INPP5D
DGKK

8.2 Sequence confirming correct cloning of LLT1 and CD161

LLT1 sequence

ATGCATGACAGTAACAATGTGGAGAAAGACATTACACCATCTGAATTGCCTGCAAACCCAGGTTGTCTGCATTC
AAAAGAGCATTCTATTAAAGCTACCTTAATTTGGCGCTTATTTTTCTTAATCATGTTTCTGACAATCATAGTGTGT
GGAATGGTTGCTGCTTTAAGCGCAATAAGAGCTAACTGCCATCAAGAGCCATCAGTATGTCTTCAAGCTGCATG
CCCAGAAAGCTGGATTGGTTTTCAAAGAAAGTGTTTCTATTTTTCTGATGACACCAAGAACTGGACATCAAGTC
AGAGGTTTTGTGACTCACAAGATGCTGATCTTGCTCAGGTTGAAAGCTTCCAGGAACTGAATTTCCTGTTGAGA
TATAAAGGCCCATCTGATCACTGGATTGGGCTGAGCAGAGAACAAGGCCAACCATGGAAATGGATAAATGGTA
CTGAATGGACAAGACAGTTTCCTATCCTGGGAGCAGGAGAGTGTGCCTATTTGAATGACAAAGGTGCCAGTAG
TGCCAGGCACTACACAGAGAGGAAGTGGATTTGTTCCAAATCAGATATACATGTCTAG

CD161 sequence

ATGGACCAACAAGCAATATATGCTGAGTTAAACTTACCCACAGACTCAGGCCCAGAAAGTTCTTCACCTTCATCT
CTTCCTCGGGATGTCTGTCAGGGTTCACCTTGGCATCAATTTGCCCTGAAACTTAGCTGTGCTGGGATTATTCTC
CTTGTCTTGGTTGTTACTGGGTTGAGTGTTTCAGTGACATCCTTAATACAGAAATCATCAATAGAAAAATGCAGT
GTGGACATTCAACAGAGCAGGAATAAAACAACAGAGAGACCGGGTCTCTTAAACTGCCCAATATATTGGCAGC
AACTCCGAGAGAAATGCTTGTTATTTTCTCACACTGTCAACCCTTGGAATAACAGTCTAGCTGATTGTTCCACCA
AAGAATCCAGCCTGCTGCTTATTCGAGATAAGGATGAATTGATACACACACAGAACCTGATACGTGACAAAGCA
ATTCTGTTTTGGATTGGATTAAATTTTTCATTATCAGAAAAGAACTGGAAGTGGATAAACGGCTCTTTTTTAAAT
TCTAATGACTTAGAAATTAGAGGTGATGCTAAAGAAAACAGCTGTATTTCCATCTCACAGACATCTGTGTATTCT
GAGTACTGTAGTACAGAAATCAGATGGATCTGCCAAAAAGAACTAACACCTGTGAGAAATAAAGTGTATCCTG
ACTCTTGA

8.3 Appendix C – Clinical parameter correlated with NK receptor expression in circulating NK cells in patients with cirrhosis and patients with cirrhosis and HCC.

Table 20 NKG2D expression (median fluorescence intensity) on circulating NK cells in patients with cirrhosis and patients with cirrhosis and HCC (spearman rank correlation shown).

	NKG2D in Cirrhosis		NKG2D in HCC	
	R value	**P value**	**R value**	**P value**
MELD	0.0353	0.8585	0.0357	0.8684
MELD-Na	0.0090	0.9677	0.2904	0.2425
INR	-0.0387	0.6217	0.0022	0.9919
Platelets	0.0716	0.7339	-0.0836	0.7416
Bilirubin	0.0340	0.8748	0.1839	0.4126
ALT	-0.0982	0.6193	-0.0343	0.8964
Albumin	-0.0137	0.9447	-0.1094	0.6107
Age	-0.1617	0.4111	0.0262	0.9034
Creatinine	0.1058	0.5920	0.1614	0.4513
AFP			-0.0079	0.9721

Table 21 DNAM-1 expression on circulating NK cells (percentage positive) and correlation with clinical parameters (Spearman rank correlation shown).

	DNAM-1 in Cirrhosis		DNAM-1 in HCC	
	R value	**P value**	**R value**	**P value**
MELD	-0.03556	0.8574	0.2023	0.3666
MELD-Na	-0.1914	0.3816	0.3453	0.1892
INR	0.04709	0.8119	0.2007	0.3705
Platelets	0.04462	0.8323	-0.09706	0.7213
Bilirubin	-0.01233	0.9503	0.1075	0.6339
ALT	-0.252	0.1959	0.1769	0.5281
Albumin	0.1051	0.5945	-0.3697	0.0904
Age	-0.3442	0.0729	0.161	0.4743
Creatinine	-0.1731	0.3782	0.1356	0.5475
AFP			0.1813	0.4444

Table 22 NKp30 expression on circulating NK cells (median fluorescence intensity) and correlation with clinical parameters (Spearman rank correlation shown).

	NKp30 in Cirrhosis		NKp30 in HCC	
	R value	**P value**	**R value**	**P value**
MELD	-0.04659	0.8139	-0.1256	0.5978
MELD-Na	-0.1283	0.5597	-0.05123	0.8626
INR	-0.185	0.3460	-0.3513	0.1288
Platelets	0.06886	0.7436	0.222	0.4448
Bilirubin	0.1458	0.4591	-0.2997	0.1992
ALT	-0.06196	0.7541	-0.1154	0.7097
Albumin	0.06916	0.7266	0.125	0.5994
Age	**-0.5243**	**0.0042 ****	0.02642	0.9120
Creatinine	-0.1995	0.3087	0.2828	0.2270
AFP			0.06832	0.7876

Table 23 NKp46 expression on circulating NK cells (median fluorescence intensity) and correlation with clinical parameters (spearman rank correlation shown).

	NKp46 in Cirrhosis		NKp46 in HCC	
	R value	**P value**	**R value**	**P value**
MELD	0.166	0.4277	0.4097	0.0728
MELD-Na	0.126	0.5966	**0.6816**	**0.0092 ****
INR	-0.1186	0.5724	0.1247	0.6005
Platelets	0.3846	0.0771	-0.2967	0.3025
Bilirubin	-0.001542	0.9942	0.3991	0.0813
ALT	0.2116	0.3098	0.05495	0.8631
Albumin	0.1212	0.5637	-0.3631	0.1156
Age	-0.1468	0.4838	-0.04679	0.8447
Creatinine	-0.1371	0.5135	0.3678	0.1106
AFP			0.1677	0.5059

Table 24 CD161 expression on circulating NK cells (percentage of NK cells that are CD161+NK cells) and correlation with clinical parameters (Spearman rank correlation shown).

	CD161 in Cirrhosis		CD161 in HCC	
	R value	**P value**	**R value**	**P value**
MELD	-0.1296	0.5111	-0.1055	0.6405
MELD-Na	-0.1979	0.3655	0.1354	0.6143
INR	**-0.3688**	**0.0490 ***	-0.1071	0.6351
Platelets	0.2724	0.1878	0.4853	0.0589
Bilirubin	-0.03316	0.8669	-0.08602	0.7035
ALT	0.01782	0.9283	0.1805	0.5197
Albumin	0.06038	0.7602	-0.03397	0.8807
Age	**-0.4484**	**0.0147 ***	0.04817	0.8314
Creatinine	0.09894	0.6164	0.05592	0.8048
AFP			0.185	0.4348

Table 25 Circulating CD56dimCD16+/-NK cell proportion (percentage of NK cells that are CD56dimCD16+/-NK cells) and correlation with clinical parameters (Spearman rank correlation shown).

	CD56dimCD16+/- NK cells in Cirrhosis		CD56dimCD16+/-NK cells in HCC	
	R value	**P value**	**R value**	**P value**
MELD	-0.0816	0.6739	-0.1539	0.4727
MELD-Na	-0.3397	0.1044	-0.192	0.4729
INR	-0.155	0.4220	-0.1984	0.3761
Platelets	-0.2626	0.1949	0.05588	0.8393
Bilirubin	-0.1983	0.3025	-0.01471	0.9482
ALT	-0.06044	0.7555	-0.2484	0.3719
Albumin	0.03433	0.8597	0.04755	0.8336
Age	-0.162	0.4011	-0.2256	0.3128
Creatinine	**0.4092**	**0.0275 ***	-0.1807	0.4209
AFP			0.1556	0.5125

Table 26 CXCR6 expression on circulating NK cells (percentage of NK cells that are CXCR6+NK cells) and correlation with clinical parameters (Spearman rank correlation shown).

	CXCR6+NK cells in Cirrhosis		CXCR6+NK cells in HCC	
	R value	**P value**	**R value**	**P value**
MELD	0.339	0.0720	-0.1436	0.5237
MELD-Na	0.2898	0.1695	-0.1318	0.6266
INR	0.06317	0.7448	-0.2246	0.3150
Platelets	-0.131	0.5237	-0.4283	0.0979
Bilirubin	**0.369**	**0.0489 ***	0.1475	0.5125
ALT	0.02294	0.9060	-0.1386	0.6222
Albumin	**-0.5883**	**0.0008 *** **	0.02378	0.9163
Age	0.07102	0.7143	0.1293	0.5665
Creatinine	**0.4132**	**0.0259 ***	-0.04294	0.8495
AFP			-0.1526	0.5206

8.4 Appendix D - Differential gene expression analyses

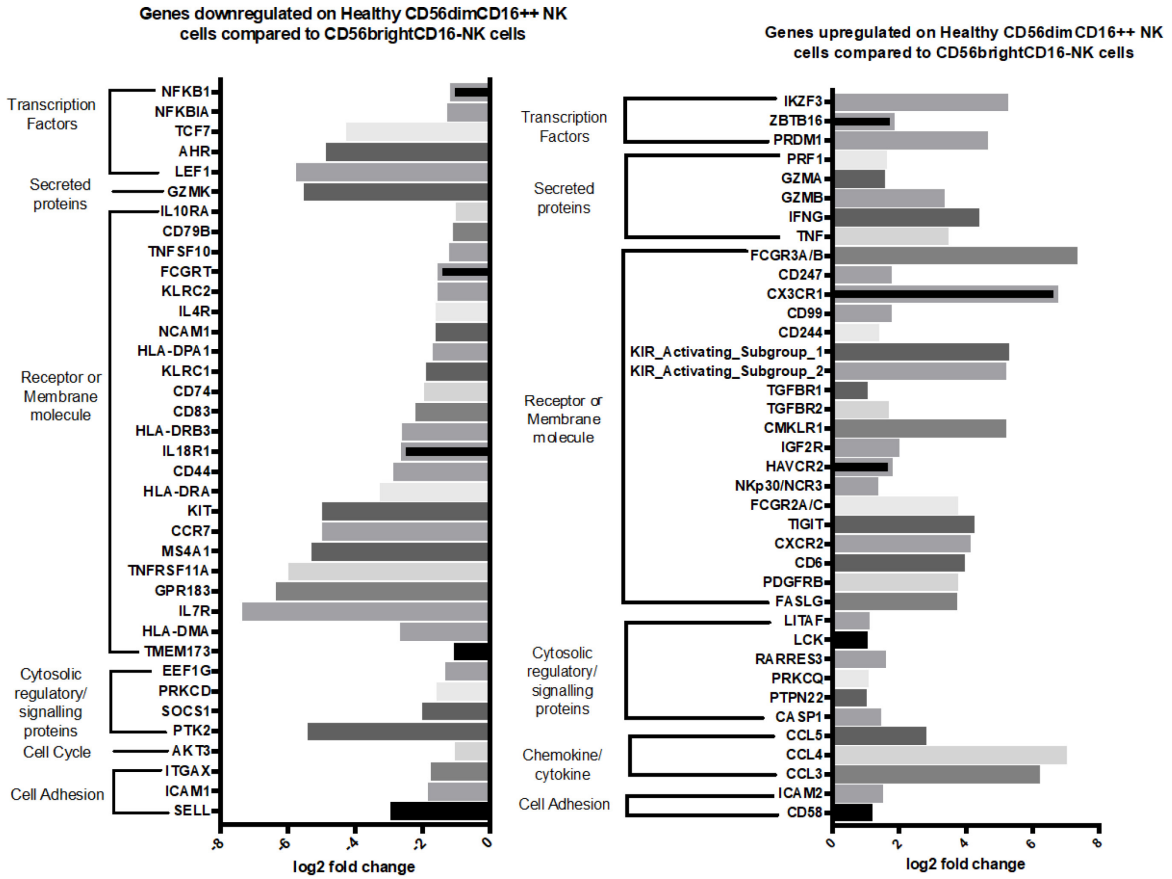


Figure 179 Gene expression in healthy circulating CD56dimCD16++ NK cells compared to CD56brightCD16- NK cells(n=3). FDR calculated for all genes and only genes with p<0.05 shown, with >30 copies in one group and at least 2 fold difference in expression

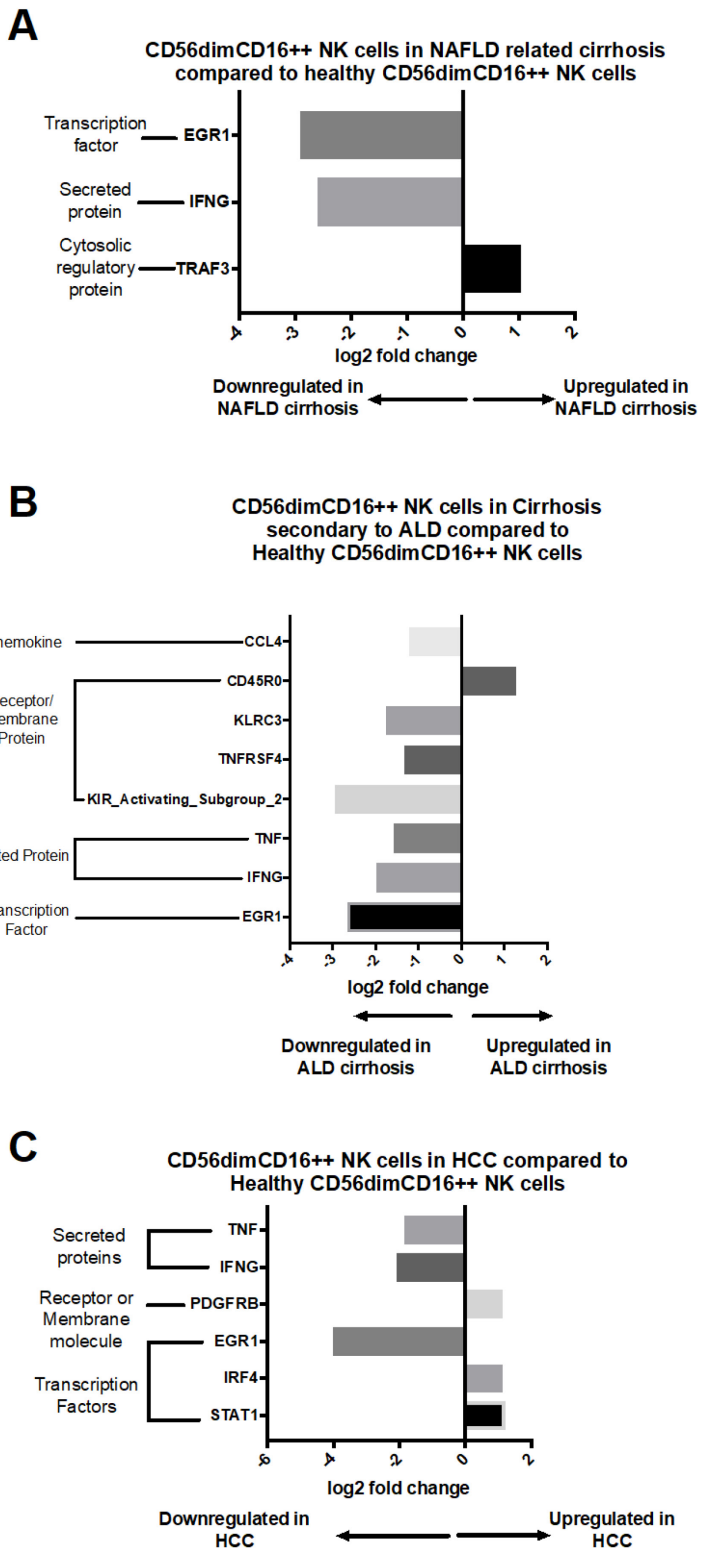


Figure 180 Gene expression in circulating CD56dimCD16++ NK cells in disease compared to circulating CD56dimCD16++ NK cells in health. Gene expression profiles from circulating CD56dimCD16++ NK cells from patients with A) cirrhosis related to non-alcoholic fatty liver disease (NAFLD), B) cirrhosis related to alcohol related liver disease (ALD) and C) NAFLD related cirrhosis with hepatocellular carcinoma (HCC) were compared with circulating CD56dimCD16++ NK cells from healthy volunteers. (Genes displayed are expressed at >20 copies, demonstrate more than a 2 fold difference in expression and $p<0.05$ and FDR value of <0.05).

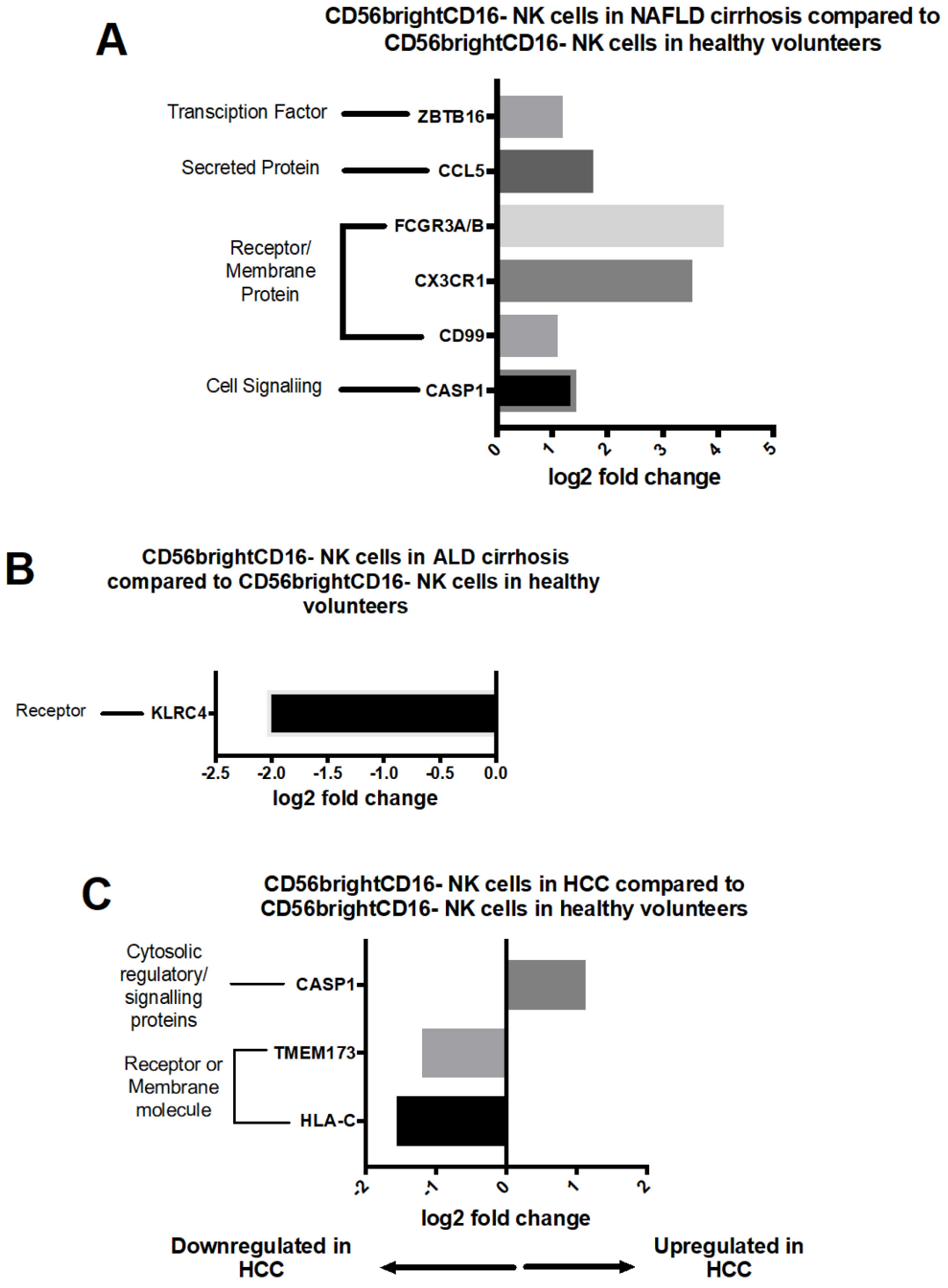


Figure 181 Gene expression in circulating CD56brightCD16- NK cells in disease compared to circulating CD56brightCD16- NK cells in health. Gene expression profiles from circulating CD56brightCD16- NK cells from patients with A) cirrhosis related to non-alcoholic fatty liver disease (NAFLD), B) cirrhosis related to alcohol related liver disease (ALD) and C) NAFLD related cirrhosis with hepatocellular carcinoma (HCC) were compared with circulating CD56brightCD16- NK cells from healthy volunteers. (Genes displayed are expressed at >20 copies, demonstrate more than a 2 fold difference in expression and p<0.05 and FDR value of <0.05).

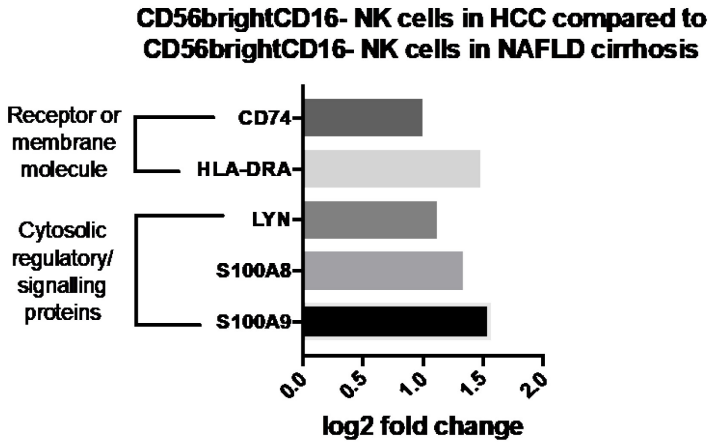


Figure 182 Gene expression in circulating CD56brightCD16- NK cells from patients with hepatocellular carcinoma (HCC) on a background of NAFLD related cirrhosis compared to circulating CD56brightCD16- NK cells from patients with NAFLD related cirrhosis without HCC (Genes displayed expressed at >20 copies, demonstrate >2 fold difference in expression, p<0.05 and FDR<0.05).

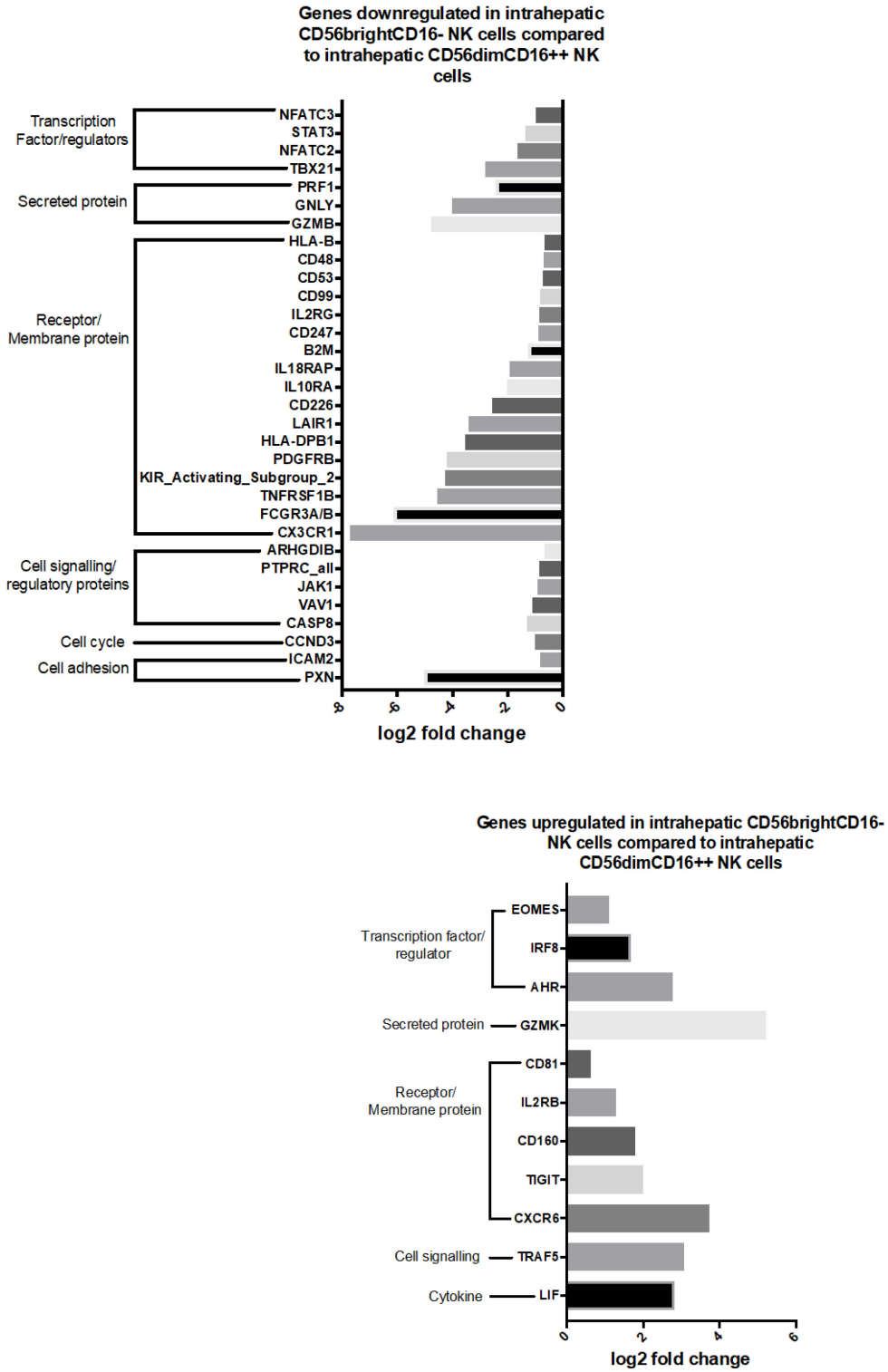


Figure 183 Gene expression in intrahepatic CD56dimCD16++ NK cells compared to CD56brightCD16- NK cells(n=3, mononuclear cells isolated from explanted livers with cirrhosis, paired samples). FDR calculated for all genes and only genes with p<0.05 shown, with >30 copies in one group and at least 2 fold difference in expression.

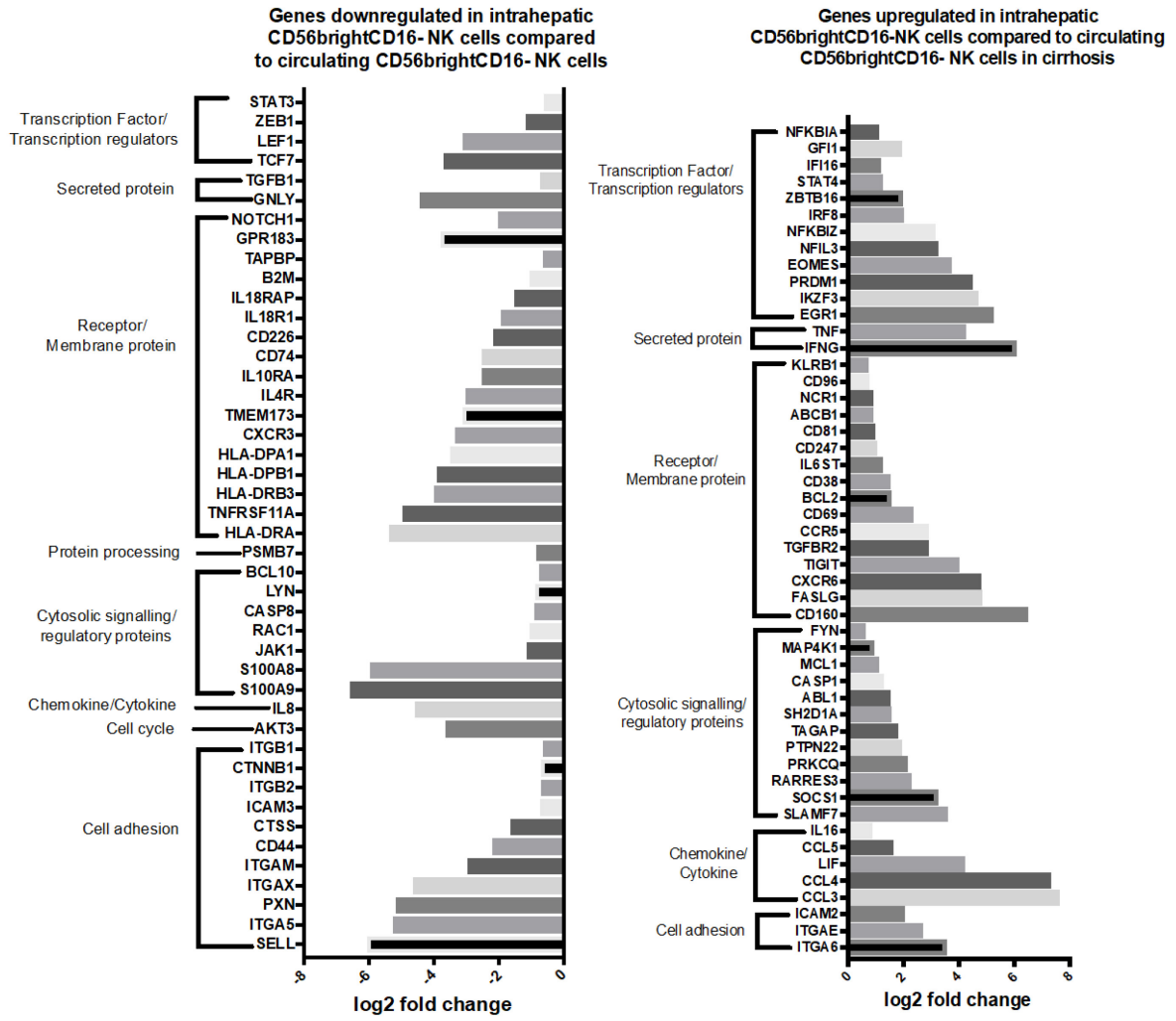


Figure 184 Comparison of gene expression in intrahepatic NAFLD cirrhosis CD56brightCD16- NK cells (n=3) and circulating CD56brightCD16- NK cells in NAFLD cirrhosis (n=4).

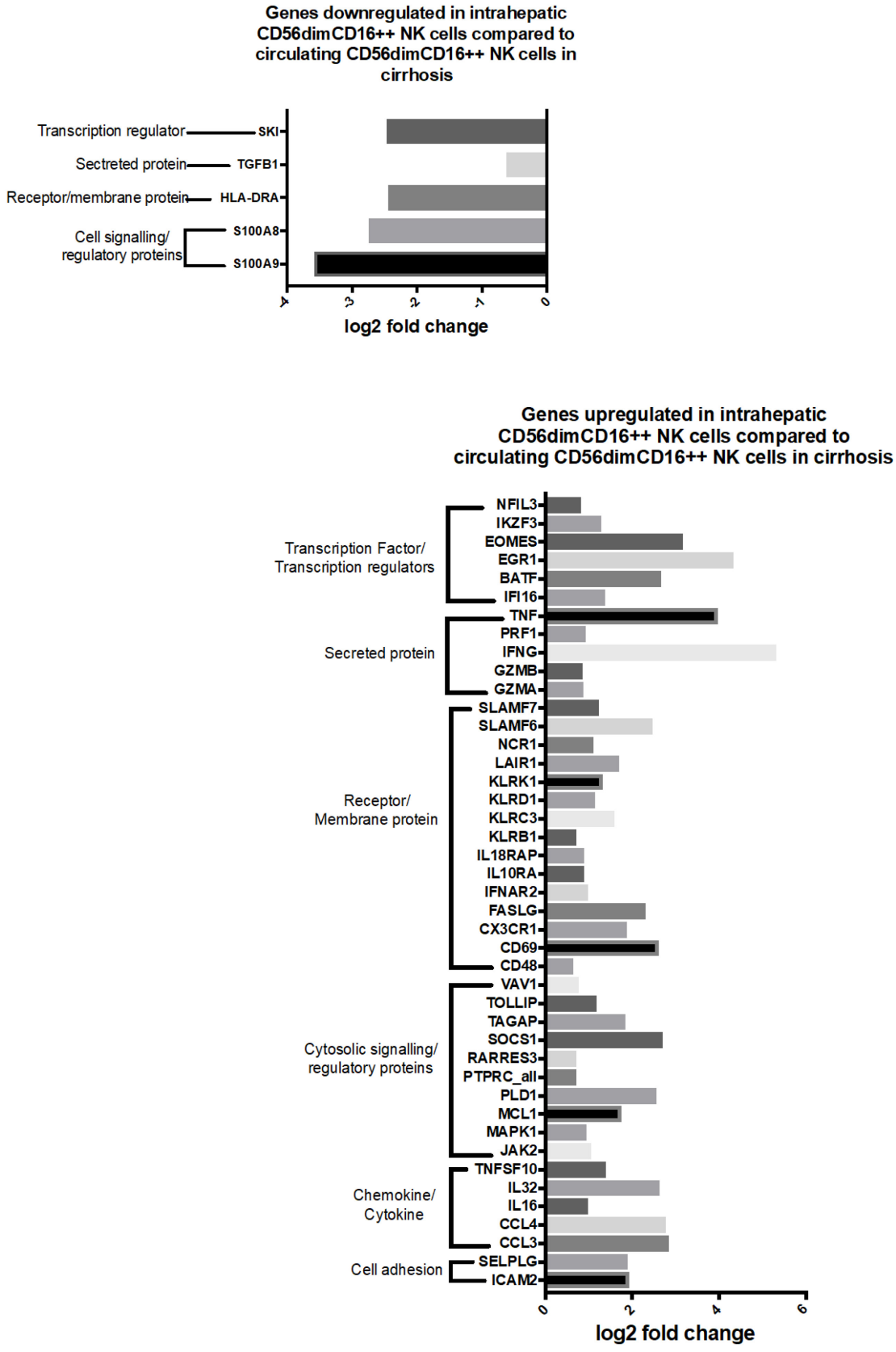


Figure 185 Comparison of gene expression in intrahepatic NAFLD cirrhosis CD56dimCD16++ NK cells (n=3) and circulating CD56dimCD16++ NK cells in NAFLD cirrhosis (n=4) (non-paired samples).

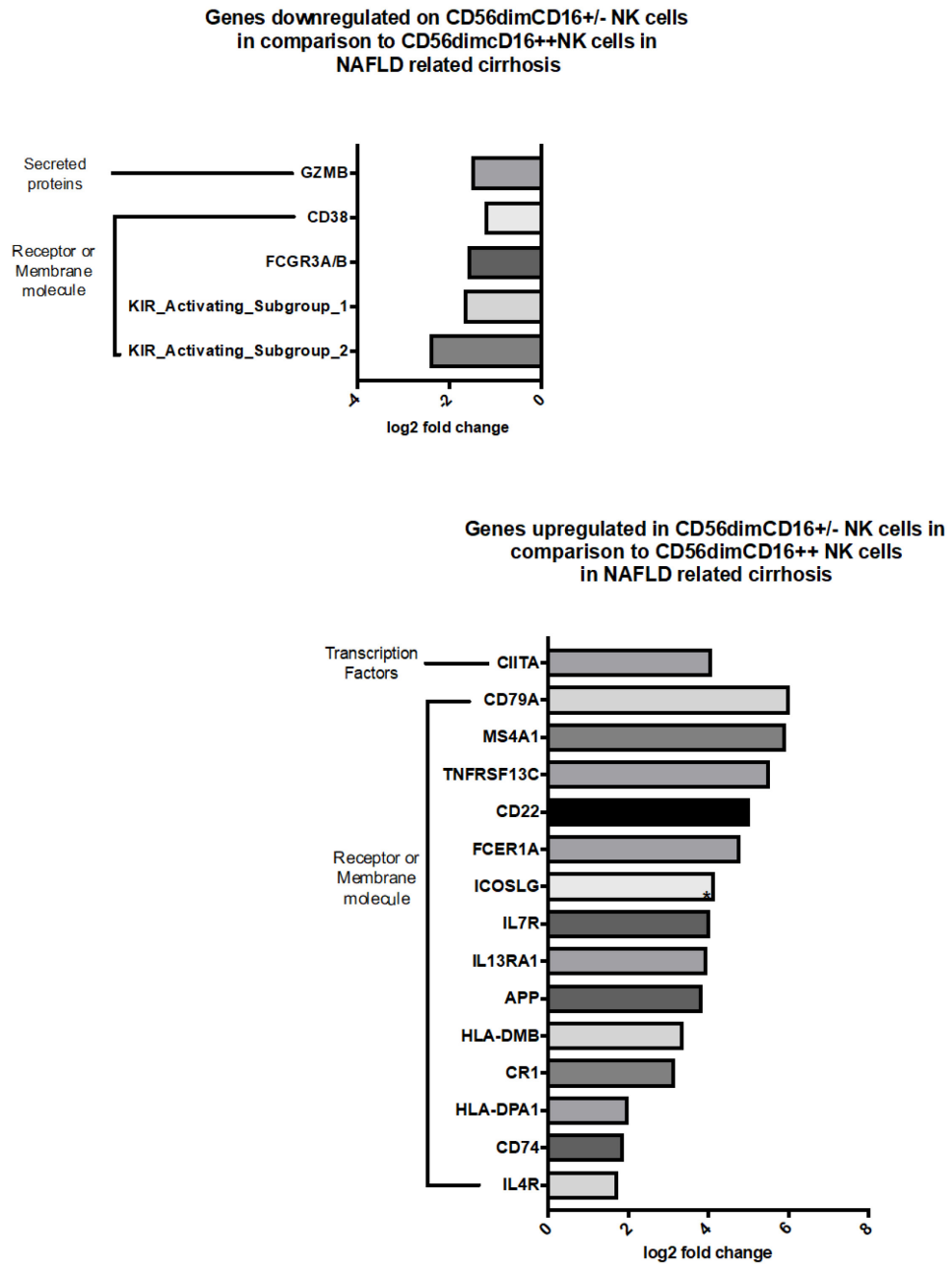


Figure 186 Gene expression in circulating CD56dimCD16+/- NK cells in comparison to circulating CD56dimCD16++ NK cells in NAFLD related cirrhosis.

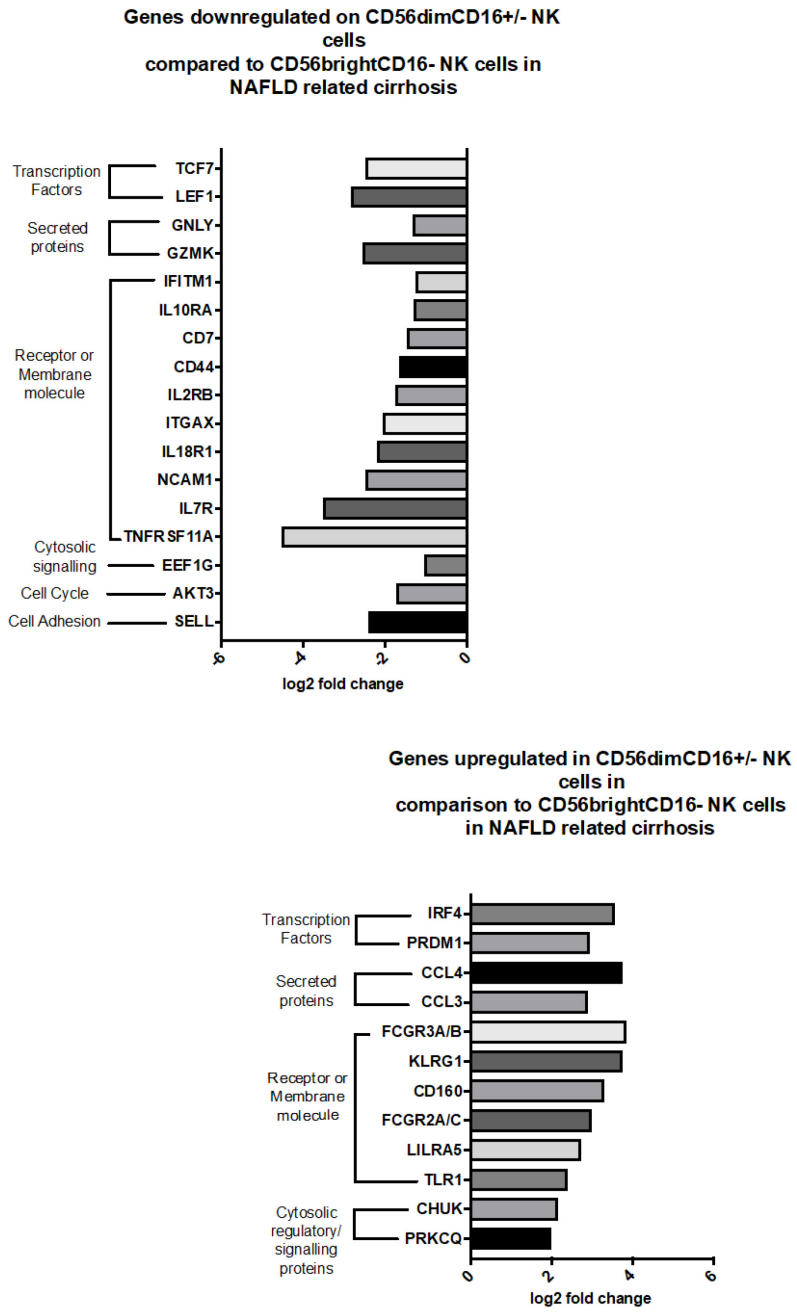
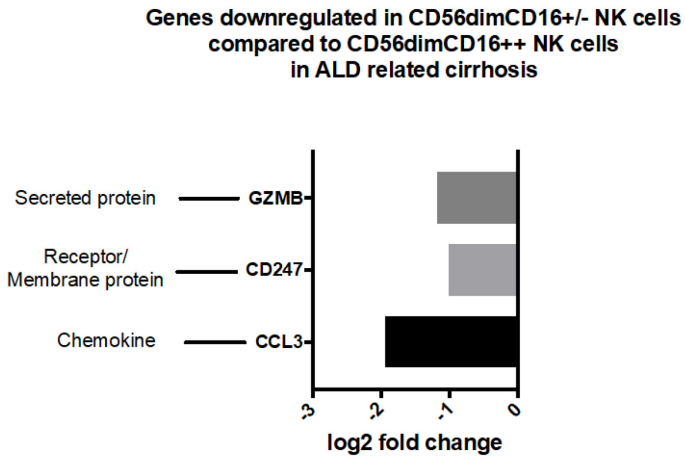


Figure 187 Gene expression in circulating CD56dimCD16+/- NK cells compared to circulating CD56brightCD16- NK cells in NAFLD related cirrhosis



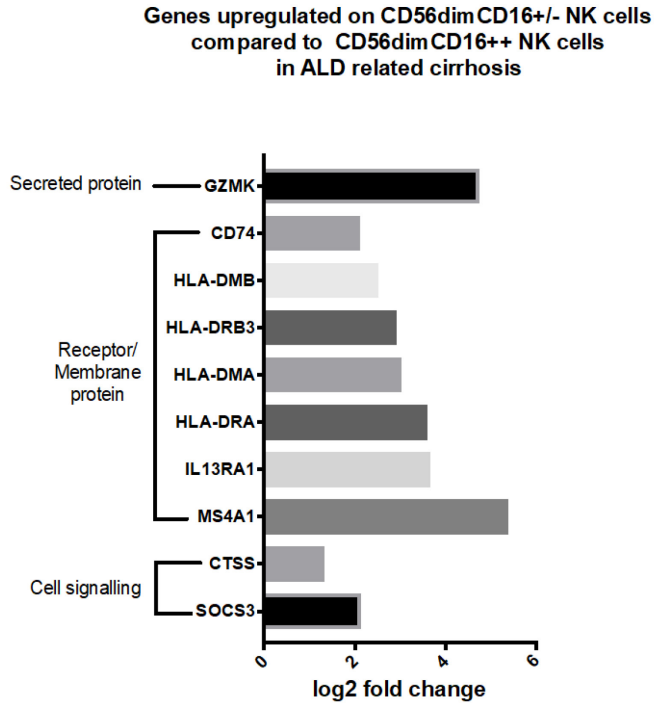


Figure 188 Gene expression in circulating CD56dimCD16+/- NK cells compared to CD56dimCD16++ NK cells in cirrhosis secondary to Alcohol related liver disease (ALD).

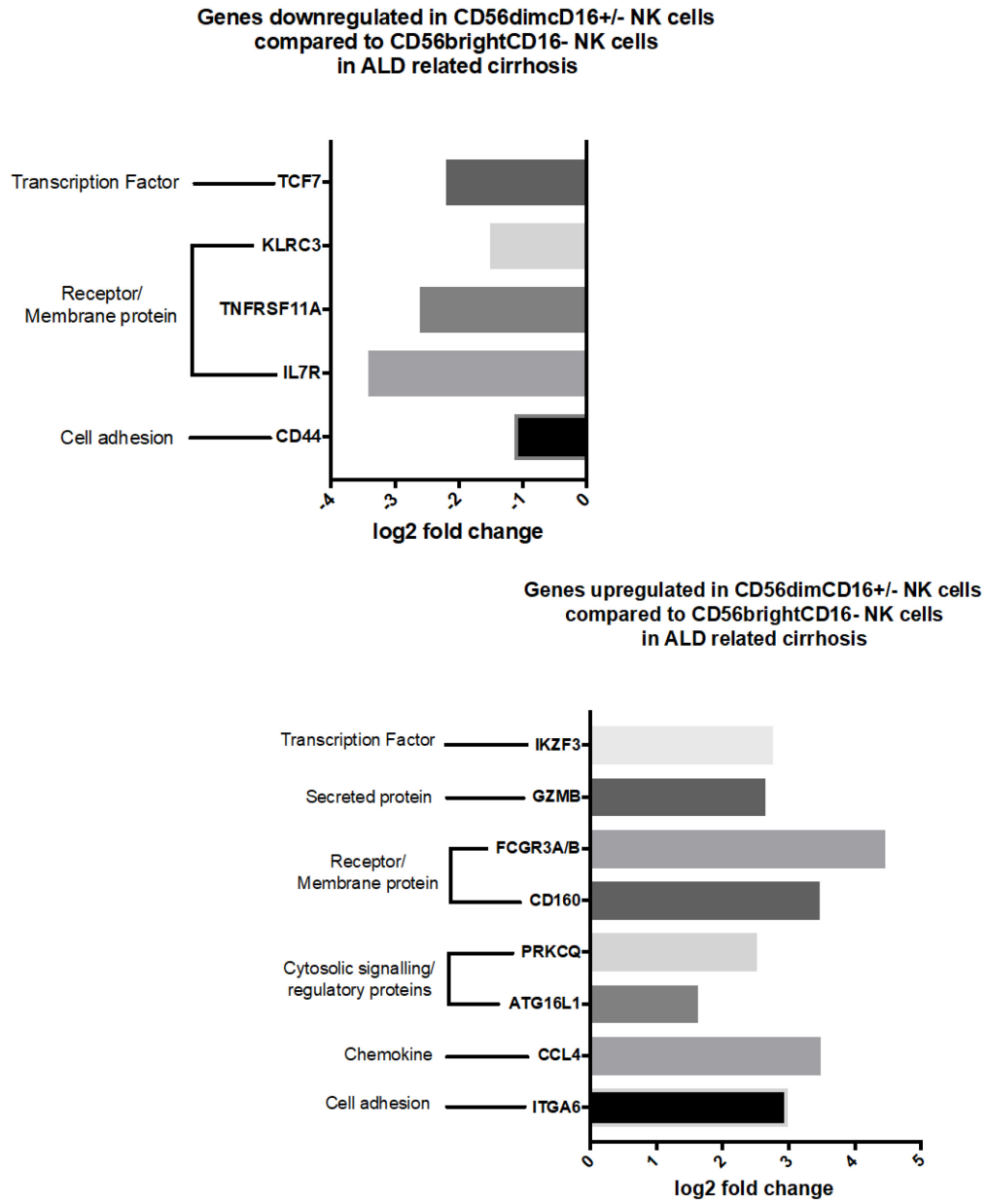


Figure 189 Gene expression in circulating CD56dimCD16+/- NK cells compared to CD56brightCD16- NK cells in ALD related cirrhosis.

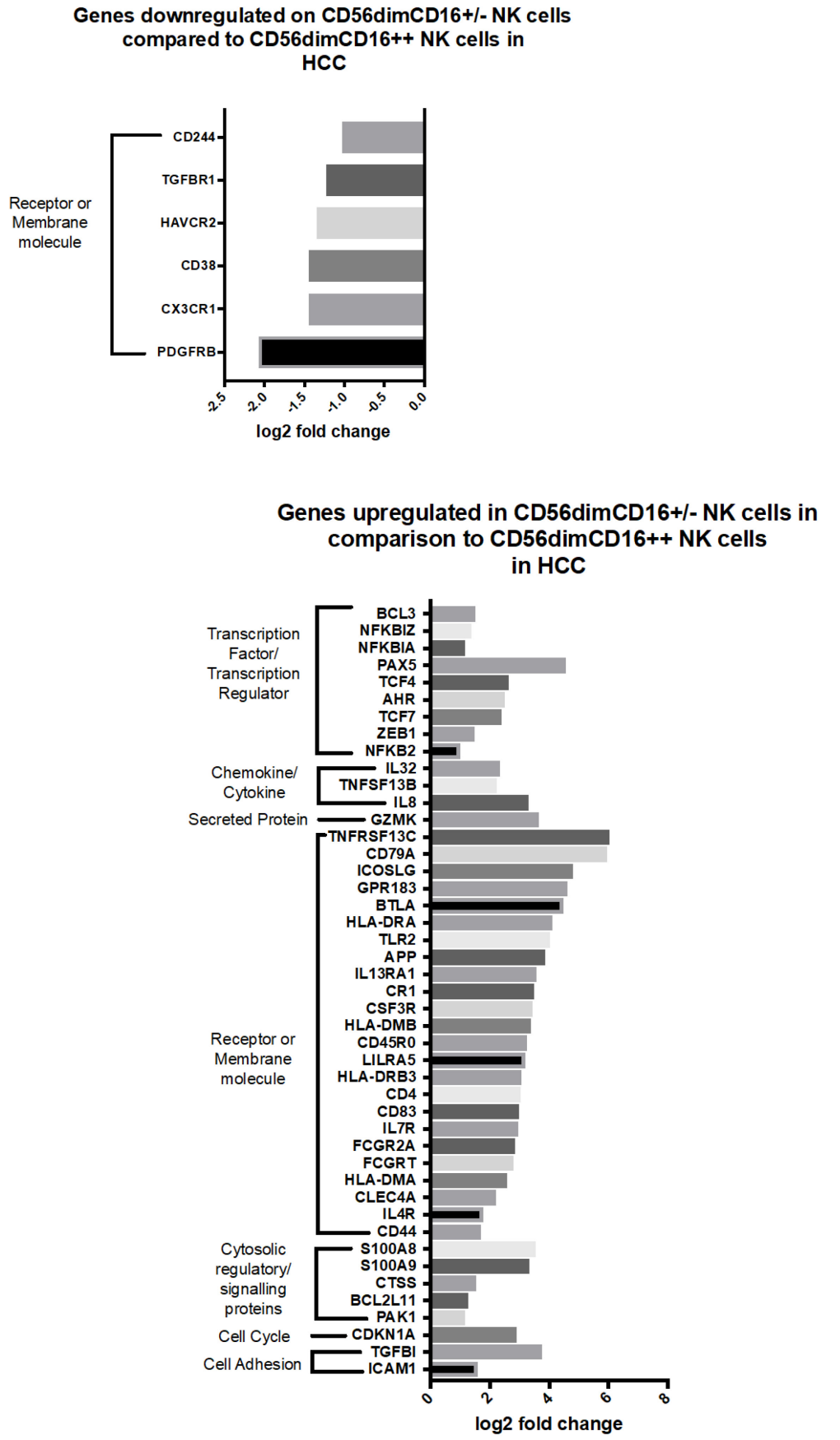
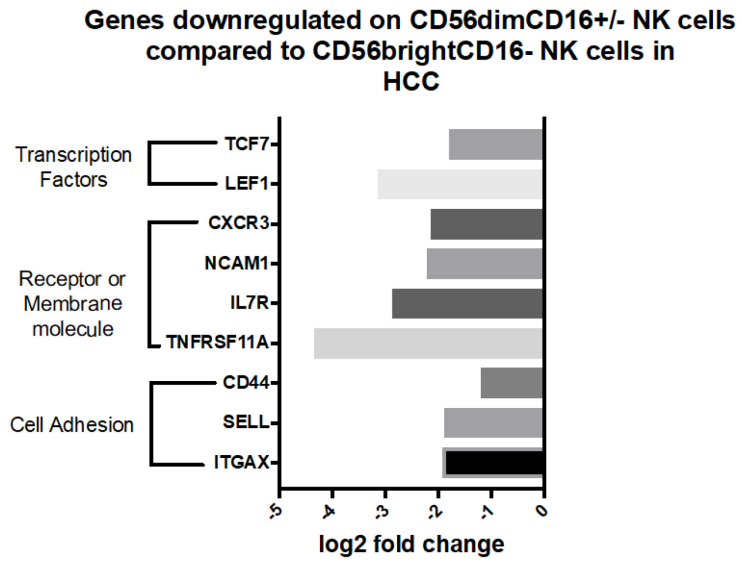


Figure 190 Gene expression in circulating CD56dimCD16+/-NK cells compared to CD56dimCD16++NK cells in HCC.



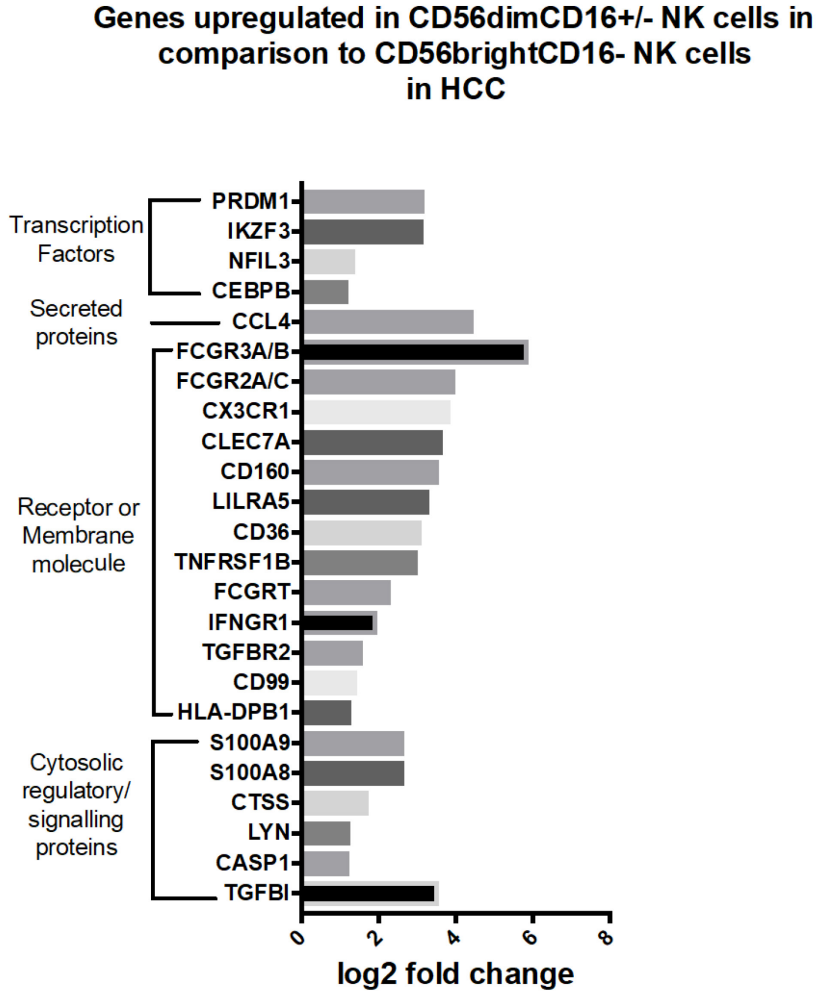


Figure 191 Gene expression in circulating CD56dimCD16+/-NK cells compared to CD56brightCD16-NK cells in HCC.

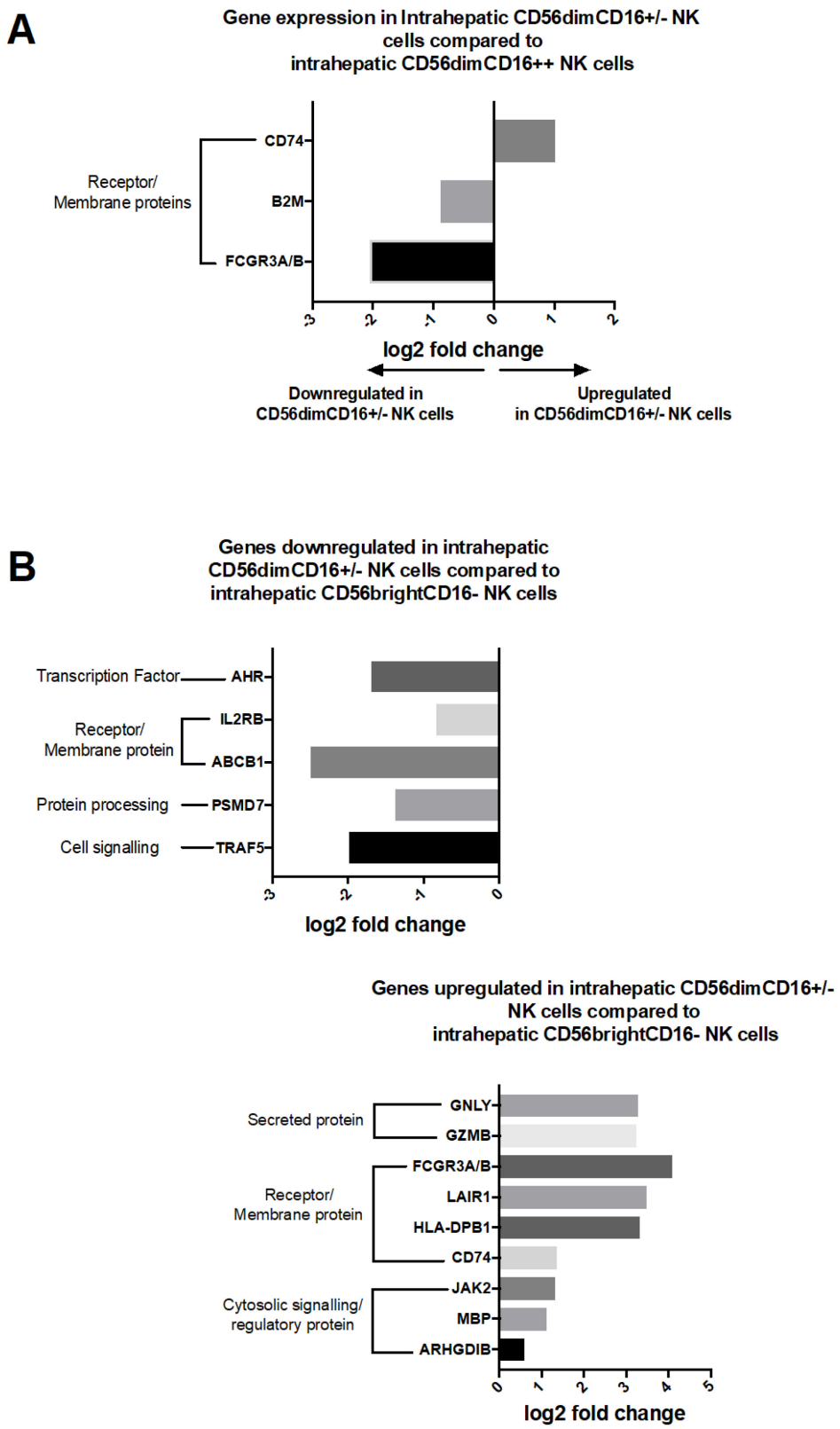


Figure 192 Gene expression in intrahepatic CD56dimCD16+/- NK cells (extracted from cirrhotic liver tissue) compared to A) intrahepatic CD56dimCD16++ NK cells and B) intrahepatic CD56brightCD16- NK cells.

8.5 Comparison of surface expression of receptors in circulatory and intrahepatic NK cells subpopulations.

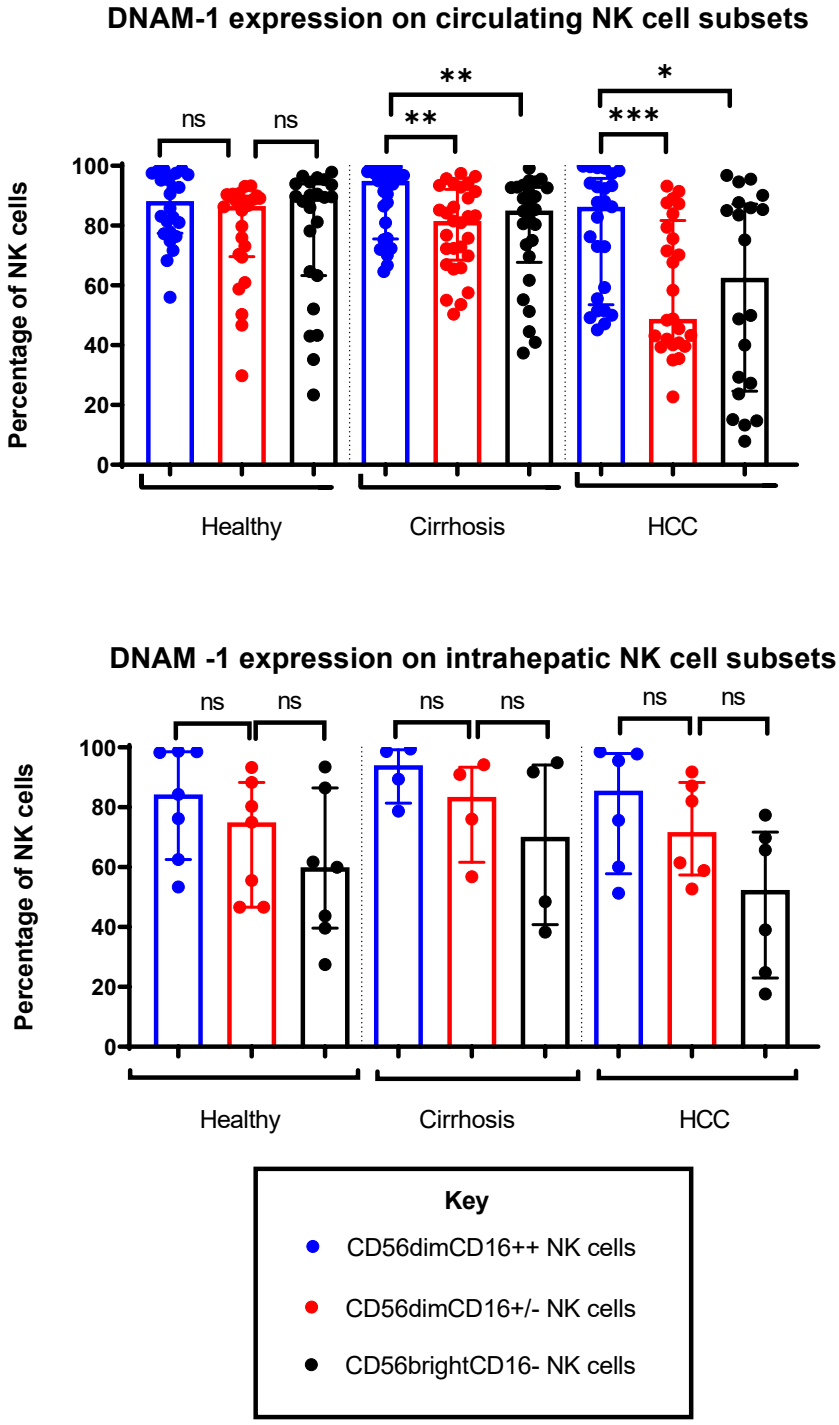


*Figure 193 DNAM-1 expression in NK cell subsets defined by CD56 and CD16 expression in the circulation and in the liver. The top graph demonstrates DNAM-1 expression in circulating NK cells on healthy, cirrhosis and HCC states regardless of underlying aetiology. The bottom graph demonstrates DNAM-1 expression on intrahepatic NK cells. Data in blue demonstrates the proportion of CD56dimCD16++NK cells expressing DNAM-1. Data in red demonstrates the proportion of CD56dimCD16+/- NK cells expressing DNAM-1. Data in black demonstrated the proportion of CD56brightCD16- NK cells expressing DNAM-1. (Graphs display individual values with the median value displayed by the bar. Comparisons between groups have been made using the Mann-Whitney test. Error bars represent the interquartile range. P values are denoted on the figures as follows: * p<0.05, ** p<0.01, *** p<0.001, **** p<0.0001). There were no differences in DNAM-1 expression*

in circulating NK cell subpopulations in healthy volunteers. DNAM-1 expression was reduced on circulating CD56dimCD16+/- NK cells proportion in cirrhosis and HCC (top graph). There were no significant differences in DNAM-1 expression between intrahepatic NK cell subpopulations (bottom graph).

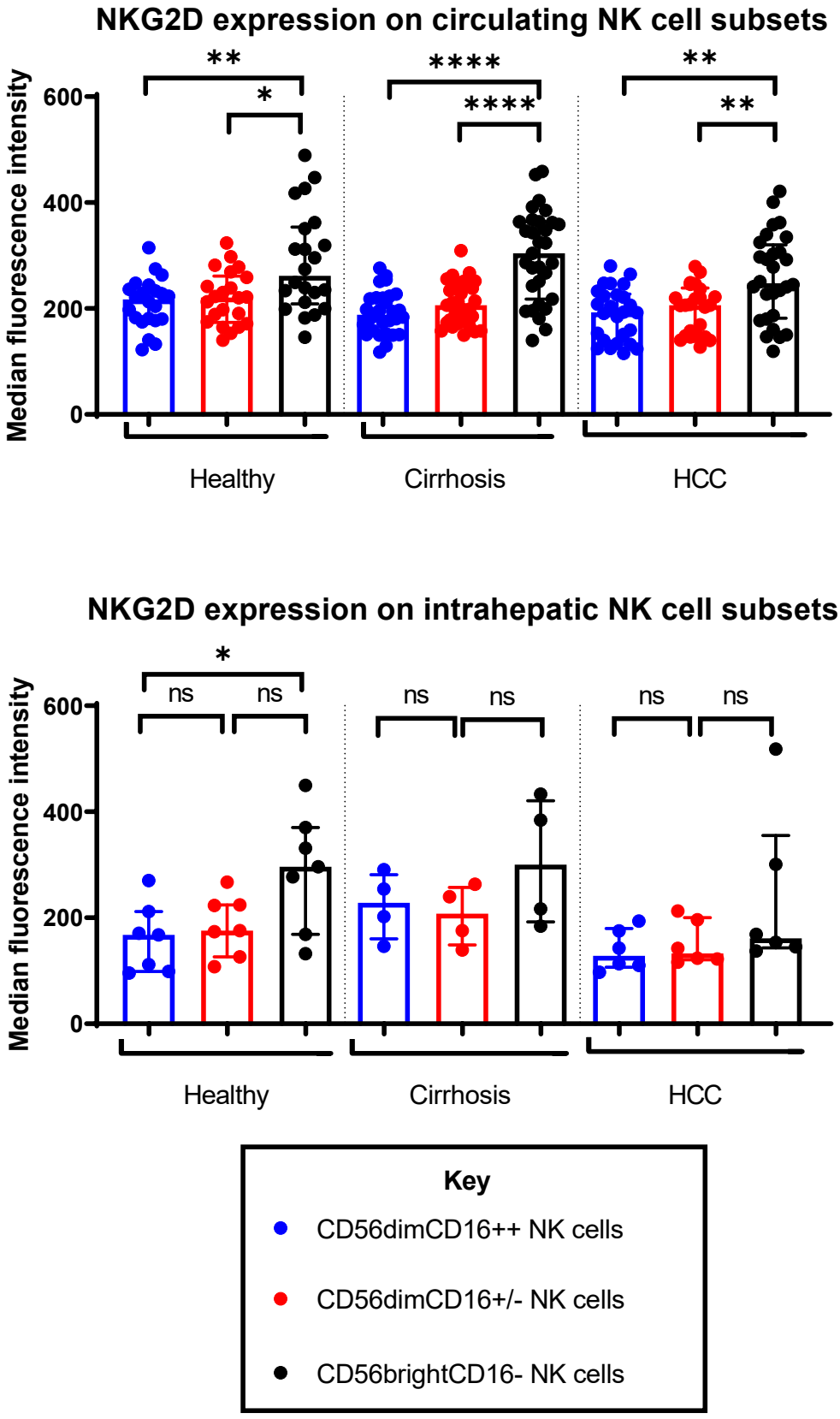


Figure 194 NKG2D expression in NK cell subsets defined by CD56 and CD16 expression in the circulation and in the liver. Circulating and intrahepatic NK cells were stained with antibodies from Phenotyping Panel 1 as described in methods. The

*top graph demonstrates NKG2D expression in circulating NK cells in healthy, cirrhosis and HCC groups regardless of underlying aetiology. The bottom graph demonstrates NKG2D expression on intrahepatic healthy, cirrhosis and HCC NK cells. Data in blue demonstrates the proportion of CD56dimCD16++NK cells expressing NKG2D. Data in red demonstrates the proportion of CD56dimCD16+/- NK cells expressing NKG2D. Data in black demonstrated the proportion of CD56brightCD16- NK cells expressing NKG2D. (Graphs display individual values with the median value displayed by the bar. Comparisons between groups have been made using the paired Wilcoxon test between the same donors. Error bars represent the interquartile range. P values are denoted on the figures as follows: * p<0.05, ** p<0.01, *** p<0.001, **** p<0.0001). There was in increased proportion of NKG2D expressing CD56dimCD16+/- NK cells in comparison to CD56dimCD16++ NK cells (top graph). There were no significant differences in NKG2D expression between intrahepatic NK cell subpopulations (bottom graph).*

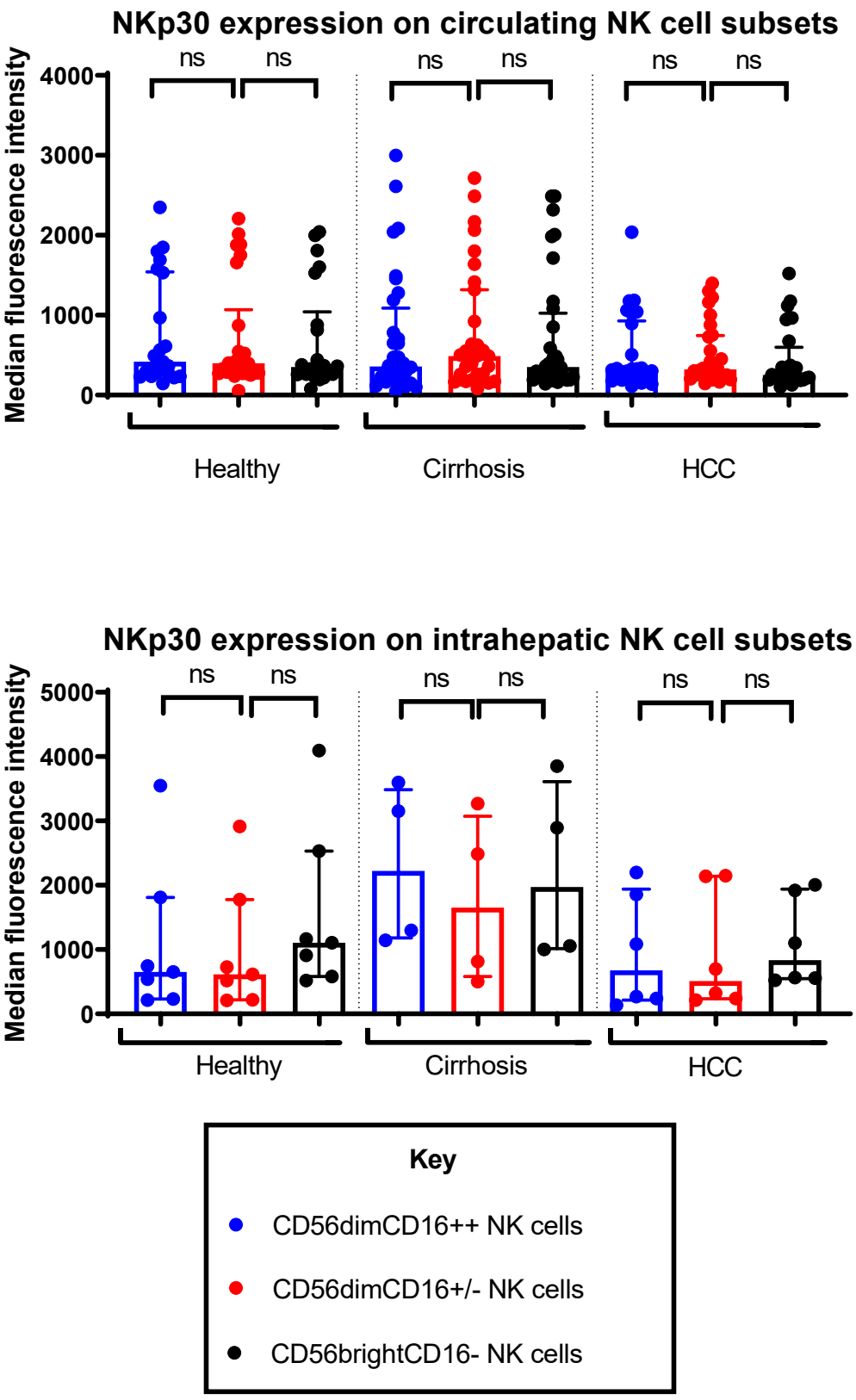


Figure 195 NKp30 expression in NK cell subsets defined by CD56 and CD16 expression in the circulation and in the liver. The top graph demonstrates NKp30 expression in circulating NK cells on healthy, cirrhosis and HCC states regardless of underlying aetiology. The bottom graph demonstrates NKp30 expression on intrahepatic NK cells. Data in blue demonstrates the proportion of CD56dimCD16++NK cells expressing NKp30. Data in red demonstrates the proportion of

*CD56dimCD16+/- NK cells expressing NKp30. Data in black demonstrated the proportion of CD56brightCD16- NK cells expressing NKp30. (Graphs display individual values with the median value displayed by the bar. Comparisons between groups have been made using the Mann-Whitney test. Error bars represent the interquartile range. P values are denoted on the figures as follows: * p<0.05, ** p<0.01, *** p<0.001, **** p<0.0001). There were no significant differences in NKp30 expression when comparing NK cells subpopulations in the circulation or in the liver.*

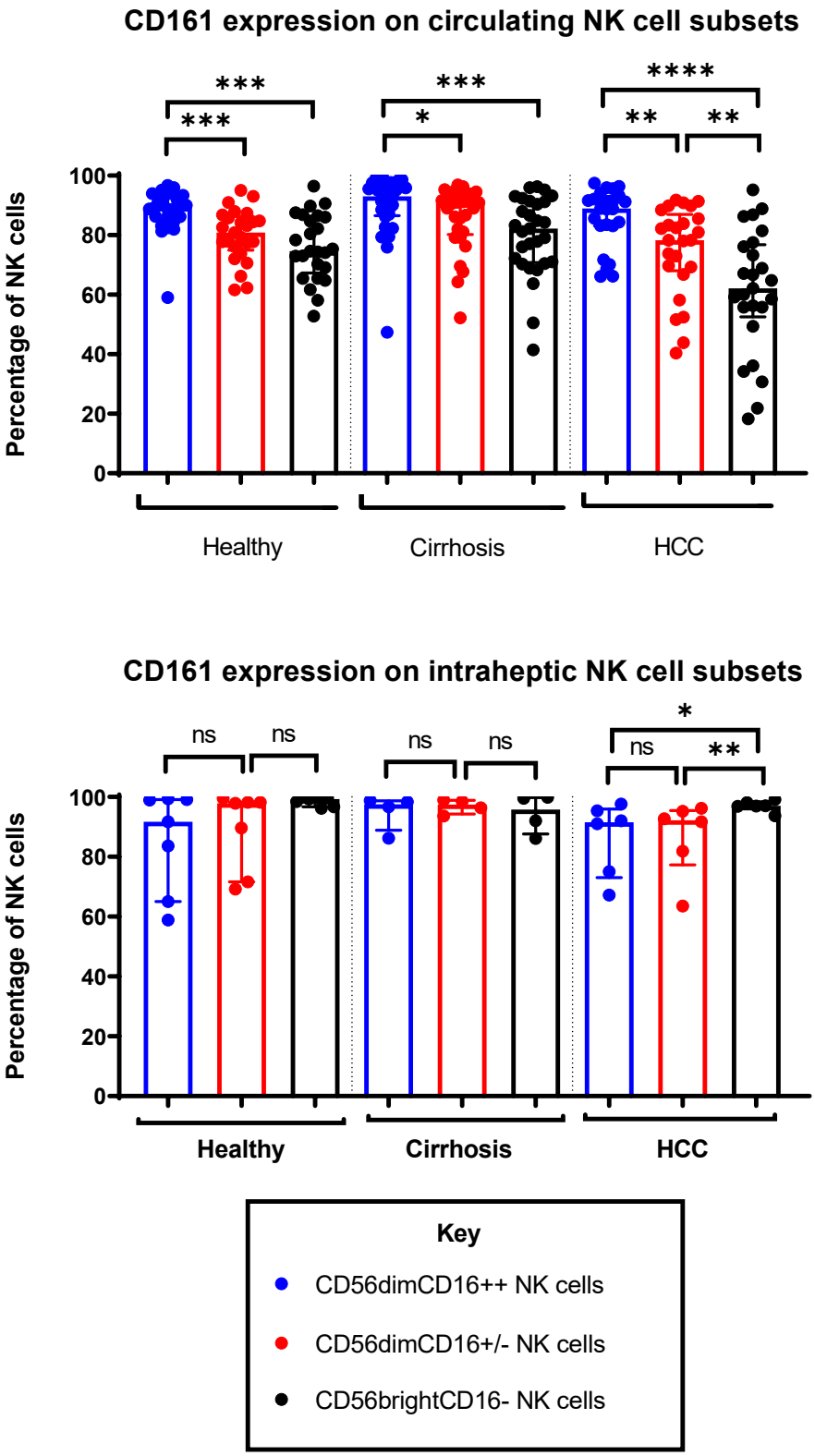


Figure 196 CD161 expression in NK cell subsets defined by CD56 and CD16 expression in the circulation and in the liver. The top graph demonstrates CD161 expression in circulating NK cells on healthy, cirrhosis and HCC states regardless of underlying aetiology. The bottom graph demonstrates CD161 expression on intrahepatic NK cells. Data in blue demonstrates the proportion of CD56dimCD16++NK cells expressing CD161. Data in red demonstrates the proportion of CD56dimCD16+/- NK cells expressing CD161. Data in black demonstrated the proportion of CD56brightCD16- NK cells expressing CD161. (Graphs display individual values with the median value displayed by the bar. Comparisons between

*groups have been made using the Mann-Whitney test. Error bars represent the interquartile range. P values are denoted on the figures as follows: * p<0.05, ** p<0.01, *** p<0.001, **** p<0.0001). The proportion of circulating CD56+CD16+/- NK cells expressing CD161 was lower compared to CD56dimCD16++ NK cell. CD56brightCD16- NK cells had the lowest proportion of CD161+cells of the three NK subpopulations in the circulation (top graph). There were no significant differences between intrahepatic NK cell subpopulations (bottom graph).*

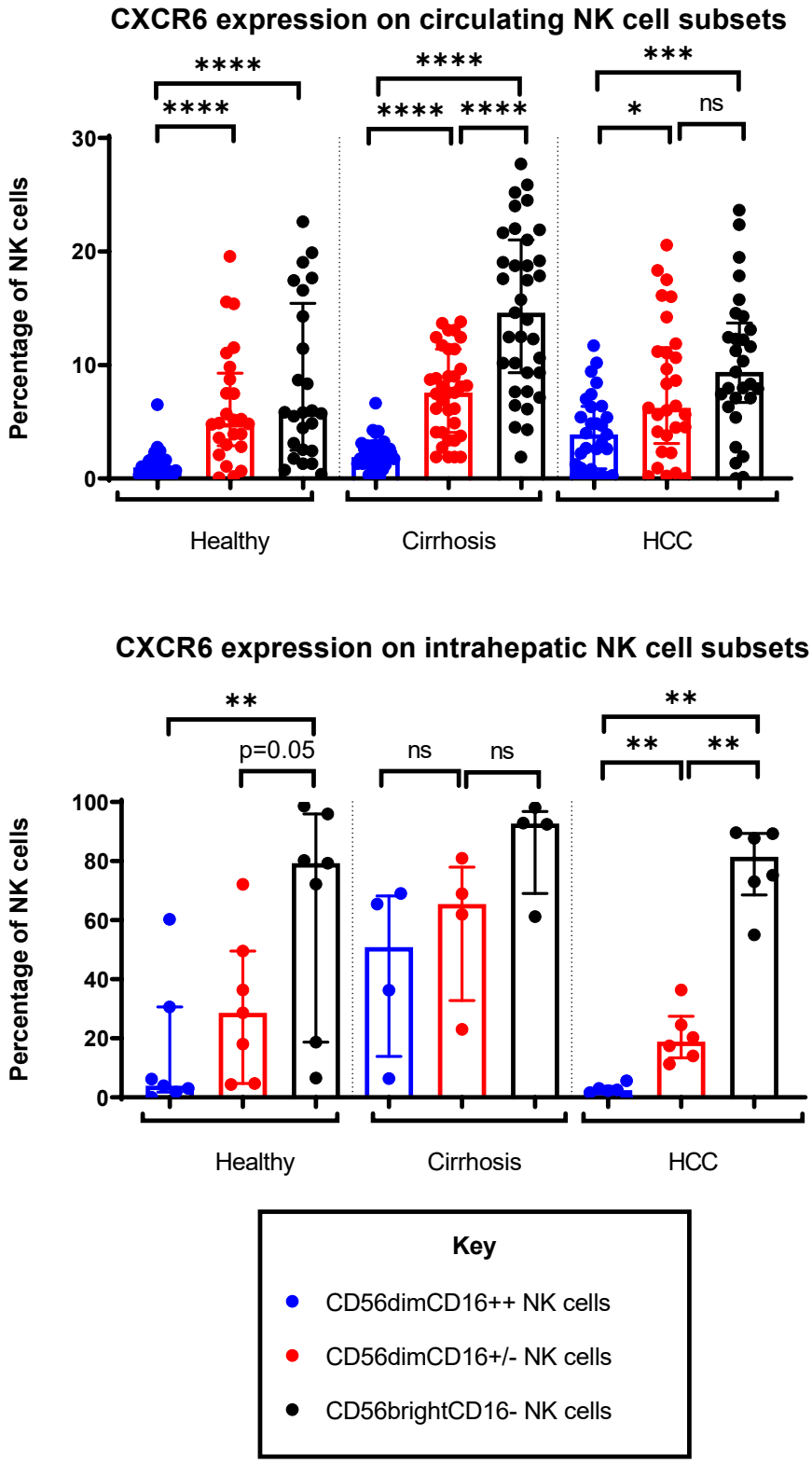


Figure 197 CXCR6 expression in NK cell subsets defined by CD56 and CD16 expression in the circulation and in the liver. The top graph demonstrates CXCR6 expression in circulating NK cells on healthy, cirrhosis and HCC states regardless of underlying aetiology. The bottom graph demonstrates CXCR6 expression on intrahepatic NK cells. Data in blue demonstrates the proportion of CD56dimCD16++NK cells expressing CXCR6. Data in red demonstrates the proportion of CD56dimCD16+/- NK

*cells expressing CXCR6. Data in black demonstrated the proportion of CD56brightCD16- NK cells expressing CXCR6. (Graphs display individual values with the median value displayed by the bar. Comparisons between groups have been made using the Mann-Whitney test. Error bars represent the interquartile range. P values are denoted on the figures as follows: * p<0.05, ** p<0.01, *** p<0.001, **** p<0.0001). There was a significantly increased proportion of CXCR6+ NK cells in the CD56dimCD16+/- subpopulation and CD56brightCD16- NK cell subpopulation compared to CD56dimCD16++ NK cells in the circulation (top graph). This trend was maintained in intrahepatic NK subpopulations (bottom graph).*

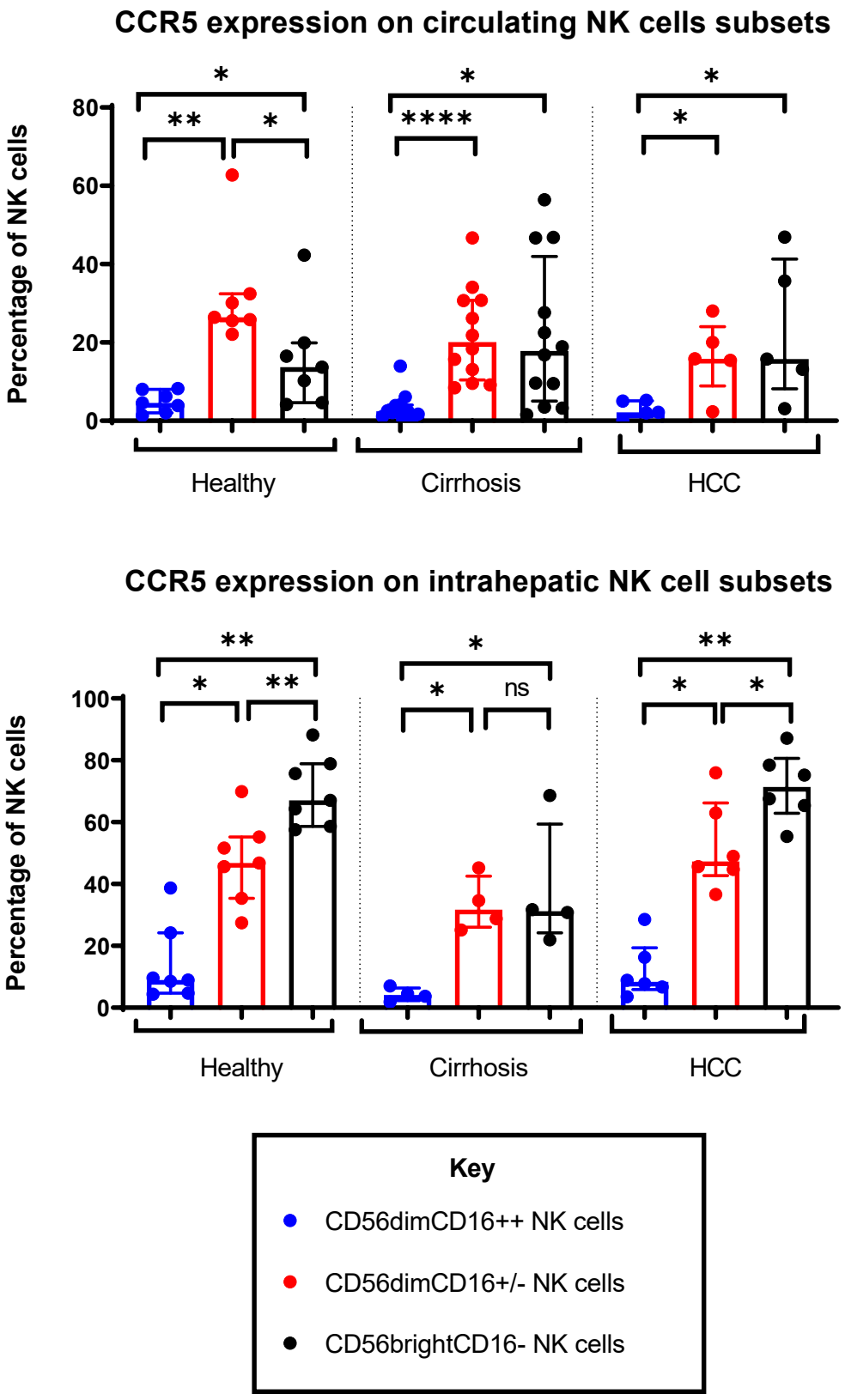


Figure 198 CCR5 expression in NK cell subsets defined by CD56 and CD16 expression in the circulation and in the liver. NK cells were stained with antibodies from the Liver phenotyping panel as described in methods. The top graph demonstrates CCR5 expression in circulating NK cells on healthy, cirrhosis and HCC states. All patients had Child-Pugh A cirrhosis, with or without HCC and all patients had an underlying alcohol related liver disease (ALD) (n=6 healthy, n=12 with cirrhosis only,

*n=5 with HCC on a background of cirrhosis). The bottom graph demonstrates CCR5 expression on intrahepatic NK cells (n=7 healthy, n=4 cirrhosis, n=6 HCC on a background of cirrhosis). Data in blue demonstrates the proportion of CD56dimCD16++NK cells expressing CCR5. Data in red demonstrates the proportion of CD56dimCD16+/- NK cells expressing CCR5. Data in black demonstrated the proportion of CD56brightCD16- NK cells expressing CCR5. (Graphs display individual values with the median value displayed by the bar. Comparisons between groups have been made using the Mann-Whitney test. Error bars represent the interquartile range. P values are denoted on the figures as follows: * p<0.05, ** p<0.01, *** p<0.001, **** p<0.0001). There was a significantly increased proportion of CCR5+ NK cells in the CD56dimCD16+/- subpopulation and CD56brightCD16- NK cell subpopulation compared to CD56dimCD16++ NK cells in the circulation (top graph). This trend was maintained in intrahepatic NK subpopulations (bottom graph).*

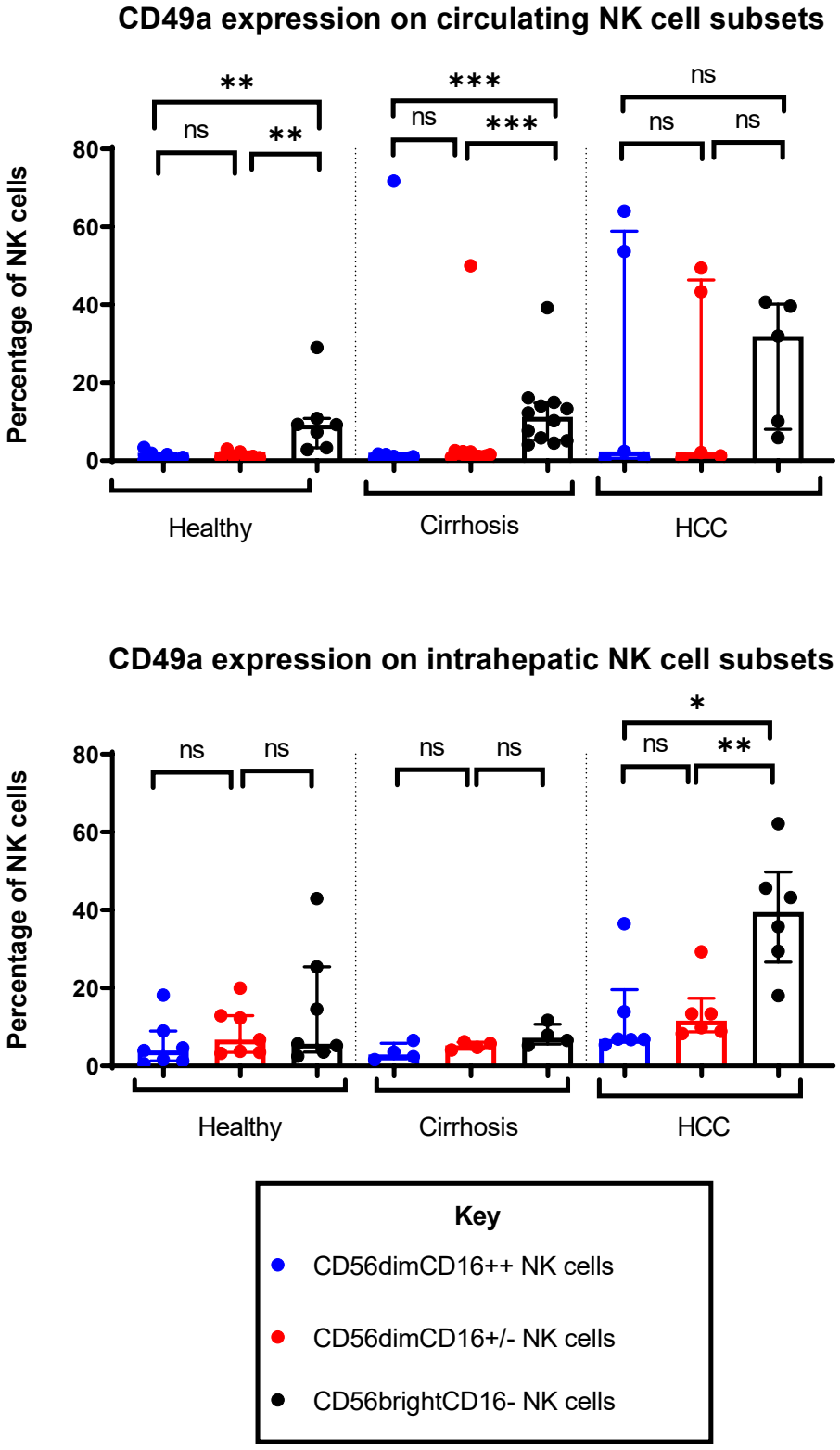


Figure 199 CD49a expression in NK cell subsets defined by CD56 and CD16 expression in the circulation and in the liver. The top graph demonstrates CD49a expression in circulating NK cells on healthy, cirrhosis and HCC states. All patients had Child-Pugh A cirrhosis, with or without HCC and all patients had an underlying alcohol related liver disease (ALD) (n=6 healthy, n=12 with cirrhosis only, n=5 with HCC on a background of cirrhosis). The bottom graph demonstrates CD49a expression on intrahepatic NK cells (n=7 healthy, n=4 cirrhosis, n=6 HCC on a background of cirrhosis). Data in blue demonstrates the proportion of CD56dimCD16++NK cells expressing CD49a. Data in red demonstrates the proportion of CD56dimCD16+/- NK

*cells expressing CD49a. Data in black demonstrated the proportion of CD56brightCD16- NK cells expressing CD49a. (Graphs display individual values with the median value displayed by the bar. Comparisons between groups have been made using the Mann-Whitney test. Error bars represent the interquartile range. P values are denoted on the figures as follows: * p<0.05, ** p<0.01, *** p<0.001, **** p<0.0001). There were no significant differences in CD49a expression in CD56dimCD16+/- NK cells in comparison to CD56dimCD16++ NK cells in the circulation (top graph). There was a significant increase in CD49a expression in CD56brightCD16- NK cells in livers with HCC, but no significant differences in CD49a expression between the two CD56dim subpopulations (bottom graph).*

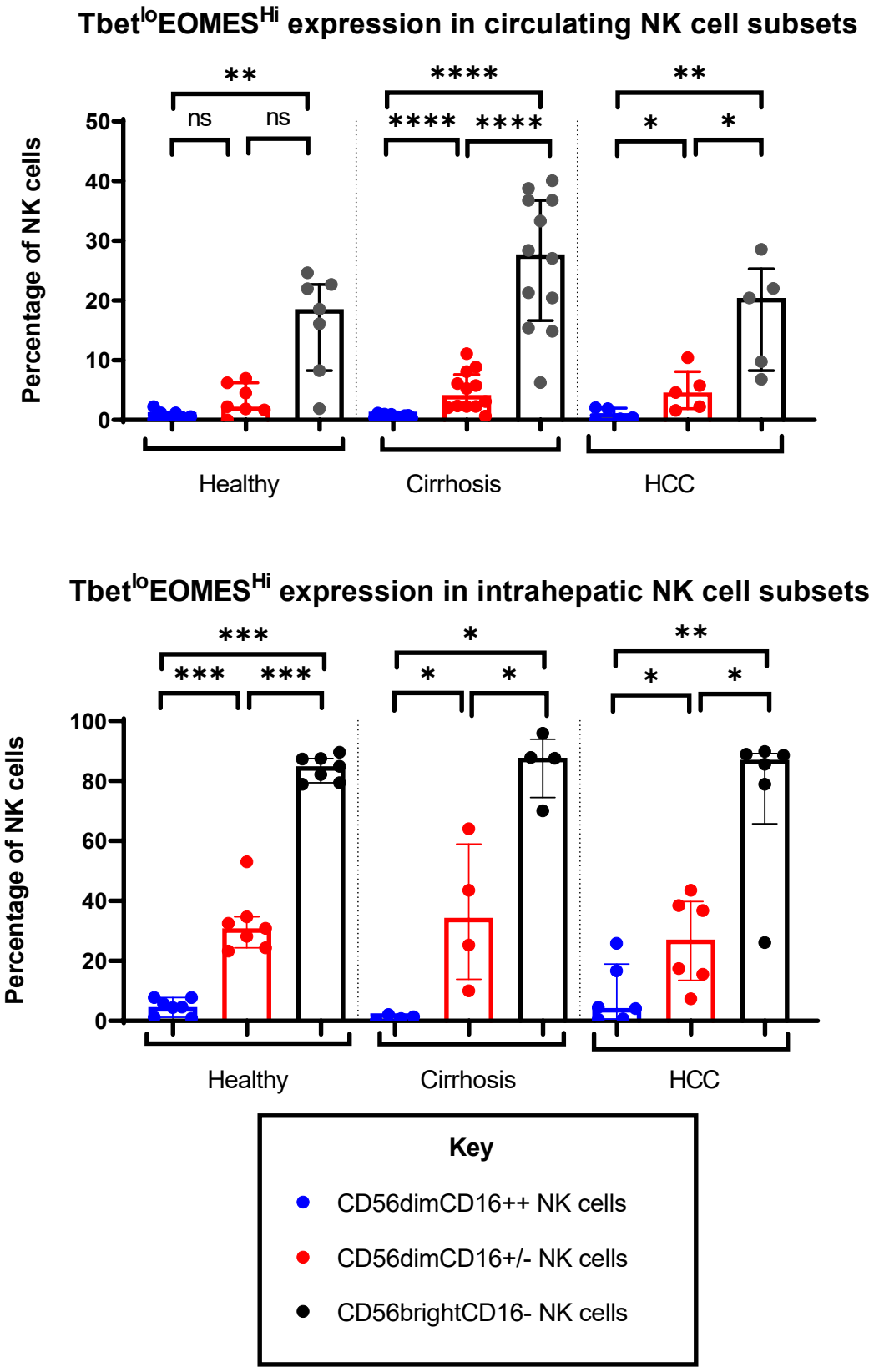


Figure 200 Tbet and EOMES expression in NK cell subsets defined by CD56 and CD16 expression in the circulation and in the liver. NK cells were stained using the Liver phenotyping panel as described in methods. The top graph demonstrates Tbet and

*EOMES expression in circulating NK cells on healthy, cirrhosis and HCC states. All patients had Child-Pugh A cirrhosis, with or without HCC and all patients had an underlying alcohol related liver disease (ALD) (n=6 healthy, n=12 with cirrhosis only, n=5 with HCC on a background of cirrhosis). The bottom graph demonstrates Tbet and EOMES expression on intrahepatic NK cells (n=7 healthy, n=4 cirrhosis, n=6 HCC on a background of cirrhosis). Data in blue demonstrates the proportion of CD56dimCD16++NK cells that are TbetloEOMESHi. Data in red demonstrates the proportion of CD56dimCD16+/- NK cells that are TbetloEOMESHi. Data in black demonstrated the proportion of CD56brightCD16- NK cells that are TbetloEOMESHi. (Graphs display individual values with the median value displayed by the bar. Comparisons between groups have been made using the Mann-Whitney test. Error bars represent the interquartile range. P values are denoted on the figures as follows: * p<0.05, ** p<0.01, *** p<0.001, **** p<0.0001). CD56dimCD16+/- NK cells had an intermediate proportion of TbetloEOMESHi NK cells, with CD56brightCD16- NK cells having the highest proportion and CD56dimCD16++ NK cells having the lowest proportion, in the circulation as well as within the liver.*

Appendix 8.6 Cytokine production in NK cell subsets following PMA/Ionomycin stimulation

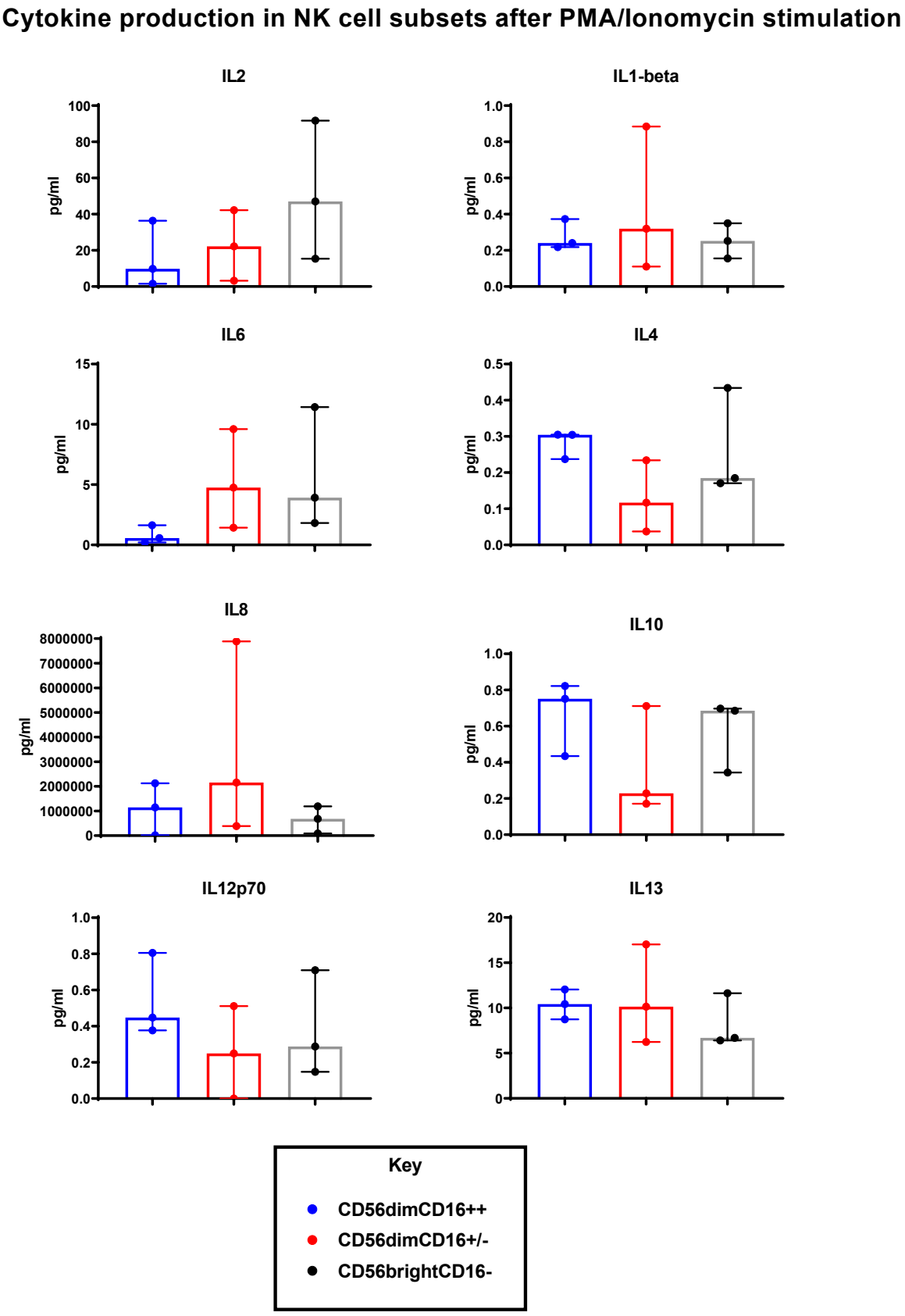


Figure 201 Cytokine production in NK cell subsets following stimulation with PMA and ionomycin. Peripheral blood mononuclear cells (PBMCs) from patients with cirrhosis secondary to Alcohol related liver disease (ALD cirrhosis, n=3) were stained with Phenotyping Panel 1 (see Table 3) and sorted in NK cells subsets based on CD56/CD16 expression as described in Figure 3. These isolated NK cell subsets were stimulated with PMA (50ng/ml) and ionomycin (500ng/ml) in duplicates for four hours. Cytokine expression was read using a V-plex pro-inflammatory panel 1 MSD plate (n=3 samples run in duplicates, data points represent an average reading of the duplicates). Comparisons were made using the paired Wilcoxon test. Graphs display individual values with the median value displayed by the bar. Error bars represent the interquartile range.

8.7 Immunohistochemistry for LLT1 in Cholangiocarcinoma

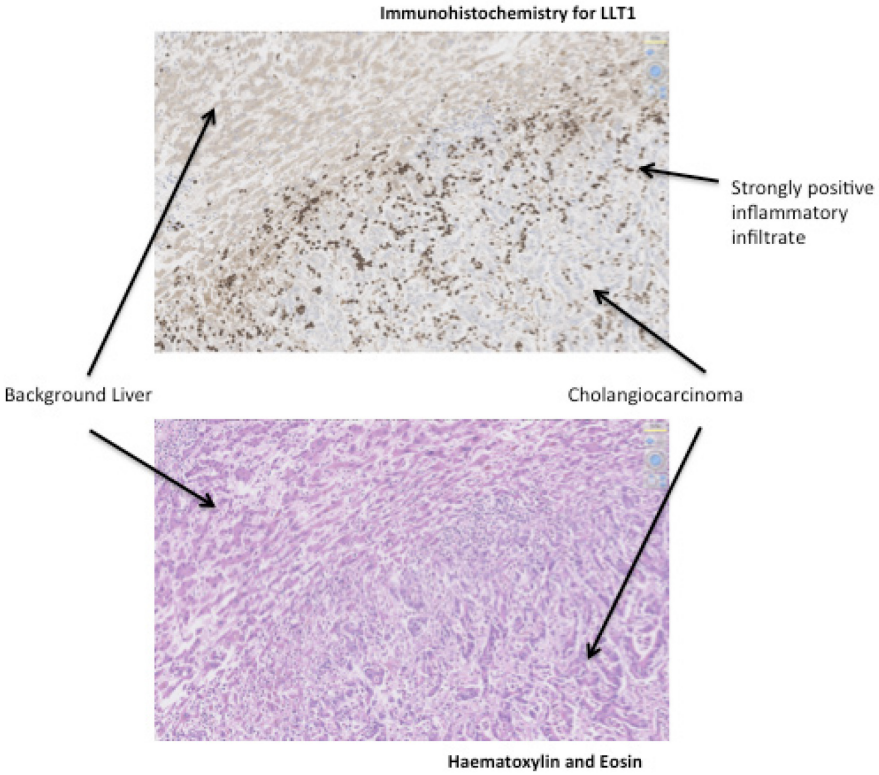


Figure 202 Immunohistochemistry for LLT1 expression on FFPE liver tissue from a resection specimen for a moderately differentiated cholangiocarcinoma. Liver resection specimens (n=17) for cholangiocarcinoma were stained for LLT1 (1:4000 dilution, Abnova) as described in methods. Immunohistochemistry for LLT1 does not demonstrate LLT1 expression on tumour tissue, and there is weak staining for LLT1 in the liver background tissue but the inflammatory infiltrate is positive for LLT1.